University of East Anglia

Phthalocyanine hybrids; old chemistry revisited and new syntheses

Nora Mobark S Farhan

This thesis is submitted in fulfilment of the requirements of the degree of Doctor of Philosophy at the University of East Anglia

School of Chemistry

University of East Anglia, Norwich, United Kingdom

November 2023

Declaration

The research described in this thesis is, to the best of my knowledge, original except where due reference has been made.

Nora Farhan

This thesis is dedicated to my beloved family

My husband Yousef

My kids Mohammed, Turki & Saba

Abstract

The work described in this thesis is concerned with the investigation of synthetic pathways toward tetrabenzoporphyrin/phthalocyanine hybrid macrocycles, specifically tetrabenzomonoazaporphyrins (TBMAPs) or other less-nitrogenous hybrids. The initial investigation was conceived to modify the latest synthetic procedure developed in the Cammidge group whereby utilisation of a less nitrogenous precursor (alkynylbenzonitrile, 1 x N) replaced phthalonitrile (2 x N) as co-macrocyclisation partner with an aminoisoindoline. Unfortunately, no hybrids were formed and instead the formation of a six-membered ring isoquinoline from the acetylene was observed under these conditions. Linstead's method to synthesise TBMAPs was then revisited, and different malonyl aminoisoindolines were synthesised and isolated. These precursors proved to be unstable under many conditions which resulted in the formation of their keto-esters and dimers during their purification process. Fusion of these precursors with zinc dust at 220°C proved to give a mixture of hybrids but no evidence for the expected TBMAPs' formation, according to MALDI-MS analysis. Isolation of the hybrids was challenging and complicated by slow decomposition during chromatography. We switched to investigate Linstead's conditions of fusion in the presence of zinc metal at high temperature on our proposed reactants (alkynylbenzonitrile with aminoisoindoline) and, interestingly, formation of ZnTBTAP, *cis*TBDAP, *trans*TBDAP and traces of ZnTBMAP were observed. However, the formation of these hybrids proved to be a result of macrocyclisation of one reactant only – the aminoisoindoline. Full analysis of all hybrids was obtained, except ZnTBMAP due to its low quantity.

In the final part of the thesis, we further explored the latest Cammidge procedure to synthesise TBTAPs by employing substituted phthalonitriles ("B") with aminoisoindolines ("A"), in this case using different metals to track the origin of each unit in the final TBTAPs. ABBB TBTAPs were selectively obtained in high yield when zinc chloride was utilised while a mixture of ABBB and ABBA TBTAPs were obtained when different metals were employed. Full characterisation of the obtained hybrids and intermediates was achieved. The formation of these hybrids is somewhat surprising and no obvious mechanisms for their formation are apparent.

Acknowledgements

First of all, I would like to express my gratitude and appreciation to Professor Andrew N. Cammidge for his continuous support, invaluable guidance and help throughout my research. I am deeply appreciative of his patience, as well as his kindness and attentiveness. Undoubtedly, he exemplifies exceptional qualities as an educator and leader in the field of science.

It is with immense gratitude that I acknowledge the constant support and the valuable scientific assistance of Dr. Isabelle Fernandes. Special thanks go to her, Dr. Joseph Wright and Dr. David Hughes for their help in running X-Ray crystallography and gathering data throughout the project.

I want to also thank the past and current members of the Cammidge team for their assistance in various ways. Extending that to all people in chemistry school, especially those who work on the third floor. Thanks, are also due to technical staff in the school of chemistry for their assistance and maintenance of instruments.

Special and massive thanks to my husband and my kids, whom without this would not have been possible. I appreciate their endless support, encouragement, and patience at every stage of my study. My appreciation also goes out to my family and friends in the UK and back home who in way or another shared their support.

Thanks, are also due to Princess Norah bint Abdulrahman University for funding my PhD research and providing me with an opportunity to achieve my goal. Thanks are extended to the Saudi Arabia Cultural Bureau in London for their support during my PhD.

List of Abbreviations

Ar	Aromatic
BINAP	2,2'-Bis(diphenylphosphino)-1,1'-binaphthyl
b.p	Boiling point
^{o}C	Degrees Celsius
cis-TBDAP	Cis-Tetrabenzodiazaporphyrin
d	Doublet
dd	Doublet of Doublets
dt	Doublet of Triplets
ddd	Doublet of Doublet of Doublets
DABCO	1,4-Diazabicyclo [2.2.2] octane
DBU	1,8-Diazabicyclo [5.4.0] undec-7-ene
DCM	Dichloromethane
DFT	Density Functional Theory
DMF	Dimethylformamide
DMSO	Dimethyl sulfoxide
DSSC	Dye Sensitised Solar Cell
ε	Extinction coefficient
eq	Equivalents
g	Grams
HOMO	Highest Occupied Molecular Orbital
IR	Infrared
i-PrOH	Isopropyl alcohol
J	Coupling Constant
L	Ligand
LUMO	Lowest Unoccupied Molecular Orbital
M	Metal

MHz	Megahertz
m	Multiplet
mg	Milligrams
mL	Millilitres
mmol	Millimol
M.p.	Melting point
M.wt	Molecular weight
nm	Nanometres
MALDI-TOF	Matrix Assisted Laser Desorption/Ionisation - Time Of Flight
MeOH	Methanol
MS	Mass Spectroscopy
m/z	Mass over Charge
NMR	Nuclear Magnetic Resonance
OPV	Organic photovoltaic
Pc	Phthalocyanine
PCE	Power Conversion Efficiency
PDT	Photodynamic therapy
PE	Petroleum Ether
PS	Photosensitiser
ppm	Parts Per Million
r.t.	Room temperature
λ	wavelength
SM	Starting Material
SubPc	Subphthalocyanine
TBMAP	Tetrabenzomonoazaporphyrin
TBTAP	Tetrabenzotriazaporphyrin
TBP	Tetrabenzoporphyrin
t-Bu	Tert-butyl
THF	Tetrahydrofuran

TLC   Thin Layer Chromatography

Trans-TBDAP   Trans-Tetrabenzodiazaporphyrin

UV-Vis   Ultraviolet-Visible

Table of Contents

X

List of figures

XIII

XV

List of schemes

Chapter 1:

Introduction to Phthalocyanines

and Tetrabenzo(aza)porphyrin

Hybrids

1.1 Introduction to Phthalocyanines

Phthalocyanines (Pcs, **2**) form a wide class of man-made macrocyclic molecules that are intensely coloured pigments. The phthalocyanine structure was elucidated by Linstead and co-workers in 1934.[1–3] It has a similar chemical structure to the naturally occurring porphyrin (**1**), as both structures consist of four pyrrole rings connected by four bridges. In porphyrin, the bridges are methine, and in phthalocyanine, they are aza-bridges (nitrogen atoms). In the Pc structure, each of the pyrrole units is fused to a benzene ring as shown in figure (1.1). Thus, tetrabenzotetraazaporphyrins are another name for these synthetic compounds.[3,4]

According to Hückel's rule of aromaticity (4n+2), Phthalocyanine macrocycle is a highly conjugated aromatic molecule with 18 π delocalised electrons. The central cavity of Pc can accommodate various metal ions to form metalated phthalocyanine (MPcs) through coordinating with the isoindolic nitrogens inside the ring.[4]
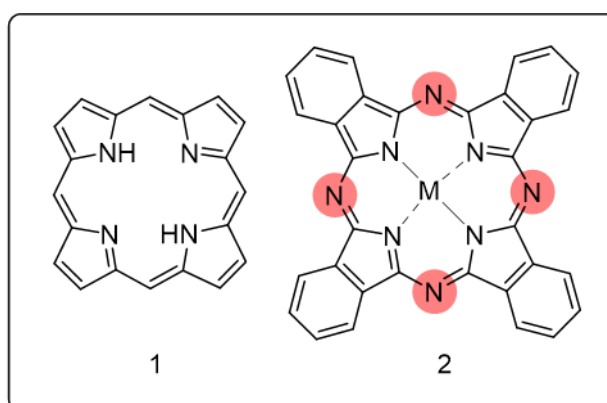
Figure 1.1: Parent structures of porphyrin (**1**) and phthalocyanine (**2**, M = 2H).

1.2 Discovery and History of Phthalocyanines

Phthalocyanine (**2**) was first reported in 1907 by Braun and Tcherniac as an unidentified blue by-product during the preparation of o-cyanobenzamide (**4**) from phthalimide (**3**).[5] Twenty years later, 23% of the blue compound was isolated by de Diesbach and Von der Weid in an attempted conversion of *o*-dibromo benzene (**5**) into phthalonitrile (**6**) using copper (I) cyanide in refluxing pyridine.[6] It was remarked on the enormous stability of that complex, but no further characterisation was made.
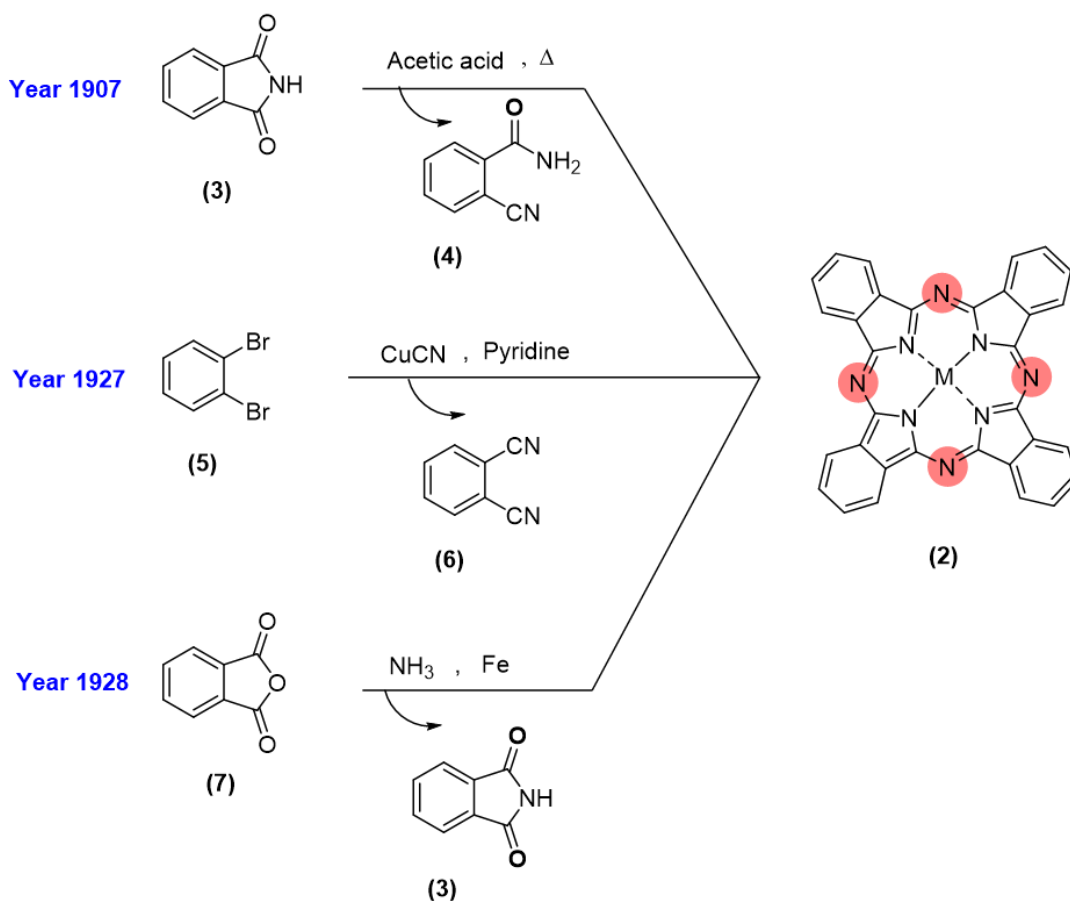
Scheme 1.1: All accidental preparations of phthalocyanine.

In 1928, Imperial Chemical Industries (ICI) (known as Scottish Dyes of Grangemouth) reported the formation of a brilliant blue impurity in an industrial preparation of phthalimide (**3**) from phthalic anhydride (**7**) and ammonia. It was later recognised to be iron phthalocyanine and the iron vessel employed in the process provided the metal ion as shown in scheme 1.1. In 1929 the first patent was issued with respect to compounds that are now known as phthalocyanines, to Dandridge, Drescher and Thomas of Scottish Dyes Ltd. In the early 1930s under the direction of Sir Patrick Linstead, the molecular structure of phthalocyanine was elucidated.[1,3] Later, Robertson confirmed the proposed structure by X-ray diffraction techniques.[7–10]

1.3 Properties of Phthalocyanines

The phthalocyanines' conjugated 18π-electron systems provide them unique optical, electrical and physical features like light absorption, intense colour, and structural shape in addition to thermal and chemical stability.[4,11] Yet, any variation of the macrocyclic complex that alters the macrocycle's symmetry and conjugation pathway may have an impact on these properties. This modification can be achieved through insertion of a metal into the macrocycle's central cavity or introduction of substituents onto the benzene rings on Pc macrocycle.[12]

1.3.1 Modification of central cavity of phthalocyanine

The size of the central cavity of Pc macrocycle is perfectly suited to bind two hydrogen atoms (H_2Pc) or a great variety of metal cations that can bind to the ionic metal-free macrocycle to form Metallophthalocyanines (MPc).[4]

For metal cations that are normally in an oxidation state of +1, such as Li and Na, the central nitrogen atoms ligate two ions to form 2:1 metal:Pc complexes.[4] However, in transition metals that are normally in oxidation state of +2, such as Cu and Fe, the central nitrogen atoms ligate one ion to form 1:1 stable metal:Pc complexes. Metals with an oxidation state higher than +2, such as Rh and Sn, usually have a high affinity for additional ligands.[13] Moreover, stacked sandwich complexes with phthalocyanines can be obtained, where the metal ion is located between two Pc macrocycles to form (MPc_2), for example when lanthanide metals M(III) are used as depicted in figure 1.2.[8,14,15]

Depending on the metal's size, it can fit in the central cavity of Pcs or lie above the plane of the Pc ring and distort the planarity of the macrocycle as in figure 1.2 (right). When the ionic radius of the metal ions is in the range of (55–80) pm such as Zn, Cu, Ni and Co, metal ions can be accommodated in the central cavity of Pcs to form square planar complexes without any significant distortion of the Pc macrocycles. However, if the ionic radius of the metal ions is over 80-90 pm such as lead, the metal ions cannot fit completely in the cavity of the macrocycle. They are located out of the plane, forming domed conformation. [16,17]
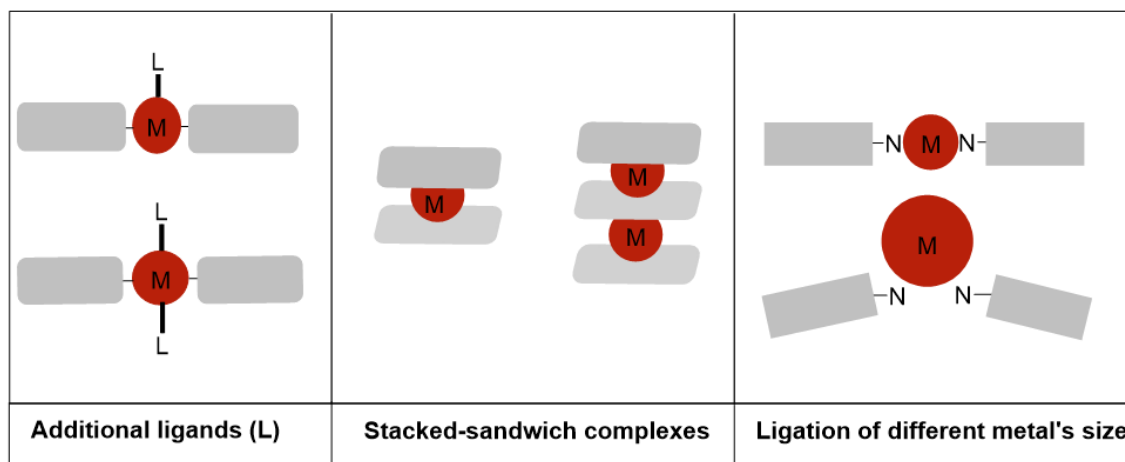
Figure 1.2:   Ligation of different size or oxidation state of metals in the Pc structures.

1.3.2 Introduction of substituents onto phthalocyanine macrocycles

Introducing substituents on the fused benzenes in Pc macrocycles are major ways of modifying the phthalocyanine structure as these benzene rings have two different sites that can be substituted. The substituents located at positions 1, 4, 8, 11, 15, 18, 22, and 25 of the phthalocyanine ring (non-peripheral positions) are named as α−substituents, while those located at positions 2, 3, 9, 10, 16, 17, 23, and 24 (peripheral positions) are regarded as β-substituents as depicted in figure 1.3.[4]
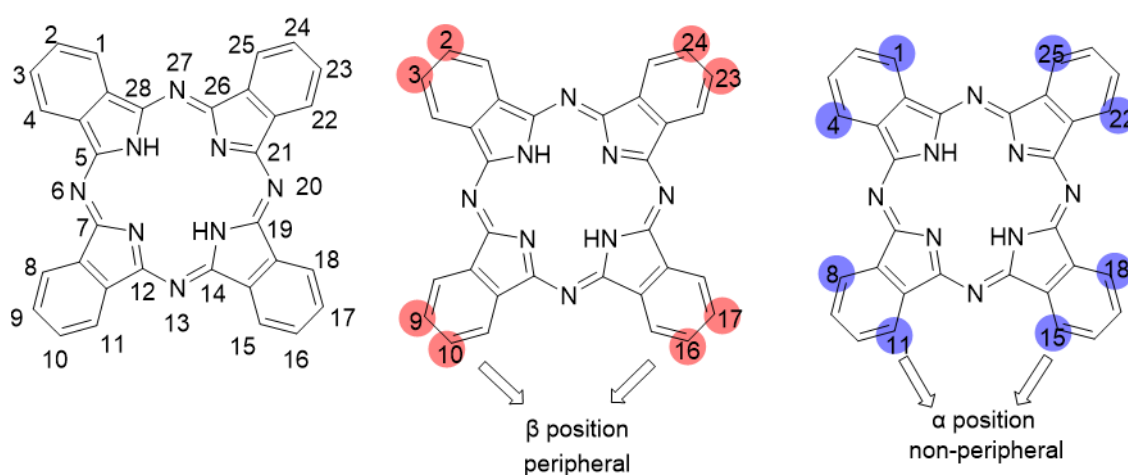
Figure 1.3: Numbering scheme for the phthalocyanine core (left) and substitution patterns: peripheral (centre) and non-peripheral (right).

There are two main different methods to introduce the α or β substituents into Pc structures. The first methodology involves an aromatic electrophilic substitution reaction with already existing Pc macrocycle such as halogenation or sulfonation of Pcs as depicted in scheme 1.2. This method produces a mixture of substituted Pcs that are challenging to isolate.[18–21]

R= SO$_2$Cl or SO$_3$H
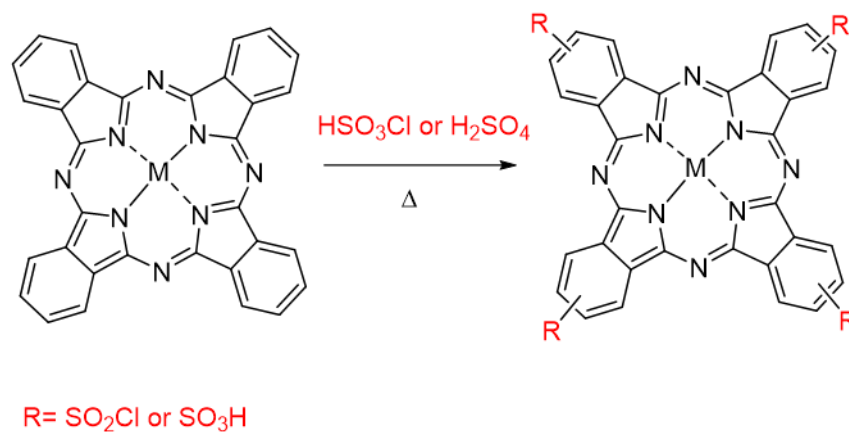
Scheme 1.2: Sulfonation and Chlorosulfonation of MPc.

Another way to generate substituted Pc is by tetramerisation of already substituted precursors. Substituted derivatives of ortho-phthalic acid, phthalimide, phthalamide, phthalonitrile and 1,3-diiminoisoindoline are good precursors for this method as shown in scheme 1.3. Also, phthalic anhydride can be used as starting materials rather than the more expensive phthalonitriles. However, the number of metal ions that can be used in this method is limited compared with the phthalonitrile. [4,22] Many substituted Pcs have been reported in the literature, they were synthesised using substituted phthalonitrile as a precursor. This method proves to produce a high yield of substituted MPc under mild conditions using different metal ions or metal salts with a catalytic amount of DBU or DBN as a base in high-boiling solvent such as quinoline, chlorobenzene or 1-chloro-naphthalene. An alkali metal such as Li and Na can be used as a template for the macrocycle by dissolving it in boiling alcohol to form metal alkoxide that reacts with phthalonitrile to produce an alkali metal Pc. The latter can be easily demetallated when dilute acid is added to form H$_2$Pc that can be refluxed with metal salts to form the desired MPc.[4,23]
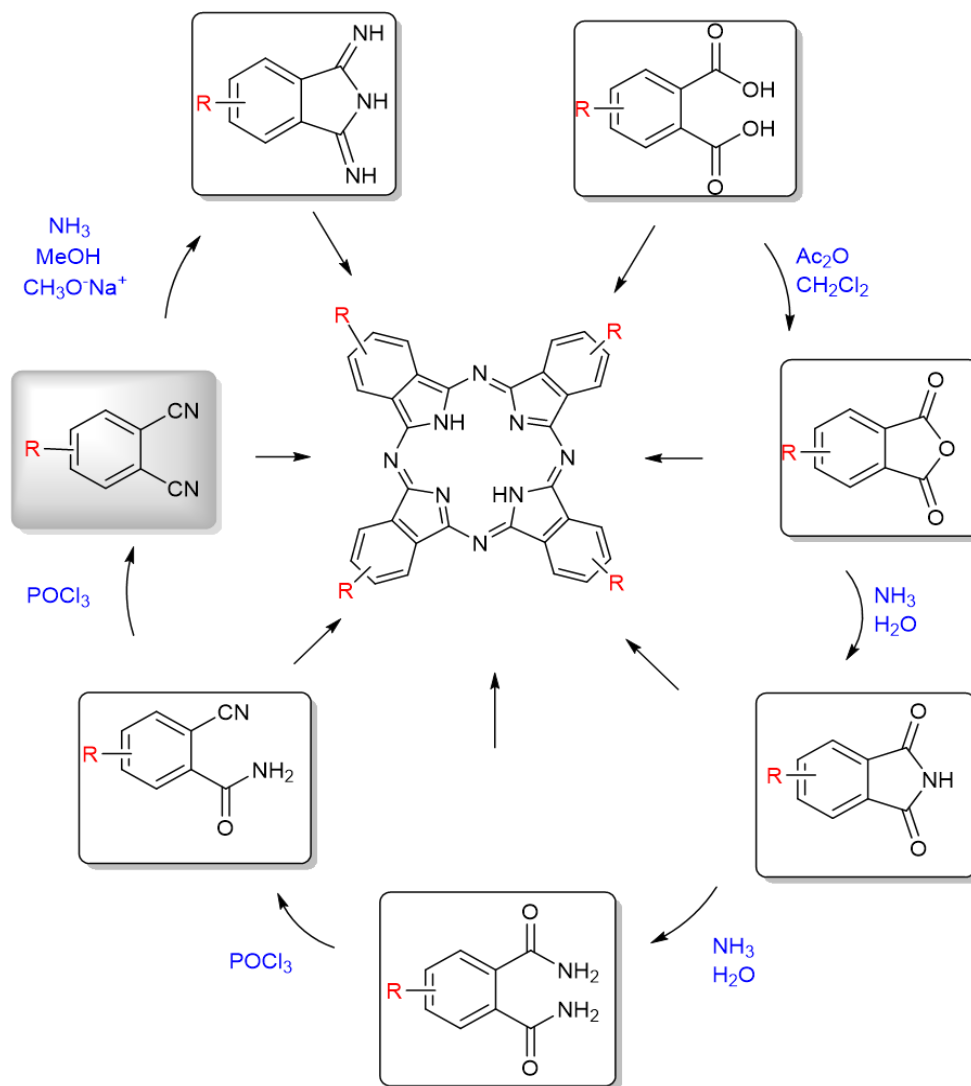
Scheme 1.3: Possible synthetic routes for preparation of substituted Pc from different precursors.

Cyclo-tetramerisation of mono-, di- or tetra-substituted phthalonitriles produces the corresponding symmetrical tetra-, octa- or 16-substituted Pcs.[24–27] The mono peripherally or non-peripherally substituted phthalonitrile can be cyclised to produce a mixture of up to four regioisomers with C_{2v}, C_{4h}, D_{2h}, and C_s symmetries. However, the steric hinderance of a substituent on non-peripheral position can modulate the ratio of the isomers and produce two or three isomers. A very bulky substituent can exclusively give only one regioisomer (C_{4h}) as illustrated in scheme 1.4.[28–30]
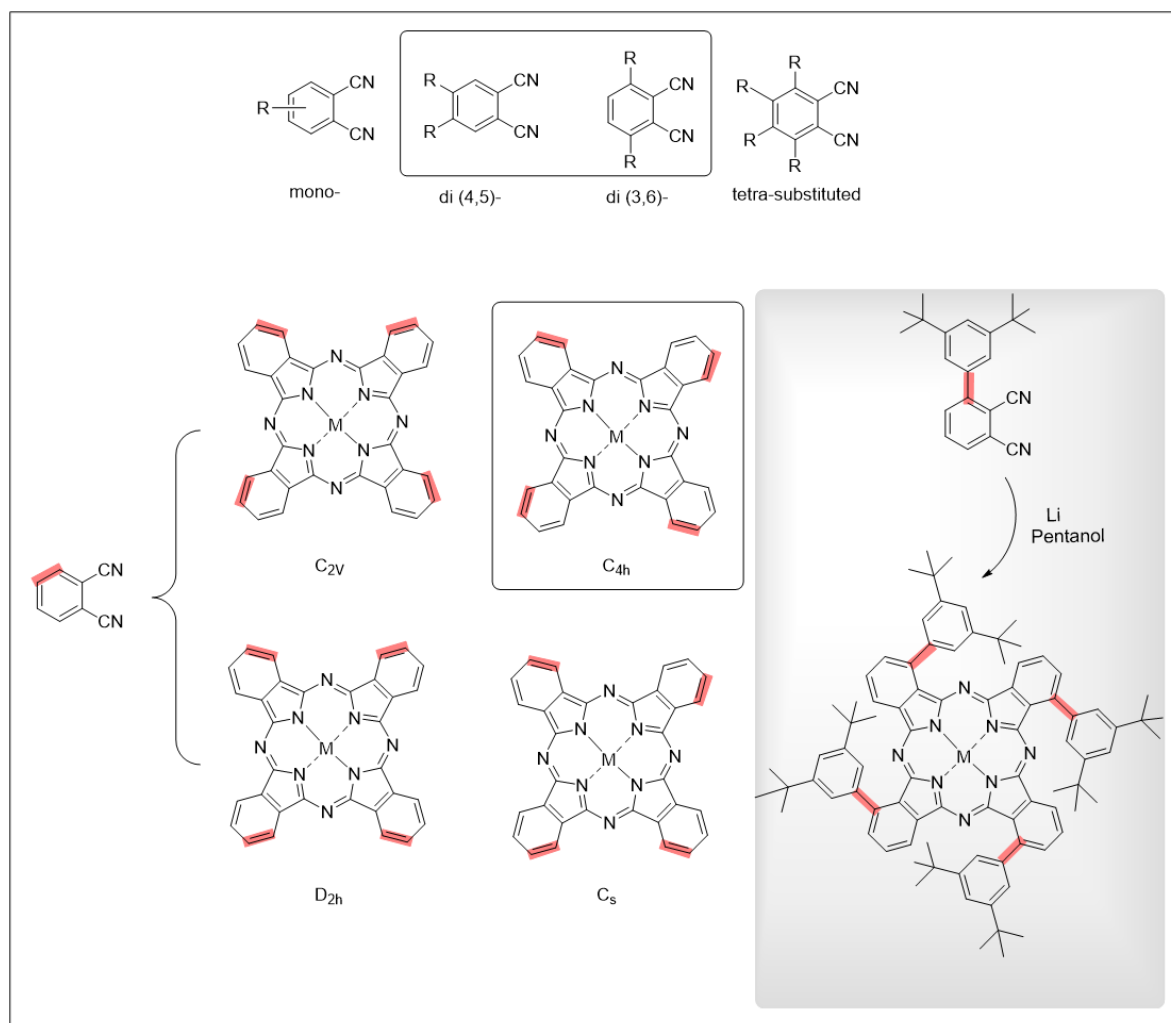
Scheme 1.4: Mono, di (4,5) or (3,6) and tetra-substituted (3,4,5,6) phthalonitriles (top), the four symmetries of isomeric mixtures and a mono-isomeric Pc bearing a very bulky substituent (right).

The most common substituents are alkyl, alkoxy and alkoxy methyl chains. It is notable that the 4 or 5-substituted derivatives of precursors provide less steric hindrance during the cyclotetramerisation reaction as compared with the corresponding 3 or 6-substituted derivatives that result in difficulty of the production of some non-peripherally octa-substituted Pcs in high yields compared to the peripheral one.[31–33]

Synthesis of unsymmetrical Pcs can be achieved by different methods such as tetramerisation of two or more different precursors. Although this method gives a mixture of all six different types of Pcs (as shown in Scheme 1.5), the ratio of the desired product can be selectively increased by controlling the precursors' ratios and reaction conditions.[34,35]
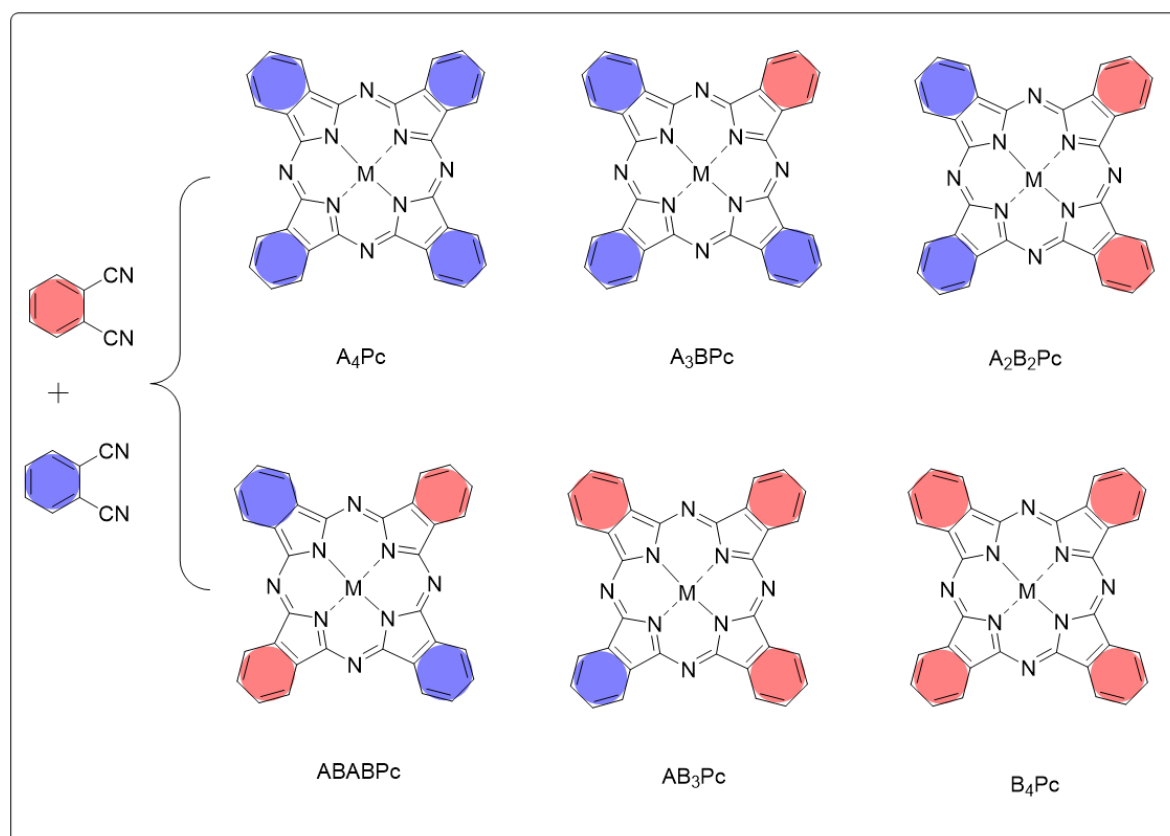
Scheme 1.5: Six possibilities of substituted Pcs formed during mixed condensation of two different substituted precursors.

Moreover, selective synthetic strategies have been reported to produce A_3B-type Pc such as Leznoff and co-workers' method in 1982 and Kobayashi and co-workers' method in 1990 as depicted in scheme 1.6. In the first method, a polymeric support was bonded to diiminoisoindoline molecule (**8**) and then, it was reacted with a substituted diiminoisoindoline derivative (**9**) in a refluxing mixture of DMF: DMEA (1:1) to give A_3B Pc (**10**) (that remained bound to the polymer) and the symmetrical A_4Pc. The side-product can be eliminated easily by washing, leaving behind the desired product that is finally cleaved from the polymer.[36]

The second strategy involves a ring expansion of subphthalocyanine (**11**) by reacting it with a substituted diiminoisoindoline precursor (**12**) to give the desired product A_3B Pc (**13**) in relatively higher yield compared to a mixed condensation strategy. However, this method is not entirely selective as it produces a mixture of isomers in small amounts, but the isolation of the desired product is quite easy using column chromatography. [29,37] Also, the reactivity of boron trihalide toward some substituents such as alkoxy or crown ether limits the substituents that can be introduced to sub-Pc.[38]
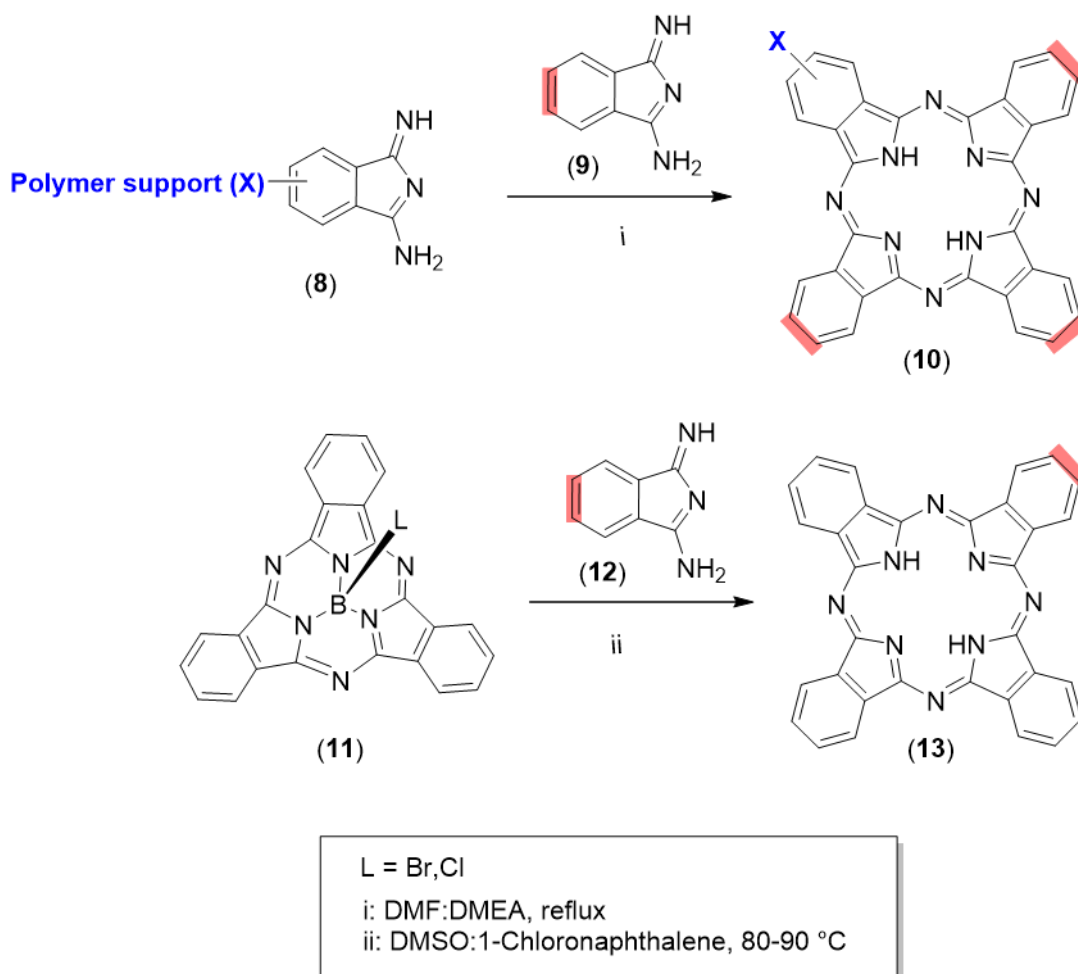
Scheme 1.6: Selective synthesis of A₃B Pc via polymeric support (top), and ring expansion of sub-Pc (bottom).

1.4. Solubility of phthalocyanines

Most unsubstituted Pc macrocycles are insoluble in the common organic solvents and even in the high boiling point solvents such as quinoline and 1-chloro- or 1-bromonaphthalene and the best method to dissolve these complexes is by protonating the nitrogen atoms that bridge the pyrrole rings with concentrated sulfuric acid. Due to the low solubility of unsubstituted Pcs, many different substituted Pcs have been reported to date, with many variations of the type of substituents, the number of the functional groups, and the position of these substituents on Pc macrocycles, to enhance their solubility and increase their potential usefulness in numerous possible applications.[22]

Enhanced solubility in aqueous or organic solvents can be achieved by introduction of non-peripheral α or peripheral β substituents in the Pc macrocycles. However, the solubility of non-peripherally substituted Pcs is generally significantly higher compared to that achieved by introduction of substituents in peripheral positions of Pcs macrocycles due to their steric hindrance which reduces the intramolecular π-π interaction and therefore their aggregation in solution. Also, tetra-substituted Pcs have been reported as highly soluble compounds in a variety of organic solvents compared to the octa-substituted analogues. In general, introduction of bulky or long hydrocarbon chain substituents into Pc macrocycles improves solubility in common organic solvents.[4,39–45]

Moreover, anionic, cationic, and neutral substituents can be substituted into Pc structures to increase their solubility in water. The hydrophilic phthalocyanines were successfully synthesised by installing bulky groups containing carboxylate or sulfonylate (anionic), quaternary pyridinium (cationic) or poly(ethylene) glycols (neutral) on the periphery of the macrocycle.[46,47]

1.5 Absorption Spectra of Phthalocyanines

The highly conjugated 18π-electron system of Pc macrocycles generates low energy π-π* transitions that can be detected in UV-vis spectra in two distinct electronic absorption regions: one in the near ultraviolet in the range 300–400nm (B band) and the other in the far-red of the visible region in the range 600–700nm (Q bands). Their strong bands in the visible region give them an intense blue green colour and render them as ideal compounds for many applications. MPc molecules are characterised by their single narrow Q bands as they are generally of D_{4h} symmetry whereas the free base phthalocyanine, the Q band splits into two, due to the reduced symmetry of the H_2Pc molecule (D_{2h}) as depicted in figure 1.4.[4,29,39]
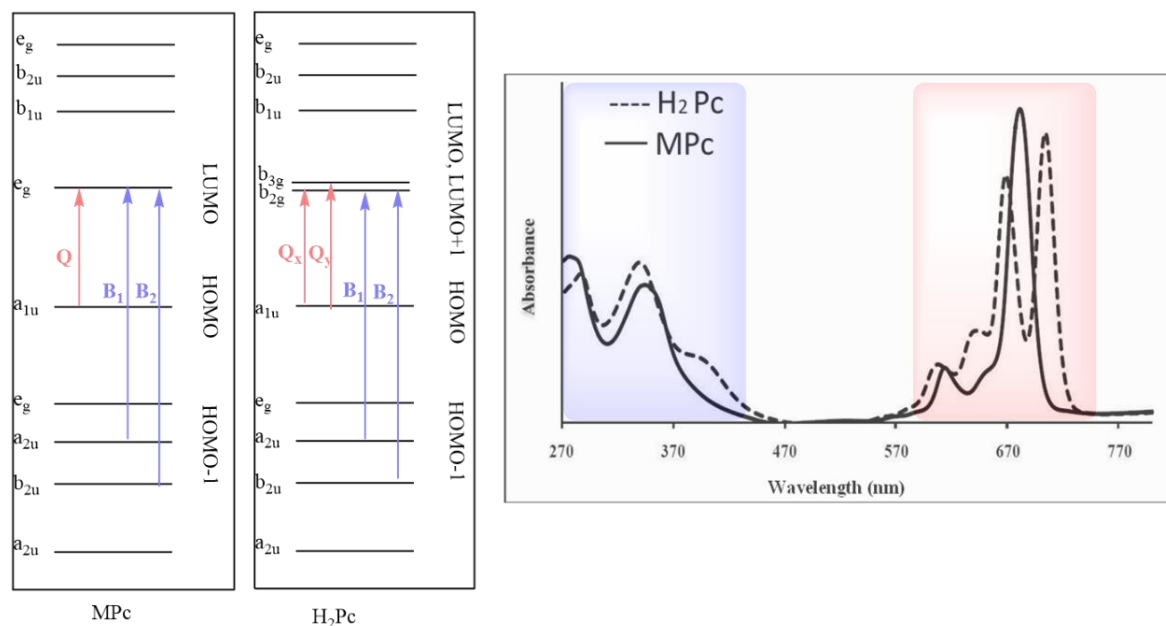
Figure 1.4: Optical absorption spectra of a typical metallated (MPc) and unmetallated (H$_2$Pc) phthalocyanines (right) and electronic energy levels in phthalocyanine complexes showing the origin of Q and B bands (left) (reproduced with permission from ref 39).

The Q and B bands are assigned based on Gouterman's four-orbital model, which emphasizes charge localisation's effect on electronic spectroscopic features. As depicted in figure 1.4, The transition from HOMO (a$_{1u}$) to LUMO (eg) causes a single Q band in MPc, while the transition between a$_{1u}$ (HOMO) to the non-generate b$_{2g}$ and b$_{3g}$ (LUMO) in H$_2$Pc causes a split in Q band. The B bands arise from the transition from a$_{2u}$ and b$_{2u}$ to the e$_g$ level and is split into two bands B$_1$ and B$_2$ that occur at about the same energy resulting in the superimposition of these bands and form the broad band.[29,48–50]

There are different factors that induce a bathochromic or hypsochromic shift in the Q-band absorption such as substituents on Pc ring, the central metal, the axial ligand, and solvent. Introduction of substituents on the Pc ring can cause a shift in the Q band depending on the type, the number and location of substituents. Functionalisation at the non-peripheral position of the Pc moiety causes a large shift when compared to similar peripherally substituted complexes. Long wavelength absorption for octa-substituted Pc with eight alkoxy groups has been reported at 750 nm.[39,51,52] Alkylthio or arylthiol substituted Pcs are redshifted compared to oxo substituted Pcs due to the electron-donating nature of sulphur. Also, incorporation of the metal inside the macrocycle offers another possibility to influence the Pc absorption properties due to electronic changes within the molecule. However, it has

been reported that the shift of the Q- band is minor in many cases unless the metal ion is located outside the central cavity where a red shift is observed.[39,53]
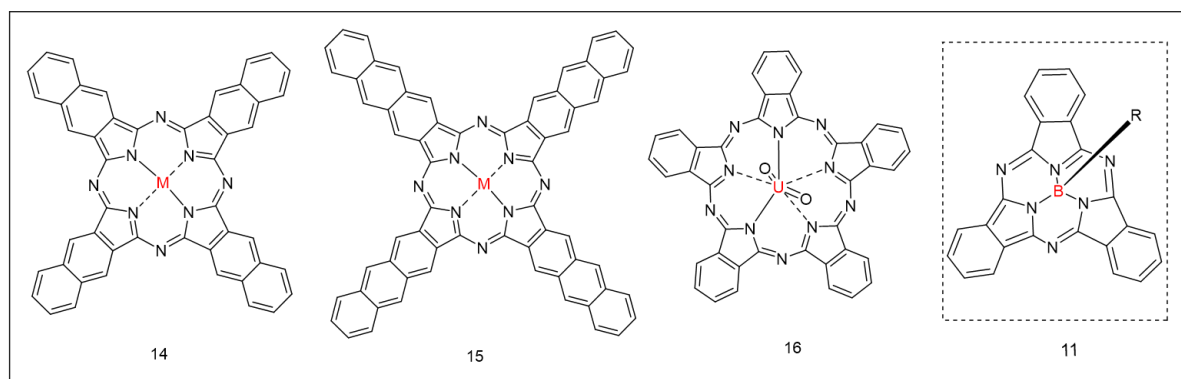
Figure 1.5: π -extended Pc derivatives (naphthalocyanine (14), anthracocyanine (15), and superphthalocyanine (16), and contracted chromophoric system subphthalocyanine (11).

Significant spectroscopic changes are also produced when the conjugated system of Pc is extended. The enlargement of π-system from phthalocyanine to naphthalocyanines (**14**) in figure 1.5) causes a shift of the intense Q absorption band by 80-100 nm to longer wavelength. Incorporation of benzene rings into the peripheral site of Pc results in a red shift of the Q band by 20-30 nm per benzene ring to the near infrared region. An extraordinarily long wavelength for 2,3-anthracocyanine (**15**) has been reported showing the Q band maximum at 935 nm. Moreover, expansion of Pc skeleton by adding one isoindoline unit to form five subunit ligand that is known as superphthalocyanine (**16**) results in λ_{max} of 945 nm whereas the contraction of its skeleton by removing of one subunit to form subphthalocyanine (**11**) leads to blue shifted Q-band peaks to 560 nm.[39,54–57]

1.6 Applications of Phthalocyanines

The delocalisation of π-electrons in the structure of Pcs, their strong absorption characteristics in far-red region with a high molar absorptivity often exceeding 10^5 L mol⁻^{1}cm^{-1}, together with their high photochemical and electrochemical and thermal stabilities and other unique features makes them promising building blocks for the construction of a new composite materials in a wide variety of industrial applications besides their use as colourants and pigments.[20,39,48] As previously discussed, the versatility of phthalocyanine, by incorporation of different metals or by functionalising the peripheral or non-peripheral sites of its benzene rings, increases their effectiveness in different fields including the area of laser printing,[48] electrochemical sensors,[58,59] non-linear optical materials,[60] liquid

crystals,[61] recordable compact discs,[62] homogenous and heterogenous catalysts,[63,64] sensitising dyes for solar cells (DSSCs),[65] semi-conductors[54] and photosensitisers PS in photodynamic therapy (PDT) for cancer treatment.[66]

1.6.1 Phthalocyanine as a dye sensitiser in dye-sensitised solar cells (DSSCs)

The use of sustainable energy sources is increased today due to the negative environmental effect of fossil fuels. Solar energy is one of the most popular renewable energies. Dye sensitised cells are one of the 3rd generations of solar cells. They have been widely explored by researchers because of low cost, simple preparation, and ability to generate the power even in low-light environments.[65]

As illustrated in figure 1.6, DSSCs consist of four components: working electrode (semi-conductor), dye sensitiser, electrolyte (redox mediator) and counter electrode. A thin layer of semi-conducting material (TiO_2) is typically deposited on transparent conductive glass plate (TCG) which is coated with ITO (indium Tin Oxide) or FTO (fluorine Tin Oxide) as transparent conductive materials to form the working electrode. Next, the desired dye sensitiser is fused into TiO_2 surface. The light harvesting efficiency of solar cells strongly depends on the dye sensitiser which converts the light into electronic excitation and promotes charge transfer to the semi-conductor surface. Then, the electrons are transported through the external circuit to platinum counter electrode that carry back the electron to the dye through redox reaction of electrolytes I_3^- to I^-.[67]
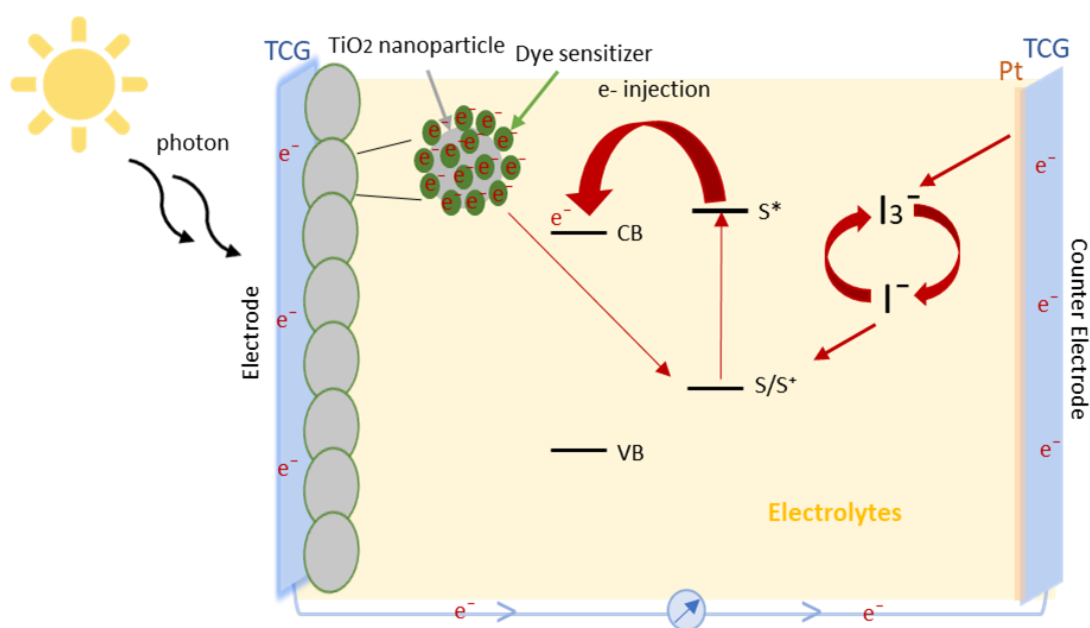
Figure 1.6: A schematic diagram of a dye-sensitised solar cell, adapted from ref 67.

Research worldwide has been conducted to design and synthesise an effective dye-sensitiser for these cells. Phthalocyanine-based dyes have been promising candidates due to their physical properties and their strong absorption in the far end region of visible light. The first use of Pc in solar cells was reported in 1958 as MgPc in organic photovoltaics (OPV), resulting in production of 0.2 V. After that, many Pc derivatives have been tailored to meet the essential condition for DSSCs so far, and lead to numerous significant developments of the performance of the devices throughout the years reaching efficiencies beyond 6%. However, the devices' performances have consistently been much lower than that for porphyrin and ruthenium- based analogs.[65,68–71]

The low power conversion efficiency (PCE) of Pc-based DSSCs is caused by many factors, and the strong tendency of aggregation of their structures on a TiO_2 surface is one of the most important that results in a reduction of electron injection efficiency in the exited states. Their aggregation is caused by a strong intermolecular π-π interaction of their macrocycles in the solutions, that can be observed by broadened absorption peaks in the visible spectra. Many different strategies were used to prevent the aggregation so far such as introduction of co-absorbent e.g., Chenodeoxycholic acid (CHINO). However, this strategy proved to be insignificant in terms of enhanced cell efficiency as CHINO: Pcs ratio of 100:1 is required to achieve maximum efficiency and that causes less adsorbed molecules on TiO_2 surface.[65,70] Insertion of anchoring groups on the Pc at a peripheral position is another strategy that has been considered. Carboxylic acid is the most common anchoring group that has been used. Also, unsymmetrically substituted dyes with A_3B design, with three bulky electron-donating groups and one or more anchoring groups on the fourth benzene ring, have been found to be effective sensitisers. This design combines steric suppression of dye aggregation, favourable push-pull effect, and improved dye binding to the semi-conductor surface. As shown in figure 1.7, unsymmetrical ZnPc bearing 2,6 di-butoxy group on peripheral phenoxy units is a good example that yields PCE of 6.4%.[68,72,73]
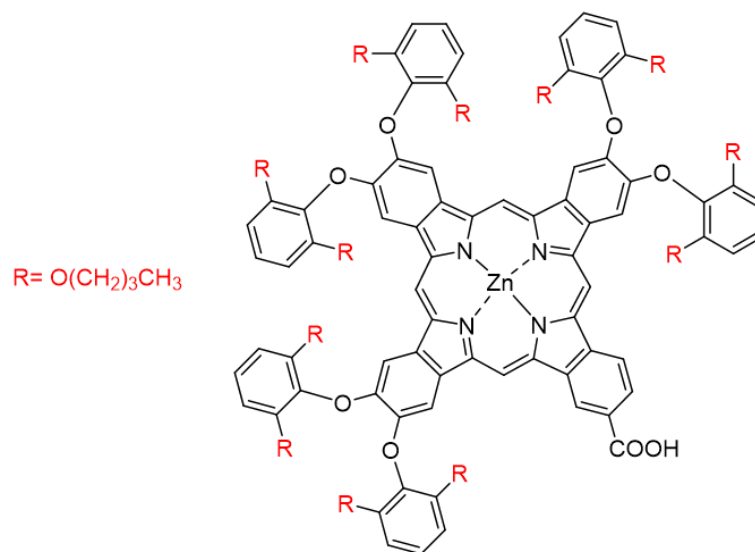
Figure 1.7: Structure of ZnPc sensitiser.

When multiple anchoring groups were introduced, greater adsorption on TiO_2 surface and faster electron injection were observed compared to the mono-analogues. Tetra-carboxylated ZnPc exhibits no J-aggregation and less H-aggregation whereas the mono-carboxylated one exhibits both J and H-aggregation as shown in figure 1.8.[74]

Mono-carboxylatedZnPc   **Tetra-carboxylatedZnPc**
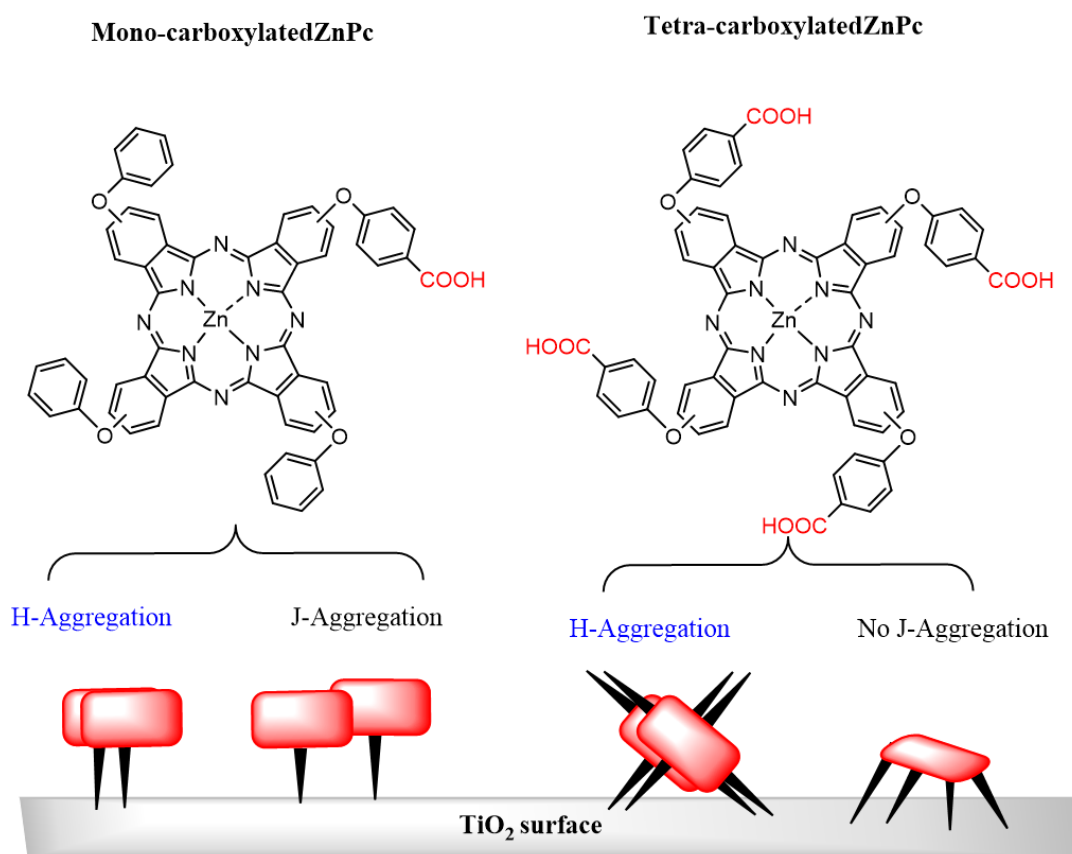
Figure 1.8: Schematic representation of aggregation behaviour of ZnPc on TiO$_2$ surface (reproduced with permission from ref 74).

Recently, in 2023, high efficiency values (9.96-10.72%) have been achieved by combining the commercially available YD2 dye and the newly synthesised Zn or TiONPcs at the ratio 3:1 respectively as shown in figure 1.9. [75]
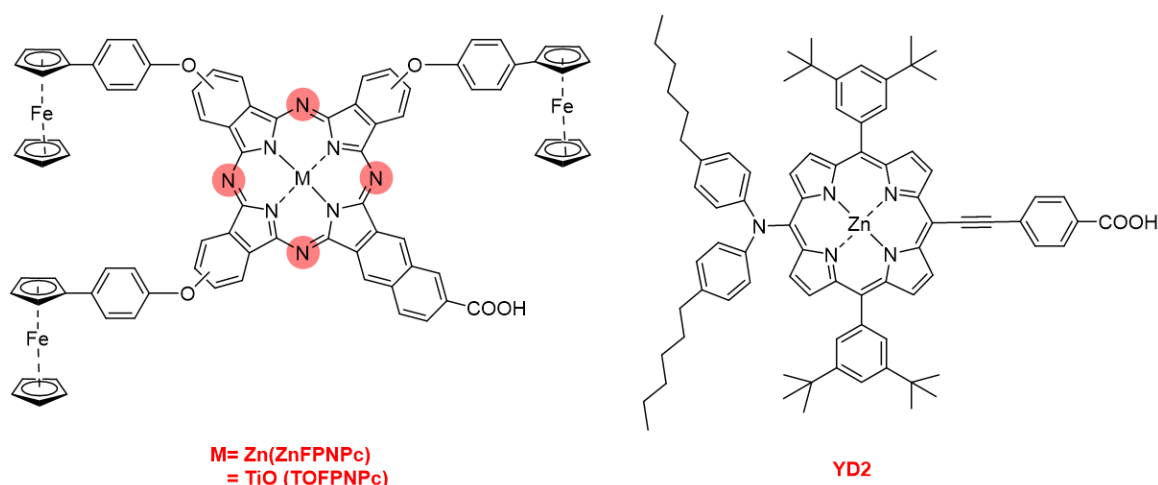
Figure 1.9: Naphthalocyanine structure (left), and YD2 porphyrin (right).

1.6.2 Phthalocyanine as photosensitiser in PDT

Photodynamic therapy is a non-toxic medical technique that involves the use of three components: a light-sensitive substance (photosensitiser PS), a light source with an appropriate wavelength and intracellular oxygen. When the photosensitiser is exposed to the light, it is activated and produces reactive oxygen species (ROS) $^1O_2$ through a photochemical reaction of electron in excited triplet state via two types of mechanisms (as illustrated in figure 1.10). The photogenerated ROS directly kills abnormal cells either by vascular damage or inducing an immune response against them. Certain types of cancer can be treated with this technique as well as some skin and eye diseases.[76–79]

The development of an effective photosensitiser has been a key topic for research. Pc derivatives are the second-generation photosensitisers after Hematoporphyrin derivatives (1st generation). The strong absorption of Pcs in the far-red region (range 650–800 nm) make them an ideal photosensitiser (PS) for PDT as long wavelength light penetrates deeper into tissues and results in good control of tumours compared to the first generation. Also, they are highly chemically pure, they produce more singlet oxygen, and target cancerous cells better. Pcs are usually used as their metalated form. Many MPc derivatives have been studied and it is concluded that diamagnetic metal ions such as Al, Zn and Ga yield high singlet oxygen quantum whereas paramagnetic metals shorten lifetime of excited states that result in a loss of photoactivity.[76,80–83]
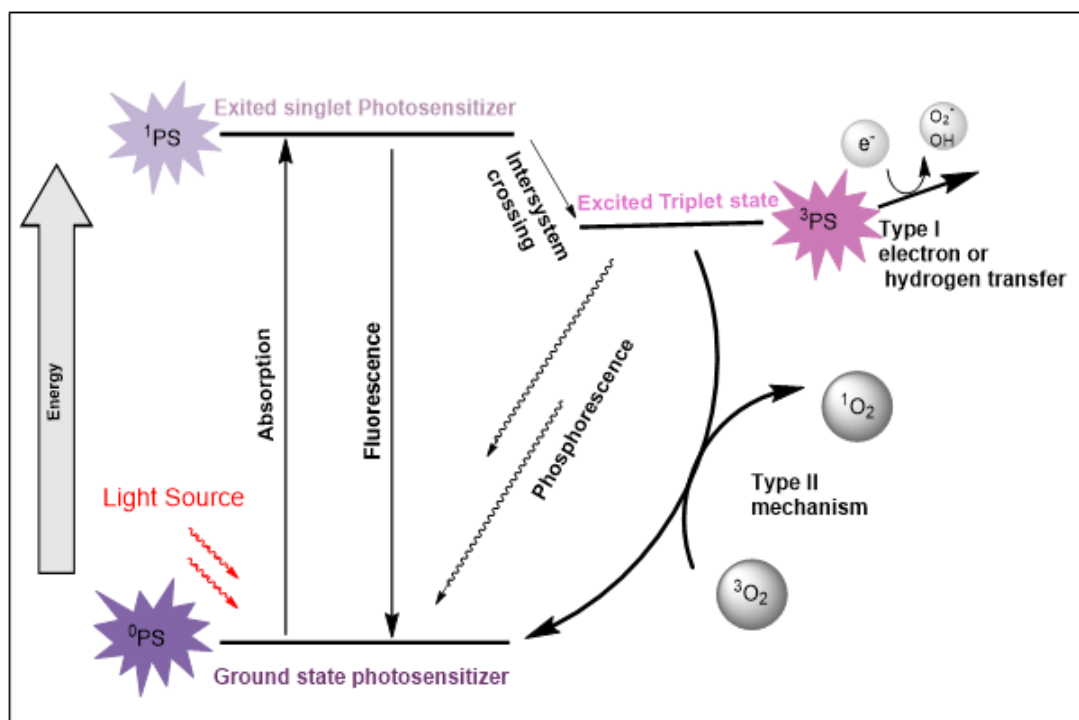
Figure 1.10: Jablonski diagram for photophysical processes involved in PDT, adapted from ref 78.

ZnPc is one of the most extensively studied Pc-based photosensitisers in PDT application. However, its low solubility in water prevents its transfer to the target tissues in the body. Great emphasis has been placed on utilisation of drug delivery vehicles for *in vivo* therapy to administer the PS by systemic routes. Liposomes, dendrimers, pH sensitive polymers and fullerenes are among the nanoparticles (NS) that are used as PS carriers. An excellent gold nanoparticle conjugation of both zinc phthalocyanine and polyethylene glycol (PEG), has been reported as an efficient method to treat a difficult type of cancers such as amelanotic melanoma (figure 1.11).[76,84–87]
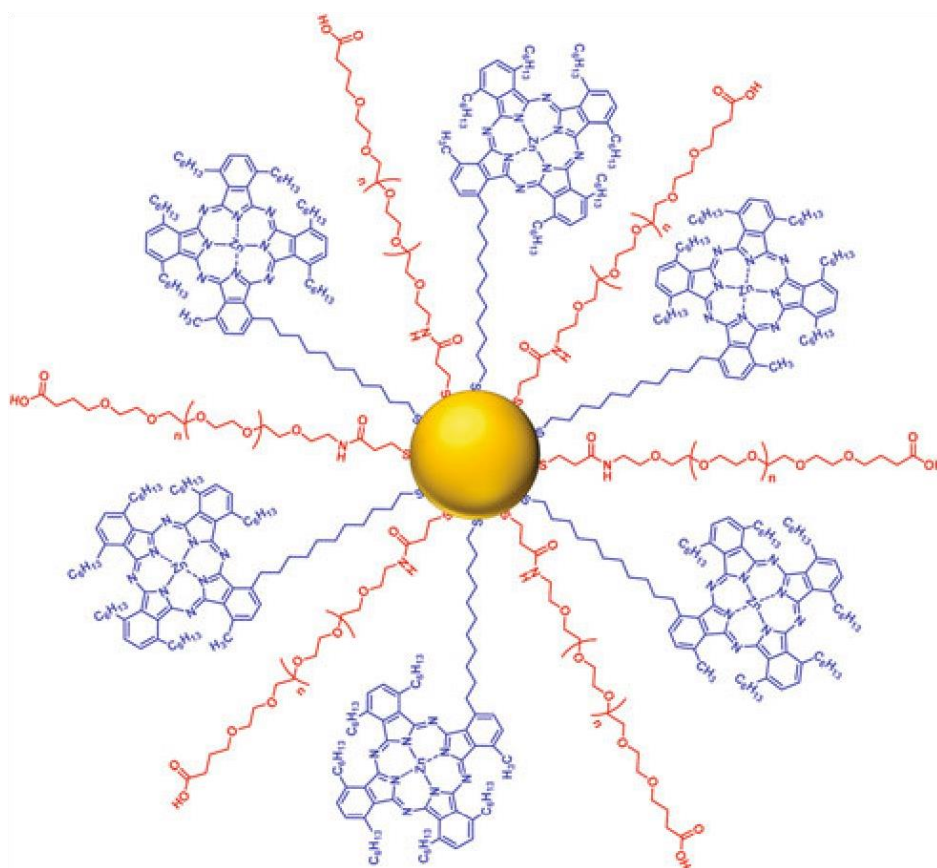
Figure 1.11: Schematic representation of phthalocyanine derivative (blue ligand) incorporated into PEG (red ligand)-functionalised gold nanoparticle (reproduced with permission from ref 85).[84,85]

Also, different substituents have been incorporated to reduce Pc self-interactions of their hydrophobic aromatic surfaces in aqueous solutions and increase water solubility. Incorporation of anionic or cationic groups, peptides, B-cyclodextrins, crown ether or glyceryl onto Pc macrocycle have been proved to reduce drug resistance and show photodynamic activities. A water soluble quaternised serotonin substituted zinc (II) phthalocyanine (figure 1.12) has been recently reported as a promising candidate as its high fluorescence quantum yield (Φ_F) was found to be 0.37- 0.42 in H_2O and DMSO respectively. Also, its absorption is within the therapeutic window ~700 nm.[88–92]
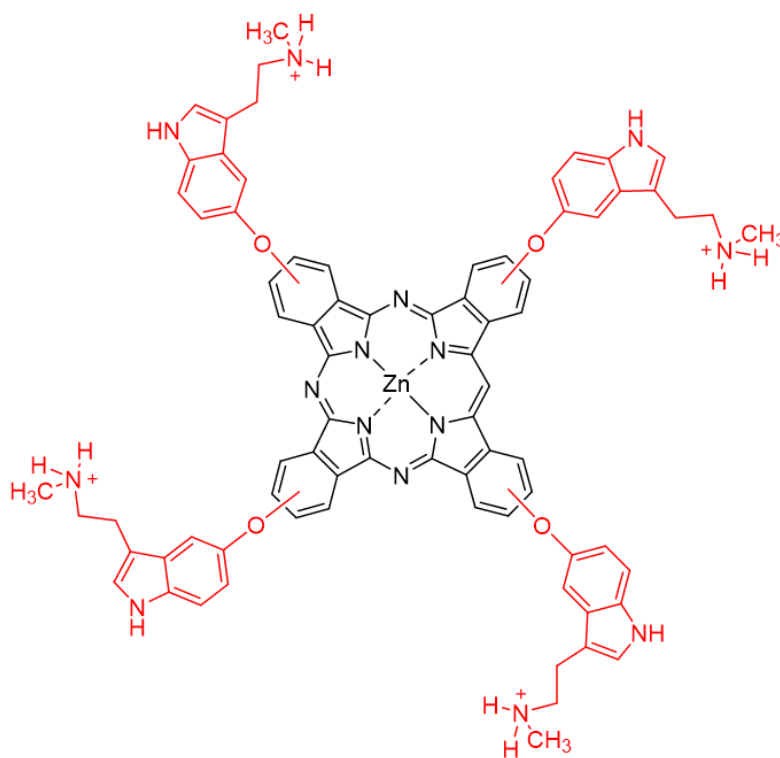
Figure 1.12: Structure of quaternised serotonin substituted zinc (II) phthalocyanine.

1.7 Introduction to Tetrabenzo(aza)porphyrin Hybrids

Another modification of phthalocyanine macrocycle can be done by replacing one or more of the bridging nitrogen atoms by sp^2 carbon atoms to form different types of hybrid macrocycles. According to the number of nitrogen bridges, there are four different hybrids known as tetrabenzo*(aza)*porphyrin: tetrabenzotriazaporphyrin (TBTAP), *cis-* and *trans-*tetrabenzodiazaporphyrin (TBDAP), tetrabenzomonoazaporphyrin (TBMAP) and tetrabenzoporphyrin (TBP). These hybrid macrocycles have structural similarities to phthalocyanine Pc and to the naturally occurring porphyrin (Pn) as shown in Figure 1.13. However, they are not as well researched as Pc and Pn due to their difficult synthesis and isolation as most reported methods produce all macrocycles in the crude mixture in small yield.[4,93–95]
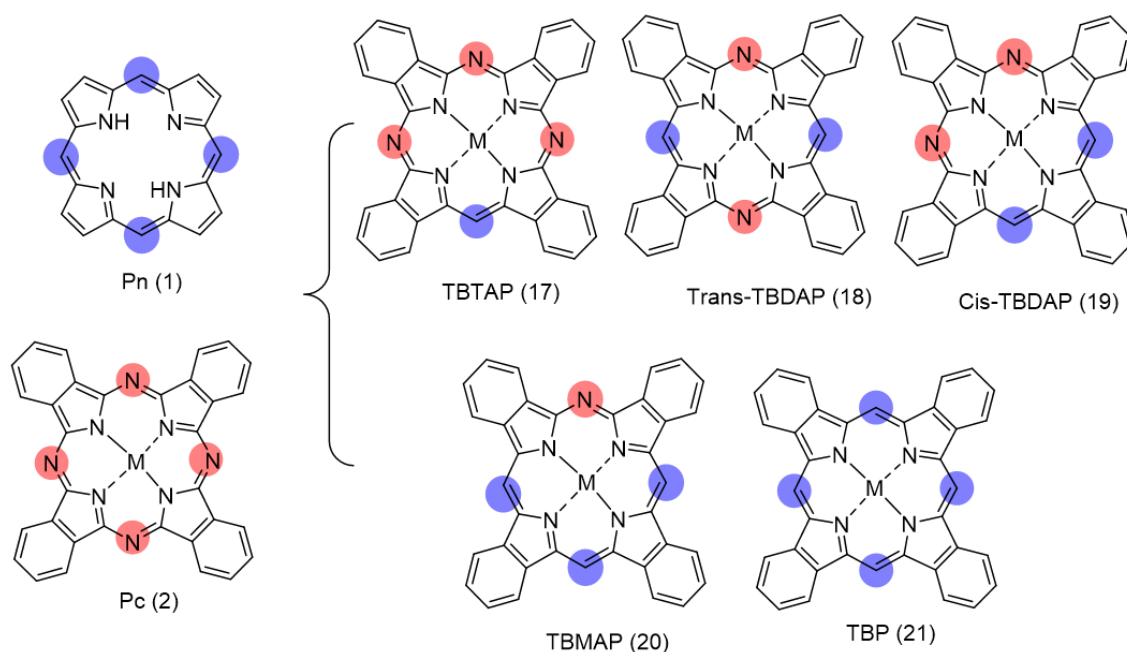
Figure 1.13: Structures of Pc, porphyrin (Pn)and the hybrid macrocycles where M = 2H or a metal.

Tetrabenzo(aza)porphyrin macrocycles are numbered as either phthalocyanine Pc or tetrabenzoporphyrin TBP. Nevertheless, phthalocyanine numbering is more common. Hence, the substituents on the benzene ring of tetrabenzo(aza)porphyrin system were numbered as Pc system, whereas the imino nitrogen atoms' number are based on those of fused tetrapyrroles. As shown in figure 1.14, every side of the porphyrin inner ring has a letter, the fusion side was assigned to the first letter of alphabet. Therefore, "a" for the side 1-2, b for the side 2-3 and so on. The position of the fused benzene rings on the pyrrole in

the porphyrin ring are indicated by the letters b, g, l, q. Tetrabenzoazaporphyrin hybrids have sixteen substituent sites as for Pc macrocycles. Substituents on benzene ring at 2, 3, 9, 10, 16, 17, 23 and 24 are known as peripheral sites (*p*), while those at 1, 4, 8, 11, 15, 18, 22 and 25 are named as non-peripheral sites (*np*) as depicted in figure 1.14 for TBTAP as an example for these hybrids.[95]
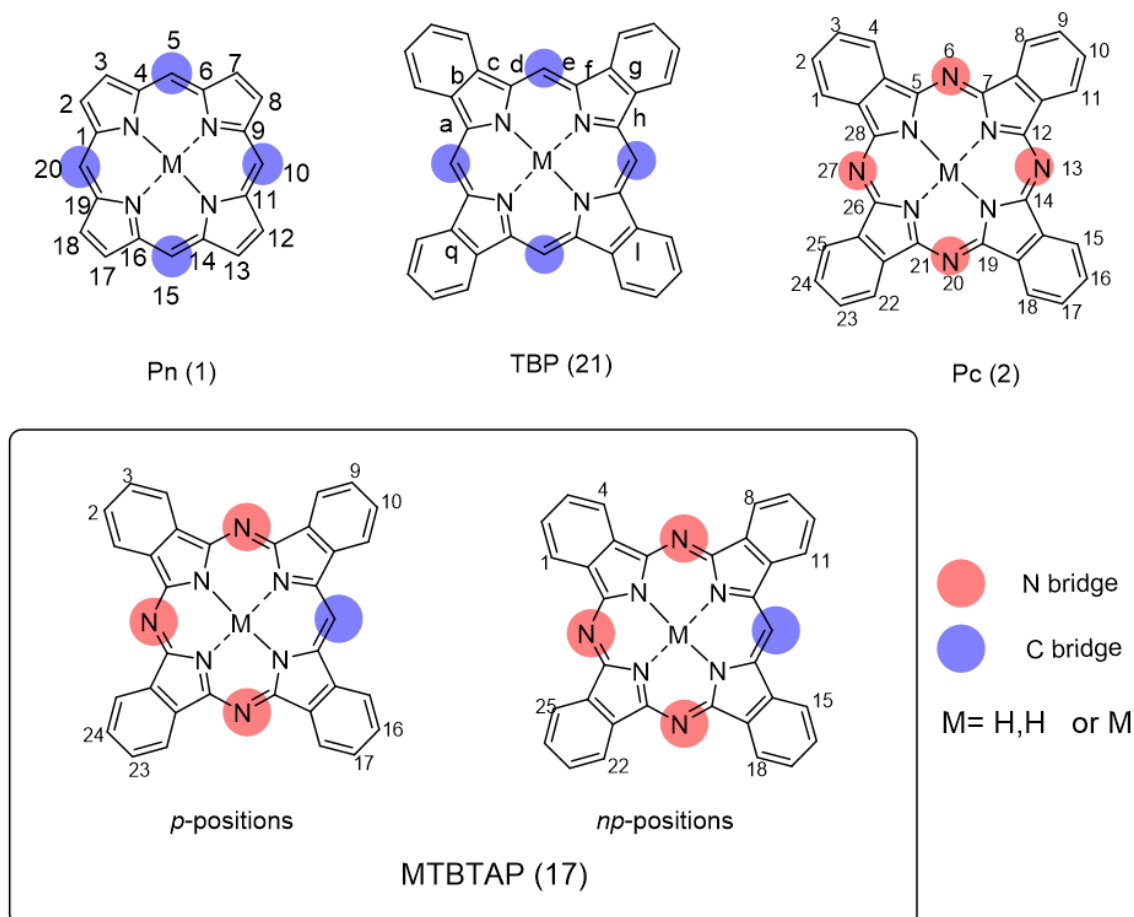
Figure 1.14: Nomenclature system of porphyrin (Pn), TBP and Pc (Top) and peripheral and non-peripheral sites of TBTAP.

1.8 The discovery and synthesis of Tetrabenzo(aza)porphyrins

The discovery and synthesis of these hybrid structures started in the 1930s. The first accidental preparation was by Lowe and Linstead. They synthesised Phthalocyanine from the reaction between methyl magnesium iodide and phthalonitrile. An unknown side product was obtained and due to its poor yield, it was difficult to characterise.[3,23] Soon, in 1936, Fischer and Friedrich synthesised the first macrocyclic molecules that are tetra pyrrole compounds cyclised through four methine groups and nitrogen atoms. Monoazaporphyrin

(MAP) was prepared at that time.[96,97] In 1937, Helberger reported the preparation of CuTBMAP with 10% yield. Its synthesis was achieved by heating *o*-halogeno acetophenone with cuprous cyanide. Formation of CuTBDAP was reported in 20% yield when phthalonitrile (**6**) was added to the reaction mixture.[98] Later, Helberger and von Rebay reported similar results when they used the preformed intermediate *o*-cyano acetophenone (**22**).[99] The formation of CuTBTAP was achieved by this method when Linstead et al, employed a molar ratio 1:1.8 of phthalonitrile: o-cyanoacetophenone in the presence of copper(I)chloride and pyridine. It was found that the reduction of the phthalonitrile (**6**) amount in the reaction mixture produced CuTBDAP whereas the absences of phthalonitrile gave CuTBMAP as shown in scheme 1.7.

MTBTAP
+
MTBDAP

(6)

(22)
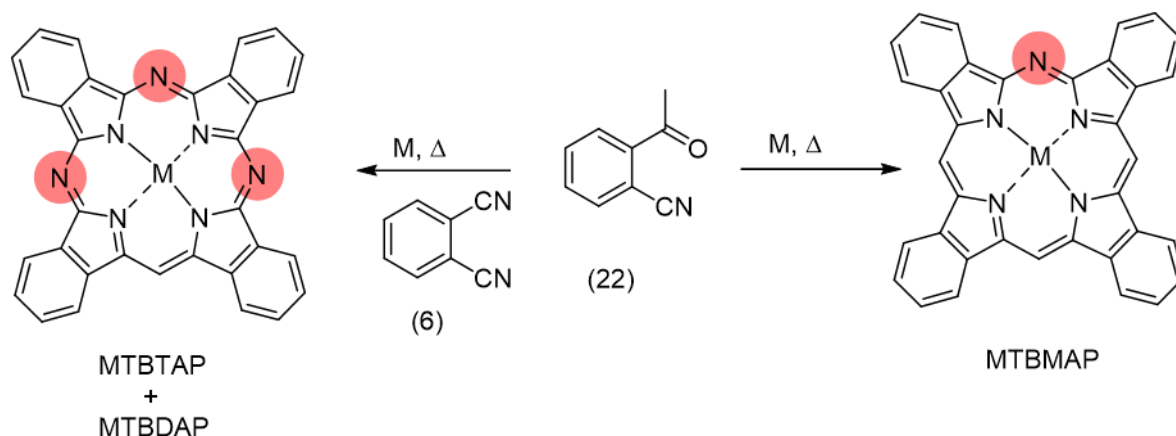
MTBMAP

Scheme 1.7: The first synthesis of MTBMAP and TBTAP hybrid structures using intermediates *o*-cyanoacetophenone (**22**).

Linstead and co-workers added malonate derivatives as another precursor to synthesise MTBMAP derivatives through fusion of imino-malonic acids (**23**) with metal dust (scheme 1.8). It was noted that the addition of phthalonitrile results in the formation of MTBTAP. Synthesis of ZnTBMAP was achieved by this method and zinc metal was removed by passing hydrogen chloride through a solution of the substance in sulphuric acid and the overall yield of the desired product was 27%. Also, the metal could be converted to another metal by treatment of the metal-free hybrid with the desired metal chloride.[100]
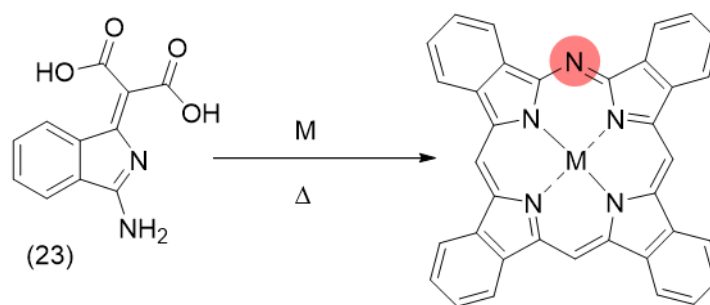
Scheme 1.8: Synthesis of MTBMAP via malonate derivative intermediates (**23**).

Later, Dent reported a successful method to prepare a copper complex of TBTAP through a mixed condensation of phthalonitrile (**6**) with methylene phthalimidine (**25**) or its precursor phthalimidine acetic acid (**24**) at 250 °C in presence of copper salt (scheme 1.9). The yield of CuTBTAP was increased up to 70% when the ratio of phthalonitrile to phthalimidine acetic acid was 3:1 whereas no green pigment was observed when a 1:3 ratio was used. Although the reaction stoichiometry was varied, none of TBDAP or TBMAP complexes were observed. [101]
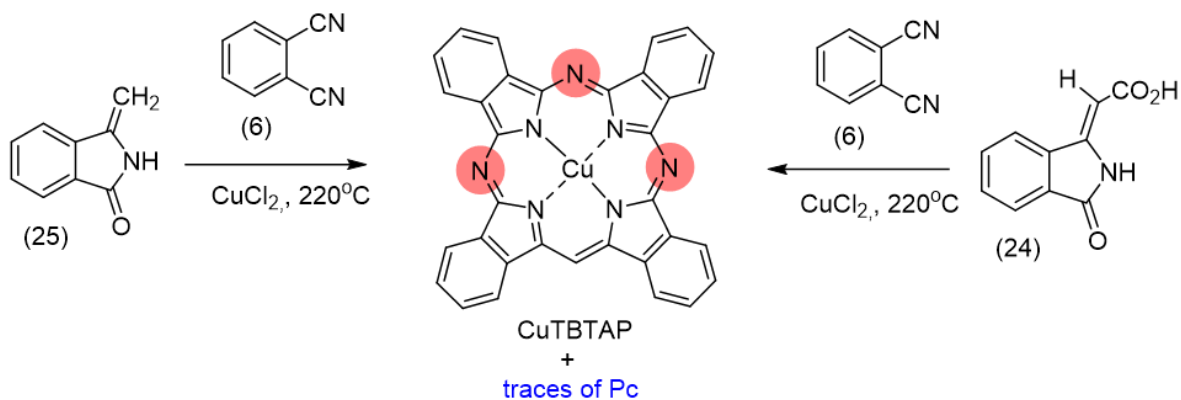
Scheme 1.9: The early syntheses of copper-TBTAPs employing mixed cyclisation between a phthalonitrile (**6**) and methylene phthalimidine (**25**) or its precursor (**24**).

Moreover, it was stated that $Cl_3CuTBTAP$ was prepared from the reaction between 4-chlorophthalonitrile (**26**) and phthalimidine acetic acid (**24**) in presence of cuprous chloride in chloronaphthalene at 250°C as depicted in scheme 1.10. Its structure was deduced by elemental analysis.[101]
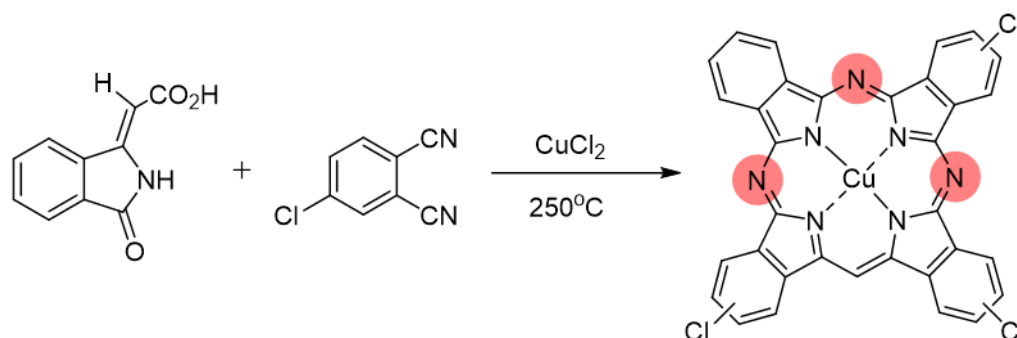
Scheme 1.10: Synthesis of Cl$_3$CuTBTAP via reaction between phthalimidine acetic acid (**24**) and 4-chlorophthalonitrile (**26**).

The results obtained by both Helberger and Dent encouraged Linstead's group to re-examine the previously formed unknown side product of their earlier work on the action of organometallic nucleophiles on phthalonitrile. This method is based on the addition of one equivalent of methyl magnesium iodide to a solution of phthalonitrile in cold diethyl ether. After the formation of a coloured intermediate, diethyl ether was distilled off and a high boiling solvent such as quinoline or cyclohexanol was added to the solid residue and heated to 200°C. MgTBTAP was obtained by this method in around 40% yield. However, when the ratio of MeMgI was increased, pigments containing more methine (CH) bridges were obtained. Treatment of 2.5 equivalents of MeMgI with phthalonitrile followed by steam at 200^{0}C resulted in the formation of TBMAP in 17 % yield as shown in scheme 1.11. Moreover, Linstead investigated the action of different organometallic nucleophiles on phthalonitrile. He was able to synthesise 15% of TBTAP derivatives when methyllithium was employed in the reaction whereas an inseparable mixture of TBTAP and Pc was obtained when butyllithium was used. Gilman et al demonstrated the high reactivity of methyllithium towards aromatic nitriles compared to the less reactive MeMgI.[23] Furthermore, it was noted that acid work-up produced a metal-free TBTAP, thus allowing further metals such as copper, zinc and iron to be incorporated. Later, Hoffman and coworkers synthesised NiTBTAP following the same method. [102]
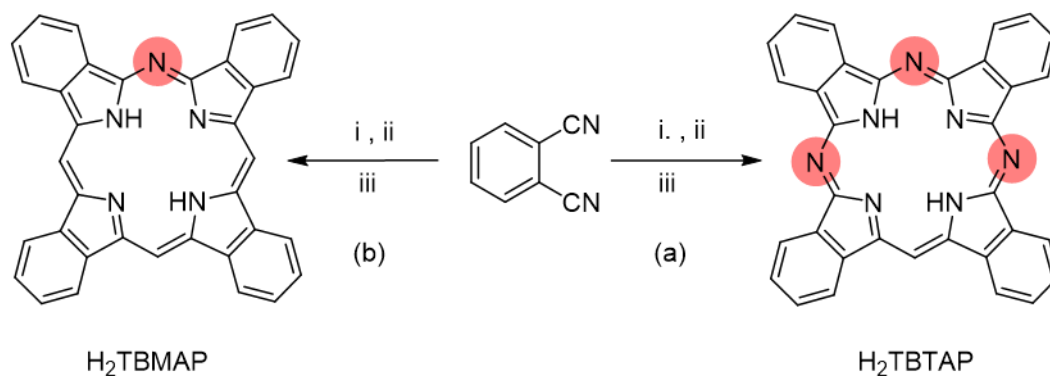
a. i. MeMgI (1 eq), Et$_2$O, 20°C   ii. quinoline, 200°C   iii. acid

b. i. MeMgI (2.5 eq) .   ii. steam heating at 200°C.   iii. acid

Scheme 1.11: The synthesis of TBTAPs and TBMAPs by action of organometallic nucleophiles on phthalonitrile.

There was an extreme challenge to investigate these hybrid materials and their properties because of their low yield and poor solubility in common organic solvents. The general mixed cyclisation methodology was employed with little change for several decades to give access to materials for further study. Substituents were introduced on the peripheral position on the hybrid macrocycles in order to increase their solubility in organic solvent and therefore make their isolation possible. Nitro-phthalimidine was introduced as a possible precursor in mixed cyclisation with diiminoisoindoline as shown in scheme 1.12. (OMe)$_3$-H$_2$TBTAP was synthesised when the methoxy group was substituted on diiminoisoindoline, whereas as OMe-H$_2$TBTAP was obtained when nitro-phthalimidine was substituted with the methoxy group.[103,104]
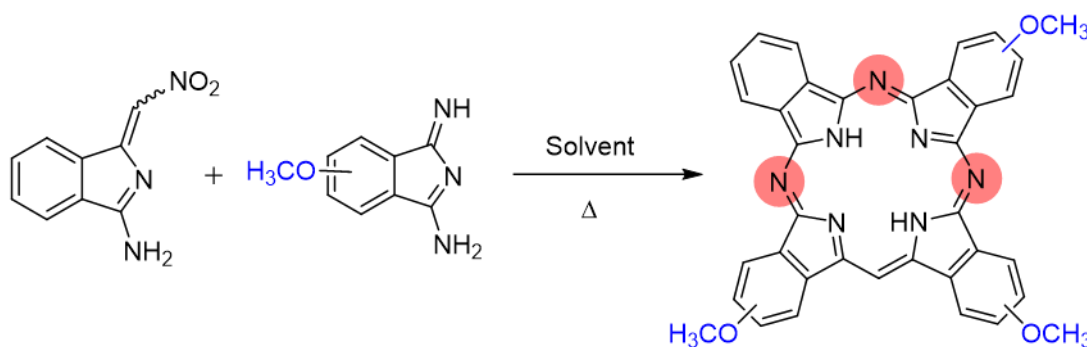
Scheme 1.12: Synthesis of (OMe)$_3$ H$_2$TBTAP via mixed cyclisation strategy.

Moreover, Kospranenkov, Luk'yanets and coworkers introduced tert-butyl groups on peripheral positions by reaction between potassium 4-t-butylphthalimide with malonic acid in the presence of zinc acetate at high temperature, then, the isolated adduct was reacted with phthalonitrile derivatives in the presence of zinc acetate in bromonaphthalene as a solvent. The resulting mixture consists of the tert-butyl-substituted mono-, di-, and tri aza analogues of zinc tetrabenzoporphyrin as shown in scheme 1.13. Tert-butyl-substituted isoindoline was used as another possible precursor for this method. These hybrids were isolated in the individual state from the mixture by chromatography on aluminium oxide. [105]
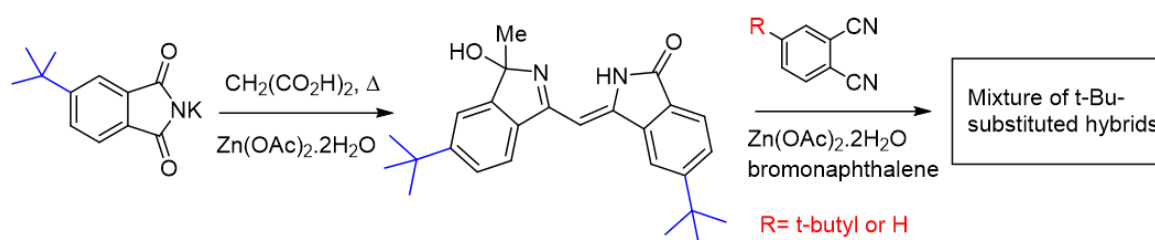
Scheme 1.13: Synthesis of t-butyl-substituted hybrids using malonic acid and t-butyl substituted phthalimide.

A variety of substituted hybrids have been successfully synthesised and reported using the mixed cyclisation method employing substituted precursors. However, despite numerous failed attempts to incorporate substituents at the meso-position of the hybrids such as Linstead's unsuccessful attempt to incorporate benzyl group using benzyl magnesium chloride instead of methyl magnesium chloride, a different result was achieved by Leznoff and McKeown in 1990. They reinvestigated the action of benzyl magnesium chloride on phthalonitrile under conditions similar to those described above and a mixture of magnesium meso-phenyl TBTAP complex in 15% yield with MgPc and sometimes traces of MgTBDAP (cis- and trans- isomers) was obtained. Moreover, comprehensive syntheses of *meso*-substituted TBTAPs were achieved from different ratios of Grignard reagents and different substituted phthalonitrile following the same method as shown in scheme 1.14. It was observed that incorporation of metal in the central cavity, bulky group at the *meso*-position and at peripheral position enhances the solubility of the hybrids and reduced their

aggregation in solution to make their isolation by chromatographic methods possible.[106]

R_1= t-Bu, H, -OCH$_2$C(CH$_3$)$_3$
R_2= Ph, CH$_2$CH$_2$CH$_3$, (CH$_2$)$_{14}$CH$_3$
X= Br, Cl
M= Mg, 2H

MgTBTAP
+
MgTBDAP
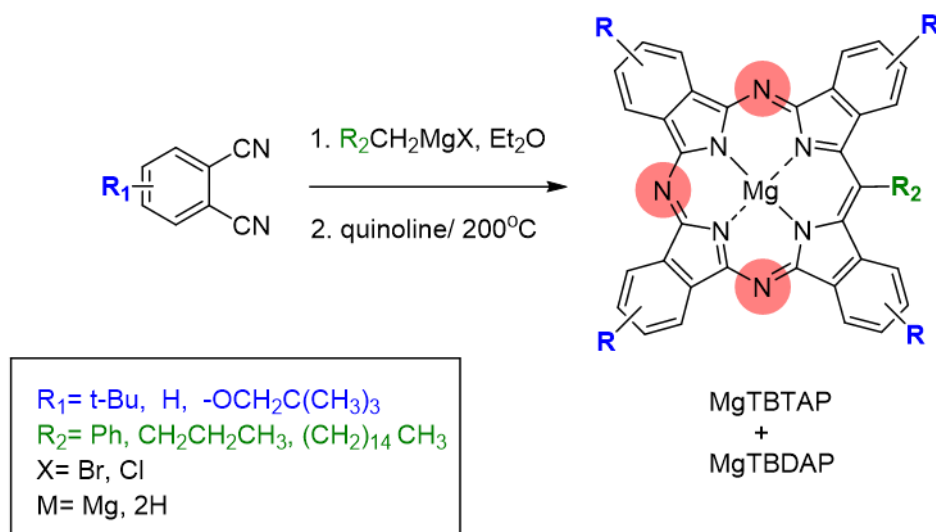
Scheme 1.14: Preparation of TBTAPs reported by Leznoff and McKeown.[106]

Leznoff and McKeown reported the synthesis of the first meso-substituted tetranaphthalo-triazaporphyrin (TNTAP) from 6-*t*-butyl-2,3-dicyanonaphthalene precursor under the same conditions (scheme 1.15). The reaction gives a mixture of TNTAP and NPc and only 3% of TNTAP was isolated as pure state as their separation proved challenging. [106]

R_1= t-Bu
R_2= (CH$_2$)$_{14}$CH$_3$
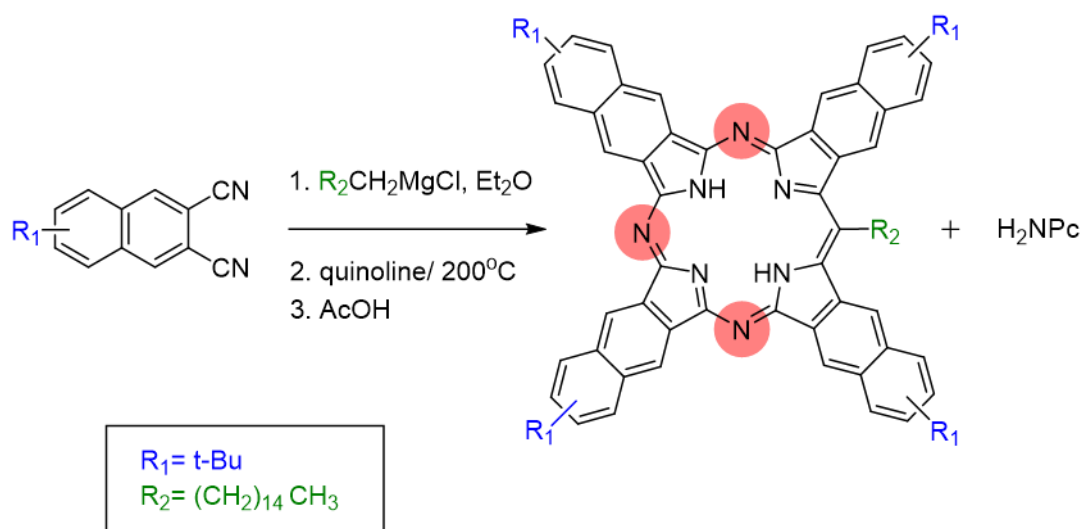
Scheme 1.15: Synthesis of TNTAP reported by Leznoff and McKeown.

In recent years, Galanin et al reported possible template synthesis of azaporphyrin derivatives using a carboxylic acid containing a CH_2 group adjacent to the carboxy group and 1,3 diiminoisoindoline derivatives and ZnO or MgO as template agent as shown in scheme 1.16. The full range of possible hybrid structures were obtained from this method as a mixture. As expected, the reaction stoichiometry has a considerable effect on the formation of these hybrids. When an excess of the carboxylic acids was added, more substituted carbon bridges were incorporated into the macrocycle core, whereas the more nitrogen bridges can be formed when the ratio of carboxylic acids was decreased compared to diiminoisoindolines. Furthermore, a very bulky 4-triphenylmethylphenoxy diiminoisoindoline was employed under the same conditions with phenylacetic acid in the presence of ZnO to produce a mixture of macrocycles and 12% of isolated ZnTBTAP. Also, meso-alkyl-ZnTBTAP was isolated as the only hybrid when longer aliphatic acids were used.[107]
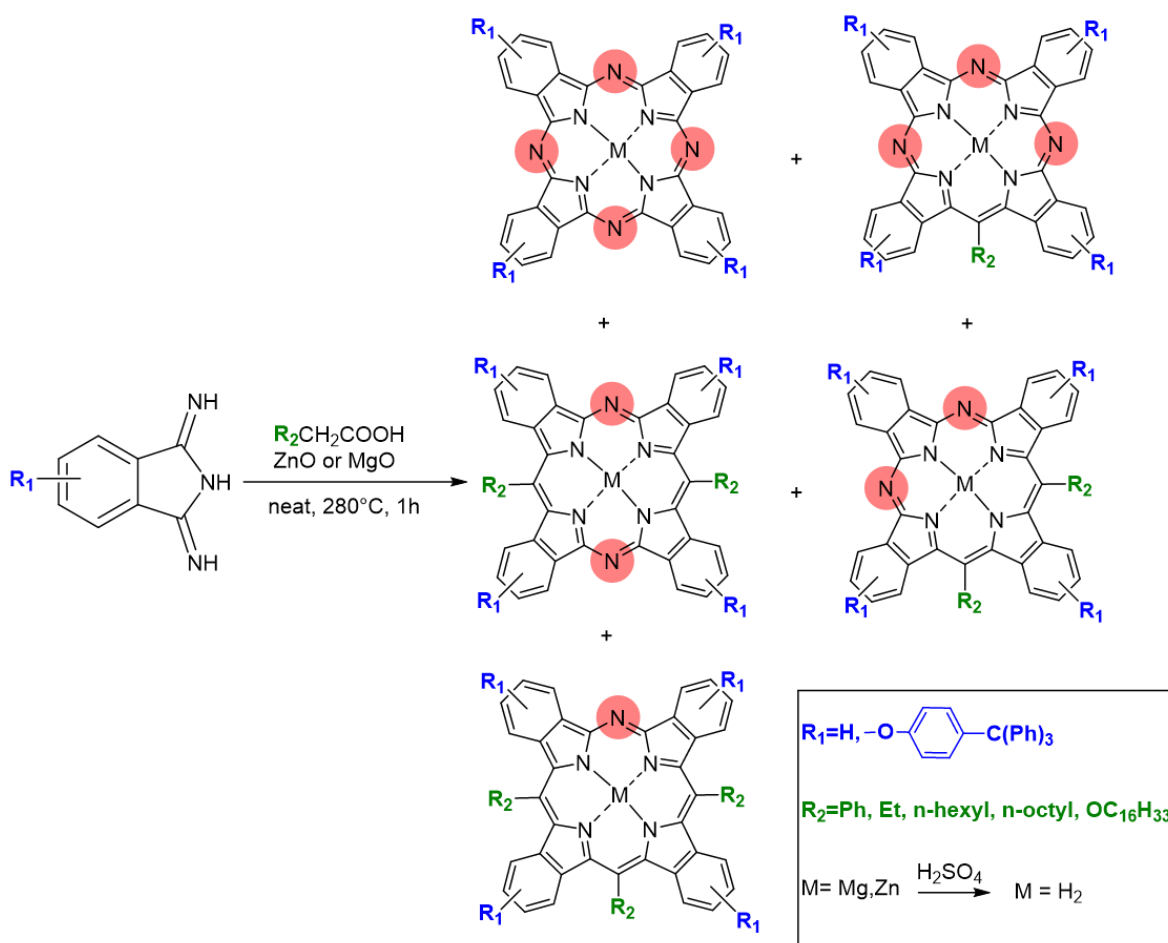
Scheme 1.16: Syntheses of substituted hybrids employing carboxylic acids reported by Galanin.

Borisov and coworkers employed this method to synthesise the substituted hybrids. They reported a successful conversion of H_2TBMAP-Ph_3 to its palladium and platinum analogues as illustrated in scheme 1.17. Also, Cis-H_2TBDAP-Ph_2 was converted to its Pd and Pt analogues under the same conditions.[108]
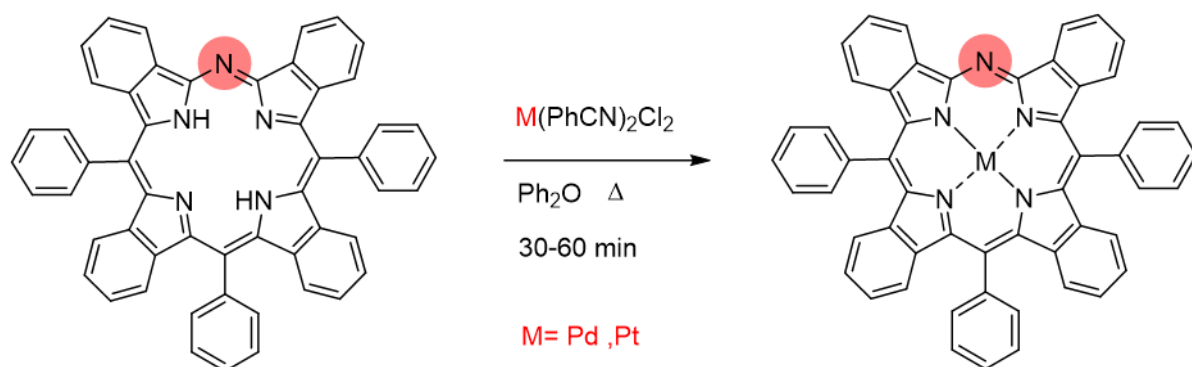
Scheme 1.17: Conversion of meso-phenyl TBMAP to its Pd and Pt analogous.

Bulavka reported similar mixed cyclisation using potassium phthalimide, potassium salt of phenyl acetic acid, urea and magnesium oxide as a template. Macrocycles were formed after 30 mins under microwave heating (scheme 1.18).[109]
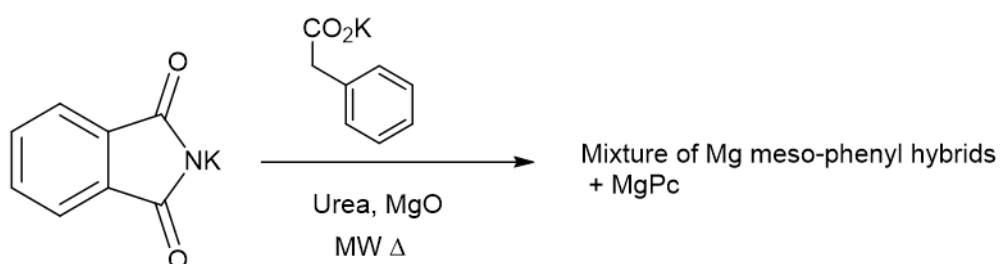
Scheme 1.18: A mixed cyclisation of phenyl acetic acid salt and phthalimide reported by Bulavka.[109]

Moreover, a selective formation of *trans*-TBP-(alkoxy)$_2$ and *trans*-TBP-(alkyl)$_2$ were successfully achieved by Galanin and co-workers. The dimeric intermediate was reacted with the appropriate carboxylic acid and zinc oxide at 300 ^{0}C for 30 min as shown in scheme 1.19. [110–113]
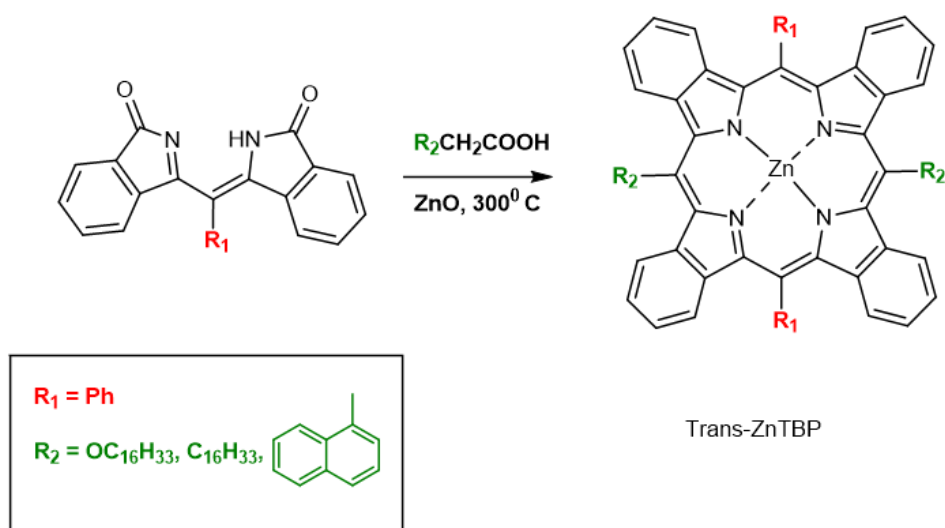
Scheme 1.19: The syntheses of trans-TBPs using dimeric intermediate and carboxylic acids.

In 2011, Tomilova and co-workers investigated the synthesis of meso-phenyl-TBTAP complexes that bears additional substituents on the meso-phenyl ring through a new synthetic route by mixed condensation of aryl acetonitrile with unsubstituted phthalonitrile in the presence of magnesium powder under conventional or microwave heating as shown in scheme 1.20. It was noted that an easy demetallation of magnesium complexes under mild conditions could be achieved in 98 % yield. The possible chromatography purification for magnesium hybrids and their high stability in air make these complexes convenient for subsequent modifications compared to other metals. [114]
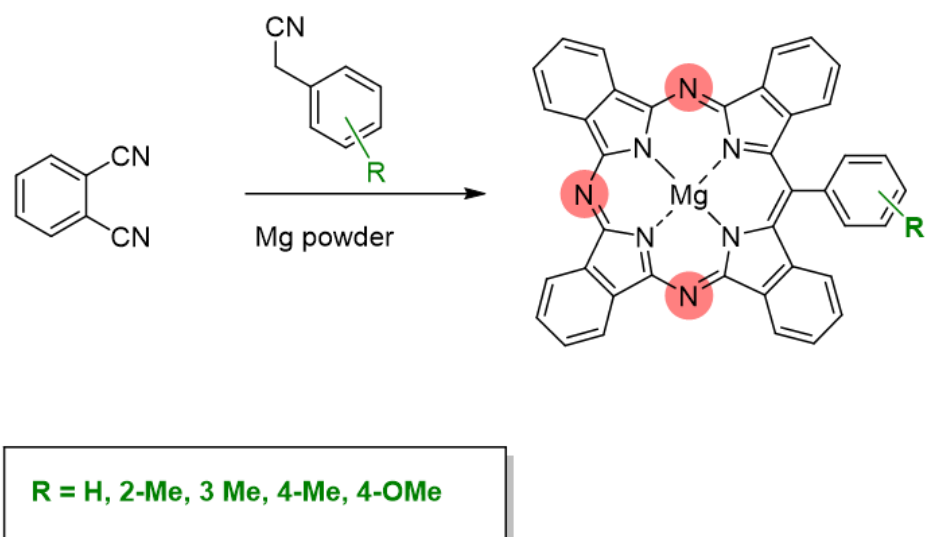
Scheme 1.20: Tomilova's syntheses of meso-aryl TBTAPs using aryl acetonitrile precursors.

The synthesis of meso-substituted ZnTBTAPs were also achieved by heating a combination of phthalonitrile and quaternary salts of triphenyl phosphonium from 200 - 300°C in the presence of zinc dust (scheme 1.21). The desired product can be purified by column chromatography as they dissolve in common organic solvents. The first x-ray crystallographic study of *meso*-substituted TBTAP was reported.[115]
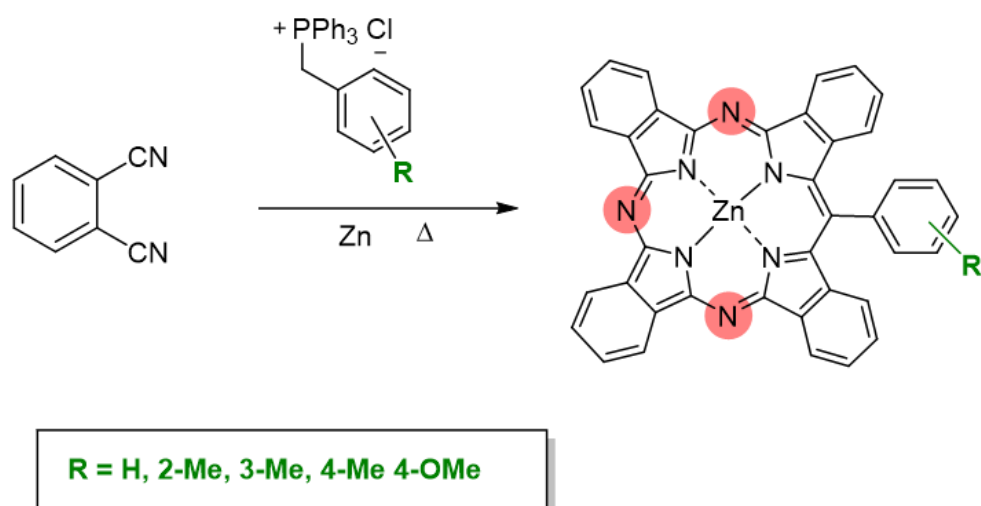
Scheme 1.21: Synthesis of meso-substituted ZnTBTAPs using benzyl phosphonium salts.

1.9 New selective synthesis of TBTAP

In 2005, unexpectedly facile access to non-peripherally substituted octaalkyl-tetrabenzotriazaporphyrins was reported by Cammidge, Cook and co-workers during a LiOPentyl-induced cyclotetramerisation of 3,6-dihexyl phthalonitrile to synthesise *np* R$_8$-H$_2$Pc (scheme 1.22). The substituted TBTAP was obtained as a green by-product (about 5% of the crude) along with the corresponding non-peripheral octa alkyl-phthalocyanine. It was observed that the use of a higher boiling solvent such as n-octanol increased the ratio of the side product (later identified as *np*-R$_8$-H$_2$TBTAP) up to 47% of the crude compared to n-pentanol. Also, when the equivalents of Li were increased to 19 from 2.1 the ratio of TBTAP was increased to 23% compared to 5%. Moreover, when freshly cut lithium metal is added to the alcohol solution of phthalonitrile, TBTAP hybrid was formed, whereas the use of the prepared lithium alkoxide leads to the formation of the phthalocyanine hybrid only. Full analysis was reported including ^{1}H NMR, ^{13}C NMR and crystal structure that proved it is the assigned product. Also, ^{13}C isotope labelling experiment was used to investigate the origin of the meso-carbon. It was proved that the hydroxyl bearing carbon atom of the alcohol solvent is the source of the *meso*-carbon. The reactions of phthalonitrile incorporating peripheral or non-peripheral substituents were investigated under the same conditions. The formation of TBTAP products was not observed when 4-t-butylphthalonitrile or 4,5- dihexylphthalonitrile were used and the reaction give only the corresponding phthalocyanines, whereas 3,6-dimethyl, 3,6-dihexyl, 3,6- dioctyl and 3,6-didecylphthalonitriles give mixtures of Pc and TBTAP. [116]
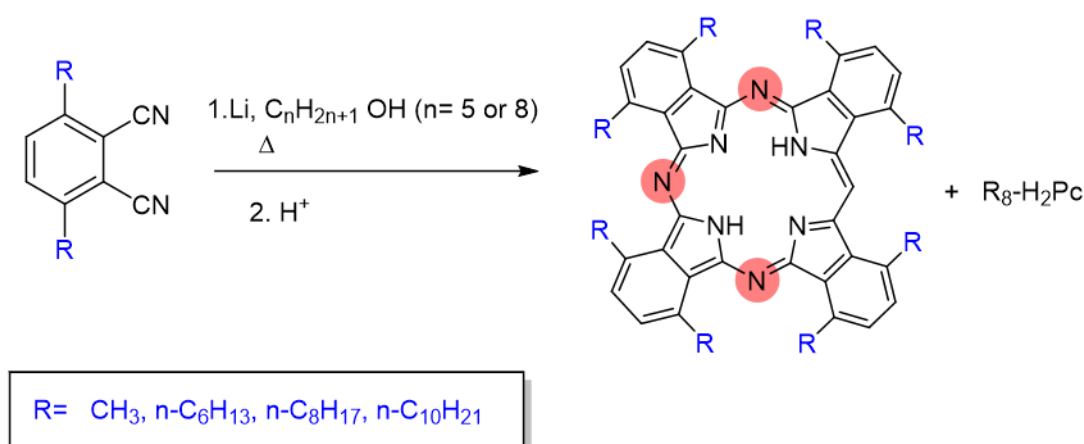
Scheme 1.22: Unexpected preparation of non-peripherally substituted octa alkyl-tetrabenzotriazaporphyrin by Cammidge and co-workers.

In 2011, Cammidge-Cook groups, reported that the non-peripherally substituted TBTAP bearing a group on the *meso*-carbon atom cannot be synthesised following Leznoff and McKeown's procedure as a result of the steric crowding, and the only TBTAP product formed was the parent $(np\text{-alkyl})_8\text{-H}_2\text{TBTAP}$. Long alkyl and benzyl Grignard reagents were used, and all give the same hybrid as depicted in scheme 1.23.[117]
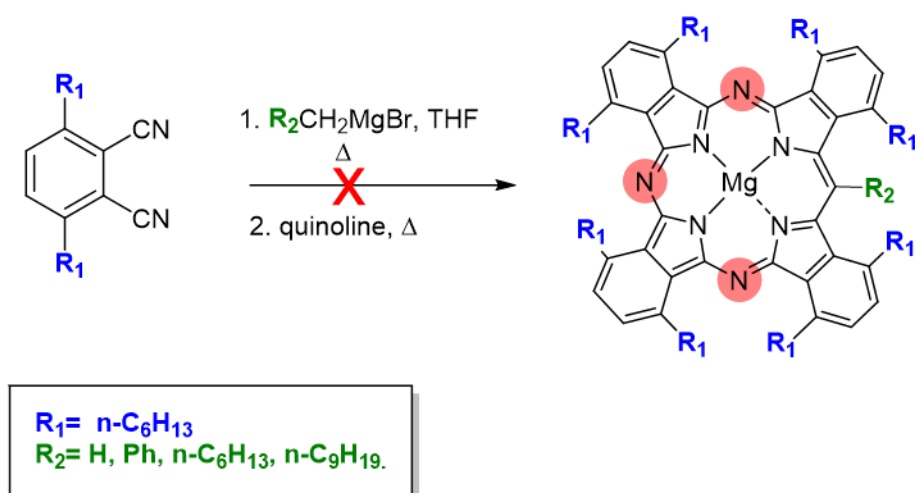
Scheme 1.23: Failed attempt to introduce bulky substituents at meso-position of np-substituted TBTAP using various Grignard reagents.

The group extended their investigation of the reaction of 3,6-dialkylphthalonitriles with varying ratios of methyl magnesium bromide as Grignard reagent based on Linstead and Galanin's previous observations on the effect of the amount of Grignard reagents/ carboxylic acids on hybrids formation.[23,107,118] Magnesium analogues of non-peripherally substituted tetrabenzo (aza)porphyrin derivatives (TBTAB, *cis/trans* TBDAP, TBMAP, TBP, Pc) were successfully synthesised following the two-step synthetic procedure of Linstead and Barrett that involves the treatment of solution of 3,6-dialkylphthalonitriles in ether or THF with methyl magnesium bromide as Grignard reagent, then exchanged the solvent to quinoline and refluxed the mixture at 200 °C (scheme 1.24). [23,117]
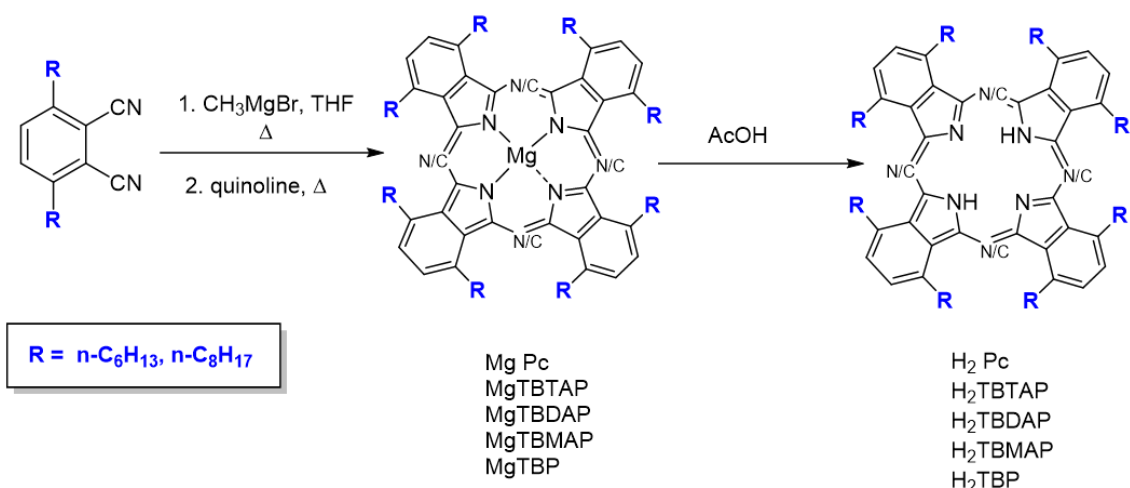
Scheme 1.24: Controlled synthesis of tetrabenzo (aza)porphyrin derivatives and their demetallation.

To understand hybrids distribution, a series of ratios of both Grignard reagent and phthalonitrile were examined. It was observed that 1:4 ratio of MeMgBr: 3,6-dialkylphthalonitriles produced no macrocyclic compounds. Thus, the ratio of Grignard reagent was increased gradually to (1:1) ratio, which give two predominant hybrids (identified later as TBTAP and TBDAP) in 24% and 14% yields after demetallation process, respectively. Increasing the ratio to 2:1 and 3:1 give all the hybrids, whereas TBP was observed as the only hybrid when the ratio increased to 4:1, but further increases in the ratio reduce its overall yield. It is important to note that, in all different ratios used, only traces of Pc were observed, and these outcomes are hugely different from Leznoff and McKeown's results which give at least 50% Pc during the preparation of *meso*-TBTAP from 4-substituted phthalonitrile. Moreover, Hexyl and Octyl chains on phthalonitrile were used to duplicate these reactions with similar outcomes. Column chromatography was used to isolate magnesium analogous except TBDAPs' isomers. Then, acetic acid was employed to de-metalate Mg-macrocycles to produce metal-free derivatives. Different metals such as Cu and Pb were successfully inserted in the central cavity of H_2-hybrids in refluxing pentanol and a large variety of MTBTAP was synthesised using this method.[117]

In 2017, another research group reported an effective procedure to synthesise a high scale of non-peripheral octaalkyl H_2TBTAP by using MeLi and cyclohexanol instead of MeMgBr. A high yield of 35% of *np* $(C_6H_{13})_8H_2$TBTAP was achieved even when six grams of phthalonitriles are used.[119]

Furthermore, Cammidge-Cook groups also investigated the reaction of 4,5 dialkyl phthalonitriles with two equivalents of MeMgBr as Grignard reagent (scheme 1.25). The reaction gives a predominant mixture of TBTAP and Pc in the ratio of 5:4, respectively. This finding is mostly the same as Leznoff and McKeown's one. Unlike 3,6 dialkyl phthalonitrile reaction, introduction of benzyl group and long alkyl chain at *meso*-position was achieved when 4,5 dialkyl phthalonitriles were employed and the formation of a product containing the unsubstituted methine bridge was not observed in this reaction. [117]
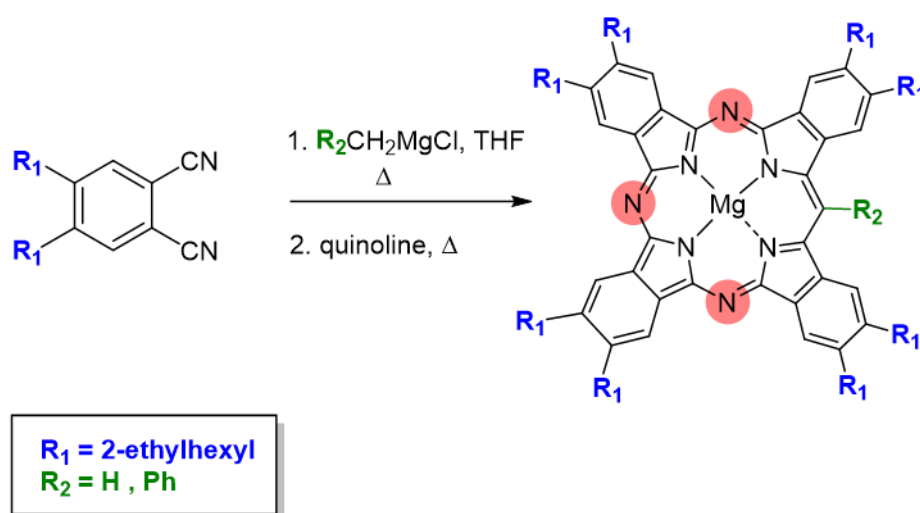
Scheme 1.25: Isolation of peripherally substituted analogues functionalised on the meso-position.

Significant emphasis has been placed on the TBM development of hybrid structures in the last decade, even though most syntheses have utilised the original procedures, albeit with some improvements. However, our group recently reported a significant breakthrough in this field, in which a novel and versatile method was disclosed to give controlled access to functionalised *meso*-phenyl TBTAPs as the only hybrid. This synthetic strategy has demonstrated a notable high yield of TBTAP and eliminates the production of any other hybrids.[120] The methodology employed in this study involves the use of a previously prepared aminoisoindoline or its derivatives following the procedure reported by Hellal and Cuny.[121] As shown in scheme 1.26, the synthesis involves two steps: the first step is treatment of a solution of 4-bromobenzonitrile in THF with a solution of lithium bis(trimethylsilyl) amide (LiHMDS) in THF, which was subsequently quenched with a mixture of isopropanol/HCl, resulting in the desired product in a high yield.[122] The next step involves cyclisation process of the resulting material with terminal aryl-acetylene through

copper-free Sonogashira cross-coupling and under microwave irradiation.[120]

Ar = 4-methoxyphenyl
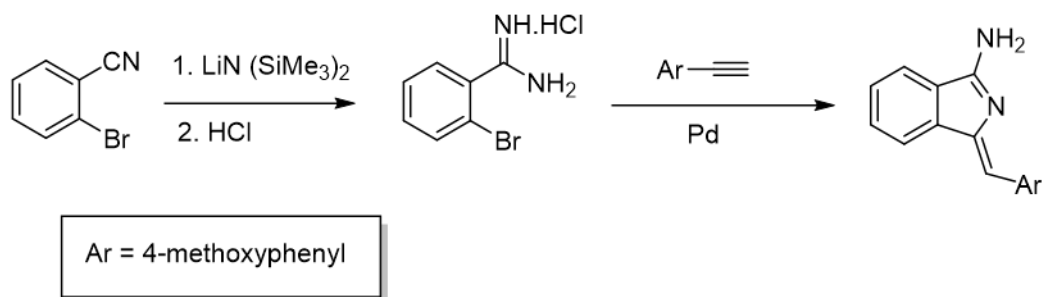
Scheme 1.26: Synthetic route for preparation of aminoisoindoline derivatives following Hellal's method.

Once the synthesis of the aminoisoindoline was achieved successfully, the first attempt to synthesise the *meso*-phenyl TBTAP involved the refluxing of a mixture of aminoisoindoline and diiminoisoindoline as a macrocyclisation partner with magnesium salt as a template in different high boiling solvents such as DMF, DMEA, quinoline and diglyme. Upon analysis, it was found that the resulting product was a mixture of the desired product *meso*-phenyl TBTAP, magnesium phthalocyanine (MgPc) and a dimeric side product as shown in scheme 1.27. Hence, the reaction was subjected to a careful investigation in order to minimise the formation of unwanted Pc and other side products and increase the overall yield of the target compound. Additional modifications were made which involved the utilisation of phthalonitrile as a less reactive precursor instead of diiminoisoindoline, controlling the addition of aminoisoindoline throughout the reaction and addition of DABCO to reaction mixture, resulting in improvement of the synthesis of the target *meso*-phenyl TBTAPs and an increase in their overall yield. Different methoxy position on the meso-phenyl TBTAP have been reported such as 3-, 3,5- and 4-methoxy phenyl.[123] Also, the first *meso*-phenol TBTAPs which bear reactive functional groups ready for further elaboration have been reported through conversion of the methoxy groups into phenolic groups. Demethylation of these macrocycles was achieved by treatment with magnesium iodide[120] or boron tribromide.[123] Subsequently, re-alkylation or acylation of these macrocycles was achieved using conventional reaction conditions in excellent yields.[120,123]
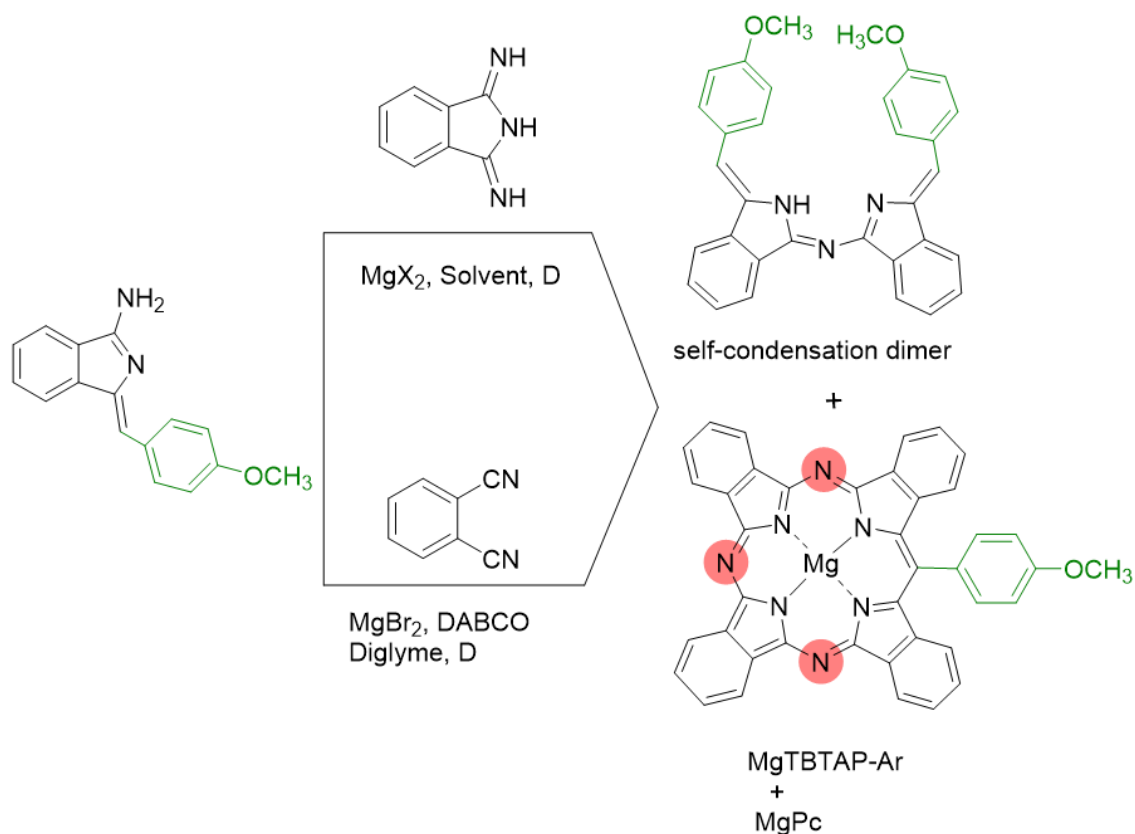
Scheme 1.27: Formation of MgTBTAP-Ar along with MgPc and dimeric intermediate using diiminoisoindoline precursor (on the top) and a modified synthetic route using phthalonitrile (on the bottom).

This new synthetic approach allows for the design and synthesis of new families of meso-aryl TBTAPs and their further elaboration into functional molecular materials. In 2014, our group chose meso-pyrenyl aminoisoindoline as co-macrocyclic compound with phthalonitrile under the optimised procedure to demonstrate the efficacy of the new synthetic protocol. The aminoisoindoline was obtained as a mixture of stereoisomers through the reaction between 1-ethynylpyrene with 2-bromobenzamidine. Then, a template co-macrocyclisation step was carried out between the mixture and phthalonitrile to give the corresponding TBTAP (scheme 1.28).[123]
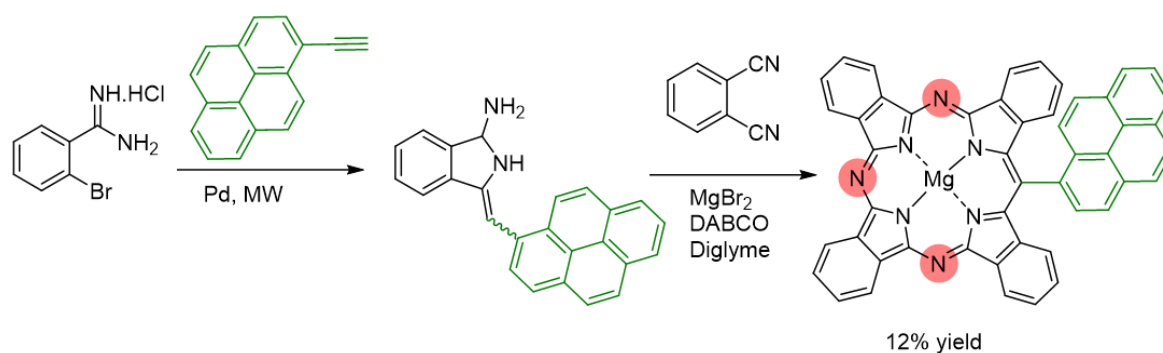
Scheme 1.28: Synthesis of meso-pyrenyl TBTAP.

Like other synthetic routes, this approach therefore also proves to be of limited value when synthesising meso-(bromophenyl) TBTAPs. The synthesis of brominated aminoisoindoline derivatives was complicated due to the generation of multiple by-products during the reaction that prevented chromatography separation of the product even when different solvent system was employed (scheme 1.29). The obtained outcome was anticipated due to the presence of the extra bromoaryl unit that could trigger numerous undesired chemical reactions.[124]
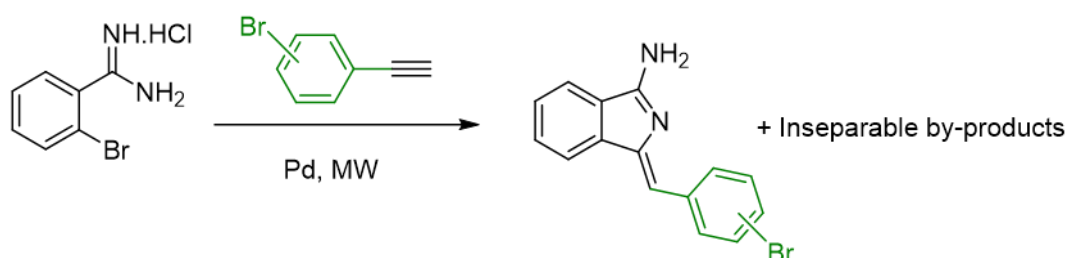
Scheme 1.29: Unsuccessful synthetic route towards brominated aminoisoindoline.

Therefore, Cammidge group extended their investigation and employed alternative strategies in order to synthesise *meso-* bromophenyl TBTAPs derivatives. These materials can be used to synthesise several novel TBTAP derivatives with reactive functional groups that are ready for further development. They reinvestigated the established strategy, that was reported originally by Linstead et al to synthesise *meso*-phenyl TBTAP by utilising Grignard reagent.[23] They successfully reported the synthesis of series of functionalised *meso*-bromophenyl TBTAPs through the reaction between phthalonitrile and a series of isomeric 2-, 3- and 4-bromobenzyl magnesium chlorides (scheme 1.30). The reaction has been

optimised further by employing diglyme as the only solvent and the reaction was done in one step with a slow addition of Grignard reagent. It is notable that the optimised conditions prevented the formation of dimeric compound and other side products and therefore increased the overall yield of the desired TBTAP. The maximum yield achieved was 56% corresponding to meso-(2-bromophenyl) TBTAP. In addition, the group investigated the utilisation of 4,5- disubstituted phthalonitrile along with 2-bromobenzyl magnesium chloride as a method of improving solubility and reducing aggregation. A chiral phthalonitrile with branched chains and a highly symmetric branched phthalonitrile were tested. The desired TBTAPs were isolated in low yields despite their straightforward synthesis.[124]
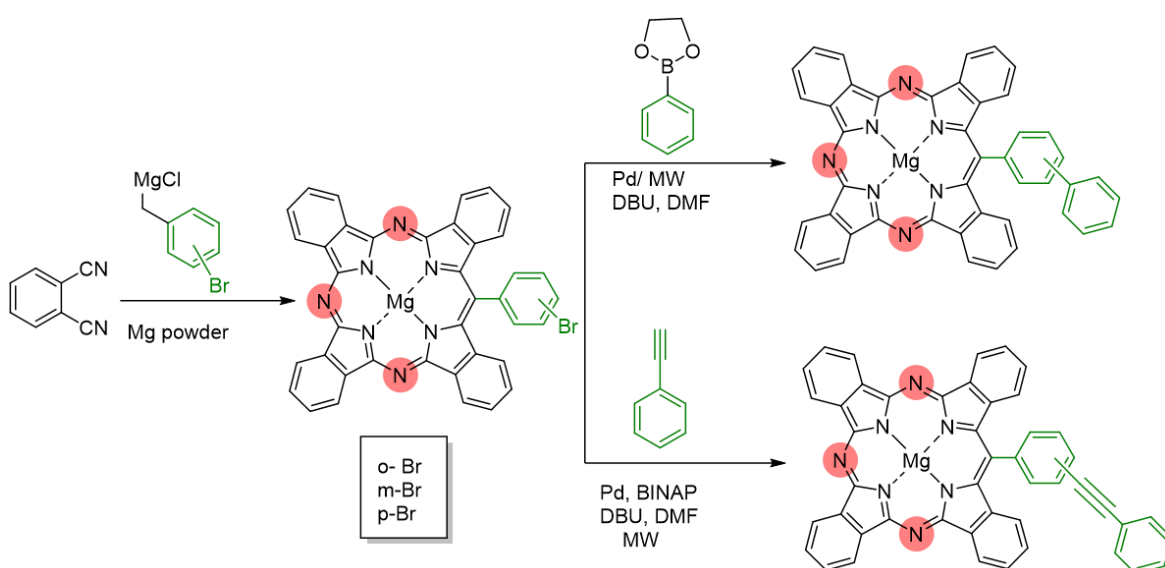
Scheme 1.30: Synthesis of isomeric series of meso-bromophenyl TBTAPs and their coupling reactions.

After the successful synthesis of *meso*-bromophenyl TBTAPs derivatives, Cammidge's group reported the first functionalisation of *meso*-phenyl TBTAP hybrids through palladium catalysed cross-coupling reactions. Suzuki and copper-free Sonogashira cross-coupling was used for this synthesis. The first coupling reaction used was the Suzuki coupling by employing bromo-aryl TBTAP as the first coupling partner and organoboronic acid reagent as the other under typical Suzuki conditions. After several attempts and various reaction conditions, it was observed that formation of debrominated products dominated when phenyl or 4-methoxyphenyl boronic acid were used. However, a successful cross-coupling reaction was achieved when boronate ester was used as a coupling partner instead of boronic acid as

illustrated in scheme 1.30. Another cross-coupling reaction was used to functionalise *meso*-phenyl TBTAP was copper-free Sonogashira reaction. A typical Sonogashira condition involves the use of aryl halides and terminal acetylene in presence of copper, palladium catalyst, and a base to yield di-aryl substituted acetylenes. The use of copper in this reaction might result in undesirable incorporation of copper metal inside TBTAP's central cavity so a copper-free reaction was employed. A successful straightforward synthesis of the desired TBTAPs was reported with a high yield (40-73%). In both strategies, a microwave reactor was used instead of conventional heating.[124]

The breakthrough synthesis of TBTAP hybrids has the potential to inspire additional modification of *meso*-phenyl TBTAP derivatives. Moreover, our group recently, have disclosed additional modifications in the synthesis of TBTAP that permits potential of incorporation of different benzo fragments regiospecifically around the macrocycles. The previously optimised procedure was used, by slowly adding aminoisoindoline to the solution of substituted phthalonitrile in refluxing diglyme in the presence of $MgBr_2$. The synthesis was straightforward. However, two distinct hybrid products were isolated, Ar-ABBB TBTAP as minor product and the unique Ar-ABBA TBTAP as the major product from all the attempts. To demonstrate the scope of this synthesis, two different series have been tested. In the first series, an identical 4-methoxyphenyl aminoisoindoline has been used as co-reactant with various peripheral substituted phthalonitriles to avoid steric clashing with substituents on the *meso*-carbon. In the first attempt, 4-tert-butylphthalonitrile was employed as it is a common precursor in Pc synthesis. Three equivalents of phthalonitrile were reacted with one equivalent of aminoisoindoline under the optimised conditions. According to the proposed mechanism, ABBB TBTAP was expected to form but a complex mixture was obtained, therefore, 4,5-disubstituted phthalonitriles were employed to simplify characterisation and analysis. Different substituents were tested such as 4,5-alkoxy, -phenoxy and -heavily branched substituents. As depicted in scheme 1.31, the desired phthalonitriles were synthesised by the Rosemund-von Braun cyanation using copper cyanide as a cyanide source. Then, they underwent a macrocyclisation reaction with aminoisoindoline to yield smooth formation of two TBTAP hybrids. Upon analysis, Ar ABBA TBTAPs with two substituted phthalonitrile units and two unsubstituted benzene units that derive from the identical aminoisoindoline were the dominant hybrids in all the attempted synthesis.[125]
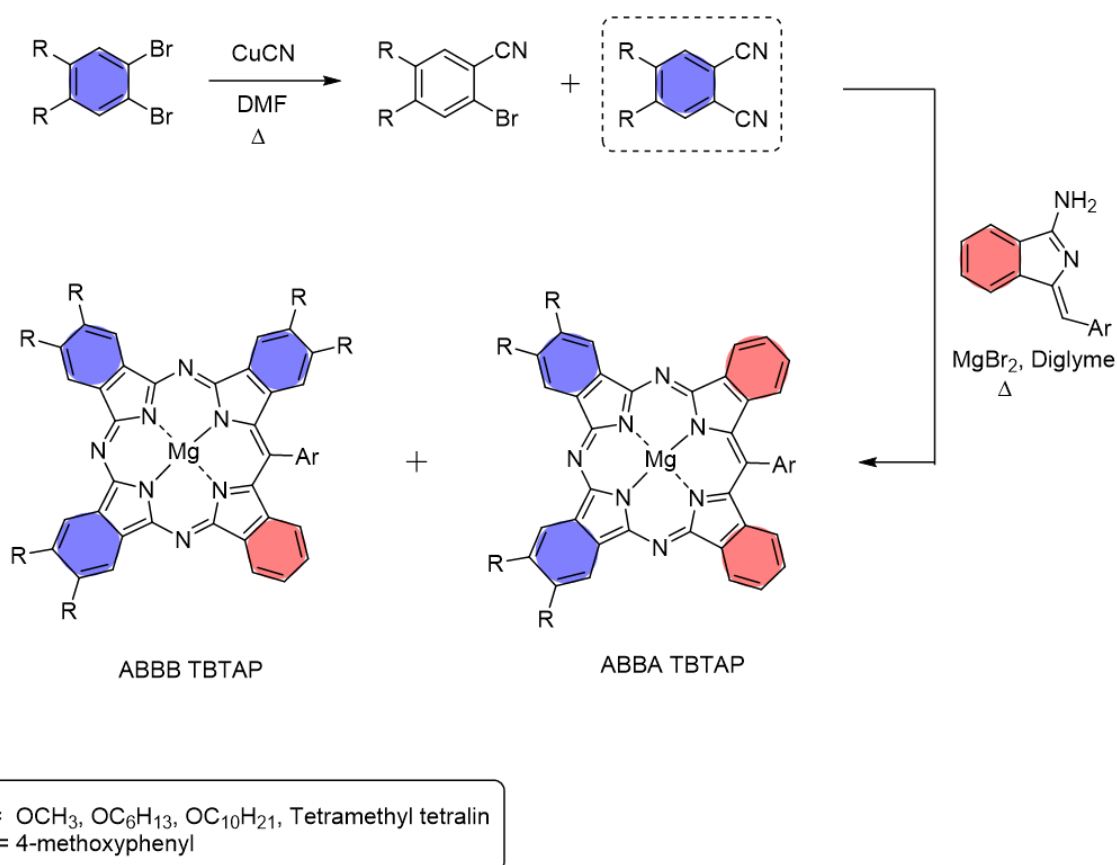
Scheme 1.31: MgTBTAP synthesis using substituted phthalonitrile and identical
aminoisoindoline.

Moreover, when the indole fragment is functionalised and unsubstituted phthalonitrile was
used as the second series, hybrids with substituents on rings close to the *meso*-Ar were
synthesised as seen in scheme 1.32. To introduce substituents on aminoisoindoline,
substituted bromobenzonitriles were used as precursor from phthalonitrile synthesis. Next,
the reaction was carried out under the same conditions and two different TBTAP hybrids
were isolated with ABBA Ar-TBTAP as the major product. The reaction was repeated with
different substituents, and the same results were obtained. Both series give ABBA Ar-
TBTAP as dominant product even when the reaction stoichiometry was changed to 2:2
aminoisoindoline: phthalonitrile stoichiometry and the rate of addition was increased.
However, the overall yield of hybrids was lowered and the relative proportion of ABBA Ar-
TBTAP hybrids in the isolated macrocyclic mixture was increased. [125]
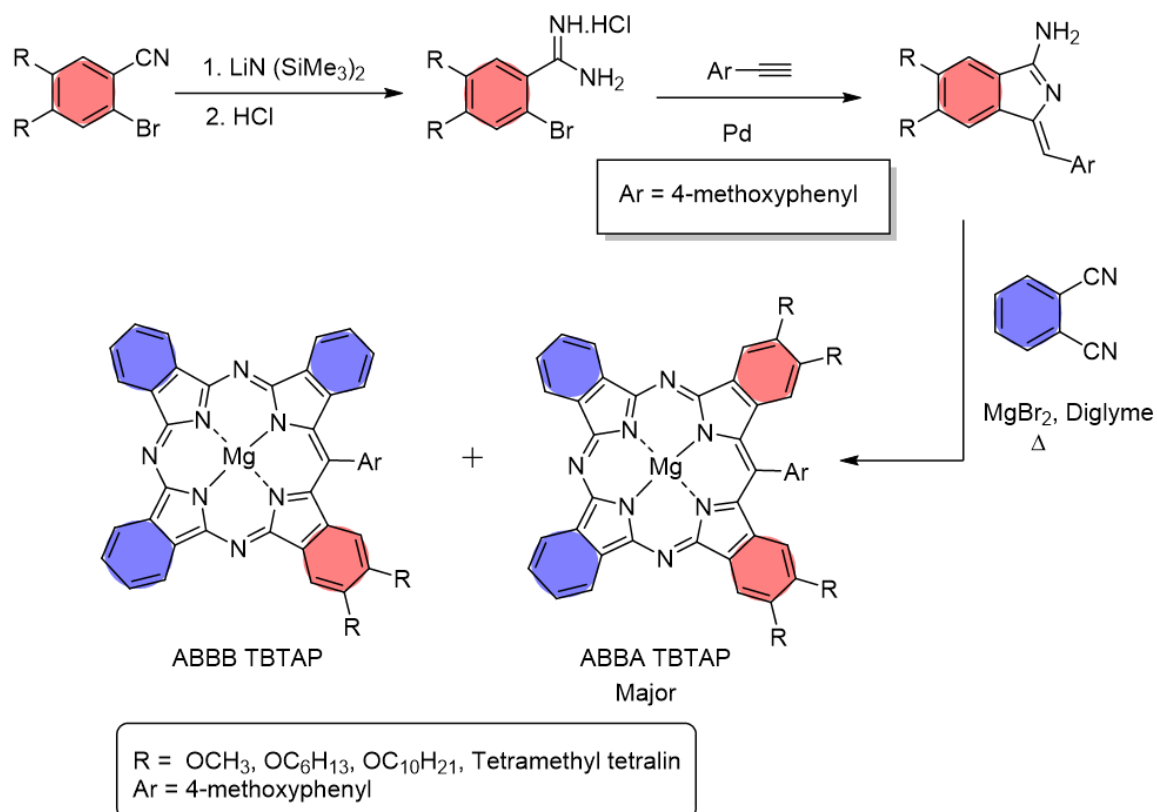
Scheme 1.32: MgTBTAPs synthesis using substituted aminoisoindoline and identical dicyano-benzene.

The proposed mechanism for the formation of both hybrids is illustrated in scheme 1.33. The first step involves the formation of AB dimeric intermediate from the reaction of aminoisoindoline with phthalonitrile. Then, the ABBB hybrid is finally produced by adding phthalonitrile units to the intermediate. However, the ABBA hybrid can form when self-condensation of intermediate dimer occurs followed by cyclisation and loss of phenyl fragment. The self-condensation step seems faster than the former step, therefore, the ABBA hybrid is the dominant macrocycle.
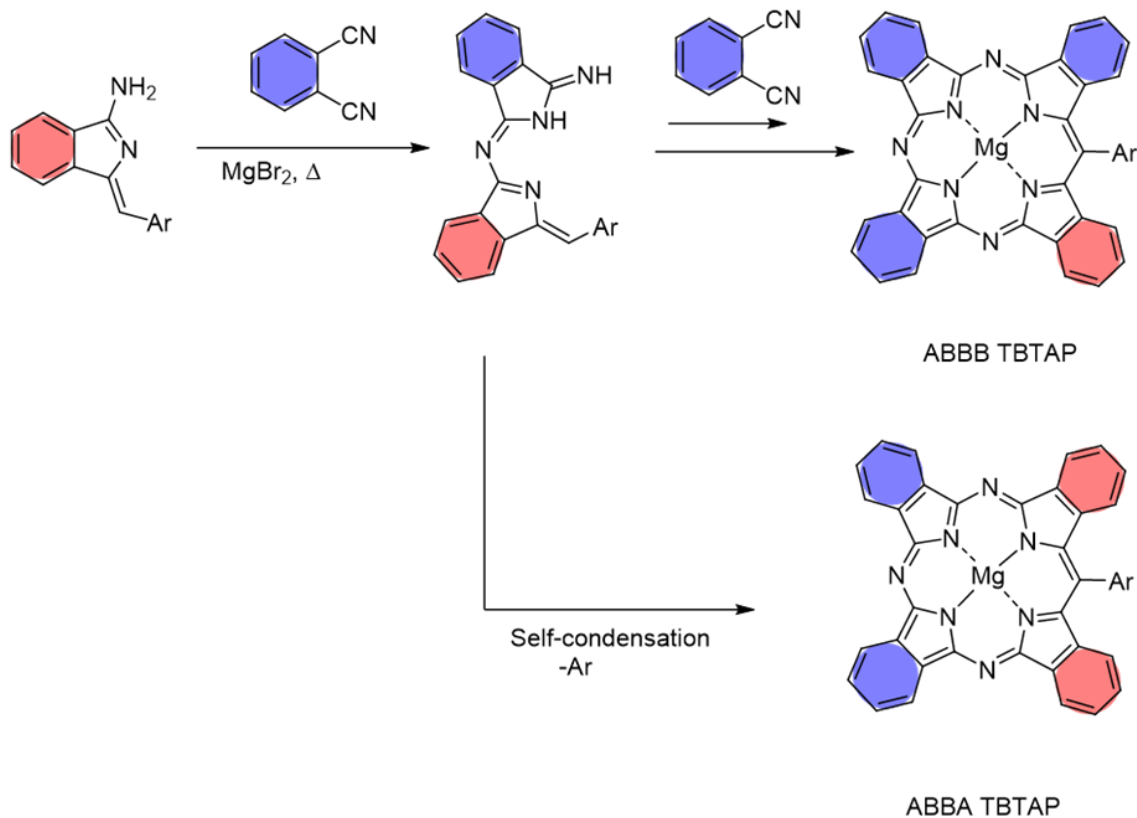
Scheme 1.33: Proposed mechanistic pathway of formation of ABBB TBTAP and ABBA TBTAP.

It should be noted that *meso*-phenyl TBTAPs have been employed as precursors to synthesise the first homo and heteroleptic lanthanide sandwich-type complexes. Complexation of metal-free meso-phenyl TBTAP with europium or lutetium acetylacetonate was carried out according to Pc double-decker synthesis to yield the title homoleptic double-decker derivatives in 85%, 81% respectively. However, complexation of preformed lutetium phthalocyanine with TBTAP leads to the formation of heteroleptic complexes as illustrated in scheme 1.34.[126–128]
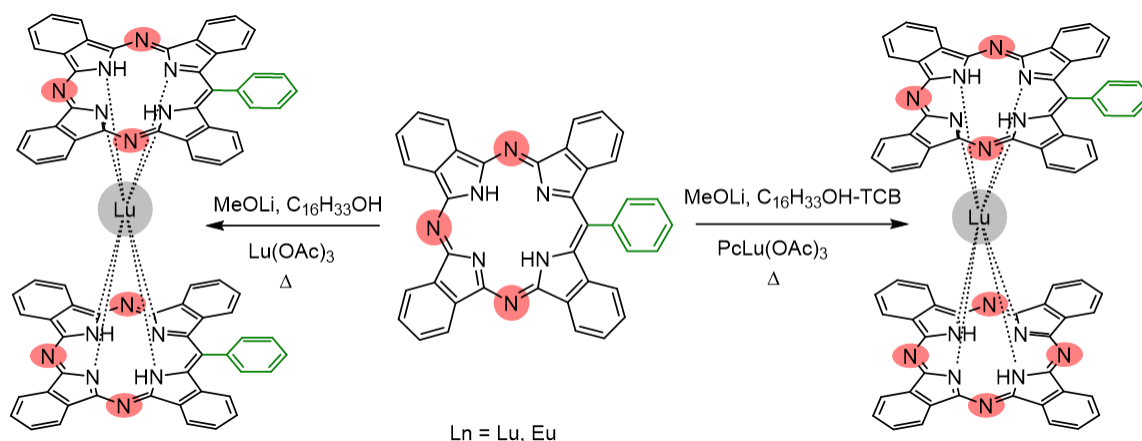
Scheme 1.34: Synthesis of homoleptic and heteroleptic meso-phenyl TBTAP double-decker.

According to a patent, TBTAP complexes can undergo a direct electrophilic aromatic substitution such as sulfonation reaction to produce water-soluble derivatives for practical applications. The patent outlined the process of sulfonating the copper complex of unsubstituted meso-TBTAP using Chloro-sulfonic acid. When the reaction was carried out at 127-135°C, three sulfonyl chloride groups were introduced, while at 143-145°C four groups were added as depicted in scheme 1.35. However, when magnesium complex of meso-phenyl TBTAP was treated with chloro-sulfonic acid at 42-46 °C, only meso-aryl group was sulfonated and this reaction demetallised magnesium ion. [129,130]
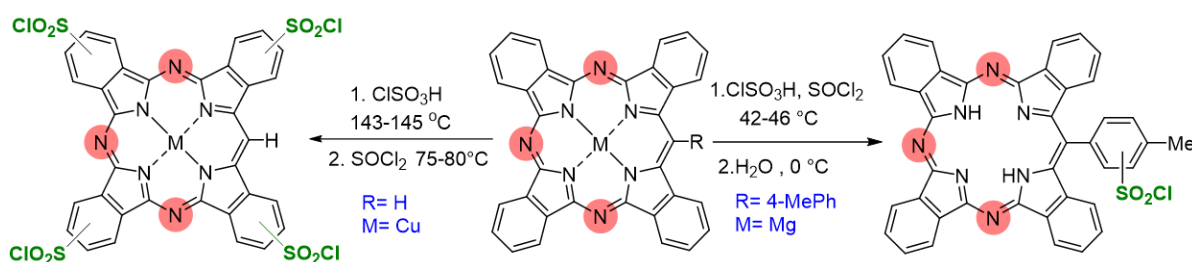
Scheme 1.35: Sulfonation of TBTAP hybrids.

1.10 Selective synthesis of tetrabenzodiazaporphyrin (TBDAP)

As described earlier, reaction of phthalonitrile with various ratios of Grignard reagents give a valuable synthesis of partially *meso*-modified TBDAP derivatives in variable quantity along with other hybrids.[131] However, there has been a growing interest to synthesise this hybrid selectively. In 2011, Okujima et al reported a successful selective synthesis of copper complex of TBDAP macrocycle by the retro Diels-Alder reaction of BCOD-fused diazaporphyrin which was obtained from 2+2 metal-templated cyclisation of dipyrromethene (scheme 1.36).[132]
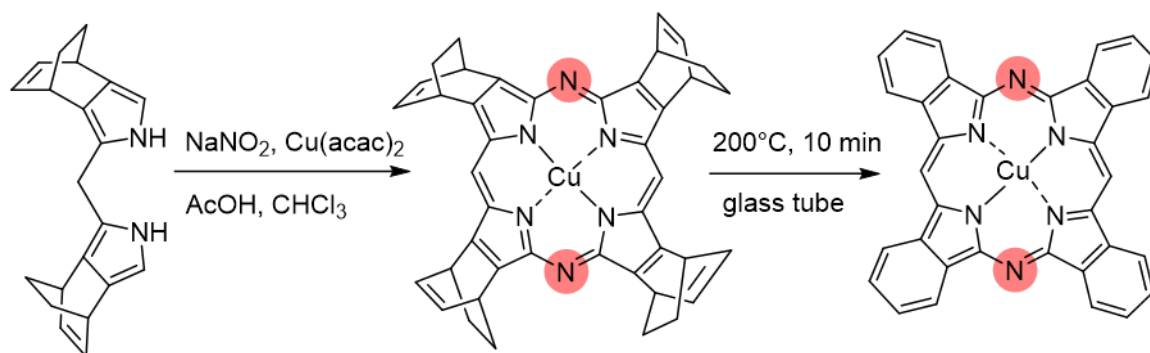
Scheme 1.36: Synthesis of BCOD CuDAP and its thermal conversion CuTBDAP.

In 2014, Cheprakov and co-workers reported the first selective synthesis of metal-free 10,20-diarylTBDAP through thermal decomposition of bis-azidocarbonyl derivatives of meso-aryldibenzodipyrromethenes in ~50% reproducible yields (scheme 1.37). [133]

R=3,5- ^{t}Bu$_2$, COOMe, 3,5-(OMe)$_2$
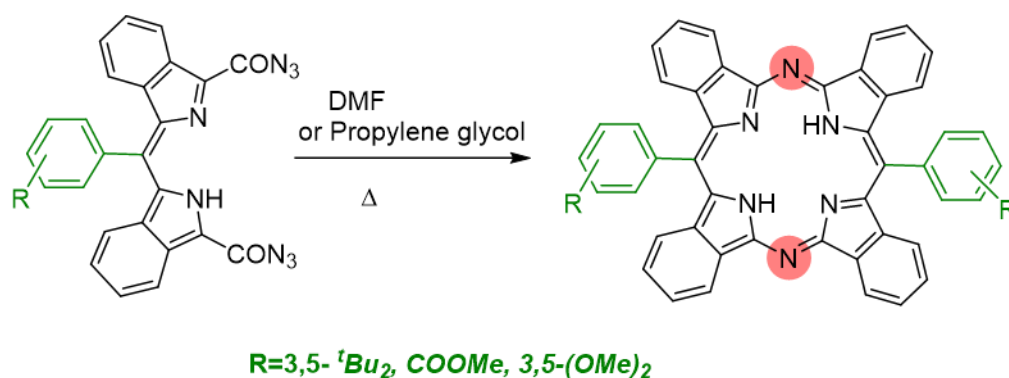
Scheme 1.37: Synthesis of H$_2$TBDAPs.

Later, they reported the first data and optical study of metalated Ar$_2$TBDAP series via direct metalation of free ligands using divalent metals such as Zn, Cu, Pd, Pt and Ni.[134] Recently, Yamada et al, reported a refined approach towards the synthesis of BCOD- fused 5,15 diazaporphyrin and their *meso*-substituted derivatives via metal-templated cyclisation reaction of bis (dibromo dipyrromethene) complexes that employ N, N′-dimethyl ethylenediamine (DMEDA) as a ligand in optimising Matano and co-workers' method (scheme 1.38). *Meso*-free BCOD-fused dipyrromethene was synthesised by acid-catalysed condensation of BCOD fused pyrrole with dimethoxy methane (methylal) whereas *meso*-substituted derivatives were prepared by the reaction between BCOD fused pyrrole with aryl aldehyde using boron trifluoride etherate as Lewis acid.   Both BCOD-fused dipyrromethene's were brominated by N-Bromo succinimide (NBS) in THF, followed by oxidation with 2,3-dichloro-5,6-dicyanobenzoquinone (DDQ) to give *meso*-substituted dibromo dipyrromethene in high yield (75-89%). [135]

R= H, Ph, 3,5- *tBu₂C₆H₃, 3,5 -(CF₃)₂Ph*
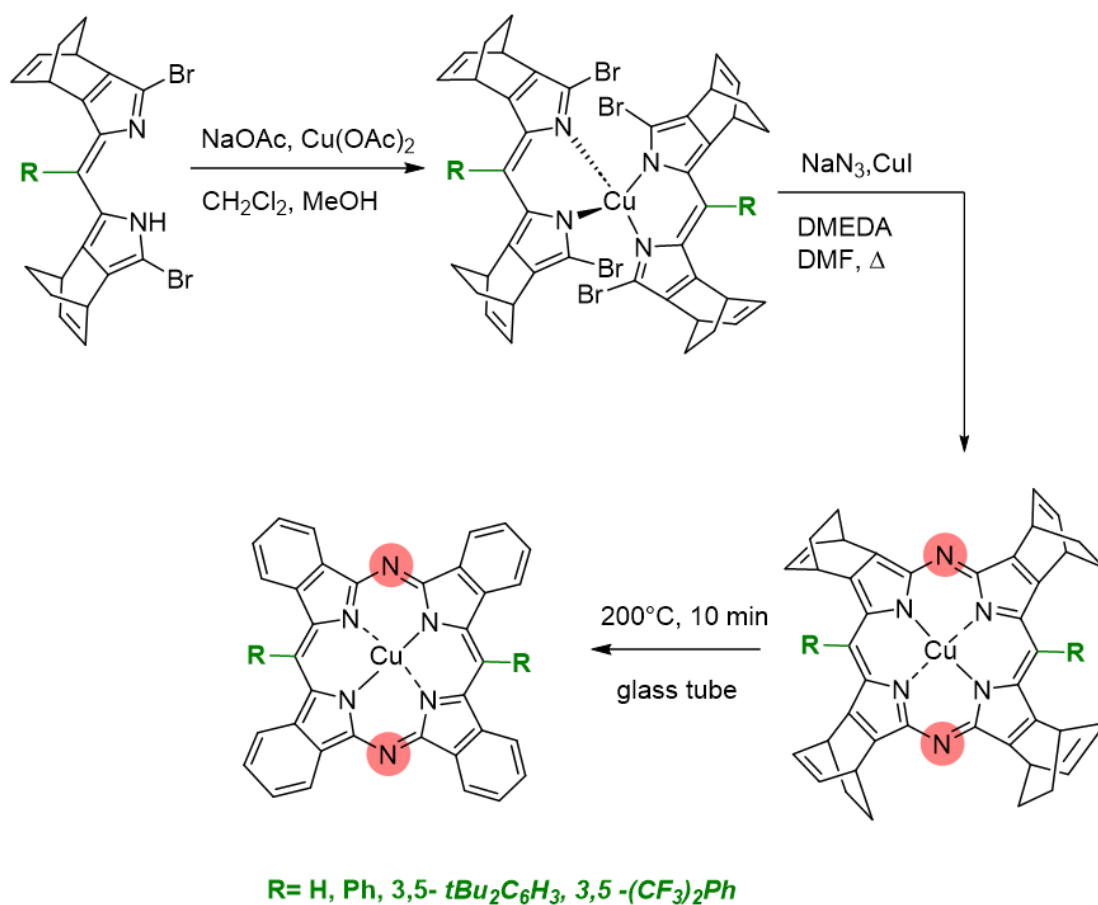
Scheme 1.38: Synthesis of CuTBDAP via bis (dibromo dipyrromethene) copper complexes.

More recently, in 2023, Yamada et al reported a 14% yield of 10,20 bis (triisopropylsilylethynyl) TBDAP using a combined method of lead-templated aza-annulation method and retro-Diels- Alder reaction as depicted in scheme 1.39. [136]
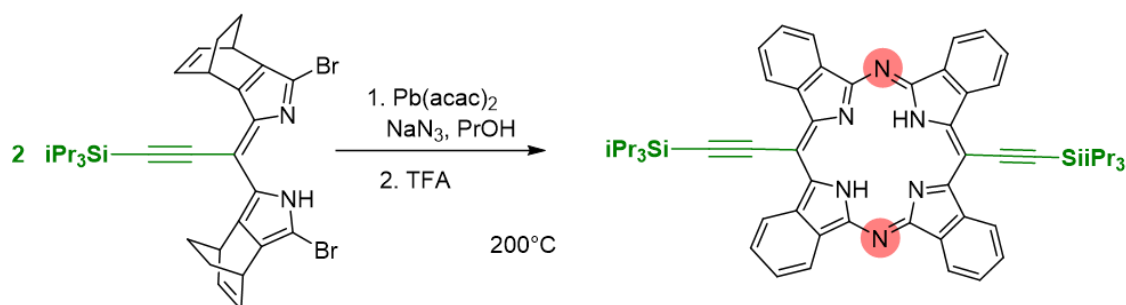
Scheme 1.39: Synthesis of 10,20-dialkynyl-TBDAP.

1.11 Properties and applications of Tetrabenzo(*aza*)porphyrins

The tetrabenzo(*aza*)porphyrin derivatives exhibit optical, electronic and chemical properties that are comparable to those of their parent phthalocyanines due to their structural similarities. However, the presence of methine bridges in place of the nitrogen atoms in Pc structure lowers the symmetry of structure from D_{4h} square planar symmetry of Pc to C_{2v} symmetry for TBTAP and the symmetry is reduced until it is restored back to D_{4h} when all nitrogen atoms are replaced by carbon atoms to give TBP. This modification causes alternation in the UV-visible absorptions for each hybrid. The replacement of nitrogen bridge by a carbon atom causes a hypsochromic shift toward shorter wavelength and lowers the intensity of Q-band, whereas the intensity of B-band is increased as depicted in figure 1.15. Furthermore, apart from TBDAP isomers, a split of Q-band can be observed in low-symmetry hybrids and a sharp single Q-band for high-symmetry Pc and TBP hybrids. The assignment of Q- and B- bands can be understood by Gouterman's four orbital model which is beyond the scope of this thesis. As discussed earlier in Pc's section, when different metals or different substituents are incorporated, the Q-band can undergo a red or blue shift. A wide range of UV-vis spectroscopy data of metalated and metal-free substituted and unsubstituted hybrids have been reported so far. [4,95,117]
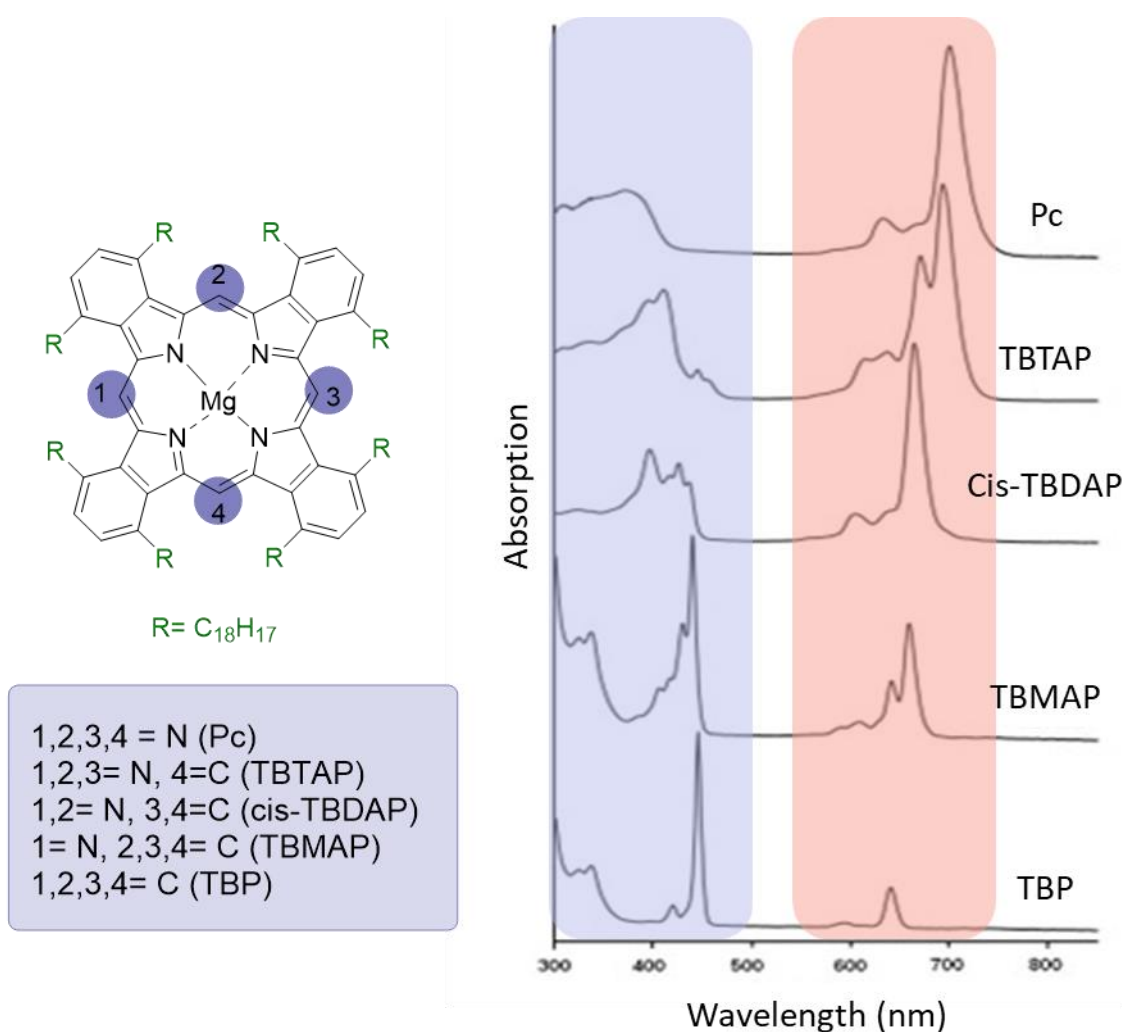
Figure 1.15: Non-peripherally substituted magnesium tetrabenzo(aza) porphyrin derivatives and their UV-visible spectra in THF as reported by Cammidge-Cook research group (reproduced with permission from ref 117).

1.11.1 Mesophase behaviour

It was anticipated that some tetrabenzo(aza) porphyrin derivatives would exhibit liquid crystalline properties due to their structural similarities with the parent phthalocyanine molecules. The latter ones are classified as thermotropic, discotic liquid crystals that have the tendency to form mesophases where the molecules are stacked in columns in a co-facial manner. These columns are often arranged in a two-dimensional lattice with either hexagonal (Col$_h$) or rectangular (Col$_r$) symmetry as illustrated in figure 1.16.[137] In 1997, polarising optical microscopy, differential scanning calorimetry (DSC) and x-ray diffraction were used to investigate the thermotropic mesophase behaviour of unsymmetrical highly substituted tetrabenzotriazaporphyrin (TBTAP) derivatives. It indicated the observation of a

weak pseudo-centred rectangular packing of these derivatives which results from their disordered hexagonal columnar mesophase packing that weakly tends to anti-parallel orientation toward neighbouring molecules. This observation contrasts with their earlier study of this system, which described the structure of the mesophase as discotic lamellar.[137–139]
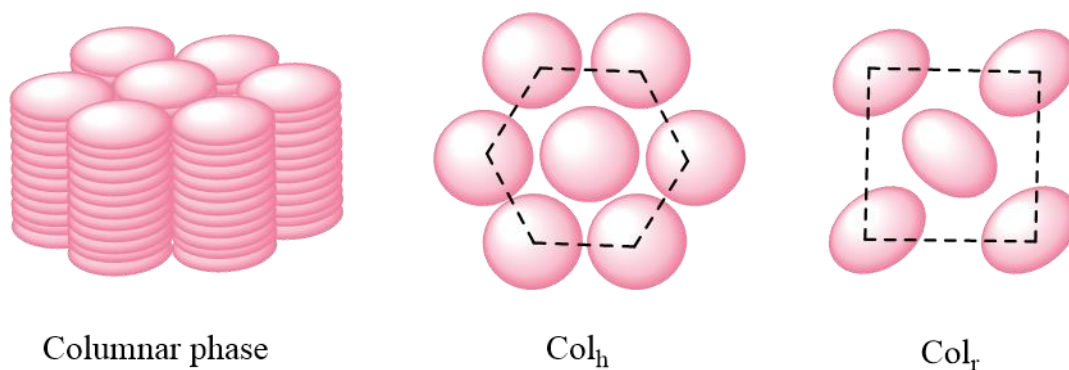
Figure 1.16: Molecular arrangement observed in columnar mesophase, columnar hexagonal in the middle and columnar rectangular in the right.

Furthermore, in 2011, Cammidge and Cook group reported mesophase data of copper, magnesium, and metal-free np-octahexyl TBTAP, TBDAP, TBMAP and TBP hybrids utilising a combination of DSC and POM techniques. A hexagonal columnar phase was observed in all hybrids. However, the interpretation of magnesium derivatives' behaviour was complicated compared to their other analogous due to the presence of solvent molecules that are bound to the crystalline structure as indicated by x-ray data. A similar trend of clearing temperature (mesophase- isotropic liquid) was observed for metal-free hybrids and the parent Pc analogous, while a low clearing temperature was observed across Cu-metalated series. [117]

As these hybrids exhibit a tendency to self-organisation in a highly-ordered columnar mesophase. This arrangement facilities effective transportation of charge carriers due to the overlap of their π- orbitals along the axis of their molecule stacking. This property together with their other appealing features such as their high solubility in most common organic solvents and their strong absorption peaks in the visible and near-infrared regions are significant for many applications. In recent years, solution processing phthalocyanine-tetrabenzoazaporphyrin hybrids have been reported as a novel type of small molecule (SM)

organic semi-conductors in electron and opto-electronic devices such as field effect transistors, sensors, organic light-emitting diodes and photovoltaic PV cells. Also, as SM donors for bulk heterojunction organic solar cells (BHJ OSCs), hole transport material in perovskite solar cells, and an ideal photo-active materials.[140–145]

Using a combination of various phthalocyanine-tetrabenzoazaporphyrin in 1-(3-methoxycarbonyl) propyl-1-phenyl-(6,6) C_{71} PCBM was reported to enhance the optical and electronic properties and photovoltaic performance of BHJ OSCs. The best power conversion efficiency PCE of 5.3% was achieved for the devices prepared from $C_6TBTAPH_2$ mixed with $PC_{70}BM$. In a different study, a high PCE exceeding 4.7% has been demonstrated in BHJ OSCs utilising miscible binary donor materials of C_6PcH_2 and $C_6TBTAPH_2$ with $PC_{70}BM$ as an acceptor at 25 mol % of C_6PcH_2 blend ratio. More recently, short alkyl substituted $np$$C_5TBTAPH_2$ and $np$$C_6TBTAPH_2$ devices were reported to exhibit a high PCE of around 4.7% whereas the longer alkyl substituted analogues C_7 and C_8 had around 2.8%. Also, the intermolecular packing apparently altered from pseudo-hexagonal 2D rectangular lattice as the pentyl to octyl substituents were extended.[146–148]

 Moreover, tetrabenzo(aza)porphyrin derivatives have been effectively utilised as a photosensitiser in DSSCs, like Pc derivatives, as discussed earlier in Pc section. In 2020, Unsymmetrical A_3B ZnTBTAP with peripherally bulky tert-butyl groups and anchoring carboxy group at its meso-phenyl was the first TBTAP macrocycle tested as photosensitiser in DSSCs with a modest PCE of around 2.4% under one-sun condition (figure 1.17). [149]

ZnTBTAP
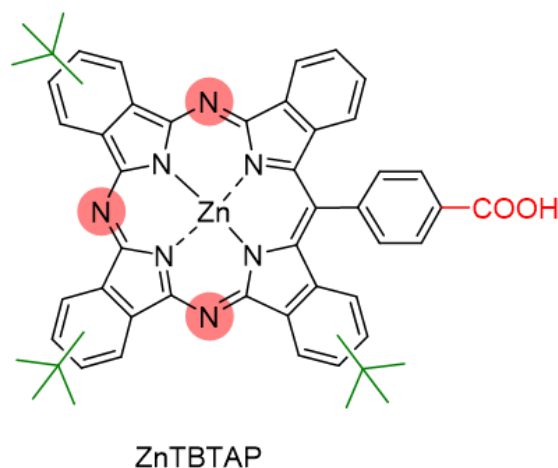
Figure 1.17: Structure of the first reported ZnTBTAP as photosensitiser in DSSCs.

Andrianov et al demonstrated the effectiveness of trans ZnTBDAP as a sensitiser for solar cells, compared to similarly substituted porphyrin and phthalocyanine. This hybrid dye possesses two noteworthy characteristics: an intense and long wavelength band in the visible region and the possibility of preparing push-pull or dipolar systems by functionalising the two meso-carbons. The CROSSDAP hybrid (its structure in figure 1.18) was employed as a sensitiser along with nanocrystalline TiO_2 based DSSCs with iodide/triiodide electrolyte. The solar cell displays a PCE of 3.37% under simulated solar spectrum AM 1.5 at 680 nm. Moreover, the light harvesting efficiency of CROSSDAP within 450-550 nm range was enhanced and a PCE of 3.82% was obtained when an imidazole ligand with a BODIPY dye was used as an additive in the electrolyte. The imidazole ligand was axially bound to the hybrid and harvests low energy photons of the visible region as depicted in figure 1.18.[150]
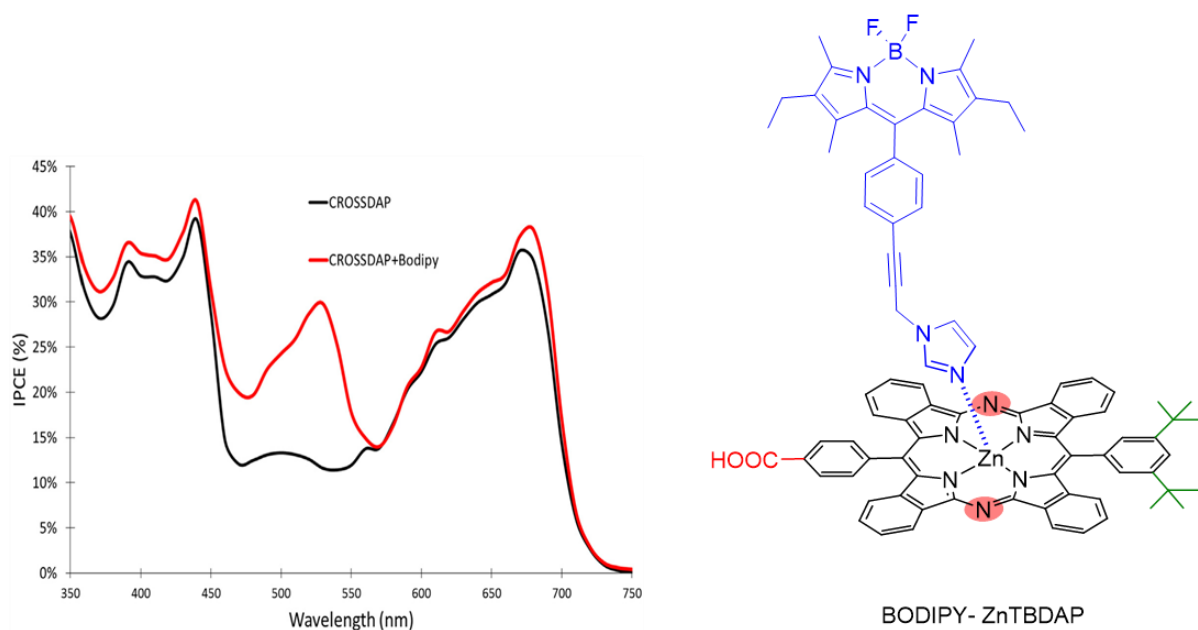
Figure 1.18: Structure of photosensitiser CROSSDAP+BODIPY right, and photaction spectra of CROSSDAP (black) and CRSOSSDAP+ BODIPY (red) (reproduced with permission from ref 150).

1.12 References

(1)   Byrne, G. T.; Linstead, R. P.; Lowe, A. R. Phthalocyanines. Part II. The Preparation of Phthalocyanine and Some Metallic Derivatives from *o*-Cyanobenzamide and Phthalimide. *J. Chem. Soc.,* **1934**, 1017–1022.

(2)   Linstead, R. P. Phthalocyanines. Part I. A New Type of Synthetic Colouring Matters. *J. Chem. Soc.,* **1934**, 1016–1017.

(3)   Dent, C. E.; Linstead, R. P.; Lowe, A. R. Phthalocyanines. Part VI. The Structure of the Phthalocyanines. *J. Chem. Soc.,* **1934**, 1033–1039.

(4)   McKeown, N. B. *Phthalocyanine Materials: Synthesis, Structure and Function*; Cambridge University Press, Cambridge, **1998**.

(5)   Braun, A.; Tcherniac, J. Über Die Produkte Der Einwirkung von Acetanhydrid Auf Phthalamid. *Ber. Dtsch. Chem. Ges.,* **1907**, *40* (2), 2709–2714.

(6)   de Diesbach, H.; von der Weid, E. Quelques Sels Complexes Des O-Dinitriles Avec Le Cuivre et La Pyridine. *Helv. Chim. Acta.,* **1927**, *10* (1), 886–888.

(7)   Robertson, J. M. An X-Ray Study of the Phthalocyanines. Part II. Quantitative Structure Determination of the Metal-Free Compound. *J. Chem. Soc (Resumed).,* **1936**, 1195–1209.

(8)   Robertson, J. M. An X-Ray Study of the Structure of the Phthalocyanines. Part I. The Metal-Free, Nickel, Copper, and Platinum Compounds. *J. Chem. Soc (Resumed).,* **1935**, 615–621.

(9)   Robertson, J. M.; Woodward, I. D. A. An X-Ray Study of the Phthalocyanines. Part III. Quantitative Structure Determination of Nickel Phthalocyanine. *J. Chem. Soc (Resumed).,* **1937**, 219–230.

(10)   Dandridge, A. G.; Drescher, H. A. E.; Thomas, J. Dye British Patent, 322, 1929.

(11)   Moser, F. H.; Thomas, A. L. Phthalocyanine Compounds. *J. Chem. Edu.,* **1964**, *41* (5), 245-249–249.

(12)   Cook, M. J. Thin Film Formulations of Substituted Phthalocyanines. *J. Mater. Chem.,* **1996**, *6* (5), 677–689.

(13)   Beltran, H. I.; Esquivel, R.; Sosa-Sanchez, A.; Sosa-Sanchez, J. L.; Hopfl, H.; Barba, V.; Farfan, N.; Galicia García, M.; Olivares-Xometl, O.; Zamudio-Rivera, L. S. Microwave Assisted Stereoselective Synthesis of Cis-Substituted Tin Phthalocyanine Dicarboxylates. Application as Corrosion Inhibitors. *Inorg. Chem.,* **2004**, *43* (12), 3555–3557.

(14)   Zvyagina, A. I. Controlled Self-Assembly of Low-Dimensional Supramolecular Systems Based on Double-Decker Lanthanide Phthalocyaninates. *Colloid J.,* **2022**, *84* (5), 633–641.

(15)   Tomilova, L. G.; Dyumaev, K. M. The First Synthesis of Sandwich-Type Titanium Bisphthalocyanines. *Mendeleev Commun.,* **1995**, *5* (3), 109–110.

(16)   Kuprikova, N. M.; Klyamer, D. D.; Sukhikh, A. S.; Krasnov, P. O.; Mrsic, I.;
        Basova, T. V. Fluorosubstituted Lead Phthalocyanines: Crystal Structure, Spectral
        and Sensing Properties. *Dyes Pigm.,* **2020**, *173*, 107939.

(17)   Engel, M. K. Single Crystal and Solid State Molecular Structures of Phthalocyanine
        Complexes. *Kawamura Rikagaku Kenkyusho Hokoku.,* **1997**, *8* (11).

(18)   Moser, F. H.; Thomas, A. L. The Phthalocyanines Properties. Vol. I. Boca Raton,
        CRC Press; Florida, 1983.

(19)   Tome, A. C.; Neves, M. G. P. M. S.; Cavaleiro, J. A. S. Porphyrins and Other
        Pyrrolic Macrocycles in Cycloaddition Reactions. *J. Porphyr Phthalocyanines*,
        2009, *13*, 408–414.

(20)   Ogunsipe, A. Metallophthalocyanines: Synthesis, Properties and Applications–a
        Review. *FUW Trends in Sci Tech. J.,* **2018**, *3* (2B), 669–681.

(21)   Ambroz, M.; Beeby, A.; MacRobert, A. J.; Simpson, M. S. C.; Svensen, R. K.;
        Phillips, D. Preparative, Analytical and Fluorescence Spectroscopic Studies of
        Sulphonated Aluminium Phthalocyanine Photosensitizers. *J. Photochem. Photobiol.
        B.,* **1991**, *9* (1), 87–95.

(22)   Nemykin, V. N.; Lukyanets, E. A. Synthesis of Substituted Phthalocyanines.
        Arkivoc., **2010**, 136–208.

(23)   Barrett, P. A.; Linstead, R. P.; Tuey, G. A. P.; Robertson, J. M. Phthalocyanines and
        Related Compounds. Part XV. Tetrabenztriazaporphin: Its Preparation from
        Phthalonitrile and a Proof of Its Structure. With a Note on a Preliminary X-Ray
        Investigation. *J. Chem. Soc. (Resumed),* **1939**, 1809–1820.

(24)   Botnar, A. A.; Domareva, N. P.; Kazaryan, K. Y.; Tikhomirova, T. V; Abramova,
        M. B.; Vashurin, A. S. Synthesis and Spectral Properties of Tetraphenoxysubstituted
        Erbium Phthalocyanines Containing Peripheral Phenyl and Cyclohexyl Fragments.
        Russ. Chem. Bull., **2022**, *71* (5), 953–961.

(25)   Bottari, G.; de la Torre, G.; Guldi, D. M.; Torres, T. Covalent and Noncovalent
        Phthalocyanine−Carbon Nanostructure Systems: Synthesis, Photoinduced Electron
        Transfer, and Application to Molecular Photovoltaics. *Chem. Rev.,* **2010**, *110* (11),
        6768–6816.

(26)   Fasiulla; Moinuddin Khan, M. H.; Harish, M. N. K.; Keshavayya, J.; Venugopala
        Reddy, K. R. Synthesis, Spectral, Magnetic and Antifungal Studies on
        Symmetrically Substituted Metal (II)Octaiminophthalocyanine Pigments. *Dyes
        Pigm.,* **2008**, *76* (2), 557–563.

(27)   McKeown, N. B. The Synthesis of Symmetrical Phthalocyanines. In *The Porphyrin
        Handbook: Vol 15 Phthalocyanines: Synthesis*, Academic Press, San Diago, 2000.

(28)   Ranta, J.; Kumpulainen, T.; Lemmetyinen, H.; Efimov, A. Synthesis and
        Characterization of Monoisomeric 1, 8, 15, 22-Substituted (A_3B and A_2B_2)
        Phthalocyanines and Phthalocyanine− Fullerene Dyads. *J. Org. Chem.,* **2010**, *75*
        (15), 5178–5194.

(29)   Brothers, P. J.; Senge, M. O. Phthalocyanines and Porphyrazines. In *Fundamentals of Porphyrin Chemistry*; John Wiley & Sons Ltd, New Jersey, 2022, pp 241–301.

(30)   Durmus, M.; Yesilot, S.; Ahsen, V. Separation and Mesogenic Properties of Tetraalkoxy-Substituted Phthalocyanine Isomers. *New. J. Chem.,* **2006**, *30* (5), 675–678.

(31)   Brewis, M.; Clarkson, G. J.; Humberstone, P.; Makhseed, S.; McKeown, N. B. The Synthesis of Some Phthalocyanines and Naphthalocyanines Derived from Sterically Hindered Phenols. *Chem. Eur. J.,* **1998**, *4* (9), 1633–1640.

(32)   Cidlina, A.; Pausimova, Z.; Miletin, M.; Zimcik, P.; Novakova, V. The Effect of Substitutents at Alkylsulfanyl/ Arylsulfanyl Non-Peripherally Substituted Phthalocyanines: Spectral and Photophysical Properties, Basicity and Photostability. *J. Porphyr Phthalocyanines.,* **2015**, *19* (10), 1095–1106.

(33)   Tillo, A.; Stolarska, M.; Kryjewski, M.; Popenda, L.; Sobotta, L.; Jurga, S.; Mielcarek, J.; Goslinski, T. Phthalocyanines with Bulky Substituents at Non-Peripheral Positions–Synthesis and Physico-Chemical Properties. *Dyes Pigm.,* **2016**, *127*, 110–115.

(34)   de Souza, T. F. M.; Torres Antonio, F. C.; Homem-de-Mello, P.; Ribeiro, A. O. Unsymmetrical Zinc (II) Phthalocyanine and Zinc (II) Naphthalocyanine with 2,3-Dicyano-1,4-Diphenylnaphthalene Precursor. *Dyes Pigm.,* **2020**, *172*, 107824.

(35)   LinBen, T. G.; Hanack, M. Synthesis, Separation and Characterization of Unsymmetrically Substituted Phthalocyanines. *Chem. Ber.*, **1994**, *127* (10), 2051–2057.

(36)   Leznoff, C. C.; Hall, T. W. The Synthesis of a Soluble, Unsymmetrical Phthalocyanine on a Polymer Support. *Tetrahedron Lett.*, **1982**, *23* (30), 3023–3026.

(37)   Kobayashi, N.; Kondo, R.; Nakajima, S.; Osa, T. New Route to Unsymmetrical Phthalocyanine Analogs by the Use of Structurally Distorted Subphthalocyanines. *J. Am. Chem. Soc.,* **1990**, *112* (26), 9640–9641.

(38)   Musluoglu, E.; Gurek, A.; Ahsen, V.; Gul, A.; Bekaroglu, O. Unsymmetrical Phthalocyanines with a Single Macrocyclic Substituent. *Chem. Ber.,* **1992**, *125* (10), 2337–2339.

(39)   Claessens, C. G.; Hahn, U.; Torres, T. Phthalocyanines: From Outstanding Electronic Properties to Emerging Applications. *Chem. Rec.,* **2008**, *8* (2), 75–97.

(40)   Durmus, M.; Nyokong, T. Synthesis and Solvent Effects on the Electronic Absorption and Fluorescence Spectral Properties of Substituted Zinc Phthalocyanines. *Polyhedron.,* **2007**, *26* (12), 2767–2776.

(41)   Artuç, G. Ö.; Altındal, A.; Eran, B. B.; Bulut, M. Synthesis, Characterization and Ethanol Sensing Properties of Peripheral and Non-Peripheral Tetrakis-(3,6-Dihexyl-7-Oxy-4-Methylcoumarin)Substituted Zinc(II), Cobalt(II), and Copper(II) Phthalocyanines. *Dyes Pigm.,* **2019**, *171*, 107741.

(42) Bottari, G.; de la Torre, G.; Guldi, D. M.; Torres, T. Covalent and Noncovalent Phthalocyanine−Carbon Nanostructure Systems: Synthesis, Photoinduced Electron Transfer, and Application to Molecular Photovoltaics. *Chem Rev.,* **2010**, *110* (11), 6768–6816.

(43) Samsunlu, T.; Akkoç, B.; Özçeşmeci, M.; Akın, M.; Şaki, N.; Hamuryudan, E. Investigation of Biological Activities of Tetra-Substituted Phthalocyanines Bearing Tetraethyleneglycol Monomethyl Ether Chains at Peripheral and Non-Peripheral Positions. *Chem. Select.,* **2023**, *8* (18), e202205001.

(44) Kim, S. H.; Namgoong, J. W.; Yuk, S. B.; Kim, J. Y.; Lee, W.; Yoon, C.; Kim, J. P. Synthesis and Characteristics of Metal-Phthalocyanines Tetra-Substituted at Non-Peripheral (α) or Peripheral (β) Positions, and Their Applications in LCD Color Filters. *J. Incl. Phenom. Macrocycl. Chem.,* **2015**, *82*, 195–202.

(45) Ekineker, G.; Göksel, M. Synthesis of Both Peripheral and Non-Peripheral Substituted Metal-Free Phthalocyanines and Characterization. *Tetrahedron,* **2020**, *76* (5), 130878.

(46) Durmus, M.; Nyokong, T. The Synthesis, Fluorescence Behaviour and Singlet Oxygen Studies of New Water-Soluble Cationic Gallium (III) Phthalocyanines. *Inorg. Chem. Commun.,* **2007**, *10* (3), 332–338.

(47) Abdulcelil Yuzer, L.; Kubra Demircioglu, P.; Derya Yetkin, L.; Ince, M.; Ayaz, F. Beyond the Conventional Photodynamic Therapy by Water-Soluble Phthalocyanines. *Chem. Select.,* **2022**, *7* (36).

(48) Gouterman, M. *Optical Spectra and Electronic Structure of Porphyrins and Related Rings.* In *The Porphyrins*, Academic Press, Cambridge Massachusetts, 1978, pp1-165.

(49) Hollebone, B. R.; Stillman, M. J. Assignment of Absorption and Magnetic Circular Dichroism Spectra of Solid, α Phase Metallophthalocyanines. *J. Chem. Soc., Faraday Trans.* **1978**, *74*, 2107–2127.

(50) Leznoff, C. C.; Lever, A. B. P. Phthalocyanines Properties and Applications. *VCH,* New York, 1989, Vol. 4, pp 23–77.

(51) Kobayashi, N.; Ogata, H.; Nonaka, N.; Luk'yanets, E. A. Effect of Peripheral Substitution on the Electronic Absorption and Fluorescence Spectra of Metal-free and Zinc Phthalocyanines. *Chem. Eur. J*., **2003**, *9* (20), 5123–5134.

(52) Cook, M. J.; Dunn, A. J.; Howe, S. D.; Thomson, A. J.; Harrison, K. J. Octa-Alkoxy Phthalocyanine and Naphthalocyanine Derivatives: Dyes with Q-Band Absorption in the Far Red or near Infrared. *J. Chem. Soc. Perkin.,* **1988**, No. 8, 2453–2458.

(53) Jiang, J. *Functional Phthalocyanine Molecular Materials.* In *Structure and Bonding*; Springer, Heidelberg, 2010.

(54) Claessens, C. G.; Blau, W. J.; Cook, M.; Hanack, M.; Nolte, R. J. M.; Torres, T.; WoEhrle, D. Phthalocyanines and Phthalocyanine Analogues: The Quest for Applicable Optical Properties. *Monatshefte fuer Chem.*, **2001**, 3–11.

(55)   Cammidge, A. N.; Gopee, H. Macrodiscotic Triphenylenophthalocyanines. *Chem. Commun.,* **2002**, *2* (9), 966–967.

(56)   Kobayashi, N.; Nakajima, S.; Ogata, H.; Fukuda, T. Synthesis, Spectroscopy, and Electrochemistry of Tetra-Tert-Butylated Tetraazaporphyrins, Phthalocyanines, Naphthalocyanines, and Anthracocyanines, Together with Molecular Orbital Calculations. *Chem. Eur. J.,* **2004**, *10* (24), 6294–6312.

(57)   Isago, H. Optical Spectra of Phthalocyanines and Related Compounds, *NIMS monographs*, *Springer*, Tokyo, 2015.

(58)   Parra, V.; Bouvet, M.; Brunet, J.; Rodriguez-Mendez, M. L.; de Saja, J. A. On the Effect of Ammonia and Wet Atmospheres on the Conducting Properties of Different Lutetium Bisphthalocyanine Thin Films. *Thin Solid Films.,* **2008**, *516* (24), 9012–9019.

(59)   Demir, E.; Silah, H.; Uslu, B. Phthalocyanine Modified Electrodes in Electrochemical Analysis. *Crit. Rev. Anal. Chem.,* **2020**, *52* (2), 425–461.

(60)   de la Torre, G.; Vazquez, P.; Agullo-Lopez, F.; Torres, T. Phthalocyanines and Related Compounds:Organic Targets for Nonlinear Optical Applications. *J. Mater. Chem.,* **1998**, *8* (8), 1671–1683.

(61)   Duro, J. A.; de la Torre, G.; Barbera, J.; Serrano, J. L.; Torres, T. Synthesis and Liquid-Crystal Behavior of Metal-Free and Metal-Containing Phthalocyanines Substituted with Long-Chain Amide Groups. *Chem. Mater.,* **1996**, *8* (5), 1061–1066.

(62)   Emmelius, M.; Pawlowski, G.; Vollmann, H. W. Materials for Optical Data Storage. *Angew. Chem. Int. Ed. Engl.,* **1989**, *28* (11), 1445–1471.

(63)   Sorokin, A. B. Phthalocyanine Metal Complexes in Catalysis. *Chem. Rev.,* **2013**, *113* (10), 8152–8191.

(64)   Wu, Y.; Liang, Y.; Wang, H. Heterogeneous Molecular Catalysts of Metal Phthalocyanines for Electrochemical CO2Reduction Reactions. *Acc. Chem. Res.,* **2021**, *54* (16), 3149–3159.

(65)   Sen, A.; Putra, M. H.; Biswas, A. K.; Behera, A. K.; Groβ, A. Insight on the Choice of Sensitizers/Dyes for Dye Sensitized Solar Cells: A Review. *Dyes Pigm.*, **2023**, 213, 111087.

(66)   Van Lier, J. E.; Brasseur, N.; Paquette, B.; Wagner, J. R.; Ali, H.; Langlois, R.; Rousseau, J. Phthalocyanines as Sensitizers for Photodynamic Therapy of Cancer. In *Photosensitisation*; Moreno, G., Pottier, R. H., Truscott, T. G., Eds.; Springer Berlin, Heidelberg, 1988, Vol. 15, pp435–444.

(67)   Sharma, K.; Sharma, V.; Sharma, S. S. Dye-Sensitized Solar Cells: Fundamentals and Current Status. *Nanoscale. Res. Lett.,* **2018**, *13* (381).

(68)   Ikeuchi, T.; Nomoto, H.; Masaki, N.; Griffith, M. J.; Mori, S.; Kimura, M. Molecular Engineering of Zinc Phthalocyanine Sensitizers for Efficient Dye-Sensitized Solar Cells. *Chem. Commun.,* **2014**, *50* (16), 1941–1943.

(69)   Yella, A.; Lee, H.-W.; Nok Tsao, H.; Yi, C.; Kumar Chandiran, A.; Nazeeruddin, M.; Wei-Guang Diau, E.; Yeh, C.-Y.; Zakeeruddin, S. M.; Gratzel, M. Porphyrin-Sensitized Solar Cells with Cobalt (II/III)-Based Redox Electrolyte Exceed 12 Percent Efficiency. *Am. Assoc. Adva. Sci.,* **2011**, *334* (6056), 629–634.

(70)   Urbani, M.; Ragoussi, M. E.; Nazeeruddin, M. K.; Torres, T. Phthalocyanines for Dye-Sensitized Solar Cells. *Coord. Chem. Rev.,* **2019**, *381*, 1–64.

(71)   Isago, H. *Optical Spectra of Phthalocyanines and Related Compounds*; Springer: Japan, 2015.

(72)   Brogdon, P.; Cheema, H.; Delcamp, J. H. Near-Infrared-Absorbing Metal-Free Organic, Porphyrin, and Phthalocyanine Sensitizers for Panchromatic Dye-Sensitized Solar Cells. *Chem. Sus. Chem.,* **2017**, *10* (1), 1–19.

(73)   Milan, R.; Selopal, G. S.; Cavazzini, M.; Orlandi, S.; Boaretto, R.; Caramori, S.; Concina, I.; Pozzi, G. Dye-Sensitized Solar Cells Based on a Push-Pull Zinc Phthalocyanine Bearing Diphenylamine Donor Groups: Computational Predictions Face Experimental Reality. *Sci. Rep.,* **2017**, *7* (15675), 1–10.

(74)   Ashokkumar, R.; Kathiravan, A.; Ramamurthy, P. Aggregation Behaviour and Electron Injection/Recombination Dynamics of Symmetrical and Unsymmetrical Zn-Phthalocyanines on TiO2 Film. *Phys. Chem.,* **2014**, *16* (3), 1015–1021.

(75)   Demirci, Y. C.; Çakar, S.; Sevim, A. M.; Gül, A.; Özacar, M. DSSCs Based on Unsymmetrical A3B Type Zn(II) and TiO(IV) Naphthalenephthalocyanine /Porphyrin Cocktail Dyes: A Potential Alternative for Ruthenium Based Sensitizers. *J. Photochem. Photobiol. A Chem.,* **2023**, *440*, 114642.

(76)   Rak, J.; Kabesova, M.; Benes, J.; Pouckova, P.; Vetvicka, D. Advances in Liposome-Encapsulated Phthalocyanines for Photodynamic Therapy. *Life.,* **2023**, *13* (2), 305.

(77)   Kwiatkowski, S.; Knap, B.; Przystupski, D.; Saczko, J.; Kędzierska, E.; Knap-Czop, K.; Kotlińska, J.; Michel, O.; Kotowski, K.; Kulbacka, J. Photodynamic Therapy – Mechanisms, Photosensitizers and Combinations. *Biomedicine Pharmacotherapy.,* **2018**, *106*, 1098–1107.

(78)   Escudero, A.; Carrillo-Carrión, C.; Castillejos, M. C.; Romero-Ben, E.; Rosales-Barrios, C.; Khiar, N. Photodynamic Therapy: Photosensitizers and Nanostructures. *Mater. Chem. Front.,* **2021**, *5* (10), 3788–3812.

(79)   Dąbrowski, J. M. Reactive Oxygen Species in Photodynamic Therapy: Mechanisms of Their Generation and Potentiation. In *Advances in Inorganic Chemistry*; van Eldik, R., Hubbard, C. D., Eds.; Elsevier, Cambridge MA, 2017; Vol. 70, pp 343–394.

(80)   Mantareva, V.; Kussovski, V.; Angelov, I.; Borisova, E.; Avramov, L.; Schnurpfeil, G.; Wöhrle, D. Photodynamic Activity of Water-Soluble Phthalocyanine Zinc(II) Complexes against Pathogenic Microorganisms. *Bioorg. Med. Chem.,* **2007**, *15* (14), 4829–4835.

(81) Nyman, E. S.; Hynninen, P. H. Research Advances in the Use of Tetrapyrrolic Photosensitizers for Photodynamic Therapy. *J. Photochem. Photobiol. B.,* **2004**, *73* (1), 1–28.

(82) Ball, D. J.; Wood, S. R.; Vernon, D. I.; Griffiths, J.; Dubbelman, T. M. A. R.; Brown, S. B. The Characterisation of Three Substituted Zinc Phthalocyanines of Differing Charge for Use in Photodynamic Therapy. A Comparative Study of Their Aggregation and Photosensitising Ability in Relation to MTHPC and Polyhaematoporphyrin. *J. Photochem. Photobiol. B.,* **1998**, *45* (1), 28–35.

(83) Durmuş, M.; Nyokong, T. The Synthesis, Fluorescence Behaviour and Singlet Oxygen Studies of New Water-Soluble Cationic Gallium (III) Phthalocyanines. *Inorg. Chem. Commun.,* **2007**, *10* (3), 332–338.

(84) Camerin, M.; Magaraggia, M.; Soncin, M.; Jori, G.; Moreno, M.; Chambrier, I.; Cook, M. J.; Russell, D. A. The in Vivo Efficacy of Phthalocyanine-Nanoparticle Conjugates for the Photodynamic Therapy of Amelanotic Melanoma. *Eur. J. Cancer.,* **2010**, *46* (10), 1910–1918.

(85) Camerin, M.; Moreno, M.; Marín, M. J.; Schofield, C. L.; Chambrier, I.; Cook, M. J.; Coppellotti, O.; Jori, G.; Russell, D. A. Delivery of a Hydrophobic Phthalocyanine Photosensitizer Using PEGylated Gold Nanoparticle Conjugates for the: In Vivo Photodynamic Therapy of Amelanotic Melanoma. *Photochem. Photobio. Sci.,* **2016**, *15* (5), 618–625.

(86) Avci, P.; Sibel Erdem, S.; Hamblin, M. R. Photodynamic Therapy: One Step Ahead with Self-Assembled Nanoparticles. *J. Biomedical Nanotechnology*, **2014**, *10*, 1937–1952.

(87) Adnane, F.; El-Zayat, E.; Fahmy, H. M. The Combinational Application of Photodynamic Therapy and Nanotechnology in Skin Cancer Treatment: A Review. *Tissue Cell.,* **2022**, *77*, 101856.

(88) EbruYabaş, F. Water-Soluble Quaternized Serotonin Substituted Zinc-Phthalocyanine for Photodynamic Therapy Applications. *Cumhuriyet. Sci. J.,* **2023**, *44* (1), 99–105.

(89) Ball, D. J.; Wood, S. R.; Vernon, D. I.; Griffiths, J.; Dubbelman, T. M. A. R.; Brown, S. B. The Characterisation of Three Substituted Zinc Phthalocyanines of Differing Charge for Use in Photodynamic Therapy. A Comparative Study of Their Aggregation and Photosensitising Ability in Relation to MTHPC and Polyhaematoporphyrin. *J. Photochem. Photobio.,* **1998**, *45*, 28–35.

(90) Mantareva, V.; Kussovski, V.; Angelov, I.; Borisova, E.; Avramov, L.; Schnurpfeil, G.; Wöhrle, D. Photodynamic Activity of Water-Soluble Phthalocyanine Zinc(II) Complexes against Pathogenic Microorganisms. *Bioorg. Med. Chem.,* **2007**, *15* (14), 4829–4835.

(91) Zhang, J.; Jiang, C.; Figueiró Longo, J. P.; Azevedo, R. B.; Zhang, H.; Muehlmann, L. A. An Updated Overview on the Development of New Photosensitizers for Anticancer Photodynamic Therapy. *Acta. Pharm. Sin. B.,* **2018**, *8* (2), 137–146.

(92)   Jiang, Z.; Shao, J.; Yang, T.; Wang, J.; Jia, L. Pharmaceutical Development, Composition and Quantitative Analysis of Phthalocyanine as the Photosensitizer for Cancer Photodynamic Therapy. *J. Pharm. Biomed. Anal.,* **2014**, *87*, 98–104.

(93)   Mack, J.; Kobayashi, N. Low Symmetry Phthalocyanines and Their Analogues. *Chem. Rev.,* **2011**, *111* (2), 281–321.

(94)   Mack, J.; Sosa-Vargas, L.; Coles, S. J.; Tizzard, G. J.; Chambrier, I.; Cammidge, A. N.; Cook, M. J.; Kobayashi, N. Synthesis, Characterization, MCD Spectroscopy, and TD-DFT Calculations of Copper-Metalated Nonperipherally Substituted Octaoctyl Derivatives of Tetrabenzotriazaporphyrin, Cis - And Trans - Tetrabenzodiazaporphyrin, Tetrabenzomonoazaporphyrin, and Tetrabenzoporphyrin. *Inorg. Chem.,* **2012**, *51*, 12820-12833.

(95)   Cammidge, A. N.; Chambrier, I.; Cook, M. J.; Sosa-Vargas, L. 75 Synthesis and Properties of the Hybrid Phthalocyanine-Tetrabenzoporphyrin Macrocycles. In *Handbook of Porphyrin Science*; World Scientific, Singapore, **2012**, Vol. 16, pp331–404.

(96)   Fischer, H.; Müller, K.; Leschhorn, O. Über Keto-phylloporphyrine Und Ihren Übergang in Desoxo-phyllerythrin-Derivate. *Justus. Liebigs. Ann. Chem.,* **1936**, *523* (1), 164–198.

(97)   Fischer, H.; Gleim, W. Synthese Des Porphins. *Justus. Liebigs. Ann. Chem.,* **1936**, *521* (1), 157–160.

(98)   Heinr. Helberger, J. Über Die Einwirkung von Kupfer-1-cyanid Auf O-Halogenacetophenone. *Justus. Liebigs. Ann. Chem.,* **1937**, *529* (1), 205–218.

(99)   Helberger, Joh. Heinr.; von Rebay, Adalb. Über Die Einwirkung von Kupfer-1-Cyanid Auf o-Halogenacetophenone. II. *Justus. Liebigs. Ann. Chem.,* **1937**, *531* (1), 279–287.

(100) Barrett, P. A.; Linstead, R. P.; Rundall, F. G.; Tuey, G. A. P. Phthalocyanines and Related Compounds. Part XIX. Tetrabenzporphin, Tetrabenzmonazaporphin and Their Metallic Derivatives. *J. Chem. Soc (Resumed).,* **1940**, 1079–1092.

(101) Dent, C. E. 1. Preparation of Phthalocyanine-like Pigments Related to the Porphyrins. *J. Chem. Soc (Resumed).,* **1938**, 1–6.

(102) Godfrey, M. R.; Newcomb, T. P.; Hoffman, B. M.; Ibers, J. A. Spin Pairing and Magnetic Coupling in Quasi One-Dimensional Semiconductors with a Trimeric Stacking Structure. *J. Am. Chem. Soc.,* **1990**, *112*, 7260–7269.

(103) DE3937716A1, 1991.

(104) EP0428214A1, 1990.

(105) Makarova, E. A.; Kopranenkov, V. N.; Shevtsov, V. K.; Luk'yanets, E. A. New Method for Synthesis of the Aza Analogs of Tetrabenzoporphin. *Chem. Heterocycl. Compd.,* **1989**, *25* (10), 1159–1164.

(106) Leznoff, C. C.; Mckeown, N. B. Preparation of Substituted Tetrabenzotriazaporphyrins and a Tetranaphthotriazaporphyrin: A Route to Mono-Meso-Substituted Phthalocyanine Analogues. *J. Org. Chem.,* **1990**, *55*, 2186–2190.

(107) Galanin, N. E.; Kudrik, E. V; Shaposhnikov, G. P. Synthesis and Properties of Meso-Phenyl-Substituted Tetrabenzoazaporphins Magnesium Complexes. *Russ. J. Org. Chem.,* **2002**, *38* (8), 1200–1203.

(108) Borisov, S. M.; Zenkl, G.; Klimant, I. Phosphorescent Platinum (II) and Palladium (II) Complexes with Azatetrabenzoporphyrinss New-Red Laser Diode-Compatible Indicators for Optical Oxygen Sensing. *ACS. Appl. Mater. Interfaces.,* **2010**, *2* (2), 366–374.

(109) Vladimir N. Bulavka. Microwave-Assisted Synthesis and Separation of Magnesium (Meso-Phenyl,Aza)Tetrabenzoporphines. In *7th International Electronic Conference on Synthetic Organic Chemistry;* **2003** E004.

(110) Galanin, N. E.; Yakubov, L. A.; Shaposhnikov, G. P. Meso-Trans-Diaryldihexadecyltetrabenzoporphyrins and Their Zinc Complexes: Synthesis and Spectra. *Russ. J. Gen. Chem.,* **2007**, *77* (8), 1448–1454.

(111) Yakubov, L. A.; Galanin, N. E.; Shaposhnikov, G. P. Synthesis and Properties of Zinc Complexes of Meso-Hexadecyloxy-Substituted Tetrabenzoporphyrin and Tetrabenzoazaporphyrins. *Russ. J. Org. Chem.,* **2008**, *44*, 755–760.

(112) Galanin, N. E.; Kudrik, E. V; Shaposhnikov, G. P. Stepwise Synthesis and Spectral Characteristics of Meso-Trans-Diphenyldi(1-Naphthyl)Tetrabenzoporphin and Its Zinc Complex. *Russ. J. Org. Chem.,* **2003**, *39* (8), 1183–1187.

(113) Bykova, V.; Usol'tseva, N.; Kudrik, E.; Galanin, N.; Shaposhnikov, G.; Yakubov, L. Synthesis and Induction of Mesomorphic Properties of Tetrabenzoporphine Derivatives. *Mol. Cryst. Liq. Cryst.,* **2008**, *494* (1), 38–47.

(114) Kalashnikov, V. V.; Pushkarev, V. E.; Tomilova, L. G. A Novel Synthetic Approach to 27-Aryltetrabenzo [5,10,15]Triazaporphyrins. *Mendeleev Commun.,* **2011**, *21* (2), 92–93.

(115) Kalashnikova, V. V; Tomilovab, L. G. New Synthetic Method for Zinc Complexes of 20-Aryltetrabenzo [5, 10, 15] Triazaporphyrin. *Macroheterocycles.,* **2011**, *4* (3), 209–210.

(116) Cammidge, A. N.; Cook, M. J.; Hughes, D. L.; Nekelson, F.; Rahman, M. A Remarkable Side-Product from the Synthesis of an Octaalkylphthalocyanine: Formation of a Tetrabenzotriazaporphyrin. *Chem. Commun.,* **2005**, 7, 930–932.

(117) Cammidge, A. N.; Chambrier, I.; Cook, M. J.; Hughes, D. L.; Rahman, M.; Sosa-Vargas, L. Phthalocyanine Analogues: Unexpectedly Facile Access to Non-Peripherally Substituted Octaalkyl Tetrabenzotriazaporphyrins, Tetrabenzodiazaporphyrins, Tetrabenzomonoazaporphyrins and Tetrabenzoporphyrins. *Chem. Eur. J.,* **2011**, *17* (11), 3136–3146.

(118) Galanin, N. E.; Kudrik, E. V; Shaposhnikov, G. P. Meso-Phenyltetrabenzoazaporphyrins and Their Zinc Complexes. Synthesis and Spectral Properties. *Russ. J. Gen. Chem.,* **2005**, *75* (4), 651–655.

(119) Fujii, A.; Itani, H.; Watanabe, K.; Dao, Q. D.; Sosa-Vargas, L.; Shimizu, Y.; Ozaki, M. Improved Synthesis of Non-Peripherally Alkyl-Substituted Tetrabenzotriazaporphyrins. *Mol. Cryst. Liq. Cryst.,* **2017**, *653* (1), 22–26.

(120) Díaz-Moscoso, A.; Tizzard, G. J.; Coles, S. J.; Cammidge, A. N. Synthesis of Meso-Substituted Tetrabenzotriazaporphyrins: Easy Access to Hybrid Macrocycles. *Angew. Chem. Int. Ed.,* **2013**, *52* (41), 10784–10787.

(121) Hellal, M.; Cuny, G. D. Microwave Assisted Copper-Free Sonogashira Coupling/5-Exo-Dig Cycloisomerization Domino Reaction: Access to 3-(Phenylmethylene) Isoindolin-1- Ones and Related Heterocycles. *Tetrahedron Lett*., **2011**, *52* (42), 5508–5511.

(122) Dalai, S.; Belov, V. N.; Nizamov, S.; Rauch, K.; Finsinger, D.; De Meijere, A. Access to Variously Substituted 5,6,7,8-Tetrahydro-3H-Quinazolin-4-Ones via Diels-Alder Adducts of Phenyl Vinyl Sulfone to Cyclobutene-Annelated Pyrimidinones. *Eur. J. Org. Chem.,* **2006**, 12, 2753–2765.

(123) Alharbi, N.; Díaz-Moscoso, A.; Tizzard, G. J.; Coles, S. J.; Cook, M. J.; Cammidge, A. N. Improved Syntheses of Meso-Aryl Tetrabenzotriazaporphyrins (TBTAPs). *Tetrahedron,* **2014**, *70* (40), 7370–7379.

(124) Alharbi, N.; Tizzard, G. J.; Coles, S. J.; Cook, M. J.; Cammidge, A. N. First Examples of Functionalisation of Meso-Aryl Tetrabenzotriazaporphyrins (TBTAPs) through Cross-Coupling Reactions. *Tetrahedron,* **2015**, *71* (39), 7227–7232.

(125) Alkorbi, F.; Díaz-Moscoso, A.; Gretton, J.; Chambrier, I.; Tizzard, G. J.; Coles, S. J.; Hughes, D. L.; Cammidge, A. N. Complementary Syntheses Giving Access to a Full Suite of Differentially Substituted Phthalocyanine-Porphyrin Hybrids. *Angew. Chem. Int. Ed.,* **2021**, *60* (14), 7632–7636.

(126) Pushkarev, V. E.; Kalashnikov, V. V.; Trashin, S. A.; Borisova, N. E.; Tomilova, L. G.; Zefirov, N. S. Bis (Tetrabenzotriazaporphyrinato) and (Tetrabenzotriazaporphyrinato) (Phthalocyaninato) Lutetium (Iii) Complexes-Novel Sandwich-Type Tetrapyrrolic Ligand Based NIR Absorbing Electrochromes. *Dalton Trans.,* **2013**, *42* (34), 12083–12086.

(127) Pushkarev, V. E.; Kalashnikov, V. V.; Tolbin, A. Y.; Trashin, S. A.; Borisova, N. E.; Simonov, S. V.; Rybakov, V. B.; Tomilova, L. G.; Zefirov, N. S. Meso-Phenyltetrabenzotriazaporphyrin Based Double-Decker Lanthanide (III) Complexes: Synthesis, Structure, Spectral Properties and Electrochemistry. *Dalton Trans.,* **2015**, *44* (37), 16553–16564.

(128) Pushkarev, V. E.; Breusova, M. O.; Shulishov, E. V; Tomilov, Y. V; Zelinsky, N. D. Selective Synthesis and Spectroscopic Properties of Alkyllsubstituted Lanthanide(III) Monoo, Dii, and Triphthalocyanines. *Russ. Chem. Bull. Int. Ed.,* **2005**, *54* (9), 2087–2093.

(129) DE 3902053A1, 1990.

(130) US5919922A. 1999.

(131) Matano, Y. Recent Advances in the Synthesis of Diazaporphyrins and Their Chalcogen Derivatives. *Org. Biomol. Chem.,* **2023**, *21*, 3034–3056.

(132) Okujima, T.; Jin, G.; Otsubo, S.; Aramaki, S.; Ono, N.; Yamada, H.; Uno, H. Tetrabenzodiazaporphyrin: The Semiconducting Hybrid of Phthalocyanine and Tetrabenzoporphyrin. *J. Porphyr Phthalocyanines.,* **2011**, *15*, 697–703.

(133) Andrianov, D. S.; Rybakov, V. B.; Cheprakov, A. V. Between Porphyrins and Phthalocyanines: 10,20-Diaryl-5,15-Tetrabenzodiazaporphyrins. *Chem. Commun.,* **2014**, *50* (59), 7953–7955.

(134) Andrianov, D. S.; Levitskiy, O. A.; Rybakov, V. B.; Magdesieva, T. V.; Cheprakov, A. V. Metal Complexes of Diaryltetrabenzodiazaporphyrins. *Chem. Select.,* **2016**, *1* (3), 360–374.

(135) Sugano, Y.; Matsuo, K.; Hayashi, H.; Aratani, N.; Yamada, H. Synthesis of 10,20-Substituted Tetrabenzo-5,15-Diazaporphyrin Copper Complexes from Soluble Precursors. *J. Porphyr Phthalocyanines.,* **2021**, *25* (10–12), 1186–1192.

(136) Sugano, Y.; Matsuo, K.; Hayashi, H.; Aratani, N.; Yamada, H. Synthesis and Properties of 10,20-Bis (Triisopropylsilylethynyl)-Tetrabenzo-5,15-Diazaporphine. *J. Porphyr Phthalocyanines.,* **2022**, *27* (01n04), 136–144.

(137) Cook, Michael J; Daniel; Mervyn F; Harrison; Kenneth J; McKeown; Neil B; Thomson; Andrew J. 1, 4, 8, 11, 15, 18, 22, 25-Octa-Alkyl Phthalocyanines: New Discotic Liquid Crystal Materials. *J. Chem. Soc., Chem. Commun.,* **1987**, No. 14, 1086-1088.

(138) McKeown, N. B.; Leznoff, C. C.; Richardson, R. M.; Cherodian, A. S. A Highly Asymmetric Disc-like Mesogen Based on the Tetrabenzotriazaporphyrin Macrocyclic Ring System. *Mol. Cryst. Liq. Cryst.,* **1992**, *213* (1), 91–98.

(139) Corsellis, E. A.; Coles, H. J.; McKeown, N. B.; Weber, P.; Guillon, D.; Skoulios, A. Studies of the Thermotropic Mesophase Behaviour Exhibited by a Highly Asymmetric Tetrabenzotriazaporphyrin Derivative. *Liq. Cryst.,* **1997**, *23* (4), 475–479.

(140) Boden, N.; Bushby, R. J.; Clements, J.; Jesudason, M. V; Knowles, P. F.; Williams, G. One-Dimensional Electronic Conductivity in Discotic Liquid Crystals. *Chem. Phys. Lett.,* **1988**, *152* (1), 94–99.

(141) Iino, H.; Usui, T.; Hanna, J. Liquid Crystals for Organic Thin-Film Transistors. *Nat Commun.,* **2015**, *6*, 6828.

(142) Duy Dao, Q.; Hori, T.; Fukumura, K.; Masuda, T.; Kamikado, T.; Fujii, A.; Shimizu, Y.; Ozaki, M. Efficiency Enhancement in Mesogenic-Phthalocyanine-Based Solar Cells with Processing Additives. *Appl. Phys. Lett.,* **2012**, *101*, 263301.

(143) Kumar, S. Discotic Liquid Crystal-Nanoparticle Hybrid Systems. *NPG. Asia Mater.*, **2014**, *6* (e82).

(144) Dao, Q. D.; Gorji, N. E.; Alhodaib, A.; Dinh, T. N.; Fujii, A.; Ozaki, M.; Hajjiah, A. Fabrication, Characterization and Simulation Analysis of Perovskite Solar Cells with Dopant-Free Solution-Processible C6PcH2 Hole Transporting Material. *Opt. Quant. Electron.,* **2022**, *54*, 278.

(145) Jimenez Tejada, J. A.; Lopez Varo, P.; Cammidge, A. N.; Chambrier, I.; Cook, M. J.; Chaure, N. B.; Ray, A. K. Compact Modeling of Organic Thin-Film Transistors with Solution Processed Octadecyl Substituted Tetrabenzotriazaporphyrin as an Active Layer. *IEEE Trans. Electron Devices.,* **2017**, *64* (6), 2629–2634.

(146) Nakagawa, D.; Nakano, C.; Ohmori, M.; Itani, H.; Shimizu, Y.; Fujii, A.; Ozaki, M. Miscibility and Carrier Transport Properties in Binary Blend System of Non-Peripherally Octa-Hexyl-Substituted Phthalocyanine Analogues. *Org. Electron.,* **2017**, *44*, 67–73.

(147) Kumar, M.; Kumar, S. Liquid Crystals in Photovoltaics: A New Generation of Organic Photovoltaics. *Polym. J.*, **2017**, *49*, 85–111.

(148) Fujita, K.; Nakagawa, D.; Nakano, C.; Dao, Q.-D.; Fujii, A.; Ozaki, M. Bulk-Heterojunction Thin-Film Solar Cells Utilizing Miscible Binary Donor Materials of Liquid Crystalline Phthalocyanine and Its Analogue. *J. Phys. Conf. Ser.*, **2017**, *924*, 012003.

(149) Tejerina, L.; Yamamoto, S.; López-Duarte, I.; Martínez-Díaz, M. V.; Kimura, M.; Torres, T. Meso-Substituted Tetrabenzotriazaporphyrins for Dye-Sensitized Solar Cells. *Helv. Chim. Acta.,* **2020**, *103*, e2000085.

(150) Andrianov, D. S.; Farré, Y.; Chen, K. J.; Warnan, J.; Planchat, A.; Jacquemin, D.; Cheprakov, A. V.; Odobel, F. Trans-Disubstituted Benzodiazaporphyrin: A Promising Hybrid Dye between Porphyrin and Phthalocyanine for Application in Dye-Sensitized Solar Cells. *J. Photochem. Photobiol. A Chem.,* **2016**, *330*, 186–194.

Chapter 2:

Results and Discussion

2.1 Introduction

The tetrabenzo(*aza*)porphyrin hybrids exhibit similar characteristics, and the potential uses in different applications, as both phthalocyanines and porphyrins due to their structural similarities as discussed previously in chapter 1. Nevertheless, the challenges and complexities inherent in synthesising these hybrids have resulted in relatively low take-up and lack of research on establishing a procedure that promotes a controlled synthesis of these hybrids. Tetrabenzotriazaporphyrin derivatives (TBTAPs), in particular, have been the most investigated hybrids recently in the UEA research group.[1–4] They have been working to establish a novel synthetic approach to synthesise TBTAP derivatives and recently they have reported a highly successful synthesis of *meso*-substituted TBTAP derivatives which is both versatile and high yielding using aminoisoindoline as an initiator for macrocyclisation. This great success allows for the availability of many novel functionalised TBTAP materials. Also, our group has reported a detailed investigation of TBTAP formation using various substituents on benzene rings in both phthalonitrile and aminoisoindoline derivatives to develop the understanding of their synthesis pathway and their mechanistic formation. Two different TBTAP hybrids were obtained in most experiments and two different pathways were hypothesised for their formation. However, their selective synthesis still proves to be difficult, and their mechanistic formation remains unclear.

On the other hand, selective synthesis routes to tetrabenzodiazaporphyrin (TBDAPs) have been successfully achieved in different research groups using different precursors as outlined in chapter 1.[5–7]

2.2 Aim of this work

Based on the recent findings, the current study was initiated with multiple objectives in mind. Nevertheless, all of them centered around the overall objective of evaluating different routes to synthesise tetrabenzo(*aza*)porphyrin hybrids especially the less studied tetrabenzomono*aza*porphyrin hybrids. The starting point of this research was repeating our group's most recent TBTAP synthesis to gain the knowledge of its synthesis and purification. With the assumption that the macrocyclisation mechanism of this method is initiated by attack of the nucleophilic amine in aminoisoindoline onto dicyano benzene (phthalonitrile) is correct, we attempted to access hybrids with more carbon bridges and by employing a mixed macrocyclisation reaction between the same aminoisoindoline but with a new complementary macrocyclisation partner (alkynyl benzonitriles) which is less nitrogenous precursor compared to phthalonitrile.

To complement the synthetic work and gain an understanding of the purification and analysis of TBMAP hybrid and assess the feasibility of its formation, Linstead's very first investigation to synthesise TBMAP hybrids using malonate aminoisoindoline as precursor was to be reinvestigated and different substitutions will be introduced on benzene ring of malonate aminoisoindoline to make the final outcome soluble and accessible to analyses.[8]

In response to recent discoveries in the group, the final phase of the work involved metal screening of TBTAP's synthesis. In this work different template metals with different oxidation state and different ionic radius have been investigated such as Li, Na, K, Mg, Ni, Cu, Pb and Zn.

2.3 Repeat of TBTAP procedure and its precursors

Before commencing work on testing our proposed pathway to synthesise tetrabenzomonoazaporphyrin hybrids (TBMAPs), we deemed it sensible to reproduce the very recent reaction reported by our group in which the isolation of 40% yield of functionalised *meso*-phenyl MgTBTAP was successfully achieved as a single product of hybrid macrocycles. Its synthesis was accomplished through the formation of aminoisoindoline (**29**) as an intermediate compound that was reacted with commercially available phthalonitrile as a complementary macrocyclisation partner in the presence of magnesium bromide as metal template and DABCO in high boiling solvent as illustrated in scheme 2.1. [4]
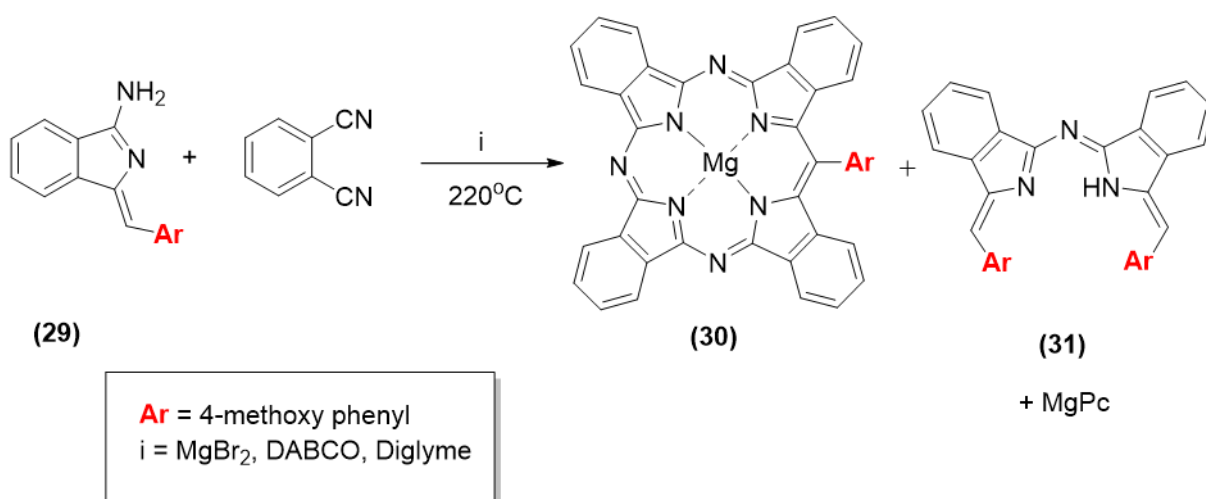
Scheme 2.1: Synthetic route of meso-phenyl TBTAP (30).

This strategy started with the synthesis of aminoisoindoline derivatives following the reported procedure by Hellal and Cuny.[9] Its preparation involves two steps reaction as shown in scheme (2.2). The first step begins by following a reported method for the formation of amidine. A solution of the commercially available 2-bromobenzonitrile (**27**) in THF was treated with a solution of lithium bis(trimethylsilyl)amide in THF which was then hydrolysed using isopropanolic HCl in order to obtain the HCl salt of the bromo benzamidine (**28**) in a good yield (76%).[10] The mechanism of this reaction includes a nucleophilic attack at the partially positive carbon atom of the nitrile group by the nitrogen of LiHMDS, then the acid work up helps to remove trimethylsilyl groups to yield the desired product.
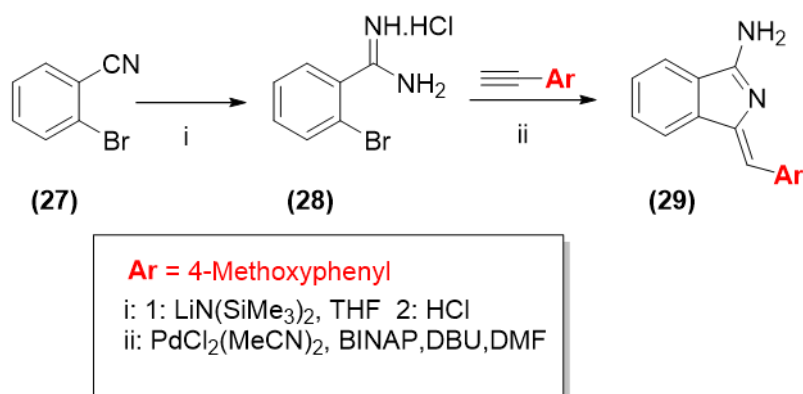
Scheme 2.2: Synthesis of aminoisoindoline (**29**).

The second step was the treatment of the solution of the intermediate with a mixture of phenyl acetylene, BINAP (as a supporting ligand), DBU and catalytic amounts of palladium in dry DMF under reflux for 4-6 hours, or 1 hour at 120°C under microwave irradiation. After workup and purification using column chromatography and recrystallisation techniques, the required product was isolated in a moderate yield of 57%. This reaction involved a copper-free Sonogashira cross-coupling and followed by a cycloisomerisation as a one-pot reaction to give the (Z)–isomer aminoisoindoline as a major product that indicates the stereoselectivity of this reaction. This result can be proved by the characteristic alkene proton that appears at δ 6.7 ppm as a singlet peak in ^{1}H NMR spectroscopy and eight protons in aromatic region as shown in figure (2.1).[9]
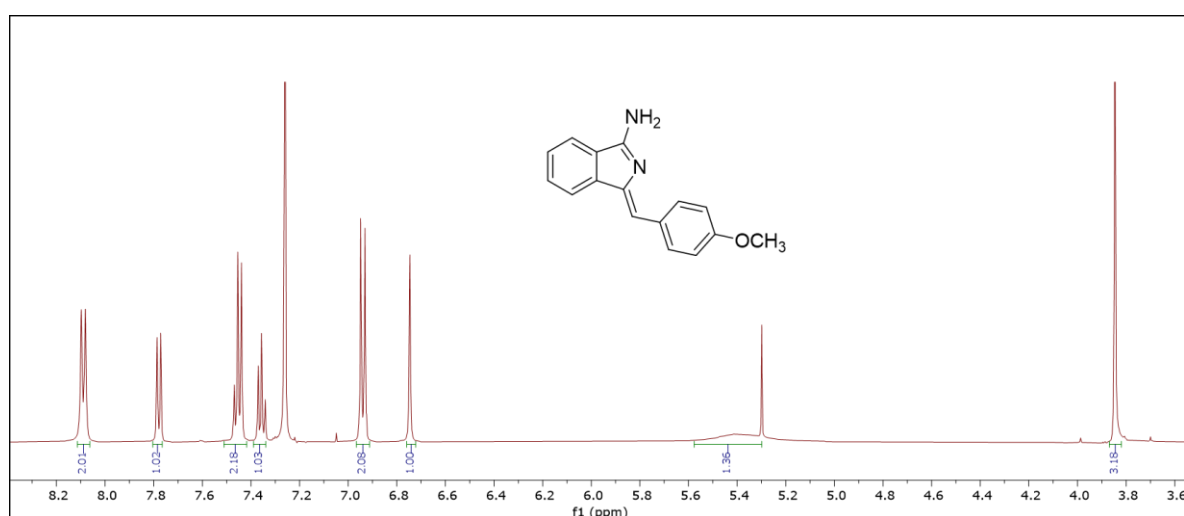
Figure 2.1: ^{1}H NMR spectrum of (Z)-1-(4-methoxyphenylmethylene)-1H-isoindol-3-amine (**29**) in CDCl_3.

The supposed catalytic cycle is depicted in detail in scheme 2.3. The mechanism is initiated by generation of an active catalyst (Pd^0) from Pd^{II} under the reaction conditions. Subsequently, an oxidative addition of the aryl halide occurs to the active catalyst to form the four-coordinated palladium complex. Then, a neutral ligand is dissociated, and a π-alkyne-palladium complex is formed that increases the acidity of the alkyne to facilitate the removal of the proton by the base. Then, trans/cis isomerisation and reductive elimination occur stepwise to release the cross coupled product and reform the catalytic species Pd^0 ready to start a new cycle. The cross-coupling product is immediately followed by a regioselective 5-exo-dig cycloisomerisation domino reaction to give the final product by coordinating the palladium catalyst to the alkyne, followed by the loss of HCl. Then, it undergoes protonolysis to recover the catalyst.[11]
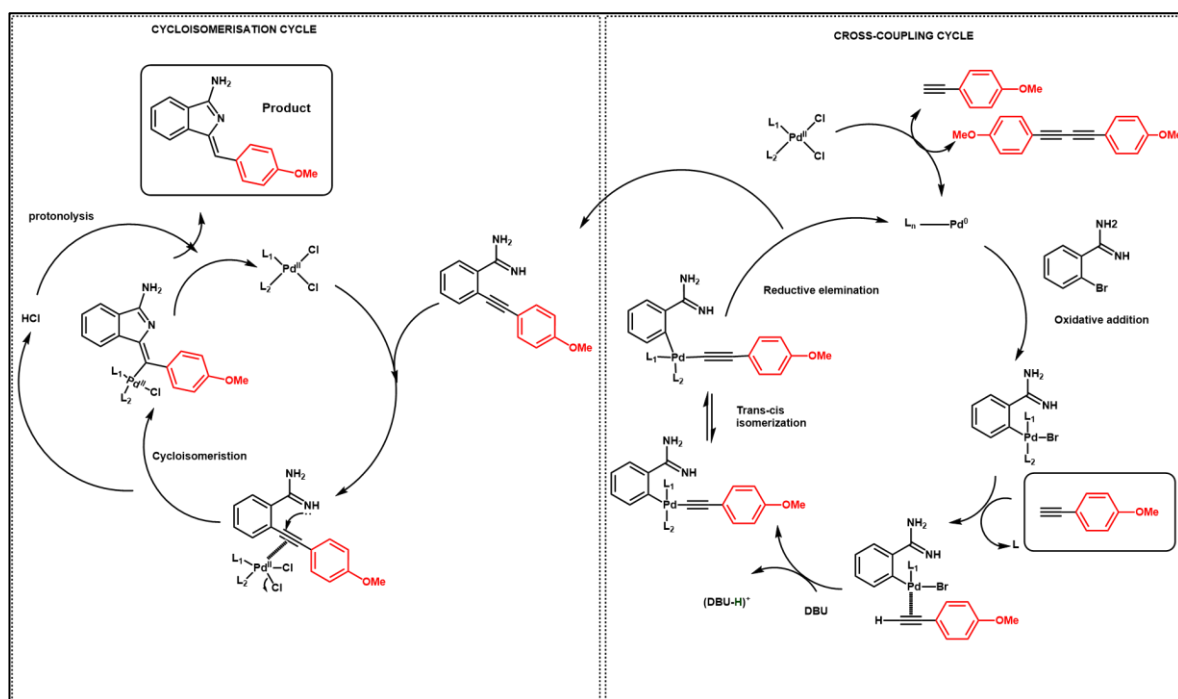
Scheme 2.3: Supposed mechanism for the formation of aminoisoindoline (**29**).

Following the process described earlier, and after the successful preparation of aminoisoindoline derivative, the macrocyclisation reaction was done by heating the mixture of aminoisoindoline derivative (**29**) and phthalonitrile as complementary macrocyclisation partner and MgBr$_2$ as template and DABCO (1,4-diazabicyclo [2.2.2] octane) in diglyme at 220°C for 4 hours. After full consumption of starting materials was observed by TLC, the solvent was removed under an argon stream while the mixture was still hot. Then, the reaction mixture was left to cool down and a mixture of DCM: MeOH (20ml) was added,

and the mixture was sonicated. Chromatographic purification was carried out using a mixture of DCM: Et₃N: distilled THF (10:1:4) as eluent leading to the isolation of a self-condensation compound (**31**) from green material and traces of blue product. The green fraction was then submitted to another column chromatography using PE: THF (5:1) as eluent to isolate the MgTBTAP (**30**). Recrystallisation of the product was difficult, and several attempts were made from different mixed organic solvents, and it was successfully recrystallised when ethanol was used as the only solvent and the mixture left in the dark until it was recrystallised and gave green crystals with purple reflex with an impressive yield of 42%. As depicted in figure 2.2, ¹H NMR spectra perfectly corresponded to the expected spectra for the product. Also, the correct molecular ion peak in the MALDI-TOF mass spectra were achieved successfully which is m/z = 640.38 and its isotopic pattern matched the theoretical one. The UV-Vis spectra clearly show the characteristic Q band that agree with the literature value.[1,12]
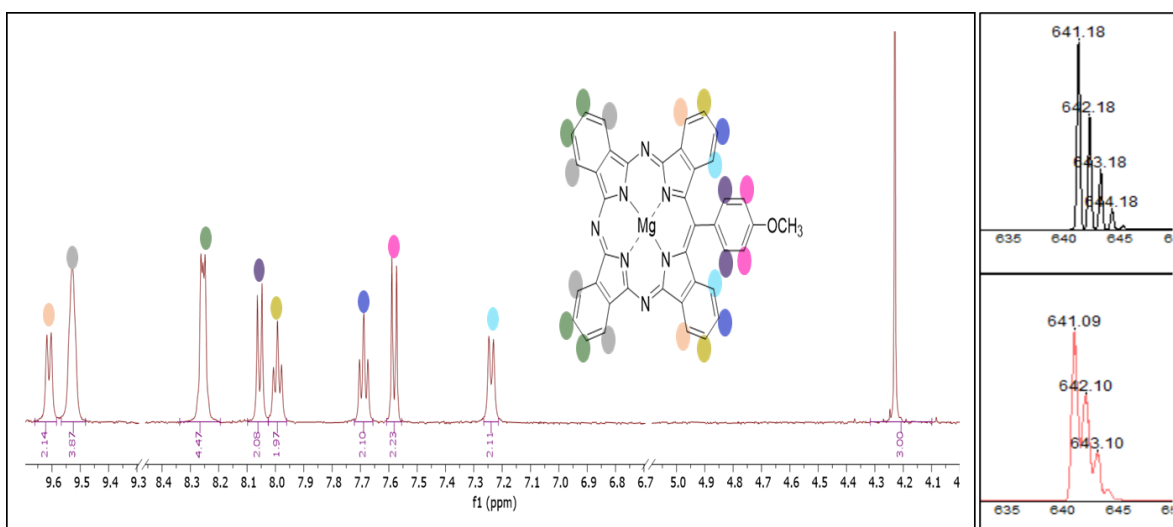
Figure 2.2: ¹H NMR spectrum of meso-(4-methoxyphenyl) MgTBTAP (**30**) in acetone-*d₆* (left) and its its MALDI-TOF MS (bottom right) plus theoretical isotopic pattern (top right).

2.4 Investigation of the proposed pathway to synthesise TBMAP hybrids:

Since the successful synthesis of MgTBTAP hybrid has been achieved in a reasonable yield, the focus of the research was moved onto the attempt of preparation of the target hybrid TBMAPs. The replacement of three *meso*-nitrogen atoms of Pc macrocycle with (substituted) carbon atoms in TBMAP structures is expected to improve solubility and

therefore increase their potential uses in many applications since the versatility of the carbon bridges and a variety of substituents at the *meso*-position can be introduced that leads to tunning the macrocycle properties. However, while several efficient syntheses of TBTAPs and TBDAPs have been reported recently, only one selective method to prepare TBMAP hybrid was reported in the 1940s by Linstead. Other methods have been reported for the synthesis of TBMAP such as the use of Grignard reagents that produce the mixture of other hybrids including TBMAPs. [8,13,14] In this section, a new approach will be tested in order to achieve TBMAP synthesis or controlled synthesis of more carbon-bridged hybrids that would give an access to a variety of substituents at *meso*-sites. The first attempt was an investigation of a mixed cyclisation of a previously synthesised aminoisoindoline (**29**) with a new complementary macrocyclisation partner which is alkynyl benzonitriles (4-methoxy phenyl acetylene) (**32**) following the proposed synthetic route in scheme 2.4.
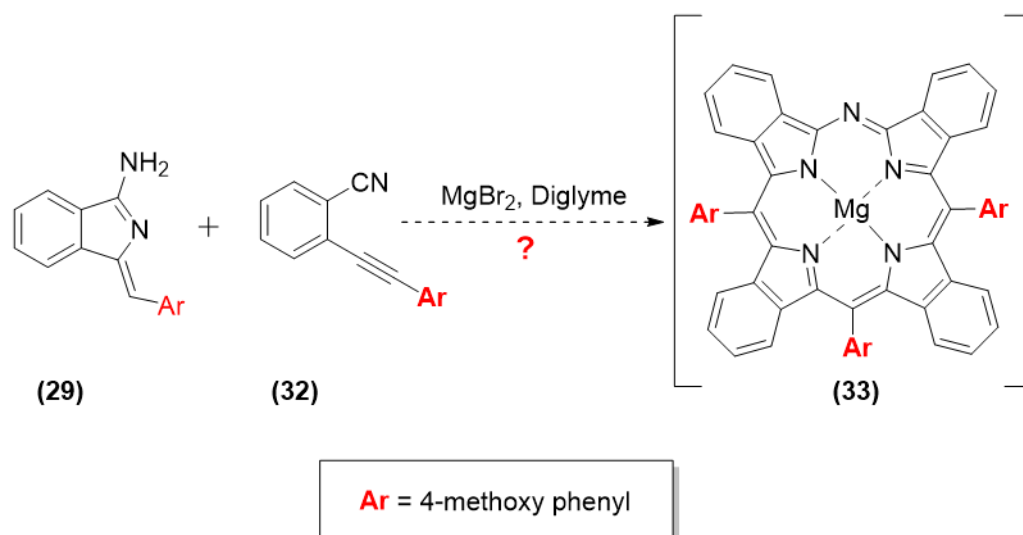
Scheme 2.4: A proposed route for synthesis of MgTBMAP (**33**).

Assuming that the proposed mechanism of aminoisoindoline initiating TBTAP macrocyclisation with phthalonitrile is correct, we are utilising a less nitrogen-rich precursor as a macrocyclisation partner instead of phthalonitrile in order to generate more carbon bridges in the hybrid. Based on the hypothesised pathway that is depicted in scheme 2.5, the anticipated outcome involved the formation of TBMAP hybrid that underwent a cyclisation through a single nitrogen bridge, that originates from aminoisoindoline, and three *meso*-

phenyl bridges that derive from the acetylene. Each bridge connects to an isoindoline unit that derived from the acetylene and one derived from the aminoisoindoline.
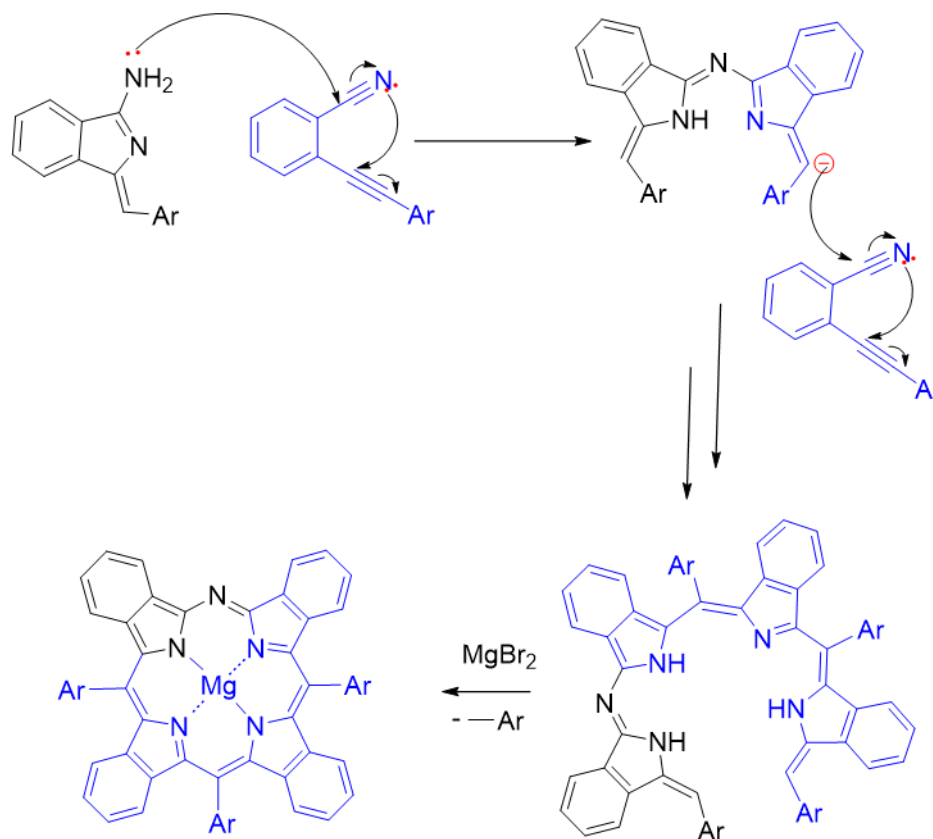
Scheme 2.5: Hypothesised macrocyclisation pathway to produce MgTBMAP (**33**).

This proposed approach started with the preparation of alkynyl benzonitriles (**32**) following the reported Sonogashira cross-coupling procedure. A terminal acetylene was mixed with bromobenzonitrile and palladium catalysts and copper iodide as co-catalysts in triethylamine (TEA) in a sealed tube at 120°C for 24 h (scheme 2.6). After the reaction was completed and cooled down, saturated solution of NH_4Cl was added and extracted with ethyl acetate, dried using magnesium sulphate, and purified by column chromatography to yield the title compound as white needles in 58% yield.[15]
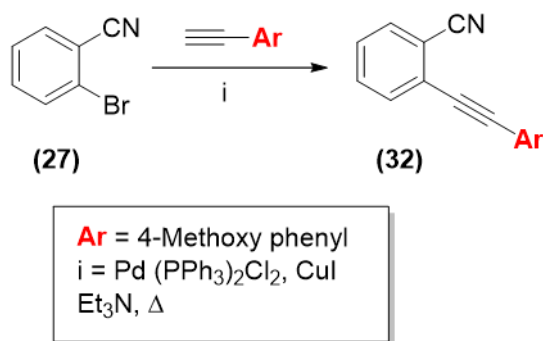
Scheme 2.6: Formation of 2-[2-(4-methoxyphenyl) ethynyl] benzonitrile (**32**).

Figure 2.3 illustrates the ^{1}H NMR spectrum of the desired product that shows the 8 protons in the aromatic region as well as the singlet peak at δ 3.84 that corresponds to methoxy protons.
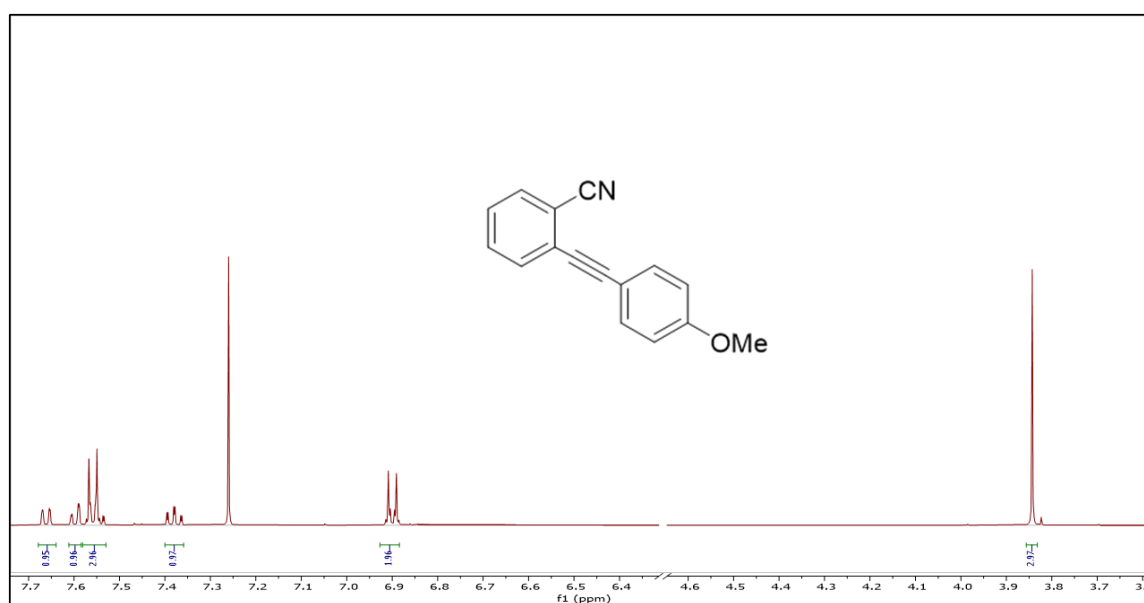
Figure 2.3: ^{1}H NMR spectrum of 2-[2-(4-methoxyphenyl) ethynyl] benzonitrile (**32**) in CDCl$_3$.

After the successful synthesis of alkynyl benzonitriles (**32**) and with aminoisoindoline (**29**) in hand, the first attempt toward the synthesis of MgTBMAP (**33**) was done as shown in scheme 2.7 by employing aminoisoindoline intermediate to initiate the macrocyclisation process around a magnesium template ion, with the alkynyl benzonitriles (**32**) under the MgTBTAP forming conditions in the presence of magnesium bromide in dry diglyme in pre-heated block at 220ºC under nitrogen.
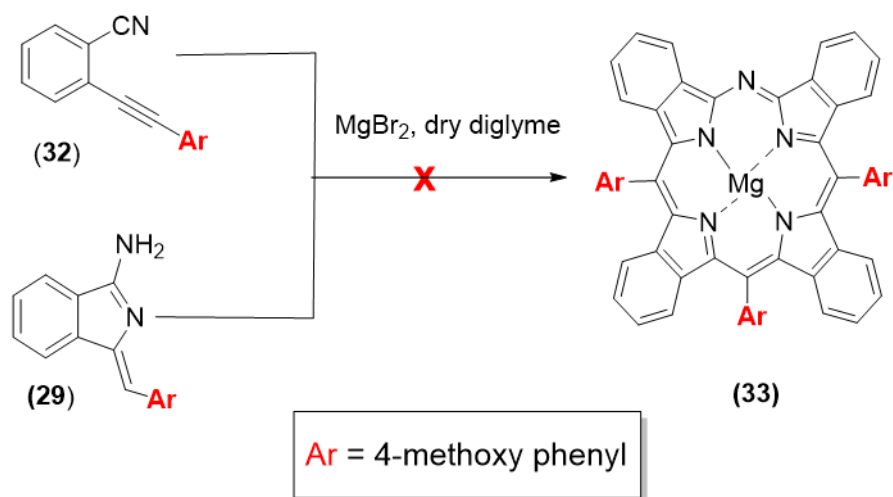
Scheme 2.7: Unsuccessful attempt to synthesise TBMAP (**33**).

The colour of the reaction changed from yellow to deep red and even when the reaction was left for longer time, it was still red, and no signs of green-dark color was observed so the reaction was checked by TLC against the starting materials and it was found that a full consumption of aminoisoindoline was observed plus unreacted acetylene and a new red spot that was identified later as self-condensation compound of aminoisoindoline (**31**). This result led us to investigate model reactivity of the acetylene using phthalocyanine cyclisation conditions as shown in scheme 2.8.[16] A mixture of acetylene (**32**) and pentanol was heated up to reflux and a small portion of lithium was added. The reaction was left to reflux until a complete conversion of the starting material was observed by TLC. However, the colour of the reaction was light yellow with no signs of any green materials, so the reaction was repeated with Li and $MgBr_2$ as template metals in pentanol, but it still gave the same outcome. It was important to analyze the outcomes to identify the reactivity of this precursor, so after the workup using dilute HCl, and an extraction with ethyl acetate and evaporation of solvent, the crude was subjected to column chromatography to isolate the product as a light brown oil.
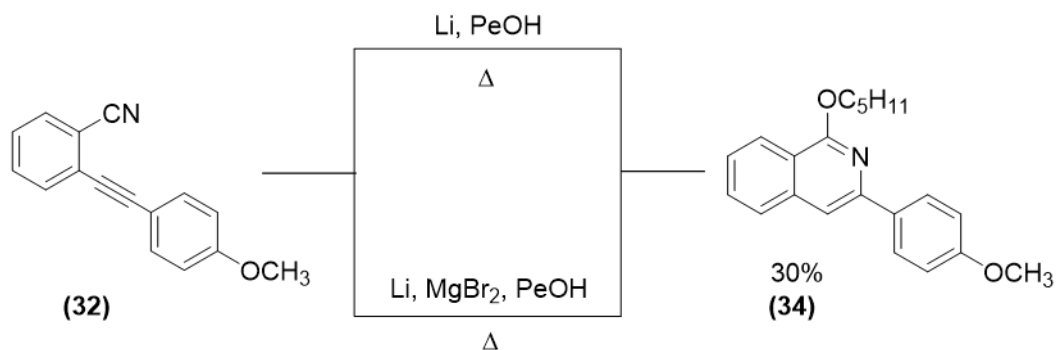
Scheme 2.8: Formation of 1-pentoxy-3-(4-metoxyphenyl) isoquinoline (**34**).

After the analysis of the compound by MALDI-TOF mass spectra it was found that m/z = 320.81 which is m/z 87 higher than the starting material molecular weight. That gives an indication of the involvement of pentyloxy group in the reaction. As shown in figure 2.4, ^{1}H NMR spectrum of the compound in deuterated chloroform gave six aromatic signals that correspond to eight aromatic protons as expected. However, the signal of alkene proton was found at an unusually high chemical shift (δ = 7. 57ppm), due to the conjugated system that helps to indicate that the compound is a 6-endo-dig compound (**34**) instead of 5-exo-dig attack that we needed. Also, two different signals appear at 4.67 and 3.88 ppm that indicates the presence of two alkoxy groups in the structure. A triplet at 4.67 ppm for pentyloxy group and singlet at 3.88 ppm for methoxy group and three different aliphatic signals at the range of 1.99-0.95 ppm that correspond to pentyloxy chain protons. As the compound is an oil, x-ray cannot be used to confirm its structure.
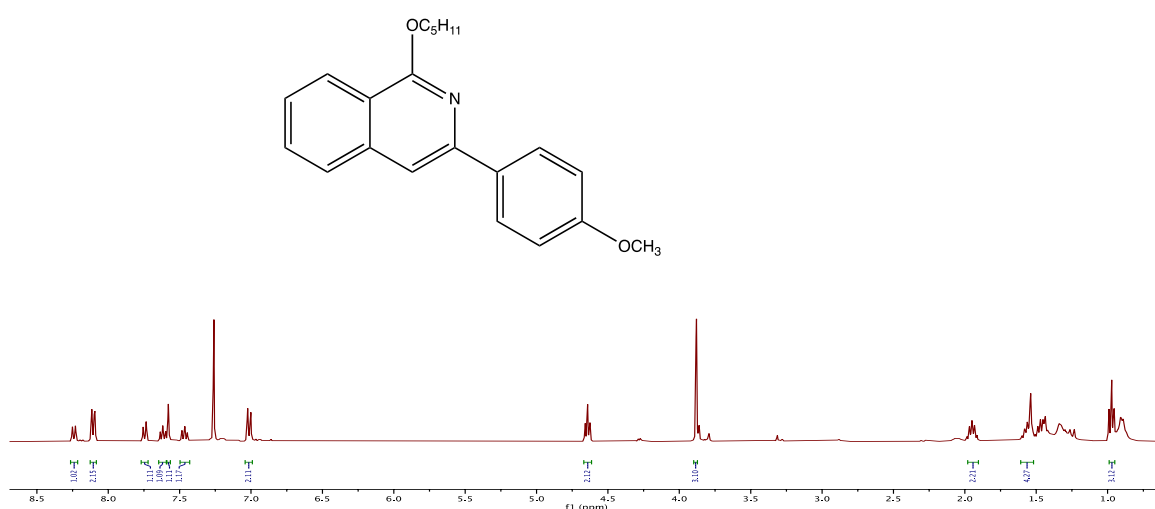
Figure 2.4: ^{1}H NMR spectrum of 1-pentoxy-3-(4-metoxyphenyl) isoquinoline (**34**) in CDCl$_3$.

It is noteworthy that this compound is favored by Baldwin's rules as well as the 5-exo-dig compound. There are many factors that affect the ring closure such as unexpected stereo-electronic interactions and neighbouring groups that modify the ideal geometry or induce polarisation at the interacting atoms. It is well-known from a thermodynamic consideration that the formation of larger rings is more favourable. However, when the larger ring requires more distortion to achieve the favourable attack trajectory, a smaller ring is faster to form. This is the case of an acetylene moiety that undergoes faster 5-exo-dig cyclisation than 6-endo-dig cyclisation. Although 5-exo-dig is more kinetically favourable over 6-endo-dig cyclisation, the latter is more thermodynamically stable, especially in our case due to its aromaticity (depicted in figure 2.5).[17–20]
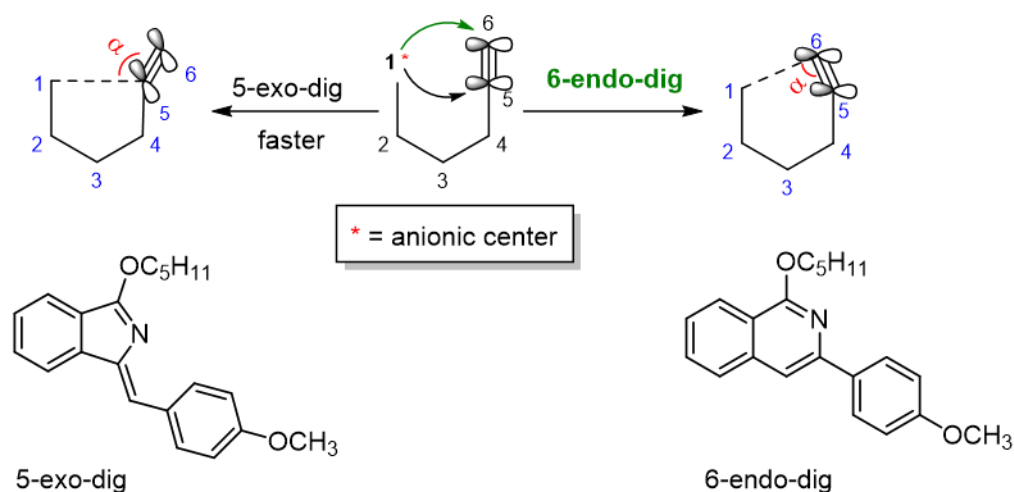
Figure 2.5: Favoured reaction of diagonal system Baldwin's rules.

This result can be a good explanation for the failed former reaction when the acetylene did not undergo full cyclisation with aminoisoindoline. Also, it directs the attention to examine the cyclisation of different substituted acetylenes when the phenyl on the remote end of the alkyne moiety is substituted with a strong electron withdrawing group on the para position in order to investigate the effect of electron-withdrawing group on the triple bond and whether it helps to produce the 5-membered ring compound. If this is successful, this acetylene will be employed as a complementary macrocyclisation partner with methoxy-aminoisoindoline to investigate the possibility of synthesis of TBMAP hybrid.

The nitro group was chosen as an electron withdrawing group and the desired acetylene was prepared in two steps as shown in scheme 2.9. In the first step, acetylenic alcohol undergoes

Sonogashira reaction with 2-bromobenzonitrile to form the substituted acetylene (**35**). Subsequently, the acetylenic alcohol was subjected directly to another Sonogashira reaction with 1-iodo-4-nitro benzene to produce the desired product (**36**).[21,22]
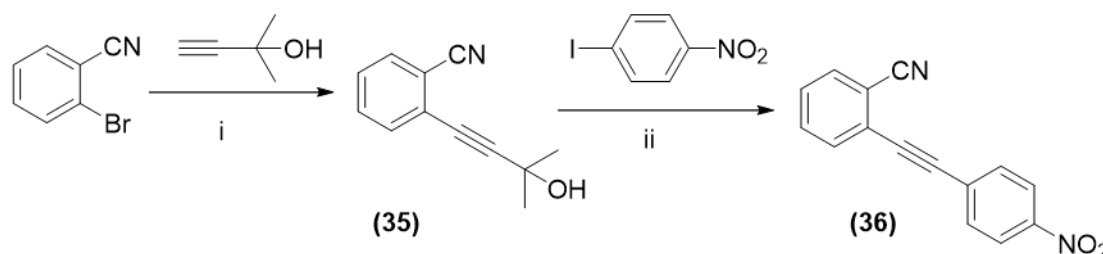
Scheme 2.9: The synthetic route to nitrophenyl acetylene (**36**).

As shown in scheme 2.9, the acetylenic alcohol (**35**) was prepared by standard Sonogashira cross–coupling reaction of commercially available 2-bromobenzonitrile using palladium as a catalyst, CuI as co-catalyst, triphenylphosphine as a supporting ligand and TEA as a basic solvent under nitrogen. Slow addition of the terminal alkyne was achieved using a syringe pump over a period of 4 hours in order to reduce alkyne-alkyne homocoupling. When the addition was finished, the heat was turned on and the reaction was left to reflux for two hours until the starting material spots disappeared in TLC. Then, the mixture was cooled down to r.t. and the reaction mixture was extracted and purified by flash chromatography on silica gel to give the coupling product (**35**) as a brown oil in excellent yield (97%). Its structure was confirmed by ^{1}H NMR spectroscopy which showed a singlet peak for 6 protons of methyl groups that appears in aliphatic region as well as a singlet peak of OH that appears at around 3.10 ppm and aromatic signals for aromatic protons appear as expected.[22]

After the successful synthesis of protected acetylene (**35**), we moved to synthesise the nitro substituted acetylene using the general procedure for the Sonogashira coupling between acetylenic alcohol (**35**) and aryl iodide under phase transfer conditions (PT Method) as shown in scheme 2.9. In a sealed tube, a mixture of aryl bromide, acetylenic alcohol, copper(I) iodide, palladium (II) dichlorobistriphenylphosphine, and tetrabutylammonium

iodide waspurged and refilled with N_2 three times. Then, a heterogeneous mixture of toluene and aqueous sodium hydroxide was added. The mixture was heated at 80 ^{0}C for 2 hours until a full consumption of starting materials was observed by TLC. Then, the mixture was allowed to cool down to room temperature and the solution was filtered through a pad of silica gel, and the filtrate was concentrated under reduced pressure. The residue was chromatographed on silica gel, to give the desired product (**36**) as colorless needles in 67% yield. From ^{1}H NMR analysis, chemical shifts and integrals as shown in figure 2.6, the structure of the desired product can be assigned as all the eight protons appear in aromatic region. [21]
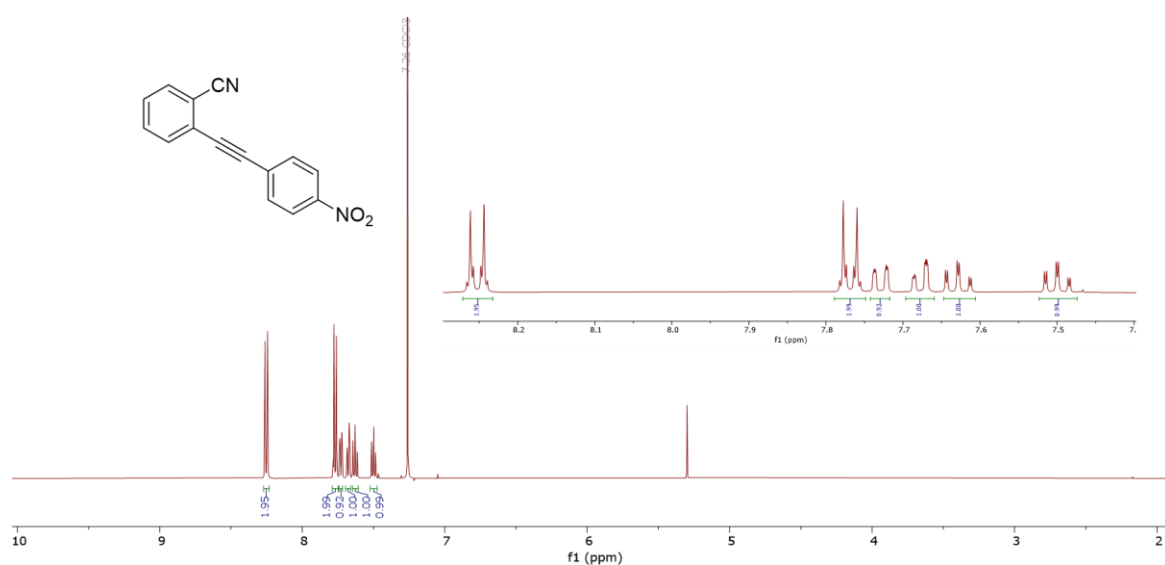
Figure 2.6: ^{1}H NMR spectrum of 2-(2-(4-nitrophenyl) ethynyl)- benzonitrile (**36**) in CDCl$_3$.

After the nitro acetylene (**36**) was successfully synthesised, we moved to investigate the cyclisation under the same conditions used for the methoxy acetylene as shown in scheme 2.10. An excess of lithium was dissolved in boiling pentanol and then the reactant was added, and the reaction was left to reflux until all starting material was consumed. The reaction was not clean as many yellow spots were observed by TLC with similar intensity. Other attempts were made with the addition of MgBr$_2$ as a template in pentanol at 160°C and in higher temperature at 220°C in diglyme and in all reactions the mixture turned light orange and many yellow spots in the TLC were observed that makes the isolation of any compound impossible by column chromatography as the differences in R$_f$ are small.
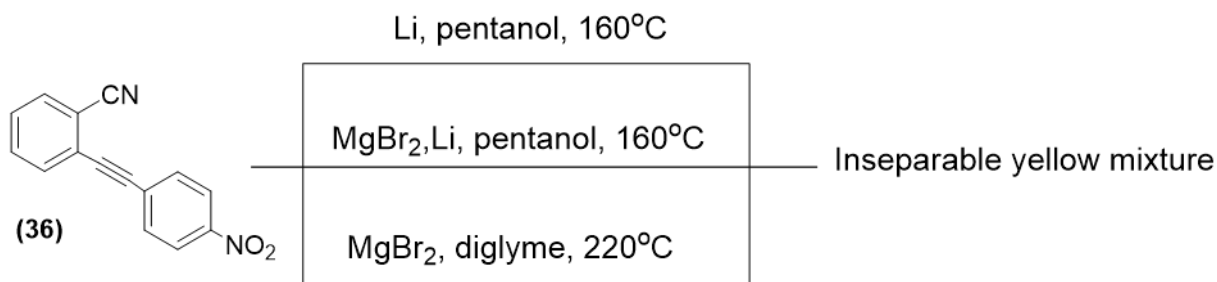
Scheme 2.10: Unsuccessful cyclisation of nitro-acetylene (**36**).

2.5 Revisiting Linstead's method to synthesise TBMAP and its precursor

After these unsuccessful attempts to synthesise the TBMAP hybrid via our proposed mixed cyclisation, we thought it necessary to reinvestigate the Linstead et al work to assess TBMAP formation. As reported, the TBMAP hybrid was synthesised selectively through fusion of malonate aminoisolindoline in presence of zinc dust at ~330°C as shown in scheme 2.11.[23]
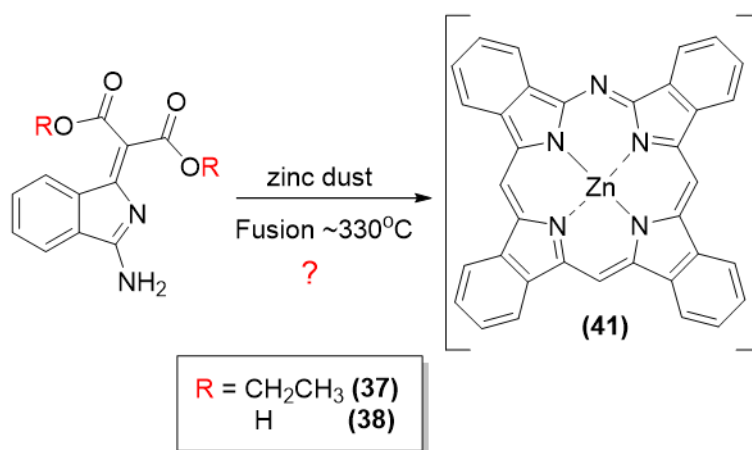
Scheme 2.11: Reported synthetic route of TMBAP (**41**) using malonic acid intermediate (**38**) or its diethyl ester as precursor (**37**).

In their paper, it was mentioned that the possibility of production of pigments when 1-imino-3-dicarboxymethylenephthalimidine or its diethyl ester was employed whereas none can be produced when the corresponding keto-ester was employed. Moreover, 27% of TBMAP was reported to be obtained when zinc was fused with imino-acid. However, a mixture of TBMAP and TBP in 60% and 40 % respectively was obtained when zinc acetate was employed and a 40% mixture of TBMAP and TBDAP pigments was obtained when copper, magnesium or magnesium acetate were employed. When a mixture of imino-acid and phthalonitrile was fused with metallic reagents, more nitrogen-bridged pigments were

obtained. A pure CuTBTAP was reported to be formed when one equiv. of phthalonitrile was fused with three equiv. of imino-acid in the presence of copper bronze as depicted in scheme 2.12.[23]
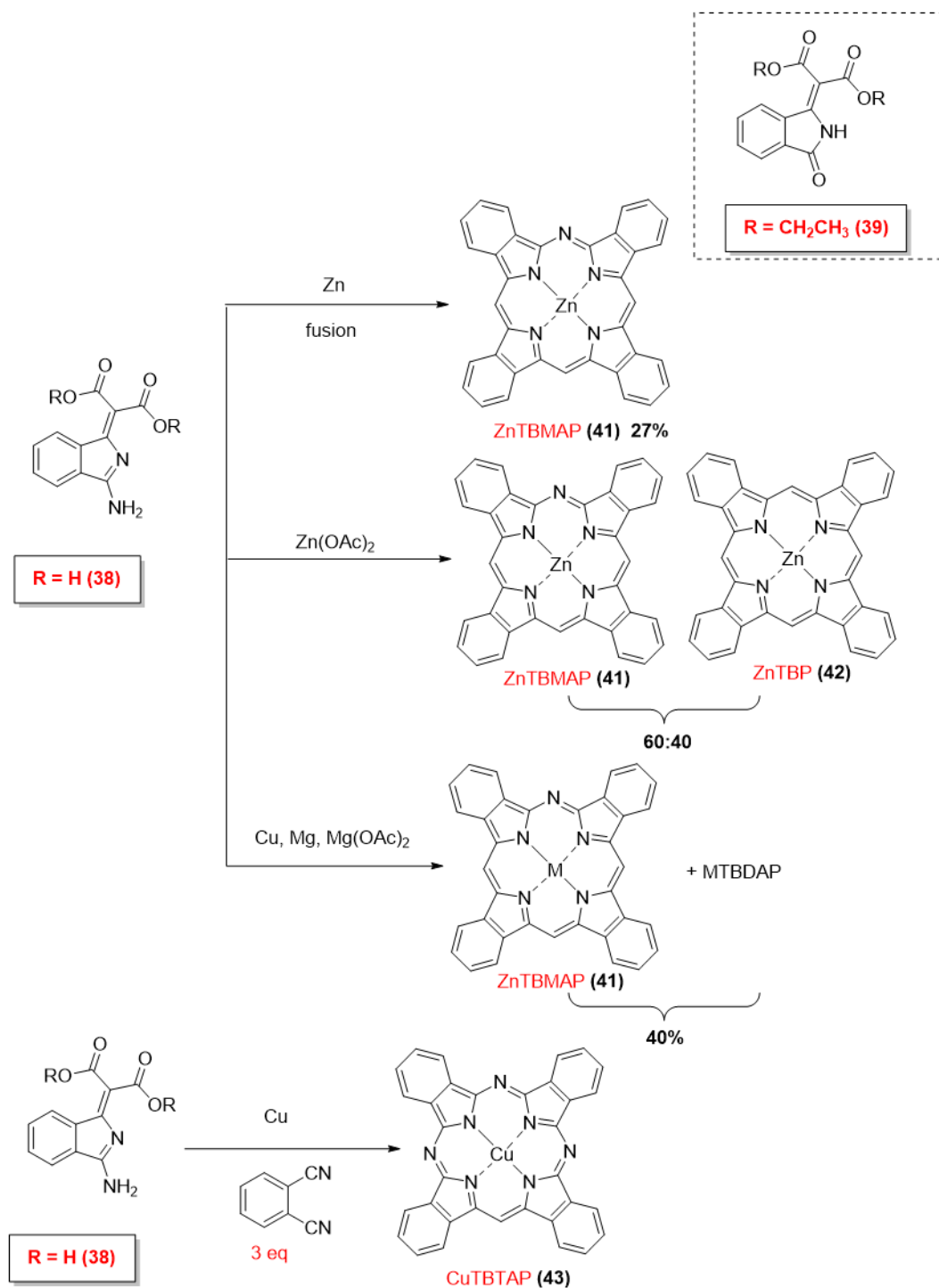
Scheme 2.12: Reported reactions of 1-imino-3-dicarboxymethylenephthalimidine and its keto-ester structure (top right).

Based on their outcomes, zinc dust and malonate aminoisoindoline (**37**) was chosen to synthesise the target hybrid (TBMAP). The first step to investigate their method is preparation of the target precursor (**37**) following their described procedure, by reacting a cold solution of sodium ethoxide (sodium in ethanol) with malonate ester and phthalonitrile (scheme 2.13).[24] Then, the mixture was heated up to nearly the boiling point. A vigorous reaction set in and when this was ceased, the dark-red solution was cooled down and poured on to a mixture of HCl and ice and kept overnight or until precipitates were formed. After that, the precipitate was filtered off and recrystallised using EtOH: H_2O in a fridge. After seven days, formation of light purple crystals was observed, then a full analysis of pure crystals by ^{1}H NMR, ^{13}C NMR, UV-vis and MALDI-TOF MS was obtained.
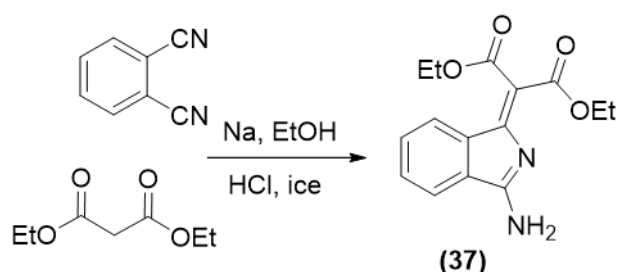
Scheme 2.13: Preparation of 1-imino-3-dicarbethoxy methylene isoindoline (**37**).

As shown in figure 2.7, the ^{1}H NMR spectrum was as expected for the desired product with 4 protons in aromatic region and two quartets at 4.3 and 4.4 ppm corresponding to CH_2 in ester group and two triplets at 1.34 and 1.40 ppm corresponding to CH_3 in ester group.
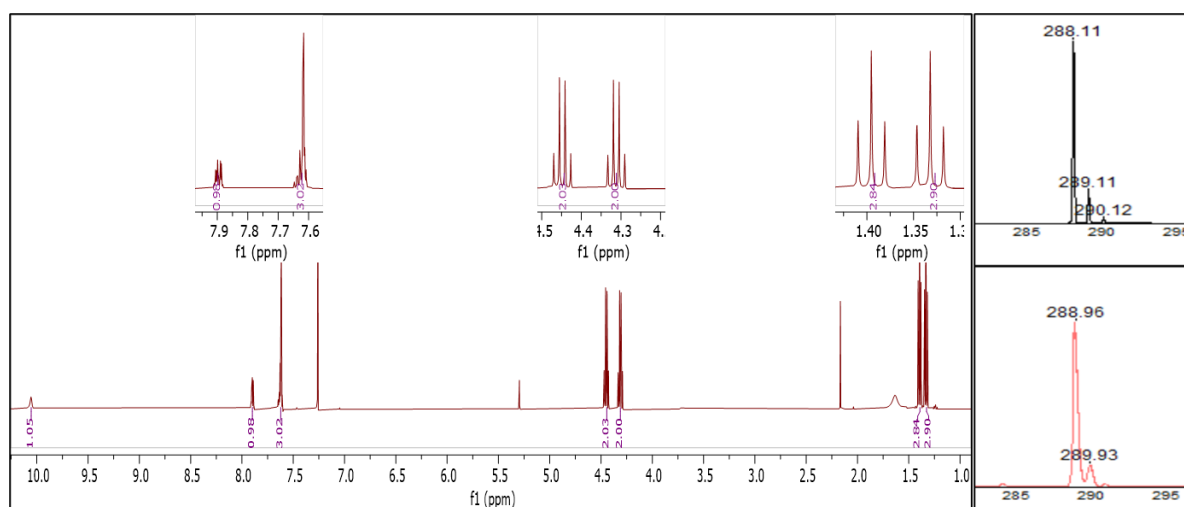
Figure 2.7: ^{1}H NMR spectrum of the isolated compound in $CDCl_3$ (left) and its MALDI-TOF MS (bottom right) plus theoretical isotopic pattern (top right).

However, the molecular ion peak in the MALDI-TOF mass spectrum was higher than the expected molecular weight which is m/z = 288.11 and what found was 288.96 (figure 2.7). The isolated crystals were submitted for x-ray diffraction analysis that proved the identification of the obtained product as the keto ester (**39**) not the desired aminoisoindoline (figure 2.8). This result agreed with the unexpected higher MALDI-MS analysis as the exact mass of keto ester is 289.09 which is closer to the observed one. Also, the melting point of the sample was taken, and it agreed with the literature value for the keto ester which is 108°C. Moreover, unsuccessful dimerisation of the compound was attempted at 120°C using toluene as solvent. This proves the isolated product is keto-ester. [24]
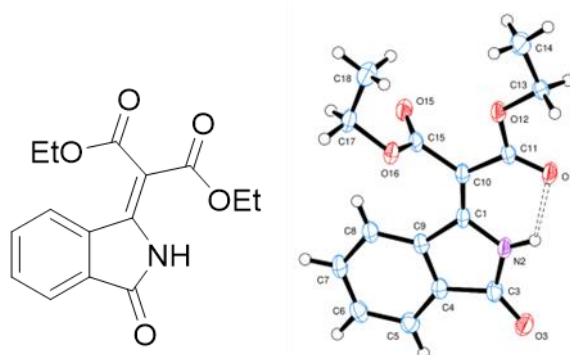
Figure 2.8: Keto ester (**39**) and its x-ray crystal structure (ORTEP).

With this unexpected result and with a sample of keto ester in hands, the reaction was repeated several times and checked by TLC. It was noticed that before acid and water work up, two yellow spots were observed in TLC whereas after acid work up many spots were observed including keto ester as major compound. The reaction was repeated with the aims of isolation and identification of the desired product spot by avoiding acid/ water work up. When the reaction was completed, the solvent was evaporated under reduced pressure and the solid was checked by TLC, two spots were observed. Then, the mixture was submitted to silica-gel column chromatography to isolate them as the difference in R_f is large. However, after the analysis of all fractions, keto-ester spot was observed in the first fractions, so we realised that even slight acidity of silica causes the formation of this compound. The isolation of top yellow spot was successful by column and was submitted for a full analysis to identify this spot later as the dimerised compound (**40**), this compound was not reported in the literature. MALDI-TOF MS gave the corresponding molecular weight for the dimer

as was m/z= 559. The NMR spectra of the pure product gave the expected proton number of the dimer structure. However, a different peak splitting of aromatic protons was observed with a slight chemical shift compared to keto ester. Moreover, the product was recrystallised using EtOH: H_2O to give red crystals that were suitable for x-ray diffraction analysis as shown in figure 2.9.
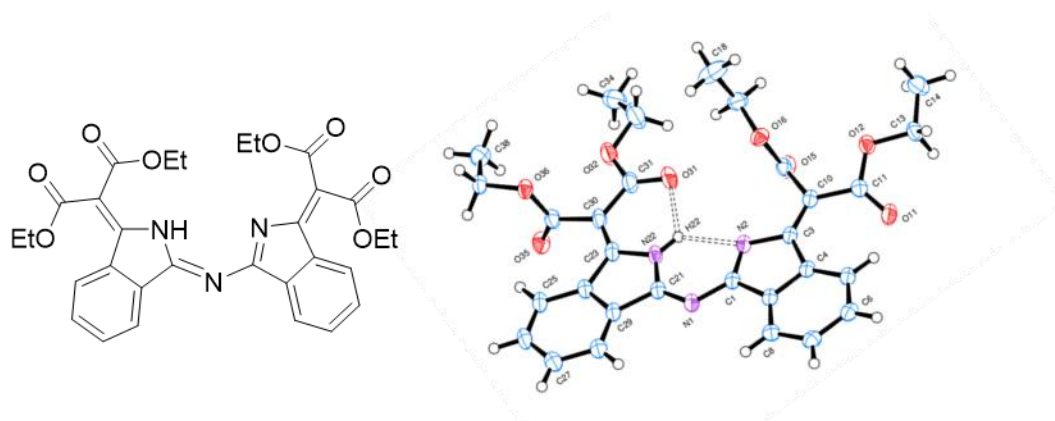
Figure 2.9: Dimer of malonate aminoisoindoline structure (**40**) and its x-ray crystal structure (ORTEP).

With use of Cammidge group's prior knowledge regarding the synthesis of self-dimerisation compound, we have decided to avoid any heat during the preparation and purification of malonate aminoisoindoline to avoid the formation of this compound. Also, the amount of sodium metal and malonate ester was doubled compared to phthalonitrile to get the reaction completed and get rid of unreacted phthalonitrile as it was observed in previous attempts. After many attempts and with all these modifications, one spot in TLC was observed and this spot does not correspond either to keto ester or to the dimer. However, the isolation of this spot from the excess of base was challenging as water work up had to be avoided. Consequently, when the reaction was finished, the mixture was cooled down overnight in the fridge with the aim to precipitate the product, but a mixture of sodium ethoxide and product was filtered off and this can be observed by ethoxide peaks that overlap with malonate peaks in the NMR spectrum and by detecting the alkalinity of the solution using litmus paper. Several attempts were made to recrystallise the compound from different organic solvents but none of them were successful and when the mixture stayed in solution for a long time, both keto-ester and dimer were observed in the TLC. Filtration of the crude after the reaction through celite was not helping to isolate the product from the base and when the amount of base was reduced in the reaction, starting materials were not fully consumed. After many attempts, the desired product (**37**) was successfully isolated by

chromatography on aluminium oxide using DCM: EtOAc 1:1 then, EtOAc 100% as eluent. The product was analysed by NMR spectroscopy and compared against keto ester and the dimer as depicted in figure 2.10. As illustrated in the figure, the most de-shielded protons were observed for the dimer compound (**40**) with clear symmetry splitting for both protons that are close to the nitrogen bridge and ethoxy groups in ester groups, whereas one de-shielded proton in both keto-ester and aminoisoindoline were observed and three protons appeared in range of 7.67-7.59 for keto-ester (**39**) and at 7.67-7.56 for aminoisoindoline (**37**). Aminoisoindoline compound failed to provide a suitable crystal for x-ray diffraction as it was dimerised and hydrolysed during the recrystallisation. TLC for the product and the keto-ester shows different R_f that makes identification of both product is possible by TLC.
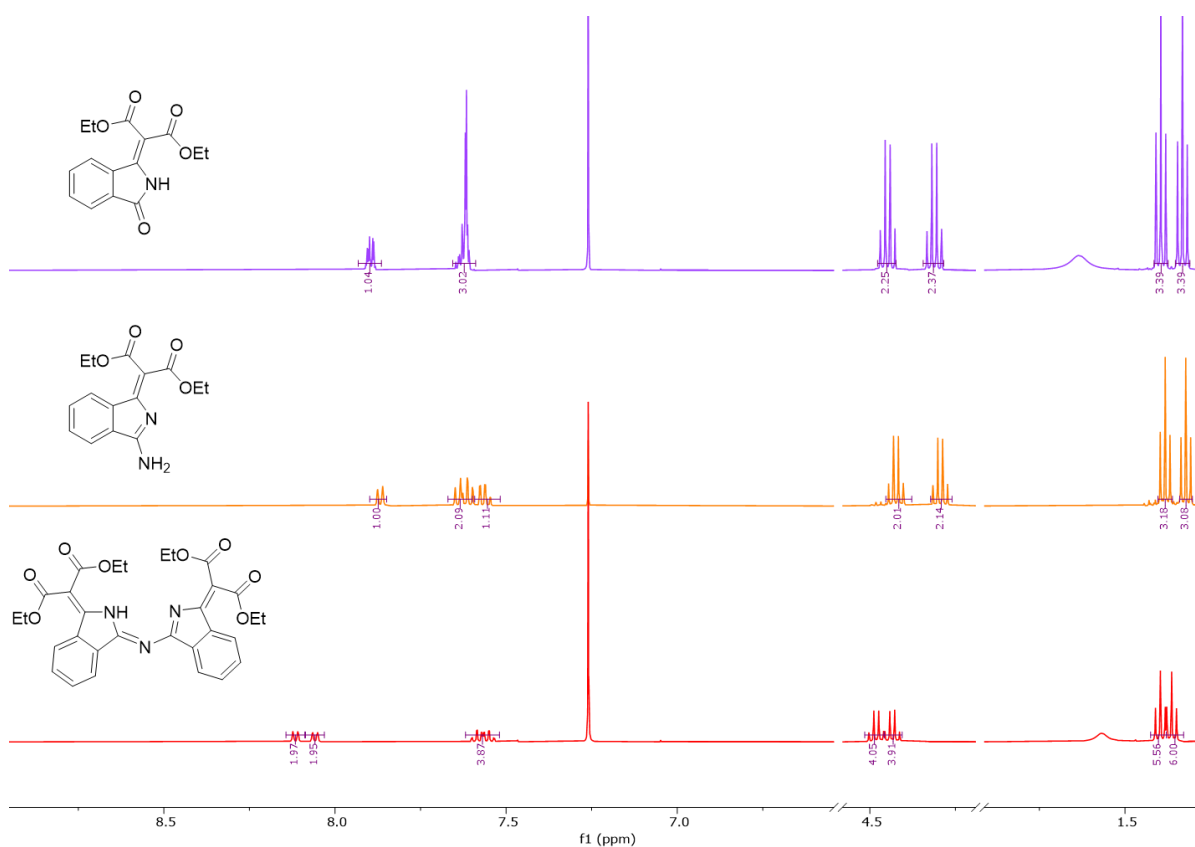
Figure 2.10: ^{1}H NMR spectra of isolated keto-ester (**39**), aminoisoindoline (**37**) and dimerisation product (**40**).

After the successful analysis and purification of malonate aminoisoindoline (**37**) and before we attempted the synthesis of TBMAP hybrid, we deemed it important to prove the structure of the isolated product by investigating its reactivity towards different aminoisoindolines and in this case 4-methoxy phenyl aminoisoindoline (**29**) that was previously prepared. The dimerisation reaction was done using our group's conditions for dimerisation reaction as depicted in scheme 2.14.
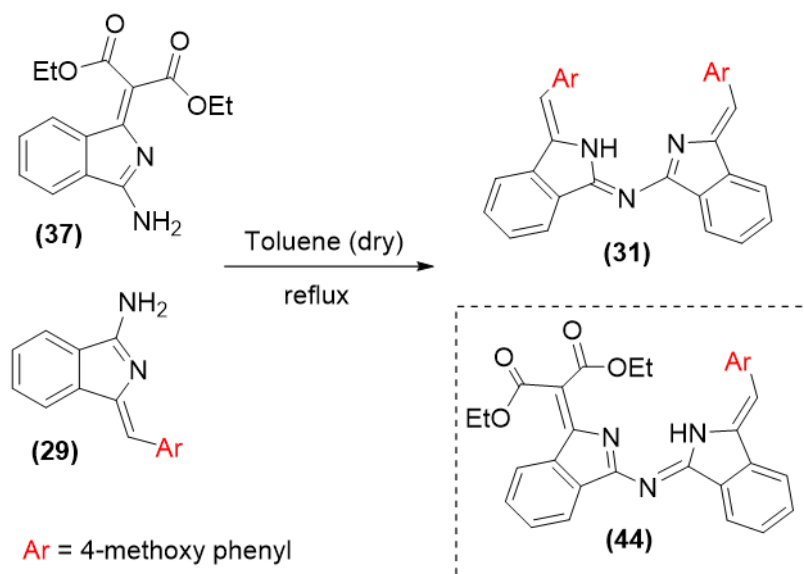
Scheme 2.14: Synthesis of unsymmetrical dimer (**44**).

Unsymmetrical dimerisation compound (**44**) was achieved by straightforward reaction between one equivalent of malonate aminoisoindoline (**37**) with one equivalent of previously prepared 4-methoxyphenylmethylene aminoisoindoline (**29**) in refluxed dry toluene under nitrogen. The reaction was monitored by TLC which resulted in the formation of an intense dark red spot but no signs of completion even after 24-36 hours. Thus, after the mixture was allowed to cool down, the solvent was evaporated under reduced pressure. Initial analysis of the mixture by TLC against the self-dimerisation product of both starting materials that were isolated from previous reactions, indicates that the unknown red spot is 4-methoxyphenyl aminoisoindoline dimer (**31**). However, no sign of malonate dimer was observed, so for certainty, the crude mixture was analysed by MALDI-TOF mass spectrometry which showed a peak around (m/z 523) corresponding to the required dimer (**44**) and the other around (m/z 485) assigning to 4-methoxyphenyl self-dimerisation product (**31**), besides starting materials peaks as shown in figure 2.11.

88
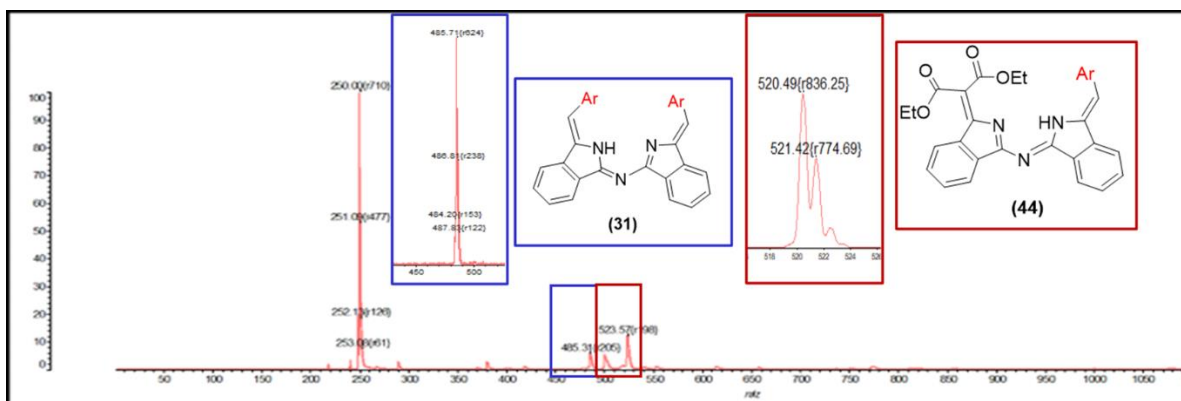
Figure 2.11: MALDI-TOF MS for reaction crude.

This result gives an indication of the overlapping of the two dimers in which the single dark red spot was present in TLC. Many attempts were made using different solvent systems to separate the two spots from each other, but their isolation proves to be challenging due to the small differences in R_f values of them in most solvents. However, the isolation of pure product was successfully achieved when 100:1 PE: DCM was used as a solvent system for the column chromatography to give the desired dimer (**44**) as the dominant product and self-dimerisation product as side-product. When all fractions were analysed by TLC, just the first two fractions and last one fraction were pure, and the rest were mixed. The ^{1}H NMR spectrum of the desired product in deuterated DCM is illustrated in figure 2.12. As expected, all signals for twelve aromatic protons in range from 8.40-7.06 ppm were observed plus the alkene proton that appeared as singlet peak at 7.27 ppm. Also, two quartet signals at 4.49 ppm and 4.37 ppm and two triplets at 1.42, 1.36 ppm that are assigned to CH_2CH_3 in malonate groups and a singlet peak appears at 3.87 ppm that corresponds to methoxy protons are all observed.
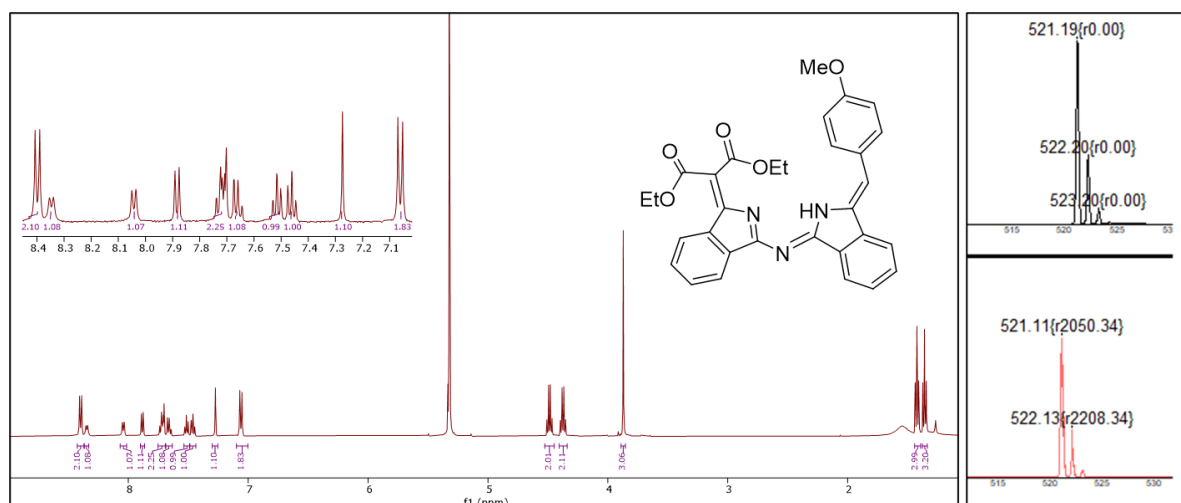
Figure 2.12: ^{1}H NMR spectrum of isolated unsymmetrical malonate-4-methoxyphenyl dimer (**44**) in DCM-d_2 (left) and its MALDI-TOF MS (bottom right) plus theoretical isotopic pattern (top right).

After the successful synthesis of unsymmetrical dimer (**44**) and with the difficulty present during its purification and separation from the symmetrical dimer, different aminoisoindoline with longer aliphatic chain was proposed to perform this reaction with the aim to increase the difference in R_f between the two dimers and reduce the possibility of overlapping, thus, ease its purification process. 4-Pentyloxyphenylmethylene aminoisoindoline (**45**) was chosen to react with malonate aminoisoindoline (**37**) and its synthetic route is depicted in scheme 2.15. Pentyloxyphenyl aminoisoindoline (**45**) was synthesised and purified following the general method of preparation of phenyl aminoisoindoline.[9] Its synthesis was straightforward and gave the desired product (**45**) in high yield 78%.
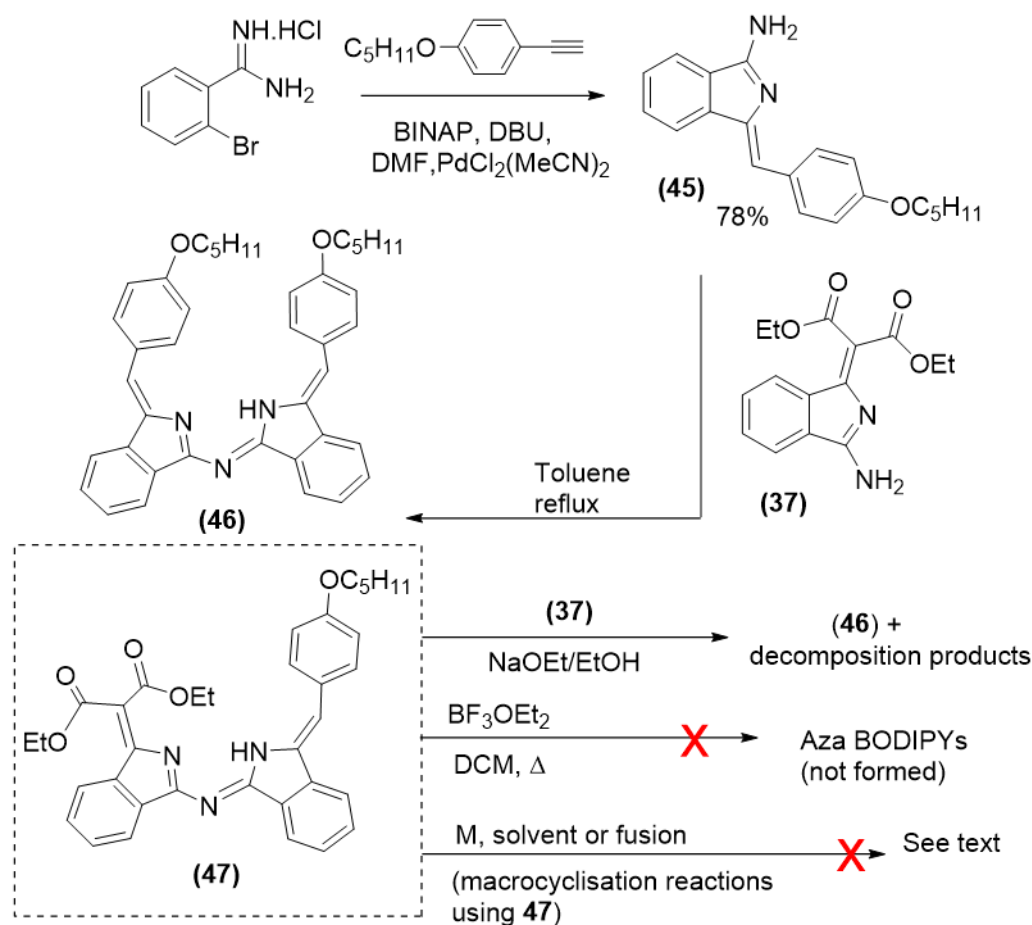
Scheme 2.15: Synthesis route of unsymmetrical dimer (**47**) and its different attempted reactions.

After successful synthesis of (**45**), it was submitted to dimerisation reaction with malonate aminoisoindoline using dry toluene under reflux. As expected, the major product was the unsymmetrical dimer (**47**) and the R_f between the symmetrical (**46**) and the unsymmetrical compounds (**47**) was larger than the previous reaction, so their separation was quite easy, and the two red bands were clearly separate when PE: DCM 100:1 was used as eluent solvent system in column chromatography. The ^{1}H NMR spectrum shown in Figure 2.13 confirms the formation of both 4-pentyloxyphenyl aminoisoindoline (**45**) and its unsymmetrical dimer (**47**). All signals of both products are observed as expected.
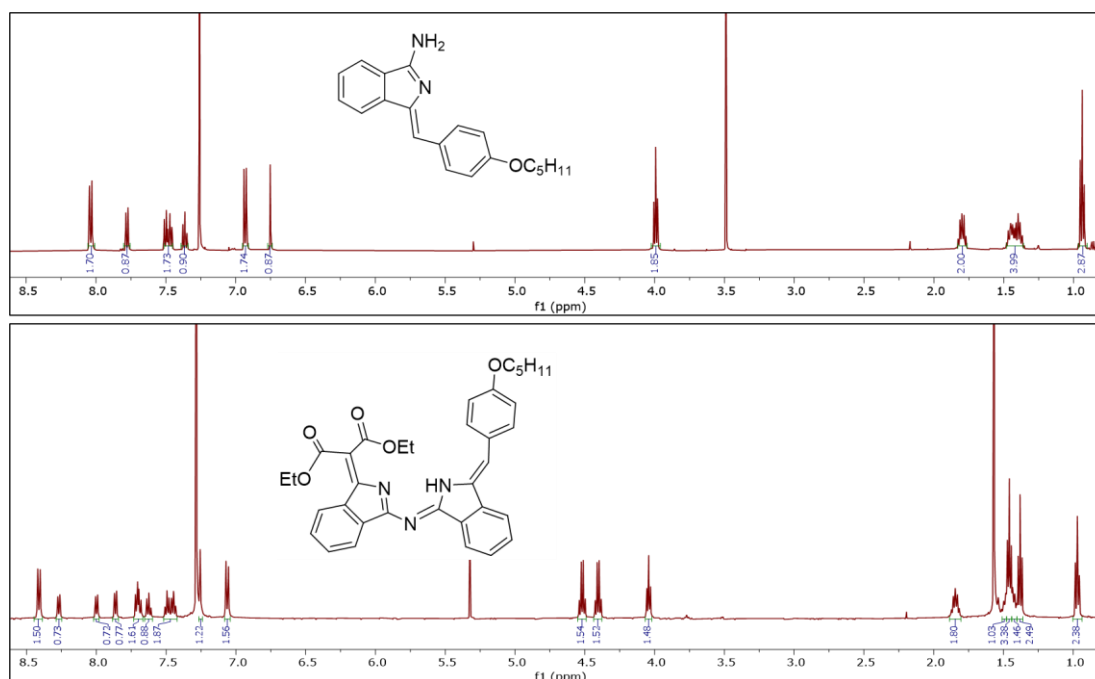
Figure 2.13: ^{1}H NMR spectra of isolated pentyloxy aminoisoindoline (**45**) (top), and unsymmetrical dimer (**47**) (bottom) in CDCl$_3$.

Further confirmation of isolation of the desired dimer (**47**) was accomplished by MALDI-TOF MS with the observation of the molecular ion peak (576.57 m/z). Also, crystals suitable for x-ray diffraction were eventually grown from a mixture of dichloromethane and methanol allowing determination of the solid-state structure as depicted in figure 2.14.
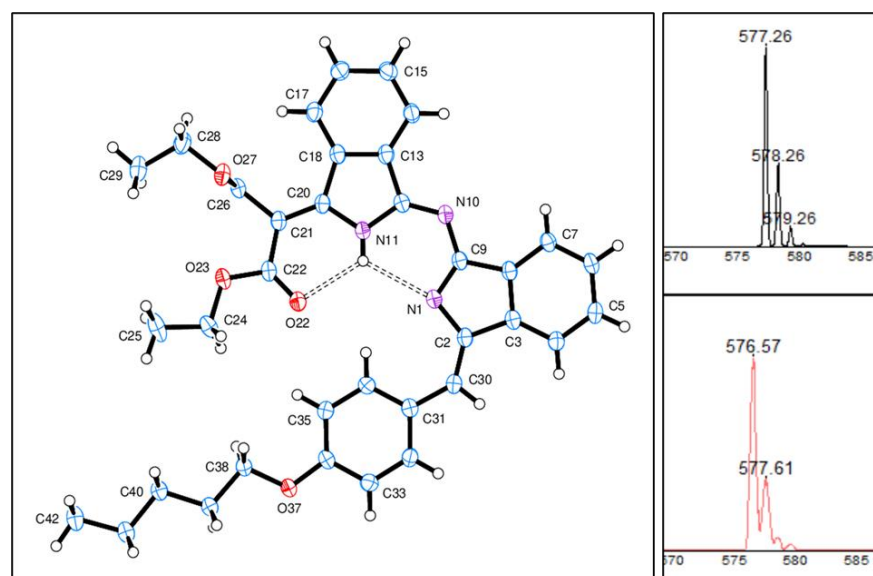
Figure 2.14: X-ray structure of the dimer (**47**) (left) and its MALDI-TOF MS (bottom right) plus theoretical isotopic pattern (top right).

The UV-Vis absorption spectra of both dimers (**44** and **47**) were obtained and shown in figure 2.15. Both dimers are red in color and their absorptions display broad profiles with a visible region maximum at around 515 nm. Also, very broad fluorescence emission peaks for both dimers (**44**) and (**47**) were observed at 625 and 624 respectively.
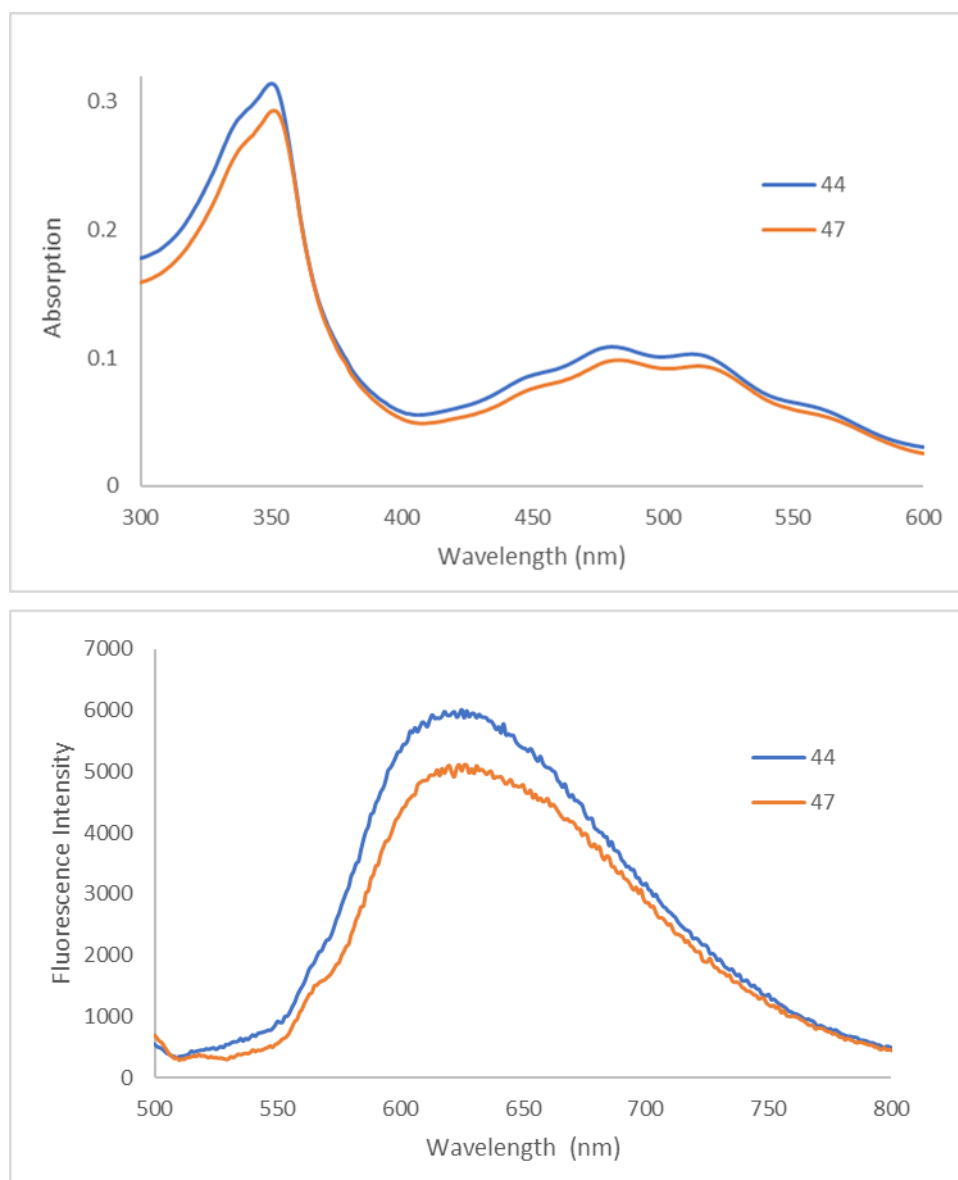
Figure 2.15: UV-Vis spectra (top), and fluorescence spectra (bottom) of unsymmetrical dimers (**44**), (**47**) in DCM.

Once the methodology of purification of malonate aminoisoindoline was optimised and its structure was confirmed by dimerising it with different aminoisoindolines, the investigation of synthesis of TBMAP hybrids was continued. However, it is worth noting that reactions employing dimer (**47**) were also investigated in parallel, but in all cases failed to produce useful products (Scheme 2.15). Briefly, reaction with aminoisoindoline (**37**) produced symmetrical dimer (**46**), decomposition products and recovered (**37**). Attempts to form BODIPY type complexes using BF$_3$ failed (likely due to steric hindrance), and high temperature reactions with various metal templates gave no evidence of macrocyclic products.

With the structure of malonate aminoisoindoline (**37**) confirmed, fusion with zinc dust was to be carried out as illustrated in scheme 2.16. Initially, the one step procedure developed by Linstead was followed in a microwave vial and using a controlled heat gun as the heat source at ~300°C for 20 minutes.[23] However, black insoluble materials were obtained so the reaction was repeated for shorter time (15, 10 and 5 mins) but in all cases black materials were obtained. We thought that the direct constant and extreme heat causes the reaction crude to be burned out, so the reaction was attempted in a pre-heated oil bath at ~ 220°C which is the TBTAP's formation temperature. Green materials were obtained which were washed with hot water and hot ethanol, then filtered off as in the reported procedure. Next, many attempts were made to dissolve the green powder using all available organic solvents in order to analyze it. However, none of the attempted low-boiling solvents dissolved it and it was only slightly soluble in high-boiling solvents such as pyridine and quinoline. No conclusive further analysis can be done due to its insolubility.
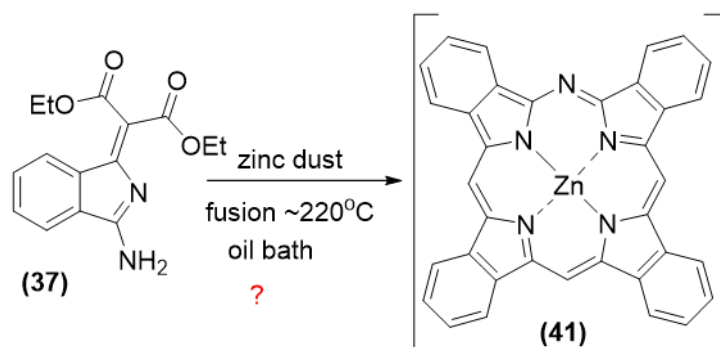
Scheme 2.16: Linstead's proposed reaction scheme for the formation of TBMAP hybrid (**41**).

2.6 Synthesis of 4,5-disubstituted malonate derivatives

At this point it was decided to introduce peripheral substituents on malonate derivative in order to enhance the solubility of the final product and then ease its analysis and purification (scheme 2.17). Preparation of zinc peripherally octa-substituted tetrabenzomono-azaporphyrin derivatives (TBMAPs) could theoretically be achieved through the formation of 4,5-dialkylsubstituted phthalonitrile unit which can be obtained via several synthetic routes that already have been reported in the literature and a variety of substituents have been attempted in our group. Some limitations of their syntheses have been reported such as low yield of phthalonitrile due to formation of mono-cyano product and other unwanted side-products that makes their purification difficult.
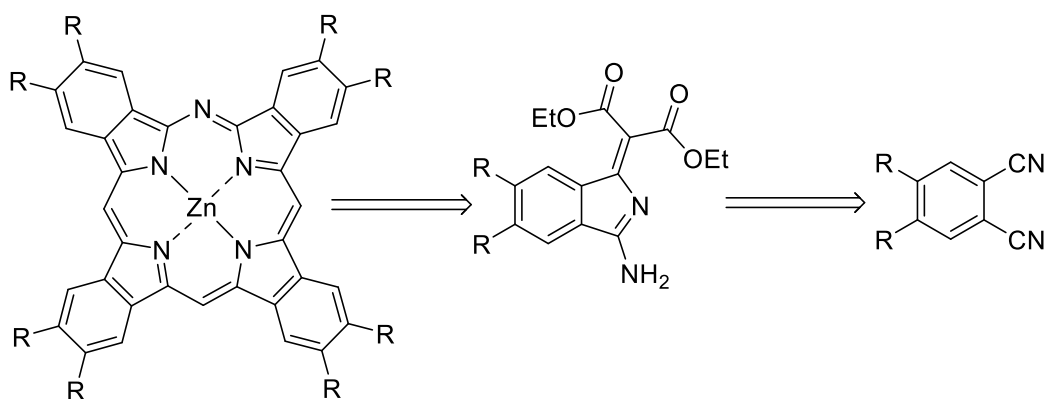
Scheme 2.17: Retrosynthetic route of target ZnTBMAP via required 4,5-dialkylmalonate aminoisoindoline and phthalonitrile precursors.

Alicyclic alkyl substituted phthalonitrile (**52**) was chosen to start with because of its easy synthetic route and its simple purification. As shown in scheme 2.18, the synthesis of 6,7-dicyano-1,1,4,4-tetramethyltetralin (**52**) starts with the conversion of the 2,5-dimethylhexane-2,5-diol into its corresponding dichloride (**48**) using concentrated hydrochloric acid.[25–28] This reaction was done in an ice bath for 30 mins and then was left at room temperature overnight. Then, the precipitate was filtered off and washed with water and extracted with DCM. The organic material was concentrated and recrystallised from methanol to give the product in a good yield. Characterisation by ^{1}H NMR spectroscopy confirmed the structure of the desired product. The second step was achieved using Bruson's procedure via Friedel-Crafts reaction.[26] The reaction involved the condensation of 2,5-dichloro-2,5-dimethylhexane (**48**) with benzene at 50°C in presence of anhydrous aluminum chloride. When the reaction was completed, diluted HCl was added, and the resulting

material was extracted with DCM and washed with diluted sodium carbonate and then dried using magnesium sulphate. If the mixture had some of the side-products (**50**), washing with methanol was needed as it precipitates the side-product and left the desired product (**49**) dissolved in methanol. The solvent was removed, and a quick column chromatography was used to get rid of benzene using PE as an eluent solvent.
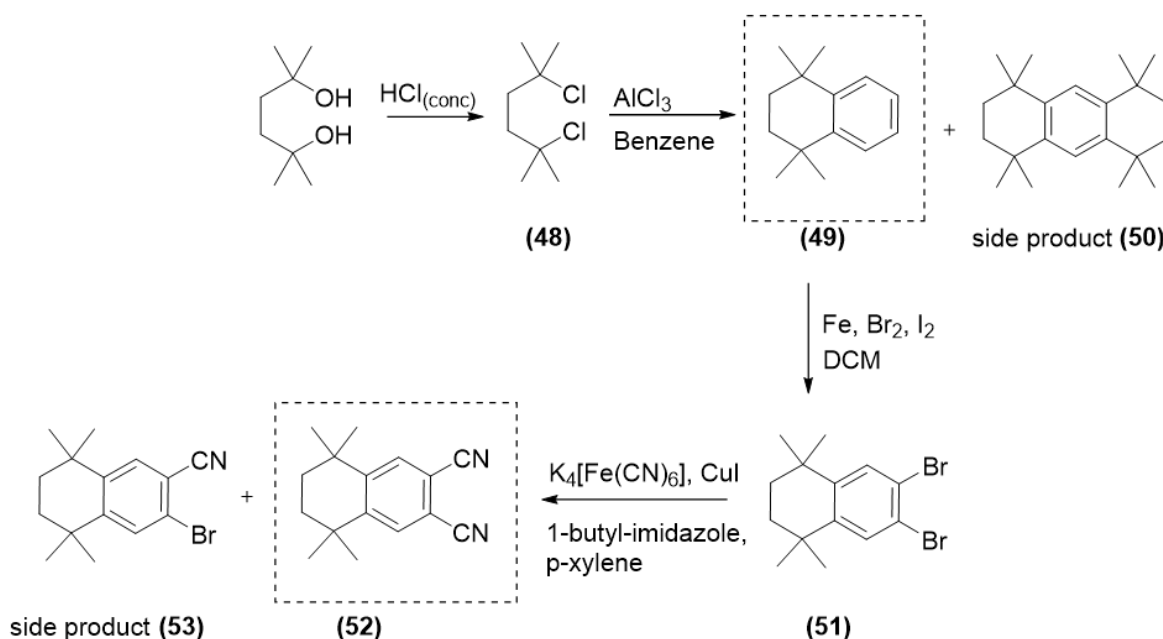
Scheme 2.18: Synthetic routes towards 4,5-disubstituted phthalonitrile (**52**).

The next step involved the bromination of 1,1,4,4-tetramethyl-1,2,3,4-tetrahydronaphthalene (**49**) using the method described by Ashton and co-workers.[29,30] A mixture of the compound with iodine and iron powder was dissolved in DCM and the mixture was cooled to 0°C. Bromine was added dropwise over 30 mins, and the mixture was left to stir at room temperature overnight. The full consumption of starting material can be monitored by NMR spectroscopy as the starting material and the product has similar R_f. After working-up and washing several times by an aqueous solution of sodium metabisulfite and sodium bicarbonate to remove the excess of bromine, the product (**51**) was purified using column chromatography with PE as eluent. Next, the final step is the cyanation reaction that was done using non-toxic anhydrous potassium hexacyanoferrate (II) $K_4[Fe(CN)_6]$, 1-butylimidazole as a ligand, copper iodide as catalyst, p-xylene as solvent.[31] The mixture was stirred under N_2 at 160°C for 4-6 days until complete consumption of starting material was

observed by TLC. After working up, the crude product was purified by column chromatography to yield the desired product (**52**) in a good yield.
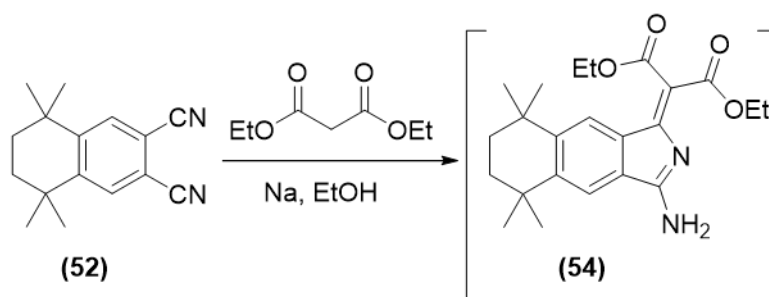
Scheme 2.19: Synthesis of alicyclic alkyl substituted malonate aminoisoindoline (**54**).

With a reasonable amount of phthalonitrile (**52**) in hand, the reaction with malonate ester and sodium ethoxide was carried out as shown in scheme 2.19.[24] The reaction was followed by TLC, and it indicates a full consumption of starting materials and formation of new yellow baseline spot on the TLC which usually indicates the formation of the aminoisoindoline. Also, the resulting crude was analysed by MALDI-TOF mass spectrometry before any purification had been done, and it showed a peak (m/z 397.60) corresponding to the required compound (**54**) (figure 2.16).
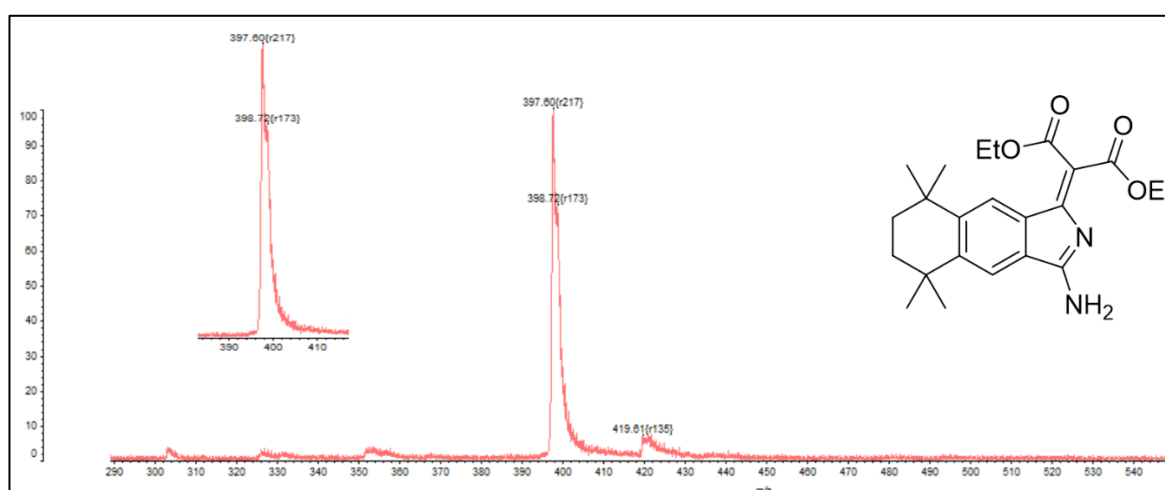
Figure 2.16: MALDI-TOF- MS of crude reaction mixture of alicyclic alkyl substituted AA (**54**).

It was observed that the product was decomposed during the work-up and purification process and no sign of the product or dimer or keto-ester has been observed either by TLC or MALDI mass spectrometry. The reaction and purification were repeated many times with more precautions in order to avoid decomposition and get the product in solid state but none of the attempts were successful and complicated mixtures were obtained and even when the reaction was put directly in the fridge or in dry ice bath to crystallise the product, the decomposition still occurred. Also, the reaction and purification were attempted in the dark as we thought it might be a light-sensitive compound but still decomposition of the product could not be avoided. After all these failed attempts, it was concluded that the observation of relatively instability of this aminoisoindoline toward different purification conditions might be due to the high steric hinderance effect between the attached alicyclic alkyl substituent and malonate chain. The failure of this reaction, towards the isolation of the required aminoisoindoline focused our attention on alternative substituents which present no steric crowding towards malonate chains and in this case methoxy group was chosen to keep the final structure simple.

As shown in scheme 2.20, the synthetic route starts with a simple bromination of commercially available veratrole (**55**) in DCM at 0°C.[32,33] Bromine was added slowly and when the addition was completed the reaction mixture was left to stir at r.t. for an hour. Then, the mixture was extracted with sodium thiosulfate or sodium metabisulfite to get rid of the excess of bromine, and finally extracted with brine solution and dried over magnesium sulphate. The desired product (**56**) was recrystallised using 2-propanol. Cyanation of dibromo-veratrole (**56**) was easily achieved following the reported procedure by the Rosemund-von Braun reaction that uses CuCN as a cyanide source.[34] Although the toxicity of CuCN and the difficulty of the isolation of the product (as there are several side products in this reaction with small difference in R_f), this reaction gave higher yield of the desired product compared to non-toxic anhydrous potassium hexacyanoferrate (II) conditions that were used previously. It is important in this reaction to control the temperature as copper phthalocyanine can be formed if the reaction temperature is above 153°C. The reaction was completed within 3-4 hours. Then, DCM was added, and copper salts were filtered off and the filtrate was washed several times with ammonia solution until no blue color was observed. Column chromatography was used to isolate the desired product (**57**) as the third fraction after the unreacted S.M and monosubstituted nitrile (**58**). All fractions are colourless

and close to each other, so a slow solvent system is recommended and collection in small fractions was needed to isolate the pure product as white solid.
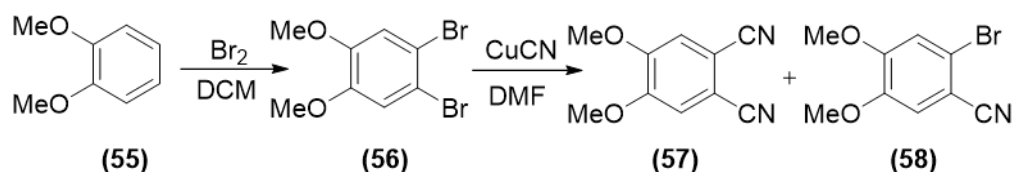
Scheme 2.20: Synthesis of dimethoxyphthalonitrile (**57**).

After a successful synthesis of 4,5-dimethoxyphthalonitrile (**57**), this phthalonitrile was submitted to the next step which involves its reaction with sodium ethoxide and diethyl malonate using the same conditions that were optimised previously (scheme 2.21). The S.M was completely consumed and gave just a yellow spot on the baseline that corresponded to the desired product (**59**). The solvent was evaporated under reduced pressure immediately to avoid dimerisation and hydrolysis of the product and the purity of the compound was checked by TLC. However, formation of keto-ester and self-condensed product was observed after the evaporation of the solvent, so column chromatography was needed to isolate the product (**59**) from keto-ester (**60**) and self-dimerisation product (**61**).
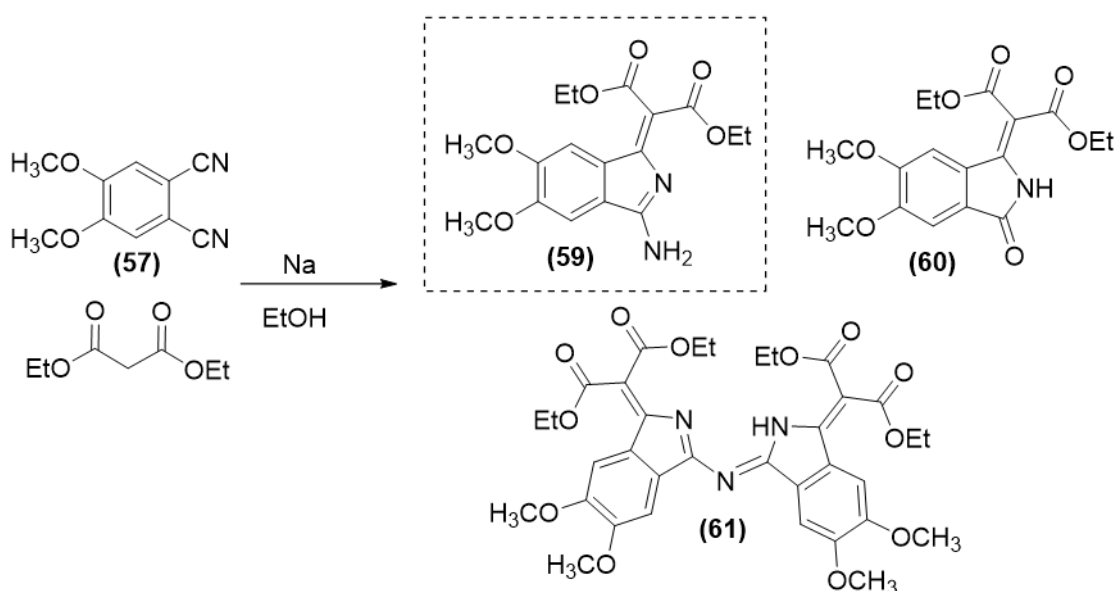
Scheme 2.21: Synthesis of 1-imino-3-dicarbethoxymethylene- 6,7 -dimethoxy isoindoline (**59**).

The product (**59**) was analysed by ^{1}H NMR spectroscopy in deuterated chloroform which gave all expected signals as illustrated in figure 2.17. Two aromatic singlets were observed for the two aromatic protons, and two singlet peaks at 3.93 and 3.87 ppm were assigned to the six protons on the methoxy groups. Also, two quartets of CH_2 in malonate group were at 4.36 and 4.23 ppm and two triplets for CH_3 in malonate were at 1.35 and 1.27 ppm. Also, the product was analysed by MALDI-TOF mass spectrometry and gave a molecular ion peak at (348.82 m/z) as expected. Both keto-ester (**60**) and self-condensed products (**61**) were isolated during the purification process and full analysis of them was successfully obtained. The x-ray structure of keto-ester compound is illustrated in figure 2.18.
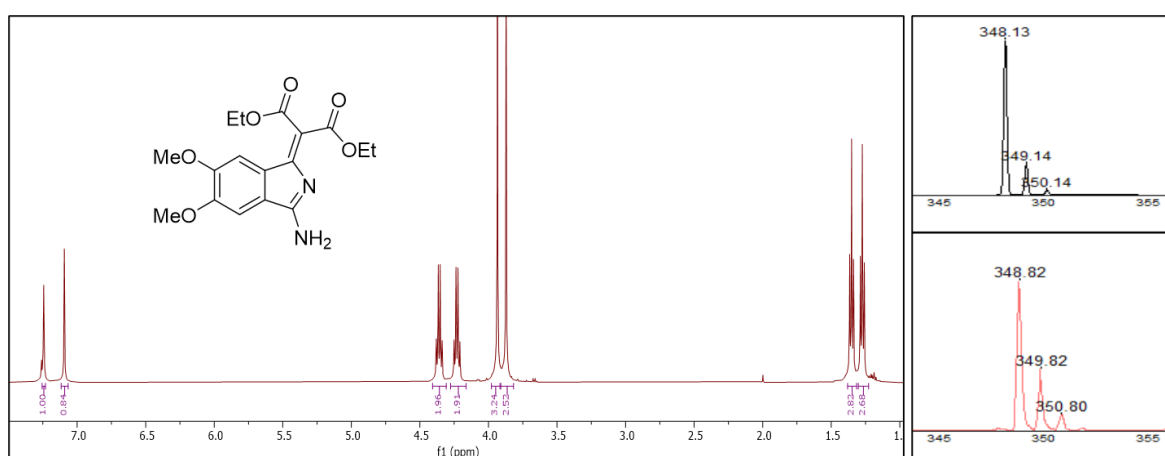
Figure 2.17: ^{1}H NMR spectrum of 4,5-dimethoxy malonate aminoisoindoline (**59**) in CDCl$_3$ (left) and its MALDI-TOF MS (bottom right) plus theoretical isotopic pattern (top right).
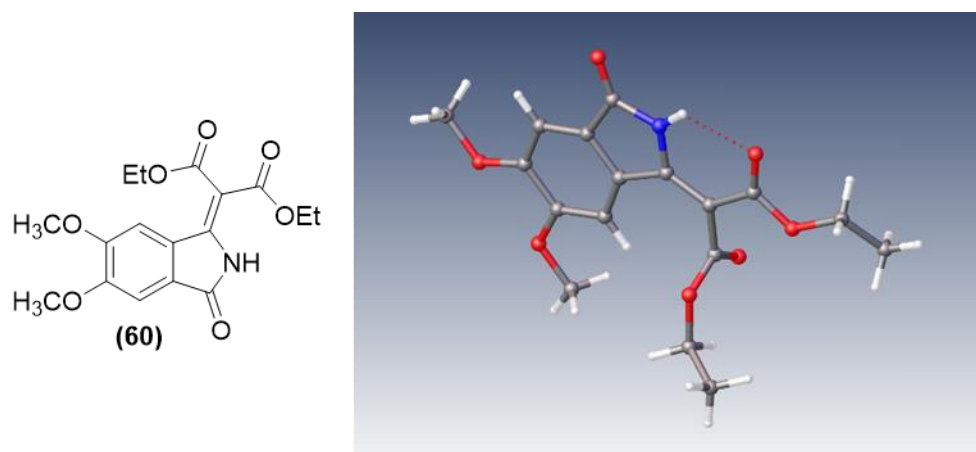
Figure 2.18: Preliminary x-ray structure of keto compound (**60**)

With our 4,5-dimethoxy malonate aminoisoindoline (**59**) in hand, we performed the macrocyclisation fusion reaction using the same conditions that were optimised previously. In a pre-heated oil bath at 220°C, a mixture of aminoisoindoline (**59**) and zinc powder was fused as depicted in scheme 2.22. The reaction was monitored by TLC until all aminoisoindoline was consumed. The crude was left to cool down to room temperature. Then, a mixture of DCM: THF was added, and the mixture was sonicated and filtered through a pad of silica to remove zinc dust and salts.
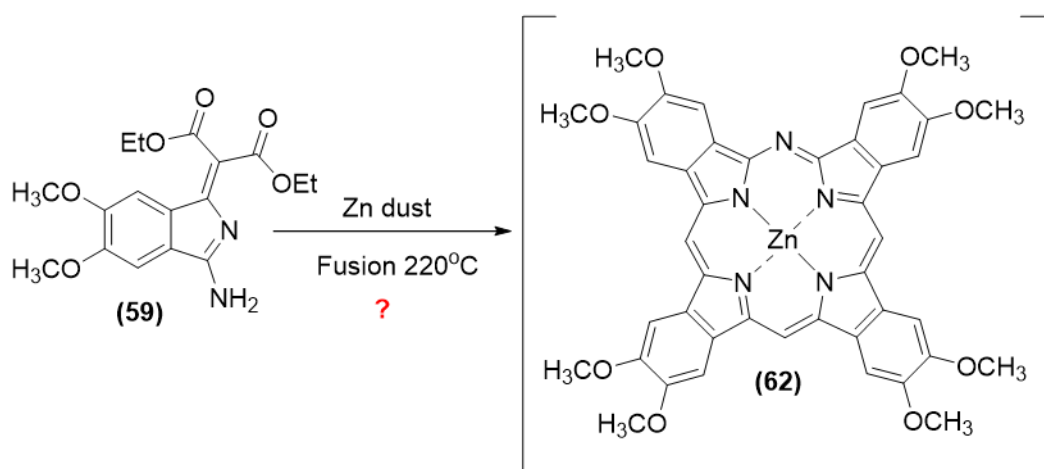
Scheme 2.22: Attempted synthesis of zinc octa-methoxy TBMAP hybrid (**62**).

It was found that the crude was very soluble in high polarity organic solvents unlike the product mixture from unsubstituted phthalonitrile, and it gave only one green band in the TLC plus brown materials. The mixture was dissolved in DCM and filtered through Celite®. The brown fraction was collected. Then, THF was added to collect the green fraction. Then, the green fraction was analysed by MALDI-TOF mass spectrometry that gave three clusters of peaks around (m/z 816.22), (m/z 887.19) (**65**) and at (m/z 958.18) (**66**); the structures are tentatively given in figure 2.19. This result indicates the presence of acetyl groups in the *meso*-position in second and third molecular mass to match the observed signals. However, the formation of the expected product (**62**) was not observed in MALDI-TOF MS.

Hypothesized Structures			
Exact mass	C= 815.17 (TBTAP) (**63**) N = 816.16 (Pc) (**64**)	887.19 (**65**)	958.22 (**66**)
Observed mass	816	887	958
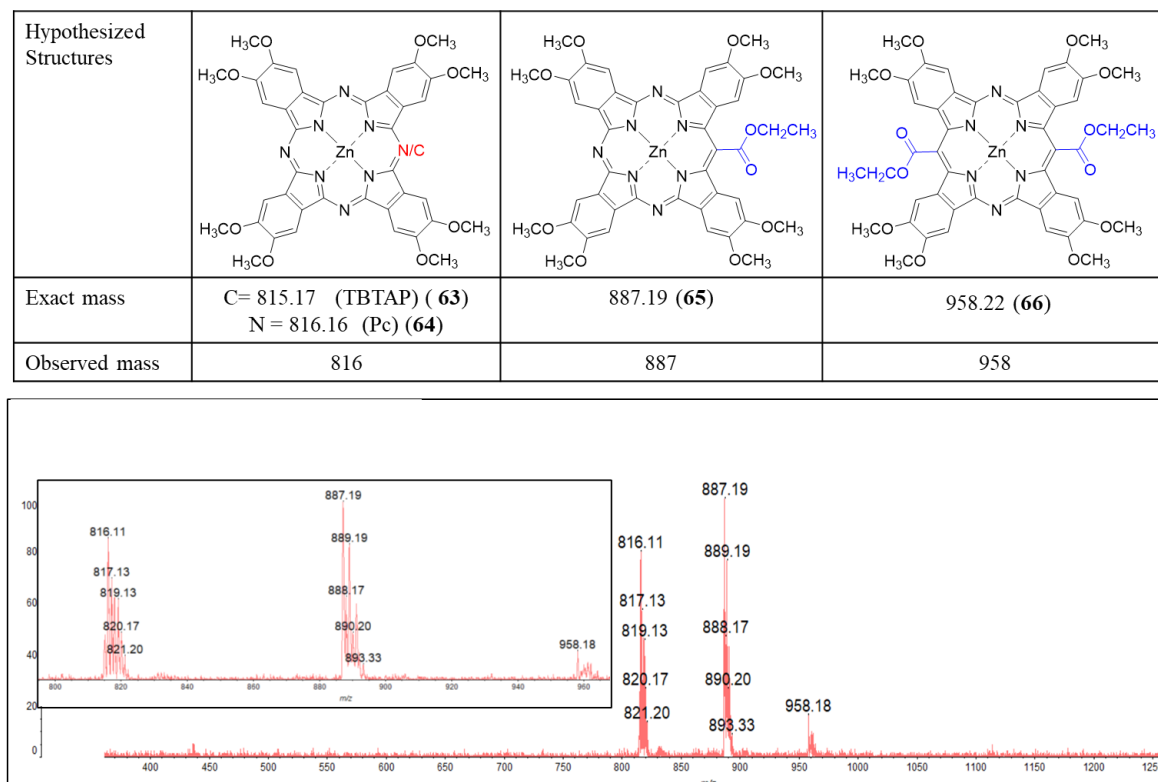
Figure 2.19: MALDI-TOF MS of green fraction and the hypothesised structures with the exact mass (top).

Thus, the green band consists of more than one product, it seems three different compounds, but we cannot be certain as the difference between CH bridge and N bridge is one atomic mass unit. Also, all compounds do not give the exact molecular ion peaks in the MALDI-TOF mass spectrum when just one nitrogen bridge is hypothesised for the structure. In all peaks, there were two more atomic mass units than the expected mass which gives an indication of more nitrogen bridges present in the crude. Many attempts have been made to isolate the green band but none of them were successful. When a slow solvent system was used none of the green products moved and when the polarity of the eluent was increased, a mixture was obtained. In some cases, two different green bands were observed but when they were collected in small tubes and were checked by the MALDI, all molecular ion peaks were presented. An observation of slow decomposition occurred during purification of the sample by getting lighter colour until we ended up with almost colourless fractions. The reaction was repeated many times in attempts to isolate the products and be more cautious to avoid decomposition as the mixture might be light-sensitive. The crude was submitted to preparative thin layer chromatography in the dark but just a small quantity of pure (**65**) was isolated as a very light green band and no more green bands were observed. The isolated

product was checked by UV-vis spectroscopy and gives a clear splitting pattern as expected for TBTAP as depicted in figure 2.20. Also, MALDI-TOF MS was used to check the isotopic pattern and whether it matched the expected pattern of TBTAP with one acetyl group attached at *meso-* position; it completely matched to the expected isotopic pattern.
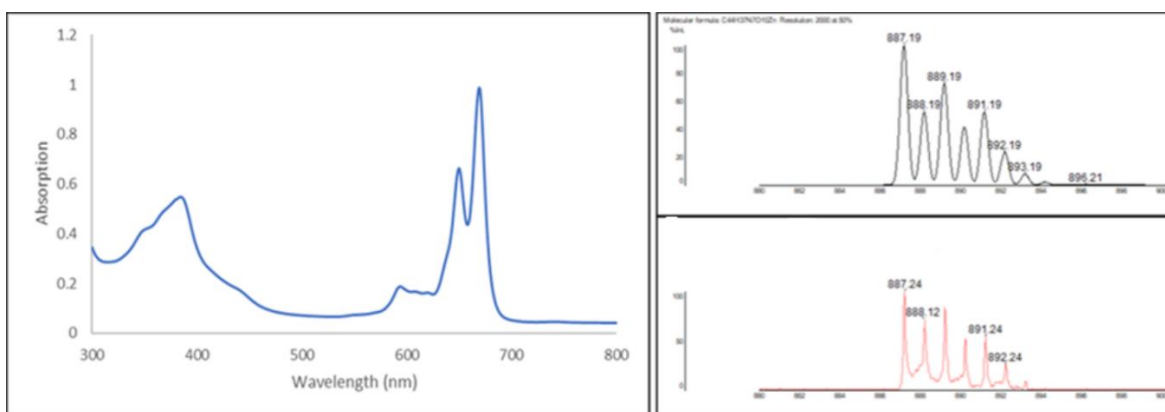
Figure 2.20: UV-vis spectrum of the isolated compound (**65**) and its its MALDI-TOF MS (bottom right) plus theoretical isotopic pattern (top right).

The reaction was repeated many times and left for longer time with the aim to remove the acetyl group and avoid its formation, but no differences were observed. Many attempts were made to isolate the compound with the molecular mass of 816 m/z to identify whether it is ZnTBTAP (**63**) or zinc phthalocyanine (**64**) but without success. The isotopic pattern of this compound was checked against both compounds but did not match either of them exactly, as illustrated in figure 2.21. A mixture of the two compounds fits this data.
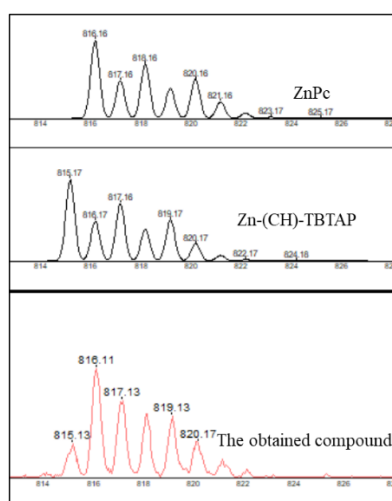
Figure 2.21: Comparison of isotopic pattern of the unknown compound against theoretical pattern of Zn (CH) TBTAP and ZnPc.

The low-solubility of the obtained crude might be the reason behind the slow-decomposition of the products during their isolation. The physical and chemical properties of hybrids are influenced by the nature of the substituents. Therefore, the focus was redirected towards long-chain 4,5-dialkoxy phthalonitrile due to its potential to facilitate the formation and isolation of the hybrids, in contrast to dimethoxy phthalonitrile. In general, 4,5-dialkoxy phthalonitrile can be synthesised by bromination of commercially available catechol (**67**), followed by simple alkylation reaction using potassium hydroxide and 1-bromohexane in DMSO to produce 1,2-dibromo-4,5-dihexyloxy benzene (**69**). Then, the final step is the cyanation reaction under the same conditions described above for dimethoxy phthalonitrile with a careful control of reaction temperature and time to avoid formation of CuPc (scheme 2.23). The desired product (**70**) was isolated by column chromatography after the work-up and its structure was checked by NMR spectroscopy.
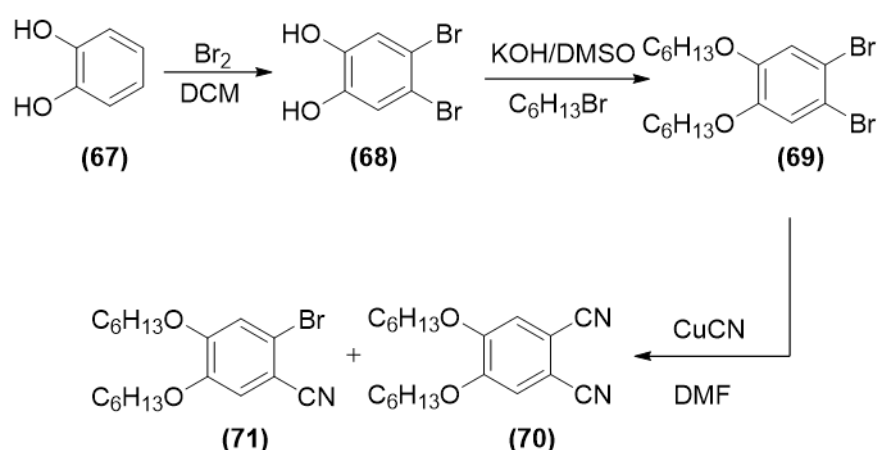
Scheme 2.23: Synthesis of 4,5-dihexyloxyphthalonitrile (**70**).

The synthesis of 4,5-dihexyloxy malonate aminoisoindoline (**72**) was attempted using the same previous conditions as illustrated in scheme 2.24. After completion of the reaction was observed by TLC against starting material spot, the solvent was evaporated under reduced pressure and at room temperature and the solid was dissolved in DCM and filtered through a pad of Celite® and washed with EtOAc to collect the baseline material. Then, the solvent was evaporated to give the desired product (**72**) as yellow solid. Many attempts to recrystallise the compound were unsuccessful and unwanted dimerisation occurred alongside keto-ester formation.
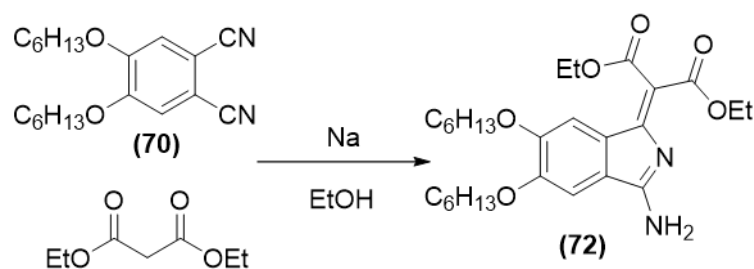
Scheme 2.24: Synthesis of 4,5-dihexyloxy malonate aminoisoindoline (**72**).

The ^{1}H NMR spectrum of both starting materials and isolated aminoisoindoline are illustrated in figure 2.22. In phthalonitrile (**70**) spectra, one singlet aromatic signal is seen corresponding to two benzene protons, whereas in aminoisoindoline (**72**) spectra two singlet peaks are observed due to low symmetry structure. Also, all hexyloxy proton peaks were observed as expected in both spectra besides malonate proton peaks in aminoisoindoline spectrum. Moreover, the isotopic patterns of malonate aminoisoindoline matched its theoretical prediction in MALDI-TOF MS.
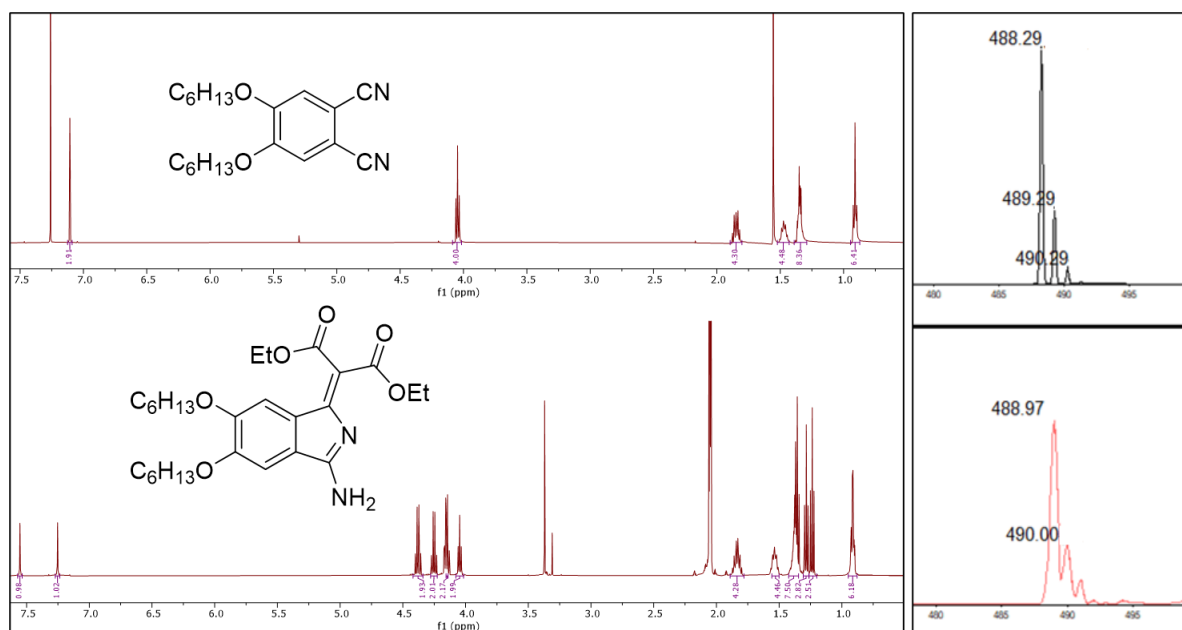
Figure 2.22: ^{1}H NMR spectra of 4,5-dihexyloxy phthalonitrile (**70**) in CDCl$_3$ (top) and 4,5-dihexyloxy malonate aminoisoindoline (**72**) in acetone-d_6 (bottom) and its MALDI-TOF MS (bottom right) plus theoretical isotopic pattern (top right).

After successful synthesis and purification of 4,5-dihexyloxy malonate aminoisoindoline (**72**), the fusion reaction was performed under the same conditions that were used for the dimethoxy analogue, as illustrated in scheme 2.25. The reaction was monitored by TLC to ensure a full consumption of the starting material. Then, the crude was dissolved in DCM, sonicated, and filtered through a pad of silica to remove zinc powder. Unlike the methoxy compound, the crude was very soluble in DCM and most organic solvents. TLC gave a green band and brown baseline. The green band was isolated by preparative thin layer chromatography and was analysed by MALDI-TOF mass spectrometry.
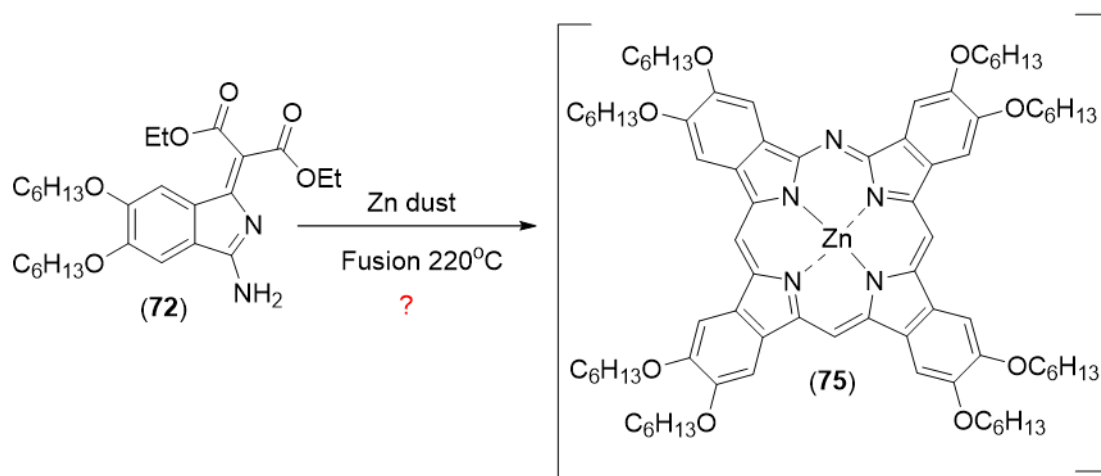
Scheme 2.25: Fusion of 4,5-dihexyloxy malonate aminoisoindoline (**72**).

As illustrated in figure 2.23, three different molecular ion peaks were observed which is similar to the results that were obtained in dimethoxy aminoisoindoline reaction. However, the observed mass is two units more and might be due to calibration failure in MALDI-TOF MS. The separation of the obtained hybrids was not successful as a fast decomposition of the crude was observed and light yellow/brownish material was obtained that does not give any identifiable molecular mass peaks in the MALDI-MS. The replacement of the methoxy group by longer chain increased the solubility of the crude which also increased its instability in solution and toward light.

Hypothesized Structures			
Exact mass	C= 1375.79 (TBTAP) (**76**) N = 1376.79 (Pc) (**77**)	1447.82 (**78**)	1518.84 (**79**)
Observed mass	1377.22	1449.20	1520.30
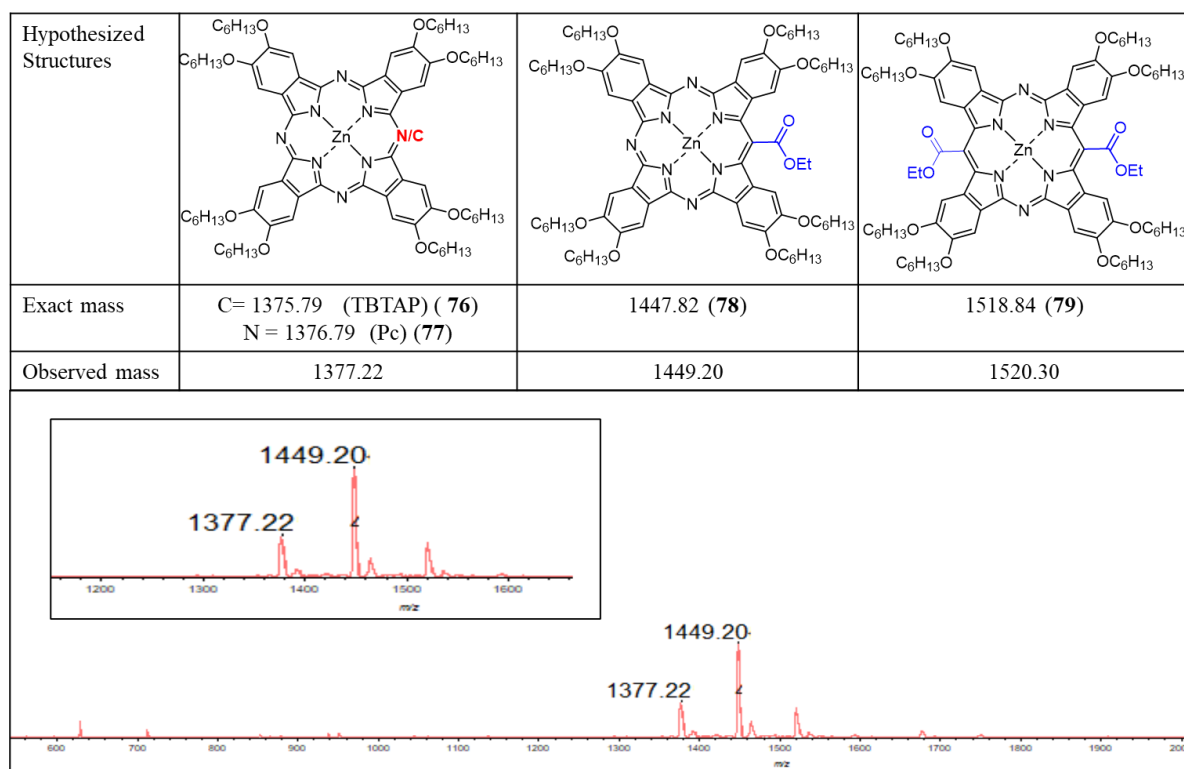
Figure 2.23: MALDI-TOF MS of green band of fusion of 4,5-dihexyloxy malonate aminoisoindoline.

2.7 Applying Linstead's conditions on our reactant

Despite unclear results that we obtained when Linstead's method was applied, formation of green materials with molecular weights that clearly correspond to macrocycles gave us an idea to apply the reaction conditions on our proposed reactants that gave no hybrids under TBTAP's condition.

2.7.1 Fusion of aminoisoinoline (29) with acetylene (32)

The first attempt was fusion of 4-methoxy aminoisoindoline (**29**) and 4-methoxy phenyl acetylene (**32**) and excess of zinc dust at controlled temperature of 220°C in pre-heated oil bath as shown in scheme 2.26.
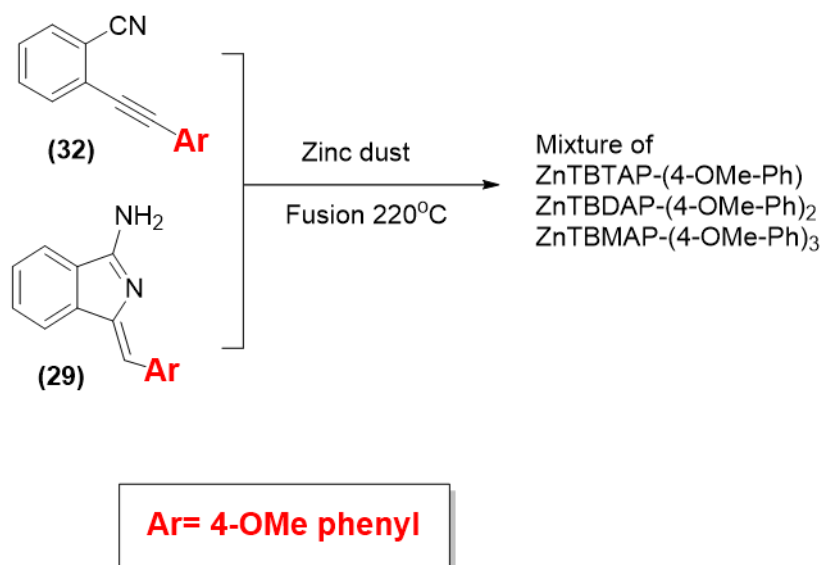
Scheme 2.26: Applying Linstead's reaction conditions on a reaction between aminoisoindoline (**29**) and cyanophenyl acetylene (**32**).

There was a visible color change, from colourless to deep green colour of the reaction mixture after heating for three hours, unlike the originally employed TBTAP's conditions, so this was a promising sign of hybrid formation. The reaction was monitored by TLC until no yellow baseline of the aminoisoindoline was observed. It was obvious that the crude mixture was partially soluble in DCM but highly soluble in polar solvents such as THF so a mixture of DCM: THF 1:1 was added to the crude after it was cooled down to room temperature, and the mixture was sonicated and filtered through a pad of silica to remove zinc powder and salts. Then, the crude was analysed by TLC and different solvent systems were attempted as eluent. It was found that the green band is clearly more than one compound when using PE: DCM: THF 30:10:0.1 as eluent.

The crude was analysed by MALDI-TOF mass spectrometry to gain a better indication of hybrid types that were formed. As illustrated in figure 2.24, there is no sign of TBMAP formation. However, there are two interesting molecular ion peaks at (m/z 682.20) and (m/z 786.72) that correspond to two or three possible macrocycles: Zn-TBTAP-(4-OCH$_3$ phenyl) (**80**), cis and/or trans Zn-TBDAP-(4-OCH$_3$ phenyl)$_2$ (**81, 82**) respectively.

Hypothesized Structures Ar = 4-OCH3- Phenyl	(83)	(80)	(81) (82)
Exact mass	378.15	681.13	786.17
Observed mass	376.91	682.20	786.72
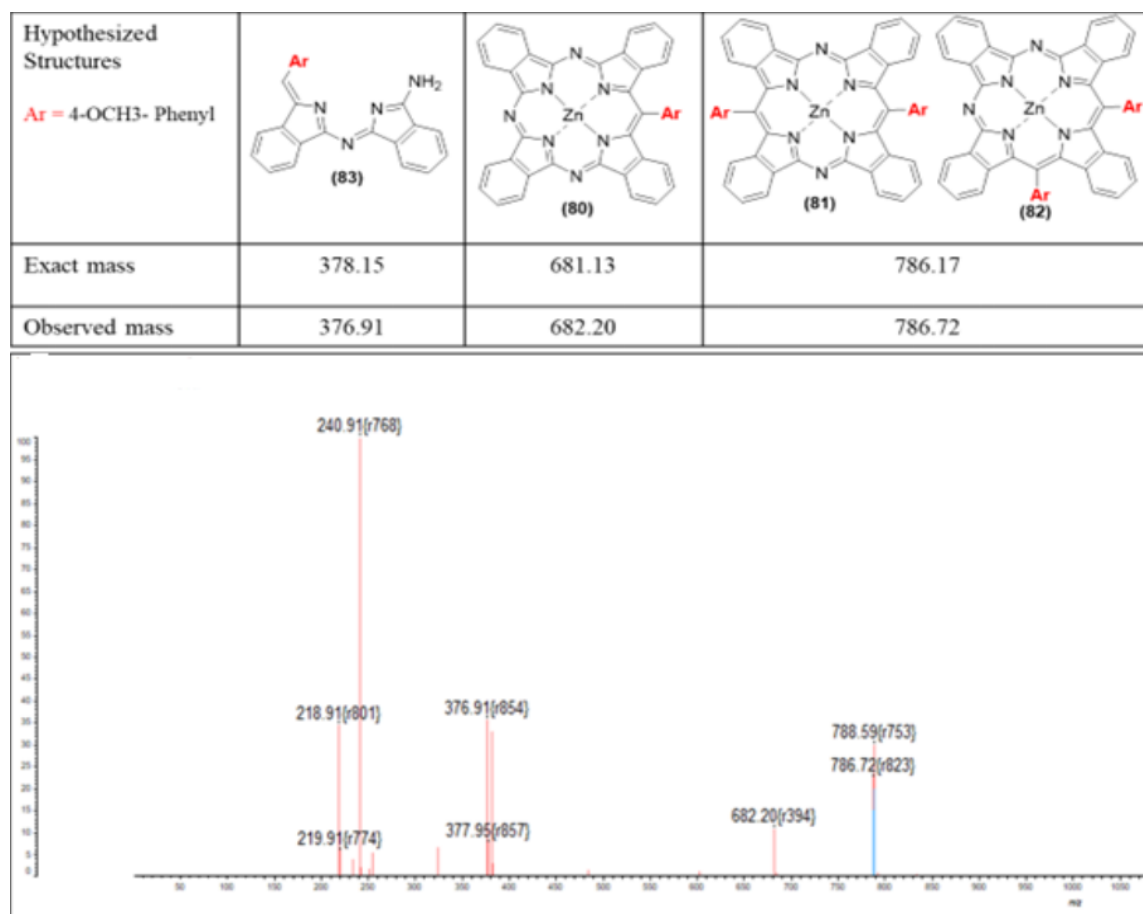
Figure 2.24: MALDI-MS of the crude of the reaction with the hypothesised structures.

Also, there is an interesting molecular ion peak at (m/z 377.95) that might give an indication of formation of intermediate compounds during the cyclisation. After analysis of possible intermediates that might be formed under this condition, unsymmetrical aminoisoindoline dimerisation compound (**83**) has the same molecular mass. This intermediate species was selectively synthesised in our group through a reaction between one equivalent of aminoisoindoline with one equivalent of phthalonitrile (its formation mechanism is illustrated in scheme 2.27). However, by looking at our reactant and without the presence of phthalonitrile, it is not possible to get this intermediate by the reaction between the two reactants and the only likely reactant that might give this intermediate is the aminoisoindoline. It appears that the aminoisoindoline underwent a homo-condensation reaction but at different attack position as illustrated in scheme 2.27 with elimination of one phenyl group.
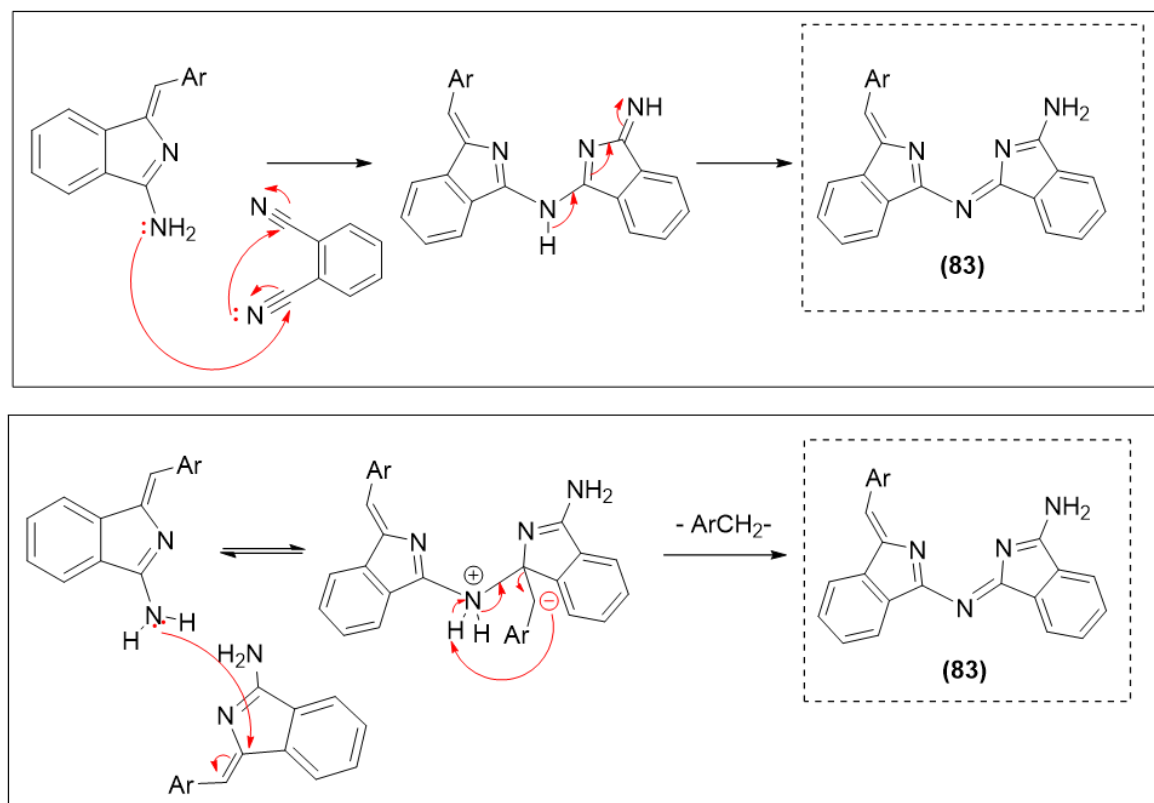
Scheme 2.27: Structure of dimer (**83**) that forms during fusion of aminoisoindoline (**29**) with cyanophenyl acetylene (**32**) and its selective synthesis route (top) and its hypothesised mechanistic formation in fusion reaction (bottom).

Although there is no sign of formation of the desired TBMAP hybrid, this outcome is still interesting to analyse. However, our choice of reactants means it is unclear whether these hybrids were formed from cyclisation of both reactants or one of them (the MeO-Ar fragment is present in both). Thus, the reaction was repeated with the need to change one reactant.

2.7.2 Fusion of 4-pentyloxy phenyl aminoisoindoline (45) with 4-methoxy phenyl acetylene (32)

4-Pentyloxyphenyl aminoisoindoline (**45**) with longer aliphatic chain was chosen to be a co-reactant with 4-methoxy phenyl acetylene (**32**). The fusion was performed as usual as illustrated in scheme 2.28. The reaction was followed by TLC until all aminoisoindoline was consumed. After the reaction cooled down, a mixture of DCM: THF 1:1 was added, and the mixture was sonicated and filtered through a pad of silica to remove zinc dust. Then, the solvent was removed under reduced pressure.
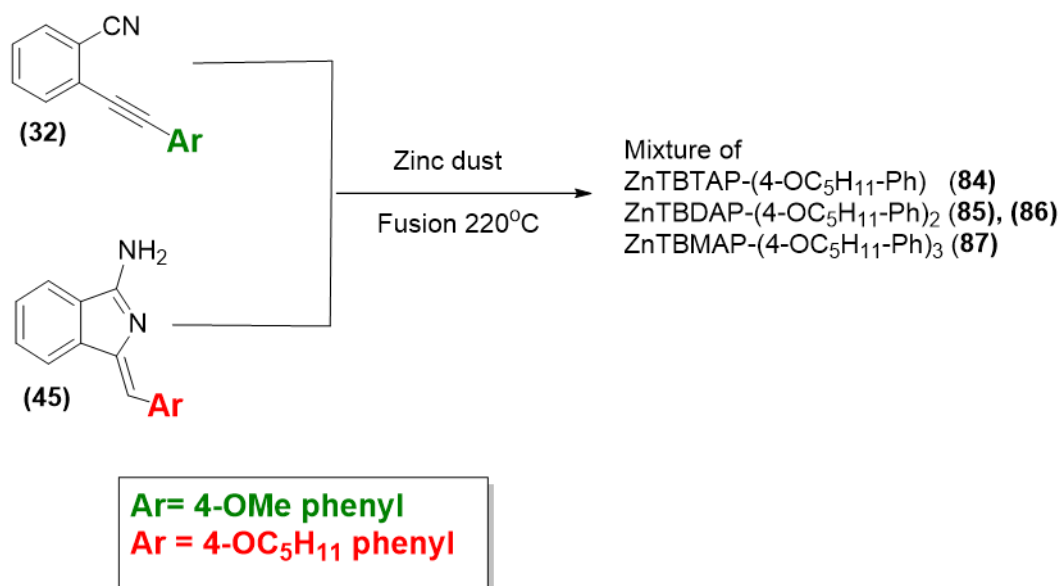
Scheme 2.28: Fusion of 4-pentyloxy phenyl aminoisoindoline (**45**) with 4-methoxy phenyl acetylene (**32**).

The TLC shows light blue spots at the top, a red/orange spot, unreacted acetylene and intense green band. The green band was isolated using preparative thin layer chromatography and submitted to another TLC using PE: DCM: THF 30:10:0.1 as eluent. It was clear that the green band consists of three to four different spots that were close to each other with some overlapping which makes their isolation challenging. Thus, the crude was analysed by MALDI-TOF MS to give some indication of the obtained hybrids. As illustrated in figure 2.25, the MALDI-MS spectra of the crude showed the molecular ion peak at (m/z 898) that corresponded to Zn-TBDAP with two pentyloxy phenyl substituents at *meso*-positions and another molecular ion peak at (m/z 737) that corresponded to Zn-TBTAP (**84**) with one pentyloxy phenyl substituent and a molecular ion peak that gave an indication of a trace amount of the desired macrocycle ZnTBMAP with three 4-pentyloxy phenyl groups (**87**).

The indication of the TBMAP is based on MALDI-TOF analysis of the mixture after the isolation of blue materials at the top and the baseline materials. Also, the spectrum showed a molecular ion peak at (m/z 595) that corresponded to the self-dimerisation compound of pentyloxy aminoisoindoline (**46**) and another molecular ion peak around (m/z 434) that might correspond to the unsymmetrical dimer (**88**) as observed in the previous reaction (structures in figure 2.26). All obtained hybrids have the same substituent and no signs of any hybrid that has a 4-methoxy phenyl substituent. This indicates the 4-pentyloxyphenyl aminoisoindoline reacts alone in different ways to give different intermediates (**46**) and (**88**). Then, with higher temperature, these intermediates underwent a cyclisation step with unreacted aminoisoindoline in presence of zinc metal to give different macrocycles. Moreover, as the acetylene is colourless, the TLC of the crude was checked under the UV-light to prove it remains unreacted, and its spot was clearly observed.
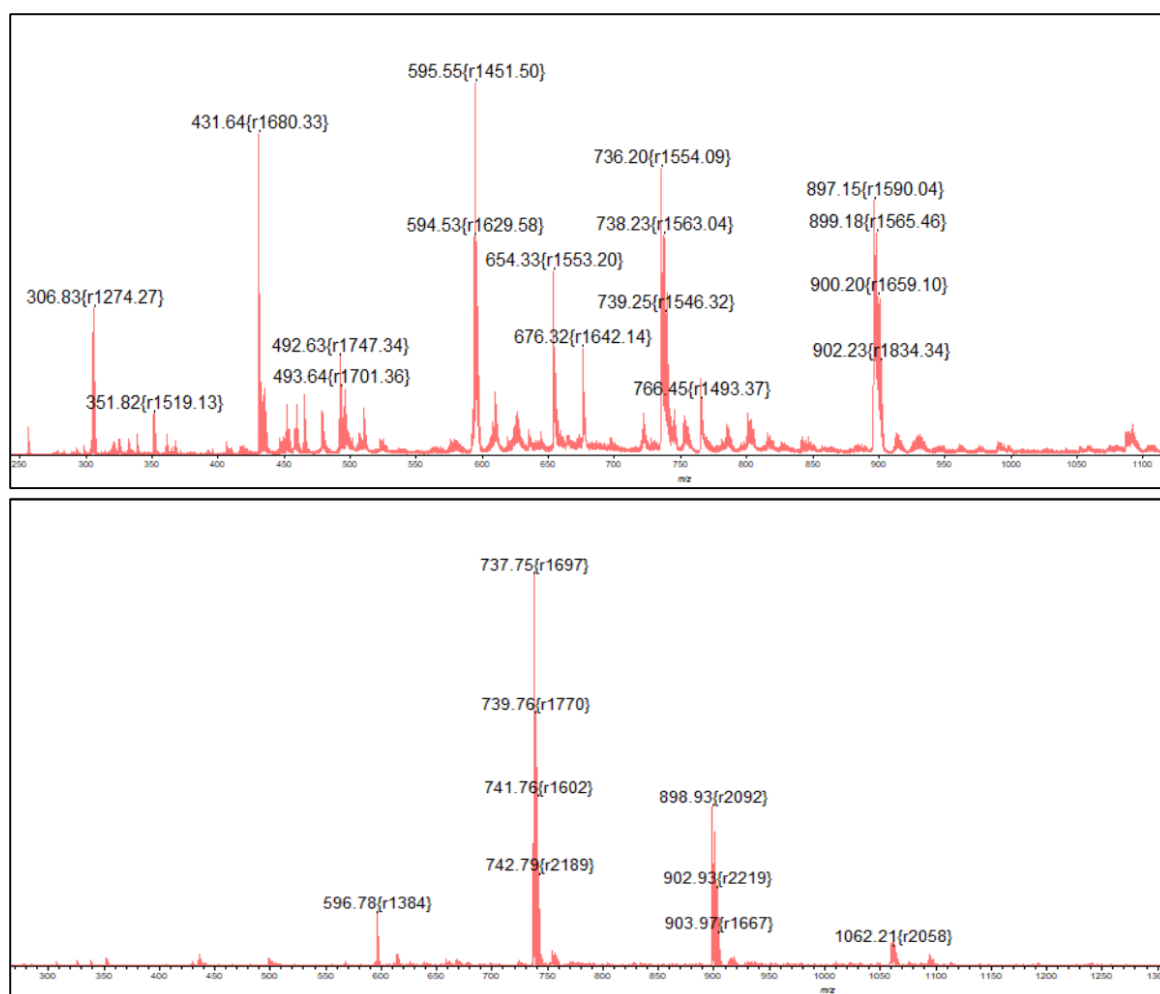
Figure 2.25: MALDI-TOF MS spectrum of crude of reaction between 4-pentyloxy phenyl aminoisoindoline and 4-methoxy acetylene (top) and its spectrum after isolation of baseline materials (bottom).
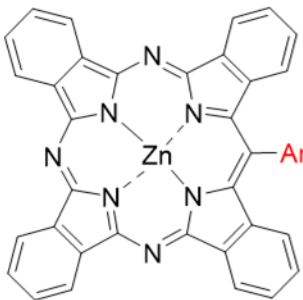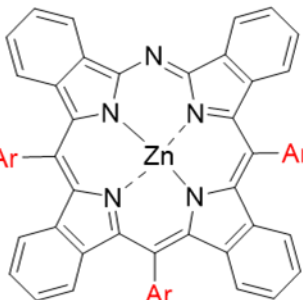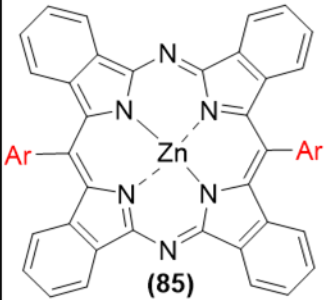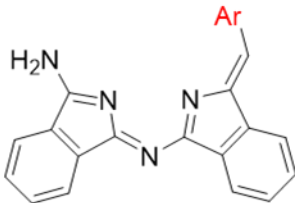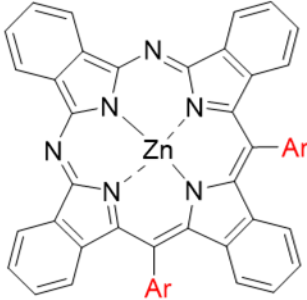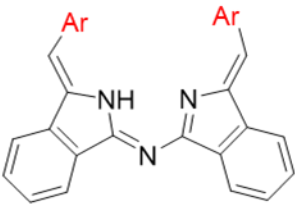
Expected structure	Exact Mass	Expected Structure	Exact Mass
(84)	737.19	(87)	1061.65
(85)	898.30	(88)	434.21
(86)		(46)	595.32

Figure 2.26: Table of masses observed and likely corresponding structures.

2.7.3 Fusion of 4-pentyloxy phenyl aminoisoindoline (45) with 4-nitro phenyl acetylene (36)

After obtaining this result and with nitro acetylene in hand (prepared previously), a test fusion of both pentyloxy aminoisoindoline (**45**) with nitro acetylene (**36**) was attempted to investigate the reactivity of nitro acetylene under this condition. One equivalent of aminoisoindoline was fused with one equivalent of nitro acetylene in presence of zinc powder in a pre-heated oil bath (scheme 2.29). After three hours, the reaction mixture turned deep green, and the reaction was monitored by TLC until the aminoisoindoline was fully

reacted. Then, after work up and evaporation of solvent, the mixture was analysed by MALDI-TOF MS, similar results were obtained as the previous reaction with no sign of the formation of any macrocyclisation that have nitro phenyl at the meso-carbon.
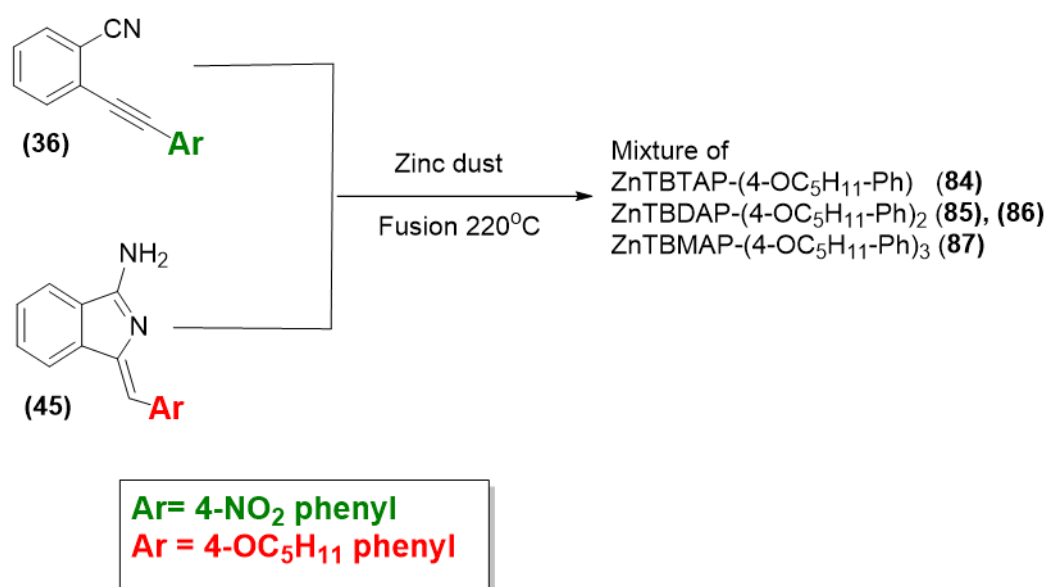
Scheme 2.29: Fusion of 4-pentyloxyphenyl aminoisoindoline (**45**) with 4-nitrophenyl acetylene (**36**).

2.7.4 Fusion of aminoisoindoline (45)

Overall, although the two different reactions gave the same results, still a final attempt needed to be conducted. As shown in scheme 2.30, 100 mg of aminoisoindoline was fused in the presence of zinc dust in pre-heated oil bath at 220°C. The reaction was monitored by TLC until a full consumption of S.M. was observed. Then, a mixture of DCM: THF 1:1 was added, and the resulting mixture was sonicated and filtered. After evaporation of the solvent, the crude was checked by TLC against previous crudes. The results were identical and both dimers' spots and hybrids were observed. Also, MALDI-TOF MS illustrated the expected hybrids peaks (figure 2.27).
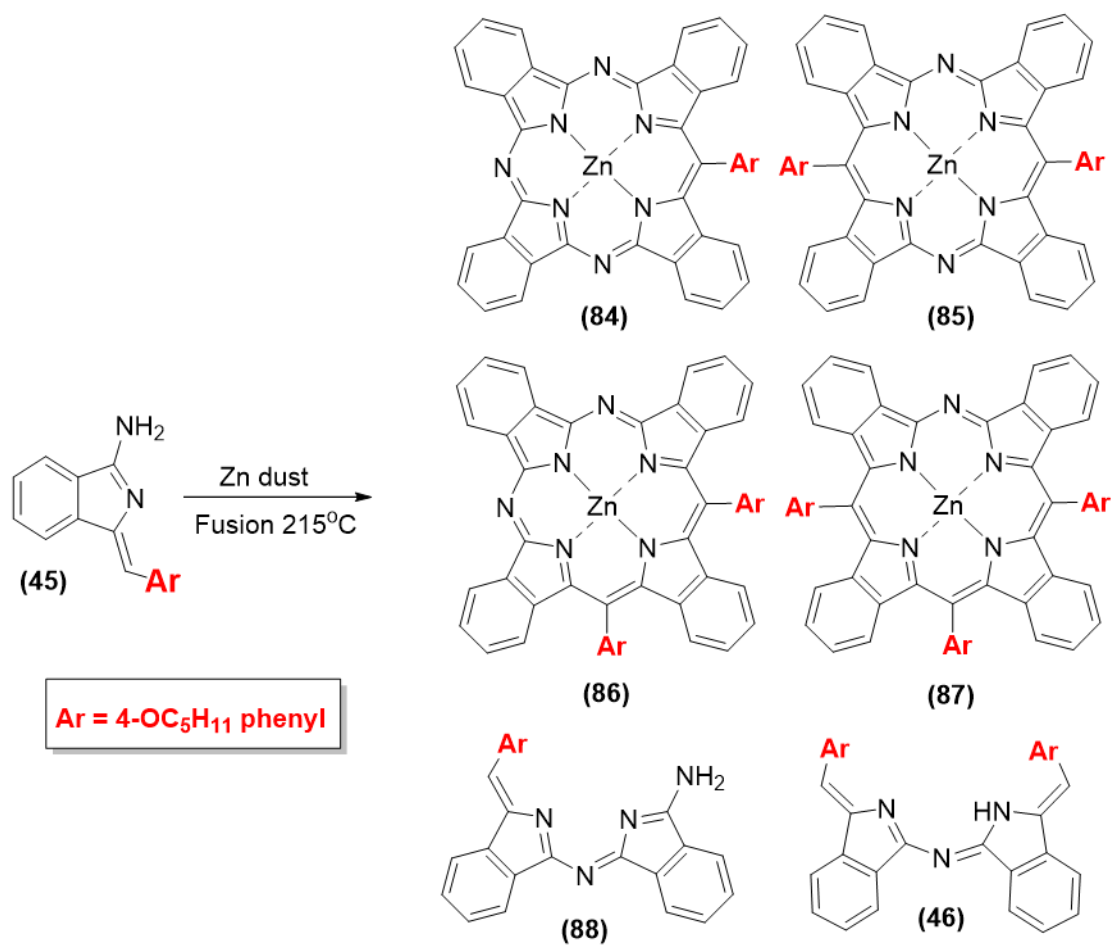
Scheme 2.30: Fusion of pentyloxy aminoisoindoline with zinc dust at 220ºC.

Structure (Ar = 4-OC$_5$H$_{11}$-phenyl)	(46)	(84)	(85)	(86)	(87)
Exact mass	595.32	737.19	898.30		1061.65
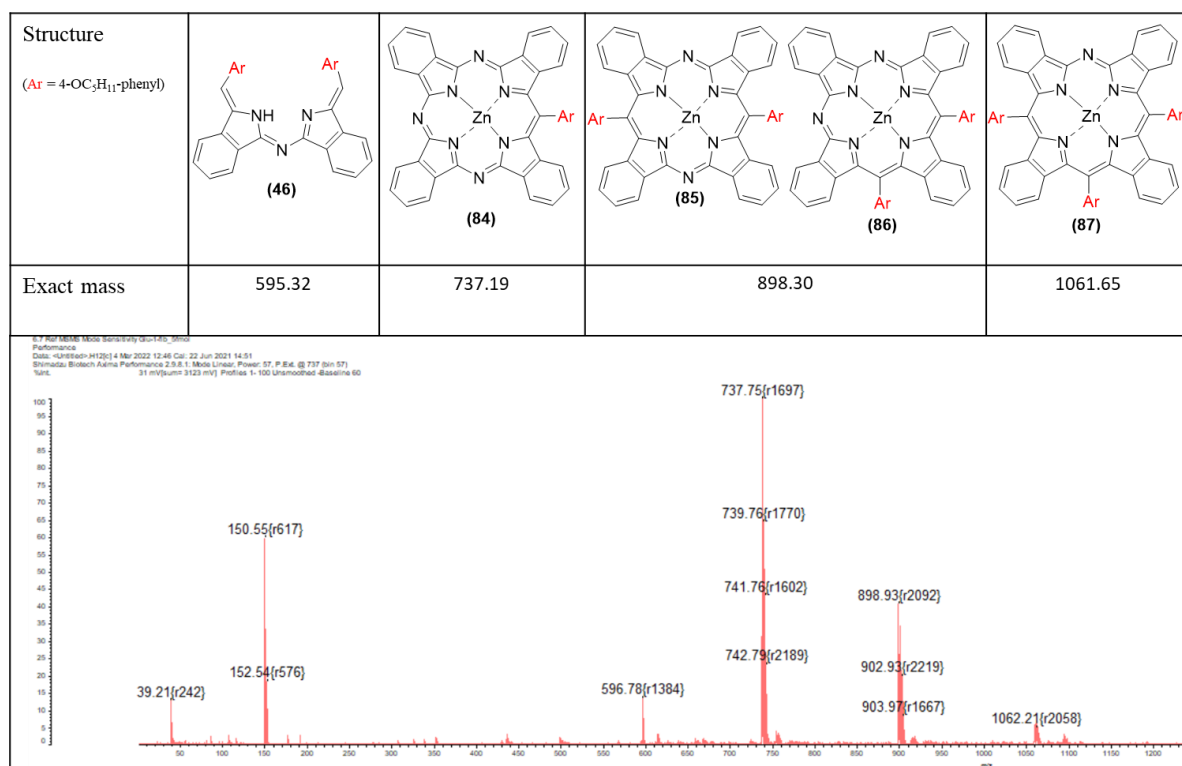
Figure 2.27: MALDI-TOF MS spectrum of crude of fusion of aminoisoindoline (**45**).

The mixture was submitted to column chromatography using PE: DCM: THF 30:10:0.1 as eluent. The fractions were collected in small tubes to get pure sample of hybrids as the TLC indicates overlapping of all spots. Then, all samples were checked by TLC to prove they were single spots. Pure samples were analysed by MALDI-TOF MS and ^{1}H NMR spectroscopy in order to identify the obtained products. The first fraction was red and gave a peak at m/z = 595 that corresponds to the self-condensed product (**46**). It was obvious that the second and the third fractions are green and gave the same molecular ion peak at m/z 898 that corresponds to ZnTBDAP with two pentyloxy phenyl groups at *meso*-positions as seen in figure 2.28. Both fractions were checked by TLC to confirm they were different compounds, and definitely they gave two different spots that indicated the formation of both isomers *cis*- and *trans*- Zn-TBDAP-(4-OC$_5$H$_{11}$ phenyl)$_2$.
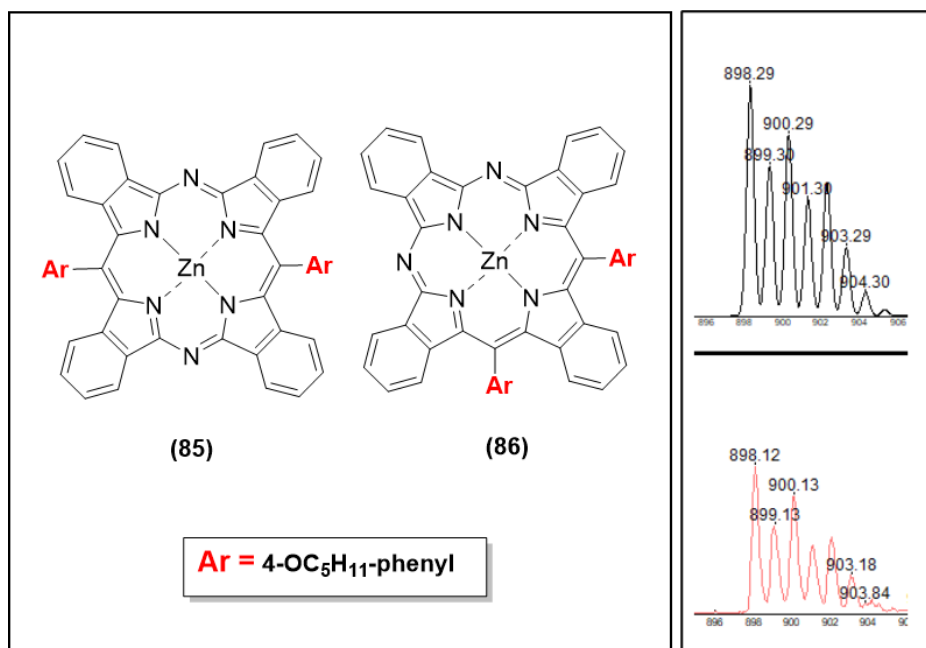
Figure 2.28: MALDI-TOF MS spectrum of fraction 2 and 3 (bottom right) plus theoretical isotopic pattern (top right).

As depicted in figure 2.29, the ^{1}H NMR spectrum in deuterated tetrahydrofuran for the second fraction shows six different signals integrating to all 24 protons in the aromatic region which indicates the symmetry of trans-TBDAP. Moreover, the protons on non-peripheral sites and close to the *meso*-phenyl groups were shielded and appears as a doublet at 7.35 ppm whereas the protons on non-peripheral sites and close to the nitrogen bridges are highly de-shielded and appears as doublet at 9.73 ppm. The triplet peak at 4.43 ppm integrates to four protons corresponding to the two-methylene groups from the alkyloxy groups. Also, the rest of the pentyloxy chain protons appeared at 2.09-1.11 ppm range as expected.
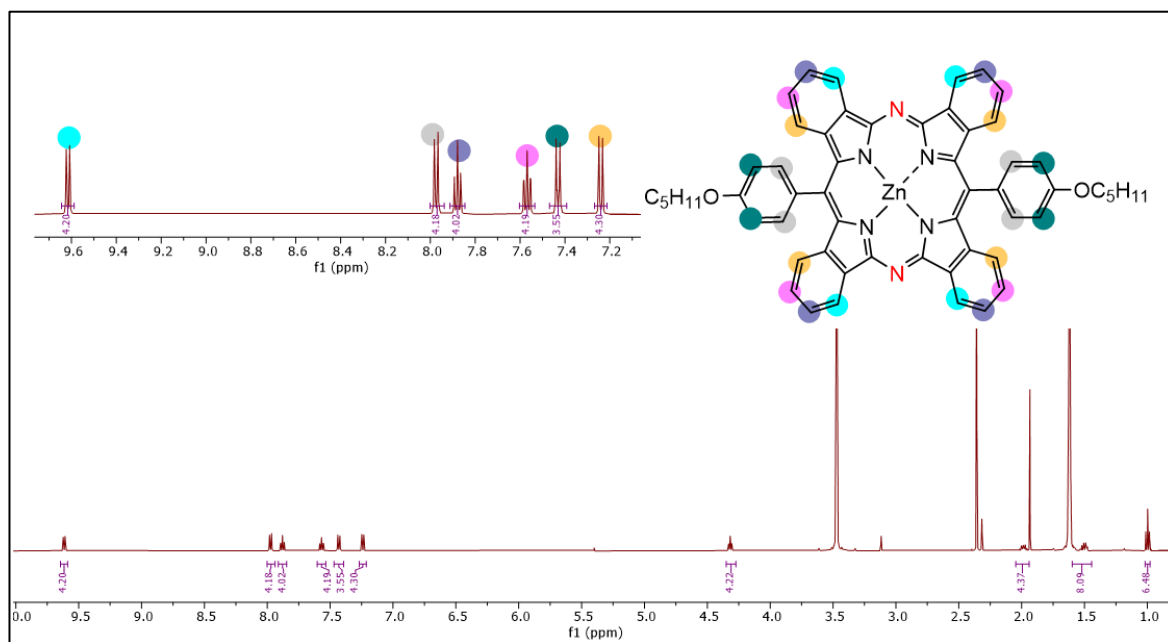
Figure 2.29: ¹H NMR spectrum of Zn-*trans*-TBDAP (**85**) in THF-d_8.

The ¹H NMR spectrum of fraction three in deuterated acetone showed all the twenty-four protons for *cis*-TBDAP as illustrated in figure 2.30. The most noticeable difference from the previous spectrum is the number of peaks in aromatic region and the peak splitting for both shielded and de-shielded protons due to the reduction in symmetry of the structure of *cis*-TBDAP. Two different peaks that integrate to four protons were found in the highly de-shielded range from 9.62- 9.52 ppm that correspond to the non-peripheral sites of the complex that close to nitrogen bridges. Moreover, two larger doublets in range 7.99- 7.54 ppm clearly indicate the eight protons from both phenyl groups at *meso*-positions. The alkoxy group protons at the *meso*-position were found as expected.
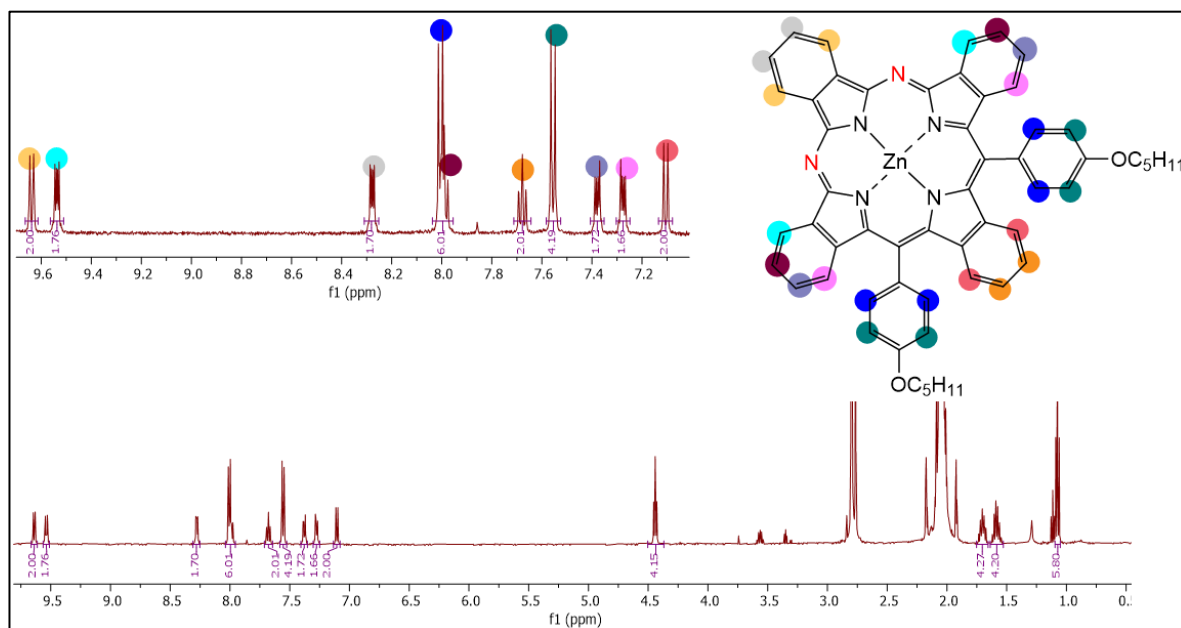
Figure 2.30: ^{1}H NMR spectrum of Zn-*Cis*-TBDAP (**86**) in d$_6$-acetone.

Both pure *cis* and *trans* products were analysed by UV-Vis spectroscopy as illustrated in figure 2.31. Each compound gave a distinctive absorption which concurs with our group's previous reported data of non-peripherally *meso*-free magnesium hybrids. It is notable that the Q band of *trans*-TBDAP is red shifted in comparison with that in *cis* product spectrum. Finally, both isomers gave suitable crystals for x-ray diffraction as depicted in figure 2.32. Full data analysis is currently being processed. Recrystallisation of *cis*-TBDAP was achieved using a mixture of distilled THF: EtOH whereas *trans*-TBDAP was recrystallised from boiling THF as its solubility was low compared to *cis*.
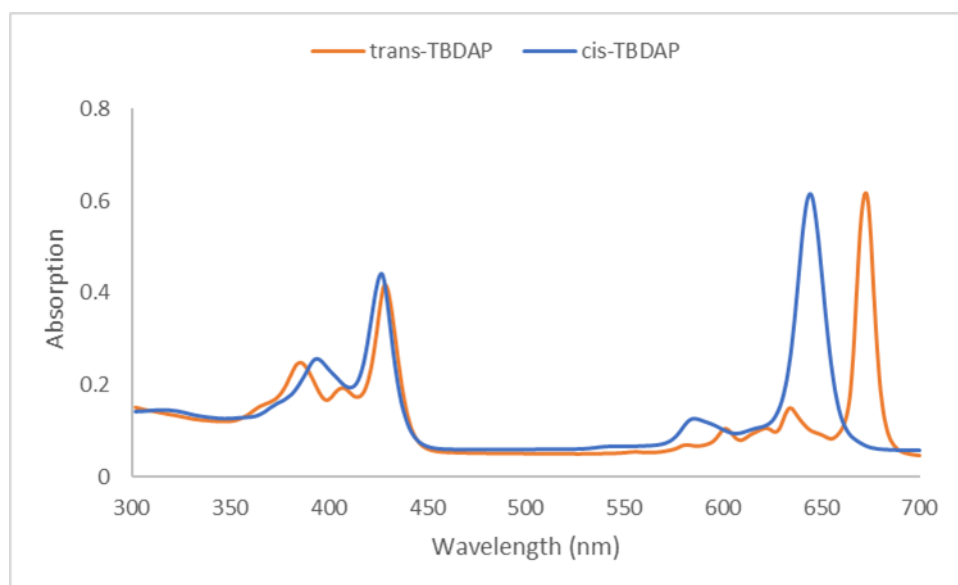
Figure 2.31: UV-Vis spectra of *trans*-ZnTBDAP (**85**) and *cis*-ZnTBDAP (**86**).
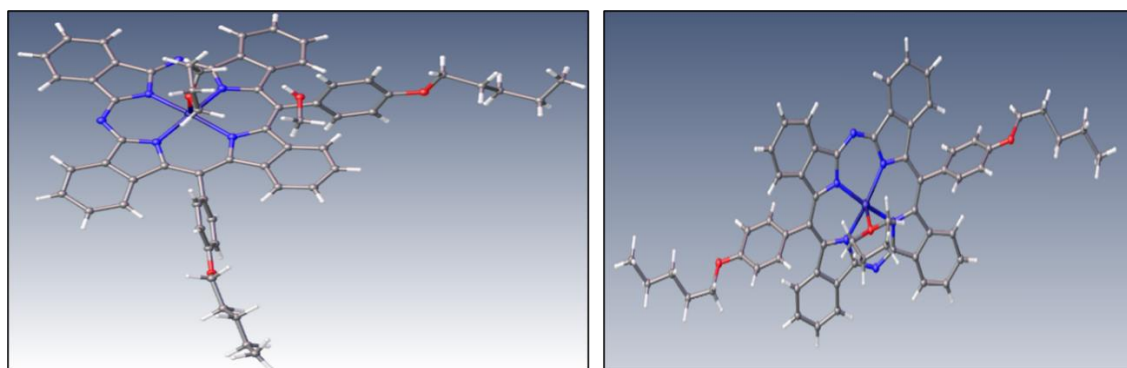
Figure 2.32: Preliminary x-ray crystal structures of both *cis* and *trans*-TBDAPs (**86**) and (**85**).

The last green fraction was analysed by MALDI-TOF MS and gave a molecular ion peak at (m/z 737) which is identified as Zn-TBTAP as illustrated in figure 2.33. The UV-Vis spectra represent a typical metalated TBTAP with split Q-band as expected. Also, the ^{1}H NMR spectrum in deuterated tetrahydrofuran gave all signals corresponding to all protons on the compound (figure 2.34). All expected signals for twenty aromatic protons from 9.58-7.25 ppm range were observed. Six protons that were on non-peripheral positions that were close to the nitrogen bridges were highly de-shielded at 9.58-9.48 ppm whereas the two protons that were on non-peripheral sites close to the *meso*-phenyl were the most shielded at 7.25

ppm. Also, the triplet peak at 4.41 ppm corresponded to the methylene group from the alkyloxy group and all protons of the alkoxy chains were at 2.09-1.08 ppm range as expected.
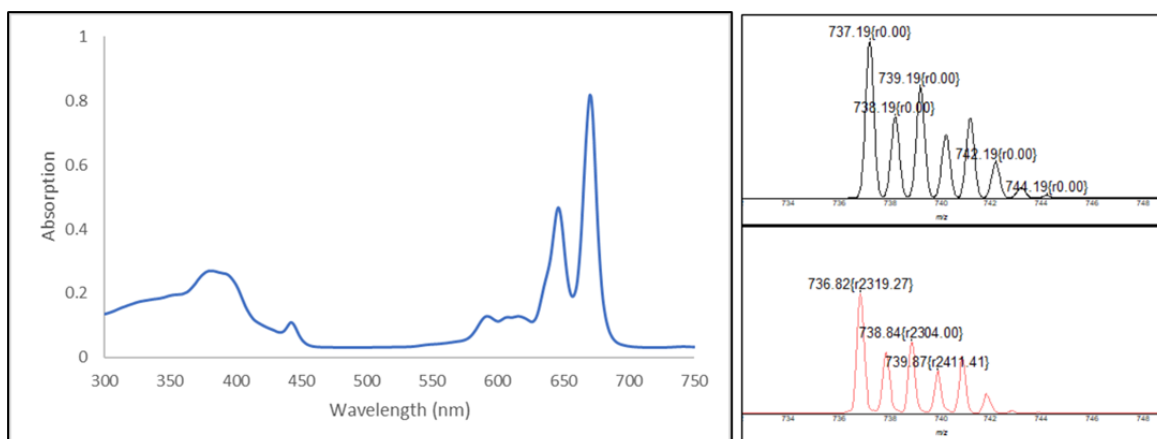
Figure 2.33: UV-Vis spectra of ZnTBTAP (**61**) and its MALDI-TOF MS (bottom right) plus theoretical isotopic pattern (top right).
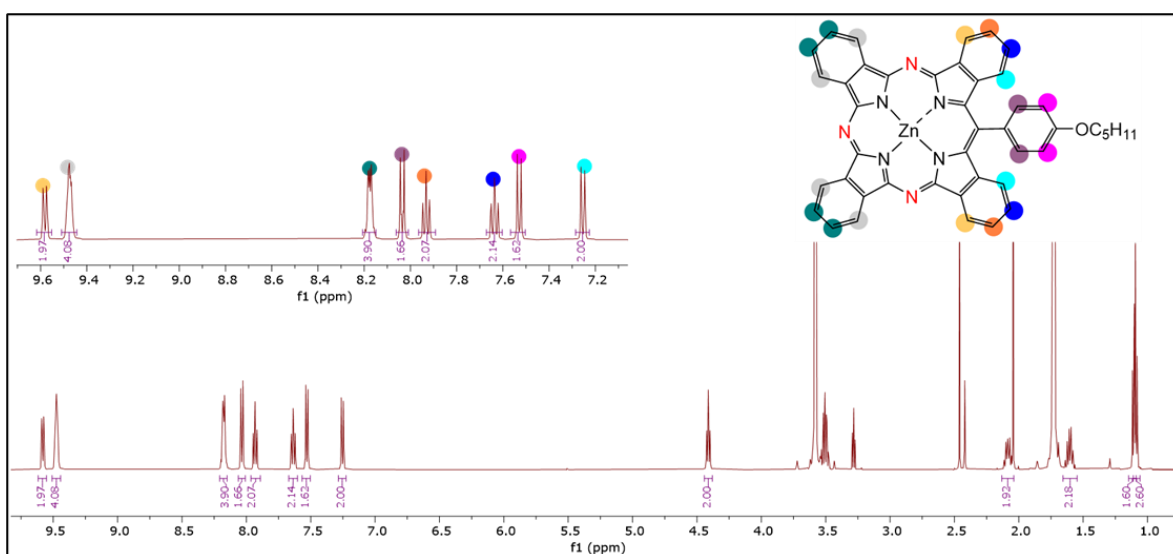
Figure 2.34: ^{1}H NMR spectrum of Zn-TBTAP (**61**) in THF-d_8.

After calculating the actual yield of this reaction, it was obvious that TBTAP macrocycle was the dominant product with 15% yield and then *Cis*-TBAP, *Trans*-TBDAP with (7% and 5% respectively) and traces of TBMAP hybrid that was not enough for any further analysis. Also, two different intermediates were isolated from the crude. The self-condensation product (**46**) that usually forms at lower temperature through elimination of NH$_3$ molecule

from two units of aminoisoindoline. Its molecular ion can be seen clearly in MALDI-TOF MS of the crude (Fig 2.27). Also, the unexpected unsymmetrical condensation product (**88**) was isolated from baseline material as orange solid that seems to result from self-condensation of aminoisoindoline with loss of phenyl group under this extreme temperature as depicted in scheme 2.31.
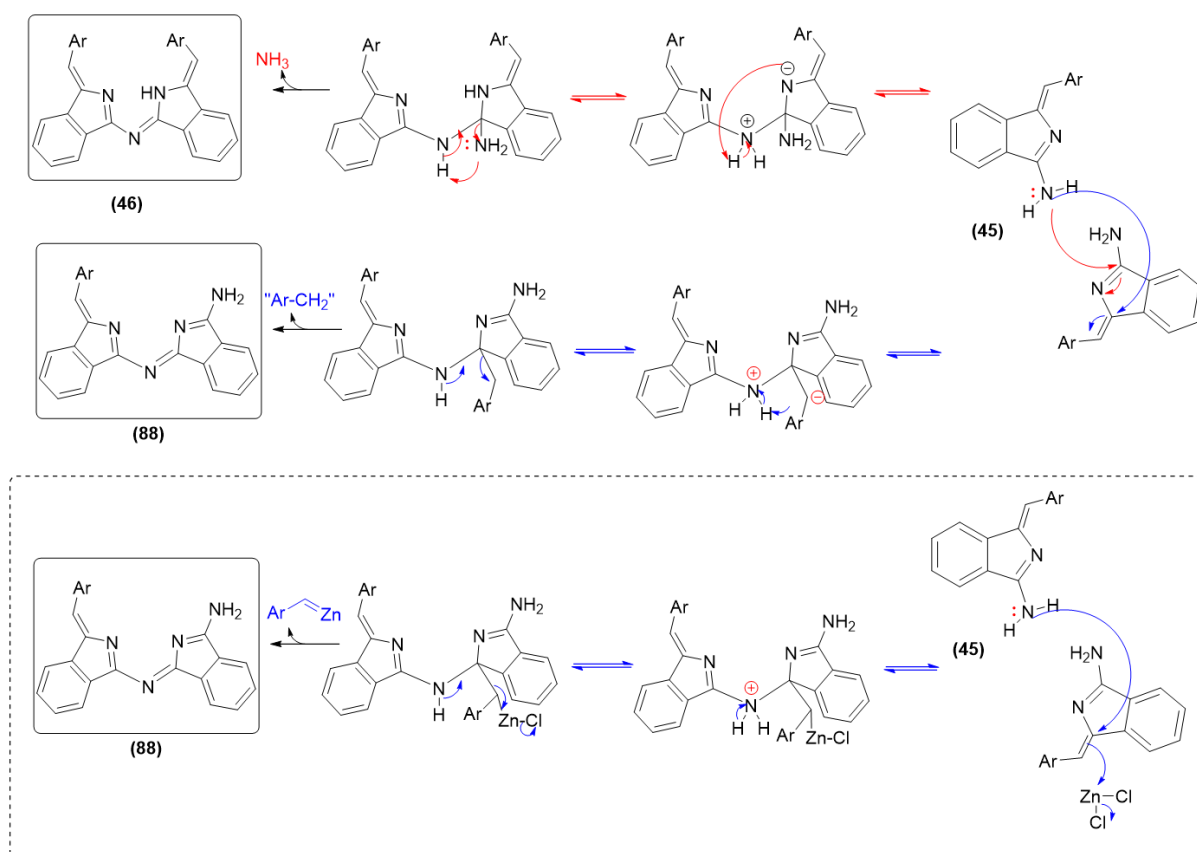
Scheme 2.31: Hypothesised mechanism of formation of self-condensation product (**46**) and unsymmetrical dimer from aminoisoindoline (**88**). Intermediate (**88**) is only observed in zinc reactions and a likely alternative mechanism invokes zinc carbenes/carbenoids (bottom)

Both symmetrical dimer (**46**) and unsymmetrical dimer (**88**) were isolated and analysed by ^{1}H NMR, ^{13}C NMR, UV-VIS and MALDI-TOF MS and they give the expected spectra. The ^{1}H NMR spectra of both dimers are illustrated in figure 2.35. A total of twelve aromatic protons from 8.15-7.03 ppm were assigned to benzene protons in dimer (**88**) whereas sixteen aromatic protons at 8.08- 6.60 ppm range corresponded to the symmetrical benzene protons in dimer (**46**). Also, a singlet for the alkene appears at 7.16 ppm with one proton integration

in (**88**) whereas it appeared at 6.83 ppm in (**46**) and integrated to two protons. The aliphatic protons in both dimers were as expected.
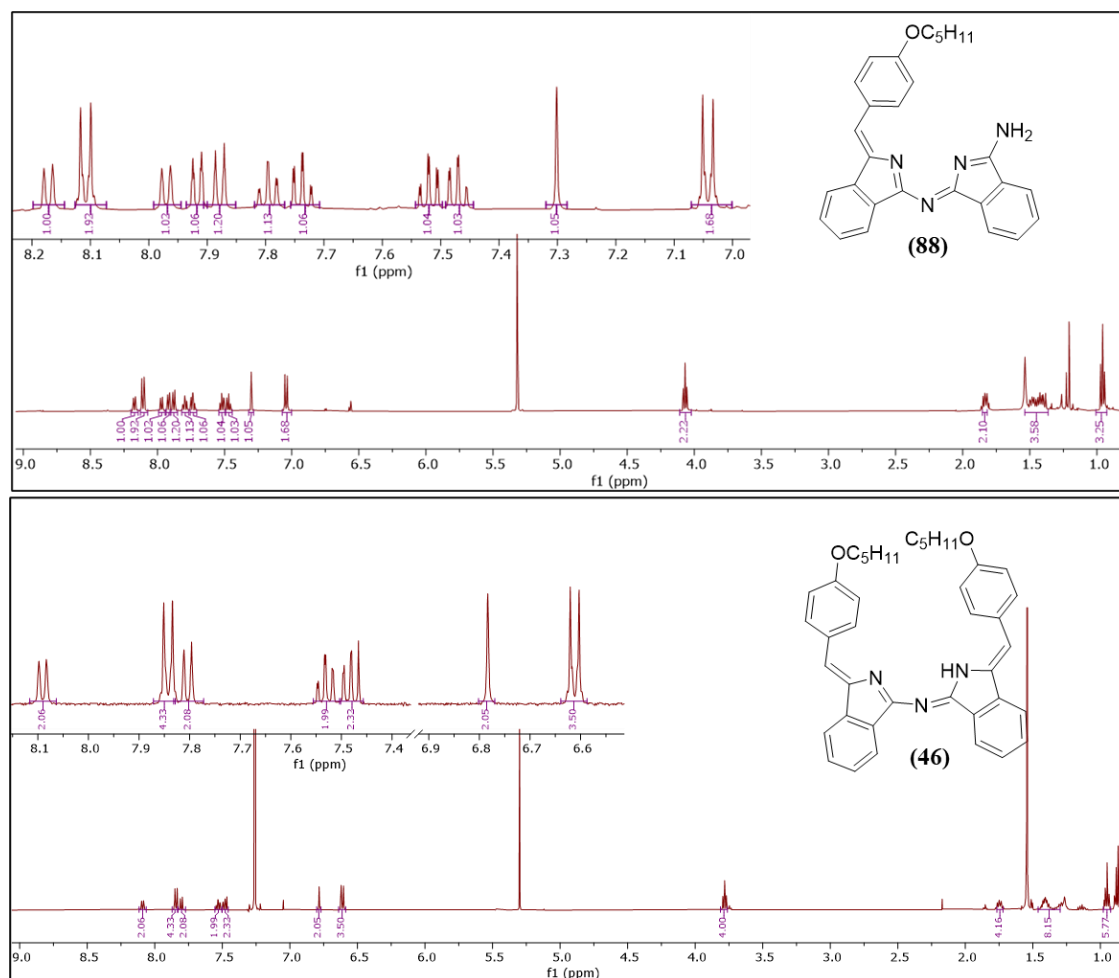
Figure 2.35: ^{1}H NMR spectra for both isolated dimers (**46**) and (**88**) in DCM-d_2.

In an attempt to isolate unsymmetrical dimer (**88**) from the crude by column chromatography (using silica gel as the stationary phase), it was noticed that the isotopic pattern of the product in MALDI-TOF MS did not exactly match the theoretical prediction. The observed spectrum is depicted in figure 2.36. After analysis of all fractions by TLC, it was noticed that two orange spots are presented with different R_f, both gave similar mass but were identified later as the expected dimer (**88**) plus its hydrolysed product (**90**). Both dimers were successfully isolated and full analysis were obtained. The hypothesised mechanism of hydrolysis of dimer (**88**) is illustrated in scheme 2.32.
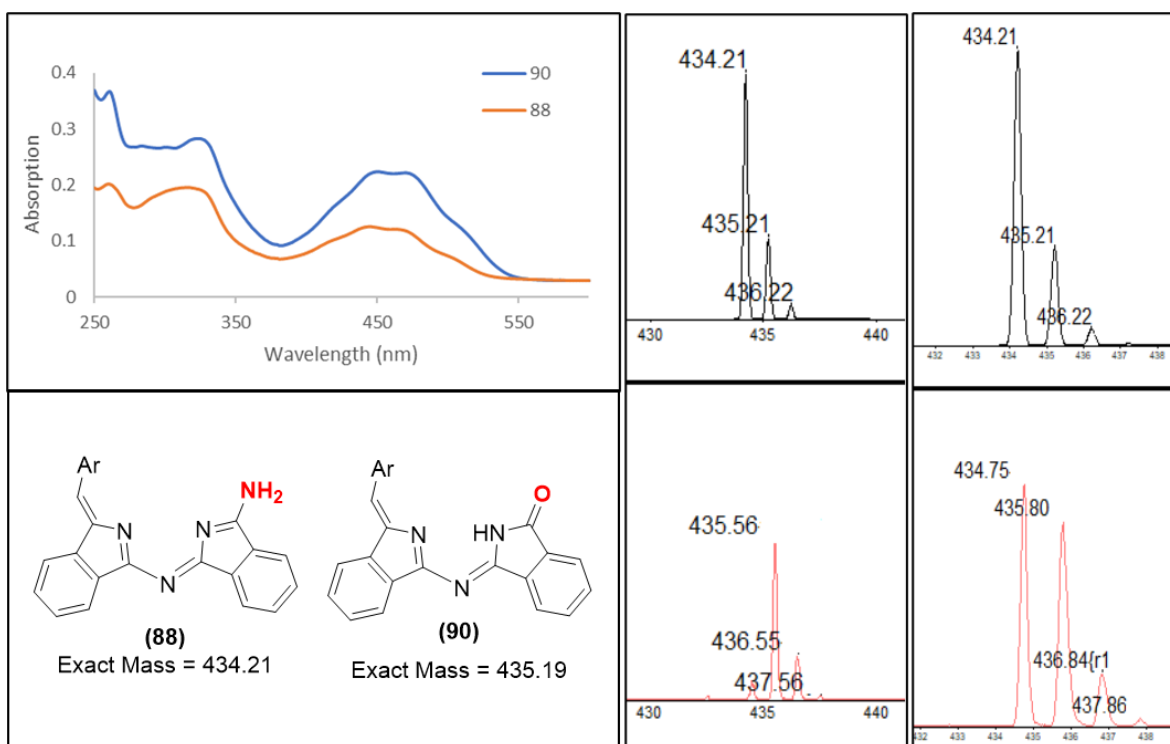
Figure 2.36: Structure and UV-Vis spectra of dimer (**88**) and its hydrolysed product (**90**) (left), MALDI-TOF MS before isolation (middle, bottom), and after isolation (right, bottom) and their theoretical isotopic pattern (top)
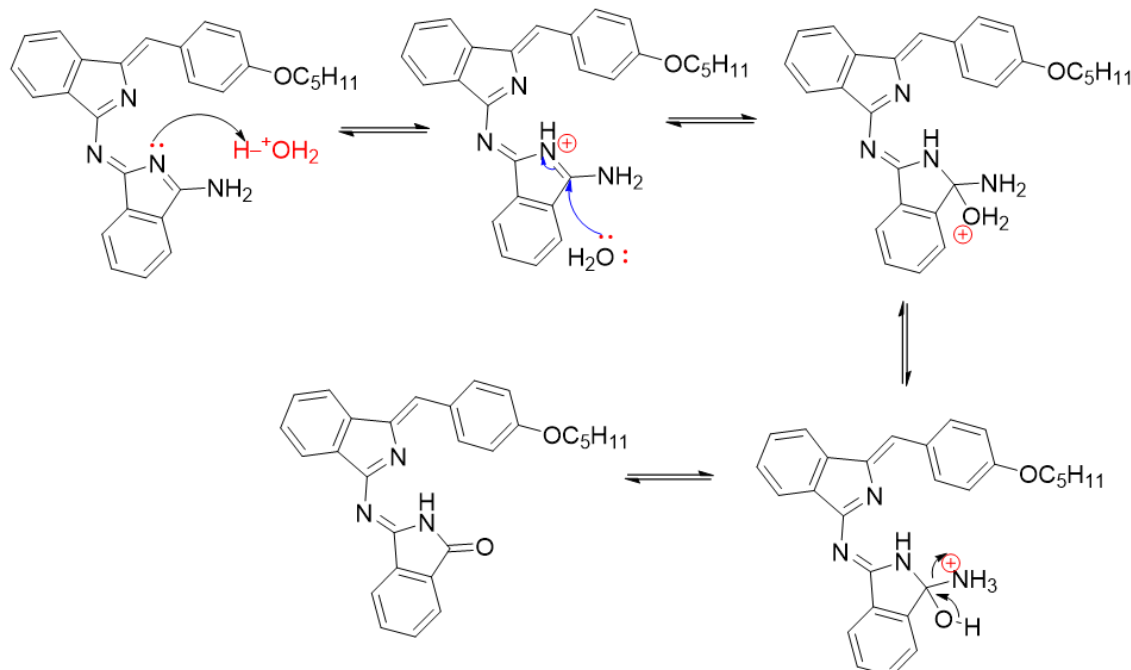
Scheme 2.32: Generic hydrolysis mechanism of unsymmetrical dimer (**88**) to produce dimer (**90**).

With the observation and isolation of two different dimerisation products, it was expected that the formation of other intermediates was likely. Two different trimeric intermediates were expected to form as there are two possible attack positions in aminoisoindoline as illustrated in scheme 2.33. However, only one trimeric product was isolated from the crude which is the symmetrical trimer (**89**). The quantity of the product was very small, and it was just analysed by MALDI-TOF MS. As shown in the scheme, the isotopic pattern of the product matches its theoretical one.
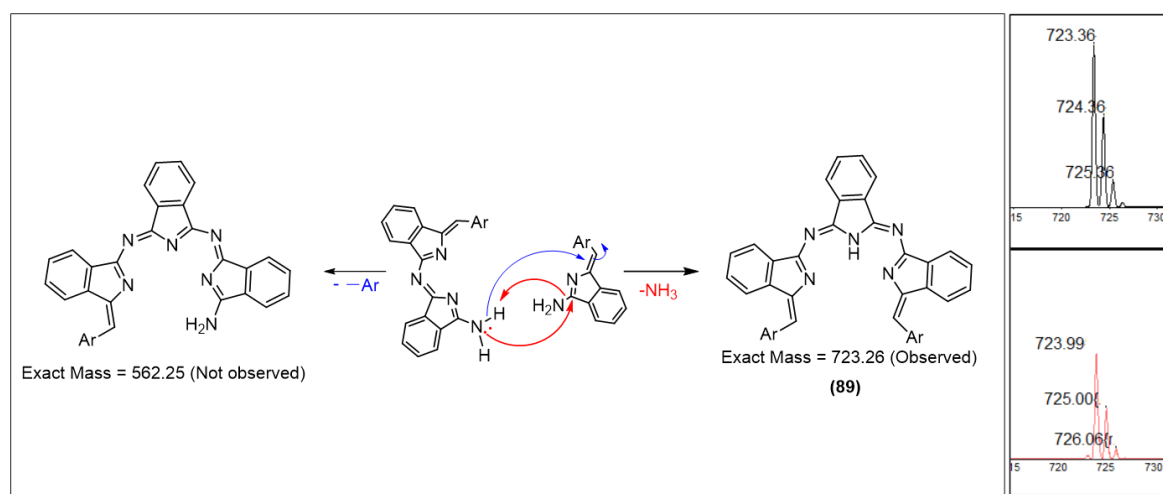
Scheme 2.33: Hypothesised mechanism of two possible trimeric products (left), and MALDI-TOF MS (bottom right) of isolated trimer (89), plus its theoretical isotopic pattern (top right).

2.8 Results from a screening of reaction conditions

After isolation and analysis of all products, the reaction has been repeated several times to ensure reliability and repeatability of the result. Also, the reactions were performed under different conditions and briefly analysed qualitatively. They included fusion reaction and in high boiling solvent at 220°C (quinoline), which gave similar outcomes. Also, activated zinc dust, zinc chloride and zinc acetate have been attempted but no differences in hybrids formation was observed. However, when the reaction was attempted with magnesium bromide, magnesium turnings or without metal in quinoline, none of the macrocycles were formed, just self-condensation product was obtained. When self-condensed compound was fused or heated up with zinc dust in quinoline, just traces of hybrids were observed by MALDI-TOF MS along with aminoisoindoline which resulted from the breaking of the dimer under the high temperature as summarised in table 2.1.

Staring Material	Metal/ metal salts	Solvent	Outcomes based on MALDI-TOF MS and TLC
Aminoisoindoline	Zinc dust	No solvent (fusion)/ freshly distilled quinoline	Mixture of hybrids and intermediates dimers/ trimer.
Aminoisoindoline	Activated zinc powder	No solvent (fusion)/ freshly distilled quinoline	Mixture of hybrids and intermediates dimers/ trimer.
Aminoisoindoline	Zinc acetate	Freshly distilled quinoline	Mixture of hybrids and intermediates dimers/ trimer.
Aminoisoindoline	Zinc chloride	Freshly distilled quinoline	Mixture of hybrids and intermediates dimers/ trimer.
Aminoisoindoline	Magnesium bromide	Fusion/ Freshly distilled quinoline	Self-condensed product
Aminoisoindoline	Magnesium turning	Fusion / Freshly distilled quinoline	Self-condensed product
Aminoisoindoline	No metal	Freshly distilled quinoline	Self-condensed product
Self-condensed compound	Zinc dust	Fusion/freshly distilled quinoline	Traces of TAP, DAP and MAP, unreacted dimer and aminoisoindoline

Table 2.1: Attempts of macrocyclisation of Pentyloxy aminoisoindoline utilising different metal salts.

2.9 Proposed mechanism of formation of *trans*-TBDAP, *cis*-TBDAP and TBTAP from dimeric intermediates

The formation of TBTAP as a dominant product under these conditions was not expected based on our previous knowledge regarding its synthesis and the essential role of phthalonitrile in its hypothesised mechanistic formation. However, the isolation of self-condensed compound (**46**), unsymmetrical dimer (**88**) and its trimeric product (**89**) from the crude leads us to suggest different mechanistic pathways to produce these macrocycles. Under these conditions at high temperature for long period of time the aminoisoindoline

molecules could condense in different ways to give these intermediate with the elimination of benzyl fragment or NH_3. With these intermediates in solution, and unreacted aminoisoindoline, it might be possible for all macrocycles to be produced.

The formation of cis-TBDAP can be hypothesised through a reaction between dimeric intermediate product (**88**) with another dimeric compound with elimination of aminoisoindoline or diiminoisoindoline to give unsymmetrical trimer which undergo a reaction with unreacted aminoisoindoline molecule or with dimer intermidates to form4-membered open chain oligomer which rapidly cyclises with loss of phenyl ring (scheme 2.34).
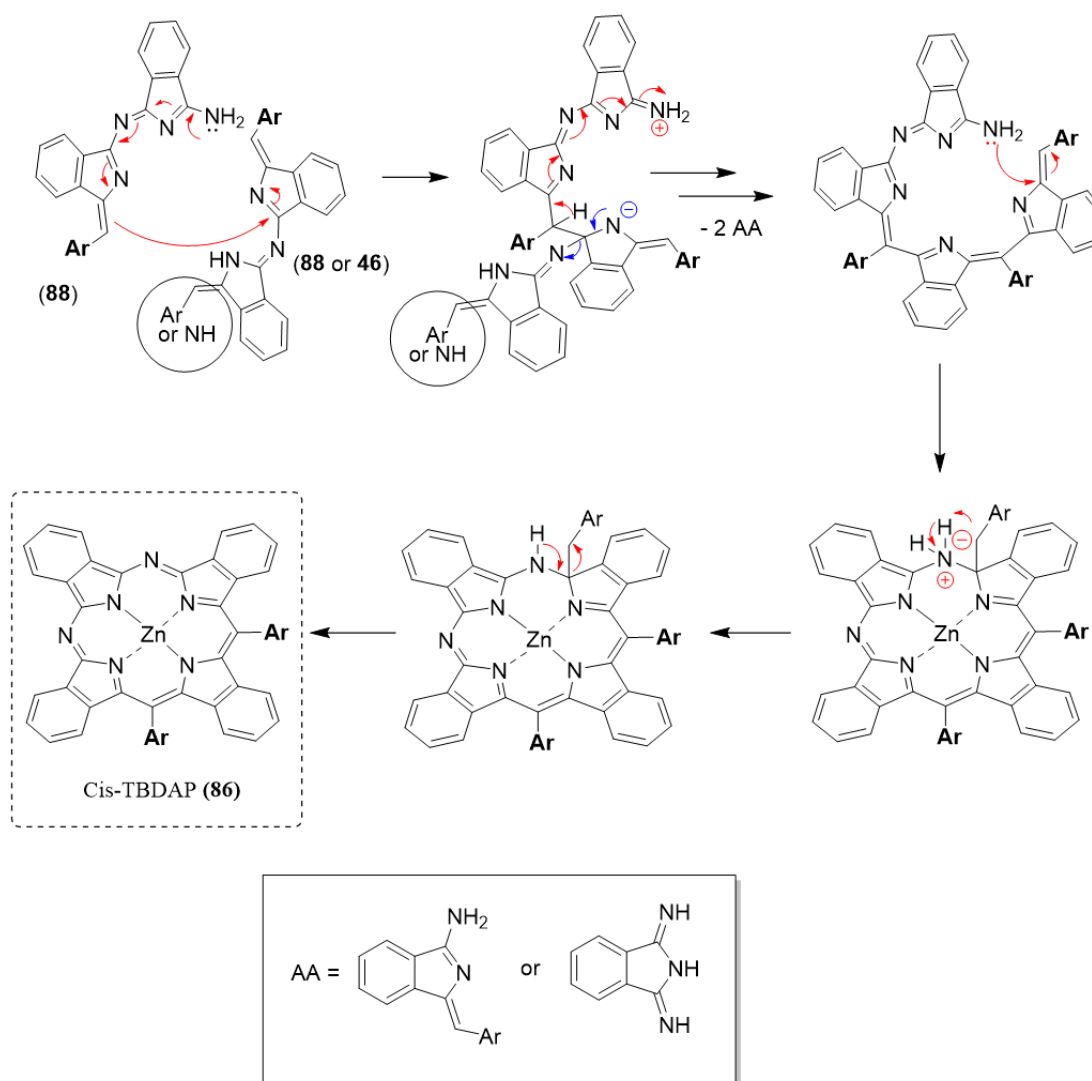
Scheme 2.34: Proposed mechanism for *cis*-TBDAP (**86**) formation from dimeric intermediate (**88**) or (**88**+**46**).

Different hypothesised pathways can be suggested to produce TBTAP and *trans*-TBDAP hybrids as illustrated in scheme 2.35. The formation of cis meso-C-Ar is difficult to explain but most likely requires loss of a benzyl fragment. Losing a PhCHZn molecule in the reaction between unsymmetrical dimer (**88**) with symmetrical dimer (**46**) could produce a 4-membered open chain oligomer. If we assume that 4-ring intermediates cyclise rapidly, cyclisation could follow two pathways, firstly producing TBTAP with loss of another PhCHZn molecule, or alternatively to produce *trans*-TBDAP with loss of an ammonia molecule.
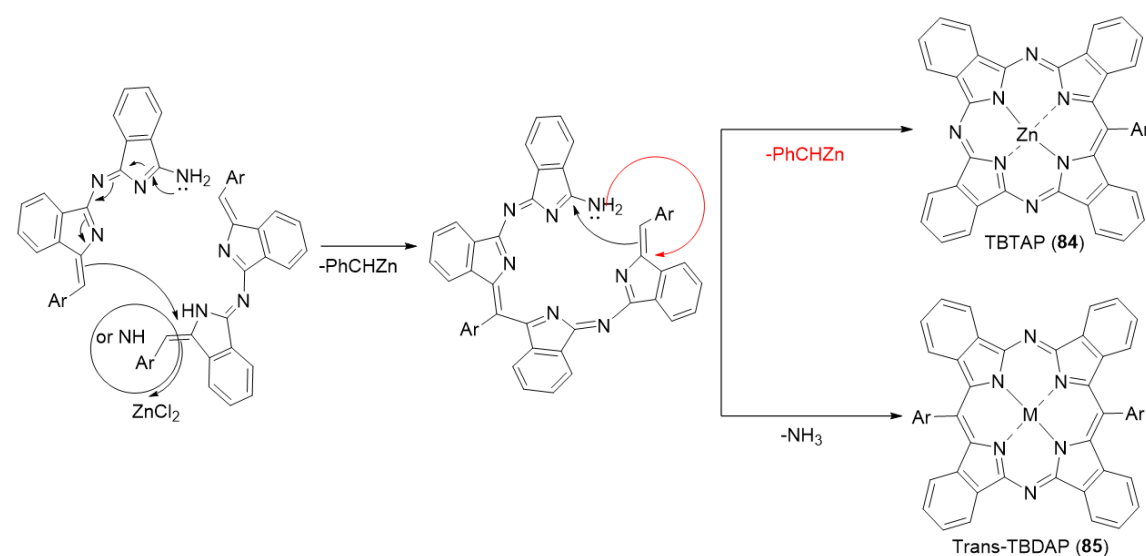
Scheme 2.35: Hypothesised consecutive addition of aminoisoindoline to form the 4-membered open chain oligomer and macrocyclisation to form TBTAP (**84**).

Based on our group's recent work, formation of 2:2 substituted ABBA TBTAP involves the elimination of an aromatic fragment during macrocyclisation process. Consequently, extensive investigations have been conducted on the potential intermediates that derived from the homo-condensation of aminoisoindoline in order to synthesise *trans*-TBDAPs selectively with the elimination of two aromatic fragments as depicted in scheme 2.36. However, the hypothesised pathway proved to be unsuccessful and did not give any TBDAPs or other hybrid products. Hence, it was concluded that the cyclisation of any hybrids should involve the elimination of ammonia molecules so the high order intermediates cannot be used as precursors for this type of reaction.
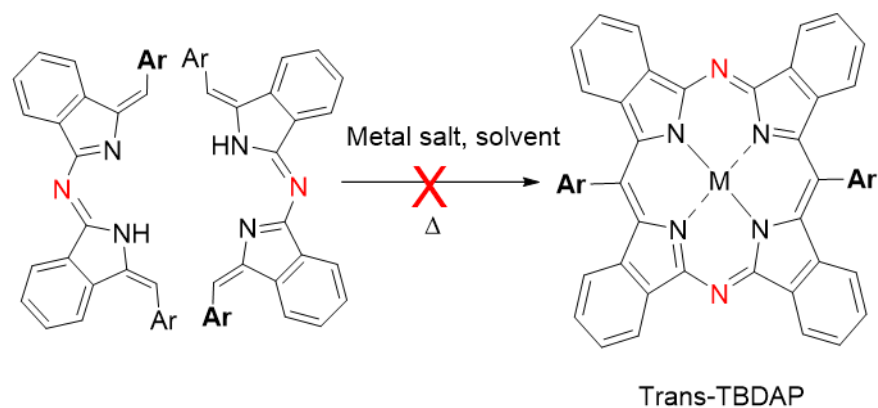
Scheme 2.36: Unsuccessful templating and macrocyclisation to synthesise *trans*-TBDAP (**85**).

Another possible pathway to yield *trans*-TBDAPs through elimination of two ammonia molecules from two units of unsymmetrical dimer was suggested as depicted in scheme 2.37. However, at the same time that this work was being carried out, other researchers in the group found that reaction of AB dimers under standard conditions (using $MgBr_2$) unexpectedly leads to AB_3 TBTAPs instead.[35]
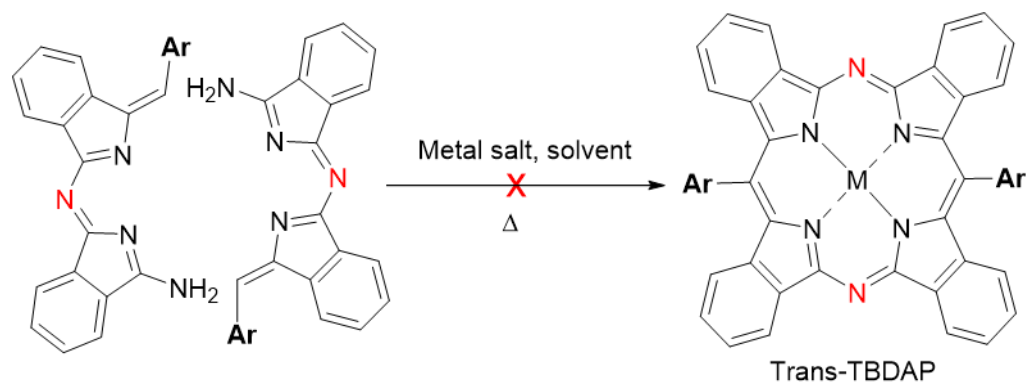
Scheme 2.37: Hypothesised templating and formation of trans-TBDAP (**85**); this reaction is found to produce only the AB_3 TBTAP and no DAP.

2.10 Synthesis of Zinc-tetrabenzotriazaporphyrin (TBTAP) using our group TBTAP's condition

The earlier mentioned unsuccessful attempt of macrocyclisation of aminoisoinoline using $MgBr_2$ as a template, and the unexpected hybrid mixture formation when zinc metal was utilised (scheme 2.38), led us to investigate the production of Zn-TBTAP following our group's recent TBTAP's procedure. This procedure mostly explored $MgBr_2$ as the metal template and other metals have not been extensively investigated under these conditions. With our previous unexpected results in mind, zinc metal might affect the reaction pathway and give a possibility of different macrocyclisation reactions occurring to yield different hybrids or even a mixture of them.
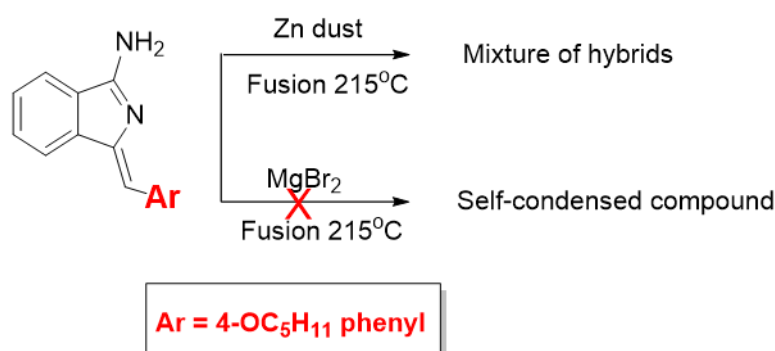
Scheme 2.38: Previous unsuccessful macrocyclisation reaction of aminoisoindoline using magnesium bromide as metal template and its successful macrocyclisation reaction with zinc metal.

As illustrated in scheme 2.39, three equivalents of phthalonitrile and one equivalent of aminoisoindoline and 1.5 equivalents of zinc chloride were dissolved in dry diglyme under argon in a preheated heating block at 215°C. After three hours, the solution started to turn to green color, but the TLC showed some unreacted starting material, so the reaction was left for longer time. After 6 hours, the solution turned to a deep green color, and a full consumption of starting material was observed by TLC. Then, the solvent was evaporated under a stream of argon and a mixture of DCM+THF was added, and the solution was sonicated and filtered off to remove inorganic and insoluble materials. Then, the solvent was evaporated under reduced pressure and the mixture was analysed by TLC. The TLC revealed the formation of intermediate products and an intense green spot that was later identified as

the desired ZnTBTAP (**84**) as the only obtained hybrid. Also, MALDI-TOF MS of the crude shows the molecular ion peak of ZnTBTAP at 737 m/z and unsymmetrical dimer ion peak at 434 m/z (figure 2.37).
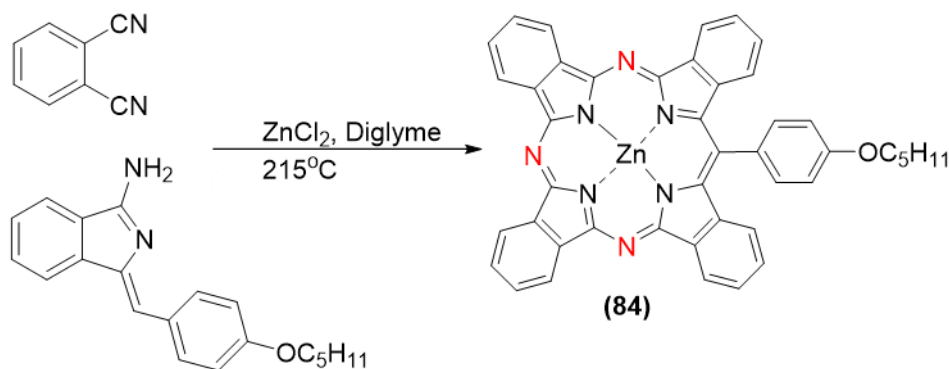
Scheme 2.39: Synthesis of Zn-TBTAP (**84**) using Cammidge's method.
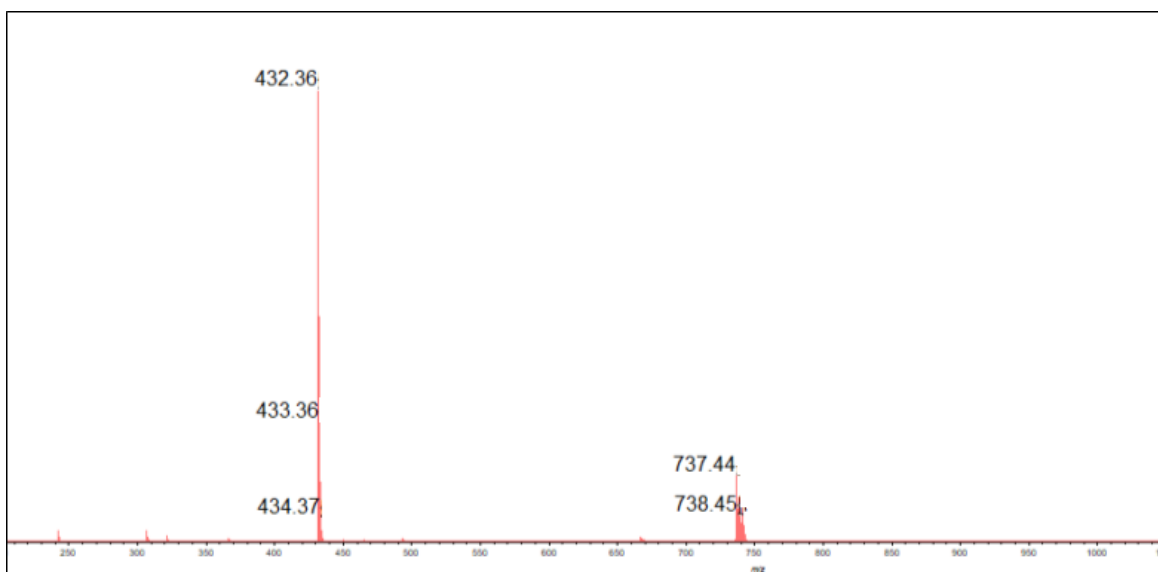
Figure 2.37: MALDI-TOF MS of reaction crude of synthesis of Zn-TBTAP (**84**)

The crude was purified by column chromatography to isolate the product. Dark crystals with purple reflex were obtained when the TBTAP was recrystallised from a mixture of acetone and ethanol. A full analysis of the product by MALDI-TOF MS, ^{1}H NMR and ^{13}C NMR spectroscopies was obtained and matched what we have from previous fusion reaction. The

solid-state structure was determined by x-ray diffraction as shown in figure 2.38. As expected, the zinc centre is bonded to an oxygen atom of coordinated ethanol. The *meso*-phenyl group is arranged approximately perpendicular to the TBTAP core plane with a disorder of alkoxy group.
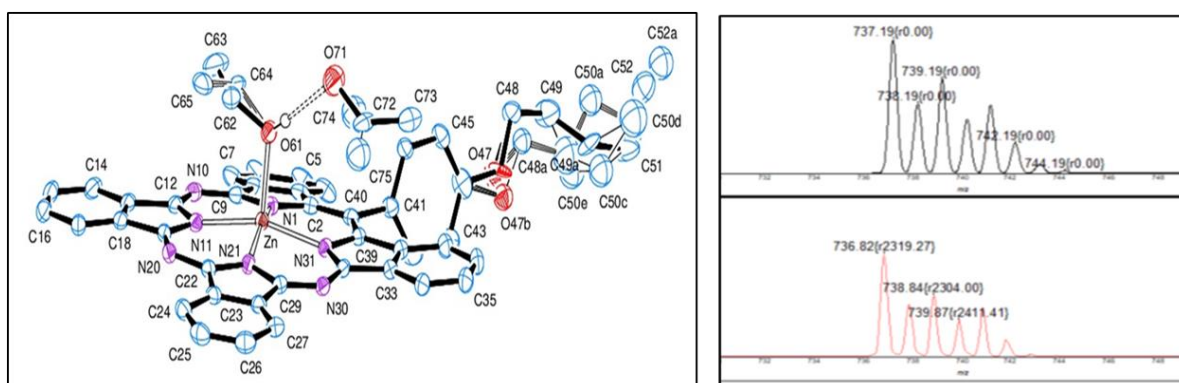
Figure 2.38: X-ray structure of Zn-TBTAP (**84**) and its MALDI-TOF MS (bottom right) plus theoretical isotopic pattern (top right).

2.11 Synthesis of Peripherally Substituted Tetrabenzotriaza Porphyrins and its Precursors

After the successful direct synthesis of zinc TBTAP, the next logical step was utilisation of substituted phthalonitrile to determine the type of the obtained TBTAP, whether it gives AB_3 or ABBA exclusively or a mixture of both types. As previously mentioned, recent Cammidge group research on peripherally substituted TBTAP revealed unexpected results that can be summarised as most derivatives (alkoxy, phenoxy and naphthalene) gave ABBA selectively whereas 1,2,3,4-tetrahydro-1,1,4,4-tetramethylnaphthyl derivatives produced a mixture of both ABBB/ ABBA TBTAP when $MgBr_2$ was employed as template (illustrated in detail in chapter one).[4]

2.11.1 Utilising 6,7-dicyanotetrahydrotetramethylnaphthalene as phthalonitrile precursor in ZnTBTAP formation conditions

The selection of this particular derivative was made in this study in order to investigate its reactivity toward zinc template. As depicted in scheme 2.40, 6,7-dicyanotetrahydrotetramethylnaphthalene (**52**) was employed as macrocyclisation partner that was mixed with pentyloxy aminoisoindoline derivative (**45**) and zinc chloride in diglyme in a pre-heated heating block at 215°C. The reaction was followed by TLC until full

consumption of starting materials was observed. The TLC revealed the appearance of single intense green spot with brown baseline materials.
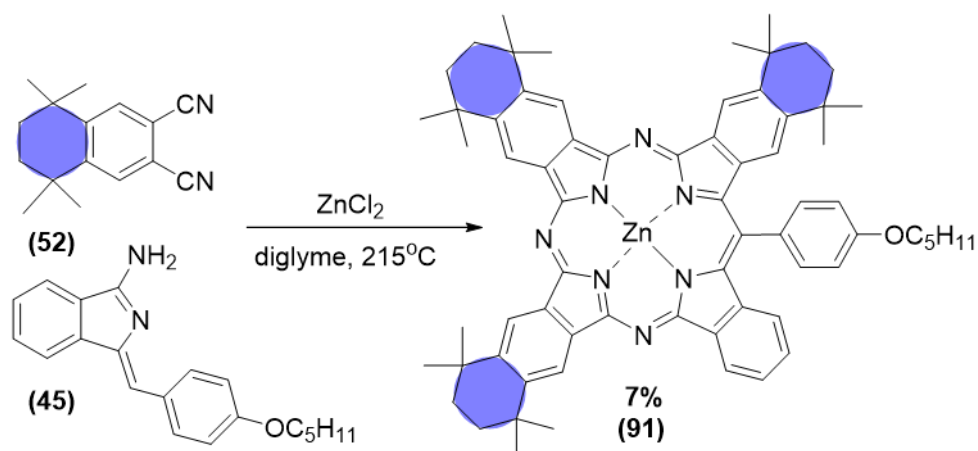
Scheme 2.40: Selective synthesis of AB$_3$ ZnTBTAP (**91**) by utilising pentyloxy aminoisoindoline (**45**) and 6,7-dicyano-1,2,3,4-tetrahydro-1,1,4,4- tetramethylnaphthalene (**52**).

After the work up and analysis of the crude by MALDI-TOF MS, it was confirmed that the only TBTAP hybrid formed from this reaction was AB$_3$ TBTAP (**91**) with a molecular ion peak at 1067.13 m/z and no sign of formation of ABBA TBTAP was observed. As illustrated in figure 2.39, the MALDI-TOF MS of the crude confirms the presence of unsymmetrical dimer with a molecular ion peak at 544 m/z and trace amount of zinc phthalocyanine (m/z 1016). This result shows significant contrast to the identical reaction using magnesium where the major product is the ABBA TBTAP and illustrates the importance of the metal ion in influencing reaction outcome.

The desired product was isolated and purified by column chromatography and crystals suitable for x-ray diffraction of TBTAP were grown from a mixture of acetone and ethanol and its crystal structure is shown in figure 2.40. Also, the MALDI-TOF MS of pure product was as expected and matched its theoretical pattern. The ^{1}H NMR spectrum is concordant with the structure proposed and gave the expected peak splitting pattern and proton integration as shown in figure 2.41.

structure			
			(91)
Exact mass	544.32	1016.52	1067.52
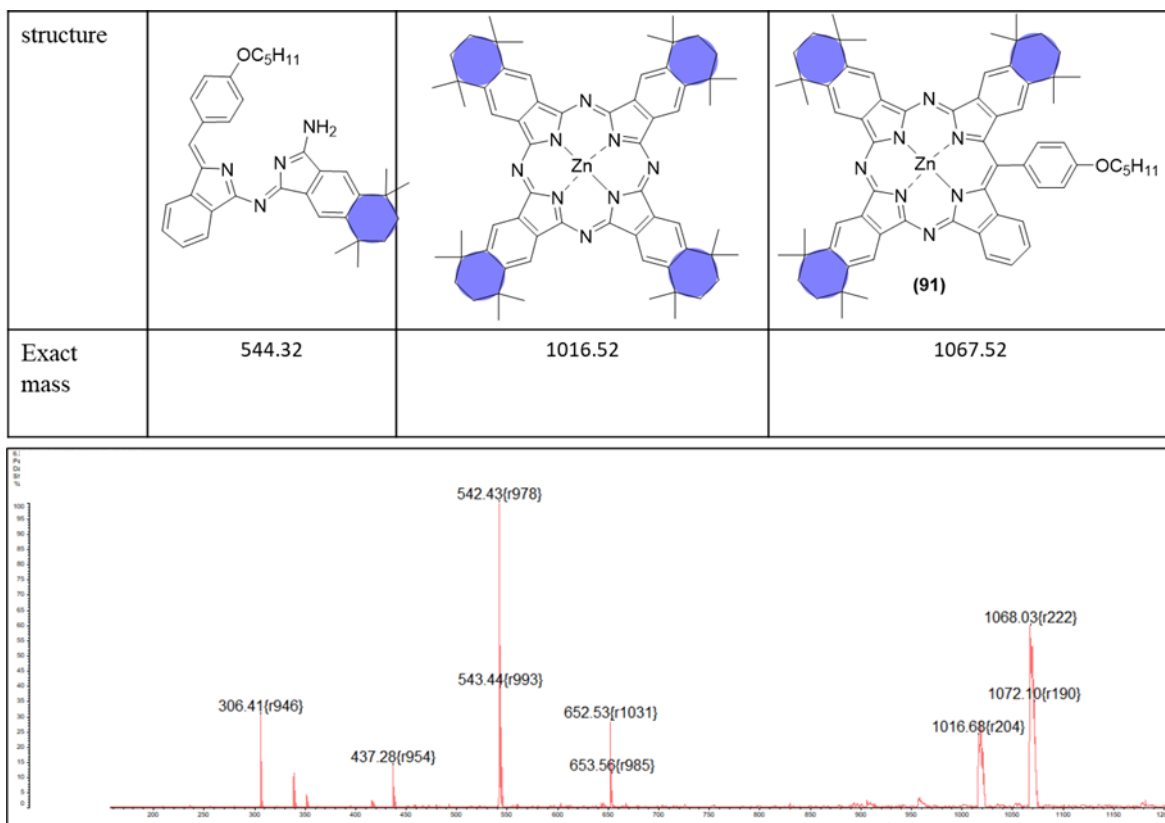
Figure 2.39: MALDI-TOF MS of crude reaction mixture of phthalonitrile (**52**) and aminoisoindoline (**45**).
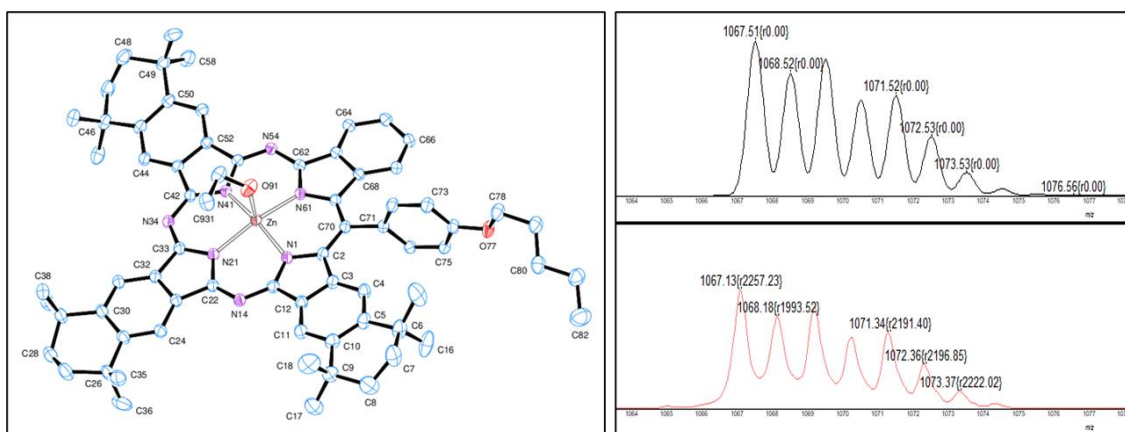
Figure 2.40: X-ray structure of AB$_3$ TBTAP (**91**) and its MALDI-TOF MS (bottom right) plus theoretical isotopic pattern (top right).
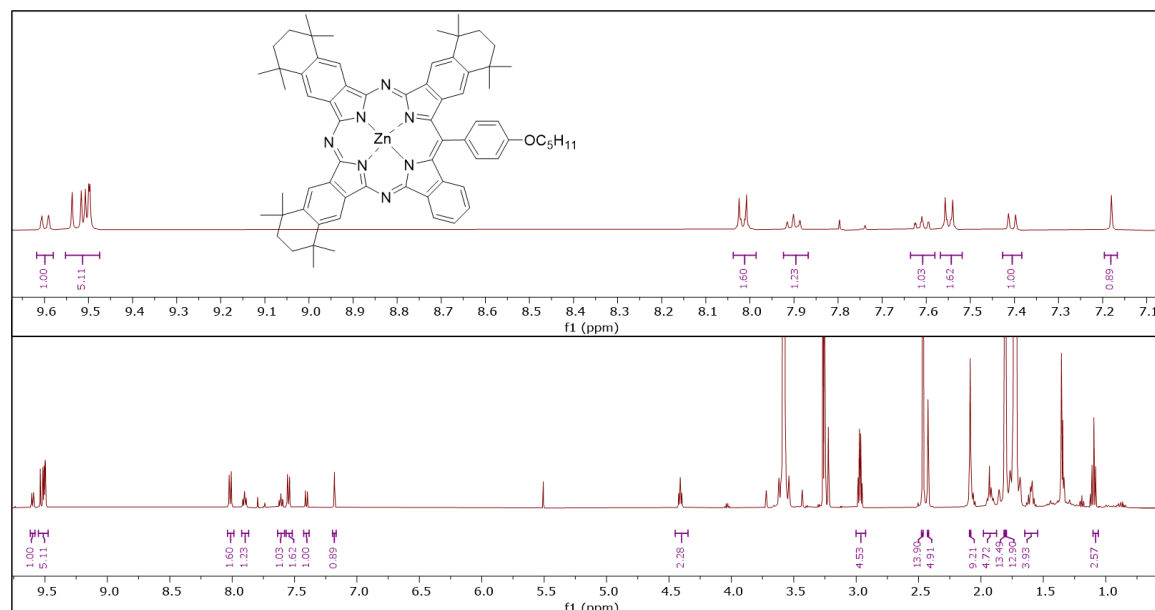
Figure 2.41: ^{1}H NMR spectra of AB$_3$ ZnTBTAP (**91**) in THF-d_8.

2.11.2 Utilising 6,7-dicyanodimethyldioxolane as phthalonitrile precursor in ZnTBTAP formation conditions

After the successful and unexpected selective synthesis of AB$_3$ ZnTBTAP when tetrahydrotetramethylnaphthalonitrile was employed, dimethyl dioxolane groups were suggested as different bulky substituents to be investigated under the same condition. As depicted in scheme 2.41, the first step was protection of the catechol diol following a reported procedure employing a slow addition of phosphorus trichloride to a solution of catechol in acetone in toluene.[36] After full consumption of starting material was observed, potassium carbonate was added to neutralise the mixture. Then, the solid was filtered off and washed with toluene. The organic phase was extracted from NaOH (10%) solution and H$_2$O. The desired product was obtained after distillation at 108°C under vacuum. The next step involves bromination by N-bromosuccinimide in DMF at r.t. in the dark for 48 h.[37] Then, water was added, and the mixture was left in the fridge until white precipitate was formed. The product was filtered off and dried under reduced pressure. The last step was cyanation using zinc cyanide and palladium catalyst in DMF at 120°C.[36] After work up and purification, the desired product was isolated and checked by ^{1}H NMR. Unlike previous cyanation methods, which gave phthalocyanine or unreacted S.M., this method successfully yields the desired dicyano-product as the major product in 71% yield.

135
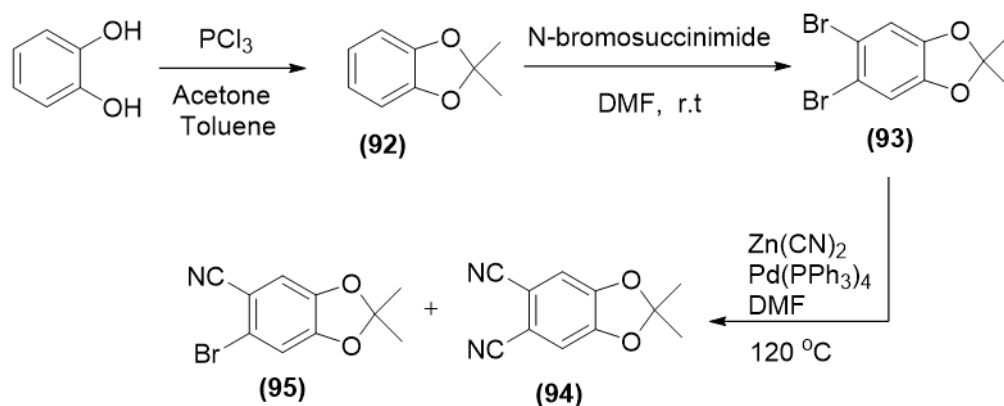
Scheme 2.41: Synthesis of dimethyl dioxolane phthalonitrile (**94**).

After successful synthesis of dimethyl dioxolane phthalonitrile (**94**), the TBTAP reaction was attempted and as expected, AB$_3$ ZnTBTAP (**96**) was obtained selectively in 8% yield (scheme 2.42).
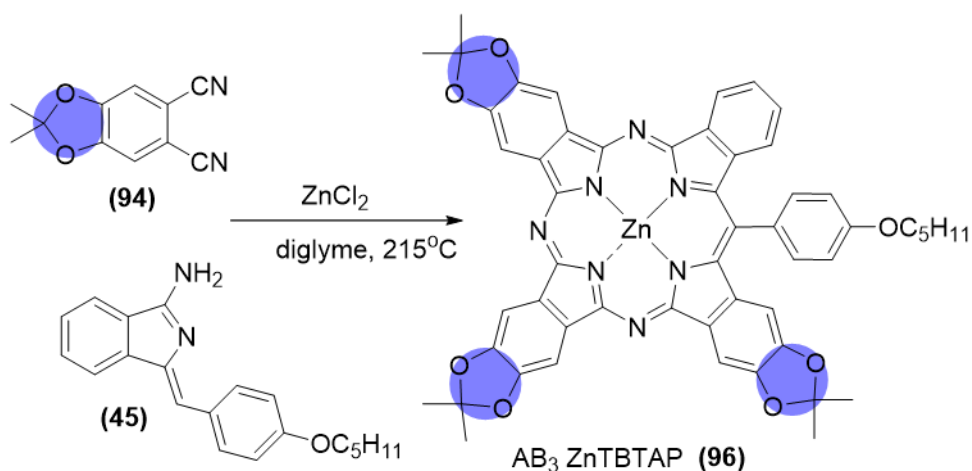
Scheme 2.42: Selective synthesis of (dimethyl dioxolane)$_3$ ZnTBTAP-(4-OC$_5$H$_{11}$-Ph) (**96**).

Formation of unsymmetrical dimer and zinc phthalocyanine were clearly visible from the MALDI-TOF MS spectrum of the crude with molecular ion peaks at 505 and 865 m/z respectively (their structures are illustrated in figure 2.42).

structure			
Exact mass	506.23	864.16	953.25
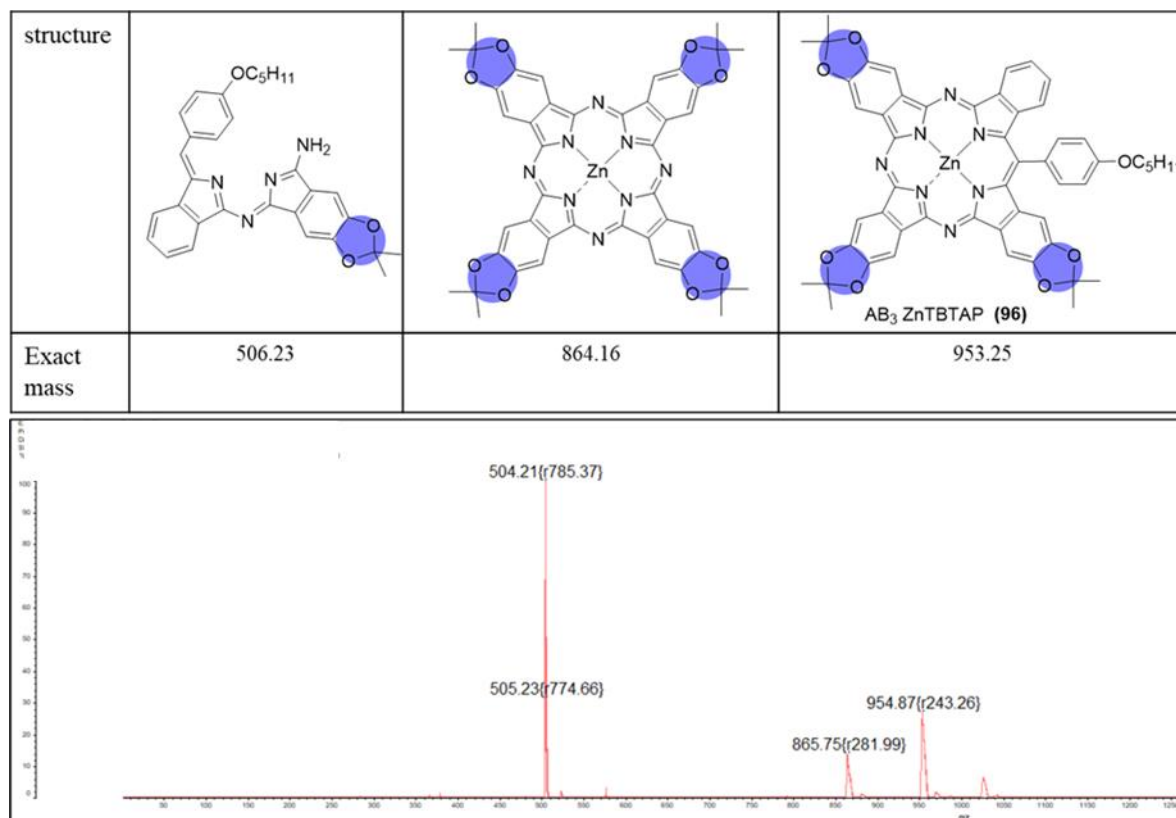
Figure 2.42: MALDI-TOF MS of crude of synthesis of ZnTBTAP (**96**), and the expected structures of observed molecular ions.

After work-up and purification by column chromatography, a full analysis of Zn-AB$_3$TBTAP (**96**) by MALDI-TOF MS, ^{1}H NMR, ^{13}C NMR and UV-Vis were obtained and were as expected. As depicted in figure 2.43, the ^{1}H NMR spectra of novel AB$_3$TBTAP gave the expected peak splitting pattern of AB$_3$ type TBTAP due to reduction of symmetry. Also, unsymmetrical dimer (**97**) and traces of trimer (**98**) were isolated from the crude, and their ^{1}H NMR spectrum are shown in figure 2.44 and were as expected. The ^{1}H NMR spectra of trimer revealed the higher symmetry of the structure compared to dimer spectra. Also, UV-vis spectra of both intermediates illustrated broad UV-visible absorbances with a λ_{max} of around 262 and molar extinction coefficient in the order of 0.51 x 10^5 for dimer (**97**) whereas a λ_{max} of around 269 and molar extinction coefficient in the order of 0.77 x 10^5 for trimer (**98**) as illustrated in figure 2.45. Very broad absorbance from 400-550 nm in both compounds can be clearly seen in the spectra.

Figure 2.43: ^{1}H NMR spectra of Zn TBTAP (**96**) in THF-d_8.

Figure 2.44: ^{1}H NMR spectra of intermediates (**97**) in DCM-d_2 and (**98**) in CDCl$_3$.
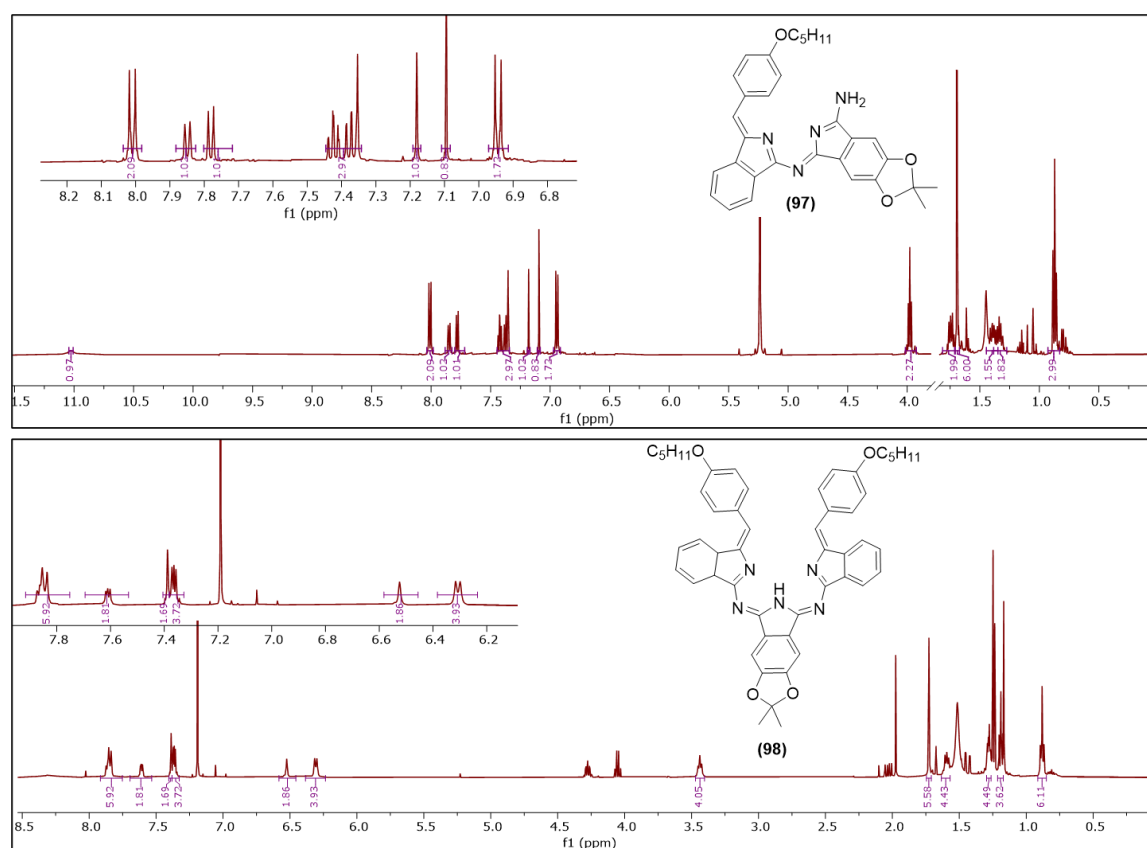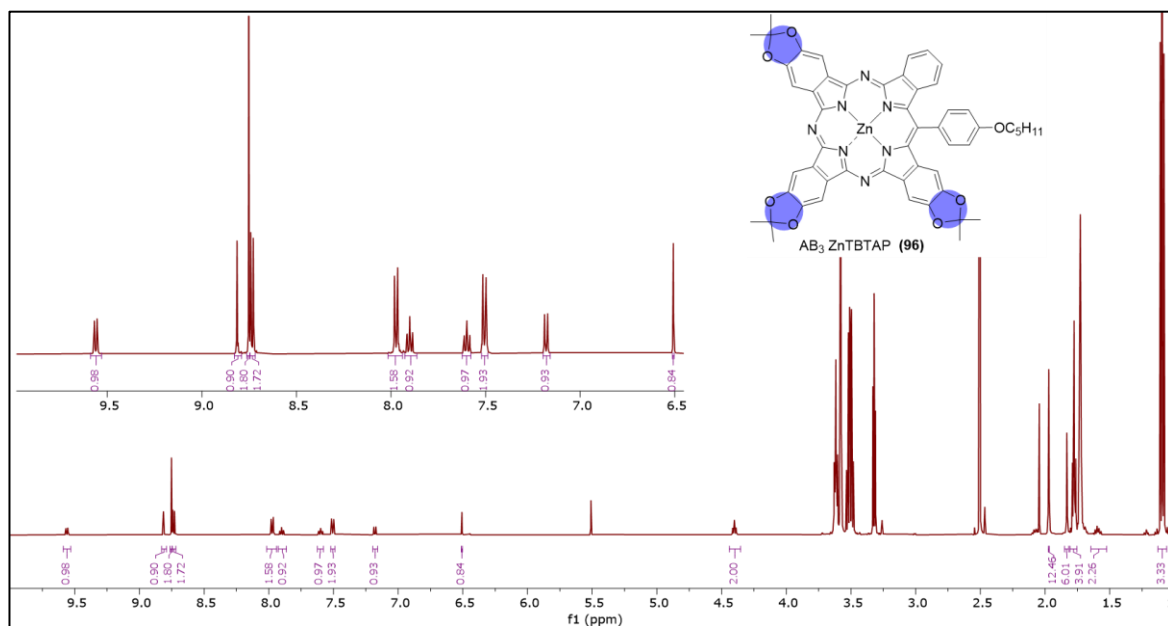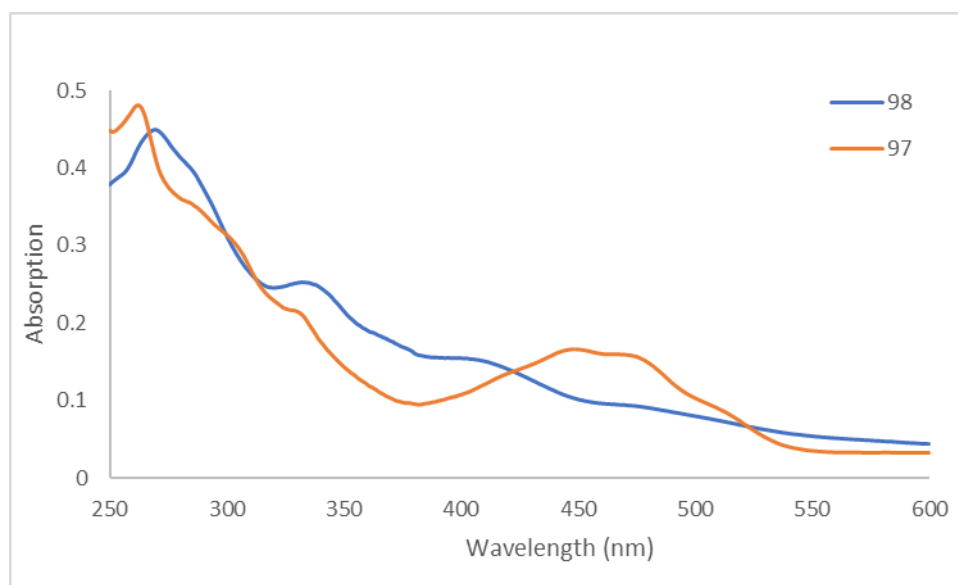
Figure 2.45: UV-Vis spectra of dimer (**97**) and its trimeric product (**98**).

As illustrated above, the two different phthalonitriles gave AB$_3$ TBTAP selectively, and this result is not easily explained. Zinc ion favours a tetrahedral geometry that could favour the formation of ABBA TBTAP via homo-condensation of previously observed intermediate as depicted in scheme 2.43 (loss of ammonia would seem logically easier than loss of benzyl). However, no sign of ABBA TBTAP was observed in two different substitutions so another pathway must be proposed to explain this result.
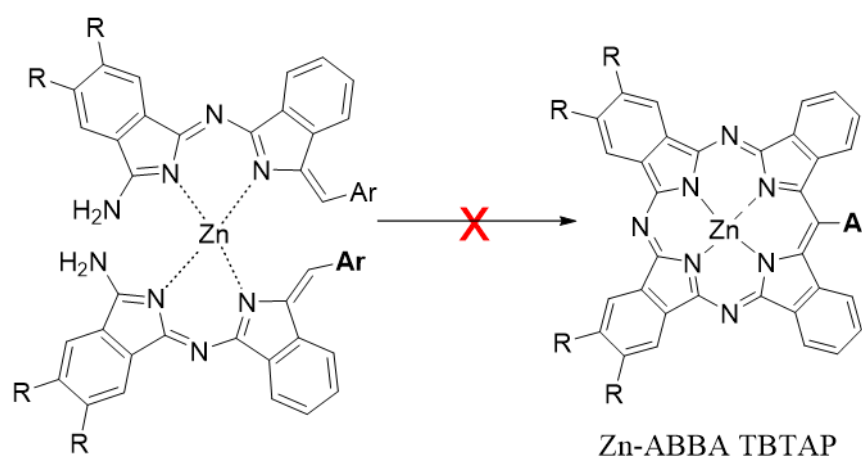
Scheme 2.43: Expected ABBA TBTAP formation via homo-condensation of the previously observed unsymmetrical dimer.

There is another possible pathway to be considered for the formation of AB$_3$ TBTAP via a macrocyclisation of an open four membered oligomer that consists of three isoinoline units that derived from phthalonitrile, and one unit derived from aminoisoindoine. This hypothesised pathway can be logical in case of zinc templating as a slow reaction rate was observed and no green material was observed before two hours. This gives a possibility of steady reaction to occur with the presence of unsymmetrical dimer in the solution and excess of phthalonitrile. (Scheme 2.44).
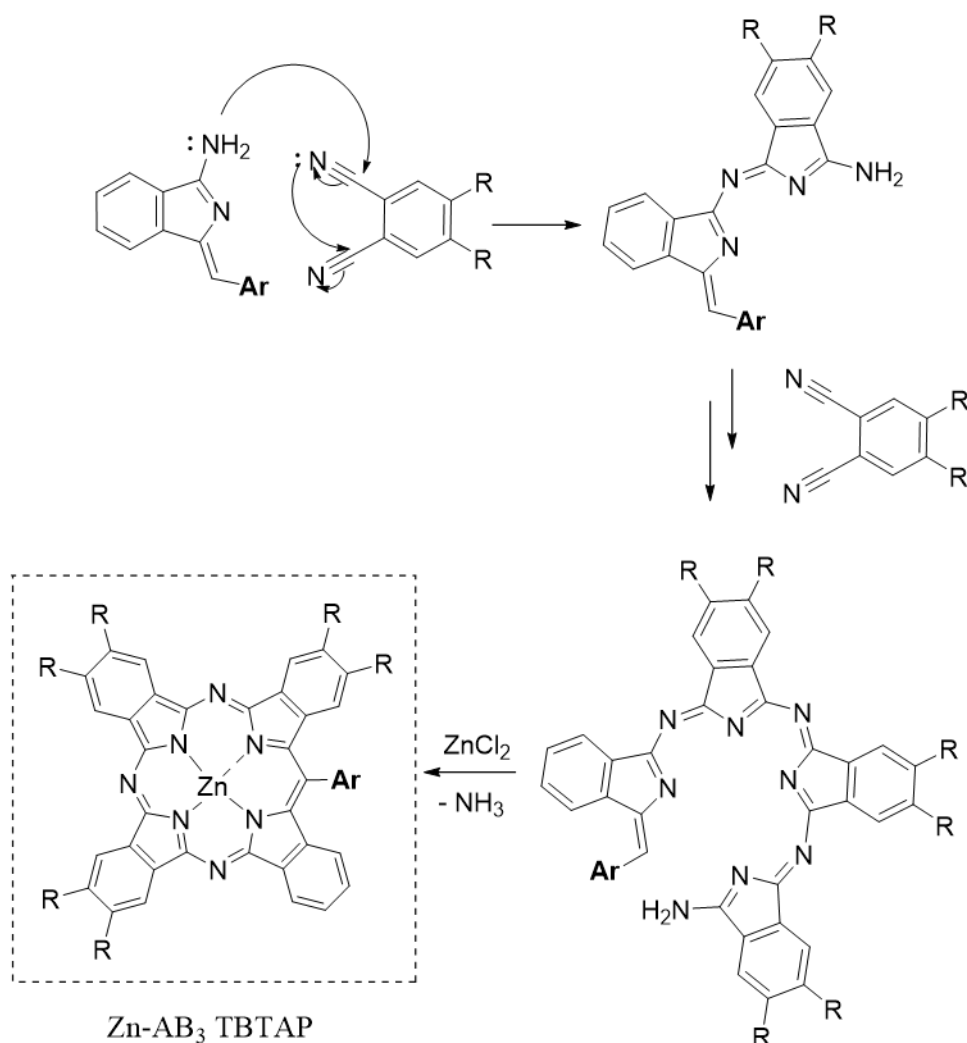
Scheme 2.44: Hypothesised consecutive addition of phthalonitrile to form the 4 membered open chain oligomer and macrocyclisation with zinc to form AB$_3$TBTAP.

2.12 Metal screening

With the observation of a selective synthesis of AB_3 TBTAP when zinc chloride was utilised as template ion, different metals with different ionic radii were suggested to be tested under this condition. Li^{1+}, Na^{1+} and K^{1+} were the first metals to be tested as they have different effective ionic radius similar and larger than Zn^{2+} (76, 102, 138 and 74 pm respectively). Also, Mg^{2+}, Ni^{2+}, mixture of Cu^{1+}/Cu^{2+} and Pb^{2+} were selected as 2+ ions with different ionic radii (72, 69, 73/77 and 119 pm respectively). The counter ions of these metals were kept the same, so we used LiCl, NaCl, KCl, $MgCl_2$, $NiCl_2$, (CuCl/Cu $(OAc)_2$ and $PbCl_2$. The reactions were attempted as illustrated in scheme 2.45.[38]
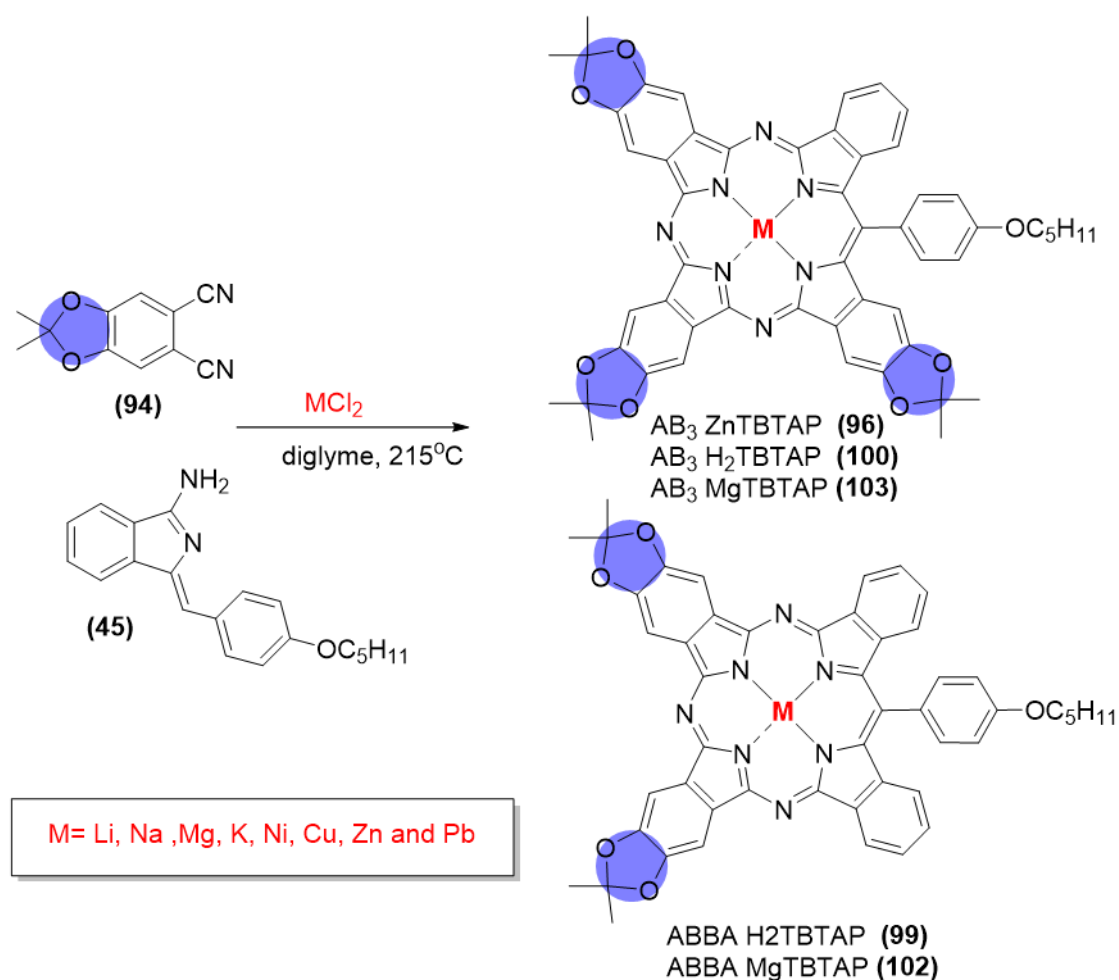
Scheme 2.45: Metal screening of macrocyclisation of phthalonitrile (**94**) and aminoisoindoline (**45**).

After work up and column chromatography purifications, the isolated products were as illustrated in table 2.3 with their calculated yields. All reactions produce unmetalated hybrids except magnesium and zinc reactions. In practice all reactions underwent a separate metalation step using zinc acetate and DMF as solvent, because the isolation of unmetalated hybrids was attempted using different solvent systems but proved unsuccessful as both hybrids have similar R_f. After many attempts to isolate these hybrids, just small amounts of H_2ABBA TBTAP was obtained in its pure state.

Metal	Solvent	Temperature	Time	Product	Calculated yield
$ZnCl_2$				Zn AB$_3$ TBTAP (**96**)	8%
LiCl				H_2 ABBA TBTAP (**99**)	10.3%
				H_2 AB$_3$ TBTAP (**100**)	6%
NaCl				H_2 ABBA TBTAP (**99**)	7%
				H_2 AB$_3$ TBTAP (**100**)	4.5%
KCl				H_2 ABBA TBTAP (**99**)	7%
				H_2 AB$_3$ TBTAP (**100**)	4.5%
$MgCl_2$	Diglyme	215°C	17 H	Mg ABBA TBTAP (**102**)	8%
				Mg AB$_3$ TBTAP (**103**)	5%
$PbCl_2$				H_2Pc	
				H_2 ABBA TBTAP	____
				H_2 AB$_3$ TBTAP	
$NiCl_2$				traces of macrocycle	____
CuCl Cu (OAc)$_2$				Cu AA CuPc	____

Table 2.2: Isolated products and their yields from metal screening of macrocyclisation of phthalonitrile (**94**) and aminoisoindoline (**45**).

Figure 2.46 shows the MALDI-TOF MS of the crude obtained when Li, Na and K were employed as the templating metals. It gave metal-free mixtures of AB$_3$ with molecular ion peak at 891 m/z and ABBA TBTAP with molecular ion peak at 819 m/z. Also, self-condensed intermediate and trimeric products were observed at 595.99 and 796.27

respectively. The crude was metalated for isolation purposes and zinc metal was used in refluxing DMF as solvent (scheme 2.46). After two hours, the crude was analysed by MALDI-TOF MS to confirm a full metalation of the crude. Figure 2.46 shows the formation of both molecular ion peaks at 881 m/z and 953 m/z that corresponded to ZnABBA and ZnAB$_3$ respectively. Then, the mixture was submitted to column chromatography to isolate both hybrids.
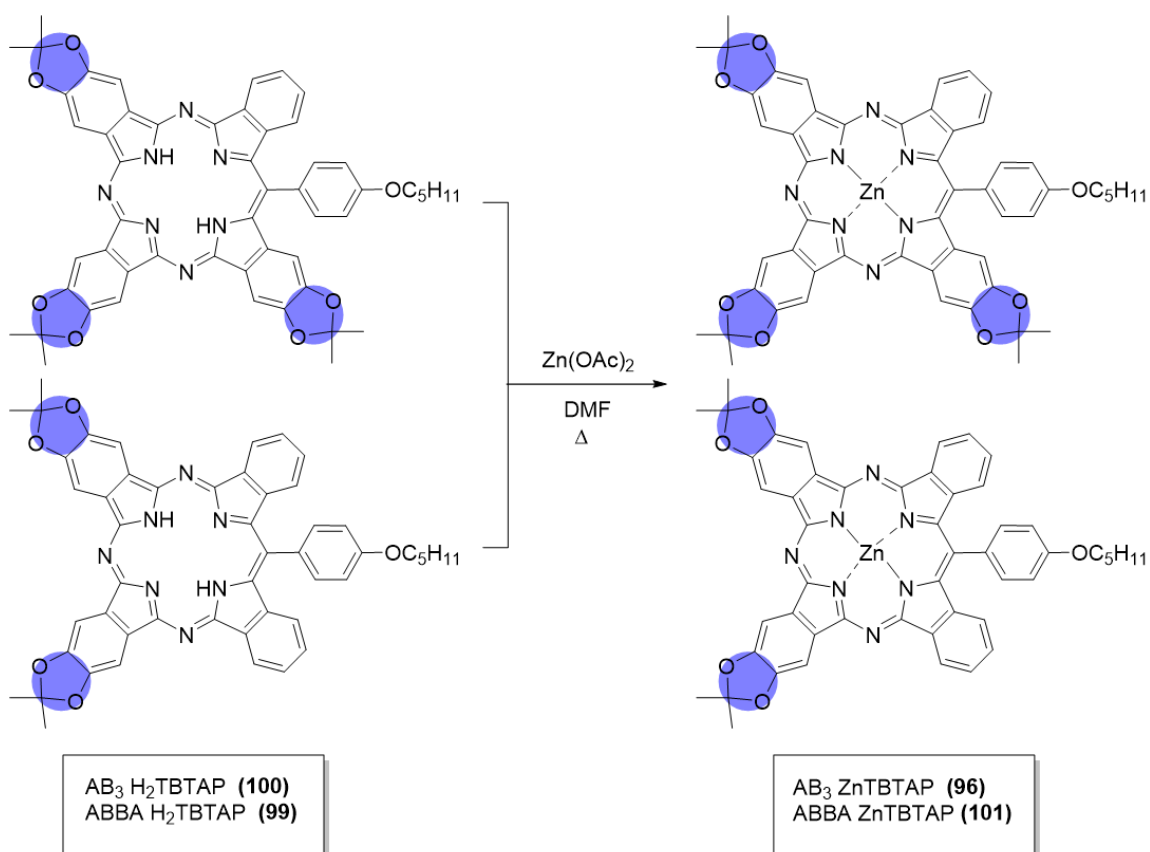
Scheme 2.46: Metalation reaction of unmetallated crude using zinc acetate and DMF as solvent.

Poposed structure				
Exact mass	595.32	795.38	M = Zn 881.23 M= 2H 819.32	M= Zn 953.2 M= 2H 891.34
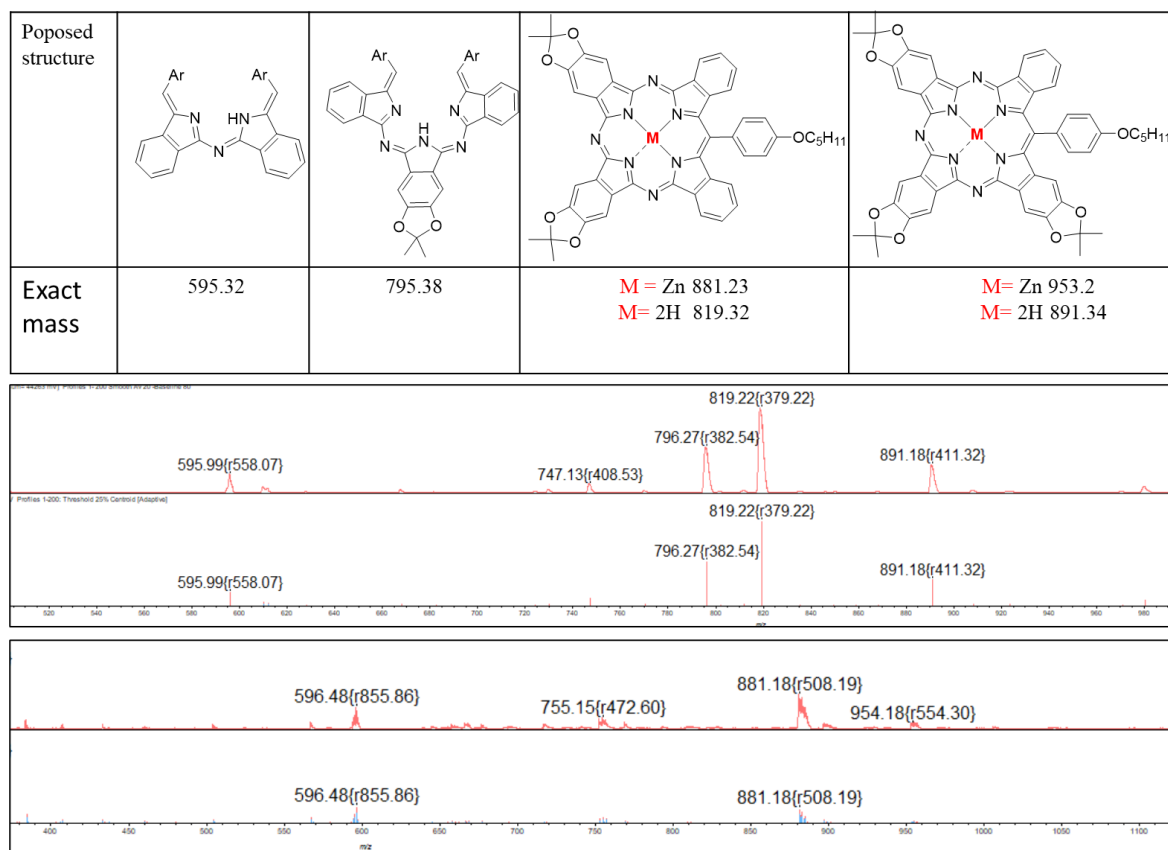
Figure 2.46: Table of observed structures and their exact mass (top), MALDI-TOF MS of metal-free crude (middle) and their zinc metalation products crude (bottom).

Both zinc ABBA (**101**) and ABBB TBTAP (**96**) were successfully isolated and analysed by ^{1}H NMR spectroscopy in THF-d_8 as illustrated in figure 2.47. As expected, the chemical shift and peak splitting differs as a result of reduction of symmetry of ABBB TBTAP compared to ABBA TBTAP. It was also possible to grow crystals of both hybrids that were suitable for x-ray diffraction (figure 2.48). It is interesting to note that ABBA hybrid (**101**) shows unusual different ligation of both ethanol molecule and THF molecule.
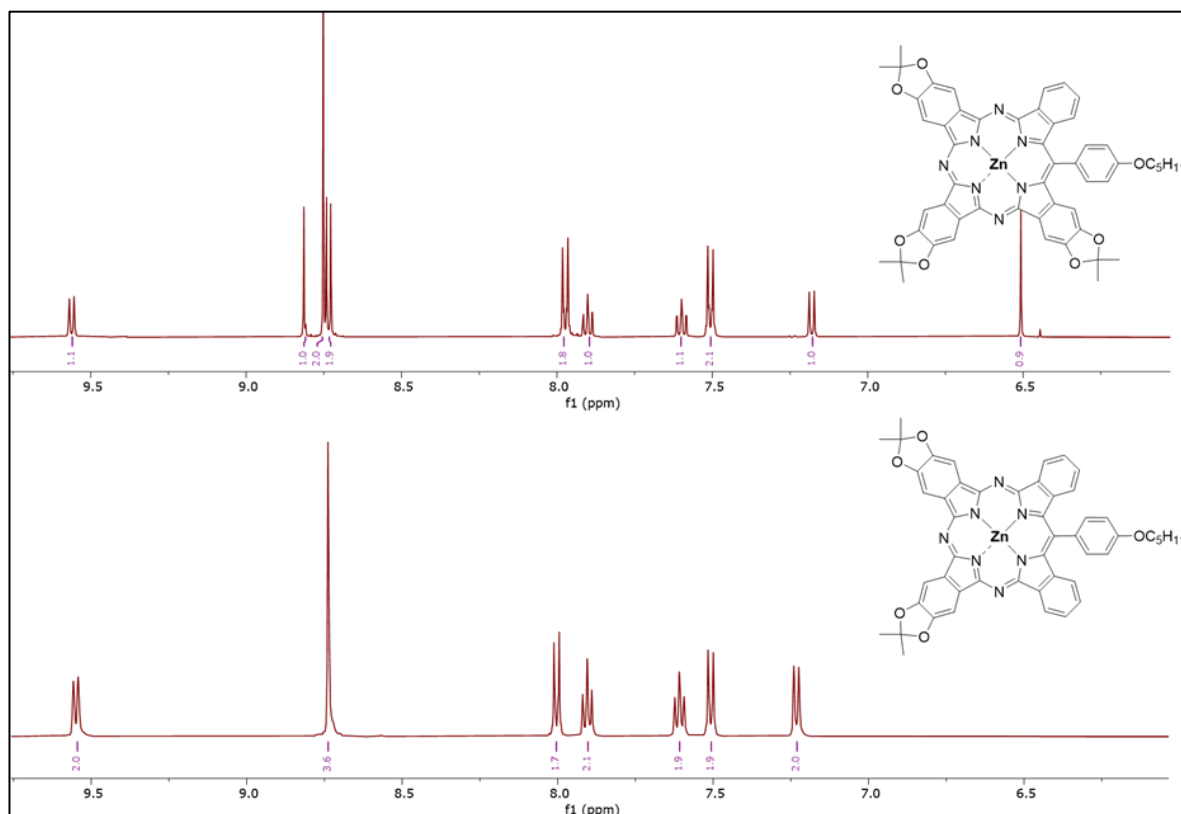
Figure 2.47: ^{1}H NMR spectra of Zn TBTAP (**96**) and (**101**) in THF-d_8.
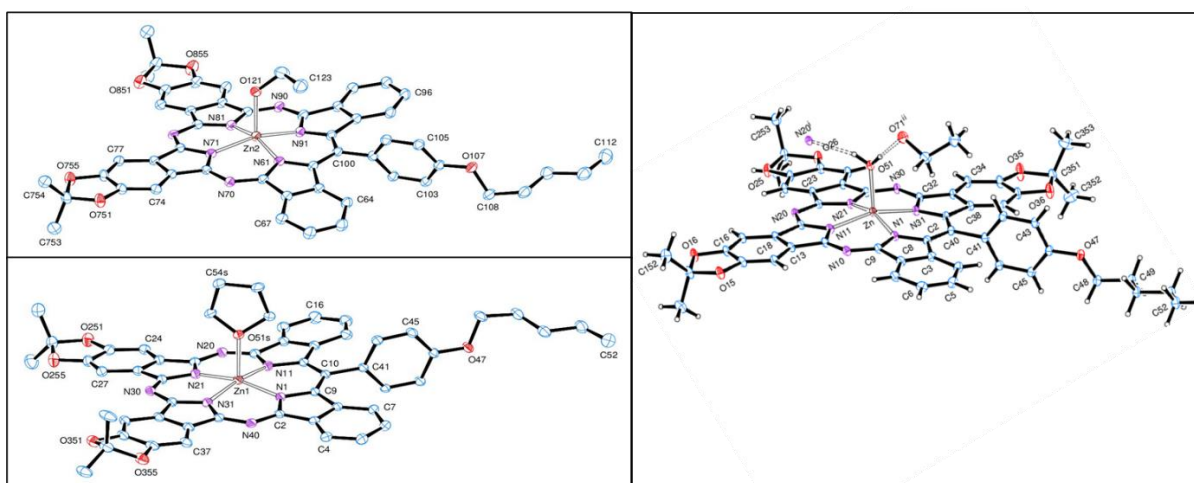
Figure 2.48: X-ray structures of (**96**) and (**101**) hybrids (ORTEP).

The reaction was attempted using magnesium chloride and both hybrids were formed as expected based on our group's previous work using magnesium as template. Both hybrids were isolated and characterised and their analysis was as expected. ^{1}H NMR spectra of zinc and magnesium ABBA hybrids in d8 THF are illustrated in figure 2.49. Their spectra are identical with a slight shift of signals.
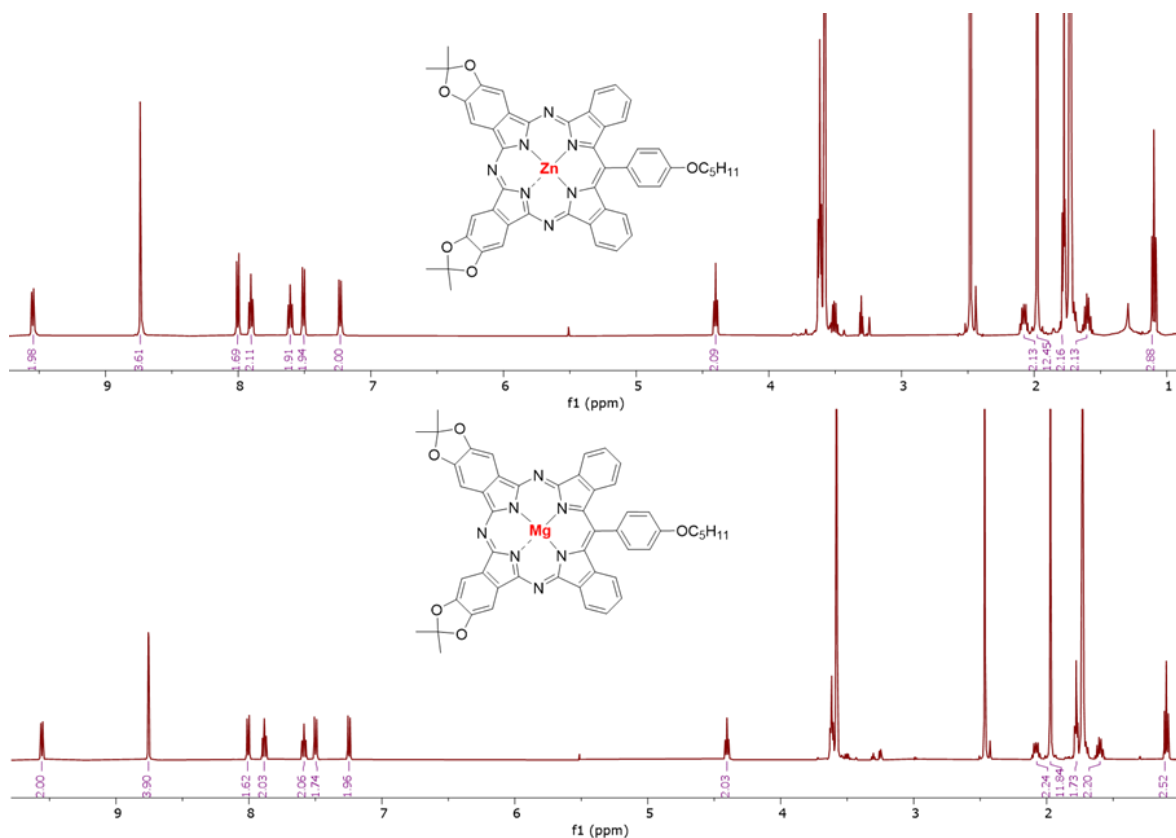
Figure 2.49: ^{1}H NMR spectra of Zn TBTAP (**101**) and MgTBTAP (**102**) in THF-d_8.

All employed metals apart from zinc gave a mixture of ABBA TBTAP and AB$_3$ TBTAP and in all these cases the ABBA hybrid was the dominant product. In contrast, zinc template gave a selective synthesis of the AB$_3$ TBTAP. NiCl$_2$ failed to give any macrocyclisation product and copper gave just Pc. The formation of the two different hybrids suggests two different pathways are occurring as illustrated above in scheme (2.43 and 2.44).
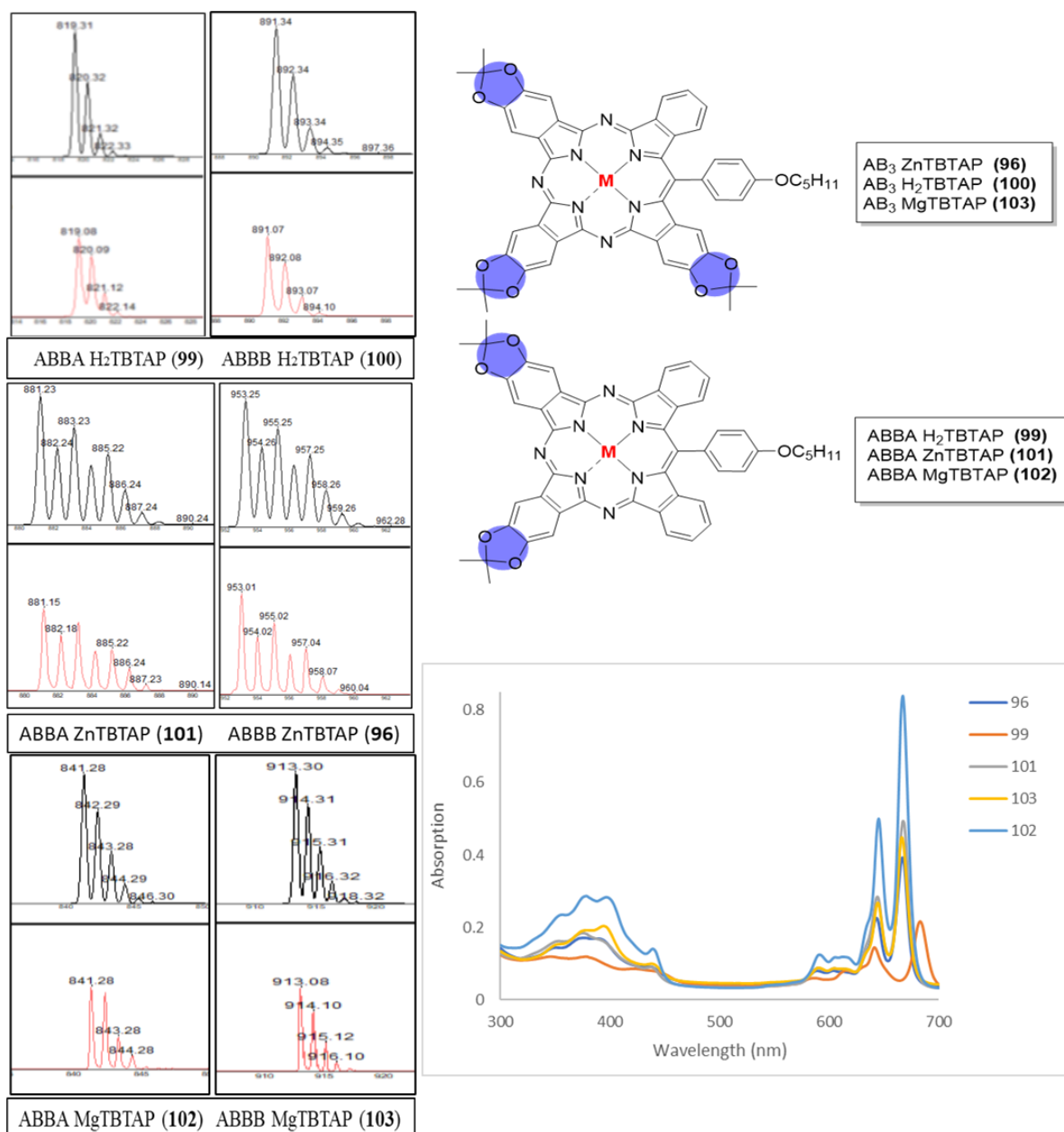
Figure 2.50: MALDI-TOF MS of metallated and unmetallated hybrids (bottom, left) plus their theoretical isotopic pattern (top, left), and their UV-Visible absorption spectra in THF.

All isolated hybrids were checked by MALDI-TOF MS and give the expected molecular ions peaks and their isotopic patterns were matched the theoretical ones as illustrated in figure 2.50. Also, UV-vis spectra of all hybrids in distilled THF were obtained. The Q-band position of all macrocycles is similar. However, the intensity of the Q-band of unmetalated hybrid is less than the metalated hybrids. It seems that the number of substituents on the macrocycle affect slightly their spectrum. This outcome is consistent with the literature. As

reported, the incorporation of substituents at both the *meso*-position of the ring and in the aromatic system of the macrocycle has only a slight effect on the absorption spectrum.[39]

2.13 Conclusion

The synthesis of tetrabenzomonoazaporphyrin hybrids (TBMAPs) was not possible using our proposed pathway by utilising alkynyl benzonitriles as a co-macrocyclisation partner with the well-investigated aminoisoindoline under our group's recent TBTAP's formation conditions. The reactivity of two different acetylenes (one bearing donating group and the other bearing withdrawing group) was tested under phthalocyanine macrocyclisation conditions but none of them gave any hybrids. However, a six membered ring intermediate (isoquinoline) was obtained which indicated that this precursor cannot be employed in macrocyclisation synthesis.

Linstead's method of TBMAP synthesis was revisited. Synthesis of its precursor proved to be challenging when acid or water was employed in purification processes. After many attempts the desired precursor was successfully isolated and TBMAP synthesis was attempted. However, insoluble material was obtained so no further analysis was possible. Thus, it was important to introduce substitutions on peripheral sites of fused benzene rings of the final hybrids to ease analysis and purification. Different phthalonitriles and different aminoisoindolines have been synthesised and the fusion reaction was attempted. Soluble crude mixtures were successfully obtained but they were unstable. At this stage, after many attempts, it was just possible to obtain MALDI-TOF MS that proved a mixture of hybrids were formed. The major hybrid was Zn (COOCH$_2$CH$_3$)-TBTAP that gave a matched splitting Q-band in UV-vis spectra to a related literature TBTAP's UV.

Unexpected results were obtained during the investigation of applying Linstead's conditions on our proposed reagents. Formation of ZnTBTAP, *cis*-TBDAP and *trans*-TBDAP hybrids were observed along with traces of the desired ZnTBMAP macrocycle from fusion of aminoisoindoline alone. Full analysis of all hybrids was obtained except ZnTBMAP due to its small quantity in the crude.

This outcome led us to reinvestigate our group's TBTAP synthesis using zinc metal and other metals as macrocyclisation templates. We aimed to explore the effect of the metal size and oxidation state on macrocyclisation. We also employed substituted phthalonitriles

(rarely employed in previous syntheses) to identify the type of hybrid and its mechanistic formation. Full analysis of isolated intermediates was successfully obtained.

Also, a selective synthesis of AB$_3$ TBTAP was successfully achieved when zinc metal was employed whereas as a mixture of AB$_3$ TBTAP and ABBA TBTAP were formed when other metals were employed. Two different pathways were hypothesised for these hybrids' formation but no clear evidence for the origin of selectivity of zinc metal has yet been deduced.

2.14 References

(1)   Alharbi, N.; Díaz-Moscoso, A.; Tizzard, G. J.; Coles, S. J.; Cook, M. J.; Cammidge, A. N. Improved Syntheses of Meso-Aryl Tetrabenzotriazaporphyrins (TBTAPs). *Tetrahedron,* **2014**, *70* (40), 7370–7379.

(2)   Alharbi, N.; Tizzard, G. J.; Coles, S. J.; Cook, M. J.; Cammidge, A. N. First Examples of Functionalisation of Meso-Aryl Tetrabenzotriazaporphyrins (TBTAPs) through Cross-Coupling Reactions. *Tetrahedron,* **2015**, *71* (39).

(3)   Díaz-Moscoso, A.; Tizzard, G. J.; Coles, S. J.; Cammidge, A. N. Synthesis of Meso-Substituted Tetrabenzotriazaporphyrins: Easy Access to Hybrid Macrocycles. *Angew. Chem.,* **2013**, *125* (41), 10984–10987.

(4)   Alkorbi, F.; Díaz-Moscoso, A.; Gretton, J.; Chambrier, I.; Tizzard, G. J.; Coles, S. J.; Hughes, D. L.; Cammidge, A. N. Complementary Syntheses Giving Access to a Full Suite of Differentially Substituted Phthalocyanine-Porphyrin Hybrids. *Angew. Chem. Int. Ed.,* **2021**, *60* (14), 7632–7636.

(5)   Sugano, Y.; Matsuo, K.; Hayashi, H.; Aratani, N.; Yamada, H. Synthesis of 10, 20-Substituted Tetrabenzo-5, 15-Diazaporphyrin Copper Complexes from Soluble Precursors. *J. Porphyr. Phthalocyanines,* **2021**, *25*, 1186–1192.

(6)   Andrianov, D. S.; Farré, Y.; Chen, K. J.; Warnan, J.; Planchat, A.; Jacquemin, D.; Cheprakov, A. V.; Odobel, F. Trans-Disubstituted Benzodiazaporphyrin: A Promising Hybrid Dye between Porphyrin and Phthalocyanine for Application in Dye-Sensitized Solar Cells. *J. Photochem. Photobiol. A Chem.,* **2016**, *330*, 186–194.

(7)   Andrianov, D. S.; Rybakov, V. B.; Cheprakov, A. V. Between Porphyrins and Phthalocyanines: 10, 20-Diaryl-5, 15-Tetrabenzodiazaporphyrins. *Chem. Commun.,* **2014**, *50* (59), 7953–7955.

(8)   A Barrett, B. P.; Linstead, R. P.; Rundall, F. G.; P Tuey, G. A. Part X I X. Tetra-Benzoporphin, Tetrabenzomonoazaporphin and Their Metallic Derivatives. *J. Chem. Soc.,* **1940**, 1079–1092.

(9)   Hellal, M.; Cuny, G. D. Microwave Assisted Copper-Free Sonogashira Coupling/5-Exo-Dig Cycloisomerization Domino Reaction: Access to 3-(Phenylmethylene)Isoindolin-1-Ones and Related Heterocycles. *Tetrahedron Lett.,* **2011**, *52* (42), 5508–5511.

(10)   Dalai, S.; Belov, V. N.; Nizamov, S.; Rauch, K.; Finsinger, D.; De Meijere, A. Access to Variously Substituted 5,6,7,8-Tetrahydro-3H-Quinazolin-4-Ones via Diels-Alder Adducts of Phenyl Vinyl Sulfone to Cyclobutene-Annelated Pyrimidinones. *Eur. J. Org. Chem.,* **2006**, No. 12, 2753–2765.

(11)   Hillier, A. C.; Grasa, G. A.; Viciu, M. S.; Lee, H. M.; Yang, C.; Nolan, S. P. Catalytic Cross-Coupling Reactions Mediated by Palladium/Nucleophilic Carbene Systems. *J. Organomet. Chem.,* **2002**, *653* (1), 69–82.

(12)   Díaz-Moscoso, A.; Tizzard, G. J.; Coles, S. J.; Cammidge, A. N. Synthesis of Meso-Substituted Tetrabenzotriazaporphyrins: Easy Access to Hybrid Macrocycles. *Angew. Chem.,* **2013**, *125* (41), 10984–10987.

(13)   McKeown, N. B. *Phthalocyanine Materials: Synthesis, Structure and Function*; Cambridge University Press, Cambridge, **1998**.

(14)   Cammidge, A. N.; Chambrier, I.; Cook, M. J.; Sosa-Vargas, L. 75 Synthesis and Properties of the Hybrid Phthalocyanine-Tetrabenzoporphyrin Macrocycles. In *Handbook of Porphyrin Science*; World Scientific, Singapore, **2012**, Vol. 16, pp331–404.

(15)   Chinchilla, R.; Nájera, C. Recent Advances in Sonogashira Reactions. *Chem. Soc. Rev.,* **2011**, *40* (10), 5084–5121.

(16)   Cook, M. J.; Dunn, A. J.; Howe, S. D.; Thomson, A. J.; Harrison, K. J. Octa-Alkoxy Phthalocyanine and Naphthalocyanine Derivatives: Dyes with Q-Band Absorption in the Far Red or near Infrared. *J. Chem. Soc. Perkin Trans. 1,* **1988**, 2453–2458.

(17)   Gilmore, K.; Mohamed, R. K.; Alabugin, I. V. The Baldwin Rules: Revised and Extended. Wiley interdisciplinary rev. *Comput. Mol. Sci.,* **2016**, *6* (5), 487–514.

(18)   Baldwin, J. E. Rules for Ring Closure. *J. Chem. Soc. Chem. Commun.*, **1976**, 18, 734–736.

(19)   Baroudi, A.; Jaradat, K.; Karton, A. 6-Endo-Dig versus 5-Exo-Dig: Exploring Radical Cyclization Preference with First-, Second-, and Third-Row Linkers Using High-Level Quantum Chemical Methods. *Chem.Phys.Chem.,* **2023**, *24* (17), e202300426.

(20)   Bengtsson, C.; Almqvist, F. A Selective Intramolecular 5-Exo-Dig or 6-Endo-Dig Cyclization En Route to 2-Furanone or 2-Pyrone Containing Tricyclic Scaffolds. *J. Org. Chem.,* **2011**, *76* (23), 9817–9825.

(21)   Nguyen, P.; Todd, S.; Van den Biggelaar, D.; Taylor, N. J.; Marder, T. B.; Wittmann, F.; Friend, R. H. Facile Route to Highly Fluorescent 9, 10-Bis (Pr-Phenylethynyl) Anthracene Chromophores via Palladium-Copper Catalyzed Cross-Coupling. *Synlett.,* **1994**, *1994*, 299–301.

(22)   Sonogashira, K.; Tohda, Y.; Hagihara, N. A Convenient Synthesis of Acetylenes: Catalytic Substitutions of Acetylenic Hydrogen with Bromoalkenes, Iodoarenes and Bromopyridines. *Tetrahedron Lett.,* **1975**, *16* (50), 4467–4470.

(23)   A Barrett, B. P.; Linstead, R. P.; Rundall, F. G.; P Tuey, G. A. 197. Phthalocyanines and related compounds. *Part X I X. Tetra-Benzprphin, Tetrabenzmnamprphin and Their Metallic Derivatives*. *J. Chem. Soc. (Resumed)*, **1940**, 1079-1092.

(24)   Barrett, P. A.; Linstead, R. P.; Leavitt, J. J.; Rowe, G. A. 196. Phthalocyanines and Related Compounds. Part XVIII. Intermediates for the Preparation of Tetrabenzporphins : The Thorpe Reaction with Phthalonitrile. *J. Chem. Soc. (Resumed),* **1940**, 1076–1079.

(25)   Kagechika, H.; Kawachi, E.; Hashimoto, Y.; Shudo, K.; Himi, T. Retinobenzoic Acids. 1. Structure-Activity Relationships of Aromatic Amides with Retinoidal Activity. *J. Med. Chem.,* **1988**, *31* (11), 2182–2192.

(26)   Bruson, H. A.; Kroeger, J. W. Cycli-Alkylation of Aromatic Compounds by the Friedel and Crafts Reaction. *J. Am. Chem. Soc.,* **1940**, *62* (1), 36–44.

(27)   Schmerling, L.; West, J. P. Condensation of Saturated Halides with Unsaturated Compounds. VIII. Condensation of Dihaloalkanes with Ethylene and Chloroethylenes1. *J. Am. Chem. Soc.,* **1952**, *74* (11), 2885–2889.

(28)   Mikhalenko, S. A.; Solov'eva, L. I.; Luk'yanets, E. A. Symmetric Sterically Hindered Phthalocyanines. *ChemInform.,* **1989**, *20* (25).

(29) Hanack, M.; Haisch, P.; Lehmann, H.; Subramanian, L. R. Synthesis of Soluble Octasubstituted Phthalocyaninatoplatinum And-Palladium Complexes. *Synthesis.,* **1993**, *1993*, 387–390.

(30) Ashton, P. R.; Girreser, U.; Giuffrida, D.; Kohnke, F. H.; Mathias, J. P.; Raymo, F. M.; Slawin, A. M. Z.; Stoddart, J. F.; Williams, D. J. Molecular Belts. 2. Substrate-Directed Syntheses of Belt-Type and Cage-Type Structures. *J. Am. Chem. Soc.,* **1993**, *115* (13), 5422–5429.

(31) Schareina, T.; Zapf, A.; Mägerlein, W.; Müller, N.; Beller, M. A State-of-the-Art Cyanation of Aryl Bromides: A Novel and Versatile Copper Catalyst System Inspired by Nature. *Chem. Eur. J.,* **2007**, *13* (21), 6249–6254.

(32) Wenderski, T.; Light, K. M.; Ogrin, D.; Bott, S. G.; Harlan, C. J. Pd Catalyzed Coupling of 1,2-Dibromoarenes and Anilines: Formation of N,N-Diaryl-*o*-Phenylenediamines. *Tetrahedron Lett.,* **2004**, *45* (37), 6851–6853.

(33) KOHN, M.; STEINER, L. The Reduction of Bromo Derivatives of Catechol, Resorcinol, and Pyrogallol. *J. Org. Chem.*, **1947**, *12* (1), 30–33.

(34) Ellis, G. P.; Romney-Alexander, T. M. Cyanation of Aromatic Halides. *Chem. Rev.,* **1987**, *87* (4), 779–794.

(35) Gretton, J. Phthalocyanine and Subphthalocyanine Hybrid Macrocycles: Improved Accessibility and Synthetic Control via New Intermediates, PhD thesis, University of East Anglia, **2022**.

(36) Gonidec, M.; Biagi, R.; Corradini, V.; Moro, F.; De Renzi, V.; Del Pennino, U.; Summa, D.; Muccioli, L.; Zannoni, C.; Amabilino, D. B.; Veciana, J. Surface Supramolecular Organization of a Terbium(III) Double-Decker Complex on Graphite and Its Single Molecule Magnet Behavior. *J. Am. Chem. Soc.,* **2011**, *133* (17), 6603–6612.

(37) Sarker, A. K.; Kang, M. G.; Hong, J. D. A Near-Infrared Dye for Dye-Sensitized Solar Cell: Catecholate- Functionalized Zinc Phthalocyanine. *Dyes Pigm.,* **2012**, *92* (3), 1160–1165.

(38) Shannon, R. Revised effective ionic radii and systematic studies of interatomic distances in halides and chalcogenides. *Acta. Cryst.*, **1976**, 32, 751-767.

(39) Fu, Y.; Forman, M.; Leznoff, C. C.; Lever, A. B. P. Effect of Stearic Acid on Molecular Orientation in Metal-Free 2, 9, 16, 23-Tetra-Tert-Butyltetrabenzotriazaporphine Langmuir-Blodgett Films. *J. Phys. Chem.*, **1994**, *98* (36), 8985–8991.

Chapter 3:

Experimental

3.1 General Methods

Solvents and reagents were obtained from commercial suppliers and used without any further purifications, with the following exceptions: Dichloromethane (DCM), triethylamine (TEA) and toluene (MePh) were dried over CaH_2. THF was distilled prior to its use as a chromatography or recrystallisation solvent. Phthalonitrile was recrystallised from hot xylene. Water refers to distilled water. Organic layers were dried using anhydrous magnesium sulphate. Evaporation of solvent was carried out on a Büchi rotary evaporator at reduced pressure.

Thin layer chromatography (TLC) was carried out on aluminum sheets coated with Alugram® Sil G/UV254 (Macherey-Nagel) and the compounds were visualised by viewing under short-wavelength UV-light at 254 nm or long-wavelength at 366 nm. Column chromatography: was carried out on silica gel 60Å mesh 70 – 230 (63 – 200 µm) under regular conditions. Solvent ratios are given as v: v.

^{1}H NMR spectra were recorded either at 400 MHz on an Ultrashield PlusTM 400 spectrometer or 500 MHz on a Bruker AscendTM 500 spectrometer in 5 mm diameter tubes at r.t. The residual solvent peaks were used as references. ^{1}H NMR signals are reported in ppm and the coupling constants J are given in Hertz. The spectra of all macrocycles are of recrystallised samples from Acetone/ EtOH, Acetone/DCM/EtOH or THF/ EtOH and display coordinated solvents in agreement with X-ray crystal structures. ^{13}C-NMR spectra were recorded at 100.5 MHz or 125.7 MHz on the same spectrometers. NMR spectra were performed in solution using deuterated chloroform, DCM, Acetone, DMSO or THF at r.t.

MALDI-TOF mass spectra were carried out using a Shimadzu Biotech Axima instrument (no matrix was used in all experiments). IR spectra were recorded using a PerkinElmer Spectrum BX FT-IR spectrometer. Ultraviolet-Visible absorption spectra were recorded on Hitachi U-3310 Spectrophotometer in solvent as stated. Melting points were taken on a Reichart Thermovar microscope with a thermopar based temperature control.

3.2 4,5-Substituted Phthalonitriles and bromobenzonitriles

3.2.1 1,1,4,4-Tetramethyl-1,2,3,4-tetrahydronaphthalene dinitrile (52)
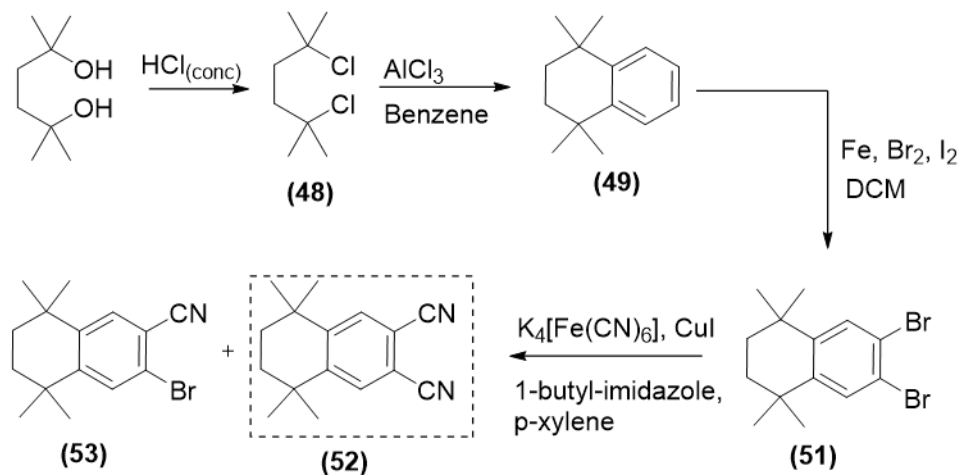
2,5-Dichloro-2,5-dimethylhexane (48)[1–3]
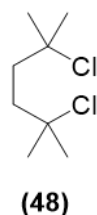
Following a known reported procedure, 2,5-dimethylhexane-2,5-diol (25 g, 171.2 mmol) was dissolved in concentrated hydrochloric acid (250 mL). The mixture was stirred at 0 °C for 30 min, then it was left stirring overnight at r.t. The light pink solid was filtered off and washed with water. The precipitate was dissolved in DCM (50 mL) and washed again with water and extracted with DCM (2 x 50 mL). The organic phase was dried (MgSO$_4$), and the solvent was evaporated under reduced pressure. The product was purified by recrystallisation from methanol to yield the desired compound as a white solid (24.5 g, 78%). **MP:** 61°C (lit. 59-60 °C)[3]

^{1}H NMR (500 MHz, Chloroform-*d*) δ 1.95 (s, 4H), 1.60 (s, 12H).

1,1,4,4-Tetramethyl-1,2,3,4-tetrahydronaphthalene (49)[2]
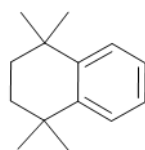
(49)

A solution of 2,5- dichloro-2,5-dimethylhexane (**48**) (20 g, 109 mmol) in benzene (250 mL) was stirred for 10 min at 50 °C. Then, anhydrous aluminum trichloride (5.8 g, 43 mmol) was added in small portions over 30 min. The thick suspension was then left stirring at 50 °C overnight. After cooling the reaction mixture to r.t., dilute hydrochloric acid (50 mL) was added and extracted with DCM (3 x 50 mL). The organic phase was washed with water and then with dilute sodium carbonate solution, dried (MgSO$_4$), filtered and the solvent was removed under reduced pressure. The resulting material was purified by column chromatography over silica gel using PE as a solvent to give the product as a colourless liquid (18.6 g, 91%).

^{1}H NMR (500 MHz, Chloroform-*d*) δ 7.55 (dd, *J* = 6.0, 3.5 Hz, 2H), 7.36 (dd, *J* = 6.0, 3.5 Hz, 2H), 1.95 (s, 4H), 1.54 (s, 12H).

6,7-Dibromo-1,1,4,4-tetramethyl-1,2,3,4-tetrahydronaphthalene (51)[4–6]
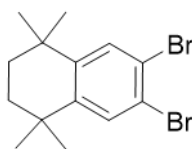
(51)

Following Ashton and co-workers' procedure, a solution of 1,1,4,4-tetramethyl-1,2,3,4-tetrahydronaphthalene (**49**) (18 g, 96 mmol), iron powder (0.612g, 10.96 mmol) and iodine (0.233g, 0.92 mmol) in DCM (180 mL) was stirred at 0 °C and then bromine (9.54 mL, 185.1 mmol) was added dropwise via dropping funnel over 30 min. After the addition was complete, the reaction mixture was left to stir at r.t. for 24 h. The resulting mixture was washed with an aqueous solution of sodium metabisulfite and then with sodium bicarbonate to remove the excess bromine. Next, water and brine (50 mL) were added, and the mixture was extracted with DCM (3 x 50 mL). The organic phase was dried over MgSO$_4$, filtered and the solvent removed under reduced pressure to give a brownish solid. The product was purified by column chromatography over silica gel using PE as eluent to give the title compound as a yellow solid (29.1g, 88%).

MP: 112- 115 °C (lit. 111-112 °C)[6]

156

¹H NMR (400 MHz, Chloroform-*d*) δ 7.50 (s, 2H), 1.66 (s, 4H), 1.25 (s, 12H).

6,7-Dicyano-1,1,4,4-tetramethyl-1,2,3,4-tetrahydronaphthalene (52)[7]

(52)
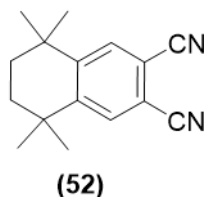
6,7-Dibromo-1,1,4,4-tetramethyl-1,2,3,4-tetrahydronaphthalene (**51**) (5 g, 15 mmol) was dissolved in anhydrous *p*-xylene (20 mL) under N₂. CuI (300 mg, 1.5 mmol), finely ground and dried K₄[Fe (CN)₆] (2.5 g, 7.5 mmol) were added followed by 1-butylimidazole (4.9mL, 37 mmol) and the solution heated to reflux at 160-170 °C. The reaction was monitored by TLC until completion (4-5 days). When the reaction was finished and cooled down, EtOAc (100 mL), H₂O (100 mL) were added, and the solution filtered to remove the precipitate formed. Then, the filtrate was transferred to a separation funnel and washed with H₂O (2 x 100 mL). The organic phase was dried (MgSO₄), and the solvent removed under reduced pressure. The crude was purified by silica gel chromatography using PE:toluene 3:1 as eluent to yield the title compound as an off-white solid (2.5 g, 70%).

MP: 205-208 °C (lit. 206-208 °C)[8]

¹H NMR (500 MHz, Chloroform-*d*) δ 7.71 (s, 2H), 1.72 (s, 4H), 1.30 (s, 12H).

6-Bromo-7-cyano-1,1,4,4-tetramethyl-1,2,3,4-tetrahydronaphthalene (53)[9]

(53)
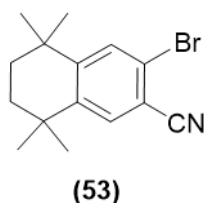
This compound was isolated as side product from the cyanation reaction (0.3 g, 7%).

MP: 157- 160 °C. (158-159°C)[9]

¹H NMR (500 MHz, Chloroform-*d*) δ 7.57 (s, 1H), 7.55 (s, 1H), 1.68 (s, 4H), 1.27 (s, 6H), 1.26 (s, 6H).

3.2.2 5,6-Dicyano-2,2-dimethyl-1,3-benzodioxole (94)[10]
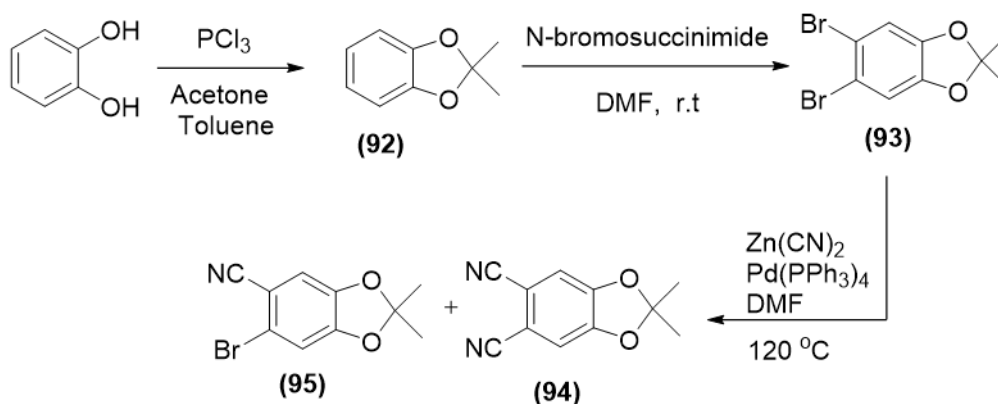
2,2-Dimethyl-1,3-benzodioxole (92)[10]

(92)
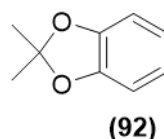
Following a reported procedure by Ivanov et al, to a suspension of pyrocatechol (33g, 0.3 mol) and acetone (29 mL, 0.39 mol) in toluene (120 mL), phosphorous trichloride (13 mL, 0.15 mol) was added dropwise over 30 min at r.t. When the addition was finished, the mixture was left to stir at r.t. until HCl ceased to evolve. Then, the mixture was poured onto 150 g of potassium carbonate, the solid filtered off and washed with toluene. The organic solution was extracted with 10% NaOH, then with water and then dried over $MgSO_4$. The solvent was removed under reduced pressure, and the residue distilled to obtain the product as a colourless liquid (23 g, 51%).

^{1}H NMR (500 MHz, Chloroform-d) δ 6.94 – 6.85 (m, 4H), 1.80 (s, 6H).

5,6-Dibromo-2,2-dimethyl-1,3-benzodioxole (93)[11]

(93)
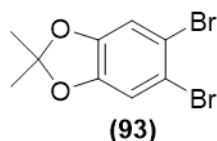
N-Bromo-succinimide (51.3 g, 0.288 mol) was added to a solution of 2,2-dimethyl-1,3-benzodioxole (**92**) (21.6 g, 0.144 mol) in dry DMF (250 mL), then, the mixture was left to stir at r.t. in darkness for two days. Then, 300 mL of water was added, and the mixture was extracted with DCM and dried over MgSO$_4$. After the solvent was evaporated under reduced pressure, a white solid was obtained as the pure product (35g, 79%)

MP: 91°C (lit 87-89°C)[11]

^{1}H NMR (500 MHz, Chloroform-d) δ 6.96 (s, 2H), 1.66 (s, 6H).

5,6-Dicyano-2,2-dimethyl-1,3-benzodioxole (94)[10]

(94)
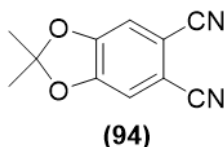
A suspension of 5,6-dibromo-2,2-dimethyl-1,3-benzodioxole (**93**) (1g, 3.24 mmol), tetrakis(triphenylphosphine) palladium (0) (0.4 g, 0.35 mmol) and zinc cyanide (0.5 g, 4.25 mmol) in DMF (7 mL) was heated to 120 °C under nitrogen for 2 h. Then aqueous ammonia (37%, 100 mL) was added, and the formed precipitate was filtered off and washed with an excess of aqueous ammonia. The product was isolated by column chromatography using PE: EtOAc 20:1 → PE: EtOAc 3:1 → EtOAc 100% as eluent. The desired product was isolated as a white solid (0.46 g, 71%)

MP: 168°C (lit 167-168 °C)[11]

^{1}H NMR (500 MHz, Chloroform-d) δ 7.03 (s, 2H), 1.76 (s, 6H).

3.2.3 Synthesis of 4,5-dimethoxyphthalonitrile (57)[12,13]
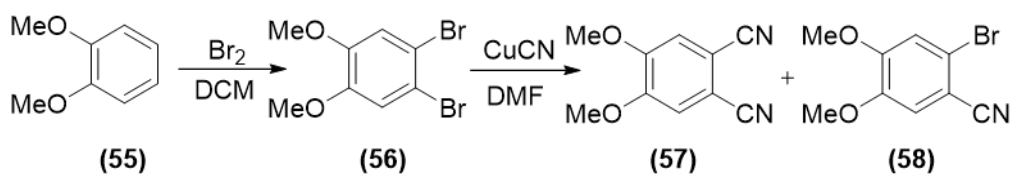
1,2-Dibromo-4,5-dimethoxybenzene (56)[14,15]

(56)
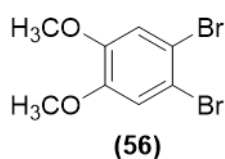
1,2-Dimethoxybenzene (40 g, 0.29 mol) was dissolved in dichloromethane (350 mL) at 0°C. Then, bromine (32.8 mL, 0.64 mol) was added dropwise over 2 h. When the addition was completed, the mixture was left to stir at r.t. for 1 h. Then, the reaction mixture was washed with sodium thiosulphate, brine and water and the organic layer was dried over magnesium sulphate (MgSO$_4$) and the solvent was evaporated. The residue was recrystallised from isopropanol to give white crystals (78.2 g, 91%).

MP: 101°C (lit 97-98°C).[16]

^{1}H NMR (500 MHz, Chloroform-*d*) δ 7.06 (s, 2H), 3.85 (s, 6H).

1,2-Dicyano-4,5-dimethoxybenzene (57)[12,13]

(57)
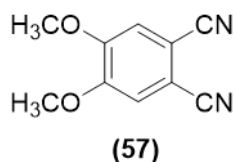
A mixture of 1,2-dibromo-4,5-dimethoxybenzene (**56**) (2.6 g, 8.73 mmol) and CuCN (3.91 g, 43.65 mmol) was heated to reflux in dry DMF (20 mL) under an inert atmosphere. After the reaction was completed, it was left to cool then 20 mL of DCM was added, and the copper salts were filtered off and the filtrate was washed with an aqueous solution of ammonia until no blue colour was observed. Finally, the organic layer was dried over

MgSO$_4$, and the solvent was evaporated under reduced pressure. The mixture was purified by column chromatography using PE:EtOAc 8:1 as eluent to give the desired product as a white solid (0.7 g, 43%).

MP: 180 °C (lit 179-181°C)[13]

^{1}H NMR (500 MHz, Chloroform-d) δ 7.15 (s, 2H), 3.97 (s, 6H).

1-Bromo-2-cyano-4,5-dimethoxybenzene (58)[7]

(58)
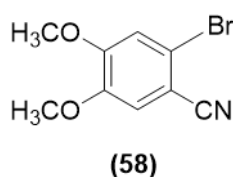
This compound was isolated as a side product from the previous cyanation reaction (1 g, 47%).

MP: 98°C (lit 113°C)[17]

^{1}H NMR (500 MHz, Chloroform-d) δ 7.07 (s, 1H), 7.05 (s, 1H), 3.93 (s, 3H), 3.89 (s, 3H).

3.2.4 Synthesis of 4,5-bis(hexyloxy)phthalonitrile (70)[12,18]
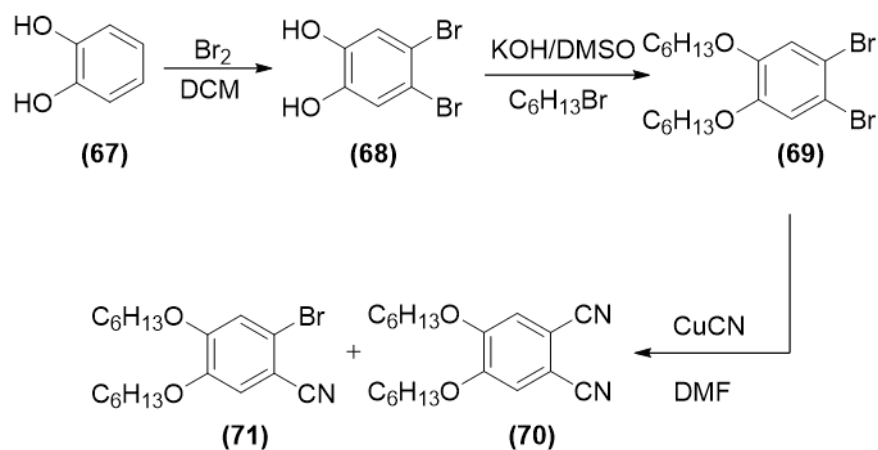
1,2-Dibromocatechol (68)[19,20]
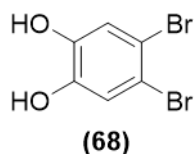
A mixture of bromine (43.5 g, 0.27 mol) and DCM (20 mL) was added slowly over 4 h to a cold mixture of pyrocatechol (15g, 0.14 mol) in DCM (150 mL). When the reaction was complete, the precipitate was filtered off and washed with sodium metabisulphite, then, the precipitate was dissolved in EtOAc, and magnesium sulphate was added and filtered off. After evaporation of solvent, the desired product was obtained as light grey solid (27 g, 74%)
MP: 115°C (lit 119°C).[20]
^{1}H NMR (400 MHz, Chloroform-*d*) δ 7.13 (s, 2H).
^{13}C NMR (101 MHz, Chloroform-*d*) δ 143.86, 119.95, 114.80.

1,2-Dibromo-4,5--bis(hexyloxy)benzene (69)[18]
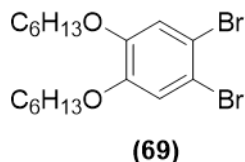
A mixture of potassium hydroxide (13.5 g, 0.24 mol) in DMSO (60 mL) was stirred for 5 mins at 20°C. Then, 1,2-dibromocatechol (**68**) (7.8 g, 0.03 mol) and 1-bromohexane (19.8 g, 0.12 mol) were added, and left to stir at 0°C for 30 mins, and then for 4.5 h at r.t. When the reaction finished, it was poured onto ice/water and extracted with DCM (4x30mL), then washed with aq. NaOH (2x30 mL) and dried over MgSO$_4$. The solvent was evaporated under reduced pressure and the pure product was obtained as brown liquid.
^{1}H NMR (500 MHz, Chloroform-*d*) δ 7.06 (s, 2H), 3.93 (t, *J* = 6.6 Hz, 4H), 1.85 – 1.74 (m, 4H), 1.49 – 1.40 (m, 4H), 1.39 – 1.27 (m, 8H), 0.94 – 0.83 (m, 6H).
^{13}C NMR (101 MHz, Chloroform-*d*) δ 149.16, 118.11, 114.77, 69.71, 31.62, 29.13, 25.72, 22.69, 14.11.

1,2-Dicyano-4,5-bis(hexyloxy)benzene (70)[12]

(70)
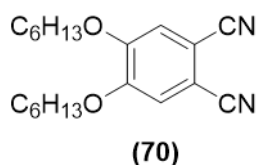
1,2-Dibromo-4,5-bis(hexyloxy)benzene (**69**) (2.6 g, 0.006 mol) and CuCN (2.7 g, 0.03 mol) was heated to reflux in dry DMF (20 mL) for 3 h or until the completion of the reaction is observed. Then, DCM (20 mL) was added, and the mixture was filtered off, and the filtrate was washed with water and then with 5% ammonia solution until no blue colour was observed. Next, the mixture was isolated by column chromatography using Hex:EtOAc 100:1 as pure white solid (0.8g, 40%).

MP: 98°C (lit 100.3°C).[10]

^{1}H NMR (500 MHz, Chloroform-*d*) δ 7.22 (s, 2H), 4.10 (t, *J* = 6.6 Hz, 4H), 2.03 – 1.91 (m, 4H), 1.65 – 1.59 (m, 4H), 1.53 – 1.47 (m, 8H), 1.10 – 1.03 (m, 6H).

1-Bromo-2-cyano-4,5-bis(hexyloxy)benzene (71)

(71)
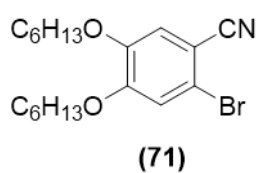
This compound was isolated as a side product from the previous cyanation reaction (1.17 g, 51%).

MP: 63°C (lit 52 °C).[10]

^{1}H NMR (500 MHz, Chloroform-*d*) δ 7.04 (s, 1H), 7.03 (s, 1H), 4.01 (t, *J* = 6.6 Hz, 2H), 3.96 (t, *J* = 6.6 Hz, 2H), 1.89 – 1.73 (m, 4H), 1.52 – 1.40 (m, 4H), 1.39 – 1.26 (m, 8H), 0.96 – 0.84 (m, 6H).

3.3 Amidines and aminoisoindolines[21,22]
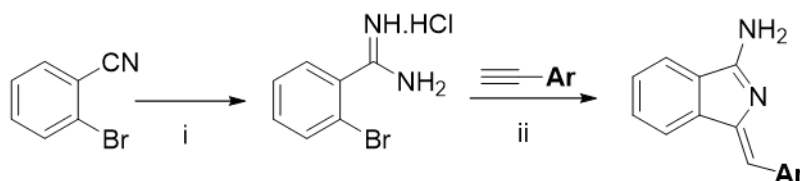
i: 1: LiN(SiMe$_3$)$_2$, THF 2: HCl
ii: PdCl$_2$(MeCN)$_2$, BINAP,DBU,DMF

Ar = 4-Methoxyphenyl (**29**)
   = 4-pentyloxyphenyl (**45**)

3.3.1 o-Bromobenzamidine hydrochloride[21]

(28)
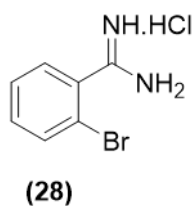
2-Bromobenzonitrile (4.18 g, 22.9 mmol, 1 eq) was dissolved in tetrahydrofuran (3.4 mL) and the mixture was added to lithium bis(trimethylsilyl)amide (1M in THF) (25 mL, 1.1 eq) and stirred for 4 hours at r.t. The reaction was cooled down in an ice bath and 15 mL of a 1:1 mixture of HCl (conc) and isopropanol was added dropwise, and then the reaction was left to stir at r.t. overnight. The reaction mixture was filtered and the solid washed with cold diethyl ether (20 mL) and dried under vacuum to yield the title compound as a white solid (4.13 g, 76.5%).

MP: > 250°C (literature > 250 °C)[21]

^{1}H NMR (500 MHz, DMSO-d_6) δ 9.32 (s, 3H), 7.86 – 7.79 (m, 1H), 7.66 – 7.61 (m, 1H), 7.60 – 7.53 (m, 2H).

^{13}C NMR (126 MHz, DMSO-d6) δ 165.89, 133.34, 133.19, 131.71, 129.99, 128.14, 119.64.

3.3.2 General synthetic procedure for the synthesis of aminoisoindolines[22]

Following the modified procedure, a solution of substituted arylacetylene (1.2 eq) and DBU (2.5 eq) in dry DMF (12 mL) was added to a mixture of amidine, BINAP (0.055 eq) and $PdCl_2(MeCN)_2$ (0.05 eq) to give a clear yellow solution with white precipitate. The mixture was left to reflux under N_2 for 5-6 h. After cooling, 50 mL of EtOAc was added and the mixture washed with a saturated solution of $NaHCO_3$ (75 mL) three times. The organic layer was dried ($MgSO_4$), filtered and concentrated. The residue was finally purified by column chromatography using DCM → EtOAc: PE (1:1) → EtOAc to give the desired product.

(Z)-1-(4-Methoxyphenylmethylene)-1H-isoindol-3-amine (29)[22]

(29)
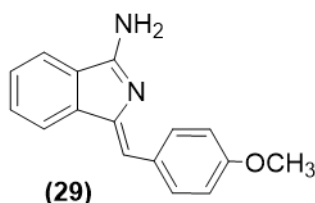
A solution of 4-ethynylanisole (2.78 g, 21 mmol) and DBU (6.66 g, 43.7mmol) in dry DMF (50 mL) was added to a mixture of o-bromobenzamidine hydrochloride (**28**) (4.12 g, 17.5 mmol), BINAP (0.60 g, 0.96 mmol) and $PdCl_2(MeCN)_2$ (0.227 g, 0.87 mmol). The reaction mixture was left at 140 °C for 6 h. After cooling, ethyl acetate (50 mL) was added, and the mixture was extracted with a saturated solution of $NaHCO_3$ (75 mL) three times, and it was purified by column chromatography using 100% dichloromethane to 1:1 ethyl acetate/petroleum ether to 100% ethyl acetate as solvent gradient. The resulting solid was recrystallised from a 1:1 mixture of dichloromethane/petroleum ether to yield the title compound as yellow solid (3.6 g, 82%).

MP: 150 °C (lit 156 -157 °C)[23]

Chemical Formula: $C_{16}H_{14}N_2O$

^{1}H NMR (500 MHz, Chloroform-*d*) δ 8.09 (d, *J* = 8.7 Hz, 2H), 7.78 (d, *J* = 7.4 Hz, 1H), 7.49 – 7.42 (m, 2H), 7.36 (td, *J* = 7.2, 0.9 Hz, 1H), 6.94 (d, *J* = 8.9 Hz, 2H), 6.75 (s, 1H), 5.39 (br s, 2H), 3.85 (s, 3H).

^{13}C NMR (126 MHz, Chloroform-d) δ 164.92, 159.16, 146.01, 143.25, 132.09, 130.92, 129.76, 129.03, 126.89, 119.66, 118.91, 115.40, 114.09, 55.42.

MS (MALDI-TOF): m/z = 250.1 [M$^+$] (100%)

Synthesis of (Z)-1-(4-pentyloxyphenylmethylene)-1H-isoindol-3-amine (45)[22]
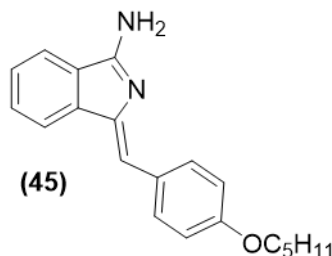
A solution of 1-ethynyl-4-(pentyloxy) benzene (4.0 g, 21 mmol) and DBU (6.66 g, 44 mmol) in dry DMF (50 mL) was added to a mixture of o-bromo benzamidine hydrochloride (**28**) (4.122 g, 17.5 mmol), BINAP (0.6 g, 0.96 mmol) and PdCl$_2$(MeCN)$_2$ (0.23 g, 0.9 mmol). Then, the mixture was stirred under N$_2$ for 5 min to give a clear yellow solution with a white solid. After that, the mixture was left at 145- 150°C for 5 h. After cooling, ethyl acetate (50 mL) was added, and the mixture was extracted with a saturated solution of NaHCO$_3$ (75 mL) three times, and it was purified by column chromatography using 100% dichloromethane to 1:1 ethyl acetate/petroleum ether to 100% ethyl acetate as solvent gradient. The resulting solid was recrystallised from a 1:1 mixture of DCM:PE to yield the title compound as orange-brown solid (4.2 g, 78.4 %).

MP: 110 °C.

Chemical Formula: C$_{20}$H$_{22}$N$_2$O

^{1}H NMR (400 MHz, Methylene Chloride-d_2) δ 8.09 (d, J = 8.8 Hz, 2H), 7.79 (dt, J = 7.7, 0.9 Hz, 1H), 7.53 – 7.43 (m, 2H), 7.37 (td, J = 7.4, 1.0 Hz, 1H), 6.92 (d, J = 8.8 Hz, 2H), 6.73 (s, 1H), 4.00 (t, J = 6.6 Hz, 2H), 1.86 – 1.72 (m, 2H), 1.52 – 1.33 (m, 4H), 0.95 (t, J = 7.1 Hz, 3H).

^{13}C NMR (101 MHz, Methylene Chloride-d_2) δ 164.81, 159.23, 145.92, 143.51, 132.41, 131.01, 129.74, 129.35, 127.21, 119.82, 119.38, 115.71, 114.79, 68.45, 29.40, 28.60, 22.90, 14.22.

MS (MALDI-TOF): m/z = 305.99 [M$^+$] (100%).

UV-vis (DCM) λ $_{max}$ /nm (ε (x10^5)) = 374 (0.3).

3.4 Acetylene and isoquinoline

3.4.1 2-[2-(4-Methoxyphenyl) ethynyl] benzonitrile [24,25]
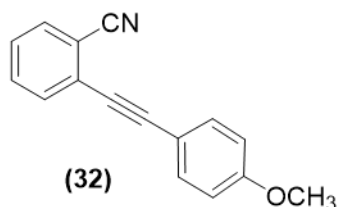
A mixture of 2-bromobenzonitrile (2.82 g, 15.49 mmol, 1 eq), 1-ethynyl-4-methoxybenzene (2.46g, 18.59 mmol, 1.2 eq), Pd $(PPh_3)_2Cl_2$ (0.21 g, 0.299 mmol), CuI (0.10g, 0.525mmol) and Et_3N (5 mL) was heated in a sealed tube at 120 °C overnight, then the reaction mixture was quenched with saturated NH_4Cl solution and extracted with EtOAc. The residue obtained was purified by chromatography on silica-gel with PE:EtOAc (20:1). The resulting solid was purified by recrystallisation using DCM:PE (1:1) to obtain the product as pure white solid (2.1 g, 58%).

Chemical Formula: $C_{16}H_{11}NO$

MP: 79°C (lit 78–79°C)[24]

¹H NMR (500 MHz, Chloroform-*d*) δ 7.68 – 7.63 (m, 1H), 7.61 – 7.58 (m, 1H), 7.58 – 7.53 (m, 3H), 7.38 (td, *J* = 7.6, 1.4 Hz, 1H), 6.90 (d, *J* = 8.9 Hz, 2H), 3.84 (s, 3H).

¹³C NMR (126 MHz, Chloroform-d) δ 160.29, 133.43, 132.42, 132.29, 131.68, 127.77, 127.37, 117.62, 114.72, 114.03, 113.89, 96.21, 84.62, 55.18.

MS (MALDI-TOF): m/z = 232.95 [M⁺] (100%)

3.4.2 1-Pentyloxy-3-(4-methoxyphenyl) isoquinoline

(34)
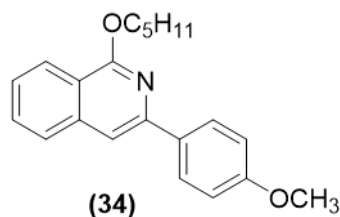
A solution of previously prepared acetylene (**32**) (100mg, 0.43 mmol) in pentanol (6 mL) was heated up to reflux and then a small pieces of lithium metal were added, and the mixture was left to reflux overnight. When the reaction cooled to r.t., diluted HCl was added and then extracted with EtOAc. The solvent was evaporated under reduced pressure and the reaction crude was subjected to column chromatography using PE:EtOAc 20:1 as eluent to yield the title compound as a brown oil (0.042 g, 30%).

Chemical Formula: $C_{21}H_{23}NO_2$

¹H NMR (400 MHz, Chloroform-d) δ 8.24 (d, J = 8.3 Hz, 1H), 8.11 (dd, J = 8.4, 1.6 Hz, 2H), 7.74 (d, J = 8.2 Hz, 1H), 7.65 – 7.59 (m, 1H), 7.58 (s, 1H), 7.50 – 7.43 (m, 1H), 7.01 (dd, J = 8.7, 1.4 Hz, 2H), 4.64 (td, J = 6.6, 1.3 Hz, 2H), 3.88 (s, 3H), 2.00 – 1.90 (m, 2H), 1.63 – 1.51 (m, 4H), 1.01 – 0.94 (m, 3H).

MS (MALDI-TOF): m/z = 320.81 [M⁺] (100%).

3.4.3 Nitro-acetylene via PT method, using a protected acetylene

2-(3-Hydroxy-3-methyl-1-butyn-1-yl)benzonitrile[26]

(35)
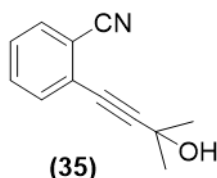
A suspension of 2-bromobenzonitrile (3 g, 16.8 mmol), bis(triphenylphosphine) palladium (II) dichloride (0.347g, 0.49 mmol), triphenylphosphine (0.52g, 1.97 mmol), and copper iodide (0.22 g, 1.15 mmol) in dry TEA (50 mL) was purged with nitrogen and then 2-methyl-3-butyn-2ol (2.77g, 32.96 mmol) in 20 mL of dry TEA was added slowly over 4h using syringe pump. After the addition was finished the mixture was refluxed at 90 °C for 2 h.

Then, the reaction mixture was cooled down and quenched with DCM (400 mL) and extracted from water (80 mL). The organic phase was dried over anhydrous magnesium sulphate and concentrated under reduced pressure. The crude product was purified by flash chromatography on silica gel using a mixture of PE: EtOAc 20:1 to yield the title compound as brown oil (3 g, 97 %).

Chemical Formula: $C_{12}H_{11}NO$

^{1}H NMR (500 MHz, Chloroform-d) δ 7.58 (dt, J = 7.8, 1.0 Hz, 1H), 7.52 – 7.45 (m, 2H), 7.39 – 7.31 (m, 1H), 3.11 (s, 1H), 1.63 (s, 6H).

^{13}C NMR (126 MHz, Chloroform-d) δ 132.16, 131.96, 131.70, 127.96, 126.29, 117.13, 114.46, 100.62, 64.85, 53.36, 30.73.

2-((Trimethylsilyl)ethynyl) benzonitrile[26]
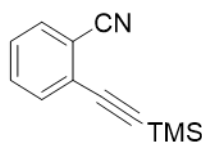
2-Bromobenzonitrile (4 g, 22 mmol), PdCl$_2$(PPh$_3$)$_2$ (300 mg, 0.44 mmol) and CuI (82 mg, 0.44 mmol) were dissolved in distilled Et$_3$N (60 mL), then trimethylsilyl acetylene (4.56 mL, 33 mmol) was added to the solution and refluxed under N$_2$ for 2 h. The reaction mixture was filtered through a silica pad using EtOAc as a solvent. After that, the filtrate was evaporated and the crude product was purified through column chromatography using PE as a solvent to give the title compound as a yellowish oil (2.6 g, 60%)

Chemical Formula: $C_{12}H_{13}NSi$

^{1}H NMR (500 MHz, Chloroform-d) δ 7.63 – 7.52 (m, 1H), 7.49 – 7.41 (m, 2H), 7.41 – 7.28 (m, 1H), 0.21 (s, 9H).

2-(2-(4-Nitrophenyl) ethynyl)benzonitrile (36)[27]
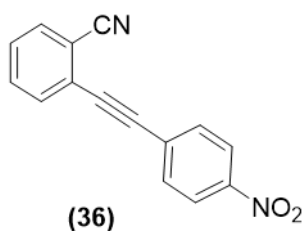
Following a PT Method, a degassed mixture of 1-iodo-4-nitrobenzene (0.75 g, 3 mmol), acetylenic alcohol **(35)** (0.55 g, 3 mmol), copper iodide (0.057 g, 0.3 mmol), palladium(II) dichlorobistriphenylphosphine (0.211g, 0.3 mmol), and tetrabutylammonium iodide (0.11g, 0.3 mmol) in a heterogeneous mixture of toluene (5.0 mL) and aqueous sodium hydroxide (5 M, 2.0 mL) was placed in a sealed tube and it was heated to 80 °C for 1 h and then cooled down to r.t. A pad of silica gel was used to filter the mixture. The filtrate was concentrated under reduced pressure. The residue was chromatographed on silica gel, eluting with PE:EtOAc 20:1 to give the desired product. Further purification was needed by recrystallisation using DCM:PE to yield colourless needles (0.5 g, 67%).

MP: 133 °C (Lit 133-134 °C)[27]

Chemical Formula: $C_{15}H_8N_2O_2$

^{1}H NMR (500 MHz, Chloroform-*d*) δ 8.29 – 8.21 (m, 2H), 7.81 – 7.74 (m, 2H), 7.73 (ddd, *J* = 7.8, 1.4, 0.6 Hz, 1H), 7.68 (ddd, *J* = 7.8, 1.4, 0.6 Hz, 1H), 7.63 (td, *J* = 7.7, 1.3 Hz, 1H), 7.50 (td, *J* = 7.7, 1.3 Hz, 1H).

^{13}C NMR (126 MHz, Chloroform-d) δ 147.77, 132.95, 132.89, 132.72, 132.51, 129.44, 128.92, 126.11, 123.84, 117.38, 115.86, 93.58, 90.26.

3.5 Dimethoxyindolines

1-Imino-3,3-dimethoxyisoindoline[28]
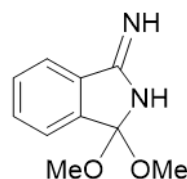
Sodium metal (2g, 0.09 mol) was dissolved in methanol (70 mL) at r.t. Then, phthalonitrile (10g, 78 mmol) was added and the mixture was left to stir until full precipitation had occurred. The solid was filtered off and washed with water and dried under vacuum to yield the product as an off white solid (10 g, 67%).

¹H NMR (500 MHz, DMSO-d_6) δ 7.72 – 7.65 (m, 1H), 7.48 – 7.39 (m, 3H), 3.20 (s, 6H).

3.6 Synthesis of malonyl aminoisoindoline and its derivatives[29]

1-Imino-3-dicarbethoxymethylene isoindoline (37)
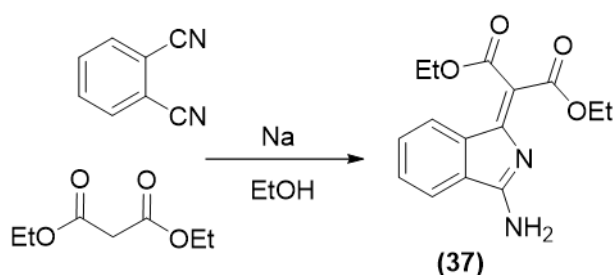
A cold solution of sodium (0.4 g, 17.4 mmol) in 9 mL of ethanol, was treated successively with diethyl malonate (2.6 mL, 17.13 mmol). Then, finely powdered phthalonitrile (2.1 g, 16.4 mmol) was added. The mixture was left to stir at r.t. until a complete consumption was observed. The solvent was removed under vacuum and the residue was purified by column chromatography using PE:EtOAc 3:1 and then EtOAc as the eluent to isolate the desired product that was dried under reduced pressure and at r.t. to give yellow powder (2.0 g, 43 %).

Chemical Formula: $C_{15}H_{16}N_2O_4$

MP: 100 °C (lit 97°C)[29]

¹H NMR (500 MHz, Chloroform-d) δ 10.06 (s, 1H), 7.95 – 7.85 (m, 1H), 7.67 – 7.59 (m, 3H), 4.45 (q, $J = 7.1$ Hz, 2H), 4.32 (q, $J = 7.1$ Hz, 2H), 1.40 (t, $J = 7.1$ Hz, 3H), 1.34 (t, $J = 7.1$ Hz, 3H).

¹³C NMR (126 MHz, Chloroform-d) δ 166.45, 166.23, 160.89, 149.63, 133.98, 132.00, 131.76, 131.38, 124.33, 122.54, 62.11, 61.41, 14.32, 14.16.

MS (MALDI-TOF): m/z = 288.73 [M⁺] (100%)

UV-vis (DCM) λ_{max} /nm (ε (x10⁵)) = 337 (0.17).

3-(Dicarbethoxymethylene) phthalimidine (39)[29]

(39)
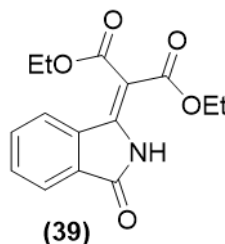
This compound was isolated as the major compound from previous reaction when following the exact reported procedure as it includes acid work up and when acid was avoided it was isolated as side product during purification process.

The reported procedure was following as:

A cold solution of sodium (0.4 g, 17.4 mmol) in 9 mL of ethanol, was treated successively with diethyl malonate (2.6 mL, 17.13 mmol). Then, finely powdered phthalonitrile (2.1 g, 16.4 mmol) was added. The mixture was left to stir at r.t. until a complete consumption was observed by TLC. Then a cold diluted HCl (20 mL) was added, and the mixture was extracted with Benzene (10 mL). Then, the aqueous layer was left overnight, and a very light solid was obtained. The obtained solid was recrystallised from EtOH: H₂O provided the title compound as a light purple crystal (3.6 g, 77%).

Chemical Formula: $C_{15}H_{15}NO_5$

MP: 109 °C (Lit 108°C)[29]

¹H NMR (500 MHz, Chloroform-d) δ 10.06 (s, 1H), 7.93 – 7.86 (m, 1H), 7.67 – 7.58 (m, 3H), 4.45 (q, J = 7.1 Hz, 2H), 4.31 (q, J = 7.1 Hz, 2H), 1.40 (t, J = 7.1 Hz, 3H), 1.33 (t, J = 7.1 Hz, 3H).

¹³C NMR (126 MHz, Chloroform-d) δ 167.32, 165.41, 165.16, 146.40, 134.41, 133.04, 132.03, 129.83, 124.12, 123.92, 102.17, 62.19, 61.65, 14.02, 13.93.

MS (MALDI-TOF): m/z = 288.96 [M⁺] (100%)

UV-vis (DCM) λ_{max} /nm (ε (x10⁵)) = 328 (0.163).

Condensation product (40)

(40)
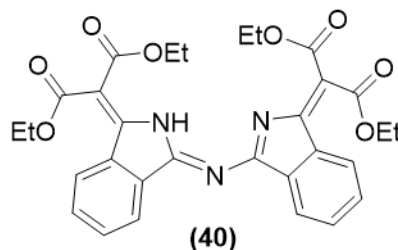
A solution of (dicarbethoxymethylene)aminoisoindoline (**37**) (50 mg, 0.174 mmol) in dry toluene (5 mL) was heated at 120 °C under an argon atmosphere and monitored by TLC until full consumption of starting material was observed. Then, the solvent was evaporated, and the crude was purified by recrystallisation using EtOH: H_2O to yield the desired compound as red crystals (20 mg, 40%).

Chemical Formula: $C_{30}H_{29}N_3O_8$

MP: 135.5- 140 °C

^{1}H NMR (500 MHz, Methylene Chloride-d_2) δ 12.50 (s, 1H), 8.13 – 8.05 (m, 4H), 7.69 – 7.48 (m, 4H), 4.45 (dq, J = 14.3, 7.2 Hz, 8H), 1.39 (t, J = 7.1 Hz, 6H), 1.36 (t, J = 7.1 Hz, 6H).

^{13}C NMR (126 MHz, Methylene Chloride-d_2) δ 167.03, 165.07, 165.01, 152.55, 137.61, 135.58, 132.06, 131.61, 125.85, 123.23, 113.74, 62.41, 62.17, 14.33, 14.26.

MS (MALDI-TOF): m/z = 560.12 [M$^+$] (100%)

UV-vis (DCM) λ $_{max}$ /nm (ε (x10^5)) = 433 (0.22), 319 (0.3).

1-Imino-3-(dicarbethoxymethylene)-6,7-dimethoxyisoindoline (59)

(59)
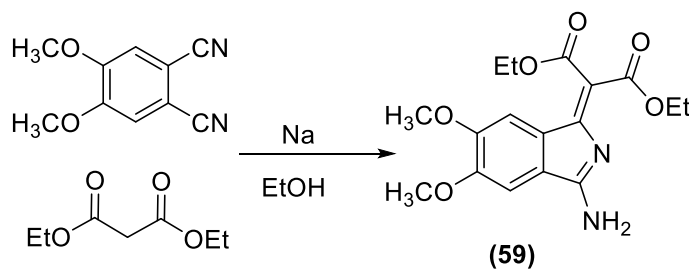
To a cold solution of sodium (0.35 g, 15.4 mmol) in ethanol (100 mL), was added diethyl malonate (1.17 mL, 7.7 mmol). Then, finely powdered 1,2-dicyano-4,5-dimethoxybenzene

(**57**) (0.724 g, 3.85 mmol) was added. The mixture was left to stir at r.t. until a complete consumption of starting material was observed. The solvent was removed under vacuum and the crude was isolated by column chromatography using PE:EtOAc 3:1 then, EtOAc 100% to afford the desired compound (0.8 g, 60%).

Chemical Formula: $C_{17}H_{20}N_2O_6$

MP: 168°C.

^{1}H NMR (500 MHz, Chloroform-*d*) δ 7.24 (s, 1H), 7.09 (s, 1H), 4.36 (q, *J* = 7.1 Hz, 2H), 4.23 (q, *J* = 7.1 Hz, 2H), 3.93 (s, 3H), 3.87 (s, 3H), 1.35 (t, *J* = 7.1 Hz, 3H), 1.27 (t, *J* = 7.1 Hz, 3H).

^{13}C NMR (126 MHz, Chloroform-*d*) δ 166.79, 166.41, 160.10, 152.49, 151.97, 150.19, 126.98, 125.86, 106.24, 104.03, 96.70, 61.81, 61.04, 56.40, 56.13, 14.21, 14.17.

MS (MALDI-TOF): m/z = 348.82 [M$^+$] (100%)

UV-vis (DCM) λ $_{max}$ /nm (ε (x10^5)) = 337 (0.29).

3-Dicarbethoxymethylene-6,7-dimethoxy phthalimidine (60)

(60)
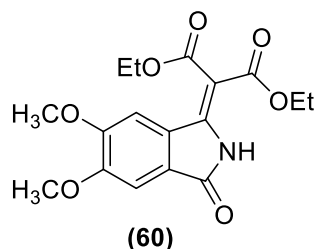
This compound was isolated as a side product during purification process of (**59**).

Chemical Formula: $C_{17}H_{19}NO_7$

MP: 191- 195 °C

^{1}H NMR (500 MHz, Methylene Chloride-*d*$_2$) δ 9.76 (s, 1H), 7.29 (s, 1H), 7.10 (s, 1H), 4.41 (q, *J* = 7.1 Hz, 2H), 4.28 (q, *J* = 7.1 Hz, 2H), 3.94 (s, 3H), 3.88 (s, 3H), 1.38 (t, *J* = 7.1 Hz, 3H), 1.31 (t, *J* = 7.1 Hz, 3H).

^{13}C NMR (126 MHz, Methylene Chloride-*d*$_2$) δ 167.78, 166.21, 165.82, 153.58, 153.33, 147.39, 128.09, 123.91, 106.65, 105.96, 101.48, 62.56, 61.99, 56.73, 56.47, 14.29.

MS (MALDI-TOF): m/z = 349.21 [M$^+$] (100%)

UV-vis (DCM) λ $_{max}$ /nm (ε (x10^5)) = 331 (0.24).

Condensation product (61)
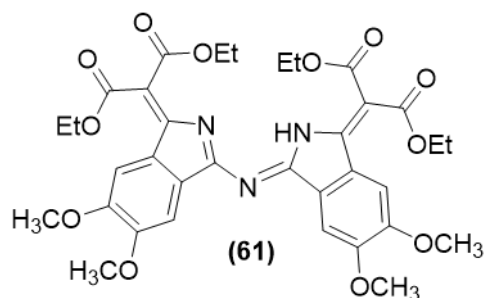
This dimer was isolated from the reaction of (**59**). The yield was not calculated as this compound formed when the mixture was left in solution or during purification process.

Chemical Formula: $C_{34}H_{37}N_3O_{12}$

MP: 197.9 – 202 °C

^{1}H NMR (500 MHz, Methylene Chloride-d_2) δ 12.27 (s, 1H), 7.73 (s, 2H), 7.53 (s, 2H), 4.49 – 4.41 (m, 4H), 4.42 – 4.36 (m, 4H), 4.03 (s, 6H), 3.93 (s, 6H), 1.39 (t, J = 7.1 Hz, 6H), 1.35 (t, J = 7.1 Hz, 6H).

^{13}C NMR (126 MHz, Methylene Chloride-d_2) δ 167.20, 165.42, 165.19, 153.08, 152.71, 152.59, 131.31, 128.88, 112.57, 108.87, 105.06, 62.28, 62.04, 56.74, 56.47, 14.33.

MS (MALDI-TOF): m/z = 679.38 [M$^+$] (100%)

UV-vis (DCM) λ $_{max}$ /nm (ε (x10^5)) = 429 (0.29).

1-Imino-3-(dicarbethoxymethylene)- 6,7-hexyloxy isoindoline (72)
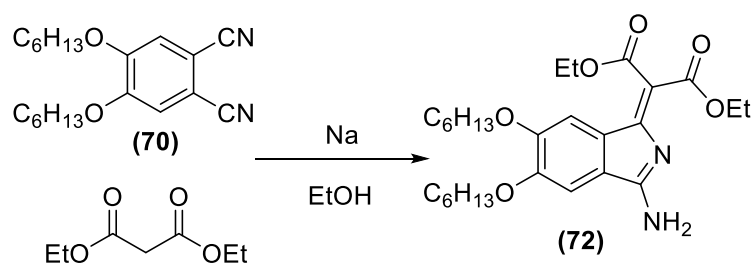
A cold solution of sodium (0.14 g, 6 mmol) in ethanol (100 mL), was treated successively with diethyl malonate (0.5 mL, 3.05 mmol). Then, finely powdered 1,2-dicyano-4,5-dihexyloxybenzene (**70**) (0.5 g, 1.5 mmol) was added. The mixture was left to stir at r.t. until a complete consumption was observed. The solvent was removed under vacuum and the residue was dissolved in DCM and NH_4Cl was added, then the solution was filtered, and the filtrate was dried under vacuum. Then, the crude was isolated by column chromatography using PE:EtOAc 3:1 then, EtOAc 100% to afford the desired compound (0.35 g, 48%).

Chemical Formula: $C_{27}H_{40}N_2O_6$

MP: 175-178 °C.

^{1}H NMR (500 MHz, Acetone-$d6$) δ 7.55 (s, 1H), 7.25 (s, 1H), 4.38 (q, J = 7.1 Hz, 2H), 4.25 (q, J = 7.1 Hz, 2H), 4.16 – 4.14 (m, 2H), 4.05 (t, J = 6.4 Hz, 2H), 1.89 – 1.78 (m, 4H), 1.56 – 1.50 (m, 4H), 1.42 – 1.34 (m, 8H), 1.28 (t, J = 7.1 Hz, 3H), 1.24 (t, J = 7.1 Hz, 3H), 0.95 – 0.88 (m, 6H).

^{13}C NMR (126 MHz, Acetone-d_6) δ 169.30, 167.88, 166.72, 166.57, 161.44, 153.56, 152.99, 150.68, 127.60, 126.11, 108.98, 106.92, 69.92, 69.86, 62.24, 61.53, 61.39, 42.50, 32.30, 32.28, 26.44, 26.43, 23.30, 14.52, 14.44, 14.41, 14.30.

MS (MALDI-TOF): m/z = 488.97 [M$^+$] (100%).

UV-vis (DCM) λ $_{max}$ /nm (ε (x10^5)) = 335 (0.19).

3.7 Unsymmetrical aza-dipyrromethene compounds

4-Methoxyphenylmethylene aminoisoindoline- 3-dicarbethoxy methylene aminoisoindoline (44)
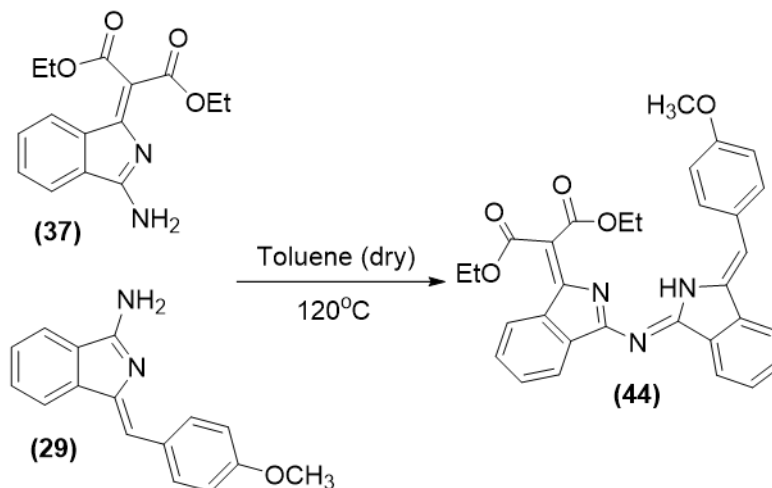
A mixture of dicarbethoxy methylene aminoisoindoline (**37**) (50 mg, 0.174 mmol) and 4-methoxyphenylmethylene aminoisoindoline (**29**) (43.5 mg, 0.174) were dissolved in dry toluene (10 mL) and heated to 120 °C under an inert atmosphere and monitored by TLC until a full consumption was observed. Then, the solvent was evaporated, and the crude was purified by column chromatography using PE:EtOAc 30:1 initially and increasing the polarity gradually. The desired product was recrystallised from DCM:MeOH and gave pure red crystals (28 mg, 31%).

Chemical Formula: $C_{31}H_{29}N_3O_5$

MP: 142-145°C

[1H] NMR (400 MHz, Methylene Chloride-d_2) δ 12.48 (s, 1H), 8.40 (d, J = 8.8 Hz, 2H), 8.34 (d, J = 7.4 Hz, 1H), 8.04 (d, J = 7.5 Hz, 1H), 7.88 (d, J = 7.7 Hz, 1H), 7.77 − 7.69 (m, 2H), 7.66 (ddd, J = 8.2, 7.1, 1.2 Hz, 1H), 7.51 (td, J = 7.4, 1.2 Hz, 1H), 7.46 (td, J = 7.4, 1.2 Hz, 1H), 7.27 (s, 1H), 7.06 (d, J = 8.8 Hz, 2H), 4.49 (q, J = 7.1 Hz, 2H), 4.37 (q, J = 7.1 Hz, 2H), 3.87 (s, 3H), 1.42 (t, J = 7.1 Hz, 3H), 1.36 (t, J = 7.1 Hz, 3H).

[13C] NMR (101 MHz, Methylene Chloride-d_2) δ 169.67, 166.14, 165.19, 160.99, 155.85, 148.39, 146.77, 142.90, 136.62, 135.50, 134.67, 134.25, 133.73, 132.43, 132.17, 129.14, 129.12, 127.57, 124.67, 124.28, 123.96, 121.50, 119.25, 114.83, 102.79, 62.62, 61.82, 55.65, 50.85, 14.44, 14.23.

MS (MALDI-TOF): m/z = 521.11 [M[+]] (100%)

UV-vis (DCM) λ $_{max}$ /nm (ε (x10^5)) = 350 (0.72), 480 (0.25), 511 (0.23).

4-Pentyloxyphenylmethylene aminoisoindoline-3-dicarbethoxy methylene aminoisoindoline (47)
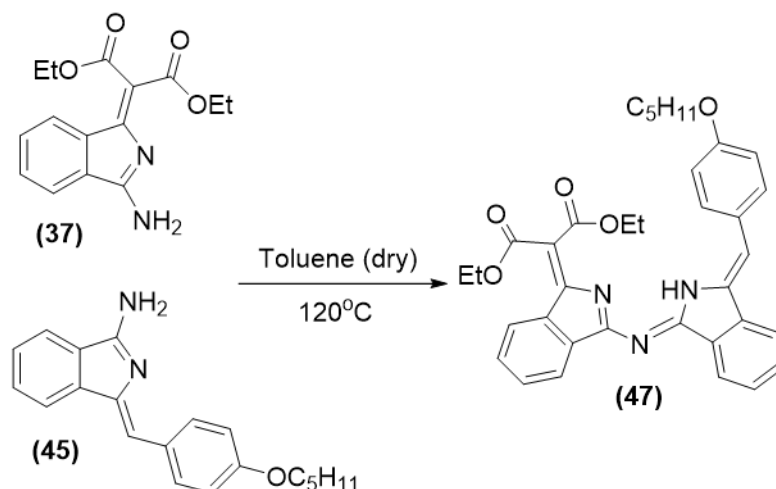
A mixture of dicarbethoxymethylene aminoisoindoline (**37**) (56.5 mg, 0.196 mmol) and 4-pentyloxyphenylmethylene aminoisoindoline (**45**) (50 mg, 0.163 mmol) were dissolved in dry toluene (10 mL) and heated to 120 °C under an inert atmosphere and monitored by TLC until a full consumption was observed. Then, the solvent was evaporated, and the crude was purified by column chromatography using PE:EtOAc 30:1 and then increasing the polarity gradually. The desired product was recrystallised from DCM: MeOH and gave pure red crystals (37 mg, 39 %).

Chemical Formula: $C_{35}H_{37}N_3O_5$

MP: 180 °C

^{1}H NMR (500 MHz, Methylene Chloride-d_2) δ 12.42 (s, 1H), 8.39 (d, J = 8.8 Hz, 2H), 8.24 (d, J = 7.3 Hz, 1H), 7.97 (dt, J = 7.4, 1.1 Hz, 1H), 7.87 (dt, J = 7.4, 1.1 Hz, 1H), 7.74 – 7.67 (m, 2H), 7.67 – 7.60 (m, 1H), 7.49 (td, J = 7.3, 1.1 Hz, 1H), 7.44 (td, J = 7.3, 1.1 Hz, 1H), 7.25 (s, 1H), 7.04 (d, J = 8.8 Hz, 2H), 4.49 (q, J = 7.1 Hz, 2H), 4.37 (q, J = 7.1 Hz, 2H), 4.03 (t, J = 6.6 Hz, 2H), 1.87 – 1.75 (m, 2H), 1.57 – 1.46 (m, 2H), 1.46 – 1.38 (m, 5H), 1.36 (t, J = 7.1 Hz, 3H), 0.96 (t, J = 7.1 Hz, 3H).

^{13}C NMR (126 MHz, Methylene Chloride-d_2) δ 169.12, 165.73, 164.74, 160.19, 155.36, 147.99, 146.23, 142.48, 136.18, 135.10, 133.85, 133.30, 131.97, 131.73, 128.65, 128.50, 127.09, 124.40, 123.85, 123.52, 121.06, 118.81, 114.94, 102.30, 68.06, 62.19, 61.38, 28.95, 28.20, 22.46, 14.01, 13.82, 13.79.

MS (MALDI-TOF): m/z = 576.43 [M$^+$] (100%)

UV-vis (DCM) λ $_{max}$ /nm (ε (x10^5)) = 351 (0.77), 483 (0.27), 514 (0.26).

Unsymmetrical Aza-dipyrromethene compound (88)
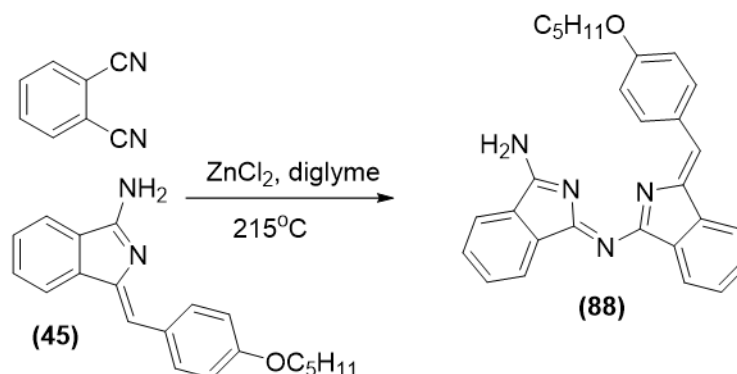
In an attempted macrocyclisation reaction, a mixture of phthalonitrile (0.25 g, 1.96 mmol, 3 eq), pentyloxy aminoisoindoline (**45**) (0.2 g, 0.65 mmol, 1 eq) and $ZnCl_2$ (0.15 g, 1 mmol, 1.5 eq), in dry diglyme (3 mL) were heated in a pre-headed heating block at 215°C under an argon atmosphere. When the reaction was finished, the solvent was removed under a stream of argon. The reaction mixture was cooled down to r.t. and 300 mL of DCM was added and the mixture was sonicated and then filtered off through a silica pad to remove the metal salt and green products. Then, the solvent was evaporated under vacuum. The mixture was subjected to dry-loading column chromatography using PE:DCM 3:2 to obtain the product as orange solid.

Also, this product was prepared selectively by a procedure which was recently optimised in our group as follows:

Pentyloxy aminoisoindoline (**45**)(0.2 g, 0.65 mmol) was mixed with phthalonitrile (0.13 g, 0.98 mmol) and sodium methoxide (0.05 g, 0.98 mmol) in methanol (12 mL). The mixture was left to stir at 60°C until a full consumption of starting materials was observed by TLC. When the reaction was finished, it was cooled down to r.t. and the solvent was evaporated and the crude was submitted to dry loading column chromatography using PE:DCM 3:2 as eluent, to isolate the desired product as orange solid (0.12 mg, 43%).

Chemical Formula: $C_{28}H_{26}N_4O$

MP: 158-162°C

^{1}H NMR (500 MHz, Chloroform-*d*) δ 8.15 (dd, *J* = 7.2, 1.6 Hz, 1H), 8.06 (d, *J* = 8.8 Hz, 1H), 7.99 (d, *J* = 7.4 Hz, 1H), 7.91 − 7.84 (m, 2H), 7.83 (d, *J* = 7.6 Hz, 1H), 7.77 − 7.75 (m, 1H), 7.73 − 7.66 (m, 1H), 7.52 − 7.41 (m, 2H), 7.16 (s, 1H), 7.03 (d, *J* = 8.8 Hz, 2H), 4.05 (t, *J* = 6.6 Hz, 2H), 1.87 − 1.80 (m, 2H), 1.51 − 1.38 (m, 4H), 0.96 (t, *J* = 7.2 Hz, 3H).**^{13}C NMR** (126 MHz, Chloroform-*d*) δ 168.80, 166.78, 160.88, 159.09, 143.74, 140.34, 135.51,

134.63, 133.30, 131.74, 131.61, 131.08, 130.96, 128.08, 127.51, 126.44, 122.59, 122.05, 121.80, 120.84, 120.52, 118.13, 113.97, 67.17, 27.92, 27.18, 21.46, 13.02.

MS (MALDI-TOF): m/z = 434 [M$^+$] (100%).

UV-vis (DCM) λ_{max} /nm (ε (x10^5)) = 314 (0.28), 445 (0.18), 453 (0.177).

Hydrolysed product (90)

(90)
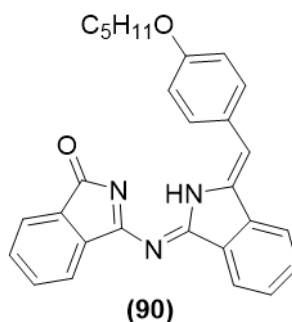
This hydrolysed bright orange compound was isolated as an amorphous solid from the previous reaction as a result of column chromatography purification.

MP: 158-162°C

Chemical Formula: C$_{28}$H$_{25}$N$_3$O$_2$

^{1}H NMR (500 MHz, Methylene Chloride-d_2) δ 11.44 (s, 1H), 8.17 (d, J = 7.4 Hz, 1H), 8.14 – 8.07 (d, J = 8.9 Hz, 2H), 7.97 (d, J = 7.4 Hz, 1H), 7.92 (dt, J = 7.3, 1.0 Hz, 1H), 7.88 (dt, J = 7.3, 1.0 Hz, 1H), 7.80 (td, J = 7.3, 1.1 Hz, 1H), 7.74 (td, J = 7.3, 1.1 Hz, 1H), 7.52 (td, J = 7.3, 1.1 Hz, 1H), 7.47 (td, J = 7.3, 1.1 Hz, 1H), 7.30 (s, 1H), 7.04 (d, J = 8.9 Hz, 2H), 4.07 (t, J = 6.6 Hz, 2H), 1.88 – 1.79 (m, 2H), 1.54 – 1.38 (m, 4H), 0.96 (t, J = 7.2 Hz, 3H).

^{13}C NMR (126 MHz, Methylene Chloride-d2) δ 169.44, 168.41, 160.62, 156.31, 145.47, 141.77, 137.15, 135.65, 133.68, 133.26, 132.89, 130.89, 129.07, 128.30, 127.46, 125.61, 123.74, 122.91, 121.18, 119.18, 114.96, 68.29, 28.91, 28.15, 22.47, 13.79.

MS (MALDI-TOF): m/z = 434.61 [M$^+$] (100%).

UV-vis (DCM) λ_{max} /nm (ε (x10^5)) = 317 (0.3), 450 (0.24), 470 (0.24).

Unsymmetrical Aza-dipyrromethene compound (97)
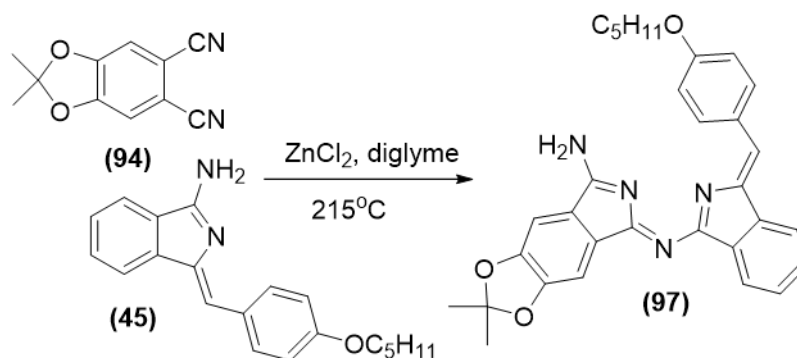
This intermediate dimer was isolated from macrocyclisation reaction of a suspension of 4,5-dimethyldioxolanephthalonitrile (**94**) (0.2 g, 0.98 mmol, 3 eq), pentyloxy aminoisoindoline (**45**) (0.1 g, 0.33 mmol, 1 eq) and zinc chloride (0.1g, 0.45 mmol, 1.5 eq) in diglyme (2 mL) in a pre-heated block at 215 °C under argon atmosphere for 18 h. Then, the solvent was evaporated under a stream of argon while the crude was still hot. After that, the reaction mixture was cooled down to r.t. and 300 mL of DCM was added, and the mixture was sonicated and then filtered through a silica pad to remove the metal salt and green products. Then, the solvent was evaporated under vacuum. The mixture was subjected to a dry-loading column chromatography using PE: DCM 3:2 to obtain the product as orange solid. Due to the many columns and recrystallisations that were done to purify this compound, its yield was not calculated from this reaction, and it was prepared selectively following the recently modified procedure in our group as follows: to 24 mL methanol, 4,5-dimethyldioxolanephthalonitrile (**94**) (0.39 g, 1.95 mmol), pentyloxy aminoisoindoline (**45**) (0.4 g, 1.3 mmol) and sodium methoxide (0.11 g, 1.95 mmol) were added and the mixture left to reflux at 60 °C overnight. Then, the desired product was isolated by column chromatography using PE: DCM 3:2 as eluent (0.15, 23%)

Chemical Formula: $C_{31}H_{30}N_4O_3$

MP: 173.5 – 180 °C.

^{1}H NMR (500 MHz, Methylene Chloride-d_2) δ 11.03 (s, 1H), 8.01 (d, J = 8.6 Hz, 2H), 7.85 (dt, J = 7.5, 1.0 Hz, 1H), 7.78 (dt, J = 7.5, 1.0 Hz, 1H), 7.46 – 7.36 (m, 2H), 7.35 (s, 1H), 7.18 (s, 1H), 7.09 (s, 1H), 6.94 (d, J = 8.6 Hz, 2H), 3.98 (t, J = 6.6 Hz, 2H), 1.81 – 1.71 (m, 2H), 1.69 (s, 6H), 1.45 – 1.35 (m, 2H), 1.38 – 1.27 (m, 2H), 0.87 (t, J = 7.2 Hz, 3H).

¹³C NMR (126 MHz, Methylene Chloride-d_2) δ 169.48, 168.05, 160.51, 152.47, 151.91, 145.55, 141.79, 133.19, 128.99, 128.36, 127.40, 125.13, 121.15, 121.01, 119.13, 114.92, 103.61, 102.88, 68.27, 28.91, 28.15, 25.70, 22.46, 13.79.

MS (MALDI-TOF): m/z = 506 [M⁺] (100%).

UV-vis (DCM) λ $_{max}$ /nm (ε (x10⁵)) = 262 (0.51), 448 (0.17), 467 (0.17).

3.8 Dimeric and trimeric condensation products

Condensation product (46)

(46)
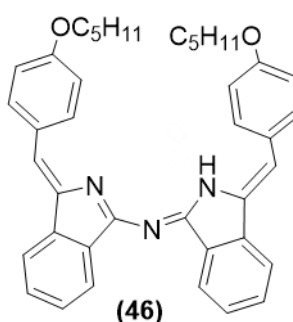
This dimer was isolated from magnesium macrocyclisation reaction of a suspension of pentyloxy aminoisoindoline (**45**) (0.2 g, 0.65 mmol, 1eq), MgCl₂ (0.13 g, 1 mmol, 1.5 eq) 4,5-dimethyldioxolanephthalonitrile (**94**) (0.5 g, 1.96 mmol, 3 eq) in diglyme (3mL) in a pre-heated 215°C heating block, under N₂ until the completion of the reaction was observed by TLC (4h). Then, the solvent was evaporated while the reaction was still hot under an argon stream. The mixture was sonicated with DCM and filtered through a short silica column to remove salts and green materials. Then, the filtrate was evaporated and the product isolated by column chromatography using PE: DCM 6:1 as eluent.

Also, this dimer was isolated from unsymmetrical dimerisation reactions of
a mixture of dicarbethoxymethylene aminoisoindoline (**37**) (56.5 mg, 0.196 mmol) and 4-pentyloxyphenylmethylene aminoisoindoline (**45**) (50 mg, 0.163 mmol) in refluxing dry toluene (10 mL) under an inert atmosphere. The reaction was monitored by TLC until a full consumption was observed. Then, the solvent was evaporated, and the crude was purified by column chromatography using PE:EtOAc 30:1 and then increasing the polarity gradually. The desired product was recrystallised from DCM: MeOH and gave pure red crystals (8 mg, 17%).

Chemical Formula: C₄₀H₄₁N₃O₂
MP: 157 °C.

¹H NMR (400 MHz, Methylene Chloride-d_2) δ 8.08 (d, J = 7.6 Hz, 2H), 7.91 – 7.81 (m, 6H), 7.57 (td, J = 7.4, 1.2 Hz, 2H), 7.51 (td, J = 7.4, 1.2 Hz, 2H), 6.83 (s, 2H), 6.65 – 6.60 (m, 4H), 3.80 (t, J = 6.7 Hz, 4H), 1.81 – 1.70 (m, 4H), 1.49 – 1.32 (m, 8H), 1.01 – 0.89 (m, 6H).

¹³C NMR (101 MHz, Methylene Chloride-d_2) δ 165.75, 159.39, 140.29, 140.20, 134.82, 131.57, 130.40, 128.54, 128.31, 122.46, 119.66, 115.47, 114.68, 68.30, 29.40, 28.59, 22.95, 14.23.

MS (MALDI-TOF): m/z = 595.32 [M⁺] (100%)

UV-vis (DCM) λ_{max} /nm (ε (x10^5)) = 493 (0.14), 360 (0.63).

Trimer (98)

(98)
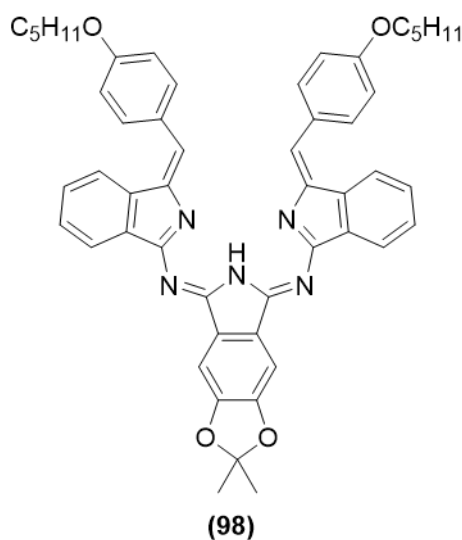
This trimer was isolated from zinc macrocyclisation reaction of a suspension of 4,5-dimethyldioxolanephthalonitrile (**94**) (0.2 g, 0.98 mmol, 3 eq), pentyloxy aminoisoindoline (**45**) (0.1 g, 0.33 mmol, 1 eq) and zinc chloride (0.1g, 0.45 mmol, 1.5 eq) in diglyme (2 mL) in a pre-heated block at 215 °C under argon atmosphere for 18 h. Then, the solvent was evaporated under a stream of argon while the crude was still hot. After that, the reaction mixture was cooled down to r.t. and 300 mL of DCM was added, and the mixture was sonicated and then filtered off through a silica pad to remove the metal salt and green products. Then, the solvent was evaporated under vacuum. The mixture was subjected to a dry-loading column chromatography using PE: DCM 3:2 to obtain the product as brown material

Chemical Formula: $C_{51}H_{49}N_5O_4$

MP: 219- 223°C

¹H NMR (500 MHz, Chloroform-*d*) δ 7.92 – 7.75 (m, 6H), 7.69 – 7.53 (m, 2H), 7.39 (s, 2H), 7.38 – 7.33 (m, 4H), 6.52 (s, 2H), 6.31 (d, *J* = 8.3 Hz, 4H), 3.44 (t, *J* = 6.8 Hz, 4H), 1.73 (s, 6H), 1.63 – 1.57 (m, 4H), 1.30 – 1.26 (m, 4H), 1.21 – 1.17 (m, 4H), 0.91 – 0.85 (m, 6H).

¹³C NMR (126 MHz, Chloroform-*d*) δ 169.08, 159.41, 151.54, 145.65, 142.46, 133.13, 128.64, 128.41, 126.95, 126.00, 121.14, 120.36, 118.75, 114.07, 103.13, 81.76, 78.98, 67.63, 42.15, 28.84, 28.09, 26.03, 25.48, 23.79, 22.49, 20.05, 14.20, 14.09.

MS (MALDI-TOF): m/z = 796.11 [M⁺] (100%).

UV-vis (DCM) λ max /nm (ε (x10⁵)) = 269 (0.774), 332 (0.43), 389 (0.27), 399 (0.267).

3.9 Macrocyclisation products

3.9.1[(4-Methoxyphenyl)-tetrabenzo-triazaporphyrin] magnesium (II) (30) [9]

(30)
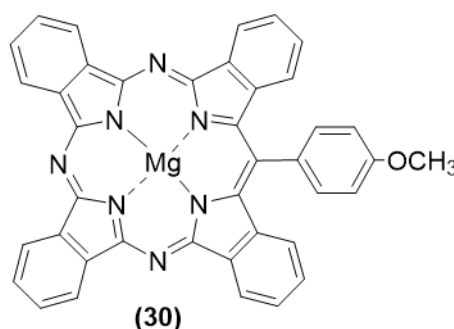
The reaction was carried out following the optimised procedure that was invented recently by Cammidge group that involves a one-step reaction. A mixture of phthalonitrile (0.1025g, 0.8 mmol, 2 eq), MgBr₂ (0.11 g, 0.6 mmol, 1.5 eq), aminoisoindoline (**29**) (0.2 g, 0.8 mmol, 2 eq) and DABCO (0.0675 g, 0.6 mmol, 1.5 eq) were dissolved in dry diglyme (3 mL) and it was heated at 220°C for 4 h under an argon atmosphere. When the reaction was finished, a stream of argon was passed through the reaction flask while it still hot, in order to remove the solvent. The reaction mixture was cooled down to r.t. and a mixture of 1:1 DCM:MeOH (20 mL) was added, and the mixture sonicated and then evaporated. Two consecutive flash chromatography columns were needed to purify the resulting mixture. Firstly, the crude was loaded on silica-gel column and eluted with 100% DCM → DCM/Et₃N (20:1) → DCM: Et₃N: THF (10:1:4) in order to remove the yellow-brown impurities and obtain a green fraction. Finally, the green fraction was then subjected to a second column chromatography

using PE/THF (5:1) as eluant to obtain the green product that finally was purified by recrystallisation using acetone; EtOH to yield (0.09 g, 18 %).

Chemical Formula: $C_{40}H_{23}MgN_7O$

MP: 294°C (literature 290 °C)[30]

^{1}H NMR (500 MHz, Acetone-d_6) δ 9.61 (d, J = 7.6 Hz, 2H), 9.53 (s, 4H), 8.28 – 8.23 (m, 4H), 8.06 (d, J = 8.3 Hz, 2H), 7.99 (t, J = 7.2 Hz, 2H), 7.69 (t, J = 7.4 Hz, 2H), 7.61 – 7.55 (m, 2H), 7.24 (d, J = 7.6 Hz, 2H), 4.23 (s, 3H).

MS (MALDI-TOF): m/z = 641.09 [M]$^+$ (100%)

3.9.2 [(4-Pentyloxyphenyl)-tetrabenzo-triazaporphyrin] zinc (84) [9]

(84)
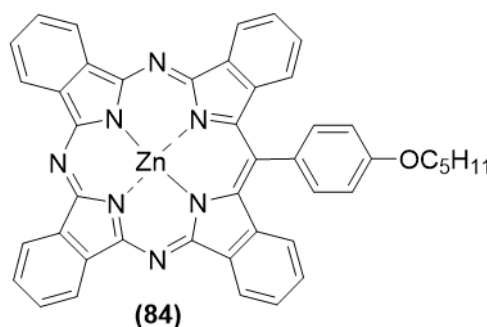
This compound was synthesised using the same previous optimised procedure as follows:

A mixture of phthalonitrile (0.25 g, 1.96 mmol, 3 eq), pentyloxy aminoisoindoline (**45**) (0.2 g, 0.65 mmol, 1 eq) and $ZnCl_2$ (0.15 g, 1 mmol, 1.5 eq), were dissolved in dry diglyme (3 mL) and it was heated at 215 °C for 6 h under an argon atmosphere. When the reaction was finished, the solvent was removed under a stream of argon. The reaction mixture was cooled down to r.t. and 300 mL of DCM was added, and the mixture was sonicated and then filtered off through a silica pad to remove the side products, then THF was added to get green materials as a separate fraction. Then, the solvent was evaporated under vacuum. The green mixture was subjected to a dry-loading column chromatography using PE: THF 20:1 to obtain the desired product that finally was purified by recrystallisation using acetone:EtOH to yield (11mg, 23%).

Also, this compound was obtained from fusion or in-solvent reaction of aminoisoindoline:

At 215 °C in an oil bath, a mixture of pentyloxy aminoisoindoline (**45**) (0.3 g, 0.98 mmol,1 eq) and Zn dust (0.13 g, 2 mmol, 1.7 eq) was sealed in a microwave vessel with a magnetic bar either in freshly distilled quinoline (2mL) or without any solvent. Then, the mixture was purged and refilled with N_2 before putting in the oil bath. The reaction was followed by TLC until full consumption of starting material was observed. After the reaction finished and while it was hot, a stream of argon was used to evaporate the solvent. Then, the crude mixture was subjected to dry loading column chromatography using DCM:PE 1:1 → DCM 100% → PE: DCM: THF 30: 10: 0.1 to give the desired product as third green fraction (0.027 g, 15%)

Chemical Formula: $C_{44}H_{31}N_7OZn$

Mp >300 °C.

¹H NMR (500 MHz, THF-d_8) δ 9.58 (d, J = 7.4 Hz, 2H), 9.48 (s, 4H), 8.21 – 8.15 (m, 4H), 8.04 (d, J = 8.4 Hz, 2H), 7.93 (t, J = 7.2 Hz, 2H), 7.68 – 7.60 (m, 2H), 7.53 (d, J = 8.4 Hz, 2H), 7.25 (d, J = 8.0 Hz, 2H), 4.41 (t, J = 6.5 Hz, 2H), 2.13 – 2.04 (m, 2H), 1.66 – 1.55 (m, 2H), 1.15 – 1.09 (m, 2H), 1.11 – 1.06 (m, 3H).

¹³C NMR (126 MHz, THF-$d8$) δ 161.72, 156.98, 153.98, 153.21, 144.38, 140.70, 140.54, 140.32, 139.73, 135.41, 134.25, 130.48, 130.18, 128.73, 127.82, 126.01, 123.94, 123.75, 123.71, 116.24, 69.54, 68.28, 30.57, 29.78, 26.15, 23.98, 14.89.

MS (MALDI-TOF): m/z = 737.19 [M⁺] (100%)

UV-vis (dist. THF) λ $_{max}$ /nm (ε (x10⁵)) = 380 (1.01), 442 (0.4), 592 (0.48), 608 (0.46), 615 (0.47), 646 (1.74), 670 (3.06).

3.9.3 [*Trans*-(4-pentyloxyphenyl) -tetrabenzo-diazaporphyrin] zinc (85)
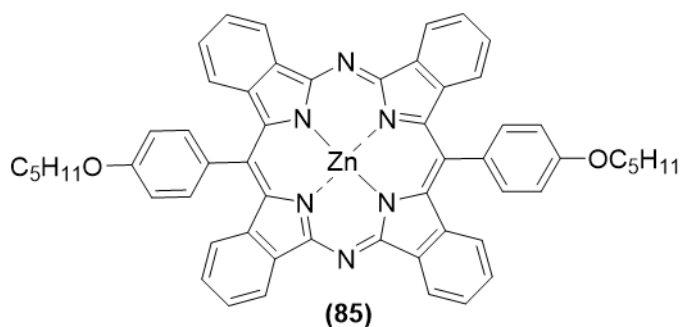
(85)

This macrocycle was isolated from the fusion reaction of pentyloxy aminoisoindoline (**45**) as the first green fraction (11 mg, 5%)

Chemical Formula: $C_{56}H_{46}N_6O_2Zn$

MP >300 °C.

^{1}H NMR (500 MHz, THF-d_8) δ 9.73 (dt, J = 7.5, 1.1 Hz, 4H), 8.12 – 8.05 (m, 4H), 8.03 – 7.94 (m, 4H), 7.71 – 7.61 (m, 4H), 7.58 – 7.51 (m, 4H), 7.37 – 7.32 (m, 4H), 4.43 (t, J = 6.5 Hz, 4H), 2.14 – 2.06 (m, 4H), 1.80 – 1.61 (m, 4H), 1.62 – 1.55 (m, 4H), 1.11 (t, J = 7.3 Hz, 6H).

^{13}C NMR (126 MHz, THF-d_8) δ 134.53, 128.49, 127.86, 126.21, 123.67, 115.98, 69.36, 68.10, 30.52, 29.61, 23.80, 14.72.

MS (MALDI-TOF): m/z = 898.29 [M$^+$] (100%).

UV-vis (dist. THF) λ_{max} /nm (ε (x10^5)) = 386 (1.13), 407 (0.88), 429 (1.89), 556 (0.25), 582 (0.32), 601 (0.47), 622 (0.48), 634 (0.68), 673 (2.79).

3.9.4 [*Cis*-(4-pentyloxyphenyl) -tetrabenzo-diazaporphyrin] zinc (86)

(86)
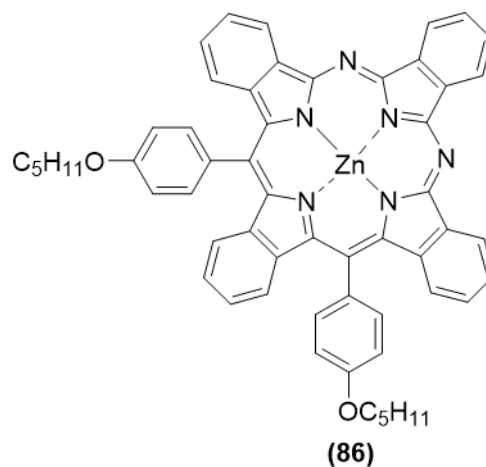
This macrocycle was isolated from the fusion reaction of pentyloxy aminosoindoline (**45**) as the second green fraction (15 mg, 7%).

Chemical Formula: $C_{56}H_{46}N_6O_2Zn$

 MP >300 °C.

^{1}H NMR (500 MHz, Acetone-d_6) δ 9.64 (d, J = 7.6 Hz, 2H), 9.56 – 9.51 (m, 2H), 8.31 – 8.25 (m, 2H), 8.04 – 7.95 (m, 6H), 7.71 – 7.64 (m, 2H), 7.58 – 7.52 (m, 4H), 7.41 – 7.35 (m, 2H), 7.30 – 7.25 (m, 2H), 7.11 (d, J = 8.1 Hz, 2H), 4.44 (t, J = 6.5 Hz, 4H), 2.20 – 2.15 (m, 2H), 1.94 – 1.90 (m, 2H), 1.74 – 1.67 (m, 4H), 1.64 – 1.53 (m, 4H), 1.07 (t, J = 7.3 Hz, 6H).

MS (MALDI-TOF): m/z = 898.29 [M$^+$] (100%).

UV-vis (dist. THF) λmax /nm (ε (x10^5)) = 394 (0.84), 427 (1.53), 585 (0.35), 644 (2.17).

3.9.5 Synthesis of peripherally substituted meso-Ar-TBTAP hybrids[9]

3.9.5.1 (Tetramethyl-tetralino)₃ZnTBTAP-(4-OC₅H₁₁-Ph) (91)

(91)
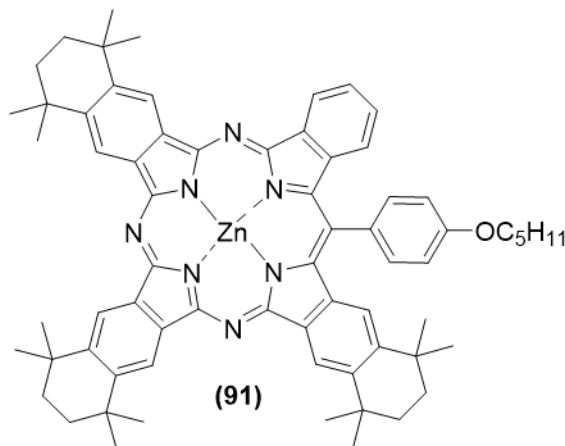
In pre-heated 215°C heating block, a suspension of pentyloxy aminoisoindoline (**45**) (0.2 g, 0.65 mmol, 1eq), $ZnCl_2$ (0.13 g, 1 mmol, 1.5 eq) and 6,7-dicyano-1,1,4,4-tetramethyl-1,2,3,4-tetrahydronaphthalene (**52**) (0.5 g, 1.96 mmol, 3 eq) in diglyme (3mL) was heated under N_2 until the completion of the reaction was observed by TLC. Then, the solvent was evaporated while the reaction was still hot under an argon stream. The mixture was sonicated with DCM and filtered through a short silica column to remove salts and baseline materials. Then, the desired product was isolated by column chromatography using PE: THF 50:1 as eluent. Recrystallisation from acetone:ethanol gave the title compound as green crystals (0.05 g, 7%)

Chemical Formula: $C_{68}H_{73}N_7OZn$

MP: 293 °C.

¹H NMR (500 MHz, THF-d_8) δ 9.60 (d, J = 7.6 Hz, 1H), 9.55 – 9.48 (m, 5H), 8.07 – 7.97 (m, 2H), 7.90 (t, J = 7.2 Hz, 1H), 7.63 – 7.59 (m, 1H), 7.55 (d, J = 8.5 Hz, 2H), 7.41 (d, J = 8.1 Hz, 1H), 7.18 (s, 1H), 4.41 (t, J = 6.3 Hz, 2H), 2.09 (s, 12H), 1.98 – 1.88 (m, 2H), 1.87 – 1.75 (m, 24H), 1.65 – 1.57 (m, 4H), 1.52 – 1.15 (m, 12H), 1.14 – 1.09 (m, 3H).

¹³C NMR (101 MHz, THF-d_8) δ 160.33, 156.24, 152.57, 152.39, 151.03, 146.93, 146.59, 144.51, 144.21, 142.61, 139.07, 138.13, 137.44, 137.15, 136.99, 136.88, 136.38, 134.53, 133.08, 126.91, 125.94, 124.53, 123.80, 123.43, 122.44, 120.66, 120.41, 120.31, 119.67, 115.02, 68.16, 66.99, 35.50, 35.46, 35.21, 34.99, 32.16, 32.05, 32.00, 29.25, 28.50, 22.53, 18.08, 13.57.

MS (MALDI-TOF): m/z = 1066.29 [M⁺] (100%)

UV-vis (dist. THF) λ_{max} /nm (ε (x10^5)) = 351 (1.3), 380 (1.37), 446 (0.63), 599 (0.73), 618 (0.74), 656 (1.79), 682 (2.87).

3.9.5.2 (Dimethyl dioxolane)₃ ZnTBTAP-(4-OC₅H₁₁-Ph) (96)
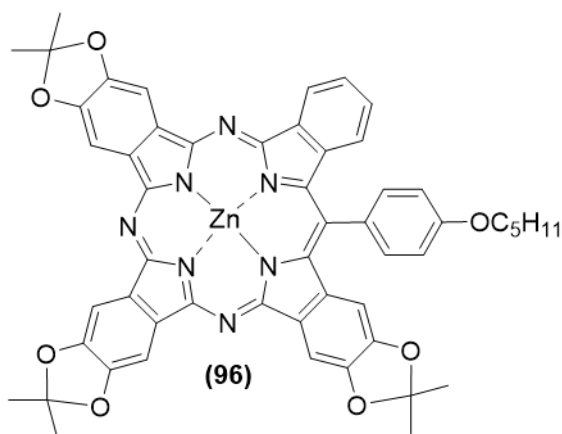
(96)

A suspension of 4,5-dimethyldioxolanephthalonitrile (**94**) (0.2 g, 0.98 mmol, 3 eq), pentyloxy aminoisoindoline (**45**) (0.1 g, 0.33 mmol, 1 eq) and zinc chloride (0.1g, 0.45 mmol, 1.5 eq) in diglyme (2 mL) was heated up in a pre-heated block at 215 °C under N$_2$ for 18 h. Then, the solvent was evaporated under a stream of argon while the crude was still hot. After that, the desired product was isolated by column chromatography using: 100% DCM → PE: DCM: THF 30: 10: 0.2 as eluent. Recrystallisation from acetone: DCM: EtOH 1:1:1.5 gave the title compound as green crystals (0.024 g, 8%).

Chemical Formula: C$_{53}$H$_{43}$N$_7$O$_7$Zn

MP: 295 °C.

¹H NMR (500 MHz, THF-d_8) δ 9.56 (dt, J = 7.6, 1.0 Hz, 1H), 8.82 – 8.81 (m, 1H), 8.75 (s, 2H), 8.75 – 8.72 (m, 2H), 8.02 – 7.94 (m, 2H), 7.93 – 7.86 (m, 1H), 7.62 – 7.58 (m, 1H), 7.54 – 7.47 (m, 2H), 7.18 (dt, J = 8.1, 0.9 Hz, 1H), 6.51 (d, J = 0.6 Hz, 1H), 4.40 (t, J = 6.5 Hz, 2H), 1.97 (s, 12H), 1.83 (s, 6H), 1.81 – 1.75 (m, 4H), 1.64 – 1.52 (m, 2H), 1.13 – 1.06 (m, 3H).

¹³C NMR (126 MHz, THF-d_8) δ 161.43, 156.41, 153.36, 152.60, 152.52, 151.55, 151.24, 150.26, 149.34, 143.55, 143.49, 140.45, 139.47, 135.75, 135.63, 135.33, 134.01, 128.25, 127.32, 125.68, 125.05, 123.48, 120.59, 119.88, 116.14, 104.69, 103.07, 102.95, 102.08, 69.33, 68.39, 68.10, 57.96, 29.57, 26.55, 26.42, 26.40, 25.98, 23.79, 19.24, 14.72.

MS (MALDI-TOF): m/z = 953.00 [M$^+$] (100%)

UV-vis (dist. THF) λ_{max} /nm (ϵ (x10^5)) = 351 (0.76), 376 (0.91), 389 (0.9), 435 (0.49), 589 (0.42), 603 (0.42), 611 (0.41), 643 (1.2), 667 (2.09).

3.9.5.3 (Dimethyl dioxolane)$_2$ H$_2$TBTAP-(4-OC$_5$H$_{11}$-Ph) (99)
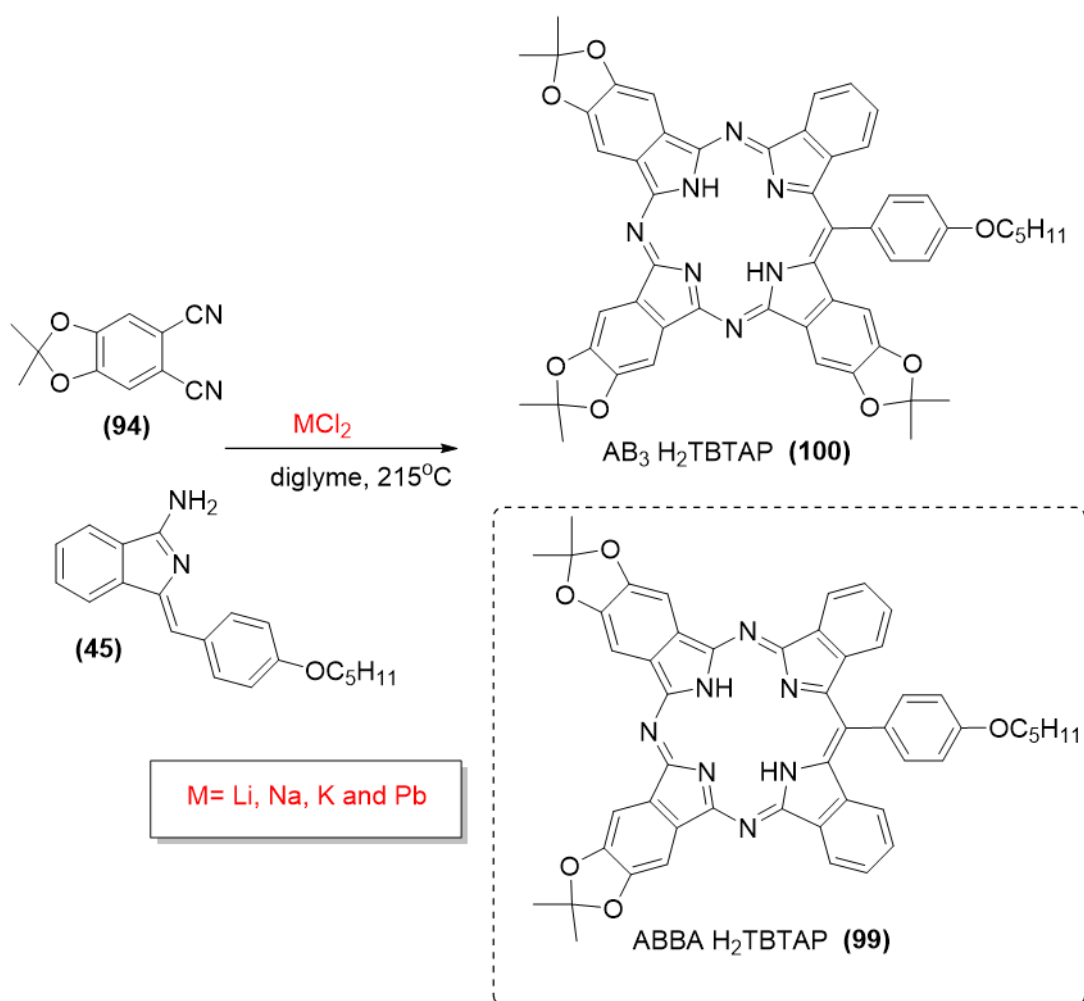
Following the previous procedure but using LiCl, NaCl or KCl as metal templates resulted in mixtures of un-metalated hybrids (AB$_3$ and A$_2$B$_2$). The isolation of the title compound was successful after several columns as dark green solids. Yield was not calculated as some of the materials were still mixed in some fractions.

Chemical Formula: C$_{50}$H$_{41}$N$_7$O$_5$

MP >300 °C.

^{1}H NMR (500 MHz, Toluene-d_8) δ 9.70 (d, J = 7.6 Hz, 2H), 8.95 (s, 2H), 8.87 (s, 2H), 7.93 (d, J = 8.1 Hz, 2H), 7.80 – 7.72 (m, 2H), 7.58 – 7.52 (m, 2H), 7.48 (d, J = 8.0 Hz, 2H), 7.35

(d, J = 8.5 Hz, 2H), 3.95 (t, J = 6.5 Hz, 2H), 2.25 – 2.18 (m, 2H), 1.99 – 1.94 (m, 2H), 1.85 – 1.77 (m, 2H), 1.00 (t, J = 7.2 Hz, 3H).

MS (MALDI-TOF): m/z = 819.08 [M$^+$] (100%)

UV-vis (dist. THF) λ_{max} /nm (ε (x10^5)) = 343 (0.39), 377 (0.39), 413 (0.29), 418 (0.29), 585 (0.21), 615 (0.26), 641 (0.41), 683 (0.59).

3.9.5.4 (Dimethyl dioxolane)$_2$ ZnTBTAP-(4-OC$_5$H$_{11}$-Ph) (101)
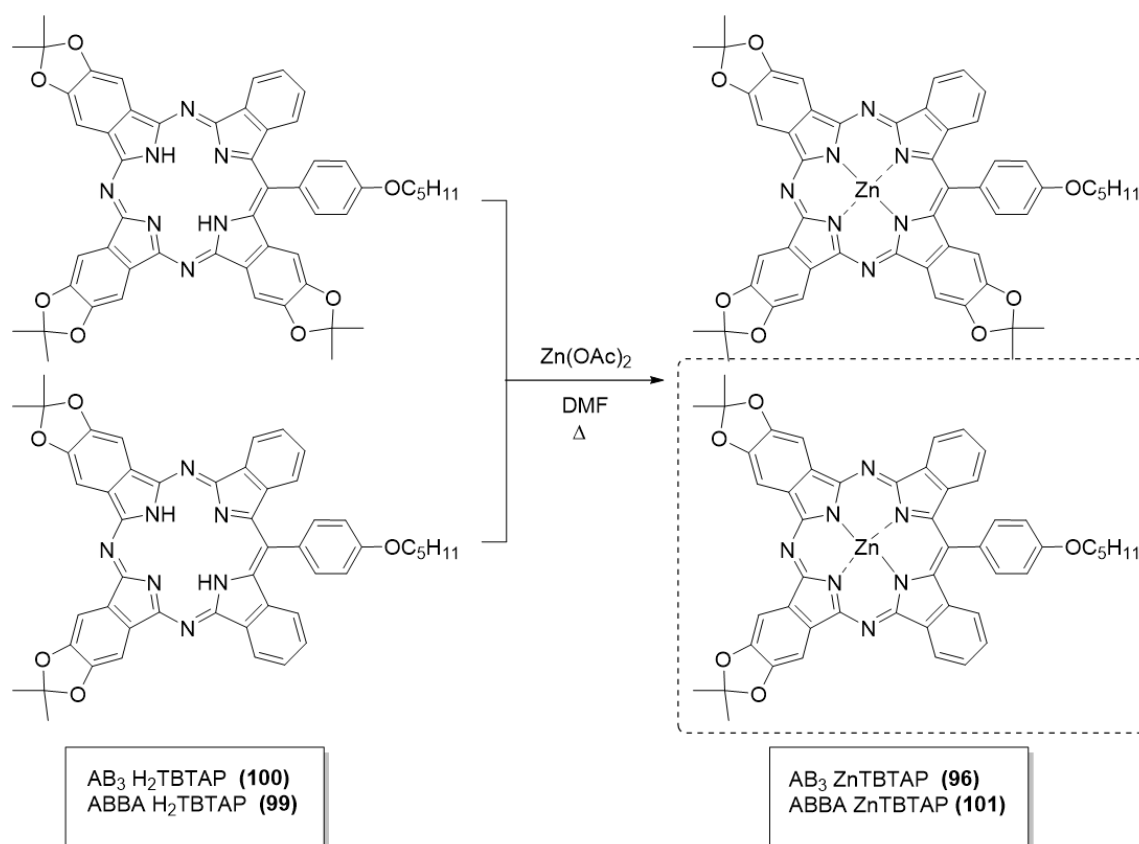
This hybrid (**101**) was isolated after metalation of metal-free crudes which were obtained when lithium, sodium and potassium chlorides were reacted as metal templates under the same conditions explained above. Yields for both hybrids are illustrated in the results and discussion chapter (table 2.3) as each metal gave different yields. A full analysis of AB$_3$ ZnTBTAP (**96**) was reported earlier.

Chemical Formula: C$_{50}$H$_{39}$N$_7$O$_5$Zn

MP >300 °C.

^{1}H NMR (500 MHz, THF-d_8) δ 9.55 (d, J = 7.6 Hz, 2H), 8.74 (s, 4H), 8.00 (d, J = 8.4 Hz, 2H), 7.91 (t, J = 7.2 Hz, 2H), 7.61 (m, 2H), 7.51 (d, J = 8.5 Hz, 2H), 7.23 (d, J = 8.0 Hz,

2H), 4.40 (t, $J = 6.5$ Hz, 2H), 2.07 (m, 2H), 1.98 (s, 12H), 1.79 (d, $J = 3.0$ Hz, 2H), 1.60 (m, 2H), 1.11 (m, 3H).

^{13}C NMR (126 MHz, THF-d_8) δ 161.46, 156.69, 153.60, 152.75, 151.61, 151.30, 143.56, 140.46, 139.46, 135.78, 135.40, 135.31, 134.07, 128.34, 127.40, 125.71, 123.51, 120.65, 115.99, 103.13, 103.00, 69.34, 68.39, 68.10, 57.96, 30.39, 29.60, 26.55, 26.40, 25.98, 23.79, 19.24, 14.71.

MS (MALDI-TOF): m/z = 881.15 [M$^+$] (100%)

UV-vis (dist. THF) λ $_{max}$ /nm (ε (x10^5)) = 353 (0.85), 357 (0.85), 375 (0.97), 437 (0.48), 590 (0.46), 604 (0.46), 612 (0.459), 644 (1.5), 667 (2.6).

3.9.5.5 (Dimethyl dioxolane)$_3$ MgTBTAP-(4-OC$_5$H$_{11}$-Ph) (102)
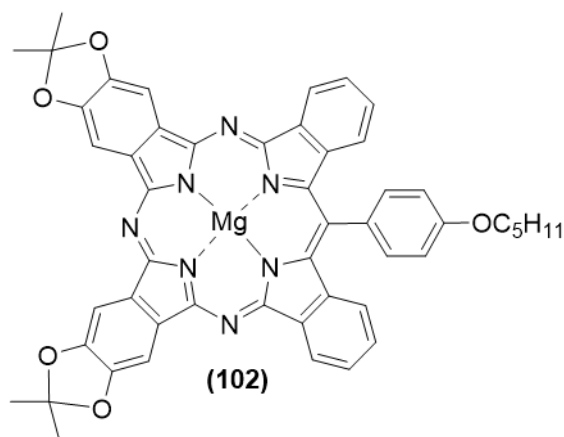
(102)

In pre-heated 215°C heating block, a suspension of pentyloxy aminoisoindoline (**45**) (0.2 g, 0.65 mmol, 1eq), MgCl$_2$ (0.13 g, 1 mmol, 1.5 eq) 4,5-dimethyldioxolanephthalonitrile (**94**) (0.5 g, 1.96 mmol, 3 eq) in diglyme (3mL) was heated under N$_2$ until the completion of the reaction was observed by TLC. Then, the solvent was evaporated while the reaction was still hot under an argon stream. The mixture was sonicated with DCM and filtered through a short silica column to remove salts and baseline materials. Then, THF was added to get green fraction. After evaporation of solvent, the desired product was isolated by column chromatography using PE: THF 50:1 as eluent. Recrystallisation from acetone: ethanol gave the title compound as the major macrocycle as green crystals (11 mg, 8%)

Chemical Formula: C$_{50}$H$_{39}$MgN$_7$O$_5$

MP >300 °C.

^{1}H NMR (500 MHz, THF-d_8) δ 9.56 (d, $J = 7.5$ Hz, 2H), 8.78 – 8.74 (m, 4H), 8.01 (d, $J = 8.4$ Hz, 2H), 7.88 (t, $J = 7.2$ Hz, 2H), 7.59 (ddd, $J = 8.0, 6.8, 1.2$ Hz, 2H), 7.50 (d, $J = 8.4$

Hz, 2H), 7.25 (d, J = 8.0 Hz, 2H), 4.40 (t, J = 6.5 Hz, 2H), 2.08 (dt, J = 14.8, 6.7 Hz, 2H), 1.97 (s, 12H), 1.79 – 1.76 (m, 2H), 1.65 – 1.54 (m, 2H), 1.11 (d, J = 7.4 Hz, 3H).

^{13}C NMR (126 MHz, THF-d_8) δ 161.35, 156.47, 153.33, 152.31, 151.37, 151.07, 142.89, 141.22, 140.10, 136.46, 135.98, 134.13, 127.98, 127.08, 126.53, 125.75, 123.53, 120.46, 115.79, 103.27, 103.14, 69.32, 68.38, 68.09, 30.40, 29.60, 26.55, 26.40, 25.97, 23.79, 14.71.

MS (MALDI-TOF): m/z = 841.28 [M$^+$] (100%)

UV-vis (dist. THF) λ_{max} /nm (ε (x10^5)) = 356 (0.76), 378 (0.93), 396 (0.92), 439 (0.45), 591 (0.4), 605 (0.38), 612 (0.38), 645 (1.62), 667 (2.71).

3.9.5.6 (Dimethyl dioxolane)$_3$ MgTBTAP-(4-OC$_5$H$_{11}$-Ph) (103)

(103)
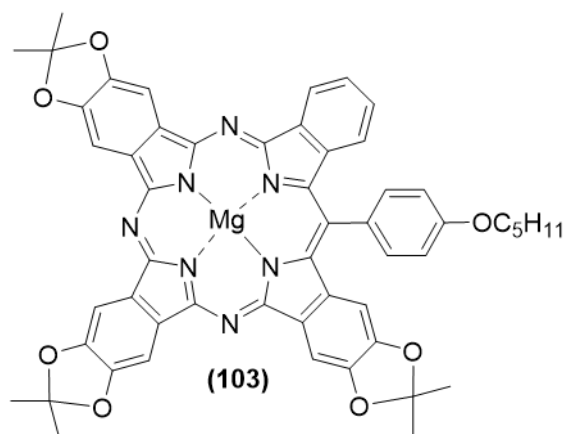
This macrocycle was isolated from the previous reaction as minor compound. Recrystallisation from acetone: ethanol gave the title compound as green solid (ca 15 mg, 5%). A pure product could not be obtained.

Chemical Formula: C$_{53}$H$_{43}$MgN$_7$O$_7$

MP >300 °C.

MS (MALDI-TOF): m/z = 913.05 [M$^+$] (100%)

UV-vis (dist. THF) λ_{max} /nm (ε (x10^5)) = 377 (0.87), 379 (0.88), 394 (0.93), 438 (0.45), 590 (0.4), 604 (0.4), 644 (1.22), 666 (2.04).

3.9.5.7 (Octamethoxy) ZnTBTAP (65)
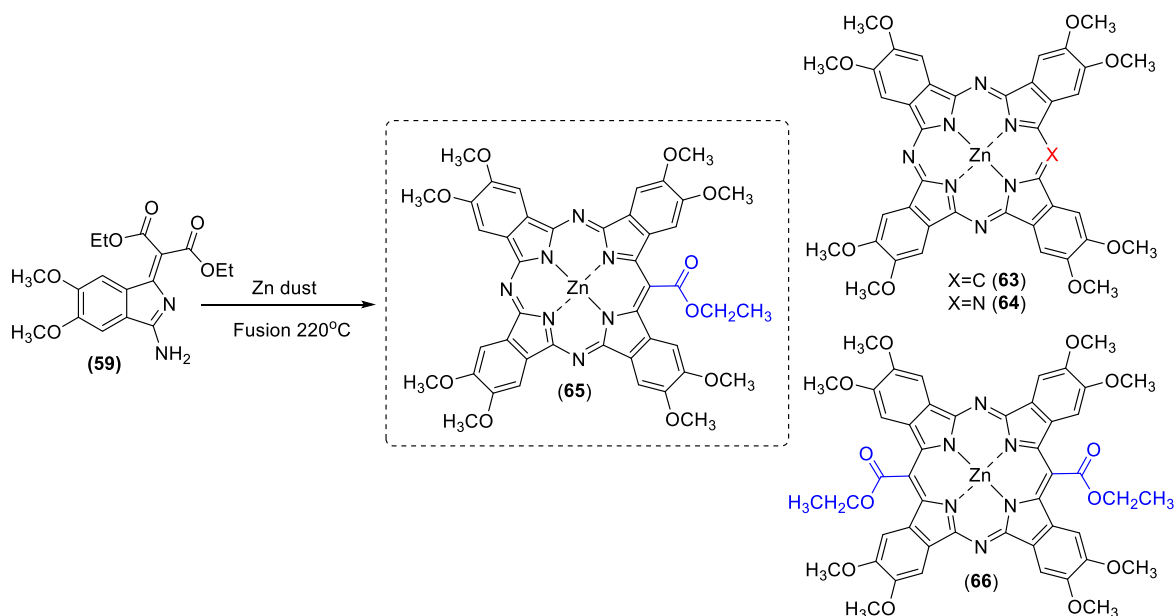
Dimethoxy malonate aminoisoindoline (**59**) (3.04 g, 0.009 mol) was fused with zinc dust (1.2 g, 0.017 mol) in a pre-heated 215°C oil bath. After 3 h, the mixture was allowed to cool down and 300 mL of DCM was added, and the mixture was sonicated to dissolve all organic materials. Then, the solution was filtered through a silica pad to remove brown materials. Then, THF was added to get a green mixture that was later analysed by TLC and one green baseline spot was obtained. However, the MALDI-TOF MS gave an indication of two hybrids. Many solvent systems were used to isolate the mixture but with no success. Precipitation with DCM: MeOH was a useful method to isolate some of the product.

Chemical Formula: $C_{44}H_{37}N_7O_{10}Zn$

MP >300 °C.

MS (MALDI-TOF): m/z = 887.86 [M$^+$] (100%)

UV-vis (dist. THF) λ_{max} /nm= 384 (0.5479), 594 (0.1875), 650 (0.6622), 669 (0.987).

3.10 References

(1)   Kagechika, H.; Kawachi, E.; Hashimoto, Y.; Shudo, K.; Himi, T. Retinobenzoic Acids. 1. Structure-Activity Relationships of Aromatic Amides with Retinoidal Activity. *J. Med. Chem.,* **1988**, *31* (11), 2182–2192.

(2)   Bruson, H. A.; Kroeger, J. W. Cycli-Alkylation of Aromatic Compounds by the Friedel and Crafts Reaction. *J. Am. Chem. Soc.,* **1940**, *62* (1), 36–44.

(3)   Schmerling, L.; West, J. P. Condensation of Saturated Halides with Unsaturated Compounds. VIII. Condensation of Dihaloalkanes with Ethylene and Chloroethylenes1. *J. Am. Chem. Soc.,* **1952**, *74* (11), 2885–2889.

(4)   Hanack, M.; Haisch, P.; Lehmann, H.; Subramanian, L. R. Synthesis of Soluble Octasubstituted Phthalocyaninatoplatinum And-Palladium Complexes. *Synthesis.,* **1993**, *1993*, 387–390.

(5)   Ashton, P. R.; Girreser, U.; Giuffrida, D.; Kohnke, F. H.; Mathias, J. P.; Raymo, F. M.; Slawin, A. M. Z.; Stoddart, J. F.; Williams, D. J. Molecular Belts. 2. Substrate-Directed Syntheses of Belt-Type and Cage-Type Structures. *J. Am. Chem. Soc.,* **1993**, *115* (13), 5422–5429.

(6)   Rose, I.; Bezzu, C. G.; Carta, M.; Comesaña-Gándara, B.; Lasseuguette, E.; Ferrari, M. C.; Bernardo, P.; Clarizia, G.; Fuoco, A.; Jansen, J. C. Polymer Ultrapermeability from the Inefficient Packing of 2D Chains. *Nat. Mater.,* **2017**, *16* (9), 932–937.

(7)   Schareina, T.; Zapf, A.; Mägerlein, W.; Müller, N.; Beller, M. A State-of-the-Art Cyanation of Aryl Bromides: A Novel and Versatile Copper Catalyst System Inspired by Nature. *Chem. Eur. J.,* **2007**, *13* (21), 6249–6254.

(8)   Mikhalenko, S. A.; Solov'eva, L. I.; Luk'yanets, E. A. Symmetric Sterically Hindered Phthalocyanines. *ChemInform.,* **1989**, *20* (25).

(9)   Alkorbi, F.; Díaz-Moscoso, A.; Gretton, J.; Chambrier, I.; Tizzard, G. J.; Coles, S. J.; Hughes, D. L.; Cammidge, A. N. Complementary Syntheses Giving Access to a Full Suite of Differentially Substituted Phthalocyanine-Porphyrin Hybrids. *Angew. Chem. Int. Ed.,* **2021**, *60* (14), 7632–7636.

(10)   Gonidec, M.; Biagi, R.; Corradini, V.; Moro, F.; De Renzi, V.; Del Pennino, U.; Summa, D.; Muccioli, L.; Zannoni, C.; Amabilino, D. B.; Veciana, J. Surface Supramolecular Organization of a Terbium(III) Double-Decker Complex on Graphite and Its Single Molecule Magnet Behavior. *J. Am. Chem. Soc.,* **2011**, *133* (17), 6603–6612.

(11)   Sarker, A. K.; Kang, M. G.; Hong, J. D. A Near-Infrared Dye for Dye-Sensitized Solar Cell: Catecholate- Functionalized Zinc Phthalocyanine. *Dyes Pigm.,* **2012**, *92* (3), 1160–1165.

(12)   Ellis, G. P.; Romney-Alexander, T. M. Cyanation of Aromatic Halides. *Chem. Rev.,* **1987**, *87* (4), 779–794.

(13)   Metz, J.; Schneider, O.; Hanack, M. Synthesis and Properties of Substituted (Phthalocyaninato)-Iron and-Cobalt Compounds and Their Pyridine Adducts. *Inorg. Chem.,* **1984**, *23* (8), 1065–1071.

(14)   Wenderski, T.; Light, K. M.; Ogrin, D.; Bott, S. G.; Harlan, C. J. Pd Catalyzed Coupling of 1,2-Dibromoarenes and Anilines: Formation of N,N-Diaryl-o-Phenylenediamines. *Tetrahedron Lett*., **2004**, *45* (37), 6851–6853.

(15)   Kohn, M.; Steiner, L. The Reduction of Bromo Derivatives of Catechol, Resorcinol, and Pyrogallol. *J. Org. Chem.,* **1947**, *12* (1), 30–33.

(16)   Platonova, Y. B.; Volov, A. N.; Tomilova, L. G. Palladium(II) Octaalkoxy- and Octaphenoxyphthalocyanines: Synthesis and Evaluation as Catalysts in the Sonogashira Reaction. *J. Catal.*, **2019**, *373*, 222–227.

(17)   Donaldson, L. R.; Wallace, S.; Haigh, D.; Patton, E. E.; Hulme, A. N. Rapid Synthesis and Zebrafish Evaluation of a Phenanthridine-Based Small Molecule Library. *Org. Biomol. Chem.,* **2011**, *9* (7), 2233–2239.

(18)   Cammidge, A. N.; Gopee, H. Structural Factors Controlling the Transition between Columnar-Hexagonal and Helical Mesophase in Triphenylene Liquid. *J. Mater Chem.*, **2001**, *11* (11), 2773–2783.

(19)   van Nostrum, C. F.; Picken, S. J.; Schouten, A.-J.; Nolte, R. J. M. Synthesis and Supramolecular Chemistry of Novel Liquid Crystalline Crown Ether-Substituted Phthalocyanines: Toward Molecular Wires and Molecular Ionoelectronics. *J. Am. Chem. Soc.*, **1995**, *117* (40), 9957–9965.

(20)   Boden, N.; Bushby, R. J.; Cammidge, A. N. Triphenylene-Based Discotic-Liquid-Crystalline Polymers: A Universal, Rational Synthesis. *J. Am. Chem. Soc.*, **1995**, *117* (3), 924–927.

(21)   Dalai, S.; Belov, V. N.; Nizamov, S.; Rauch, K.; Finsinger, D.; De Meijere, A. Access to Variously Substituted 5,6,7,8-Tetrahydro-3H-Quinazolin-4-Ones via Diels-Alder Adducts of Phenyl Vinyl Sulfone to Cyclobutene-Annelated Pyrimidinones. *Eur. J. Org. Chem.,* **2006**, No. 12, 2753–2765.

(22)   Hellal, M.; Cuny, G. D. Microwave Assisted Copper-Free Sonogashira Coupling/5-Exo-Dig Cycloisomerization Domino Reaction: Access to 3-(Phenylmethylene)Isoindolin-1-Ones and Related Heterocycles. *Tetrahedron Lett.*, **2011**, *52* (42), 5508–5511.

(23)   Alharbi, N. Synthesis and Functionalization of Novel Meso-Substituted. PhD thesis. University of East Anglia, **2014**.

(24)   He, Y.; Zhang, X.; Fan, X. Synthesis of Naphthalene Amino Esters and Arylnaphthalene Lactone Lignans through Tandem Reactions of 2-Alkynylbenzonitriles. *Chem. Commun.,* **2014**, *50* (42), 5641–5643.

(25)   Ye, P.; Shao, Y.; Xie, L.; Shen, K.; Cheng, T.; Chen, J. Lanthanide-Catalyzed Tandem Insertion of Secondary Amines with 2-Alkynylbenzonitriles: Synthesis of Aminoisoindoles. *Chem. Asian. J.,* **2018**, *13* (23), 3681–3690.

(26)   Sonogashira, K. Development of Pd–Cu Catalyzed Cross-Coupling of Terminal Acetylenes with Sp2-Carbon Halides. *J. Organomet. Chem.,* **2002**, *653* (1), 46–49.

(27)   Chow, H. F.; Wan, C. W.; Low, K. H.; Yeung, Y. Y. A Highly Selective Synthesis of Diarylethynes and Their Oligomers by a Palladium-Catalyzed Sonogashira Coupling Reaction under Phase Transfer Conditions. *J. Org. Chem.,* **2001**, *66* (5), 1910–1913.

(28)   Chambrier, I.; Cook, M. J. Reaction of Phthalonitrile with Alkoxide Ions. *J. Chem. Research. Synopses (Print).,* **1990**, 10, 322–323.

(29)   Barrett, P. A.; Linstead, R. P.; Leavitt, J. J.; Rowe, G. A. 196. Phthalocyanines and Related Compounds. Part XVIII. Intermediates for the Preparation of Tetrabenzporphins : The Thorpe Reaction with Phthalonitrile. *J. Chem. Soc (Resumed).,* **1940**, 1076–1079.

(30)   Díaz-Moscoso, A.; Tizzard, G. J.; Coles, S. J.; Cammidge, A. N. Synthesis of Meso-Substituted Tetrabenzotriazaporphyrins: Easy Access to Hybrid Macrocycles. *Angew. Chem.,* **2013**, *125* (41), 10984–10987.

Chapter 4:

Appendix

Crystal data and structure refinement for an isoindoline dimer (40)

_____

Identification code   noraf2

Elemental formula   C30 H29 N3 O8

Formula weight   559.56

Crystal system, space group   Orthorhombic,   Pbcn
(no. 60)

Unit cell dimensions   a = 30.827(2) Å   α = 90 °
                              b = 7.91493(9) Å   β = 90 °
                              c = 23.2060(2) Å   γ = 90 °

Volume   5662.0(4) Å^3

Z, Calculated density   8,   1.313 Mg/m^3

F(000)   2352

Absorption coefficient   0.801 mm^{-1}

Temperature   121(30) K

Wavelength   1.54184 Å

Crystal colour, shape   orange rod

Crystal size   0.02 x 0.06 x 0.32 mm

Crystal mounting: on a small loop, in oil, fixed in cold
N$_2$ stream

On the diffractometer:

   Theta range for data collection   2.867 to 72.488 °

   Limiting indices   -38<=h<=38, -9<=k<=7, -
28<=l<=28

   Completeness to theta = 67.684   100.0 %

Absorption correction   Semi-empirical from
equivalents

Max. and min. transmission   1.00000 and 0.69628

Reflections collected (not including absences) 152327

No. of unique reflections   5619 [R(int) for
equivalents = 0.082]

No. of 'observed' reflections (I > 2σ$_I$)   5113

Structure determined by: dual methods, in SHELXT

_____

 Refinement: Full-matrix least-squares on F^2, in
SHELXL

        Data / restraints / parameters   5619 / 0 / 371

        Goodness-of-fit on F^2 1.045

        Final R indices ('observed' data) R_1 = 0.044, wR_2 = 0.110

        Final R indices (all data) R_1 = 0.048, wR_2 = 0.112

        Reflections weighted:
           w = $[\sigma^2(Fo^2)+(0.0484P)^2+3.815P]^{-1}$ where P=$(Fo^2+2Fc^2)/3$

        Extinction coefficient   n/a

    Largest diff. peak and hole   0.34 and -0.29 e.$\mathring{A}^{-3}$

    Location of largest difference peak   near H(18b)

_____
_

    Table 1.   Atomic coordinates (x 10^5) and equivalent isotropic
               displacement parameters ($\mathring{A}^2$ x 10^4). U(eq) is
defined
               as one third of the trace of the orthogonalized
Uij

               tensor.   E.s.ds are in parentheses.

_____

                      x   y   z   U(eq)

_____

        N(1)   75696(4)   36578(15)   74041(5)   254(3)
        C(1)   74009(5)   27484(17)   78533(6)   231(3)
        N(2)   69905(4)   24447(14)   79701(5)   239(3)
        C(3)   69841(5)   14890(16)   84856(6)   223(3)
        C(4)   74379(5)   11843(17)   86824(6)   229(3)
        C(5)   76348(5)   2988(17)   91300(6)   252(3)
        C(6)   80860(5)   2424(18)   91459(7)   282(3)
        C(7)   83402(5)   10305(19)   87306(7)   291(3)
        C(8)   81468(5)   19279(18)   82833(7)   264(3)
        C(9)   76983(5)   19773(17)   82696(6)   234(3)
        C(10)   65974(5)   9920(17)   87045(6)   237(3)
        C(11)   65409(5)   1482(18)   92668(6)   250(3)
        O(11)   67927(4)   1750(16)   96641(5)   352(3)
        O(12)   61518(3)   -6127(13)   92953(5)   285(2)
        C(13)   60601(5)   -14230(20)   98454(7)   313(3)
        C(14)   55963(6)   -19590(20)   98375(9)   423(4)
        C(15)   61805(5)   13517(18)   83909(6)   252(3)
        O(15)   59297(4)   24451(14)   85294(5)   342(3)
        O(16)   61132(3)   2457(13)   79668(5)   289(2)
        C(17)   56946(5)   3510(20)   76845(7)   346(4)
        C(18)   56919(7)   -9820(30)   72283(11)   637(7)

C(21)	73185(5)	44041(17)	70335(6)	243(3)
N(22)	68759(4)	44642(15)	70051(5)	260(3)
C(23)	67326(5)	53570(17)	65246(6)	261(3)
C(24)	71273(5)	59473(17)	62245(6)	261(3)
C(25)	71933(6)	68635(18)	57185(6)	289(3)
C(26)	76176(6)	71488(19)	55481(6)	317(4)
C(27)	79691(6)	65613(19)	58672(7)	325(4)
C(28)	79060(5)	56532(19)	63724(7)	295(3)
C(29)	74826(5)	53587(17)	65391(6)	258(3)
C(30)	63128(5)	55426(18)	63713(6)	286(3)
C(31)	59593(6)	47790(20)	67034(7)	345(4)
O(31)	60005(4)	39586(18)	71388(6)	468(3)
O(32)	55733(4)	51249(17)	64593(5)	397(3)
C(33)	51935(7)	44270(30)	67415(10)	570(6)
C(34)	48131(6)	54300(30)	65588(10)	515(5)
C(35)	61873(5)	65861(19)	58581(6)	278(3)
O(35)	61678(4)	81002(14)	58571(5)	360(3)
O(36)	60994(3)	56008(13)	54028(4)	274(2)
C(37)	59477(5)	64820(20)	48889(7)	288(3)
C(38)	54793(6)	69770(20)	49427(8)	371(4)

_____

Table 2. Molecular dimensions. Bond lengths are in Ångstroms,
angles in degrees. E.s.ds are in parentheses.

_____
____

N(1)-C(1)	1.3694(18)	N(1)-C(21)	1.2991(19)
C(1)-N(2)	1.3161(19)	C(21)-N(22)	1.367(2)
C(1)-C(9)	1.465(2)	C(21)-C(29)	1.464(2)
N(2)-C(3)	1.4155(18)	N(22)-C(23)	1.3920(18)
C(3)-C(10)	1.354(2)	C(23)-C(30)	1.350(2)
C(3)-C(4)	1.491(2)	C(23)-C(24)	1.478(2)
C(4)-C(5)	1.392(2)	C(24)-C(25)	1.395(2)
C(4)-C(9)	1.399(2)	C(24)-C(29)	1.396(2)
C(5)-C(6)	1.392(2)	C(25)-C(26)	1.385(2)
C(6)-C(7)	1.390(2)	C(26)-C(27)	1.392(2)
C(7)-C(8)	1.392(2)	C(27)-C(28)	1.389(2)
C(8)-C(9)	1.384(2)	C(28)-C(29)	1.381(2)
C(10)-C(11)	1.476(2)	C(30)-C(31)	1.465(2)
C(10)-C(15)	1.504(2)	C(30)-C(35)	1.500(2)
C(11)-O(11)	1.2054(19)	C(31)-O(31)	1.208(2)
C(11)-O(12)	1.3436(18)	C(31)-O(32)	1.346(2)
O(12)-C(13)	1.4562(18)	O(32)-C(33)	1.451(2)
C(13)-C(14)	1.492(2)	C(33)-C(34)	1.478(3)
C(15)-O(15)	1.2043(18)	C(35)-O(35)	1.1999(19)
C(15)-O(16)	1.3334(18)	C(35)-O(36)	1.3408(18)
O(16)-C(17)	1.4496(19)	O(36)-C(37)	1.4587(17)
C(17)-C(18)	1.495(3)	C(37)-C(38)	1.501(2)
C(21)-N(1)-C(1)	121.10(13)	C(5)-C(4)-C(3)	135.96(14)
N(2)-C(1)-N(1)	128.17(13)	C(9)-C(4)-C(3)	104.84(12)
N(2)-C(1)-C(9)	112.93(12)	C(6)-C(5)-C(4)	118.14(14)
N(1)-C(1)-C(9)	118.90(13)	C(7)-C(6)-C(5)	122.04(14)
C(1)-N(2)-C(3)	106.56(12)	C(6)-C(7)-C(8)	120.29(15)
C(10)-C(3)-N(2)	118.97(13)	C(9)-C(8)-C(7)	117.37(14)
C(10)-C(3)-C(4)	131.61(13)	C(8)-C(9)-C(4)	123.04(14)
N(2)-C(3)-C(4)	109.40(12)	C(8)-C(9)-C(1)	130.71(14)
C(5)-C(4)-C(9)	119.12(14)	C(4)-C(9)-C(1)	106.23(13)

C(3)-C(10)-C(11)	124.53(13)	C(25)-C(24)-C(23)	132.94(15)
C(3)-C(10)-C(15)	121.05(13)	C(29)-C(24)-C(23)	107.09(13)
C(11)-C(10)-C(15)	114.36(13)	C(26)-C(25)-C(24)	117.57(15)
O(11)-C(11)-O(12)	123.02(14)	C(25)-C(26)-C(27)	121.91(14)
O(11)-C(11)-C(10)	126.31(14)	C(28)-C(27)-C(26)	120.85(16)
O(12)-C(11)-C(10)	110.59(12)	C(29)-C(28)-C(27)	117.14(15)
C(11)-O(12)-C(13)	114.44(12)	C(28)-C(29)-C(24)	122.58(14)
O(12)-C(13)-C(14)	107.49(14)	C(28)-C(29)-C(21)	129.28(15)
O(15)-C(15)-O(16)	124.66(14)	C(24)-C(29)-C(21)	108.12(14)
O(15)-C(15)-C(10)	123.75(14)	C(23)-C(30)-C(31)	121.97(14)
O(16)-C(15)-C(10)	111.47(12)	C(23)-C(30)-C(35)	121.09(14)
C(15)-O(16)-C(17)	115.76(12)	C(31)-C(30)-C(35)	116.92(14)
O(16)-C(17)-C(18)	106.54(14)	O(31)-C(31)-O(32)	123.67(16)
		O(31)-C(31)-C(30)	125.70(16)
N(1)-C(21)-N(22)	129.99(13)	O(32)-C(31)-C(30)	110.63(13)
N(1)-C(21)-C(29)	123.20(14)	C(31)-O(32)-C(33)	116.49(14)
N(22)-C(21)-C(29)	106.80(13)	O(32)-C(33)-C(34)	107.83(16)
C(21)-N(22)-C(23)	111.91(12)	O(35)-C(35)-O(36)	124.70(14)
C(30)-C(23)-N(22)	124.78(14)	O(35)-C(35)-C(30)	124.36(14)
C(30)-C(23)-C(24)	129.09(14)	O(36)-C(35)-C(30)	110.94(12)
N(22)-C(23)-C(24)	106.07(13)	C(35)-O(36)-C(37)	115.53(11)
C(25)-C(24)-C(29)	119.94(15)	O(36)-C(37)-C(38)	111.42(13)

_____

Table 3.   Anisotropic displacement parameters (Å^2 x 10^4) for the
           expression:
               exp {-2π^2(h^{2}a*^{2}U$_{11}$ + ... + 2hka*b*U$_{12}$)}
           E.s.ds are in parentheses.

	U$_{11}$	U$_{22}$	U$_{33}$	U$_{23}$	U$_{13}$	U$_{12}$
N(1)	421(7)	145(6)	197(6)	-19(5)	7(5)	-5(5)
C(1)	380(8)	118(6)	194(7)	-36(5)	-3(6)	4(5)
N(2)	395(7)	135(5)	188(6)	-8(4)	-18(5)	16(5)
C(3)	380(8)	104(6)	186(7)	-24(5)	-27(6)	19(5)
C(4)	357(8)	118(6)	211(7)	-46(5)	-18(6)	4(5)
C(5)	402(8)	138(7)	217(7)	-12(5)	-22(6)	10(6)
C(6)	393(8)	185(7)	269(8)	-24(6)	-76(6)	25(6)
C(7)	343(8)	220(7)	309(8)	-48(6)	-45(6)	8(6)
C(8)	369(8)	160(7)	264(7)	-47(6)	3(6)	-19(6)
C(9)	390(8)	107(6)	204(7)	-40(5)	-15(6)	3(5)
C(10)	369(8)	137(6)	205(7)	-23(5)	-20(6)	30(6)
C(11)	320(7)	185(7)	244(7)	-8(6)	18(6)	25(6)
O(11)	381(6)	456(7)	220(5)	58(5)	-24(5)	-7(5)
O(12)	382(6)	228(5)	245(5)	32(4)	5(4)	0(4)
C(13)	407(9)	252(8)	280(8)	48(6)	29(6)	-27(6)
C(14)	446(10)	342(9)	480(11)	75(8)	30(8)	-71(8)
C(15)	370(8)	170(7)	216(7)	17(5)	11(6)	3(6)
O(15)	440(6)	277(6)	310(6)	-23(5)	-30(5)	116(5)
O(16)	349(6)	235(5)	282(6)	-44(4)	-44(4)	4(4)
C(17)	343(8)	326(9)	368(9)	0(7)	-67(7)	-37(7)
C(18)	518(12)	790(16)	602(14)	-329(13)	-179(10)	-20(11)

C(21)	423(8)	125(6)	182(7)	-47(5)	14(6)	-4(6)
N(22)	428(7)	173(6)	181(6)	17(5)	11(5)	0(5)
C(23)	467(9)	137(6)	179(7)	-11(5)	14(6)	9(6)
C(24)	464(9)	123(6)	195(7)	-31(5)	33(6)	-2(6)
C(25)	526(9)	155(7)	185(7)	-14(5)	11(6)	7(6)
C(26)	586(10)	179(7)	188(7)	-29(6)	80(7)	-32(7)
C(27)	500(10)	209(7)	268(8)	-52(6)	90(7)	-42(7)
C(28)	462(9)	186(7)	237(7)	-50(6)	35(6)	-9(6)
C(29)	460(8)	137(7)	177(6)	-42(5)	19(6)	-4(6)
C(30)	475(9)	182(7)	200(7)	28(6)	18(6)	0(6)
C(31)	464(9)	303(8)	268(8)	74(7)	-15(7)	-17(7)
O(31)	527(8)	526(8)	351(7)	234(6)	-24(6)	-92(6)
O(32)	422(7)	442(7)	328(6)	144(5)	34(5)	-22(5)
C(33)	497(11)	714(15)	498(12)	280(11)	71(9)	-79(10)
C(34)	421(10)	527(12)	597(13)	130(10)	-77(9)	-139(9)
C(35)	390(8)	219(8)	225(7)	20(6)	23(6)	7(6)
O(35)	591(8)	199(6)	289(6)	26(4)	-27(5)	13(5)
O(36)	403(6)	207(5)	211(5)	18(4)	-5(4)	24(4)
C(37)	374(8)	277(8)	214(7)	45(6)	-8(6)	17(6)
C(38)	388(9)	344(9)	382(9)	9(7)	-24(7)	34(7)

Table 4. Hydrogen coordinates (x 10^4) and isotropic displacement parameters ($Å^2$ x 10^3). All hydrogen atoms were included in idealised positions with U(iso)'s set at 1.2*U(eq) or, for the methyl group hydrogen atoms, 1.5*U(eq) of the parent carbon atoms.

	x	y	z	U(iso)
H(5)	7466	-252	9416	30
H(6)	8224	-353	9450	34
H(7)	8647	956	8752	35
H(8)	8316	2485	7999	32
H(13A)	6112	-622	10166	38
H(13B)	6251	-2416	9900	38
H(14A)	5524	-2511	10203	63
H(14B)	5411	-966	9785	63
H(14C)	5549	-2753	9519	63
H(17A)	5654	1482	7511	41
H(17B)	5458	151	7965	41
H(18A)	5413	-959	7025	96
H(18B)	5928	-769	6954	96
H(18C)	5733	-2093	7407	96
H(22)	6702	3995	7260	49(6)
H(25)	6956	7277	5499	35
H(26)	7670	7763	5203	38
H(27)	8256	6784	5738	39
H(28)	8144	5252	6594	35
H(33A)	5228	4485	7165	68
H(33B)	5155	3228	6630	68
H(34A)	4551	4983	6744	77
H(34B)	4854	6612	6672	77
H(34C)	4781	5360	6139	77
H(37A)	5984	5740	4549	35

H(37B)	6126	7507	4828	35
H(38A)	5387	7565	4592	56
H(38B)	5302	5962	4996	56
H(38C)	5443	7728	5275	56

Table 5. Torsion angles, in degrees. E.s.ds are in parentheses.

C(21)-N(1)-C(1)-N(2)	2.3(2)
C(21)-N(1)-C(1)-C(9)	-178.04(12)
N(1)-C(1)-N(2)-C(3)	-178.51(13)
C(9)-C(1)-N(2)-C(3)	1.81(15)
C(1)-N(2)-C(3)-C(10)	-179.70(12)
C(1)-N(2)-C(3)-C(4)	-1.01(15)
C(10)-C(3)-C(4)-C(5)	1.7(3)
N(2)-C(3)-C(4)-C(5)	-176.74(15)
C(10)-C(3)-C(4)-C(9)	178.30(14)
N(2)-C(3)-C(4)-C(9)	-0.17(14)
C(9)-C(4)-C(5)-C(6)	0.0(2)
C(3)-C(4)-C(5)-C(6)	176.17(15)
C(4)-C(5)-C(6)-C(7)	-0.3(2)
C(5)-C(6)-C(7)-C(8)	0.7(2)
C(6)-C(7)-C(8)-C(9)	-0.7(2)
C(7)-C(8)-C(9)-C(4)	0.4(2)
C(7)-C(8)-C(9)-C(1)	-177.64(14)
C(5)-C(4)-C(9)-C(8)	0.0(2)
C(3)-C(4)-C(9)-C(8)	-177.32(12)
C(5)-C(4)-C(9)-C(1)	178.43(12)
C(3)-C(4)-C(9)-C(1)	1.16(14)
N(2)-C(1)-C(9)-C(8)	176.36(14)
N(1)-C(1)-C(9)-C(8)	-3.3(2)
N(2)-C(1)-C(9)-C(4)	-1.95(16)
N(1)-C(1)-C(9)-C(4)	178.34(12)
N(2)-C(3)-C(10)-C(11)	-173.36(12)
C(4)-C(3)-C(10)-C(11)	8.3(2)
N(2)-C(3)-C(10)-C(15)	3.6(2)
C(4)-C(3)-C(10)-C(15)	-174.72(13)
C(3)-C(10)-C(11)-O(11)	20.8(2)
C(15)-C(10)-C(11)-O(11)	-156.41(15)
C(3)-C(10)-C(11)-O(12)	-162.39(13)
C(15)-C(10)-C(11)-O(12)	20.45(17)
O(11)-C(11)-O(12)-C(13)	-0.6(2)
C(10)-C(11)-O(12)-C(13)	-177.63(12)
C(11)-O(12)-C(13)-C(14)	171.24(13)
C(3)-C(10)-C(15)-O(15)	-103.82(18)
C(11)-C(10)-C(15)-O(15)	73.45(18)
C(3)-C(10)-C(15)-O(16)	80.04(16)
C(11)-C(10)-C(15)-O(16)	-102.68(14)
O(15)-C(15)-O(16)-C(17)	-3.5(2)
C(10)-C(15)-O(16)-C(17)	172.56(12)
C(15)-O(16)-C(17)-C(18)	179.73(16)
C(1)-N(1)-C(21)-N(22)	0.2(2)
C(1)-N(1)-C(21)-C(29)	-178.59(12)
N(1)-C(21)-N(22)-C(23)	-177.86(14)
C(29)-C(21)-N(22)-C(23)	1.12(15)
C(21)-N(22)-C(23)-C(30)	176.35(14)
C(21)-N(22)-C(23)-C(24)	-1.10(15)
C(30)-C(23)-C(24)-C(25)	1.3(3)

N(22)-C(23)-C(24)-C(25)	178.55(15)
C(30)-C(23)-C(24)-C(29)	-176.68(15)
N(22)-C(23)-C(24)-C(29)	0.62(15)
C(29)-C(24)-C(25)-C(26)	0.1(2)
C(23)-C(24)-C(25)-C(26)	-177.60(15)
C(24)-C(25)-C(26)-C(27)	-0.4(2)
C(25)-C(26)-C(27)-C(28)	0.2(2)
C(26)-C(27)-C(28)-C(29)	0.3(2)
C(27)-C(28)-C(29)-C(24)	-0.6(2)
C(27)-C(28)-C(29)-C(21)	177.71(13)
C(25)-C(24)-C(29)-C(28)	0.4(2)
C(23)-C(24)-C(29)-C(28)	178.65(13)
C(25)-C(24)-C(29)-C(21)	-178.22(12)
C(23)-C(24)-C(29)-C(21)	0.03(15)
N(1)-C(21)-C(29)-C(28)	-0.1(2)
N(22)-C(21)-C(29)-C(28)	-179.19(14)
N(1)-C(21)-C(29)-C(24)	178.39(13)
N(22)-C(21)-C(29)-C(24)	-0.69(15)
N(22)-C(23)-C(30)-C(31)	-0.8(2)
C(24)-C(23)-C(30)-C(31)	176.04(14)
N(22)-C(23)-C(30)-C(35)	177.57(13)
C(24)-C(23)-C(30)-C(35)	-5.6(2)
C(23)-C(30)-C(31)-O(31)	1.4(3)
C(35)-C(30)-C(31)-O(31)	-177.07(17)
C(23)-C(30)-C(31)-O(32)	-179.09(14)
C(35)-C(30)-C(31)-O(32)	2.5(2)
O(31)-C(31)-O(32)-C(33)	-1.1(3)
C(30)-C(31)-O(32)-C(33)	179.33(16)
C(31)-O(32)-C(33)-C(34)	158.85(17)
C(23)-C(30)-C(35)-O(35)	-79.1(2)
C(31)-C(30)-C(35)-O(35)	99.4(2)
C(23)-C(30)-C(35)-O(36)	101.06(17)
C(31)-C(30)-C(35)-O(36)	-80.49(17)
O(35)-C(35)-O(36)-C(37)	-3.5(2)

C(30)-C(35)-O(36)-C(37)	176.39(12)
C(35)-O(36)-C(37)-C(38)	-77.59(17)

Table 6.   Hydrogen bonds, in Ångstroms and degrees.

_____
_____

D-H...A	d(D-H)	d(H...A)	d(D...A)	<(DHA)
C(13)-H(13A)...O(35)#1	0.99	2.57	3.541(2)	168.0
C(17)-H(17A)...O(31)	0.99	2.39	3.263(2)	146.2
N(22)-H(22)...N(2)	0.88	2.24	2.7740(17)	119.0
N(22)-H(22)...O(31)	0.88	2.18	2.7455(19)	121.5
C(34)-H(34A)...O(15)#2	0.98	2.58	3.296(2)	130.4

_____
_____

Symmetry transformations used to generate equivalent atoms:
#1 : x, 1-y, z+½   #2 : 1-x, y, 1½-z

Crystal structure analysis of an isoindoline dimer (40)

Crystal data: $C_{30}H_{29}N3O8$, M = 559.56. Orthorhombic, space group Pbcn (no. 60), a = 30.827(2), b = 7.91493(9), c = 23.2060(2) Å, V = 5662.0(4) Å^3. Z = 8, Dc = 1.313 g cm^{-3}, F(000) = 2352, T = 121(30) K, μ(Cu-Kα) = 8.0 cm^{-1}, λ(Cu-Kα) = 1.54184 Å.

The crystal was an orange rod. From a sample under oil, one, *ca* 0.02 x 0.06 x 0.32 mm, was mounted on a small loop and fixed in the cold nitrogen stream on a Rigaku Oxford Diffraction XtaLAB Synergy diffractometer, equipped with Cu-Kα radiation, HyPix detector and mirror monochromator. Intensity data were measured by thin-slice ω-scans. Total no. of reflections recorded, to θ_{max} = 72.5°, was 152327 of which 5619 were unique (Rint = 0.082); 5113 were 'observed' with I > 2σ_I.

Data were processed using the CrysAlisPro-CCD and -RED (1) programs. The structure was determined by the intrinsic phasing routines in the SHELXT program (2A) and refined by full-matrix least-squares methods, on F^2's, in SHELXL (2B). The non-hydrogen atoms were refined with anisotropic thermal parameters. The hydrogen atom on N(22) was located in a difference map and was refined freely. The remaining hydrogen atoms were included in idealised positions and their Uiso values were set to ride on the Ueq values of the parent carbon atoms. At the conclusion of the refinement, wR$_2$ = 0.112 and R$_1$ = 0.048 (2B) for all 5619 reflections weighted w = [$\sigma^2(F_o^2)$ + (0.0484 P)^2 + 3.815 P]$^{-1}$ with P = (F$_o^2$ + 2F$_c^2$)/3; for the 'observed' data only, R$_1$ = 0.044.

In the final difference map, the highest peak (*ca* 0.35 eÅ^{-3}) was near H(18b).

Scattering factors for neutral atoms were taken from reference (3). Computer programs used in this analysis have been noted above, and were run through WinGX (4) on a Dell Optiplex 780 PC at the University of East Anglia.

References

(1) Programs CrysAlisPro, Rigaku Oxford Diffraction Ltd., Abingdon, UK (2018).

(2) G. M. Sheldrick, Programs for crystal structure determination (SHELXT), *Acta Cryst.* (2015) A**71**, 3-8, and refinement (SHELXL), *Acta Cryst.* (2008) A**64**, 112-122 and (2015) C**71**, 3-8.

(3) 'International Tables for X-ray Crystallography', Kluwer Academic Publishers, Dordrecht (1992). Vol. C, pp. 500, 219 and 193.

(4) L. J. Farrugia, *J. Appl. Cryst.* (2012) **45**, 849–854.

Legends for Figures

Figure 1.   View of a molecule of the isoindoline dimer, indicating the atom numbering scheme. Thermal ellipsoids are drawn at the 50% probability level.

Figure 2.   View down the *a* axis, showing the stacking of molecules parallel to the *b* axis (which is horizontal across the page).

Notes on the structure

There are three N atoms in the molecule which might form NH groups. Each was refined as an –NH group in a fixed trigonal planar arrangement with only the isotropic thermal parameter free to refine; the results show that this arrangement was found acceptable only around the N(22) atom; the H(22)'s Uiso value here refined well whereas those for the N(1)-H and N(2)-H groups indicated that there were no H atoms bound in those sites.

The H(22) atom was found to form good intramolecular hydrogen bonds with N(2) and O(31), Figure 1. There are further, 'weak hydrogen bonds', e.g. C(5)-H(5)…O(11), C(17)-H(17A)…O(31) and C(33)-H(33a)…O(31), which support the planar conformation.

The two isoindoline groups are essentially coplanar through the central nitrogen atom, N(1). There are small angles of rotation about the C(3)-C(10) and C(23)-C(30) bonds, viz 5.80(9) and 3.18(11) ° respectively. There is more variation in the torsion angles of the carboxylate groups, as C(11)-O(12)-C(13)-C(14), C(15)-O(16)-C(17)-C(18), C(31)-O(32)-C(33)-C(34) and C(35)-O(36)-C(37)-C(38) where the angles are 171.2, 179.7, 158.9 and -77.6°, respectively; all these C-C-O-C-C chains are all-*trans* except in the last case.

The aromatic planar sections of the bis-isoindoline molecules are overlaid by parallel molecules related by a glide plane normal to the *a* axis with a shift parallel to the *b* axis, resulting in the stacking of molecules, 3.28 Å apart, in columns along the *b* axis, Figure 2. Contacts between the columns are at van der Waals' distances.

Crystal data and structure refinement for $(EtOCO)_2C-C_8H_4NH-N-C_8H_4N-CO-C_6H_4-C_5H_{11}$ (47)

_____

    Identification code   IsabF1045

    Elemental formula   C35 H35 N3 O5

    Formula weight   577.66

    Crystal system, space group   Monoclinic, P2$_1$/c (no. 14)

    Unit cell dimensions   a = 7.64750(10) Å α = 90 °
                                   b = 15.7892(3) Å β = 95.263(2) °

                                   c = 24.3771(4) Å γ = 90 °

    Volume   2931.07(8) Å^3

    Z, Calculated density   4,   1.309 Mg/m^3

    F(000)   1224

    Absorption coefficient   0.711 mm^{-1}

    Temperature   100.01(10) K

    Wavelength   1.54184 Å

    Crystal colour, shape   ? ?

    Crystal size   ? x ? x ? mm

    Crystal mounting: on a small loop, in oil, fixed in cold N$_2$ stream

    On the diffractometer:

      Theta range for data collection   7.677 to 72.494 °

      Limiting indices   -9<=h<=6, -18<=k<=18, -30<=l<=29

      Completeness to theta = 67.684   99.6 %

    Absorption correction   Semi-empirical from equivalents

    Max. and min. transmission   1.00000 and 0.31070

    Reflections collected (not including absences) 22790

    No. of unique reflections   5644 [R(int) for equivalents = 0.055]

    No. of 'observed' reflections (I > 2σ_I)   4861

    Structure determined by: dual methods, in SHELXT

         Refinement: Full-matrix least-squares on F^2, in
SHELXL

         Data / restraints / parameters   5644 / 0 / 388

         Goodness-of-fit on F^2 1.038

         Final R indices ('observed' data) R_1 = 0.047, wR_2 = 0.123

         Final R indices (all data) R_1 = 0.054, wR_2 = 0.127

         Reflections weighted:
           $w = [\sigma^2(Fo^2)+(0.0739P)^2+0.7810P]^{-1}$ where $P=(Fo^2+2Fc^2)/3$

         Extinction coefficient   n/a

       Largest diff. peak and hole   0.31 and -0.25 e.Å^{-3}

       Location of largest difference peak   near C(18)

Table 1. Atomic coordinates (x 10^5) and equivalent isotropic
          displacement parameters (Å^2 x 10^4). U(eq) is defined
          as one third of the trace of the orthogonalized Uij
          tensor. E.s.ds are in parentheses.

---

	x	y	z	U(eq)
N(1)	82996(15)	54193(8)	71329(5)	243(3)
C(2)	90162(18)	46585(9)	73614(6)	245(3)
C(3)	91399(18)	47175(10)	79671(6)	245(3)
C(4)	97034(19)	41648(10)	83915(6)	276(3)
C(5)	95780(20)	44266(11)	89321(6)	302(3)
C(6)	88990(20)	52228(10)	90479(6)	284(3)
C(7)	83520(19)	57795(10)	86266(6)	256(3)
C(8)	84968(18)	55134(10)	80873(6)	241(3)
C(9)	80123(18)	59138(9)	75529(6)	234(3)
N(10)	73711(16)	67280(8)	75381(5)	248(3)
N(11)	69197(16)	68513(8)	65415(5)	242(3)
C(12)	69203(17)	71209(10)	70786(6)	239(3)
C(13)	63362(18)	80002(10)	70540(6)	255(3)
C(14)	61060(20)	85564(11)	74804(6)	303(3)
C(15)	56160(20)	93774(11)	73447(7)	332(4)
C(16)	53570(20)	96301(11)	67950(7)	320(3)
C(17)	55498(19)	90657(10)	63677(6)	284(3)
C(18)	60451(18)	82415(10)	65011(6)	247(3)
C(20)	63926(18)	74903(9)	61675(6)	240(3)
C(21)	62208(18)	74094(10)	56111(6)	253(3)
C(22)	64511(19)	65926(10)	53413(6)	264(3)
O(22)	69004(15)	59400(7)	55768(4)	319(3)
O(23)	60382(14)	66490(7)	47980(4)	299(3)
C(24)	60830(20)	58663(11)	44875(6)	351(4)
C(25)	56050(30)	60790(14)	38956(7)	462(5)
C(26)	56832(19)	81566(10)	52530(6)	267(3)
O(26)	66895(14)	86685(7)	50929(5)	345(3)
O(27)	39434(14)	81746(7)	51460(4)	304(3)
C(28)	32110(20)	88560(12)	47927(7)	352(4)
C(29)	34900(20)	87049(13)	41989(7)	392(4)
C(30)	95243(18)	39706(10)	70822(6)	255(3)

C(31)	95042(18)	37927(10)	64976(6)	252(3)
C(32)	101138(19)	29988(10)	63372(6)	274(3)
C(33)	101036(19)	27792(10)	57891(6)	281(3)
C(34)	94556(19)	33428(10)	53810(6)	254(3)
C(35)	88590(20)	41381(10)	55277(6)	274(3)
C(36)	88957(19)	43573(10)	60812(6)	269(3)
O(37)	94790(14)	30588(7)	48548(4)	283(2)
C(38)	86010(20)	35522(10)	44178(6)	268(3)
C(39)	86208(19)	30312(10)	38996(6)	263(3)
C(40)	78940(20)	34978(10)	33804(6)	273(3)
C(41)	80610(20)	29681(11)	28653(6)	292(3)
C(42)	73600(20)	34027(12)	23325(7)	364(4)

Table 2.   Molecular dimensions.   Bond lengths are in Ångstroms,
angles in degrees.   E.s.ds are in parentheses.

N(1)-C(9)
1.3218(19)

N(1)-C(2)
1.4134(19)

C(2)-C(30)
1.357(2)

C(2)-C(3)
1.474(2)

C(3)-C(8)
1.390(2)

C(3)-C(4)
1.391(2)

C(4)-C(5)
1.393(2)

C(5)-C(6)
1.399(2)

C(6)-C(7)
1.387(2)

C(7)-C(8)
1.394(2)

C(8)-C(9)
1.465(2)

C(9)-N(10)
1.375(2)

N(10)-C(12)
1.2990(19)

N(11)-C(12)
1.3768(18)

N(11)-C(20)
1.3943(19)

C(12)-C(13)
1.458(2)

C(13)-C(14)
1.384(2)

C(13)-C(18)
1.399(2)

C(14)-C(15)
1.381(2)

C(15)-C(16)
1.395(2)

C(16)-C(17)
1.389(2)

C(17)-C(18)
1.386(2)

C(18)-C(20)
1.476(2)

C(20)-C(21)
1.357(2)

C(21)-C(22)
1.466(2)

C(21)-C(26)
1.502(2)

C(22)-O(22)
1.2138(19)

C(22)-O(23)
1.3361(18)

O(23)-C(24)
1.451(2)

C(24)-C(25)
1.494(2)

C(26)-O(26)
1.2055(19)

C(26)-O(27)
1.3324(18)

O(27)-C(28)
1.4577(19)

C(28)-C(29)
1.502(2)

C(30)-C(31)
1.451(2)

C(31)-C(36)
1.398(2)

C(31)-C(32)
1.405(2)

C(32)-C(33)
1.380(2)

C(33)-C(34)
1.392(2)

C(34)-O(37)
1.3605(17)

C(34)-C(35)
1.394(2)

C(35)-C(36)
1.391(2)

O(37)-C(38)
1.4359(18)

C(38)-C(39)
1.509(2)

C(39)-C(40)	1.524(2)	C(41)-C(42)	1.522(2)
C(40)-C(41)	1.524(2)		

C(9)-N(1)-C(2)	106.42(12)	C(18)-C(17)-C(16)	118.17(14)
C(30)-C(2)-N(1)	126.94(13)	C(17)-C(18)-C(13)	119.87(14)
C(30)-C(2)-C(3)	123.91(13)	C(17)-C(18)-C(20)	133.20(13)
N(1)-C(2)-C(3)	109.15(12)	C(13)-C(18)-C(20)	106.93(13)
C(8)-C(3)-C(4)	120.10(14)	C(21)-C(20)-N(11)	125.53(14)
C(8)-C(3)-C(2)	106.07(12)	C(21)-C(20)-C(18)	128.37(14)
C(4)-C(3)-C(2)	133.82(14)	N(11)-C(20)-C(18)	106.09(12)
C(3)-C(4)-C(5)	118.29(15)	C(20)-C(21)-C(22)	121.80(14)
C(4)-C(5)-C(6)	121.10(14)	C(20)-C(21)-C(26)	120.21(14)
C(7)-C(6)-C(5)	120.83(14)	C(22)-C(21)-C(26)	117.91(12)
C(6)-C(7)-C(8)	117.55(15)	O(22)-C(22)-O(23)	123.81(14)
C(3)-C(8)-C(7)	122.10(14)	O(22)-C(22)-C(21)	125.12(13)
C(3)-C(8)-C(9)	105.55(13)	O(23)-C(22)-C(21)	111.04(13)
C(7)-C(8)-C(9)	132.30(14)	C(22)-O(23)-C(24)	116.45(12)
N(1)-C(9)-N(10)	128.03(13)	O(23)-C(24)-C(25)	107.27(15)
N(1)-C(9)-C(8)	112.80(13)	O(26)-C(26)-O(27)	125.31(14)
N(10)-C(9)-C(8)	119.16(13)	O(26)-C(26)-C(21)	124.47(13)
C(12)-N(10)-C(9)	122.33(13)	O(27)-C(26)-C(21)	110.22(13)
C(12)-N(11)-C(20)	111.90(12)	C(26)-O(27)-C(28)	117.02(12)
N(10)-C(12)-N(11)	130.50(14)	O(27)-C(28)-C(29)	111.79(14)
N(10)-C(12)-C(13)	123.11(13)	C(2)-C(30)-C(31)	132.03(14)
N(11)-C(12)-C(13)	106.37(12)	C(36)-C(31)-C(32)	117.61(13)
C(14)-C(13)-C(18)	122.06(14)	C(36)-C(31)-C(30)	124.22(14)
C(14)-C(13)-C(12)	129.25(14)	C(32)-C(31)-C(30)	118.16(13)
C(18)-C(13)-C(12)	108.68(13)	C(33)-C(32)-C(31)	121.41(14)
C(15)-C(14)-C(13)	117.77(14)	C(32)-C(33)-C(34)	120.10(14)
C(14)-C(15)-C(16)	120.67(15)	O(37)-C(34)-C(33)	115.38(13)
C(17)-C(16)-C(15)	121.44(15)	O(37)-C(34)-C(35)	124.87(14)

C(33)-C(34)-C(35) 119.75(14)		O(37)-C(38)-C(39) 106.59(12)
C(36)-C(35)-C(34) 119.68(14)		C(38)-C(39)-C(40) 113.62(13)
C(35)-C(36)-C(31) 121.43(14)		C(41)-C(40)-C(39) 111.54(13)
C(34)-O(37)-C(38) 118.36(12)		C(42)-C(41)-C(40) 113.96(14)

Table 3.   Anisotropic displacement parameters ($Å^2$ x 10^4) for the expression:

$$\exp\{-2\pi^2(h^2a*^2U_{11} + ... + 2hka*b*U_{12})\}$$

E.s.ds are in parentheses.

	U_{11}	U_{22}	U_{33}	U_{23}	U_{13}	U_{12}
N(1)	238(6)	286(7)	205(6)	4(5)	20(5)	-14(5)
C(2)	220(6)	301(8)	212(7)	21(6)	16(5)	-23(5)
C(3)	207(6)	315(8)	211(7)	4(6)	13(5)	-41(5)
C(4)	271(7)	319(8)	235(7)	15(6)	7(6)	5(6)
C(5)	308(8)	369(9)	220(7)	52(6)	-22(6)	-12(6)
C(6)	305(7)	357(9)	187(7)	-15(6)	4(6)	-58(6)
C(7)	257(7)	295(8)	215(7)	-14(6)	10(6)	-52(6)
C(8)	216(6)	294(8)	210(7)	8(6)	4(5)	-47(5)
C(9)	212(6)	284(8)	205(7)	1(6)	14(5)	-33(5)
N(10)	248(6)	294(7)	199(6)	15(5)	15(5)	-3(5)
N(11)	265(6)	268(7)	190(6)	5(5)	13(5)	-3(5)
C(12)	195(6)	307(8)	214(7)	-6(6)	20(5)	-22(5)
C(13)	197(6)	330(8)	232(7)	13(6)	-5(5)	0(5)
C(14)	307(7)	382(9)	217(7)	-5(6)	10(6)	68(6)
C(15)	336(8)	384(9)	274(8)	-40(7)	18(6)	93(7)
C(16)	280(7)	351(9)	324(8)	7(7)	2(6)	73(6)
C(17)	252(7)	347(8)	247(7)	29(6)	0(6)	24(6)
C(18)	196(6)	325(8)	218(7)	6(6)	7(5)	-16(5)
C(20)	202(6)	296(8)	219(7)	27(6)	5(5)	-26(5)
C(21)	227(7)	313(8)	214(7)	22(6)	1(5)	-18(5)
C(22)	249(7)	342(8)	198(7)	25(6)	9(5)	-25(6)
O(22)	416(6)	309(6)	225(5)	5(4)	1(4)	6(5)

O(23)	345(6)	366(6)	183(5)	−6(4)	1(4)	−18(4)
C(24)	392(9)	421(10)	241(8)	−71(7)	30(6)	−58(7)
C(25)	499(10)	672(13)	219(8)	−56(8)	44(7)	−220(9)
C(26)	286(7)	325(8)	185(7)	−10(6)	−4(6)	−15(6)
O(26)	330(6)	377(7)	318(6)	86(5)	−17(5)	−71(5)
O(27)	273(5)	391(6)	245(5)	64(4)	1(4)	13(4)
C(28)	321(8)	420(10)	306(8)	72(7)	−12(6)	73(7)
C(29)	351(8)	533(11)	285(8)	103(8)	−6(7)	8(8)
C(30)	239(7)	301(8)	223(7)	36(6)	12(5)	−13(6)
C(31)	234(7)	291(8)	233(7)	2(6)	22(5)	−23(5)
C(32)	293(7)	286(8)	240(7)	32(6)	0(6)	7(6)
C(33)	295(7)	265(8)	282(8)	−17(6)	19(6)	5(6)
C(34)	251(7)	303(8)	209(7)	−23(6)	32(5)	−33(6)
C(35)	305(7)	276(8)	239(7)	28(6)	21(6)	7(6)
C(36)	295(7)	266(8)	249(7)	−5(6)	38(6)	14(6)
O(37)	342(6)	306(6)	198(5)	−19(4)	11(4)	33(4)
C(38)	291(7)	292(8)	218(7)	−1(6)	13(6)	8(6)
C(39)	264(7)	296(8)	231(7)	−11(6)	33(6)	−11(6)
C(40)	262(7)	320(8)	239(7)	0(6)	28(6)	−17(6)
C(41)	274(7)	370(9)	232(7)	−7(6)	23(6)	−30(6)
C(42)	322(8)	523(11)	247(8)	31(7)	15(6)	−38(7)

Table 4. Hydrogen coordinates (x 10^4) and isotropic displacement parameters (Å^2 x 10^3). All hydrogen atoms were included in idealised positions with U(iso)'s set at 1.2*U(eq) or, for the methyl group hydrogen atoms, 1.5*U(eq) of the parent carbon or nitrogen atoms.

	x	y	z	U(iso)
H(4)	10152	3634	8316	33
H(5)	9952	4066	9221	36
H(6)	8814	5381	9412	34
H(7)	7905	6311	8701	31
H(11)	7210	6349	6448	29
H(14)	6277	8383	7846	36
H(15)	5456	9766	7623	40

H(16)	5050	10189	6713	38
H(17)	5352	9236	6002	34
H(24A)	5253	5462	4614	42
H(24B)	7248	5619	4535	42
H(25A)	5622	5573	3678	69
H(25B)	4450	6322	3854	69
H(25C)	6436	6478	3775	69
H(28A)	3758	9387	4912	42
H(28B)	1962	8903	4830	42
H(29A)	2992	9165	3979	59
H(29B)	4726	8669	4160	59
H(29C)	2931	8185	4078	59
H(30)	9968	3531	7308	31
H(32)	10533	2613	6606	33
H(33)	10530	2254	5692	34
H(35)	8439	4520	5257	33
H(36)	8507	4891	6176	32
H(38A)	9207	4085	4378	32
H(38B)	7403	3671	4494	32
H(39A)	7934	2522	3939	32
H(39B)	9819	2860	3857	32
H(40A)	6668	3633	3407	33
H(40B)	8527	4026	3351	33
H(41A)	9289	2831	2844	35
H(41B)	7432	2440	2899	35
H(42A)	7506	3035	2026	55
H(42B)	6136	3528	2345	55
H(42C)	7995	3919	2290	55

Table 5.   Torsion angles, in degrees.   E.s.ds are in parentheses.
_____

C(9)-N(1)-C(2)-C(30)   -179.53(14)

C(9)-N(1)-C(2)-C(3)   0.48(15)

C(30)-C(2)-C(3)-C(8)   179.91(14)

N(1)-C(2)-C(3)-C(8)   -0.10(15)

C(30)-C(2)-C(3)-C(4)   -1.3(3)

N(1)-C(2)-C(3)-C(4)   178.73(15)

C(8)-C(3)-C(4)-C(5)   1.0(2)

C(2)-C(3)-C(4)-C(5)   -177.74(15)

C(3)-C(4)-C(5)-C(6)   0.2(2)

C(4)-C(5)-C(6)-C(7)   -0.9(2)

C(5)-C(6)-C(7)-C(8)   0.3(2)

C(4)-C(3)-C(8)-C(7)   -1.5(2)

C(2)-C(3)-C(8)-C(7)   177.49(13)

C(4)-C(3)-C(8)-C(9)   -179.31(13)

C(2)-C(3)-C(8)-C(9)   -0.28(15)

C(6)-C(7)-C(8)-C(3)   0.9(2)

C(6)-C(7)-C(8)-C(9)   177.97(14)

C(2)-N(1)-C(9)-N(10)   -177.99(13)

C(2)-N(1)-C(9)-C(8)   -0.68(16)

C(3)-C(8)-C(9)-N(1)   0.63(16)

C(7)-C(8)-C(9)-N(1)   -176.82(15)

C(3)-C(8)-C(9)-N(10)   -178.17(12)

C(7)-C(8)-C(9)-N(10)   4.4(2)

N(1)-C(9)-N(10)-C(12)   1.3(2)

C(8)-C(9)-N(10)-C(12)   179.86(13)

C(9)-N(10)-C(12)-N(11)   1.7(2)

C(9)-N(10)-C(12)-C(13)   -176.27(13)

C(20)-N(11)-C(12)-N(10)   -177.75(14)

_____

C(20)-N(11)-C(12)-C(13)
0.48(15)

N(10)-C(12)-C(13)-C(14)   -
1.8(2)

N(11)-C(12)-C(13)-C(14)
179.77(15)

N(10)-C(12)-C(13)-C(18)
176.83(13)

N(11)-C(12)-C(13)-C(18)   -
1.56(15)

C(18)-C(13)-C(14)-C(15)   -
1.6(2)

C(12)-C(13)-C(14)-C(15)
176.91(15)

C(13)-C(14)-C(15)-C(16)
0.2(2)

C(14)-C(15)-C(16)-C(17)
1.3(2)

C(15)-C(16)-C(17)-C(18)   -
1.3(2)

C(16)-C(17)-C(18)-C(13)
0.0(2)

C(16)-C(17)-C(18)-C(20)   -
179.02(15)

C(14)-C(13)-C(18)-C(17)
1.5(2)

C(12)-C(13)-C(18)-C(17)   -
177.27(13)

C(14)-C(13)-C(18)-C(20)   -
179.24(14)

C(12)-C(13)-C(18)-C(20)
1.97(15)

C(12)-N(11)-C(20)-C(21)   -
178.30(13)

C(12)-N(11)-C(20)-C(18)
0.71(15)

C(17)-C(18)-C(20)-C(21)   -
3.6(3)

C(13)-C(18)-C(20)-C(21)
177.31(14)

C(17)-C(18)-C(20)-N(11)
177.43(15)

C(13)-C(18)-C(20)-N(11)   -
1.66(15)

N(11)-C(20)-C(21)-C(22)
5.0(2)

C(18)-C(20)-C(21)-C(22)   -
173.78(14)

N(11)-C(20)-C(21)-C(26)   -
178.46(13)

C(18)-C(20)-C(21)-C(26)
2.7(2)

C(20)-C(21)-C(22)-O(22)   -
4.3(2)

C(26)-C(21)-C(22)-O(22)
179.08(14)

C(20)-C(21)-C(22)-O(23)
173.42(13)

C(26)-C(21)-C(22)-O(23)   -
3.19(18)

O(22)-C(22)-O(23)-C(24)
2.3(2)

C(21)-C(22)-O(23)-C(24)   -
175.47(12)

C(22)-O(23)-C(24)-C(25)   -
179.29(13)

C(20)-C(21)-C(26)-O(26)
87.6(2)

C(22)-C(21)-C(26)-O(26)   -
95.77(18)

C(20)-C(21)-C(26)-O(27)   -
91.64(16)

C(22)-C(21)-C(26)-O(27)
85.02(16)

O(26)-C(26)-O(27)-C(28)
1.9(2)

C(21)-C(26)-O(27)-C(28)   -
178.85(12)

C(26)-O(27)-C(28)-C(29)
75.20(18)

N(1)-C(2)-C(30)-C(31)   -
0.1(3)

C(3)-C(2)-C(30)-C(31)
179.84(14)

C(2)-C(30)-C(31)-C(36)
0.0(3)

C(2)-C(30)-C(31)-C(32)   -
179.20(15)

C(36)-C(31)-C(32)-C(33)   -
0.4(2)

C(30)-C(31)-C(32)-C(33)
178.79(14)

C(31)-C(32)-C(33)-C(34)   -
1.0(2)

C(32)-C(33)-C(34)-O(37)   -
178.98(13)

C(32)-C(33)-C(34)-C(35)
1.6(2)

O(37)-C(34)-C(35)-C(36)
179.85(14)

C(33)-C(34)-C(35)-C(36)   -
0.8(2)

C(34)-C(35)-C(36)-C(31)   -
0.6(2)

C(32)-C(31)-C(36)-C(35)
1.3(2)

C(30)-C(31)-C(36)-C(35)   -
177.91(14)

C(33)-C(34)-O(37)-C(38)
171.06(13)

C(35)-C(34)-O(37)-C(38)   -
9.6(2)

C(34)-O(37)-C(38)-C(39)   -
172.20(12)

O(37)-C(38)-C(39)-C(40)   -
174.34(12)

C(38)-C(39)-C(40)-C(41)
176.02(12)

C(39)-C(40)-C(41)-C(42)   -
179.87(12)

_____

Table 6. Hydrogen bonds, in Ångstroms and degrees.

_____

D-H...A	d(D-H)	d(H...A)	d(D...A)
<(DHA)			
N(11)-H(11)...N(1)	0.86	2.32	2.8329(18)
118.5			
N(11)-H(11)...O(22)	0.86	2.21	2.7557(16)
121.1			

_____

Crystal structure analysis of $(EtOCO)_2C-C_8H_4NH-N-C_8H_4N-CO-C_6H_4-C_5H_{11}$ (47)

Crystal data: $C_{35}H_{35}N_3O_5$, M = 577.66. Monoclinic, space group $P2_1/c$ (no. 14), a = 7.64750(10), b = 15.7892(3), c = 24.3771(4) Å, β = 95.263(2) °, V = 2931.07(8) Å^3. Z = 4, Dc = 1.309 g cm^{-3}, F(000) = 1224, T = 100.01(10) K, μ(Cu-Kα) = 7.11 cm^{-1}, λ(Cu-Kα) = 1.54184 Å.

The crystal was a colourless shard. From a sample under oil, one, *ca* 0. x 0. x 0. mm, was mounted on a small loop and fixed in the cold nitrogen stream on a Rigaku Oxford Diffraction XtaLAB Synergy diffractometer, equipped with Cu-Kα radiation, HyPix detector and mirror monochromator. Intensity data were measured by thin-slice ω-scans. Total no. of reflections recorded, to θ_{max} = 72.5°, was 22790 of which 5644 were unique (Rint = 0.055); 4861 were 'observed' with I > $2\sigma_I$.

Data were processed using the CrysAlisPro-CCD and -RED (1) programs. The structure was determined by the intrinsic phasing routines in the SHELXT program (2A) and refined by full-matrix least-squares methods, on F^2's, in SHELXL (2B). The non-hydrogen atoms were refined with anisotropic thermal parameters. The hydrogen atom on N(11) was located in a difference map; this and all the remaining hydrogen atoms were included in idealised positions and their Uiso values were set to ride on the Ueq values of the parent carbon and nitrogen atoms. At the conclusion of the refinement, wR_2 = 0.127 and R_1 = 0.054 (2B) for all 5644 reflections weighted w = $[\sigma^2(F_o^2) + (0.0739\ P)^2 + 0.781\ P]^{-1}$ with P = $(F_o^2 + 2F_c^2)/3$; for the 'observed' data only, R_1 = 0.047.

In the final difference map, the highest peak (*ca* 0.3 eÅ^{-3}) was near C18).

Scattering factors for neutral atoms were taken from reference (3). Computer programs used in this analysis have been noted above, and were run through WinGX (4) on a Dell Optiplex 780 PC at the University of East Anglia.

References

(1) Programs CrysAlisPro, Rigaku Oxford Diffraction Ltd., Abingdon, UK (2018).

(2) G. M. Sheldrick, Programs for crystal structure determination (SHELXT), *Acta Cryst.* (2015) A**71**, 3-8, and refinement (SHELXL), *Acta Cryst.* (2008) A**64**, 112-122 and (2015) C**71**, 3-8.

(3) 'International Tables for X-ray Crystallography', Kluwer Academic Publishers, Dordrecht (1992). Vol. C, pp. 500, 219 and 193.

(4) L. J. Farrugia, *J. Appl. Cryst.* (2012) **45**, 849–854.

Legends for Figures

Figure 1.   View of the bis-isoindole molecule, indicating the atom numbering scheme. Thermal ellipsoids are drawn at the 50% probability level.

Figure 2.   View of the packing of molecules, along the *c* axis.

Figure 3.   View of the packing of molecules, along the *a* axis.

Notes on the structure

The N(11)-H(11) group of one isoindole system was established in the structure analysis and was shown to form bifurcated hydrogen bonds to N(1) and O(22) of the same molecule.

Crystal data and structure refinement for [Zn (OEt){(C$_{16}$ H$_{18}$ N$_2$)$_3$(C$_{24}$ H$_{19}$ N O)}],2EtOH (91)

_____

Identification code   isabf1046

Elemental formula   C70 H68 N7 O2 Zn, 2(C2 H6 O)

Formula weight   1204.88

Crystal system, space group   Monoclinic, P 2$_1$/c (no. 14)

Unit cell dimensions   a = 11.81403(15) Å α = 90 °
                                             b = 32.9326(4) Å   β = 103.4190(10) °

                                             c = 17.3242(2) Å   γ = 90 °

Volume   6556.23(16) Å^3

Z, Calculated density   4, 1.221 Mg/m^3

F(000)   2572

Absorption coefficient   0.941 mm^{-1}

Temperature   99.99(10) K

Wavelength   1.54184 Å

Crystal colour, shape   purple block

Crystal size   0.49 x 0.15 x 0.11 mm

Crystal mounting: on a small loop, in oil, fixed in cold N$_2$ stream

On the diffractometer:

Theta range for data collection   7.666 to 69.999 °

Limiting indices   -14<=h<=14, -38<=k<=40, -20<=l<=21

Completeness to theta = 67.684   99.4 %

Absorption correction   Semi-empirical from equivalents

Max. and min. transmission   1.00000 and 0.48207

Reflections collected (not including absences) 49477

No. of unique reflections   12191 [R(int) for equivalents = 0.051]

No. of 'observed' reflections (I > 2σ$_I$)   10680

Structure determined by: dual methods, in SHELXT

Refinement: Full-matrix least-squares on F^2, in SHELXL

Data / restraints / parameters   12191 / 0 / 816

Goodness-of-fit on F^2 1.032

Final R indices ('observed' data) $R_1 = 0.063$, $wR_2 = 0.175$

Final R indices (all data) $R_1 = 0.069$, $wR_2 = 0.180$

Reflections weighted:
   $w = [\sigma^2(Fo^2)+(0.1053P)^2+4.9425P]^{-1}$ where $P=(Fo^2+2Fc^2)/3$

Extinction coefficient   n/a

Largest diff. peak and hole   0.76 and -0.54 e.Å^{-3}

Location of largest difference peak   near C(931)

Table 1. Atomic coordinates (x 10^5) and equivalent isotropic
          displacement parameters (Å^2 x 10^4). U(eq) is defined
          as one third of the trace of the orthogonalized Uij
          tensor. E.s.ds are in parentheses.

	x	y	z	U(eq)	S.o.f.#
Zn	39358(3)	42283(2)	33547(2)	348(1)	
N(1)	34571(19)	38535(6)	41519(12)	373(5)	
C(2)	28740(20)	39703(8)	47126(15)	374(5)	
C(3)	24110(20)	36088(8)	50163(16)	404(6)	
C(4)	17370(30)	35298(9)	55661(17)	461(6)	
C(5)	14340(30)	31323(9)	57102(18)	512(7)	
C(6)	7030(30)	30760(11)	63260(20)	634(9)	
C(7)	2210(40)	26495(12)	62900(30)	829(13)	
C(8)	10330(40)	23311(13)	62070(30)	929(15)	
C(9)	15320(30)	23599(10)	54580(20)	589(8)	
C(10)	18130(30)	28025(9)	53145(19)	497(7)	
C(11)	24740(30)	28828(9)	47585(18)	466(6)	
C(12)	27670(20)	32785(8)	46177(16)	412(6)	
C(13)	34200(20)	34435(8)	40807(15)	394(5)	
N(14)	38870(20)	32023(6)	36094(13)	397(5)	
C(15)	-3260(40)	33817(14)	61900(40)	1002(17)	
C(16)	14390(40)	31744(17)	71480(20)	959(16)	
C(17)	26210(40)	20997(11)	56130(30)	756(11)	
C(18)	6270(50)	22081(13)	47420(30)	960(15)	
N(21)	46250(20)	37372(6)	29068(13)	386(5)	
C(22)	44440(20)	33405(8)	30828(15)	385(5)	
C(23)	49480(20)	30747(8)	25712(15)	393(5)	
C(24)	50450(20)	26586(8)	25052(16)	424(6)	
C(25)	55640(30)	24949(8)	19247(17)	456(6)	
C(26)	57240(30)	20334(9)	19170(20)	539(7)	
C(27)	60810(40)	18997(10)	11380(30)	708(10)	
C(28)	69140(40)	21741(10)	8890(20)	668(9)	
C(29)	64510(30)	25988(9)	7056(19)	519(7)	
C(30)	59640(20)	27607(8)	13956(17)	443(6)	
C(31)	58950(20)	31767(8)	14902(16)	422(6)	
C(32)	53990(20)	33327(8)	20776(15)	396(5)	
C(33)	52020(20)	37468(8)	23088(15)	387(5)	

N(34)	55660(20)	40692(6)	19718(12)	389(5)
C(35)	45840(30)	18127(9)	19000(20)	618(8)
C(36)	66410(40)	19121(11)	26380(30)	834(12)
C(37)	74350(30)	28740(11)	5460(20)	667(9)
C(38)	54870(30)	26093(11)	-584(19)	621(8)
N(41)	48214(18)	45777(6)	27331(12)	349(4)
C(42)	53840(20)	44501(7)	21749(14)	358(5)
C(43)	57690(20)	48015(7)	17897(15)	367(5)
C(44)	64000(20)	48396(8)	12147(15)	400(6)
C(45)	65920(20)	52252(8)	9298(15)	410(6)
C(46)	74180(30)	52587(9)	3658(16)	474(6)
C(47)	76820(30)	57064(10)	2450(20)	606(8)
C(48)	66130(40)	59643(10)	840(20)	639(9)
C(49)	60520(30)	59880(9)	7971(17)	493(7)
C(50)	60420(20)	55672(8)	11795(15)	399(6)
C(51)	54590(20)	55240(8)	17942(15)	385(5)
C(52)	53540(20)	51450(7)	21087(14)	356(5)
C(53)	48250(20)	49958(7)	27414(14)	334(5)
N(54)	44813(18)	52375(6)	32510(12)	347(4)
C(55)	85830(30)	50504(12)	7392(19)	610(8)
C(56)	68860(30)	50503(10)	-4191(17)	539(7)
C(57)	48000(30)	61355(10)	4990(20)	663(9)
C(58)	67290(30)	62868(9)	14050(19)	615(9)
N(61)	37334(18)	47208(6)	40067(12)	342(4)
C(62)	40330(20)	51039(7)	38490(14)	339(5)
C(63)	37430(20)	53798(7)	44266(14)	353(5)
C(64)	39290(20)	57961(7)	45262(16)	392(6)
C(65)	35620(30)	59819(8)	51432(17)	450(6)
C(66)	30290(30)	57566(8)	56384(17)	445(6)
C(67)	28500(20)	53429(8)	55480(15)	390(5)
C(68)	32160(20)	51466(7)	49219(14)	349(5)
C(69)	32140(20)	47252(7)	46416(14)	343(5)
C(70)	27630(20)	43805(8)	49357(14)	347(5)
C(71)	20570(20)	44483(8)	55404(14)	365(5)
C(72)	8700(20)	45203(9)	52968(16)	445(6)
C(73)	1790(20)	45689(10)	58375(16)	476(6)
C(74)	6940(20)	45437(9)	66431(16)	427(6)
C(75)	18870(20)	44803(8)	68949(15)	393(5)
O(77)	1110(16)	45804(7)	72360(11)	512(5)
C(76)	25600(20)	44297(7)	63500(15)	361(5)
C(78)	-11390(30)	45961(13)	70175(19)	597(8)
C(79)	-15480(30)	45629(12)	77785(19)	588(8)
C(80)	-12400(30)	41679(12)	82010(20)	598(8)
C(81)	-16240(40)	41433(13)	89800(20)	717(10)
C(82)	-12850(50)	37585(16)	94330(30)	991(15)
O(91)	22428(19)	42571(8)	25861(13)	609(6)
C(921)	19300(50)	42009(18)	18080(30)	622(12)
0.7				
C(922)	20460(100)	39150(40)	18650(70)	470(20)*
0.3				
C(931)	15610(70)	37600(20)	16820(50)	590(30)
0.473(15)				
C(932)	8390(90)	40470(70)	13580(60)	1780(90)
0.527(15)				
O(94)	3630(40)	8364(17)	81910(20)	1330(17)
C(95)	-7120(80)	6440(20)	78940(70)	1550(30)
C(961)	-14780(100)	7730(70)	75400(100)	1440(80)
0.5				

C(962)	-15840(150)	9850(40)	71020(90)	1460(80)
0.5				
O(97)	81120(70)	19280(30)	86770(50)	1990(40)
0.8				
C(98)	91070(120)	18730(60)	84130(110)	2260(110)
0.7				
C(99)	96480(110)	14850(40)	88590(50)	1450(40)
0.8				
C(100)	99130(190)	18330(120)	83400(200)	2010(180)
0.4				
C(101)	94400(200)	18560(70)	77990(140)	1860(100)
0.5				

\# - site occupancy, if different from 1.

* - U(iso) ($\mathring{A}^2$ x 10^4)

Table 2.   Molecular dimensions. Bond lengths are in Ångstroms,
angles in degrees. E.s.ds are in parentheses.

Zn-N(61)	2.022(2)	Zn-N(21)	2.043(2)
Zn-N(41)	2.025(2)	Zn-O(91)	2.132(2)
Zn-N(1)	2.028(2)		
N(61)-Zn-N(41)	89.08(8)	N(1)-Zn-N(21)	88.61(8)
N(61)-Zn-N(1)	91.14(8)	N(61)-Zn-O(91)	95.60(9)
N(41)-Zn-N(1)	165.47(9)	N(41)-Zn-O(91)	99.68(8)
N(61)-Zn-N(21)	163.00(9)	N(1)-Zn-O(91)	94.76(9)
N(41)-Zn-N(21)	86.97(8)	N(21)-Zn-O(91)	101.36(10)
N(1)-C(13)	1.356(3)	C(6)-C(15)	1.554(6)
N(1)-C(2)	1.370(3)	C(7)-C(8)	1.451(6)
C(2)-C(70)	1.419(4)	C(8)-C(9)	1.548(5)
C(2)-C(3)	1.458(4)	C(9)-C(17)	1.517(5)
C(3)-C(4)	1.400(4)	C(9)-C(18)	1.522(6)
C(3)-C(12)	1.404(4)	C(9)-C(10)	1.528(4)
C(4)-C(5)	1.395(4)	C(10)-C(11)	1.398(4)
C(5)-C(10)	1.412(4)	C(11)-C(12)	1.384(4)
C(5)-C(6)	1.531(4)	C(12)-C(13)	1.446(4)
C(6)-C(7)	1.511(5)	C(13)-N(14)	1.346(3)
C(6)-C(16)	1.522(6)	N(14)-C(22)	1.323(3)

N(21)-C(33)	1.366(3)
N(21)-C(22)	1.370(3)
C(22)-C(23)	1.467(4)
C(23)-C(24)	1.382(4)
C(23)-C(32)	1.396(4)
C(24)-C(25)	1.402(4)
C(25)-C(30)	1.425(4)
C(25)-C(26)	1.532(4)
C(26)-C(36)	1.505(5)
C(26)-C(35)	1.525(5)
C(26)-C(27)	1.567(5)
C(27)-C(28)	1.472(5)
C(28)-C(29)	1.509(4)
C(29)-C(38)	1.533(5)
C(29)-C(30)	1.537(4)
C(29)-C(37)	1.549(5)
C(30)-C(31)	1.385(4)
C(31)-C(32)	1.385(4)
C(32)-C(33)	1.455(4)
C(33)-N(34)	1.330(3)
N(34)-C(42)	1.334(3)
N(41)-C(42)	1.360(3)
N(41)-C(53)	1.377(3)
C(42)-C(43)	1.460(3)
C(43)-C(44)	1.382(4)
C(43)-C(52)	1.397(4)
C(44)-C(45)	1.400(4)
C(45)-C(50)	1.417(4)
C(45)-C(46)	1.537(4)
C(46)-C(56)	1.523(4)
C(46)-C(47)	1.531(4)
C(46)-C(55)	1.540(5)
C(47)-C(48)	1.493(5)
C(48)-C(49)	1.534(4)
C(49)-C(58)	1.525(4)
C(49)-C(57)	1.528(5)
C(49)-C(50)	1.537(4)
C(50)-C(51)	1.403(4)
C(51)-C(52)	1.379(4)
C(52)-C(53)	1.467(3)
C(53)-N(54)	1.321(3)
N(54)-C(62)	1.342(3)
N(61)-C(62)	1.355(3)
N(61)-C(69)	1.379(3)
C(62)-C(63)	1.450(3)
C(63)-C(64)	1.393(3)
C(63)-C(68)	1.401(4)
C(64)-C(65)	1.385(4)
C(65)-C(66)	1.391(4)
C(66)-C(67)	1.382(4)
C(67)-C(68)	1.413(3)
C(68)-C(69)	1.470(3)
C(69)-C(70)	1.399(3)
C(70)-C(71)	1.499(3)
C(71)-C(72)	1.388(4)
C(71)-C(76)	1.392(4)
C(72)-C(73)	1.387(4)
C(73)-C(74)	1.389(4)
C(74)-O(77)	1.368(3)
C(74)-C(75)	1.391(4)

C(75)-C(76) 1.378(3)	O(91)-C(922) 1.657(14)
O(77)-C(78) 1.438(3)	C(921)-C(922) 0.952(12)
C(78)-C(79) 1.510(4)	C(921)-C(932) 1.436(14)
C(79)-C(80) 1.495(5)	C(921)-C(931) 1.518(9)
C(80)-C(81) 1.523(5)	C(922)-C(931) 0.779(13)
C(81)-C(82) 1.495(6)	C(922)-C(932) 1.553(16)
O(91)-C(921) 1.325(5)	C(931)-C(932) 1.310(19)
C(13)-N(1)-C(2) 109.5(2)	C(18)-C(9)-C(10) 108.6(3)
C(13)-N(1)-Zn 123.52(17)	C(17)-C(9)-C(8) 106.8(3)
C(2)-N(1)-Zn 125.28(17)	C(18)-C(9)-C(8) 109.4(4)
N(1)-C(2)-C(70) 123.6(2)	C(10)-C(9)-C(8) 109.5(3)
N(1)-C(2)-C(3) 108.6(2)	C(11)-C(10)-C(5) 118.7(3)
C(70)-C(2)-C(3) 127.8(2)	C(11)-C(10)-C(9) 118.0(3)
C(4)-C(3)-C(12) 118.2(2)	C(5)-C(10)-C(9) 123.3(3)
C(4)-C(3)-C(2) 135.8(3)	C(12)-C(11)-C(10) 120.1(3)
C(12)-C(3)-C(2) 106.0(2)	C(11)-C(12)-C(3) 121.8(2)
C(5)-C(4)-C(3) 120.4(3)	C(11)-C(12)-C(13) 131.3(2)
C(4)-C(5)-C(10) 120.7(3)	C(3)-C(12)-C(13) 106.9(2)
C(4)-C(5)-C(6) 116.6(3)	N(14)-C(13)-N(1) 129.4(2)
C(10)-C(5)-C(6) 122.6(3)	N(14)-C(13)-C(12) 121.6(2)
C(7)-C(6)-C(16) 111.3(4)	N(1)-C(13)-C(12) 109.0(2)
C(7)-C(6)-C(5) 110.6(3)	C(22)-N(14)-C(13) 123.7(2)
C(16)-C(6)-C(5) 109.5(3)	C(22)-N(21)-Zn 125.01(17)
C(7)-C(6)-C(15) 108.8(3)	C(33)-N(21)-Zn 125.63(17)
C(16)-C(6)-C(15) 105.1(4)	C(33)-N(21)-C(22) 108.8(2)
C(5)-C(6)-C(15) 111.3(3)	N(14)-C(22)-N(21) 127.6(2)
C(8)-C(7)-C(6) 115.1(3)	N(14)-C(22)-C(23) 123.2(2)
C(7)-C(8)-C(9) 115.3(4)	N(21)-C(22)-C(23) 109.1(2)
C(17)-C(9)-C(18) 111.4(4)	C(24)-C(23)-C(32) 120.1(2)
C(17)-C(9)-C(10) 111.1(3)	C(24)-C(23)-C(22) 134.0(2)

C(32)-C(23)-C(22) 105.9(2)	C(48)-C(47)-C(46) 112.5(3)
C(23)-C(24)-C(25) 119.9(3)	C(47)-C(48)-C(49) 112.5(3)
C(24)-C(25)-C(30) 119.4(2)	C(58)-C(49)-C(57) 109.8(3)
C(24)-C(25)-C(26) 117.6(3)	C(58)-C(49)-C(48) 109.5(3)
C(30)-C(25)-C(26) 122.9(3)	C(57)-C(49)-C(48) 108.0(3)
C(36)-C(26)-C(35) 110.6(3)	C(58)-C(49)-C(50) 109.8(2)
C(36)-C(26)-C(25) 108.8(3)	C(57)-C(49)-C(50) 109.2(2)
C(35)-C(26)-C(25) 111.3(3)	C(48)-C(49)-C(50) 110.4(3)
C(36)-C(26)-C(27) 110.8(3)	C(51)-C(50)-C(45) 119.5(2)
C(35)-C(26)-C(27) 105.2(3)	C(51)-C(50)-C(49) 118.2(2)
C(25)-C(26)-C(27) 110.2(3)	C(45)-C(50)-C(49) 122.3(2)
C(28)-C(27)-C(26) 114.3(3)	C(52)-C(51)-C(50) 119.8(2)
C(27)-C(28)-C(29) 113.4(3)	C(51)-C(52)-C(43) 120.3(2)
C(53)-N(41)-Zn 124.27(16)	C(51)-C(52)-C(53) 133.7(2)
N(34)-C(42)-N(41) 127.8(2)	C(43)-C(52)-C(53) 105.9(2)
N(34)-C(42)-C(43) 122.5(2)	N(54)-C(53)-N(41) 127.5(2)
N(41)-C(42)-C(43) 109.6(2)	N(54)-C(53)-C(52) 123.2(2)
C(44)-C(43)-C(52) 120.6(2)	N(41)-C(53)-C(52) 109.1(2)
C(44)-C(43)-C(42) 132.8(2)	C(53)-N(54)-C(62) 123.8(2)
C(52)-C(43)-C(42) 106.6(2)	C(62)-N(61)-C(69) 109.7(2)
C(43)-C(44)-C(45) 119.7(2)	C(62)-N(61)-Zn 124.31(16)
C(44)-C(45)-C(50) 119.4(2)	C(69)-N(61)-Zn 125.91(16)
C(44)-C(45)-C(46) 117.9(2)	N(54)-C(62)-N(61) 129.0(2)
C(50)-C(45)-C(46) 122.7(2)	N(54)-C(62)-C(63) 121.7(2)
C(56)-C(46)-C(47) 111.5(3)	N(61)-C(62)-C(63) 109.2(2)
C(56)-C(46)-C(45) 110.1(2)	C(64)-C(63)-C(68) 122.9(2)
C(47)-C(46)-C(45) 109.6(2)	C(64)-C(63)-C(62) 130.3(2)
C(56)-C(46)-C(55) 108.5(3)	C(68)-C(63)-C(62) 106.8(2)
C(47)-C(46)-C(55) 107.2(3)	C(65)-C(64)-C(63) 117.5(2)
C(45)-C(46)-C(55) 109.8(2)	C(64)-C(65)-C(66) 120.5(2)

C(67)-C(66)-C(65) 122.3(2)

C(66)-C(67)-C(68) 118.2(2)

C(63)-C(68)-C(67) 118.6(2)

C(63)-C(68)-C(69) 106.4(2)

C(67)-C(68)-C(69) 135.0(2)

N(61)-C(69)-C(70) 124.0(2)

N(61)-C(69)-C(68) 107.9(2)

C(70)-C(69)-C(68) 128.1(2)

C(69)-C(70)-C(2) 127.3(2)

C(69)-C(70)-C(71) 117.0(2)

C(2)-C(70)-C(71) 115.7(2)

C(72)-C(71)-C(76) 118.6(2)

C(28)-C(29)-C(38) 111.3(3)

C(28)-C(29)-C(30) 109.9(3)

C(38)-C(29)-C(30) 109.1(2)

C(28)-C(29)-C(37) 109.3(3)

C(38)-C(29)-C(37) 105.7(3)

C(30)-C(29)-C(37) 111.6(2)

C(31)-C(30)-C(25) 119.6(2)

C(31)-C(30)-C(29) 118.6(3)

C(25)-C(30)-C(29) 121.8(2)

C(30)-C(31)-C(32) 120.0(3)

C(31)-C(32)-C(23) 120.7(2)

C(31)-C(32)-C(33) 132.2(2)

C(23)-C(32)-C(33) 107.1(2)

O(94)-C(95) 1.405(10)

C(95)-C(961) 1.057(17)

C(95)-C(962) 1.883(15)

O(97)-C(98) 1.369(14)

N(34)-C(33)-N(21) 128.3(2)

N(34)-C(33)-C(32) 122.6(2)

N(21)-C(33)-C(32) 109.1(2)

C(33)-N(34)-C(42) 123.1(2)

C(42)-N(41)-C(53) 108.4(2)

C(42)-N(41)-Zn 126.89(17)

C(72)-C(71)-C(70) 120.0(2)

C(76)-C(71)-C(70) 121.4(2)

C(73)-C(72)-C(71) 121.7(2)

C(72)-C(73)-C(74) 118.9(2)

O(77)-C(74)-C(73) 124.8(2)

O(77)-C(74)-C(75) 115.3(2)

C(73)-C(74)-C(75) 119.9(2)

C(76)-C(75)-C(74) 120.5(2)

C(74)-O(77)-C(78) 118.1(2)

C(75)-C(76)-C(71) 120.4(2)

O(77)-C(78)-C(79) 106.5(2)

C(80)-C(79)-C(78) 113.6(3)

C(79)-C(80)-C(81) 113.0(3)

C(82)-C(81)-C(80) 114.3(4)

C(921)-O(91)-Zn 128.9(3)

C(922)-O(91)-Zn 112.8(4)

O(91)-C(921)-C(931) 106.5(5)

C(932)-C(922)-O(91) 100.8(10)

C(961)-C(95)-O(94) 127.7(14)

O(94)-C(95)-C(962) 107.1(6)

C(98)-C(100) 1.00(2)

```
      C(98)-C(101)                        C(100)-C(98)-O(97)
1.22(2)                          168(3)
      C(98)-C(99)                         C(101)-C(98)-O(97)
1.55(3)                          141(2)
      O(97)-C(98)-C(99)
103.3(17)
```

Table 3.   Anisotropic displacement parameters ($Å^2$ x 10^4) for the
           expression:
                  exp $\{-2\pi^2(h^2a*^2U_{11} + ... + 2hka*b*U_{12})\}$
           E.s.ds are in parentheses.

	U_{11}	U_{22}	U_{33}	U_{23}	U_{13}	U_{12}
Zn	430(2)	309(2)	332(2)	-15.2(12)	140.0(14)	-13.9(13)
N(1)	460(12)	336(10)	351(11)	-15(8)	150(9)	-10(9)
C(2)	403(13)	398(13)	337(12)	-8(10)	116(10)	-40(10)
C(3)	446(14)	404(13)	379(13)	-32(10)	132(11)	-57(11)
C(4)	507(15)	462(15)	460(15)	-62(12)	208(12)	-113(12)
C(5)	556(17)	535(17)	495(16)	-50(13)	224(13)	-165(13)
C(6)	670(20)	670(20)	660(20)	-89(16)	351(17)	-279(17)
C(7)	1000(30)	680(20)	1000(30)	-150(20)	630(30)	-310(20)
C(8)	1020(30)	660(20)	1360(40)	260(20)	790(30)	-10(20)
C(9)	602(19)	497(17)	730(20)	39(15)	275(16)	-138(14)
C(10)	508(16)	472(16)	548(17)	19(13)	200(13)	-125(13)
C(11)	524(16)	413(14)	503(16)	-31(12)	204(13)	-63(12)
C(12)	473(14)	389(13)	403(14)	-7(11)	161(11)	-45(11)
C(13)	482(14)	345(12)	373(13)	-7(10)	133(11)	-37(11)
N(14)	509(12)	333(11)	384(11)	-8(9)	173(9)	-20(9)
C(15)	940(30)	820(30)	1540(50)	-150(30)	870(30)	-210(20)
C(16)	1090(30)	1300(40)	630(20)	-220(20)	480(20)	-590(30)
C(17)	790(30)	516(19)	1080(30)	59(19)	470(20)	-42(17)
C(18)	1110(40)	650(20)	1070(40)	-30(20)	160(30)	-400(20)
N(21)	503(12)	312(10)	377(11)	4(8)	171(9)	-15(9)
C(22)	482(14)	347(12)	347(12)	-15(10)	140(11)	1(10)
C(23)	487(14)	349(13)	361(13)	-31(10)	135(11)	4(11)
C(24)	528(15)	343(13)	421(14)	-19(10)	152(12)	-13(11)

C(25)	536(16)	353(13)	502(15)	-61(11)	169(12)	2(11)
C(26)	644(19)	369(14)	659(19)	-97(13)	267(15)	21(13)
C(27)	910(30)	412(16)	950(30)	-123(17)	500(20)	8(16)
C(28)	850(20)	524(18)	740(20)	-40(16)	400(20)	161(17)
C(29)	608(18)	434(15)	580(18)	-102(13)	272(14)	21(13)
C(30)	492(15)	399(14)	466(15)	-63(11)	170(12)	27(11)
C(31)	515(15)	387(14)	393(13)	-24(11)	166(11)	15(11)
C(32)	494(14)	360(13)	358(13)	-10(10)	151(11)	-1(11)
C(33)	472(14)	359(13)	350(13)	-30(10)	136(11)	0(11)
N(34)	503(12)	343(11)	351(11)	-14(8)	164(9)	-12(9)
C(35)	820(20)	374(15)	740(20)	-1(14)	341(18)	-68(15)
C(36)	960(30)	471(19)	990(30)	-23(19)	60(20)	242(19)
C(37)	680(20)	610(20)	840(20)	-118(17)	430(19)	23(16)
C(38)	790(20)	640(20)	504(17)	-62(15)	281(16)	85(17)
N(41)	401(11)	330(10)	327(10)	-2(8)	106(8)	3(8)
C(42)	402(13)	365(12)	321(12)	-16(10)	111(10)	-16(10)
C(43)	429(13)	353(12)	320(12)	-3(9)	86(10)	-26(10)
C(44)	473(14)	391(13)	356(13)	-12(10)	138(11)	-30(11)
C(45)	472(14)	440(14)	320(12)	-4(10)	95(11)	-91(11)
C(46)	551(16)	531(16)	369(14)	-1(12)	164(12)	-114(13)
C(47)	780(20)	619(19)	490(17)	-24(14)	300(16)	-189(17)
C(48)	930(30)	549(18)	477(17)	88(14)	240(17)	-139(17)
C(49)	675(19)	408(15)	408(14)	49(11)	150(13)	-92(13)
C(50)	456(14)	398(14)	332(12)	19(10)	66(10)	-90(11)
C(51)	426(13)	362(13)	352(12)	-3(10)	62(10)	-31(10)
C(52)	385(13)	362(12)	312(12)	-1(9)	61(10)	-25(10)
C(53)	340(12)	330(12)	329(12)	2(9)	70(9)	-17(9)
N(54)	366(10)	333(10)	341(10)	1(8)	80(8)	-5(8)
C(55)	518(17)	890(20)	457(16)	-26(16)	177(13)	-99(16)
C(56)	585(18)	672(19)	390(15)	-48(13)	172(13)	-98(15)

C(57)	830(20)	492(17)	640(20)	222(15)	114(18)	33(16)
C(58)	920(30)	445(16)	503(17)	−13(13)	211(17)	−198(16)
N(61)	369(10)	345(10)	330(10)	−13(8)	121(8)	−4(8)
C(62)	342(12)	319(12)	354(12)	0(9)	79(10)	17(9)
C(63)	365(12)	344(12)	345(12)	−3(10)	76(10)	26(10)
C(64)	441(14)	341(13)	395(13)	−8(10)	99(11)	26(10)
C(65)	568(16)	332(13)	449(15)	−57(11)	117(12)	19(11)
C(66)	532(16)	423(14)	389(14)	−84(11)	126(12)	77(12)
C(67)	445(14)	404(13)	330(12)	−17(10)	109(10)	35(11)
C(68)	346(12)	365(12)	325(12)	−19(9)	55(9)	25(10)
C(69)	360(12)	359(12)	310(11)	−23(9)	78(9)	14(10)
C(70)	351(12)	394(13)	300(11)	−18(10)	85(9)	4(10)
C(71)	389(13)	385(13)	336(12)	−24(10)	113(10)	−12(10)
C(72)	411(14)	595(16)	321(13)	−15(11)	68(10)	25(12)
C(73)	332(13)	695(19)	394(14)	−7(13)	70(11)	62(12)
C(74)	381(13)	547(16)	378(13)	−20(11)	139(10)	16(12)
C(75)	386(13)	481(14)	316(12)	−10(10)	91(10)	−13(11)
O(77)	354(9)	847(15)	357(10)	−30(9)	128(8)	31(9)
C(76)	332(12)	380(13)	381(13)	−5(10)	104(10)	−6(10)
C(78)	382(15)	970(30)	467(16)	35(16)	149(12)	99(15)
C(79)	377(14)	910(20)	515(17)	35(16)	179(13)	101(15)
C(80)	457(16)	770(20)	614(19)	−57(16)	212(15)	−51(15)
C(81)	660(20)	870(30)	680(20)	114(19)	273(18)	4(19)
C(82)	1030(40)	950(30)	1040(40)	280(30)	340(30)	30(30)
O(91)	449(11)	873(17)	476(12)	66(11)	50(9)	−130(10)
C(921)	630(30)	790(40)	420(20)	20(20)	80(20)	−80(20)
C(931)	580(50)	560(40)	620(50)	−210(30)	110(40)	−140(40)
C(932)	600(60)	4100(300)	620(60)	450(100)	30(40)	−50(100)
O(94)	920(30)	2280(50)	850(20)	320(30)	340(20)	420(30)
C(95)	1120(50)	1440(60)	2390(100)	480(60)	1020(60)	−40(50)

C(961)	580(60)	2500(200)	1120(100)	-970(120)	0(60)	-50(90)
C(962)	1900(150)	850(70)	1150(100)	250(70)	-640(100)	-650(80)
O(97)	1440(60)	2440(90)	1920(70)	-730(70)	20(50)	130(60)
C(98)	1040(80)	3200(200)	2690(190)	-2310(190)	700(100)	-570(110)
C(99)	1440(80)	1750(90)	930(50)	-400(50)	-220(50)	990(80)
C(100)	670(100)	2900(400)	2300(300)	-1600(300)	20(150)	-530(170)
C(101)	1660(170)	2300(200)	2030(190)	1270(180)	1310(160)	920(160)

Table 4. Hydrogen coordinates (x 10^4) and isotropic displacement
        parameters (Å^2 x 10^3). All hydrogen atoms were
        included in idealised positions with U(iso)'s set at
        1.2*U(eq) or, for the methyl group hydrogen atoms,
        1.5*U(eq) of the parent carbon atoms.

	x	y	z	U(iso)
H(4)	1491	3744	5837	55
H(7A)	-46	2600	6771	99
H(7B)	-450	2632	5847	99
H(8A)	645	2071	6201	111
H(8B)	1677	2335	6671	111
H(11)	2717	2670	4483	56
H(15A)	-30	3654	6211	150
H(15B)	-835	3334	5680	150
H(15C)	-750	3346	6596	150
H(16A)	1733	3446	7153	144
H(16B)	971	3151	7531	144
H(16C)	2079	2988	7280	144
H(17A)	3174	2203	6066	113
H(17B)	2424	1825	5712	113
H(17C)	2954	2107	5157	113
H(18A)	-50	2378	4659	144
H(18B)	945	2216	4280	144
H(18C)	415	1934	4835	144
H(24)	4766	2487	2846	51
H(27A)	6420	1630	1217	85
H(27B)	5385	1882	712	85
H(28A)	7118	2062	422	80
H(28B)	7619	2187	1308	80
H(31)	6181	3352	1159	51
H(35A)	4010	1893	1436	93
H(35B)	4707	1525	1885	93
H(35C)	4318	1881	2366	93
H(36A)	7351	2054	2639	125
H(36B)	6383	1981	3108	125
H(36C)	6772	1625	2627	125
H(37A)	7144	3145	429	100
H(37B)	8069	2879	1007	100
H(37C)	7704	2769	103	100
H(38A)	5210	2883	-160	93
H(38B)	5791	2515	-494	93
H(38C)	4857	2437	1	93
H(44)	6697	4610	1018	48

H(47A)	8222	5806	717	73
H(47B)	8055	5729	-196	73
H(48A)	6053	5854	-368	77
H(48B)	6813	6236	-54	77
H(51)	5144	5750	1989	46
H(55A)	8930	5179	1235	91
H(55B)	8449	4769	829	91
H(55C)	9098	5074	386	91
H(56A)	6731	4771	-323	81
H(56B)	6172	5184	-669	81
H(56C)	7419	5065	-760	81
H(57A)	4378	5946	117	99
H(57B)	4434	6155	938	99
H(57C)	4802	6397	256	99
H(58A)	7514	6193	1590	92
H(58B)	6733	6549	1163	92
H(58C)	6365	6307	1845	92
H(64)	4286	5944	4191	47
H(65)	3674	6259	5227	54
H(66)	2783	5889	6045	53
H(67)	2499	5198	5890	47
H(72)	529	4536	4757	53
H(73)	-615	4618	5664	57
H(75)	2233	4472	7435	47
H(76)	3355	4383	6524	43
H(78A)	-1445	4374	6664	72
H(78B)	-1399	4850	6750	72
H(79A)	-1207	4782	8130	71
H(79B)	-2386	4596	7659	71
H(80A)	-403	4130	8307	72
H(80B)	-1601	3948	7857	72
H(81A)	-1290	4371	9312	86
H(81B)	-2464	4171	8869	86
H(82A)	-1555	3765	9914	149
H(82B)	-1628	3532	9115	149
H(82C)	-453	3732	9559	149

Table 5. Torsion angles, in degrees. E.s.ds are in parentheses.

```
  C(13)-N(1)-C(2)-C(70)                C(3)-C(4)-C(5)-C(10)
179.2(2)                             1.0(5)
  Zn-N(1)-C(2)-C(70)          -        C(3)-C(4)-C(5)-C(6)
15.4(4)                              179.6(3)
  C(13)-N(1)-C(2)-C(3)        -        C(4)-C(5)-C(6)-C(7)
0.9(3)                               167.6(3)
  Zn-N(1)-C(2)-C(3)                    C(10)-C(5)-C(6)-C(7)       -
164.47(17)                           13.9(5)
  N(1)-C(2)-C(3)-C(4)         -        C(4)-C(5)-C(6)-C(16)       -
178.3(3)                             69.4(4)
  C(70)-C(2)-C(3)-C(4)                 C(10)-C(5)-C(6)-C(16)
1.5(5)                               109.2(4)
  N(1)-C(2)-C(3)-C(12)                 C(4)-C(5)-C(6)-C(15)
0.9(3)                               46.5(4)
  C(70)-C(2)-C(3)-C(12)       -        C(10)-C(5)-C(6)-C(15)      -
179.3(3)                             135.0(4)
  C(12)-C(3)-C(4)-C(5)                 C(16)-C(6)-C(7)-C(8)       -
0.1(4)                               79.4(5)
  C(2)-C(3)-C(4)-C(5)                  C(5)-C(6)-C(7)-C(8)
179.2(3)                             42.6(6)
```

C(15)-C(6)-C(7)-C(8)
165.2(4)
C(6)-C(7)-C(8)-C(9)   –
59.3(6)
C(7)-C(8)-C(9)-C(17)
161.4(4)
C(7)-C(8)-C(9)-C(18)   –
77.9(5)
C(7)-C(8)-C(9)-C(10)
41.1(5)
C(4)-C(5)-C(10)-C(11)   –
1.7(5)
C(6)-C(5)-C(10)-C(11)
179.7(3)
C(4)-C(5)-C(10)-C(9)
178.7(3)
C(6)-C(5)-C(10)-C(9)
0.2(5)
C(17)-C(9)-C(10)-C(11)
50.3(4)
C(18)-C(9)-C(10)-C(11)   –
72.6(4)
C(8)-C(9)-C(10)-C(11)
168.0(3)
C(17)-C(9)-C(10)-C(5)   –
130.2(4)
C(18)-C(9)-C(10)-C(5)
106.9(4)
C(8)-C(9)-C(10)-C(5)   –
12.4(5)
C(5)-C(10)-C(11)-C(12)
1.5(5)
C(9)-C(10)-C(11)-C(12)   –
179.0(3)
C(10)-C(11)-C(12)-C(3)   –
0.5(4)
C(10)-C(11)-C(12)-C(13)   –
179.4(3)
C(4)-C(3)-C(12)-C(11)   –
0.3(4)
C(2)-C(3)-C(12)-C(11)   –
179.7(3)
C(4)-C(3)-C(12)-C(13)
178.9(2)
C(2)-C(3)-C(12)-C(13)   –
0.6(3)
C(2)-N(1)-C(13)-N(14)   –
179.2(3)
Zn-N(1)-C(13)-N(14)
15.1(4)
C(2)-N(1)-C(13)-C(12)
0.6(3)
Zn-N(1)-C(13)-C(12)   –
165.13(18)
C(11)-C(12)-C(13)-N(14)   –
1.1(5)
C(3)-C(12)-C(13)-N(14)
179.8(2)
C(11)-C(12)-C(13)-N(1)
179.1(3)

C(3)-C(12)-C(13)-N(1)
0.0(3)
N(1)-C(13)-N(14)-C(22)   –
3.5(5)
C(12)-C(13)-N(14)-C(22)
176.7(3)
C(13)-N(14)-C(22)-N(21)   –
1.5(4)
C(13)-N(14)-C(22)-C(23)   –
179.9(3)
C(33)-N(21)-C(22)-N(14)   –
177.9(3)
Zn-N(21)-C(22)-N(14)   –
6.0(4)
C(33)-N(21)-C(22)-C(23)
0.7(3)
Zn-N(21)-C(22)-C(23)
172.55(17)
N(14)-C(22)-C(23)-C(24)   –
3.2(5)
N(21)-C(22)-C(23)-C(24)
178.1(3)
N(14)-C(22)-C(23)-C(32)
177.0(3)
N(21)-C(22)-C(23)-C(32)   –
1.6(3)
C(32)-C(23)-C(24)-C(25)   –
2.0(4)
C(22)-C(23)-C(24)-C(25)
178.3(3)
C(23)-C(24)-C(25)-C(30)   –
1.4(4)
C(23)-C(24)-C(25)-C(26)
175.8(3)
C(24)-C(25)-C(26)-C(36)   –
69.6(4)
C(30)-C(25)-C(26)-C(36)
107.6(4)
C(24)-C(25)-C(26)-C(35)
52.5(4)
C(30)-C(25)-C(26)-C(35)   –
130.4(3)
C(24)-C(25)-C(26)-C(27)
168.8(3)
C(30)-C(25)-C(26)-C(27)   –
14.1(4)
C(36)-C(26)-C(27)-C(28)   –
80.5(4)
C(35)-C(26)-C(27)-C(28)
160.0(3)
C(25)-C(26)-C(27)-C(28)
40.0(5)
C(26)-C(27)-C(28)-C(29)   –
61.6(5)
C(27)-C(28)-C(29)-C(38)   –
70.1(4)
C(27)-C(28)-C(29)-C(30)
50.8(4)
C(27)-C(28)-C(29)-C(37)
173.5(3)

C(24)-C(25)-C(30)-C(31) 3.6(4)	C(53)-N(41)-C(42)-N(34) - 179.4(2)
C(26)-C(25)-C(30)-C(31) - 173.5(3)	Zn-N(41)-C(42)-N(34) - 6.9(4)
C(24)-C(25)-C(30)-C(29) - 175.0(3)	C(53)-N(41)-C(42)-C(43) - 0.5(3)
C(26)-C(25)-C(30)-C(29) 7.9(5)	Zn-N(41)-C(42)-C(43) 72.01(16)
C(28)-C(29)-C(30)-C(31) 156.7(3)	N(34)-C(42)-C(43)-C(44) - 3.6(5)
C(38)-C(29)-C(30)-C(31) - 81.1(3)	N(41)-C(42)-C(43)-C(44) 177.4(3)
C(37)-C(29)-C(30)-C(31) 35.3(4)	N(34)-C(42)-C(43)-C(52) 175.6(2)
C(28)-C(29)-C(30)-C(25) - 24.7(4)	N(41)-C(42)-C(43)-C(52) - 3.4(3)
C(38)-C(29)-C(30)-C(25) 97.6(3)	C(52)-C(43)-C(44)-C(45) - 2.2(4)
C(37)-C(29)-C(30)-C(25) - 146.0(3)	C(42)-C(43)-C(44)-C(45) 176.9(3)
C(25)-C(30)-C(31)-C(32) - 2.4(4)	C(43)-C(44)-C(45)-C(50) - 6.0(4)
C(29)-C(30)-C(31)-C(32) 176.3(3)	C(43)-C(44)-C(45)-C(46) 172.8(2)
C(30)-C(31)-C(32)-C(23) - 1.0(4)	C(44)-C(45)-C(46)-C(56) 67.2(3)
C(30)-C(31)-C(32)-C(33) - 179.5(3)	C(50)-C(45)-C(46)-C(56) - 114.0(3)
C(24)-C(23)-C(32)-C(31) 3.3(4)	C(44)-C(45)-C(46)-C(47) - 169.8(3)
C(22)-C(23)-C(32)-C(31) - 176.9(3)	C(50)-C(45)-C(46)-C(47) 9.0(4)
C(24)-C(23)-C(32)-C(33) - 177.9(2)	C(44)-C(45)-C(46)-C(55) - 52.3(3)
C(22)-C(23)-C(32)-C(33) 1.9(3)	C(50)-C(45)-C(46)-C(55) 126.5(3)
C(22)-N(21)-C(33)-N(34) - 178.6(3)	C(56)-C(46)-C(47)-C(48) 76.0(3)
Zn-N(21)-C(33)-N(34) 9.6(4)	C(45)-C(46)-C(47)-C(48) - 46.2(3)
C(22)-N(21)-C(33)-C(32) 0.5(3)	C(55)-C(46)-C(47)-C(48) - 165.3(3)
Zn-N(21)-C(33)-C(32) - 171.29(17)	C(46)-C(47)-C(48)-C(49) 66.0(4)
C(31)-C(32)-C(33)-N(34) - 3.8(5)	C(47)-C(48)-C(49)-C(58) 78.4(3)
C(23)-C(32)-C(33)-N(34) 177.6(3)	C(47)-C(48)-C(49)-C(57) - 162.0(3)
C(31)-C(32)-C(33)-N(21) 177.0(3)	C(47)-C(48)-C(49)-C(50) - 42.7(4)
C(23)-C(32)-C(33)-N(21) - 1.5(3)	C(44)-C(45)-C(50)-C(51) 9.5(4)
N(21)-C(33)-N(34)-C(42) - 1.5(4)	C(46)-C(45)-C(50)-C(51) - 169.3(2)
C(32)-C(33)-N(34)-C(42) 179.5(2)	C(44)-C(45)-C(50)-C(49) - 170.2(2)
C(33)-N(34)-C(42)-N(41) - 0.1(4)	C(46)-C(45)-C(50)-C(49) 11.0(4)
C(33)-N(34)-C(42)-C(43) - 178.8(2)	C(58)-C(49)-C(50)-C(51) 65.2(3)

C(57)-C(49)-C(50)-C(51)	-	55.3(3)
C(48)-C(49)-C(50)-C(51)	-	173.9(3)
C(58)-C(49)-C(50)-C(45)	-	115.2(3)
C(57)-C(49)-C(50)-C(45)		124.3(3)
C(48)-C(49)-C(50)-C(45)		5.7(4)
C(45)-C(50)-C(51)-C(52)	-	4.7(4)
C(49)-C(50)-C(51)-C(52)		174.9(2)
C(50)-C(51)-C(52)-C(43)	-	3.5(4)
C(50)-C(51)-C(52)-C(53)		179.3(2)
C(44)-C(43)-C(52)-C(51)		7.0(4)
C(42)-C(43)-C(52)-C(51)	-	172.3(2)
C(44)-C(43)-C(52)-C(53)	-	175.1(2)
C(42)-C(43)-C(52)-C(53)		5.6(3)
C(42)-N(41)-C(53)-N(54)	-	172.2(2)
Zn-N(41)-C(53)-N(54)		15.1(3)
C(42)-N(41)-C(53)-C(52)		4.1(3)
Zn-N(41)-C(53)-C(52)	-	168.65(15)
C(51)-C(52)-C(53)-N(54)	-	12.2(4)
C(43)-C(52)-C(53)-N(54)		170.3(2)
C(51)-C(52)-C(53)-N(41)		171.3(3)
C(43)-C(52)-C(53)-N(41)	-	6.2(3)
N(41)-C(53)-N(54)-C(62)	-	1.8(4)
C(52)-C(53)-N(54)-C(62)	-	177.6(2)
C(53)-N(54)-C(62)-N(61)	-	7.4(4)
C(53)-N(54)-C(62)-C(63)		175.7(2)
C(69)-N(61)-C(62)-N(54)	-	174.9(2)
Zn-N(61)-C(62)-N(54)		1.6(4)
C(69)-N(61)-C(62)-C(63)		2.4(3)
Zn-N(61)-C(62)-C(63)		178.78(16)
N(54)-C(62)-C(63)-C(64)	-	5.5(4)

N(61)-C(62)-C(63)-C(64)		177.1(3)
N(54)-C(62)-C(63)-C(68)		175.4(2)
N(61)-C(62)-C(63)-C(68)	-	2.1(3)
C(68)-C(63)-C(64)-C(65)	-	0.4(4)
C(62)-C(63)-C(64)-C(65)	-	179.4(3)
C(63)-C(64)-C(65)-C(66)	-	0.1(4)
C(64)-C(65)-C(66)-C(67)		0.7(4)
C(65)-C(66)-C(67)-C(68)	-	0.7(4)
C(64)-C(63)-C(68)-C(67)		0.4(4)
C(62)-C(63)-C(68)-C(67)		179.6(2)
C(64)-C(63)-C(68)-C(69)	-	178.2(2)
C(62)-C(63)-C(68)-C(69)		1.0(3)
C(66)-C(67)-C(68)-C(63)		0.2(4)
C(66)-C(67)-C(68)-C(69)		178.3(3)
C(62)-N(61)-C(69)-C(70)		177.5(2)
Zn-N(61)-C(69)-C(70)		1.1(3)
C(62)-N(61)-C(69)-C(68)	-	1.7(3)
Zn-N(61)-C(69)-C(68)	-	178.04(15)
C(63)-C(68)-C(69)-N(61)		0.3(3)
C(67)-C(68)-C(69)-N(61)	-	177.9(3)
C(63)-C(68)-C(69)-C(70)	-	178.8(2)
C(67)-C(68)-C(69)-C(70)		3.0(5)
N(61)-C(69)-C(70)-C(2)		8.1(4)
C(68)-C(69)-C(70)-C(2)	-	172.9(2)
N(61)-C(69)-C(70)-C(71)	-	170.3(2)
C(68)-C(69)-C(70)-C(71)		8.7(4)
N(1)-C(2)-C(70)-C(69)	-	0.4(4)
C(3)-C(2)-C(70)-C(69)		179.8(3)
N(1)-C(2)-C(70)-C(71)		178.0(2)
C(3)-C(2)-C(70)-C(71)	-	1.8(4)

C(69)-C(70)-C(71)-C(72) 87.5(3)	C(73)-C(74)-C(75)-C(76) – 2.0(4)
C(2)-C(70)-C(71)-C(72) – 91.0(3)	C(73)-C(74)-O(77)-C(78) 8.1(5)
C(69)-C(70)-C(71)-C(76) – 94.2(3)	C(75)-C(74)-O(77)-C(78) – 172.5(3)
C(2)-C(70)-C(71)-C(76) 87.2(3)	C(74)-C(75)-C(76)-C(71) 1.1(4)
C(76)-C(71)-C(72)-C(73) – 0.8(4)	C(72)-C(71)-C(76)-C(75) 0.3(4)
C(70)-C(71)-C(72)-C(73) 177.5(3)	C(70)-C(71)-C(76)-C(75) – 177.9(2)
C(71)-C(72)-C(73)-C(74) – 0.1(5)	C(74)-O(77)-C(78)-C(79) 170.4(3)
C(72)-C(73)-C(74)-O(77) – 179.1(3)	O(77)-C(78)-C(79)-C(80) – 63.5(4)
C(72)-C(73)-C(74)-C(75) 1.5(5)	C(78)-C(79)-C(80)-C(81) 178.2(3)
O(77)-C(74)-C(75)-C(76) 178.5(2)	C(79)-C(80)-C(81)-C(82) – 177.6(4)

Crystal structure analysis of the zinc complex, isabf1046 (91)

Crystal data: $C_{70}H_{68}N7O2Zn$, 2(EtOH), M = 1204.88. Monoclinic, space group $P2_1/c$ (no. 14), a = 11.81403(15), b = 32.9326(4), c = 17.3242(2) Å, β = 103.4190(10) °, V = 6556.23(16) $Å^3$. Z = 4, Dc = 1.221 g cm^{-3}, F(000) = 2572, T = 99.99(10) K, μ(Cu-Kα) = 9.4 cm^{-1}, λ(Cu-Kα) = 1.54184 Å.

The crystal was a purple block. From a sample under oil, one, ca 0.49 x 0.15 x 0.11 mm, was mounted on a small loop and fixed in the cold nitrogen stream on a Rigaku Oxford Diffraction XtaLAB Synergy diffractometer, equipped with Cu-Kα radiation, HyPix detector and mirror monochromator. Intensity data were measured by thin-slice ω-scans. Total no. of reflections recorded, to $θ_{max}$ = 70.0°, was 49477 of which 12191 were unique (Rint = 0.051); 10680 were 'observed' with I > $2σ_I$.

Data were processed using the CrysAlisPro-CCD and -RED (1) programs. The structure was determined by the intrinsic phasing routines in the SHELXT program (2A) and refined by full-matrix least-squares methods, on F^2's, in SHELXL (2B). In the zinc complex molecule, non-hydrogen atoms were refined with anisotropic thermal parameters. Hydrogen atoms were included in idealised positions and their Uiso values were set to ride on the Ueq values of the parent carbon atoms. I have assumed that the O-ligand on the zinc centre is of an EtO⁻ group; there is no sign of a hydroxyl H atom here but we note that there is an EtOH molecule nearby, with the O…O distance at 2.684 Å. There are two discrete EtOH molecules in the crystal, each with a realistic O atom and disordered ethyl groups. At the conclusion of the refinement, wR_2 = 0.180 and R_1 = 0.069 (2B) for all 12191 reflections weighted w = $[σ^2(F_o^2) + (0.01053 P)^2 + 4.943 P]^{-1}$ with P = $(F_o^2 + 2F_c^2)/3$; for the 'observed' data only, R_1 = 0.063.

In the final difference map, the highest peak (*ca* 0.8 e$Å^{-3}$) was near C(931).

Scattering factors for neutral atoms were taken from reference (3). Computer programs used in this analysis have been noted above, and were run through WinGX (4) on a Dell Optiplex 780 PC at the University of East Anglia.

References

(1) Programs CrysAlisPro, Rigaku Oxford Diffraction Ltd., Abingdon, UK (2018).

(2) G. M. Sheldrick, Programs for crystal structure determination (SHELXT), *Acta Cryst.* (2015) A**71**, 3-8, and refinement (SHELXL), *Acta Cryst.* (2008) A**64**, 112-122 and (2015) C**71**, 3-8.

(3) 'International Tables for X-ray Crystallography', Kluwer Academic Publishers, Dordrecht (1992). Vol. C, pp. 500, 219 and 193.

(4) L. J. Farrugia, *J. Appl. Cryst.* (2012) **45**, 849–854.

Legends for Figures

Figure 1.   View of a molecule of the zinc complex molecule, indicating the atom numbering scheme. Thermal ellipsoids are drawn at the 30% probability level.

Figure 2.   View of the packing of molecules, along the *b* axis. Molecules are stacked in pairs about centres of symmetry

Figure 3.   View of the packing of molecules, along the *c* axis. Molecules are stacked in pairs about centres of symmetry

Notes on the structure

The Zn-isoindole fragment of N(61)-C(69) is overlaid about a centre of symmetry by its related group at a distance of *ca* 3.55 Å.

Crystal data and structure refinement for [Zn (TBTAP) EtOH].EtOH (84)

_____

Identification code   isabf1063z

Elemental formula   C46 H37 N7 O2 Zn, C2 H6 O

Formula weight   831.26

Crystal system, space group   Monoclinic, P2$_1$/c (no. 14)

Unit cell dimensions   a = 12.24290(10) Å   α = 90°

                                             b = 24.68004(19) Å   β = 96.3005(7)°

                                             c = 13.24798(10) Å   γ = 90°

Volume   3978.77(6) Å^3

Z, Calculated density   4,   1.388 Mg/m^3

F(000)   1736

Absorption coefficient   1.282 mm^{-1}

Temperature   100(2) K

Wavelength   1.54184 Å

Crystal colour, shape   purple prism

Crystal size   0.26 x 0.25 x 0.26 mm

Crystal mounting: on a small loop, in oil, fixed in cold N2 stream

On the diffractometer:

  Theta range for data collection   7.887 to 72.465 °

  Limiting indices   -14<=h<=14, -29<=k<=30, -15<=l<=16

  Completeness to theta = 67.684   99.6 %

Reflections collected (not including absences) 31127

No. of unique reflections   7727 [R(int) for equivalents = 0.033]

No. of 'observed' reflections (I > 2σ$_I$)   7053

Structure determined by: dual methods, in SHELXT

Refinement: Full-matrix least-squares on F^2, in SHELXL

Data / restraints / parameters   7727 / 0 / 620

Goodness-of-fit on F^2 1.029

Final R indices ('observed' data) $R_1 = 0.041$, $wR_2 = 0.103$

Final R indices (all data) $R_1 = 0.045$, $wR_2 = 0.105$

Reflections weighted:
   $w = [\sigma^2(Fo^2)+(0.0466P)^2+4.0016P]^{-1}$ where $P=(Fo^2+2Fc^2)/3$

Extinction coefficient   n/a

Largest diff. peak and hole   0.68 and -0.44 e.Å^{-3}

Location of largest difference peak   near C(6)

Table 1. Atomic coordinates (x 10^5) and equivalent isotropic
          displacement parameters (Å^2 x 10^4). U(eq) is defined
          as one third of the trace of the orthogonalized Uij
          tensor. E.s.ds are in parentheses.

	x	y	z	U(eq)	S.o.f.#
Zn	26122(2)	92649(2)	44038(2)	188.3(9)	
N(1)	36856(13)	87508(7)	51721(12)	217(3)	
C(2)	37550(15)	82004(8)	50247(14)	221(4)	
C(3)	46596(16)	79898(9)	57482(15)	265(4)	
C(4)	51705(18)	74859(9)	59286(18)	327(5)	
C(5)	60814(19)	74622(10)	66590(20)	401(6)	
C(6)	64849(19)	79140(10)	72113(19)	408(6)	
C(7)	60017(18)	84109(10)	70335(17)	335(5)	
C(8)	50931(17)	84394(9)	63047(15)	271(4)	
C(9)	44645(16)	89051(9)	59288(14)	240(4)	
N(10)	46900(13)	94015(7)	63145(12)	253(4)	
N(11)	34366(13)	98996(7)	51239(12)	217(3)	
C(12)	42214(15)	98489(8)	59436(14)	230(4)	
C(13)	44999(16)	103877(9)	63575(15)	269(4)	
C(14)	52423(18)	105622(10)	71619(16)	329(5)	
C(15)	53173(19)	111212(11)	73340(18)	380(6)	
C(16)	46878(18)	114878(10)	67254(18)	358(5)	
C(17)	39549(18)	113146(9)	59249(17)	302(5)	
C(18)	38678(16)	107561(9)	57557(15)	258(4)	
C(19)	32137(15)	104354(8)	49788(14)	223(4)	
N(20)	25286(13)	106645(7)	42505(13)	232(3)	
N(21)	19725(13)	98289(6)	33755(12)	204(3)	
C(22)	19945(16)	103766(8)	34965(14)	217(4)	
C(23)	13113(16)	106328(8)	26563(15)	227(4)	
C(24)	10628(17)	111737(8)	24164(16)	275(4)	
C(25)	3578(18)	112740(9)	15437(17)	318(5)	
C(26)	-991(19)	108506(9)	9343(16)	315(5)	
C(27)	1379(17)	103137(9)	11824(15)	261(4)	
C(28)	8650(16)	102111(8)	20390(14)	218(4)	
C(29)	12986(15)	97089(8)	25096(14)	199(4)	
N(30)	10274(13)	92246(6)	21295(12)	200(3)	
N(31)	21509(12)	86749(6)	33770(11)	191(3)	
C(32)	14139(15)	87571(8)	25439(13)	191(4)	
C(33)	10609(16)	82390(8)	21120(14)	220(4)	
C(34)	2866(17)	81177(9)	12905(15)	269(4)	

Atom	x	y	z	U(eq)	Occ.
C(35)	990(20)	75778(9)	10562(16)	340(5)	
C(36)	6750(20)	71731(9)	16272(17)	359(5)	
C(37)	14353(19)	72898(8)	24496(16)	305(5)	
C(38)	16372(16)	78368(8)	27039(14)	229(4)	
C(39)	23344(15)	81278(8)	35043(14)	205(4)	
C(40)	30947(16)	79073(8)	42741(14)	219(4)	
C(41)	32066(17)	73046(8)	43138(15)	242(4)	
C(42)	38270(20)	70186(9)	36747(17)	349(5)	
C(43)	39280(20)	64618(10)	37590(20)	441(6)	
C(44)	34090(20)	61798(9)	44840(20)	394(5)	
C(45)	27833(17)	64576(9)	51179(16)	293(4)	
C(46)	26916(16)	70152(8)	50308(14)	246(4)	
O(47)	37300(70)	56470(60)	46220(140)	290(20)	0.4
O(471)	33890(70)	56190(60)	45300(120)	280(20)	0.4
C(48)	30240(30)	53323(13)	53160(30)	317(6)	0.75
C(49)	33870(40)	47523(14)	53120(30)	555(10)	0.8
C(50)	29080(60)	44630(20)	43050(40)	377(14)	0.45
C(51)	33300(70)	38870(20)	42460(50)	660(20)	0.55
C(52)	28240(40)	35270(20)	50130(40)	500(10)	0.7
C(48A)	31800(90)	52720(50)	48310(100)	330(20)*	0.25
C(49A)	33500(110)	46650(50)	44390(100)	690(30)*	0.35
C(50A)	29290(80)	42560(40)	50990(80)	500(20)*	0.3
C(51A)	30670(120)	37340(60)	45340(130)	660(40)*	0.3
C(52A)	26850(90)	32340(50)	52860(90)	570(30)*	0.3
O(47B)	36620(130)	56140(50)	41660(80)	350(30)*	0.2
C(50C)	28680(140)	44410(70)	37540(150)	560(40)*	0.2
C(50D)	19480(160)	40810(80)	40600(150)	740(50)*	0.2
C(50E)	39500(150)	45020(80)	44380(130)	620(40)*	0.2
O(61)	12818(14)	92027(7)	52899(12)	347(4)	
C(62)	10660(40)	96280(20)	59800(40)	382(13)	0.648(9)
C(63)	17090(40)	94930(30)	69810(40)	633(18)	0.648(9)
C(64)	14140(60)	93800(30)	63730(50)	236(19)	0.352(9)
C(65)	10380(70)	99560(30)	63620(70)	450(30)	0.352(9)
O(71)	-7473(15)	87466(8)	48604(14)	483(4)	
C(72)	-10520(20)	86233(17)	37980(20)	639(10)	0.826(5)
C(73)	-12650(30)	80595(15)	35190(30)	499(9)	0.826(5)
O(74)	-1730(110)	84390(50)	44790(100)	610(40)*	0.174(5)

_____

```
      C(75)   -10520(20)    86233(17)    37980(20)    639(10)
0.174(5)
      C(76)   -12750(100)   89060(50)    31200(100)   290(30)*
0.174(5)
```

_____

```
           # - site occupancy, if different from 1.
           * - U(iso) (Å² x 10⁴)
```

Table 2. Molecular dimensions. Bond lengths are in Ångstroms,
              angles in degrees. E.s.ds are in parentheses.

_____

Zn-N(1)	Zn-N(21)
2.0197(16)	2.0427(16)
Zn-N(31)	Zn-O(61)
2.0301(16)	2.1152(16)
Zn-N(11)	
2.0424(16)	

N(1)-Zn-N(31)	N(11)-Zn-N(21)
90.28(6)	85.56(7)
N(1)-Zn-N(11)	N(1)-Zn-O(61)
89.17(7)	99.95(7)
N(31)-Zn-N(11)	N(31)-Zn-O(61)
161.81(6)	98.36(6)
N(1)-Zn-N(21)	N(11)-Zn-O(61)
160.87(6)	99.65(6)
N(31)-Zn-N(21)	N(21)-Zn-O(61)
89.07(6)	99.05(7)

N(1)-C(9)	C(13)-C(18)
1.360(2)	1.388(3)
N(1)-C(2)	C(13)-C(14)
1.376(3)	1.391(3)
C(2)-C(40)	C(14)-C(15)
1.410(3)	1.400(3)
C(2)-C(3)	C(15)-C(16)
1.477(3)	1.388(4)
C(3)-C(4)	C(16)-C(17)
1.401(3)	1.380(3)
C(3)-C(8)	C(17)-C(18)
1.404(3)	1.399(3)
C(4)-C(5)	C(18)-C(19)
1.395(3)	1.465(3)
C(5)-C(6)	C(19)-N(20)
1.394(4)	1.333(3)
C(6)-C(7)	N(20)-C(22)
1.371(3)	1.337(3)
C(7)-C(8)	N(21)-C(22)
1.393(3)	1.361(2)
C(8)-C(9)	N(21)-C(29)
1.441(3)	1.370(2)
C(9)-N(10)	C(22)-C(23)
1.344(3)	1.461(3)
N(10)-C(12)	C(23)-C(28)
1.314(3)	1.397(3)
N(11)-C(19)	C(23)-C(24)
1.360(3)	1.398(3)
N(11)-C(12)	C(24)-C(25)
1.374(2)	1.387(3)
C(12)-C(13)	C(25)-C(26)
1.464(3)	1.399(3)

C(26)-C(27)
1.388(3)
C(27)-C(28)
1.387(3)
C(28)-C(29)
1.461(3)
C(29)-N(30)
1.325(2)
N(30)-C(32)
1.341(2)
N(31)-C(32)
1.362(2)
N(31)-C(39)
1.376(2)
C(32)-C(33)
1.447(3)
C(33)-C(34)
1.395(3)
C(33)-C(38)
1.406(3)
C(34)-C(35)
1.382(3)
C(35)-C(36)
1.396(3)
C(36)-C(37)
1.384(3)
C(37)-C(38)
1.407(3)
C(38)-C(39)
1.473(3)
C(39)-C(40)
1.412(3)
C(40)-C(41)
1.494(3)
C(41)-C(42)
1.390(3)
C(41)-C(46)
1.393(3)
C(42)-C(43)
1.383(3)
C(43)-C(44)
1.395(4)
C(44)-O(47)
1.378(14)
C(44)-C(45)
1.379(3)
C(44)-O(471)
1.386(15)
C(44)-O(47B)
1.501(11)

C(45)-C(46)
1.384(3)
O(47)-C(48)
1.540(16)
O(471)-C(48)
1.374(14)
C(48)-C(49)
1.499(4)
C(48)-H(481)
1.04(4)
C(48)-H(482)
0.94(3)
C(49)-C(50)
1.568(8)
C(50)-C(51)
1.518(7)
C(51)-C(52)
1.531(7)
C(48A)-C(49A)
1.607(17)
C(49A)-C(50A)
1.466(16)
C(50A)-C(51A)
1.510(17)
C(51A)-C(52A)
1.68(2)
C(50C)-C(50D)
1.52(3)
C(50C)-C(50E)
1.53(2)
O(61)-C(62)
1.435(5)
O(61)-C(64)
1.493(7)
O(61)-H(61)
0.70(3)
C(62)-C(63)
1.504(8)
C(64)-C(65)
1.493(11)

O(71)-C(72)
1.448(3)
C(72)-C(73)
1.456(5)
O(74)-C(75)
1.402(13)
C(75)-C(76)
1.146(13)

C(9)-N(1)-C(2)
109.37(16)
C(9)-N(1)-Zn
124.09(14)
C(2)-N(1)-Zn
126.54(13)
N(1)-C(2)-C(40)
124.52(17)
N(1)-C(2)-C(3)
107.98(17)

C(40)-C(2)-C(3)
127.44(18)
C(4)-C(3)-C(8)
118.43(19)
C(4)-C(3)-C(2)
135.4(2)
C(8)-C(3)-C(2)
106.02(18)
C(5)-C(4)-C(3)
117.6(2)

243

C(6)-C(5)-C(4)	C(22)-N(21)-C(29)
122.7(2)	108.40(16)
C(7)-C(6)-C(5)	C(22)-N(21)-Zn
120.3(2)	126.66(13)
C(6)-C(7)-C(8)	C(29)-N(21)-Zn
117.5(2)	124.24(13)
C(7)-C(8)-C(3)	N(20)-C(22)-N(21)
123.5(2)	128.14(18)
C(7)-C(8)-C(9)	N(20)-C(22)-C(23)
129.5(2)	122.11(18)
C(3)-C(8)-C(9)	N(21)-C(22)-C(23)
106.99(17)	109.75(16)
N(10)-C(9)-N(1)	C(28)-C(23)-C(24)
129.30(19)	121.12(19)
N(10)-C(9)-C(8)	C(28)-C(23)-C(22)
121.06(18)	106.14(17)
N(1)-C(9)-C(8)	C(24)-C(23)-C(22)
109.63(18)	132.74(19)
C(12)-N(10)-C(9)	C(25)-C(24)-C(23)
124.09(17)	117.38(19)
C(19)-N(11)-C(12)	C(24)-C(25)-C(26)
108.21(16)	121.36(19)
C(19)-N(11)-Zn	C(27)-C(26)-C(25)
126.77(13)	121.1(2)
C(12)-N(11)-Zn	C(28)-C(27)-C(26)
124.47(14)	117.8(2)
N(10)-C(12)-N(11)	C(27)-C(28)-C(23)
127.62(18)	121.17(18)
N(10)-C(12)-C(13)	C(27)-C(28)-C(29)
123.28(18)	132.44(18)
N(11)-C(12)-C(13)	C(23)-C(28)-C(29)
109.08(18)	106.36(17)
C(18)-C(13)-C(14)	N(30)-C(29)-N(21)
120.9(2)	128.03(17)
C(18)-C(13)-C(12)	N(30)-C(29)-C(28)
106.72(17)	122.61(17)
C(14)-C(13)-C(12)	N(21)-C(29)-C(28)
132.4(2)	109.34(16)
C(13)-C(14)-C(15)	C(29)-N(30)-C(32)
117.1(2)	123.91(16)
C(16)-C(15)-C(14)	C(32)-N(31)-C(39)
121.7(2)	109.28(15)
C(17)-C(16)-C(15)	C(32)-N(31)-Zn
121.2(2)	123.16(12)
C(16)-C(17)-C(18)	C(39)-N(31)-Zn
117.4(2)	126.30(12)
C(13)-C(18)-C(17)	N(30)-C(32)-N(31)
121.71(19)	129.23(17)
C(13)-C(18)-C(19)	N(30)-C(32)-C(33)
106.08(18)	121.43(16)
C(17)-C(18)-C(19)	N(31)-C(32)-C(33)
132.2(2)	109.34(16)
N(20)-C(19)-N(11)	C(34)-C(33)-C(38)
127.99(17)	122.69(18)
N(20)-C(19)-C(18)	C(34)-C(33)-C(32)
122.10(18)	130.22(19)
N(11)-C(19)-C(18)	C(38)-C(33)-C(32)
109.90(17)	107.06(16)
C(19)-N(20)-C(22)	C(35)-C(34)-C(33)
122.20(17)	117.6(2)

C(34)-C(35)-C(36)
120.4(2)
C(37)-C(36)-C(35)
122.3(2)
C(36)-C(37)-C(38)
118.3(2)
C(33)-C(38)-C(37)
118.67(18)
C(33)-C(38)-C(39)
105.84(16)
C(37)-C(38)-C(39)
135.47(19)
N(31)-C(39)-C(40)
123.53(17)
N(31)-C(39)-C(38)
108.44(16)
C(40)-C(39)-C(38)
128.02(18)
C(2)-C(40)-C(39)
126.36(18)
C(2)-C(40)-C(41)
116.26(17)
C(39)-C(40)-C(41)
117.37(17)
C(42)-C(41)-C(46)
118.23(19)
C(42)-C(41)-C(40)
122.56(18)
C(46)-C(41)-C(40)
119.20(18)
C(43)-C(42)-C(41)
120.3(2)
C(42)-C(43)-C(44)
120.5(2)
O(47)-C(44)-C(45)
124.3(8)
C(45)-C(44)-O(471)
117.2(6)
O(47)-C(44)-C(43)
115.0(7)
C(45)-C(44)-C(43)
119.8(2)
O(471)-C(44)-C(43)
122.7(6)
C(45)-C(44)-O(47B)
141.2(6)
C(43)-C(44)-O(47B)
98.4(5)
C(44)-C(45)-C(46)
119.3(2)
C(45)-C(46)-C(41)
121.9(2)
C(44)-O(47)-C(48)
112.9(10)

C(48)-O(471)-C(44)
123.8(12)
O(471)-C(48)-C(49)
111.6(7)
C(49)-C(48)-O(47)
107.1(6)
O(471)-C(48)-H(481)
99.1(19)
C(49)-C(48)-H(481)
108.3(19)
O(47)-C(48)-H(481)
114.4(19)
O(471)-C(48)-H(482)
115(2)
C(49)-C(48)-H(482)
111.6(19)
O(47)-C(48)-H(482)
105(2)
H(481)-C(48)-H(482)
110(3)
C(48)-C(49)-C(50)
110.8(3)
C(51)-C(50)-C(49)
111.9(5)
C(50)-C(51)-C(52)
110.2(4)
C(49A)-C(48A)-H(481)
111.7(17)
C(50A)-C(49A)-C(48A)
112.5(10)
C(49A)-C(50A)-C(51A)
103.0(11)
C(50A)-C(51A)-C(52A)
106.2(11)
C(50D)-C(50C)-C(50E)
121.2(16)
C(62)-O(61)-Zn
120.46(18)
C(64)-O(61)-Zn
120.2(3)
C(62)-O(61)-H(61)
105(3)
C(64)-O(61)-H(61)
113(3)
Zn-O(61)-H(61)
126(2)
O(61)-C(62)-C(63)
106.6(5)
O(61)-C(64)-C(65)
105.6(7)

O(71)-C(72)-C(73)
117.9(3)
C(76)-C(75)-O(74)
143.3(9)

Table 3.   Anisotropic displacement parameters (Å^2 x 10^4) for the
expression:
$$\exp\{-2\pi^2(h^2a^{*2}U_{11} + \ldots + 2hka^*b^*U_{12})\}$$
E.s.ds are in parentheses.

	U_{11}	U_{22}	U_{33}	U_{23}	U_{13}	U_{12}
Zn	182.0(14)	208.3(14)	173.7(14)	-23.1(9)	14.7(9)	-11.5(9)
N(1)	206(8)	267(8)	178(7)	9(6)	24(6)	-4(6)
C(2)	201(9)	260(10)	212(9)	59(7)	61(7)	15(7)
C(3)	219(10)	336(11)	247(10)	119(8)	57(8)	-9(8)
C(4)	268(11)	308(11)	405(12)	148(9)	40(9)	-5(9)
C(5)	292(11)	374(13)	531(15)	242(11)	17(10)	23(10)
C(6)	278(11)	451(14)	467(14)	228(11)	-87(10)	-84(10)
C(7)	273(11)	412(13)	307(11)	150(9)	-21(8)	-80(9)
C(8)	236(10)	359(11)	223(9)	96(8)	42(8)	-48(8)
C(9)	190(9)	362(11)	175(9)	42(8)	44(7)	-26(8)
N(10)	207(8)	368(10)	186(8)	-20(7)	34(6)	-55(7)
N(11)	183(8)	278(9)	193(8)	-34(6)	38(6)	-43(6)
C(12)	175(9)	341(11)	180(9)	-43(8)	48(7)	-62(8)
C(13)	210(10)	380(12)	233(10)	-97(8)	96(7)	-94(8)
C(14)	250(10)	493(13)	254(10)	-126(9)	67(8)	-91(10)
C(15)	292(11)	526(15)	343(12)	-242(11)	125(9)	-178(11)
C(16)	312(11)	394(13)	393(12)	-187(10)	159(10)	-130(10)
C(17)	274(10)	307(11)	352(11)	-125(9)	150(9)	-91(9)
C(18)	201(9)	341(11)	249(10)	-93(8)	99(8)	-83(8)
C(19)	194(9)	248(10)	240(9)	-66(8)	84(7)	-64(7)
N(20)	222(8)	224(8)	258(8)	-49(6)	64(6)	-46(6)
N(21)	202(8)	204(8)	207(8)	-29(6)	25(6)	-8(6)
C(22)	211(9)	211(9)	241(9)	-16(7)	84(7)	-13(7)
C(23)	211(9)	227(9)	255(10)	2(7)	84(7)	-8(7)
C(24)	298(11)	212(10)	330(11)	11(8)	109(8)	-7(8)
C(25)	355(12)	251(10)	362(12)	105(9)	106(9)	52(9)
C(26)	325(11)	357(12)	267(10)	86(9)	50(8)	56(9)

C(27)	270(10)	304(11)	216(9)	22(8)	52(8)	17(8)
C(28)	226(9)	221(9)	219(9)	8(7)	80(7)	8(7)
C(29)	187(9)	226(9)	188(9)	−1(7)	38(7)	12(7)
N(30)	204(8)	214(8)	186(7)	−17(6)	36(6)	1(6)
N(31)	188(7)	204(8)	185(7)	−11(6)	34(6)	11(6)
C(32)	182(9)	218(9)	177(8)	−29(7)	34(7)	−6(7)
C(33)	241(9)	221(9)	204(9)	−16(7)	46(7)	−27(7)
C(34)	289(10)	283(10)	231(9)	−20(8)	13(8)	−51(8)
C(35)	407(13)	339(12)	264(10)	−58(9)	−1(9)	−128(10)
C(36)	513(14)	225(10)	344(11)	−50(9)	63(10)	−119(10)
C(37)	408(12)	212(10)	299(11)	−4(8)	50(9)	−39(9)
C(38)	265(10)	217(9)	215(9)	−11(7)	65(7)	−16(8)
C(39)	219(9)	203(9)	202(9)	−7(7)	65(7)	−5(7)
C(40)	217(9)	237(10)	217(9)	27(7)	86(7)	11(7)
C(41)	272(10)	224(10)	231(9)	41(7)	33(8)	27(8)
C(42)	455(13)	280(11)	339(11)	58(9)	169(10)	86(10)
C(43)	553(16)	313(12)	487(14)	34(10)	186(12)	169(11)
C(44)	428(13)	248(11)	495(14)	102(10)	8(11)	65(10)
C(45)	300(11)	281(11)	286(10)	86(8)	−28(8)	−34(8)
C(46)	261(10)	266(10)	207(9)	22(8)	2(7)	−38(8)
O(47)	250(50)	150(20)	470(50)	50(20)	50(50)	30(40)
O(471)	210(50)	280(40)	410(50)	180(30)	240(40)	110(40)
C(48)	447(19)	257(15)	257(16)	69(13)	78(14)	33(13)
C(49)	860(30)	349(18)	500(20)	151(15)	259(19)	166(18)
C(50)	780(50)	230(30)	140(30)	79(19)	130(20)	190(30)
C(51)	1170(60)	340(30)	590(40)	200(30)	560(40)	260(30)
C(52)	550(20)	470(20)	490(20)	−40(20)	90(20)	90(20)
O(61)	249(8)	462(10)	348(9)	−177(7)	115(7)	−152(7)
C(62)	350(20)	400(30)	440(30)	−110(20)	213(19)	−76(19)
C(63)	440(30)	1150(50)	340(30)	−240(30)	180(20)	−330(30)

C(64)	240(30)	320(40)	150(40)	−10(30)	60(30)	−50(30)
C(65)	500(50)	350(50)	580(50)	−70(40)	350(40)	−70(30)
O(71)	362(9)	609(12)	476(10)	−120(9)	37(8)	−56(8)
C(72)	325(14)	1160(30)	451(16)	−267(18)	114(12)	−250(16)
C(73)	484(19)	620(20)	409(17)	−11(15)	111(14)	26(16)
C(75)	325(14)	1160(30)	451(16)	−267(18)	114(12)	−250(16)

Table 4. Hydrogen coordinates (x 10^4) and isotropic displacement
        parameters (Å^2 x 10^3). The hydroxyl hydrogen of O(61)
        and the methylene hydrogens of C(48) were clear in
        difference maps and were refined freely; all remaining
        hydrogen atoms were included in idealised positions with
        U(iso)'s set at 1.2*U(eq) or, for the methyl group
        hydrogen atoms, 1.5*U(eq) of the parent carbon atoms.

	x	y	z	U(iso)	S.o.f.#
H(4)	4906	7172	5567	39	
H(5)	6442	7124	6786	48	
H(6)	7097	7877	7713	49	
H(7)	6276	8724	7394	40	
H(14)	5680	10313	7577	39	
H(15)	5812	11253	7882	46	
H(16)	4763	11865	6862	43	
H(17)	3526	11565	5505	36	
H(24)	1365	11461	2835	33	
H(25)	182	11638	1356	38	
H(26)	-579	10932	341	38	
H(27)	-187	10026	779	31	
H(34)	-98	8397	906	32	
H(35)	-425	7481	503	41	
H(36)	539	6805	1445	43	
H(37)	1811	7008	2833	37	
H(42)	4183	7207	3178	42	
H(43)	4354	6270	3319	53	
H(45)	2420	6268	5609	35	
H(46)	2266	7206	5472	30	
H(49A)	3134	4561	5901	67	0.8
H(49B)	4199	4736	5376	67	0.8
H(50A)	2096	4457	4267	45	0.45
H(50B)	3113	4672	3716	45	0.45
H(51A)	4141	3884	4394	80	0.55
H(51B)	3138	3743	3552	80	0.55
H(52A)	3102	3156	4968	60	0.7
H(52B)	3023	3667	5700	60	0.7
H(52C)	2022	3526	4860	60	0.7
H(49C)	2970	4626	3744	82	0.35
H(49D)	4144	4601	4405	82	0.35
H(50C)	2147	4324	5184	60	0.3
H(50D)	3362	4251	5776	60	0.3
H(51C)	3841	3686	4402	80	0.3
H(51D)	2597	3734	3876	80	0.3

H(52D)	2759	2884	4952	68	0.3
H(52E)	3156	3240	5934	68	0.3
H(52F)	1918	3288	5410	68	0.3
H(62A)	271	9647	6053	46	0.648(9)
H(62B)	1304	9982	5727	46	0.648(9)
H(63A)	1586	9774	7479	95	0.648(9)
H(63B)	1466	9142	7221	95	0.648(9)
H(63C)	2493	9475	6897	95	0.648(9)
H(64A)	2192	9353	6664	28	0.352(9)
H(64B)	961	9154	6782	28	0.352(9)
H(65A)	1106	10097	7058	68	0.352(9)
H(65B)	1493	10174	5952	68	0.352(9)
H(65C)	269	9976	6069	68	0.352(9)
H(72A)	-457	8756	3412	77	0.826(5)
H(72B)	-1720	8835	3566	77	0.826(5)
H(73A)	-597	7845	3695	75	0.826(5)
H(73B)	-1485	8035	2786	75	0.826(5)
H(73C)	-1856	7919	3887	75	0.826(5)
H(75A)	-1367	8276	3528	77	0.174(5)
H(75B)	-1569	8749	4272	77	0.174(5)
H(76A)	-1366	8692	2492	44	0.174(5)
H(76B)	-686	9171	3082	44	0.174(5)
H(76C)	-1963	9095	3205	44	0.174(5)
H(481)	2190(30)	5346(14)	5090(30)	65(10)	
H(482)	3180(30)	5490(13)	5960(20)	56(9)	
H(61)	770(30)	9084(13)	5140(20)	43(9)	

- site occupancy, if different from 1.

Table 5. Torsion angles, in degrees. E.s.ds are in parentheses.

C(9)-N(1)-C(2)-C(40)	- 177.69(17)	Zn-N(1)-C(2)-C(3) 179.64(12)
Zn-N(1)-C(2)-C(40) 2.2(3)		N(1)-C(2)-C(3)-C(4) - 175.2(2)
C(9)-N(1)-C(2)-C(3) 0.3(2)	-	C(40)-C(2)-C(3)-C(4) 2.1(4)

Angle	Value	Angle	Value
N(1)-C(2)-C(3)-C(8)	0.0(2)	N(11)-C(12)-C(13)-C(18)	-0.5(2)
C(40)-C(2)-C(3)-C(8)	177.34(18)	N(10)-C(12)-C(13)-C(14)	-0.2(3)
C(8)-C(3)-C(4)-C(5)	0.3(3)	N(11)-C(12)-C(13)-C(14)	-179.0(2)
C(2)-C(3)-C(4)-C(5)	175.2(2)	C(18)-C(13)-C(14)-C(15)	0.2(3)
C(3)-C(4)-C(5)-C(6)	0.6(4)	C(12)-C(13)-C(14)-C(15)	178.4(2)
C(4)-C(5)-C(6)-C(7)	-1.5(4)	C(13)-C(14)-C(15)-C(16)	-0.6(3)
C(5)-C(6)-C(7)-C(8)	1.3(3)	C(14)-C(15)-C(16)-C(17)	0.3(3)
C(6)-C(7)-C(8)-C(3)	-0.4(3)	C(15)-C(16)-C(17)-C(18)	0.4(3)
C(6)-C(7)-C(8)-C(9)	-176.5(2)	C(14)-C(13)-C(18)-C(17)	0.5(3)
C(4)-C(3)-C(8)-C(7)	-0.4(3)	C(12)-C(13)-C(18)-C(17)	-178.12(18)
C(2)-C(3)-C(8)-C(7)	-176.68(19)	C(14)-C(13)-C(18)-C(19)	178.45(18)
C(4)-C(3)-C(8)-C(9)	176.44(18)	C(12)-C(13)-C(18)-C(19)	-0.2(2)
C(2)-C(3)-C(8)-C(9)	0.2(2)	C(16)-C(17)-C(18)-C(13)	-0.8(3)
C(2)-N(1)-C(9)-N(10)	179.71(18)	C(16)-C(17)-C(18)-C(19)	-178.1(2)
Zn-N(1)-C(9)-N(10)	-0.2(3)	C(12)-N(11)-C(19)-N(20)	177.81(18)
C(2)-N(1)-C(9)-C(8)	0.4(2)	Zn-N(11)-C(19)-N(20)	-10.5(3)
Zn-N(1)-C(9)-C(8)	-179.51(12)	C(12)-N(11)-C(19)-C(18)	-1.2(2)
C(7)-C(8)-C(9)-N(10)	-3.1(3)	Zn-N(11)-C(19)-C(18)	170.47(12)
C(3)-C(8)-C(9)-N(10)	-179.75(17)	C(13)-C(18)-C(19)-N(20)	-178.23(17)
C(7)-C(8)-C(9)-N(1)	176.2(2)	C(17)-C(18)-C(19)-N(20)	-0.6(3)
C(3)-C(8)-C(9)-N(1)	-0.4(2)	C(13)-C(18)-C(19)-N(11)	0.9(2)
N(1)-C(9)-N(10)-C(12)	-6.0(3)	C(17)-C(18)-C(19)-N(11)	178.5(2)
C(8)-C(9)-N(10)-C(12)	173.22(18)	N(11)-C(19)-N(20)-C(22)	-4.2(3)
C(9)-N(10)-C(12)-N(11)	0.2(3)	C(18)-C(19)-N(20)-C(22)	174.79(17)
C(9)-N(10)-C(12)-C(13)	-178.26(18)	C(19)-N(20)-C(22)-N(21)	5.6(3)
C(19)-N(11)-C(12)-N(10)	-177.56(18)	C(19)-N(20)-C(22)-C(23)	-175.11(17)
Zn-N(11)-C(12)-N(10)	10.5(3)	C(29)-N(21)-C(22)-N(20)	178.43(18)
C(19)-N(11)-C(12)-C(13)	1.1(2)	Zn-N(21)-C(22)-N(20)	7.8(3)
Zn-N(11)-C(12)-C(13)	-170.84(12)	C(29)-N(21)-C(22)-C(23)	-0.9(2)
N(10)-C(12)-C(13)-C(18)	178.20(18)	Zn-N(21)-C(22)-C(23)	-171.60(12)

N(20)-C(22)-C(23)-C(28) 178.33(17)	-	Zn-N(31)-C(32)-C(33) 166.00(12)	-
N(21)-C(22)-C(23)-C(28) 1.1(2)		N(30)-C(32)-C(33)-C(34) 3.2(3)	-
N(20)-C(22)-C(23)-C(24) 1.0(3)		N(31)-C(32)-C(33)-C(34) 176.89(19)	
N(21)-C(22)-C(23)-C(24) 179.6(2)	-	N(30)-C(32)-C(33)-C(38) 178.40(17)	
C(28)-C(23)-C(24)-C(25) 0.0(3)		N(31)-C(32)-C(33)-C(38) 1.5(2)	-
C(22)-C(23)-C(24)-C(25) 179.3(2)	-	C(38)-C(33)-C(34)-C(35) 0.6(3)	-
C(23)-C(24)-C(25)-C(26) 0.9(3)		C(32)-C(33)-C(34)-C(35) 178.8(2)	-
C(24)-C(25)-C(26)-C(27) 0.0(3)		C(33)-C(34)-C(35)-C(36) 0.2(3)	-
C(25)-C(26)-C(27)-C(28) 1.7(3)	-	C(34)-C(35)-C(36)-C(37) 0.9(4)	
C(26)-C(27)-C(28)-C(23) 2.5(3)		C(35)-C(36)-C(37)-C(38) 0.7(3)	-
C(26)-C(27)-C(28)-C(29) 179.4(2)	-	C(34)-C(33)-C(38)-C(37) 0.8(3)	
C(24)-C(23)-C(28)-C(27) 1.7(3)	-	C(32)-C(33)-C(38)-C(37) 179.35(18)	
C(22)-C(23)-C(28)-C(27) 177.74(17)		C(34)-C(33)-C(38)-C(39) 178.02(18)	-
C(24)-C(23)-C(28)-C(29) 179.76(17)		C(32)-C(33)-C(38)-C(39) 0.5(2)	
C(22)-C(23)-C(28)-C(29) 0.8(2)	-	C(36)-C(37)-C(38)-C(33) 0.1(3)	-
C(22)-N(21)-C(29)-N(30) 178.07(18)	-	C(36)-C(37)-C(38)-C(39) 178.3(2)	
Zn-N(21)-C(29)-N(30) 7.1(3)	-	C(32)-N(31)-C(39)-C(40) 177.07(17)	
C(22)-N(21)-C(29)-C(28) 0.4(2)		Zn-N(31)-C(39)-C(40) 15.5(3)	-
Zn-N(21)-C(29)-C(28) 171.38(12)		C(32)-N(31)-C(39)-C(38) 1.6(2)	-
C(27)-C(28)-C(29)-N(30) 0.6(3)		Zn-N(31)-C(39)-C(38) 165.86(12)	
C(23)-C(28)-C(29)-N(30) 178.84(17)		C(33)-C(38)-C(39)-N(31) 0.6(2)	
C(27)-C(28)-C(29)-N(21) 178.0(2)	-	C(37)-C(38)-C(39)-N(31) 177.9(2)	-
C(23)-C(28)-C(29)-N(21) 0.3(2)		C(33)-C(38)-C(39)-C(40) 177.94(18)	-
N(21)-C(29)-N(30)-C(32) 1.8(3)	-	C(37)-C(38)-C(39)-C(40) 3.5(4)	
C(28)-C(29)-N(30)-C(32) 179.88(17)		N(1)-C(2)-C(40)-C(39) 5.9(3)	
C(29)-N(30)-C(32)-N(31) 2.1(3)	-	C(3)-C(2)-C(40)-C(39) 170.98(18)	-
C(29)-N(30)-C(32)-C(33) 178.01(17)		N(1)-C(2)-C(40)-C(41) 173.19(17)	-
C(39)-N(31)-C(32)-N(30) 177.97(18)	-	C(3)-C(2)-C(40)-C(41) 9.9(3)	
Zn-N(31)-C(32)-N(30) 14.1(3)		N(31)-C(39)-C(40)-C(2) 1.2(3)	
C(39)-N(31)-C(32)-C(33) 1.9(2)		C(38)-C(39)-C(40)-C(2) 179.51(18)	

N(31)-C(39)-C(40)-C(41) -179.76(17)	C(40)-C(41)-C(46)-C(45) -178.69(18)
C(38)-C(39)-C(40)-C(41) -1.4(3)	C(45)-C(44)-O(47)-C(48) 19.5(11)
C(2)-C(40)-C(41)-C(42) -100.9(2)	O(471)-C(44)-O(47)-C(48) -52(4)
C(39)-C(40)-C(41)-C(42) 79.9(3)	C(43)-C(44)-O(47)-C(48) -172.0(6)
C(2)-C(40)-C(41)-C(46) 77.7(2)	O(47)-C(44)-O(471)-C(48) 101(5)
C(39)-C(40)-C(41)-C(46) -101.5(2)	C(45)-C(44)-O(471)-C(48) -16.8(11)
C(46)-C(41)-C(42)-C(43) -0.3(3)	C(43)-C(44)-O(471)-C(48) 170.4(6)
C(40)-C(41)-C(42)-C(43) 178.3(2)	C(44)-O(471)-C(48)-C(49) -163.9(7)
C(41)-C(42)-C(43)-C(44) 0.1(4)	C(44)-O(471)-C(48)-O(47) -88(5)
C(42)-C(43)-C(44)-O(47) -168.6(6)	C(44)-O(47)-C(48)-O(471) 65(4)
C(42)-C(43)-C(44)-C(45) 0.5(4)	C(44)-O(47)-C(48)-C(49) 174.3(7)
C(42)-C(43)-C(44)-O(471) 173.1(6)	O(471)-C(48)-C(49)-C(50) -61.2(7)
C(42)-C(43)-C(44)-O(47B) 173.4(6)	O(47)-C(48)-C(49)-C(50) -77.1(7)
O(47)-C(44)-C(45)-C(46) 167.2(6)	C(48)-C(49)-C(50)-C(51) 175.8(5)
O(471)-C(44)-C(45)-C(46) -173.8(6)	C(49)-C(50)-C(51)-C(52) 70.8(8)
C(43)-C(44)-C(45)-C(46) -0.7(3)	C(48A)-C(49A)-C(50A)-C(51A) 174.3(10)
O(47B)-C(44)-C(45)-C(46) -169.6(9)	C(49A)-C(50A)-C(51A)-C(52A) 176.0(10)
C(44)-C(45)-C(46)-C(41) 0.5(3)	Zn-O(61)-C(62)-C(63) -90.1(3)
C(42)-C(41)-C(46)-C(45) 0.0(3)	Zn-O(61)-C(64)-C(65) 93.1(5)

Table 6. Hydrogen bonds, in Ångstroms and degrees.

D-H...A	d(D-H)	d(H...A)	d(D...A)	<(DHA)
O(61)-H(61)...O(71^c)	0.70(3)	2.03(3)	2.730(2)	174(3)
O(61)-H(61)...O(74^d)	0.70(3)	2.10(3)	2.732(13)	150(3)

Crystal structure analysis of [Zn (TBTAP) EtOH]. EtOH (84)

Crystal data: $C_{46}H_{37}N_7O_2Zn$, C_2H_6O, M = 831.26. Monoclinic, space group $P2_1/c$ (no. 14), a = 12.24290(10), b = 24.68004(19), c = 13.24798(10) Å, β = 96.3005(7) °, V = 3978.77(6) $Å^3$. Z = 4, Dc = 1.388 g cm^{-3}, F(000) = 1736, T = 100(2) K, μ(Cu-Kα) = 12.82 cm^{-1}, λ(Cu-Kα) = 1.54184 Å.

The crystal was a purple prism. From a sample under oil, one, 0.26 x 0.25 x 0.26 mm, was mounted on a small loop and fixed in the cold nitrogen stream on a Rigaku Oxford Diffraction XtaLAB Synergy diffractometer, equipped with Cu-Kα radiation, HyPix detector and mirror monochromator. Intensity data were measured by thin-slice ω-scans. Total no. of reflections recorded, to $θ_{max} = 72.5°$, was 31127 of which 7727 were unique (Rint = 0.033); 7053 were 'observed' with $I > 2σ_I$.

Data were processed using the CrysAlisPro-CCD and -RED (1) programs. The structure was determined by the intrinsic phasing routines in the SHELXT program (2A) and refined by full-matrix least-squares methods, on F^2's, in SHELXL (2B). The non-hydrogen atoms (except those with site occupancies less than 0.38 were refined with anisotropic thermal parameters. The hydrogen atom on O(61) was located in a difference map and was refined freely as were the hydrogen atoms of the methylene group of C(48). The remaining hydrogen atoms were included in idealised positions and their Uiso values were set to ride on the Ueq values of the parent carbon atoms. At the conclusion of the refinement, $wR_2 = 0.105$ and $R_1 = 0.045$ (2B) for all 7727 reflections weighted $w = [σ^2(F_o^2) + (0.0466 \, P)^2 + 4.00 \, P]^{-1}$ with $P = (F_o^2 + 2F_c^2)/3$; for the 'observed' data only, $R_1 = 0.042$.

In the final difference map, the highest peak (*ca* 0.7 e$Å^{-3}$) was near C(6).

Scattering factors for neutral atoms were taken from reference (3). Computer programs used in this analysis have been noted above, and were run through WinGX (4) on a Dell Optiplex 780 PC at the University of East Anglia.

References

(1) Programs CrysAlisPro, Rigaku Oxford Diffraction Ltd., Abingdon, UK (2018).

(2) G. M. Sheldrick, Programs for crystal structure determination (SHELXT), *Acta Cryst.* (2015) A**71**, 3-8, and refinement (SHELXL), *Acta Cryst.* (2008) A**64**, 112-122 and (2015) C**71**, 3-8.

(3) 'International Tables for X-ray Crystallography', Kluwer Academic Publishers, Dordrecht (1992). Vol. C, pp. 500, 219 and 193.

(4) L. J. Farrugia, *J. Appl. Cryst.* (2012) **45**, 849–854.

Legends for Figures

Figure 1.   View of a molecule of the zinc complex, [Zn (TBTAP) EtOH] indicating the atom numbering scheme. Thermal ellipsoids are drawn at the 50% probability level.

Figure 2.   View of the packing of molecules, along the *b* axis. Pairs of molecules lie overlapping about centres of symmetry, e.g. at (½, 1, ½).

Notes on the structure

The TBTAP ligand is tetradentate, bonded to the zinc atom through the four isoindole N atoms. The zinc centre is also bonded to O(61) of the coordinated EtOH molecule. The coordination about the zinc atom is approximately square pyramidal, with O(61) in the apical site; all the O(61)-Zn-N angles lie in the range 98.36(6)-99.95(7) ° and the zinc atom lies 0.3269(8) A from the mean-plane of the four isoindole N atoms. The phenyl ring is arranged approximately perpendicular to the TBTAP core plane, with close contacts of H(37) and N(4) to the ring mean-plane at *ca* 2.47 Å.

The TBTAP ligand lies against a centrosymmetrically related group with an interplanar distance of *ca* 3.38 Å through the inversion centre.

Both the coordinated and the solvent EtOH molecules are disordered. In the coordinated EtOH, O(61) is common to the two orientations of the ethanol molecule and there are two distinct ethyl group orientations; the hydroxyl hydrogen H(61) was located in a difference map and is donor in hydrogen bonds to the two component O atoms of the EtOH solvent molecule. This solvent molecule is disordered in two orientations, with the methylene C atom common to both orientations; the dimensions of the minor component are not reliable since the methylene carbon, C(75), has an occupancy factor of 0.174 and may be hidden close to the major component, C(72), rather than coincident with it. No hydrogen atom was located bonded to either of the two O part-atoms of this molecule.

Crystal data and structure refinement for [Zn cyclo-{$(C_{11}H_8N_2O_2)_3$-C_8H_4N-$(C$-C_6H_4-$OC_5H_{11})$}OH_2],solvents (96)

_____

Identification code   isabf1163

Elemental formula   C53 H45 N7 O8 ZN, C5.6 H10, C2 H5-
                                          O, C2.1, C4 H8 O, C1.8

Formula weight   1214.66

Crystal system, space group   Triclinic, P-1 (no. 2)

Unit cell dimensions   a = 11.6669(3) Å α = 109.644(2) °
                            b = 15.8147(4) Å β = 106.969(2) °
                            c = 17.6852(3) Å γ = 9 4.356(2) °

Volume   2883.96(12) Å^3

Z, Calculated density   2, 1.399 Mg/m^3

F(000)   1276

Absorption coefficient   1.161 mm^{-1}

Temperature   100.00(10) K

Wavelength   1.54184 Å

Crystal colour, shape   purple block

Crystal size   0.27 x 0.11 x 0.02 mm

Crystal mounting: on a small loop, in oil, fixed in cold N$_2$ stream

On the diffractometer:

  Theta range for data collection   7.726 to 69.989 °

  Limiting indices   -14<=h<=14, -19<=k<=19, -14<=l<=21

  Completeness to theta = 67.684   99.5 %

Absorption correction   Semi-empirical from equivalents

Max. and min. transmission   1.00000 and 0.71916

Reflections collected (not including absences) 37452

No. of unique reflections   10814 [R(int) for equivalents = 0.058]

No. of 'observed' reflections (I > 2σ_I)   9687

Structure determined by: dual methods, in SHELXT

Refinement: Full-matrix least-squares on F^2, in SHELXL

  Data / restraints / parameters   10814 / 0 / 806

  Goodness-of-fit on F^2 1.020

Final R indices ('observed' data) $R_1 = 0.068$, $wR_2 = 0.189$

Final R indices (all data) $R_1 = 0.072$, $wR_2 = 0.193$

Reflections weighted:
   $w = [\sigma^2(Fo^2)+(0.1201P)^2+3.2288P]^{-1}$ where $P=(Fo^2+2Fc^2)/3$

Extinction coefficient   n/a

Largest diff. peak and hole   0.99 and -0.64 e.Å^{-3}

Location of largest difference peak   near O(81)

_____

Table 1.   Atomic coordinates (x 10^5) and equivalent isotropic
           displacement parameters (Å^2 x 10^4).   U(eq) is defined
           as one third of the trace of the orthogonalized Uij
           tensor.   E.s.ds are in parentheses.

	x	y	z	U(eq)	S.o.f.#
Zn	80816(3)	35966(2)	80656(2)	278.1(14)	
O(51)	72530(20)	44351(15)	88317(15)	306(4)	
N(1)	73430(20)	36868(18)	69068(15)	311(5)	
C(2)	62950(30)	31520(20)	62552(18)	324(6)	
C(3)	60490(30)	35190(20)	55694(19)	341(6)	
C(4)	51540(30)	32750(20)	47650(20)	402(7)	
C(5)	52480(30)	38030(20)	42910(20)	437(8)	
C(6)	61910(30)	45450(30)	45870(20)	445(8)	
C(7)	70900(30)	47950(30)	53750(20)	414(7)	
C(8)	69990(30)	42690(20)	58586(19)	356(7)	
C(9)	77910(30)	43470(20)	66872(19)	326(6)	
N(10)	88260(20)	49847(18)	71161(16)	330(5)	
N(11)	96030(20)	45080(17)	83025(15)	290(5)	
C(12)	96440(30)	50440(20)	78347(19)	312(6)	
C(13)	107820(30)	57090(20)	82468(19)	316(6)	
C(14)	112350(30)	63880(20)	80070(20)	349(6)	
C(15)	123670(30)	68850(20)	85430(20)	358(7)	
O(15)	130290(20)	75978(17)	84797(16)	439(6)	
C(151)	142120(30)	78420(20)	91430(20)	438(8)	
C(152)	144930(40)	88320(30)	96340(30)	582(10)	
C(153)	151470(40)	74810(30)	87290(30)	597(10)	
O(16)	141080(20)	73457(16)	96821(16)	434(6)	
C(16)	130220(30)	67330(20)	92700(20)	348(6)	
C(17)	125910(30)	60740(20)	95138(19)	319(6)	
C(18)	114290(30)	55540(20)	89724(19)	298(6)	
C(19)	106540(20)	47884(19)	89881(18)	277(6)	
N(20)	109840(20)	44324(16)	95922(15)	266(5)	
N(21)	91760(20)	32478(16)	90037(15)	285(5)	
C(22)	102970(20)	37060(19)	95810(17)	268(5)	
C(23)	106740(20)	32887(19)	102211(18)	280(6)	
C(24)	117380(30)	34640(20)	109239(19)	303(6)	
C(25)	117140(30)	28950(20)	113660(19)	328(6)	
O(25)	126280(20)	29013(15)	120644(14)	410(5)	
C(251)	121320(30)	22410(20)	123520(20)	390(7)	
C(252)	129970(30)	15930(20)	124370(20)	420(7)	
C(253)	118390(30)	27380(30)	131430(20)	474(8)	
O(26)	109950(20)	17305(16)	116761(15)	431(6)	
C(26)	107250(30)	21860(20)	111314(19)	331(6)	
C(27)	96990(30)	20040(20)	104522(19)	326(6)	
C(28)	96960(30)	25764(19)	99971(18)	292(6)	
C(29)	87820(30)	25616(19)	92336(18)	289(6)	
N(30)	77630(20)	19441(17)	88436(15)	301(5)	
N(31)	69160(20)	23790(17)	76273(15)	300(5)	
C(32)	69240(30)	18642(19)	81083(18)	294(6)	
C(33)	58510(30)	11480(20)	76998(19)	320(6)	
C(34)	55000(30)	4560(20)	79750(20)	396(7)	
C(35)	44270(30)	-1280(20)	74440(20)	453(8)	
O(35)	38930(30)	-8780(20)	75450(20)	754(10)	
C(351)	27460(30)	-12540(30)	68410(20)	470(8)	
C(352)	27040(60)	-22500(40)	63680(30)	776(14)	
C(353)	17280(50)	-11100(40)	71750(30)	782(15)	
O(36)	27300(30)	-7480(20)	62922(18)	645(8)	

C(36)	37330(30)	-480(20)	66860(20)	407(7)	
C(37)	40600(30)	6190(20)	64100(20)	354(6)	
C(38)	51760(30)	12390(20)	69434(19)	318(6)	
C(39)	58800(30)	20270(20)	69102(18)	298(6)	
C(40)	56040(30)	23880(20)	62635(18)	312(6)	
C(41)	44960(30)	18700(20)	54958(18)	317(6)	
C(42)	33590(30)	21210(20)	54240(20)	367(7)	
C(43)	23330(30)	16160(20)	47190(20)	363(7)	
C(44)	24340(30)	8540(20)	40785(19)	338(6)	
C(45)	35670(30)	5990(20)	41442(19)	340(6)	
C(46)	45840(30)	11130(20)	48525(19)	327(6)	
O(47)	13820(19)	4064(15)	34067(13)	368(5)	
C(48)	14170(30)	-4600(20)	28090(20)	385(7)	
C(49)	1510(30)	-8620(20)	21520(20)	389(7)	
C(50)	-1980(30)	-3960(20)	15150(20)	393(7)	
C(51)	-14630(30)	-8260(20)	8440(20)	395(7)	
C(52)	-18260(30)	-3220(30)	2400(20)	474(8)	
C(61)	110750(50)	24060(40)	63360(40)	789(14)	
C(62)	107890(60)	15070(60)	61400(50)	1080(20)	
C(63)	94920(60)	12210(50)	56070(40)	921(17)	
C(64)	89270(70)	20420(50)	59320(50)	985(19)	
C(65)	100710(90)	27210(70)	64860(90)	2150(70)	
C(66)	99700(200)	23800(180)	52620(160)	1090(70)*	0.3
C(67)	92500(200)	24970(160)	69170(150)	970(60)*	0.3
O(71)	47990(20)	49296(18)	16388(17)	505(6)	
C(72)	53840(40)	52530(30)	25360(30)	539(9)	
C(73)	67540(40)	53770(40)	27890(30)	666(11)	
C(75)	56900(200)	45400(170)	33370(160)	1340(70)*	0.4
C(76)	50340(170)	38310(130)	35110(110)	1240(50)*	0.5
C(77)	63870(180)	52160(140)	41310(120)	1350(60)*	0.5
C(78)	47800(300)	50000(200)	28300(190)	1610(90)*	0.4
C(79)	66200(400)	41100(300)	28400(300)	1780(150)*	0.3
O(81)	55130(30)	61460(20)	10300(20)	653(8)	
C(82)	55240(40)	70520(30)	15770(30)	595(10)	
C(83)	65330(40)	76870(30)	15720(30)	663(11)	
C(84)	73120(60)	70620(30)	12340(40)	884(17)	
C(85)	63920(40)	62000(30)	6230(30)	557(10)	
C(91)	97650(180)	55490(130)	43710(120)	780(40)*	0.3
C(92)	96410(70)	47790(60)	44580(70)	690(30)	0.5
C(93)	100330(70)	38730(60)	41990(50)	547(19)	0.5
C(94)	94390(110)	63070(100)	50490(80)	970(40)	0.5

\# - site occupancy, if different from 1.
* - U(iso) (Å^2 x 10^4)

Table 2.   Molecular dimensions.   Bond lengths are in Ångstroms,
           angles in degrees.   E.s.ds are in parentheses.

Zn-N(31)	2.035(2)	N(1)-Zn-N(21)	159.95(10)
Zn-N(1)	2.037(2)	N(31)-Zn-N(11)	159.34(10)
Zn-N(21)	2.043(2)	N(1)-Zn-N(11)	89.57(10)
Zn-N(11)	2.044(2)	N(21)-Zn-N(11)	85.06(9)
Zn-O(51)	2.069(2)	N(31)-Zn-O(51)	100.28(9)
		N(1)-Zn-O(51)	104.37(9)
N(31)-Zn-N(1)	88.94(10)	N(21)-Zn-O(51)	95.59(9)
N(31)-Zn-N(21)	89.35(9)	N(11)-Zn-O(51)	100.05(9)
O(51)-H(51X)	0.83(5)	O(25)-C(251)	1.456(4)
O(51)-H(51Y)	0.82(5)	C(251)-O(26)	1.450(4)
N(1)-C(9)	1.350(4)	C(251)-C(252)	1.505(5)
N(1)-C(2)	1.380(4)	C(251)-C(253)	1.508(5)
C(2)-C(40)	1.407(4)	O(26)-C(26)	1.368(3)
C(2)-C(3)	1.479(4)	C(26)-C(27)	1.355(4)
C(3)-C(8)	1.399(5)	C(27)-C(28)	1.398(4)
C(3)-C(4)	1.403(4)	C(28)-C(29)	1.448(4)
C(4)-C(5)	1.387(5)	C(29)-N(30)	1.318(4)
C(5)-C(6)	1.384(5)	N(30)-C(32)	1.339(4)
C(6)-C(7)	1.382(5)	N(31)-C(32)	1.360(4)
C(7)-C(8)	1.397(4)	N(31)-C(39)	1.381(4)
C(8)-C(9)	1.445(4)	C(32)-C(33)	1.441(4)
C(9)-N(10)	1.348(4)	C(33)-C(38)	1.401(4)
N(10)-C(12)	1.316(4)	C(33)-C(34)	1.417(4)
N(11)-C(19)	1.363(4)	C(34)-C(35)	1.362(5)
N(11)-C(12)	1.376(3)	C(35)-O(35)	1.387(4)
C(12)-C(13)	1.452(4)	C(35)-C(36)	1.401(5)
C(13)-C(18)	1.397(4)	O(35)-C(351)	1.451(4)
C(13)-C(14)	1.401(4)	C(351)-O(36)	1.447(4)
C(14)-C(15)	1.368(4)	C(351)-C(353)	1.474(6)
C(15)-O(15)	1.372(3)	C(351)-C(352)	1.504(6)
C(15)-C(16)	1.398(4)	O(36)-C(36)	1.375(4)
O(15)-C(151)	1.448(4)	C(36)-C(37)	1.375(5)
C(151)-O(16)	1.448(4)	C(37)-C(38)	1.419(4)
C(151)-C(152)	1.469(5)	C(38)-C(39)	1.467(4)
C(151)-C(153)	1.527(5)	C(39)-C(40)	1.411(4)
O(16)-C(16)	1.370(4)	C(40)-C(41)	1.501(4)
C(16)-C(17)	1.370(4)	C(41)-C(46)	1.381(4)
C(17)-C(18)	1.405(4)	C(41)-C(42)	1.397(4)
C(18)-C(19)	1.468(4)	C(42)-C(43)	1.392(4)
C(19)-N(20)	1.343(4)	C(43)-C(44)	1.391(4)
N(20)-C(22)	1.341(4)	C(44)-O(47)	1.368(4)
N(21)-C(22)	1.363(4)	C(44)-C(45)	1.395(4)
N(21)-C(29)	1.373(3)	C(45)-C(46)	1.393(4)
C(22)-C(23)	1.472(4)	O(47)-C(48)	1.434(4)
C(23)-C(28)	1.403(4)	C(48)-C(49)	1.515(4)
C(23)-C(24)	1.406(4)	C(49)-C(50)	1.520(4)
C(24)-C(25)	1.379(4)	C(50)-C(51)	1.527(4)
C(25)-O(25)	1.373(3)	C(51)-C(52)	1.522(4)
C(25)-C(26)	1.404(4)		
Zn-O(51)-H(51X)	129(3)	N(1)-C(2)-C(40)	124.4(3)
Zn-O(51)-H(51Y)	127(4)	N(1)-C(2)-C(3)	108.4(3)
H(51X)-O(51)-H(51Y)	96(4)	C(40)-C(2)-C(3)	127.2(3)
C(9)-N(1)-C(2)	109.2(2)	C(8)-C(3)-C(4)	119.5(3)
C(9)-N(1)-Zn	123.3(2)	C(8)-C(3)-C(2)	105.3(3)
C(2)-N(1)-Zn	127.33(19)	C(4)-C(3)-C(2)	135.2(3)

C(5)-C(4)-C(3)	117.8(3)		O(25)-C(251)-C(253)	109.7(3)
C(6)-C(5)-C(4)	122.0(3)		C(252)-C(251)-C(253)	115.6(3)
C(7)-C(6)-C(5)	121.3(3)		C(26)-O(26)-C(251)	107.1(2)
C(6)-C(7)-C(8)	117.1(3)		C(27)-C(26)-O(26)	127.8(3)
C(7)-C(8)-C(3)	122.3(3)		C(27)-C(26)-C(25)	122.9(3)
C(7)-C(8)-C(9)	130.2(3)		O(26)-C(26)-C(25)	109.3(2)
C(3)-C(8)-C(9)	107.5(3)		C(26)-C(27)-C(28)	114.9(3)
N(10)-C(9)-N(1)	128.9(3)		C(27)-C(28)-C(23)	123.1(3)
N(10)-C(9)-C(8)	121.6(3)		C(27)-C(28)-C(29)	129.8(3)
N(1)-C(9)-C(8)	109.5(3)		C(23)-C(28)-C(29)	107.1(2)
C(12)-N(10)-C(9)	124.8(3)		N(30)-C(29)-N(21)	128.4(3)
C(19)-N(11)-C(12)	108.4(2)		N(30)-C(29)-C(28)	122.0(2)
C(19)-N(11)-Zn	127.65(18)		N(21)-C(29)-C(28)	109.6(2)
C(12)-N(11)-Zn	123.28(19)		C(29)-N(30)-C(32)	124.4(2)
N(10)-C(12)-N(11)	127.9(3)		C(32)-N(31)-C(39)	108.5(2)
N(10)-C(12)-C(13)	122.9(3)		C(32)-N(31)-Zn	122.61(19)
N(11)-C(12)-C(13)	109.2(2)		C(39)-N(31)-Zn	127.78(19)
C(18)-C(13)-C(14)	122.8(3)		N(30)-C(32)-N(31)	129.0(3)
C(18)-C(13)-C(12)	107.0(2)		N(30)-C(32)-C(33)	121.3(2)
C(14)-C(13)-C(12)	130.2(3)		N(31)-C(32)-C(33)	109.6(2)
C(15)-C(14)-C(13)	114.4(3)		C(38)-C(33)-C(34)	124.0(3)
C(14)-C(15)-O(15)	127.5(3)		C(38)-C(33)-C(32)	107.5(3)
C(14)-C(15)-C(16)	123.1(3)		C(34)-C(33)-C(32)	128.5(3)
O(15)-C(15)-C(16)	109.4(3)		C(35)-C(34)-C(33)	114.6(3)
C(15)-O(15)-C(151)	107.0(2)		C(34)-C(35)-O(35)	126.6(3)
O(16)-C(151)-O(15)	106.0(2)		C(34)-C(35)-C(36)	122.4(3)
O(16)-C(151)-C(152)	110.3(3)		O(35)-C(35)-C(36)	111.0(3)
O(15)-C(151)-C(152)	109.5(3)		C(35)-O(35)-C(351)	105.9(3)
O(16)-C(151)-C(153)	107.4(3)		O(36)-C(351)-O(35)	106.4(3)
O(15)-C(151)-C(153)	108.4(3)		O(36)-C(351)-C(353)	109.6(3)
C(152)-C(151)-C(153)	114.9(3)		O(35)-C(351)-C(353)	109.1(4)
C(16)-O(16)-C(151)	107.0(2)		O(36)-C(351)-C(352)	110.2(3)
O(16)-C(16)-C(17)	127.2(3)		O(35)-C(351)-C(352)	109.0(4)
O(16)-C(16)-C(15)	109.6(3)		C(353)-C(351)-C(352)	112.3(4)
C(17)-C(16)-C(15)	123.3(3)		C(36)-O(36)-C(351)	108.4(3)
C(16)-C(17)-C(18)	114.6(3)		C(37)-C(36)-O(36)	128.4(3)
C(13)-C(18)-C(17)	121.8(3)		C(37)-C(36)-C(35)	123.7(3)
C(13)-C(18)-C(19)	105.8(2)		O(36)-C(36)-C(35)	107.9(3)
C(17)-C(18)-C(19)	132.4(3)		C(36)-C(37)-C(38)	115.6(3)
N(20)-C(19)-N(11)	127.3(2)		C(33)-C(38)-C(37)	119.6(3)
N(20)-C(19)-C(18)	123.2(2)		C(33)-C(38)-C(39)	105.5(2)
N(11)-C(19)-C(18)	109.5(2)		C(37)-C(38)-C(39)	135.0(3)
C(22)-N(20)-C(19)	122.9(2)		N(31)-C(39)-C(40)	123.2(3)
C(22)-N(21)-C(29)	108.2(2)		N(31)-C(39)-C(38)	109.0(2)
C(22)-N(21)-Zn	128.16(18)		C(40)-C(39)-C(38)	127.8(3)
C(29)-N(21)-Zn	122.94(19)		C(2)-C(40)-C(39)	126.4(3)
N(20)-C(22)-N(21)	126.9(2)		C(2)-C(40)-C(41)	117.7(3)
N(20)-C(22)-C(23)	123.2(2)		C(39)-C(40)-C(41)	115.8(3)
N(21)-C(22)-C(23)	109.9(2)		C(46)-C(41)-C(42)	118.7(3)
C(28)-C(23)-C(24)	121.3(2)		C(46)-C(41)-C(40)	119.9(3)
C(28)-C(23)-C(22)	105.2(2)		C(42)-C(41)-C(40)	121.4(3)
C(24)-C(23)-C(22)	133.5(3)		C(43)-C(42)-C(41)	120.6(3)
C(25)-C(24)-C(23)	114.5(3)		C(44)-C(43)-C(42)	120.0(3)
O(25)-C(25)-C(24)	126.9(3)		O(47)-C(44)-C(43)	115.9(3)
O(25)-C(25)-C(26)	109.7(2)		O(47)-C(44)-C(45)	124.3(3)
C(24)-C(25)-C(26)	123.3(3)		C(43)-C(44)-C(45)	119.7(3)
C(25)-O(25)-C(251)	106.5(2)		C(46)-C(45)-C(44)	119.5(3)
O(26)-C(251)-O(25)	105.8(2)		C(41)-C(46)-C(45)	121.4(3)
O(26)-C(251)-C(252)	108.5(3)		C(44)-O(47)-C(48)	116.9(2)
O(25)-C(251)-C(252)	108.6(3)		O(47)-C(48)-C(49)	108.3(3)
O(26)-C(251)-C(253)	108.0(3)		C(48)-C(49)-C(50)	113.8(3)

C(49)-C(50)-C(51)	113.0(3)	C(52)-C(51)-C(50)	112.4(3)
C(61)-C(62)	1.334(9)	C(62)-C(61)-C(65)	103.6(7)
C(61)-C(65)	1.368(10)	C(61)-C(62)-C(63)	106.4(6)
C(62)-C(63)	1.469(9)	C(62)-C(63)-C(64)	104.7(6)
C(63)-C(64)	1.516(9)	C(65)-C(64)-C(63)	98.4(6)
C(64)-C(65)	1.485(12)	C(61)-C(65)-C(64)	111.7(7)
O(71)-C(72)	1.419(5)	O(71)-C(72)-C(73)	112.5(3)
C(72)-C(73)	1.506(6)		
		C(77)-C(75)-C(76)	107(2)
C(75)-C(77)	1.40(3)	C(77)-C(75)-C(78)	108(2)
C(75)-C(76)	1.47(3)	C(76)-C(75)-C(78)	111(2)
C(75)-C(78)	1.57(4)	C(77)-C(75)-C(79)	108(2)
C(75)-C(79)	1.63(5)	C(76)-C(75)-C(79)	110(2)
		C(78)-C(75)-C(79)	112(2)
O(81)-C(85)	1.428(5)		
O(81)-C(82)	1.430(5)	C(85)-O(81)-C(82)	108.3(3)
C(82)-C(83)	1.492(6)	O(81)-C(82)-C(83)	108.0(3)
C(83)-C(84)	1.489(7)	C(84)-C(83)-C(82)	103.3(4)
C(84)-C(85)	1.512(7)	C(83)-C(84)-C(85)	102.7(4)
		O(81)-C(85)-C(84)	104.1(3)
C(91)-C(92)	1.28(2)		
C(91)-C(94)	1.55(2)	C(92)-C(91)-C(94)	112.2(14)
C(92)-C(93)	1.501(13)	C(91)-C(92)-C(93)	140.4(11)
C(92)-C(92)#1	1.71(2)	C(94)#1-C(93)-C(92)	107.9(9)
C(93)-C(94)#1	1.427(14)	C(93)#1-C(94)-C(91)	102.2(12)

Symmetry transformation used to generate equivalent atoms:
    #1 : 2-x, 1-y, 1-z

Table 3. Anisotropic displacement parameters (Å^2 x 10^4) for the
          expression:
                  exp {-2π^2(h^{2}a*^{2}U$_{11}$ + ... + 2hka*b*U$_{12}$)}
          E.s.ds are in parentheses.

	U$_{11}$	U$_{22}$	U$_{33}$	U$_{23}$	U$_{13}$	U$_{12}$
Zn	227(2)	298(2)	324(2)	193(2)	37(2)	5(2)
O(51)	246(10)	307(11)	363(11)	160(10)	67(8)	23(9)
N(1)	271(12)	371(13)	321(12)	209(10)	60(10)	27(10)
C(2)	292(14)	382(16)	291(14)	155(12)	53(11)	67(12)
C(3)	334(15)	387(16)	340(15)	203(13)	85(12)	84(13)
C(4)	405(17)	419(18)	364(16)	203(14)	38(13)	75(14)
C(5)	510(20)	465(19)	345(16)	227(14)	63(14)	95(16)
C(6)	510(20)	560(20)	415(17)	337(16)	172(15)	183(17)
C(7)	371(17)	540(20)	443(17)	317(16)	133(14)	100(15)
C(8)	316(15)	462(18)	350(15)	251(14)	79(12)	92(13)
C(9)	267(14)	403(16)	354(15)	228(13)	75(12)	45(12)
N(10)	279(12)	401(14)	368(13)	243(11)	85(10)	26(10)
N(11)	265(11)	322(12)	342(12)	218(10)	79(10)	40(10)
C(12)	272(14)	337(15)	378(15)	214(13)	98(12)	16(12)
C(13)	248(13)	353(15)	412(16)	229(13)	106(12)	49(12)
C(14)	295(14)	395(16)	445(16)	288(14)	105(13)	48(12)
C(15)	307(15)	370(16)	518(18)	311(14)	150(13)	46(12)
O(15)	344(12)	471(13)	595(14)	387(12)	101(10)	-37(10)
C(151)	321(16)	456(19)	630(20)	380(17)	110(15)	-17(14)
C(152)	570(20)	460(20)	710(30)	320(20)	110(20)	64(18)
C(153)	480(20)	620(30)	830(30)	390(20)	280(20)	114(19)
O(16)	304(11)	435(13)	583(14)	340(11)	43(10)	-82(9)
C(16)	254(14)	343(15)	472(17)	229(13)	85(13)	-5(12)
C(17)	252(13)	345(15)	400(15)	233(13)	66(12)	22(12)
C(18)	258(13)	313(14)	385(15)	215(12)	105(12)	28(11)
C(19)	208(12)	294(14)	352(14)	178(12)	67(11)	25(11)
N(20)	229(11)	262(11)	329(12)	170(10)	64(9)	15(9)
N(21)	235(11)	287(12)	341(12)	182(10)	44(9)	18(9)
C(22)	233(13)	279(14)	319(13)	172(11)	62(11)	44(11)
C(23)	241(13)	267(13)	350(14)	180(11)	59(11)	17(11)
C(24)	225(13)	295(14)	391(15)	200(12)	37(11)	-8(11)
C(25)	252(14)	327(15)	379(15)	208(12)	-4(11)	-3(11)
O(25)	318(11)	394(12)	467(12)	296(10)	-66(9)	-56(9)
C(251)	308(15)	403(17)	428(17)	281(14)	-38(13)	-38(13)
C(252)	436(18)	404(17)	437(17)	268(15)	55(14)	39(14)
C(253)	363(17)	550(20)	497(19)	288(17)	17(15)	85(15)
O(26)	377(12)	428(12)	451(12)	333(11)	-67(10)	-88(10)
C(26)	301(14)	332(15)	395(15)	246(13)	54(12)	8(12)
C(27)	274(14)	318(15)	391(15)	222(13)	35(12)	-15(11)
C(28)	238(13)	276(14)	346(14)	169(12)	33(11)	-14(11)
C(29)	257(13)	269(14)	338(14)	165(11)	50(11)	4(11)
N(30)	237(11)	300(12)	352(12)	181(10)	26(10)	-9(9)
N(31)	242(11)	319(12)	322(12)	168(10)	26(9)	6(10)
C(32)	250(13)	282(14)	361(14)	175(12)	65(11)	19(11)
C(33)	250(13)	310(15)	365(15)	158(12)	35(12)	-7(11)
C(34)	327(16)	395(17)	426(17)	229(14)	18(13)	-62(13)
C(35)	354(17)	456(19)	524(19)	282(16)	43(15)	-103(14)
O(35)	559(17)	820(20)	753(19)	570(17)	-160(14)	-339(15)
C(351)	371(17)	490(20)	504(19)	266(16)	31(15)	-76(15)
C(352)	1010(40)	710(30)	630(30)	270(20)	240(30)	360(30)
C(353)	680(30)	1230(50)	770(30)	630(30)	360(30)	460(30)
O(36)	488(15)	704(19)	626(16)	414(15)	-82(13)	-251(14)

C(36)	281(15)	416(18)	438(17)	181(14)	16(13)	−102(13)
C(37)	237(14)	406(17)	358(15)	156(13)	15(12)	−10(12)
C(38)	249(13)	330(15)	363(15)	157(12)	61(12)	26(12)
C(39)	245(13)	291(14)	315(14)	122(11)	34(11)	19(11)
C(40)	279(14)	316(15)	319(14)	132(12)	54(11)	57(12)
C(41)	286(14)	330(15)	313(14)	166(12)	24(11)	26(12)
C(42)	332(15)	368(16)	344(15)	131(13)	34(12)	79(13)
C(43)	278(14)	386(16)	382(16)	158(13)	31(12)	80(12)
C(44)	315(15)	341(15)	326(14)	168(12)	22(12)	23(12)
C(45)	347(15)	333(15)	324(14)	152(12)	58(12)	60(12)
C(46)	283(14)	352(15)	348(15)	182(12)	50(12)	70(12)
O(47)	296(10)	356(11)	358(11)	117(9)	2(9)	30(9)
C(48)	337(16)	340(16)	404(16)	131(13)	37(13)	33(13)
C(49)	342(16)	330(16)	422(17)	144(13)	40(13)	−19(13)
C(50)	346(16)	354(16)	421(17)	164(14)	52(13)	−46(13)
C(51)	321(16)	392(17)	437(17)	201(14)	47(13)	−27(13)
C(52)	394(18)	480(20)	530(20)	275(17)	46(15)	−23(15)
C(61)	630(30)	760(30)	770(30)	90(30)	180(20)	120(30)
C(62)	790(40)	1810(80)	1100(50)	1000(50)	440(40)	340(50)
C(63)	780(40)	1060(50)	950(40)	500(40)	210(30)	140(30)
C(64)	1000(50)	920(40)	1220(50)	600(40)	400(40)	230(40)
C(65)	1070(70)	1290(80)	3050(160)	−530(90)	780(90)	240(60)
O(71)	429(13)	535(15)	564(15)	272(12)	110(11)	93(11)
C(72)	490(20)	650(20)	530(20)	297(19)	150(17)	118(18)
C(73)	510(20)	800(30)	620(30)	280(20)	80(20)	140(20)
O(81)	659(19)	479(16)	820(20)	225(15)	285(16)	78(14)
C(82)	630(20)	450(20)	750(30)	181(19)	360(20)	56(18)
C(83)	560(20)	600(30)	820(30)	230(20)	270(20)	60(20)
C(84)	900(40)	570(30)	1320(50)	320(30)	650(40)	50(30)
C(85)	650(30)	530(20)	680(20)	320(20)	370(20)	186(19)
C(92)	390(40)	590(50)	1240(80)	290(50)	550(50)	50(40)
C(93)	440(40)	740(50)	460(40)	300(40)	90(30)	0(40)
C(94)	760(70)	1270(110)	770(70)	450(70)	90(60)	−70(70)

Table 4. Hydrogen coordinates (x 10^4) and isotropic displacement
parameters (Å^2 x 10^3). All hydrogen atoms were
included in idealised positions with U(iso)'s set at
1.2*U(eq) or, for the methyl group hydrogen atoms,
1.5*U(eq) of the parent carbon atoms.

	x	y	z	U(iso)	S.o.f.#
H(51X)	6630(40)	4640(30)	8690(20)	42(10)	
H(51Y)	7590(50)	4870(40)	9290(30)	68(15)	
H(4)	4505	2765	4551	48	
H(5)	4646	3652	3746	52	
H(6)	6222	4890	4242	53	
H(7)	7740	5302	5579	50	
H(14)	10794	6494	7514	42	
H(15A)	14560	9160	9262	87	
H(15B)	13839	9007	9863	87	
H(15C)	15268	8991	10106	87	
H(15D)	15239	7803	8358	90	
H(15E)	15935	7582	9174	90	
H(15F)	14867	6824	8390	90	
H(17)	13042	5976	10009	38	
H(24)	12417	3935	11081	36	
H(25A)	13771	1929	12892	63	
H(25B)	12637	1110	12577	63	
H(25C)	13146	1318	11897	63	
H(25D)	12595	3089	13610	71	
H(25E)	11293	3155	13030	71	
H(25F)	11437	2293	13305	71	
H(27)	9032	1524	10297	39	
H(34)	5975	403	8488	47	
H(35A)	2715	-2585	6745	116	
H(35B)	1955	-2499	5869	116	
H(35C)	3415	-2315	6180	116	
H(35D)	1740	-1453	7546	117	
H(35E)	1815	-457	7502	117	
H(35F)	951	-1325	6699	117	
H(37)	3571	661	5895	42	
H(42)	3285	2642	5859	44	
H(43)	1563	1793	4676	44	
H(45)	3644	79	3709	41	
H(46)	5355	940	4894	39	
H(48A)	1674	-878	3109	46	
H(48B)	2011	-378	2526	46	
H(49A)	-453	-815	2451	47	
H(49B)	105	-1519	1837	47	
H(50A)	415	-428	1225	47	
H(50B)	-178	258	1828	47	
H(51A)	-1471	-1471	509	47	
H(51B)	-2073	-824	1133	47	
H(52A)	-2640	-621	-178	71	
H(52B)	-1836	314	566	71	
H(52C)	-1234	-333	-58	71	
H(61A)	11218	2534	5857	118	
H(61B)	11814	2689	6850	118	
H(62A)	10923	1374	6664	162	
H(62B)	11297	1179	5823	162	
H(63A)	9108	681	5671	138	

H(63B)	9395	1068	4998	138
H(64A)	8447	2217	5466	148
H(64B)	8411	1940	6262	148
H(65A)	10020	3296	6381	323
H(65B)	10160	2859	7092	323
H(72A)	5085	4812	2755	65
H(72B)	5162	5845	2804	65
H(73A)	7116	5600	3411	100
H(73B)	6981	4790	2535	100
H(73C)	7058	5822	2584	100
H(82A)	5657	7078	2164	71
H(82B)	4732	7232	1370	71
H(83A)	6214	8021	1197	80
H(83B)	6994	8134	2155	80
H(84A)	7912	6945	1696	106
H(84B)	7753	7316	933	106
H(85A)	6008	6245	63	67
H(85B)	6784	5658	538	67

Table 5.   Torsion angles, in degrees. E.s.ds are in parentheses.
_____

C(9)-N(1)-C(2)-C(40)	178.6(3)	C(15)-C(16)-C(17)-C(18)	0.1(5)
Zn-N(1)-C(2)-C(40)	-5.6(4)	C(14)-C(13)-C(18)-C(17)	-0.1(5)
C(9)-N(1)-C(2)-C(3)	-1.1(3)	C(12)-C(13)-C(18)-C(17)	178.9(3)
Zn-N(1)-C(2)-C(3)	174.7(2)	C(14)-C(13)-C(18)-C(19)	-179.3(3)
N(1)-C(2)-C(3)-C(8)	0.5(3)	C(12)-C(13)-C(18)-C(19)	-0.4(3)
C(40)-C(2)-C(3)-C(8)	-179.2(3)	C(16)-C(17)-C(18)-C(13)	0.0(4)
N(1)-C(2)-C(3)-C(4)	179.2(4)	C(16)-C(17)-C(18)-C(19)	179.0(3)
C(40)-C(2)-C(3)-C(4)	-0.5(6)	C(12)-N(11)-C(19)-N(20)	-178.6(3)
C(8)-C(3)-C(4)-C(5)	-0.7(5)	Zn-N(11)-C(19)-N(20)	10.3(4)
C(2)-C(3)-C(4)-C(5)	-179.3(3)	C(12)-N(11)-C(19)-C(18)	0.1(3)
C(3)-C(4)-C(5)-C(6)	0.5(5)	Zn-N(11)-C(19)-C(18)	-170.94(19)
C(4)-C(5)-C(6)-C(7)	0.0(6)	C(13)-C(18)-C(19)-N(20)	179.0(3)
C(5)-C(6)-C(7)-C(8)	-0.3(5)	C(17)-C(18)-C(19)-N(20)	-0.2(5)
C(6)-C(7)-C(8)-C(3)	0.1(5)	C(13)-C(18)-C(19)-N(11)	0.2(3)
C(6)-C(7)-C(8)-C(9)	179.0(3)	C(17)-C(18)-C(19)-N(11)	-179.0(3)
C(4)-C(3)-C(8)-C(7)	0.4(5)	N(11)-C(19)-N(20)-C(22)	1.8(5)
C(2)-C(3)-C(8)-C(7)	179.4(3)	C(18)-C(19)-N(20)-C(22)	-176.8(3)
C(4)-C(3)-C(8)-C(9)	-178.7(3)	C(19)-N(20)-C(22)-N(21)	-2.8(5)
C(2)-C(3)-C(8)-C(9)	0.3(3)	C(19)-N(20)-C(22)-C(23)	177.5(3)
C(2)-N(1)-C(9)-N(10)	-176.5(3)	C(29)-N(21)-C(22)-N(20)	-178.8(3)
Zn-N(1)-C(9)-N(10)	7.5(5)	Zn-N(21)-C(22)-N(20)	-8.4(4)
C(2)-N(1)-C(9)-C(8)	1.3(4)	C(29)-N(21)-C(22)-C(23)	1.0(3)
Zn-N(1)-C(9)-C(8)	-174.7(2)	Zn-N(21)-C(22)-C(23)	171.34(19)
C(7)-C(8)-C(9)-N(10)	-2.0(5)	N(20)-C(22)-C(23)-C(28)	178.3(3)
C(3)-C(8)-C(9)-N(10)	177.0(3)	N(21)-C(22)-C(23)-C(28)	-1.5(3)
C(7)-C(8)-C(9)-N(1)	180.0(3)	N(20)-C(22)-C(23)-C(24)	-2.9(5)
C(3)-C(8)-C(9)-N(1)	-1.0(4)	N(21)-C(22)-C(23)-C(24)	177.4(3)
N(1)-C(9)-N(10)-C(12)	3.9(5)	C(28)-C(23)-C(24)-C(25)	-1.2(4)
C(8)-C(9)-N(10)-C(12)	-173.6(3)	C(22)-C(23)-C(24)-C(25)	-179.9(3)
C(9)-N(10)-C(12)-N(11)	-2.4(5)	C(23)-C(24)-C(25)-O(25)	178.8(3)
C(9)-N(10)-C(12)-C(13)	176.1(3)	C(23)-C(24)-C(25)-C(26)	1.2(5)
C(19)-N(11)-C(12)-N(10)	178.3(3)	C(24)-C(25)-O(25)-C(251)	174.5(3)
Zn-N(11)-C(12)-N(10)	-10.2(4)	C(26)-C(25)-O(25)-C(251)	-7.6(4)
C(19)-N(11)-C(12)-C(13)	-0.4(3)	C(25)-O(25)-C(251)-O(26)	11.9(3)
Zn-N(11)-C(12)-C(13)	171.17(19)	C(25)-O(25)-C(251)-C(252)	128.2(3)
N(10)-C(12)-C(13)-C(18)	-178.2(3)	C(25)-O(25)-C(251)-C(253)	-104.4(3)
N(11)-C(12)-C(13)-C(18)	0.5(3)	O(25)-C(251)-O(26)-C(26)	-12.0(4)
N(10)-C(12)-C(13)-C(14)	0.6(5)	C(252)-C(251)-O(26)-C(26)	-128.4(3)
N(11)-C(12)-C(13)-C(14)	179.3(3)	C(253)-C(251)-O(26)-C(26)	105.5(3)
C(18)-C(13)-C(14)-C(15)	0.1(5)	C(251)-O(26)-C(26)-C(27)	-173.7(3)
C(12)-C(13)-C(14)-C(15)	-178.6(3)	C(251)-O(26)-C(26)-C(25)	7.6(4)
C(13)-C(14)-C(15)-O(15)	-178.9(3)	O(25)-C(25)-C(26)-C(27)	-178.7(3)
C(13)-C(14)-C(15)-C(16)	0.0(5)	C(24)-C(25)-C(26)-C(27)	-0.7(5)
C(14)-C(15)-O(15)-C(151)	-174.5(3)	O(25)-C(25)-C(26)-O(26)	0.0(4)
C(16)-C(15)-O(15)-C(151)	6.5(4)	C(24)-C(25)-C(26)-O(26)	178.0(3)
C(15)-O(15)-C(151)-O(16)	-10.2(4)	O(26)-C(26)-C(27)-C(28)	-178.3(3)
C(15)-O(15)-C(151)-C(152)	-129.2(3)	C(25)-C(26)-C(27)-C(28)	0.1(5)
C(15)-O(15)-C(151)-C(153)	104.7(3)	C(26)-C(27)-C(28)-C(23)	-0.2(5)
O(15)-C(151)-O(16)-C(16)	10.3(4)	C(26)-C(27)-C(28)-C(29)	177.9(3)
C(152)-C(151)-O(16)-C(16)	128.8(3)	C(24)-C(23)-C(28)-C(27)	0.7(5)
C(153)-C(151)-O(16)-C(16)	-105.4(3)	C(22)-C(23)-C(28)-C(27)	179.8(3)
C(151)-O(16)-C(16)-C(17)	174.5(3)	C(24)-C(23)-C(28)-C(29)	-177.7(3)
C(151)-O(16)-C(16)-C(15)	-6.6(4)	C(22)-C(23)-C(28)-C(29)	1.3(3)
C(14)-C(15)-C(16)-O(16)	-179.0(3)	C(22)-N(21)-C(29)-N(30)	-178.4(3)
O(15)-C(15)-C(16)-O(16)	0.1(4)	Zn-N(21)-C(29)-N(30)	10.6(4)
C(14)-C(15)-C(16)-C(17)	0.0(5)	C(22)-N(21)-C(29)-C(28)	-0.1(3)
O(15)-C(15)-C(16)-C(17)	179.0(3)	Zn-N(21)-C(29)-C(28)	-171.09(19)
O(16)-C(16)-C(17)-C(18)	178.8(3)	C(27)-C(28)-C(29)-N(30)	-0.7(5)

C(23)-C(28)-C(29)-N(30)	177.6(3)	C(36)-C(37)-C(38)-C(33)	-0.8(5)
C(27)-C(28)-C(29)-N(21)	-179.1(3)	C(36)-C(37)-C(38)-C(39)	179.2(3)
C(23)-C(28)-C(29)-N(21)	-0.8(3)	C(32)-N(31)-C(39)-C(40)	-178.4(3)
N(21)-C(29)-N(30)-C(32)	2.4(5)	Zn-N(31)-C(39)-C(40)	13.6(4)
C(28)-C(29)-N(30)-C(32)	-175.7(3)	C(32)-N(31)-C(39)-C(38)	0.6(3)
C(29)-N(30)-C(32)-N(31)	-1.2(5)	Zn-N(31)-C(39)-C(38)	-167.41(19)
C(29)-N(30)-C(32)-C(33)	177.5(3)	C(33)-C(38)-C(39)-N(31)	-0.5(3)
C(39)-N(31)-C(32)-N(30)	178.4(3)	C(37)-C(38)-C(39)-N(31)	179.5(3)
Zn-N(31)-C(32)-N(30)	-12.9(4)	C(33)-C(38)-C(39)-C(40)	178.4(3)
C(39)-N(31)-C(32)-C(33)	-0.4(3)	C(37)-C(38)-C(39)-C(40)	-1.6(6)
Zn-N(31)-C(32)-C(33)	168.34(19)	N(1)-C(2)-C(40)-C(39)	-2.3(5)
N(30)-C(32)-C(33)-C(38)	-178.8(3)	C(3)-C(2)-C(40)-C(39)	177.3(3)
N(31)-C(32)-C(33)-C(38)	0.1(3)	N(1)-C(2)-C(40)-C(41)	-179.0(3)
N(30)-C(32)-C(33)-C(34)	0.6(5)	C(3)-C(2)-C(40)-C(41)	0.6(5)
N(31)-C(32)-C(33)-C(34)	179.5(3)	N(31)-C(39)-C(40)-C(2)	-1.8(5)
C(38)-C(33)-C(34)-C(35)	-0.5(5)	C(38)-C(39)-C(40)-C(2)	179.4(3)
C(32)-C(33)-C(34)-C(35)	-179.9(3)	N(31)-C(39)-C(40)-C(41)	175.0(3)
C(33)-C(34)-C(35)-O(35)	177.9(4)	C(38)-C(39)-C(40)-C(41)	-3.8(5)
C(33)-C(34)-C(35)-C(36)	0.2(6)	C(2)-C(40)-C(41)-C(46)	94.2(3)
C(34)-C(35)-O(35)-C(351)	177.7(4)	C(39)-C(40)-C(41)-C(46)	-82.9(4)
C(36)-C(35)-O(35)-C(351)	-4.4(5)	C(2)-C(40)-C(41)-C(42)	-87.5(4)
C(35)-O(35)-C(351)-O(36)	6.4(5)	C(39)-C(40)-C(41)-C(42)	95.4(3)
C(35)-O(35)-C(351)-C(353)	-111.8(4)	C(46)-C(41)-C(42)-C(43)	0.3(5)
C(35)-O(35)-C(351)-C(352)	125.3(4)	C(40)-C(41)-C(42)-C(43)	-178.0(3)
O(35)-C(351)-O(36)-C(36)	-6.3(4)	C(41)-C(42)-C(43)-C(44)	0.0(5)
C(353)-C(351)-O(36)-C(36)	111.6(4)	C(42)-C(43)-C(44)-O(47)	-179.2(3)
C(352)-C(351)-O(36)-C(36)	-124.3(4)	C(42)-C(43)-C(44)-C(45)	-0.2(5)
C(351)-O(36)-C(36)-C(37)	-177.6(4)	O(47)-C(44)-C(45)-C(46)	179.1(3)
C(351)-O(36)-C(36)-C(35)	3.6(4)	C(43)-C(44)-C(45)-C(46)	0.0(4)
C(34)-C(35)-C(36)-C(37)	-0.3(6)	C(42)-C(41)-C(46)-C(45)	-0.4(4)
O(35)-C(35)-C(36)-C(37)	-178.3(4)	C(40)-C(41)-C(46)-C(45)	178.0(3)
C(34)-C(35)-C(36)-O(36)	178.5(4)	C(44)-C(45)-C(46)-C(41)	0.3(4)
O(35)-C(35)-C(36)-O(36)	0.5(5)	C(43)-C(44)-O(47)-C(48)	-170.2(3)
O(36)-C(36)-C(37)-C(38)	-178.0(4)	C(45)-C(44)-O(47)-C(48)	10.7(4)
C(35)-C(36)-C(37)-C(38)	0.5(5)	C(44)-O(47)-C(48)-C(49)	176.6(2)
C(34)-C(33)-C(38)-C(37)	0.8(5)	O(47)-C(48)-C(49)-C(50)	73.8(4)
C(32)-C(33)-C(38)-C(37)	-179.7(3)	C(48)-C(49)-C(50)-C(51)	178.4(3)
C(34)-C(33)-C(38)-C(39)	-179.2(3)	C(49)-C(50)-C(51)-C(52)	177.0(3)
C(32)-C(33)-C(38)-C(39)	0.3(3)		
C(65)-C(61)-C(62)-C(63)	39.8(9)	C(82)-O(81)-C(85)-C(84)	26.1(5)
C(61)-C(62)-C(63)-C(64)	-32.1(7)	C(83)-C(84)-C(85)-O(81)	-36.6(5)
C(62)-C(63)-C(64)-C(65)	10.8(9)		
C(62)-C(61)-C(65)-C(64)	-33.6(14)	C(94)-C(91)-C(92)-C(93)	-161.7(13)
C(63)-C(64)-C(65)-C(61)	12.7(13)	C(94)-C(91)-C(92)-C(92)#1	-45.3(14)
		C(91)-C(92)-C(93)-C(94)#1	127.4(19)
C(85)-O(81)-C(82)-C(83)	-5.4(5)	C(92)#1-C(92)-C(93)-C(94)#1	13.3(9)
O(81)-C(82)-C(83)-C(84)	-17.8(6)	C(92)-C(91)-C(94)-C(93)#1	40.9(17)
C(82)-C(83)-C(84)-C(85)	32.6(6)		

Symmetry transformation used to generate equivalent atoms:
    #1 : 2-x, 1-y, 1-z

Table 6.   Hydrogen bonds, in Ångstroms and degrees.
_____

D-H...A	d(D-H)	d(H...A)	d(D...A)	<(DHA)
C(17)-H(17)...O(51)#2	0.95	2.45	3.246(3)	140.9
C(24)-H(24)...O(51)#2	0.95	2.52	3.280(3)	136.7
C(85)-H(85B)...N(20)#1	0.99	2.69	3.377(5)	126.7
O(51)-H(51X)...O(71)#3	0.83(5)	1.86(5)	2.683(3)	178(4)
O(51)-H(51Y)...N(20)#2	0.82(5)	2.06(6)	2.819(3)	154(5)

_____

Symmetry transformations used to generate equivalent atoms:
   #1 : 2-x, 1-y, 1-z   #2 : 2-x, 1-y, 2-z   #3 : 1-x, 1-y, 1-z

Crystal structure analysis of [Zn cyclo-{(C₁₁H₈N₂O₂)₃-C₈H₄N-(C-C₆H₄-OC₅H₁₁)} **OH₂], solvents (96)**

Crystal data: $C_{53} H_{45} N_7 O_8 Zn$, $C_{5.6} H_{10}$, $C_2 H_5 O$, $C_{2.1}$, $C_4 H_8 O$, $C_{1.8}$, M = 1214.66. Triclinic, space group P-1 (no. 2), a = 11.6669(3), b = 15.8147(4), c = 17.6852(3) Å, α = 109.644(2), β = 106.969(2), γ = 94.356(2) °, V = 2883.96(12) Å³. Z = 2, Dc = 1.399 g cm⁻³, F(000) = 1276, T = 100.00(10) K, μ(Cu-Kα) = 11.6 cm⁻¹, λ(Cu-Kα) = 1.54184 Å.

The crystal was a purple block. From a sample under oil, one, *ca* 0.02 x 0.11 x 0.27 mm, was mounted on a small loop and fixed in the cold nitrogen stream on a Rigaku Oxford Diffraction XtaLAB Synergy diffractometer, equipped with Cu-Kα radiation, HyPix detector and mirror monochromator. Intensity data were measured by thin-slice ω-scans. Total no. of reflections recorded, to θ_{max} = 70.0°, was 37,452 of which 10,814 were unique (Rint = 0.058); 9,687 were 'observed' with I > 2σ_I.

Data were processed using the CrysAlisPro-CCD and -RED (1) programs. The structure was determined by the intrinsic phasing routines in the SHELXT program (2A) and refined by full-matrix least-squares methods, on F^2's, in SHELXL (2B). The non-hydrogen atoms were refined with anisotropic thermal parameters. The hydrogen atoms of the ligand water molecules were located in difference maps and were refined freely. The remaining hydrogen atoms were included in idealised positions and their Uiso values were set to ride on the Ueq values of the parent carbon atoms. At the conclusion of the refinement, wR_2 = 0.193 and R_1 = 0.072 (2B) for all 10,814 reflections weighted w = $[\sigma^2(F_o^2) + (0.1201 P)^2 + 3.229 P]^{-1}$ with P = $(F_o^2 + 2F_c^2)/3$; for the 'observed' data only, R_1 = 0.068.

In the final difference map, the highest peak (*ca* 1.0 eÅ⁻³) was near O(81).

Scattering factors for neutral atoms were taken from reference (3). Computer programs used in this analysis have been noted above, and were run through WinGX (4) on a Dell Optiplex 780 PC at the University of East Anglia.

References

(1)   Programs CrysAlisPro, Rigaku Oxford Diffraction Ltd., Abingdon, UK (2018).

(2)   G. M. Sheldrick, Programs for crystal structure determination (SHELXT), *Acta Cryst.* (2015) A**71**, 3-8, and refinement (SHELXL), *Acta Cryst.* (2008) A**64**, 112-122 and (2015) C**71**, 3-8.

(3)   *'International Tables for X-ray Crystallography'*, Kluwer Academic Publishers, Dordrecht (1992). Vol. C, pp. 500, 219 and 193.

(4)   L. J. Farrugia, *J. Appl. Cryst.* (2012) **45**, 849–854.

Legends for Figures

Figure 1.   View of the phthalocyanine derivative molecule, indicating the atom numbering scheme. The ligated water molecule is shown, with its hydrogen bonded neighbours. Thermal ellipsoids are drawn at the 50% probability level.

Figure 2.   The hydrogen bonding contacts in the dimer unit.

Figure 3.   The overlaying of the phthalocyanine-type ring systems in the dimer unit.

Figure 4.   Packing of the parallel phthalocyanine-type rings, omitting the C_5H_{11} chains and most of the solvent and disordered atoms.

Notes on the structure

The principal phthalocyanine derivative molecule is clearly defined and well refined. The zinc centre has a square pyramidal coordination, with a water molecule in the apical site. The two hydrogen atoms of the water molecule were clearly identified in difference maps and were refined independently and satisfactorily. The three isopropyl-dioxy-isoindole (??) groups are very similar; the fourth isoindole group is unsubstituted but there is evidence of a partially occupied, separate isopropyl-dioxo group (as neo-pentane) close to the end of that isoindole group, presumably a case of disorder in the phthalocyanine alignment. There are also solvent molecules (ethanol, thf, and some less-well defined, disordered molecules) in the crystal lattice.

The water molecule is hydrogen bonded to an ethanol molecule and to N(20) of a centrosymmerically related phthalocyanine ligand, thus forming a dimer about an inversion centre. The indole ring of C(12)…C(19) and N(20) lies under N(20') and the indole group of C(22')…C(29').

Crystal data and structure refinement for a Zn-phthalocyanine complex with THF/EtOH ligands, plus solvents (101)

Identification code   isabf1337

Elemental formula
              C54 H47 N7 O6 ZN, C52 H44 N7 O6 ZN, C3.6 H4.8 O, *ca* 7.7C

Formula weight   1020.11

Crystal system, space group   Triclinic, P-1 (no. 2)

Unit cell dimensions   a = 14.7577(3) Å   α = 83.6288(12) °

                                  b = 15.4422(3) Å   β = 79.7051(13) °

                                  c = 22.5632(3) Å   γ = 75.3302(15) °

Volume   4882.57(16) Å^3

Z, Calculated density   2, 1.388 Mg/m^3

F(000)   2123

Absorption coefficient   1.211 mm^{-1}

Temperature   100.3(8) K

Wavelength   1.54184 Å

Crystal colour, shape   dark blue needle

Crystal size   0.55 x 0.03 x 0.02 mm

Crystal mounting: on a small loop, in oil, fixed in cold N$_2$ stream

On the diffractometer:

  Theta range for data collection   7.646 to 69.998 °

    Limiting indices   -17<=h<=17, -18<=k<=18, -27<=l<=27

    Completeness to theta = 67.684   99.3 %

Absorption correction   Semi-empirical from equivalents

Max. and min. transmission   1.00000 and 0.71194

Reflections collected (not including absences) 62951

No. of unique reflections   18253 [R(int) for equivalents = 0.084]

No. of 'observed' reflections (I > 2σ_I)   14581

Structure determined by: dual methods, in SHELXT

Refinement: Full-matrix least-squares on F^2, in SHELXL

Data / restraints / parameters   18253 / 0 / 1301

Goodness-of-fit on F^2 1.077

Final R indices ('observed' data) $R_1 = 0.066$, $wR_2 = 0.187$

Final R indices (all data) $R_1 = 0.079$, $wR_2 = 0.198$

Reflections weighted:
   $w = [\sigma2(Fo^2)+(0.1342P)^2+0.3100P]^{-1}$ where $P=(Fo^2+2Fc^2)/3$

Extinction coefficient   n/a

Largest diff. peak and hole   0.87 and -0.77 e.$Å^{-3}$

Location of largest difference peak   near Zn(2)

Table 1. Atomic coordinates (x 10^5) and equivalent isotropic
              displacement parameters ($Å^2$ x 10^4). U(eq) is defined
              as one third of the trace of the orthogonalized Uij
              tensor. E.s.ds are in parentheses.

---

	x	y	z	U(eq) S.o.f.#
Zn(1)	100133(2)	33239(2)	9013(2)	286.5(12)
N(1)	102555(16)	27613(15)	1063(10)	280(5)
C(2)	98700(19)	31613(18)	-3900(12)	287(6)
C(3)	101530(20)	25464(19)	-8614(13)	316(6)
C(4)	99330(20)	26480(20)	-14442(13)	381(7)
C(5)	102810(20)	19310(20)	-18026(14)	419(7)
C(6)	108520(20)	11300(20)	-15804(14)	393(7)
C(7)	110720(20)	10240(20)	-10065(13)	342(6)
C(8)	107120(19)	17471(19)	-6299(13)	301(6)
C(9)	107704(19)	19021(18)	-119(12)	275(5)
C(10)	112421(19)	12988(18)	4151(12)	279(5)
N(11)	109972(16)	23114(16)	12301(11)	306(5)
C(12)	113522(19)	14828(18)	9897(13)	288(6)
C(13)	118860(20)	8725(19)	14258(13)	304(6)
C(14)	123840(20)	-330(20)	14545(14)	382(7)
C(15)	128570(30)	-3620(20)	19415(15)	458(8)
C(16)	128380(30)	1760(20)	24028(15)	473(8)
C(17)	123350(20)	10590(20)	23951(14)	387(7)
C(18)	118610(20)	13994(19)	19027(13)	325(6)
C(19)	112900(20)	22823(19)	17732(13)	313(6)
N(20)	111034(17)	29400(16)	21501(11)	322(5)
N(21)	100326(17)	40420(16)	15911(11)	310(5)
C(22)	105400(20)	37427(19)	20622(13)	318(6)
C(23)	103440(20)	44400(20)	24817(13)	337(6)
C(24)	106640(20)	44670(20)	30283(14)	362(6)
C(25)	102720(20)	52440(20)	33098(14)	382(7)
O(251)	104249(19)	54461(17)	38541(11)	485(6)
C(252)	97880(30)	63110(20)	39940(17)	501(8)

C(253)	103570(30)	69310(30)	41210(20)	613(10)
C(254)	89860(30)	61700(30)	44800(20)	645(11)
O(255)	93946(19)	66588(17)	34417(12)	520(6)
C(26)	96260(20)	59710(20)	30732(15)	400(7)
C(27)	93020(20)	59570(20)	25432(14)	371(7)
C(28)	96840(20)	51660(20)	22511(13)	336(6)
C(29)	95120(20)	48934(19)	16888(13)	316(6)
N(30)	89291(16)	54344(15)	13477(11)	317(5)
N(31)	92744(17)	44718(16)	5201(11)	317(5)
C(32)	88491(19)	52313(18)	8055(13)	300(6)
C(33)	82590(20)	58638(19)	4108(14)	327(6)
C(34)	76610(20)	67102(19)	5158(15)	368(7)
C(35)	71890(20)	70919(19)	409(15)	379(7)
O(351)	65360(16)	79029(15)	175(12)	469(6)
C(352)	60500(20)	78470(20)	-4757(18)	480(9)
C(353)	52090(30)	74420(30)	-2390(20)	626(12)
C(354)	57920(30)	87610(20)	-8030(20)	558(10)
O(355)	67412(16)	72374(15)	-8749(11)	464(6)
C(36)	73130(20)	66880(20)	-4954(15)	379(7)
C(37)	79080(20)	58610(20)	-6086(15)	353(6)
C(38)	83800(20)	54486(19)	-1255(14)	326(6)
C(39)	90229(19)	45703(19)	-447(13)	304(6)
N(40)	92935(16)	39815(16)	-4617(11)	311(5)
C(41)	116698(19)	3644(18)	2442(12)	282(6)
C(42)	126022(19)	1126(18)	-528(13)	303(6)
C(43)	130040(20)	-7629(19)	-1905(14)	337(6)
C(44)	124850(20)	-14206(19)	-177(14)	343(6)
C(45)	115490(20)	-11710(20)	2678(14)	356(6)
C(46)	111550(20)	-2861(19)	3913(14)	335(6)
O(47)	129545(15)	-22735(13)	-1505(11)	406(5)
C(48)	125050(20)	-29810(20)	1212(18)	459(8)
C(49)	131990(20)	-38650(20)	-65(17)	453(8)
C(50)	133420(20)	-41030(20)	-6552(17)	461(8)
C(51)	139610(30)	-50330(20)	-7712(19)	546(9)
C(52)	139800(40)	-53140(30)	-13880(20)	722(12)
O(51S)	87869(14)	27685(13)	12816(9)	339(4)
C(52S)	88000(20)	18440(20)	12589(14)	389(7)
C(53S)	78150(30)	17630(30)	15682(16)	491(9)
C(54S)	75090(20)	25010(20)	20133(15)	424(7)
C(55S)	82580(30)	30440(20)	18515(14)	432(8)
Zn(2)	47640(3)	79379(2)	48954(2)	302.7(12)
N(61)	51691(18)	69882(16)	42820(10)	309(5)
C(62)	47540(20)	62941(18)	42463(12)	311(6)
C(63)	53360(20)	57130(20)	37775(13)	334(6)
C(64)	53150(20)	48960(20)	35676(14)	398(7)
C(65)	60550(30)	45040(20)	31393(16)	481(8)
C(66)	68090(30)	48990(20)	29168(16)	487(8)
C(67)	68450(20)	56990(20)	31114(14)	409(7)
C(68)	60990(20)	61020(20)	35442(13)	341(6)
C(69)	59740(20)	68877(19)	38603(12)	314(6)
N(70)	65930(17)	74145(16)	37430(10)	310(5)
N(71)	59870(17)	83475(16)	45898(10)	307(5)
C(72)	65890(20)	80748(19)	40688(12)	292(6)
C(73)	72870(20)	86018(19)	39255(12)	312(6)
C(74)	80210(20)	85580(20)	34311(13)	346(6)
O(751)	92988(17)	92984(17)	29911(10)	466(6)
C(752)	97080(20)	99440(20)	32079(14)	405(7)
C(753)	106510(30)	94590(30)	33819(17)	514(8)
C(754)	97430(30)	106980(20)	27284(15)	470(8)
O(755)	90512(17)	102818(17)	37408(10)	458(6)

C(75)	85620(20)	91670(20)	34262(13)	353(6)
C(76)	84060(20)	97600(20)	38749(13)	364(7)
C(77)	76890(20)	98050(20)	43648(13)	336(6)
C(78)	71140(20)	91928(19)	43763(12)	295(6)
C(79)	62910(20)	90080(18)	47967(12)	291(6)
N(80)	59363(17)	94082(15)	53153(10)	291(5)
N(81)	47093(18)	85896(16)	56421(10)	316(5)
C(82)	52130(20)	91955(19)	57093(12)	301(6)
C(83)	48440(20)	96039(18)	62877(12)	308(6)
C(84)	51000(20)	102540(20)	65745(13)	346(6)
C(85)	45480(20)	104830(20)	71138(13)	377(7)
O(851)	46476(19)	110913(16)	74803(10)	474(6)
C(852)	38420(30)	111940(20)	79680(14)	456(8)
C(853)	31670(30)	120820(30)	78703(16)	510(9)
C(854)	42030(30)	110440(30)	85579(16)	601(10)
O(855)	33720(20)	104845(17)	79080(10)	536(7)
C(86)	37860(30)	101120(20)	73713(13)	399(7)
C(87)	35270(20)	94770(20)	71060(13)	401(7)
C(88)	40890(20)	92283(19)	65532(13)	338(6)
C(89)	40150(20)	85955(19)	61419(12)	319(6)
N(90)	33499(19)	81399(16)	62501(11)	351(5)
N(91)	38465(18)	72443(16)	53739(11)	329(5)
C(92)	32620(20)	75460(20)	58841(13)	351(6)
C(93)	24640(20)	71280(20)	59948(13)	359(6)
C(94)	16660(20)	72640(20)	64434(14)	401(7)
C(95)	9850(20)	67990(20)	64199(15)	449(8)
C(96)	10990(20)	62240(20)	59621(15)	437(8)
C(97)	18890(20)	60920(20)	55149(15)	401(7)
C(98)	25870(20)	65504(19)	55353(13)	346(6)
C(99)	34850(20)	66277(19)	51476(13)	331(6)
C(100)	39240(20)	61673(19)	46288(13)	323(6)
C(101)	34970(20)	54600(20)	44729(13)	324(6)
C(102)	36320(20)	46330(20)	47920(13)	342(6)
C(103)	32750(20)	39450(20)	46476(14)	367(6)
C(104)	27530(20)	41040(20)	41739(14)	368(6)
C(105)	26200(20)	49300(20)	38464(14)	389(7)
C(106)	29860(20)	56030(20)	39932(14)	370(6)
O(107)	23333(18)	34879(14)	40053(10)	431(5)
C(108)	27020(30)	25620(20)	41893(18)	483(8)
C(109)	21180(30)	20010(30)	40030(20)	581(10)
C(110)	11800(30)	20160(30)	44504(19)	569(9)
C(111)	6350(40)	13670(30)	43210(20)	637(11)
C(112)	-2400(40)	13510(30)	47710(20)	693(12)
O(121)	37004(15)	89585(14)	45391(9)	352(4)
C(122)	28520(30)	89300(30)	43070(20)	695(12)
C(123)	29990(40)	83250(30)	38270(20)	635(11)
O(131)	49760(70)	32430(70)	18650(40)	1090(20)
0.6				
C(132)	41320(60)	37640(70)	19450(50)	900(30)
0.6				
C(133)	35290(60)	32300(70)	24120(40)	850(30)
0.6				
C(134)	41230(90)	24130(90)	26290(60)	1060(30)
0.6				
C(135)	50330(70)	23620(70)	22190(40)	840(20)
0.6				
C(137)	49940(90)	33660(80)	22490(60)	680(30)
0.4				
C(136)	46280(150)	29680(140)	27880(90)	1150(50)
0.4				

O(138)	50000(70)	28010(80)	17130(50)	840(30)
0.4				
C(139)	41700(120)	22320(110)	22800(80)	880(40)
0.4				
C(201)	42470(80)	74090(70)	17900(50)	1440(30)
C(202)	43040(110)	70030(100)	24070(70)	1420(40)
0.7				
C(203)	35400(120)	67290(110)	24010(70)	1460(40)
0.7				
C(204)	26410(100)	71470(90)	26880(50)	1670(40)
C(205)	18560(120)	66880(120)	24640(70)	1680(50)
0.8				
C(206)	23420(140)	60050(130)	20710(80)	1730(60)
0.7				
C(207)	33900(200)	63350(190)	17900(120)	1480(80)
0.4				
C(208)	36400(120)	72300(110)	14210(70)	1370(50)
0.6				
C(210)	20160(140)	73530(130)	23030(80)	1270(50)
0.5				
C(211)	39290(180)	75810(160)	29040(100)	1320(70)
0.4				
C(212)	29400(200)	77140(180)	30980(120)	1470(80)
0.4				
C(213)	26850(170)	71310(160)	17500(100)	1490(70)
0.5				

- site occupancy, if different from 1.
* - U(iso) (Å^2 x 10^4)

Table 2. Molecular dimensions. Bond lengths are in Ångstroms,
         angles in degrees. E.s.ds are in parentheses.

Zn(1)-N(1)	2.015(2)	Zn(2)-N(91)	2.025(2)
Zn(1)-N(21)	2.017(2)	Zn(2)-N(61)	2.033(2)
Zn(1)-N(11)	2.020(2)	Zn(2)-N(81)	2.036(2)
Zn(1)-N(31)	2.022(2)	Zn(2)-N(71)	2.042(2)
Zn(1)-O(51S)	2.1944(18)	Zn(2)-O(121)	2.124(2)
N(1)-Zn(1)-N(21)	165.34(9)	N(11)-Zn(1)-O(51S)	96.29(8)
N(1)-Zn(1)-N(11)	91.30(10)	N(31)-Zn(1)-O(51S)	96.45(8)
N(21)-Zn(1)-N(11)	88.77(10)	N(91)-Zn(2)-N(61)	89.35(9)
N(1)-Zn(1)-N(31)	89.46(10)	N(91)-Zn(2)-N(81)	89.66(9)
N(21)-Zn(1)-N(31)	87.26(10)	N(61)-Zn(2)-N(81)	160.53(10)
N(11)-Zn(1)-N(31)	167.11(9)	N(91)-Zn(2)-N(71)	160.55(10)
N(1)-Zn(1)-O(51S)	95.16(8)	N(61)-Zn(2)-N(71)	89.64(10)
N(21)-Zn(1)-O(51S)	99.40(8)	N(81)-Zn(2)-N(71)	84.88(9)

N(91)-Zn(2)-O(121)
94.93(9)
N(61)-Zn(2)-O(121)
105.09(9)

N(1)-C(2)
1.362(4)
N(1)-C(9)
1.380(4)
C(2)-N(40)
1.346(4)
C(2)-C(3)
1.439(4)
C(3)-C(4)
1.393(4)
C(3)-C(8)
1.404(4)
C(4)-C(5)
1.380(5)
C(5)-C(6)
1.407(5)
C(6)-C(7)
1.373(5)
C(7)-C(8)
1.415(4)
C(8)-C(9)
1.462(4)
C(9)-C(10)
1.412(4)
C(10)-C(12)
1.403(4)
C(10)-C(41)
1.485(4)
N(11)-C(19)
1.363(4)
N(11)-C(12)
1.385(4)
C(12)-C(13)
1.474(4)
C(13)-C(14)
1.407(4)
C(13)-C(18)
1.409(4)
C(14)-C(15)
1.386(5)
C(15)-C(16)
1.394(5)
C(16)-C(17)
1.378(5)
C(17)-C(18)
1.401(4)
C(18)-C(19)
1.439(4)
C(19)-N(20)
1.340(4)
N(20)-C(22)
1.323(4)
N(21)-C(29)
1.364(4)
N(21)-C(22)
1.380(4)

N(81)-Zn(2)-O(121)
94.38(9)
N(71)-Zn(2)-O(121)
104.09(8)

C(22)-C(23)
1.453(4)
C(23)-C(24)
1.405(4)
C(23)-C(28)
1.405(4)
C(24)-C(25)
1.365(4)
C(25)-O(251)
1.370(4)
C(25)-C(26)
1.401(5)
O(251)-C(252)
1.455(5)
C(252)-O(255)
1.460(5)
C(252)-C(253)
1.502(5)
C(252)-C(254)
1.505(6)
O(255)-C(26)
1.359(4)
C(26)-C(27)
1.369(5)
N(61)-C(69)
1.369(4)
N(61)-C(62)
1.378(4)
C(62)-C(100)
1.411(4)
C(62)-C(63)
1.469(4)
C(63)-C(68)
1.403(4)
C(63)-C(64)
1.404(4)
C(64)-C(65)
1.382(5)
C(65)-C(66)
1.393(5)
C(66)-C(67)
1.371(5)
C(67)-C(68)
1.399(4)
C(68)-C(69)
1.430(4)
C(69)-N(70)
1.345(4)
N(70)-C(72)
1.320(4)
N(71)-C(79)
1.368(4)
N(71)-C(72)
1.377(4)
C(72)-C(73)
1.441(4)

C(73)-C(78)	C(32)-C(33)
1.389(4)	1.470(4)
C(73)-C(74)	C(33)-C(38)
1.403(4)	1.394(4)
C(74)-C(75)	C(33)-C(34)
1.377(4)	1.397(4)
O(751)-C(75)	C(34)-C(35)
1.369(3)	1.378(5)
O(751)-C(752)	C(35)-O(351)
1.456(4)	1.376(4)
C(752)-O(755)	C(35)-C(36)
1.457(4)	1.384(5)
C(752)-C(753)	O(351)-C(352)
1.501(5)	1.448(5)
C(752)-C(754)	C(352)-O(355)
1.503(5)	1.453(5)
O(755)-C(76)	C(352)-C(354)
1.371(3)	1.509(4)
C(75)-C(76)	C(352)-C(353)
1.390(4)	1.516(4)
C(76)-C(77)	O(355)-C(36)
1.381(4)	1.378(4)
C(77)-C(78)	C(36)-C(37)
1.416(4)	1.376(5)
C(78)-C(79)	C(37)-C(38)
1.470(4)	1.404(4)
C(79)-N(80)	C(38)-C(39)
1.343(4)	1.459(4)
N(80)-C(82)	C(39)-N(40)
1.345(4)	1.320(4)
N(81)-C(82)	C(41)-C(46)
1.370(4)	1.385(4)
N(81)-C(89)	C(41)-C(42)
1.380(4)	1.397(4)
C(82)-C(83)	C(42)-C(43)
1.467(4)	1.378(4)
C(83)-C(88)	C(43)-C(44)
1.396(4)	1.404(4)
C(83)-C(84)	C(44)-O(47)
1.411(4)	1.362(4)
C(84)-C(85)	C(44)-C(45)
1.366(4)	1.393(4)
C(85)-O(851)	C(45)-C(46)
1.369(4)	1.380(4)
C(85)-C(86)	O(47)-C(48)
1.396(4)	1.442(3)
O(851)-C(852)	C(48)-C(49)
1.458(4)	1.506(5)
C(27)-C(28)	C(49)-C(50)
1.394(4)	1.514(6)
C(28)-C(29)	C(50)-C(51)
1.462(4)	1.516(5)
C(29)-N(30)	C(51)-C(52)
1.327(4)	1.497(7)
N(30)-C(32)	O(51S)-C(55S)
1.328(4)	1.427(4)
N(31)-C(32)	O(51S)-C(52S)
1.354(4)	1.429(4)
N(31)-C(39)	C(52S)-C(53S)
1.372(4)	1.526(4)

C(53S)-C(54S) 1.530(5)	C(97)-C(98) 1.399(4)
C(54S)-C(55S) 1.522(4)	C(98)-C(99) 1.477(4)
C(852)-O(855) 1.467(4)	C(99)-C(100) 1.406(4)
C(852)-C(854) 1.494(5)	C(100)-C(101) 1.492(4)
C(852)-C(853) 1.497(6)	C(101)-C(102) 1.381(4)
O(855)-C(86) 1.372(4)	C(101)-C(106) 1.395(4)
C(86)-C(87) 1.367(5)	C(102)-C(103) 1.390(4)
C(87)-C(88) 1.402(4)	C(103)-C(104) 1.391(4)
C(88)-C(89) 1.456(4)	C(104)-O(107) 1.377(4)
C(89)-N(90) 1.321(4)	C(104)-C(105) 1.389(4)
N(90)-C(92) 1.344(4)	C(105)-C(106) 1.381(4)
N(91)-C(92) 1.359(4)	O(107)-C(108) 1.438(4)
N(91)-C(99) 1.383(4)	C(108)-C(109) 1.502(5)
C(92)-C(93) 1.452(4)	C(109)-C(110) 1.558(6)
C(93)-C(94) 1.397(4)	C(110)-C(111) 1.515(5)
C(93)-C(98) 1.400(4)	C(111)-C(112) 1.498(7)
C(94)-C(95) 1.385(5)	O(121)-C(122) 1.452(5)
C(95)-C(96) 1.397(5)	C(122)-C(123) 1.461(6)
C(96)-C(97) 1.387(5)	C(123)-C(212) 2.01(3)

C(2)-N(1)-C(9) 109.3(2)	C(4)-C(5)-C(6) 120.1(3)
C(2)-N(1)-Zn(1) 124.28(19)	C(7)-C(6)-C(5) 122.1(3)
C(9)-N(1)-Zn(1) 126.26(19)	C(6)-C(7)-C(8) 118.6(3)
N(40)-C(2)-N(1) 128.8(3)	C(3)-C(8)-C(7) 118.6(3)
N(40)-C(2)-C(3) 122.1(3)	C(3)-C(8)-C(9) 105.9(2)
N(1)-C(2)-C(3) 109.0(2)	C(7)-C(8)-C(9) 135.5(3)
C(4)-C(3)-C(8) 122.4(3)	N(1)-C(9)-C(10) 123.6(3)
C(4)-C(3)-C(2) 130.1(3)	N(1)-C(9)-C(8) 108.3(2)
C(8)-C(3)-C(2) 107.4(3)	C(10)-C(9)-C(8) 128.1(3)
C(5)-C(4)-C(3) 118.2(3)	C(12)-C(10)-C(9) 127.1(3)

C(12)-C(10)-C(41)
115.8(2)

C(9)-C(10)-C(41)
117.1(2)

C(19)-N(11)-C(12)
109.3(2)

C(69)-N(61)-C(62)
107.9(2)

C(69)-N(61)-Zn(2)
124.4(2)

C(62)-N(61)-Zn(2)
127.43(18)

N(61)-C(62)-C(100)
123.6(3)

N(61)-C(62)-C(63)
109.2(2)

C(100)-C(62)-C(63)
127.1(3)

C(68)-C(63)-C(64)
119.1(3)

C(68)-C(63)-C(62)
105.4(2)

C(64)-C(63)-C(62)
135.4(3)

C(65)-C(64)-C(63)
118.4(3)

C(19)-N(11)-Zn(1)
125.0(2)

C(12)-N(11)-Zn(1)
124.8(2)

N(11)-C(12)-C(10)
124.2(3)

N(11)-C(12)-C(13)
108.2(2)

C(10)-C(12)-C(13)
127.6(3)

C(14)-C(13)-C(18)
118.7(3)

C(14)-C(13)-C(12)
135.8(3)

C(18)-C(13)-C(12)
105.5(2)

C(15)-C(14)-C(13)
118.5(3)

C(14)-C(15)-C(16)
121.9(3)

C(17)-C(16)-C(15)
120.9(3)

C(16)-C(17)-C(18)
117.6(3)

C(17)-C(18)-C(13)
122.4(3)

C(17)-C(18)-C(19)
130.0(3)

C(13)-C(18)-C(19)
107.7(3)

N(20)-C(19)-N(11)
128.2(3)

N(20)-C(19)-C(18)
122.6(3)

C(64)-C(65)-C(66)
121.6(3)

C(67)-C(66)-C(65)
121.2(3)

C(66)-C(67)-C(68)
117.7(3)

C(67)-C(68)-C(63)
122.0(3)

C(67)-C(68)-C(69)
130.4(3)

C(63)-C(68)-C(69)
107.5(3)

N(70)-C(69)-N(61)
127.7(3)

N(70)-C(69)-C(68)
122.2(3)

N(61)-C(69)-C(68)
110.0(2)

C(72)-N(70)-C(69)
125.1(2)

C(79)-N(71)-C(72)
107.7(2)

C(79)-N(71)-Zn(2)
128.02(18)

C(72)-N(71)-Zn(2)
123.68(19)

N(11)-C(19)-C(18)
109.2(3)

C(22)-N(20)-C(19)
124.2(3)

C(29)-N(21)-C(22)
108.0(2)

C(29)-N(21)-Zn(1)
125.9(2)

C(22)-N(21)-Zn(1)
126.0(2)

N(20)-C(22)-N(21)
127.2(3)

N(20)-C(22)-C(23)
123.0(3)

N(21)-C(22)-C(23)
109.9(3)

C(24)-C(23)-C(28)
121.8(3)

C(24)-C(23)-C(22)
132.1(3)

C(28)-C(23)-C(22)
106.1(3)

C(25)-C(24)-C(23)
114.3(3)

C(24)-C(25)-O(251)
127.2(3)

C(24)-C(25)-C(26)
123.7(3)

O(251)-C(25)-C(26)
109.1(3)

C(25)-O(251)-C(252)
107.4(3)

O(251)-C(252)-O(255)
105.2(3)

280

O(251)-C(252)-C(253) 109.0(3)

O(255)-C(252)-C(253) 108.3(3)

O(251)-C(252)-C(254) 109.3(3)

O(255)-C(252)-C(254) 108.0(3)

C(253)-C(252)-C(254) 116.5(3)

C(26)-O(255)-C(252) 106.9(3)

O(255)-C(26)-C(27) 127.1(3)

O(255)-C(26)-C(25) 110.0(3)

C(27)-C(26)-C(25) 122.9(3)

C(26)-C(27)-C(28) 114.4(3)

C(27)-C(28)-C(23) 122.9(3)

C(27)-C(28)-C(29) 130.7(3)

C(23)-C(28)-C(29) 106.4(3)

N(30)-C(29)-N(21) 128.3(3)

N(30)-C(29)-C(28) 122.1(3)

N(21)-C(29)-C(28) 109.7(3)

C(29)-N(30)-C(32) 122.3(3)

C(32)-N(31)-C(39) 108.8(2)

C(32)-N(31)-Zn(1) 125.5(2)

C(39)-N(31)-Zn(1) 125.27(19)

N(30)-C(32)-N(31) 128.7(3)

N(30)-C(32)-C(33) 122.0(3)

N(31)-C(32)-C(33) 109.3(3)

C(38)-C(33)-C(34) 123.4(3)

C(38)-C(33)-C(32) 106.3(3)

C(34)-C(33)-C(32) 130.3(3)

C(35)-C(34)-C(33) 113.5(3)

O(351)-C(35)-C(34) 127.0(3)

N(70)-C(72)-N(71) 128.0(2)

N(70)-C(72)-C(73) 122.3(2)

N(71)-C(72)-C(73) 109.7(2)

C(78)-C(73)-C(74) 124.1(3)

C(78)-C(73)-C(72) 107.4(2)

C(74)-C(73)-C(72) 128.6(3)

C(75)-C(74)-C(73) 113.8(3)

C(75)-O(751)-C(752) 106.9(2)

O(751)-C(752)-O(755) 105.4(2)

O(751)-C(752)-C(753) 108.4(3)

O(755)-C(752)-C(753) 109.9(3)

O(751)-C(752)-C(754) 108.3(3)

O(755)-C(752)-C(754) 109.5(3)

C(753)-C(752)-C(754) 114.9(3)

C(76)-O(755)-C(752) 107.3(2)

O(751)-C(75)-C(74) 126.7(3)

O(751)-C(75)-C(76) 110.2(2)

C(74)-C(75)-C(76) 123.1(3)

O(755)-C(76)-C(77) 127.1(3)

O(755)-C(76)-C(75) 109.3(2)

C(77)-C(76)-C(75) 123.5(3)

C(76)-C(77)-C(78) 114.5(3)

C(73)-C(78)-C(77) 121.0(2)

C(73)-C(78)-C(79) 105.7(2)

C(77)-C(78)-C(79) 133.3(3)

N(80)-C(79)-N(71) 126.5(2)

N(80)-C(79)-C(78) 123.9(2)

N(71)-C(79)-C(78) 109.5(2)

C(79)-N(80)-C(82) 123.0(2)

C(82)-N(81)-C(89) 108.0(2)

C(82)-N(81)-Zn(2) 128.11(18)

C(89)-N(81)-Zn(2) 123.1(2)

N(80)-C(82)-N(81)	126.8(3)
N(80)-C(82)-C(83)	123.5(3)
N(81)-C(82)-C(83)	109.7(2)
C(88)-C(83)-C(84)	121.1(3)
C(88)-C(83)-C(82)	106.0(2)
C(84)-C(83)-C(82)	132.9(3)
C(85)-C(84)-C(83)	114.9(3)
C(84)-C(85)-O(851)	126.4(3)
C(84)-C(85)-C(86)	123.6(3)
O(851)-C(85)-C(86)	110.0(3)
C(85)-O(851)-C(852)	107.2(2)
O(851)-C(852)-O(855)	105.2(2)
O(851)-C(852)-C(854)	108.8(3)
O(855)-C(852)-C(854)	109.7(3)
O(851)-C(852)-C(853)	109.3(3)
O(351)-C(35)-C(36)	109.7(3)
C(34)-C(35)-C(36)	123.4(3)
C(35)-O(351)-C(352)	103.9(3)
O(351)-C(352)-O(355)	104.8(2)
O(351)-C(352)-C(354)	109.5(3)
O(355)-C(352)-C(354)	109.6(3)
O(351)-C(352)-C(353)	109.7(3)
O(355)-C(352)-C(353)	109.1(3)
C(354)-C(352)-C(353)	113.8(3)
C(36)-O(355)-C(352)	103.9(3)
C(37)-C(36)-O(355)	127.1(3)
C(37)-C(36)-C(35)	123.8(3)
O(355)-C(36)-C(35)	109.2(3)
C(36)-C(37)-C(38)	113.9(3)
C(33)-C(38)-C(37)	122.0(3)

O(855)-C(852)-C(853)	108.3(3)
C(854)-C(852)-C(853)	115.1(3)
C(86)-O(855)-C(852)	107.1(2)
C(87)-C(86)-O(855)	127.6(3)
C(87)-C(86)-C(85)	122.8(3)
O(855)-C(86)-C(85)	109.5(3)
C(86)-C(87)-C(88)	114.5(3)
C(83)-C(88)-C(87)	123.1(3)
C(83)-C(88)-C(89)	106.9(2)
C(87)-C(88)-C(89)	129.9(3)
N(90)-C(89)-N(81)	128.1(3)
N(90)-C(89)-C(88)	122.5(3)
N(81)-C(89)-C(88)	109.4(2)
C(89)-N(90)-C(92)	124.3(3)
C(33)-C(38)-C(39)	106.4(3)
C(37)-C(38)-C(39)	131.6(3)
N(40)-C(39)-N(31)	127.3(3)
N(40)-C(39)-C(38)	123.5(3)
N(31)-C(39)-C(38)	109.3(2)
C(39)-N(40)-C(2)	124.2(3)
C(46)-C(41)-C(42)	118.4(3)
C(46)-C(41)-C(10)	120.3(2)
C(42)-C(41)-C(10)	121.3(2)
C(43)-C(42)-C(41)	120.9(2)
C(42)-C(43)-C(44)	120.0(3)
O(47)-C(44)-C(45)	124.8(2)
O(47)-C(44)-C(43)	115.9(2)
C(45)-C(44)-C(43)	119.3(3)
C(46)-C(45)-C(44)	119.6(2)

C(45)-C(46)-C(41)
121.7(3)

C(44)-O(47)-C(48)
116.7(2)

O(47)-C(48)-C(49)
108.0(3)

C(48)-C(49)-C(50)
114.0(3)

C(49)-C(50)-C(51)
114.1(3)

C(52)-C(51)-C(50)
113.6(4)

C(55S)-O(51S)-C(52S)
107.1(2)

C(55S)-O(51S)-Zn(1)
118.76(17)

C(52S)-O(51S)-Zn(1)
122.46(17)

O(51S)-C(52S)-C(53S)
104.5(3)

C(52S)-C(53S)-C(54S)
104.0(3)

C(55S)-C(54S)-C(53S)
104.6(2)

O(51S)-C(55S)-C(54S)
106.4(2)

C(92)-N(91)-C(99)
108.8(2)

C(92)-N(91)-Zn(2)
122.06(19)

C(99)-N(91)-Zn(2)
125.54(18)

N(90)-C(92)-N(91)
128.6(3)

N(90)-C(92)-C(93)
122.0(3)

N(91)-C(92)-C(93)
109.4(3)

C(94)-C(93)-C(98)
122.4(3)

C(94)-C(93)-C(92)
129.9(3)

C(98)-C(93)-C(92)
107.6(3)

C(95)-C(94)-C(93)
117.2(3)

C(94)-C(95)-C(96)
120.8(3)

C(97)-C(96)-C(95)
121.9(3)

C(96)-C(97)-C(98)
117.9(3)

C(97)-C(98)-C(93)
119.7(3)

C(97)-C(98)-C(99)
135.0(3)

C(93)-C(98)-C(99)
105.3(3)

N(91)-C(99)-C(100)
123.9(3)

N(91)-C(99)-C(98)
108.9(2)

C(100)-C(99)-C(98)
127.1(3)

C(99)-C(100)-C(62)
125.9(3)

C(99)-C(100)-C(101)
117.7(2)

C(62)-C(100)-C(101)
116.4(3)

C(102)-C(101)-C(106)
118.5(3)

C(102)-C(101)-C(100)
120.1(3)

C(106)-C(101)-C(100)
121.3(3)

C(101)-C(102)-C(103)
122.0(3)

C(102)-C(103)-C(104)
118.8(3)

O(107)-C(104)-C(105)
116.2(3)

O(107)-C(104)-C(103)
124.0(3)

C(105)-C(104)-C(103)
119.8(3)

C(106)-C(105)-C(104)
120.6(3)

C(105)-C(106)-C(101)
120.3(3)

C(104)-O(107)-C(108)
116.8(2)

O(107)-C(108)-C(109)
109.2(3)

C(108)-C(109)-C(110)
112.5(3)

C(111)-C(110)-C(109)
113.9(4)

C(112)-C(111)-C(110)
113.6(4)

C(122)-O(121)-Zn(2)
132.2(2)

O(121)-C(122)-C(123)
115.5(4)

C(122)-C(123)-C(212)
166.3(9)

O(131)-C(132)
1.295(13)

O(131)-C(135)
1.491(13)

C(132)-C(133)
1.558(13)

C(133)-C(134)
1.433(16)

C(134)-C(135)
1.479(15)

C(137)-C(136)
1.38(2)

283

C(137)-O(138)
1.565(17)
C(136)-C(139)
2.01(3)
O(138)-C(139)
1.909(18)

C(132)-O(131)-C(135)
112.6(9)
O(131)-C(132)-C(133)
105.2(9)
C(134)-C(133)-C(132)
110.3(8)

C(201)-C(208)
1.420(17)
C(201)-C(202)
1.471(16)
C(201)-C(203)
1.953(18)
C(202)-C(203)
1.304(18)
C(202)-C(211)
1.45(2)
C(203)-C(204)
1.395(18)
C(203)-C(207)
1.64(3)
C(204)-C(210)
1.33(2)
C(204)-C(212)
1.53(3)
C(204)-C(205)
1.674(19)

C(208)-C(201)-C(202)
123.3(12)
C(203)-C(202)-C(211)
97.4(16)
C(203)-C(202)-C(201)
89.2(12)
C(211)-C(202)-C(201)
118.0(15)
C(202)-C(203)-C(204)
123.9(15)
C(202)-C(203)-C(207)
119.9(16)
C(204)-C(203)-C(207)
107.0(15)
C(204)-C(203)-C(201)
119.9(12)
C(210)-C(204)-C(203)
111.0(14)
C(210)-C(204)-C(212)
132.4(17)
C(203)-C(204)-C(212)
98.4(15)
C(203)-C(204)-C(205)
107.4(12)
C(210)-C(205)-C(206)
112.6(18)

C(133)-C(134)-C(135)
103.0(9)
C(134)-C(135)-O(131)
107.7(9)
C(136)-C(137)-O(138)
109.9(12)
C(137)-C(136)-C(139)
86.2(12)
C(137)-O(138)-C(139)
85.0(8)
O(138)-C(139)-C(136)
76.2(8)

C(205)-C(210)
1.12(2)
C(205)-C(206)
1.42(2)
C(205)-C(213)
2.01(3)
C(206)-C(207)
1.74(3)
C(206)-C(213)
1.96(3)
C(207)-C(213)
1.40(3)
C(207)-C(208)
1.62(3)
C(208)-C(213)
1.51(3)
C(210)-C(213)
1.46(3)
C(211)-C(212)
1.41(3)

C(206)-C(205)-C(204)
109.5(14)
C(205)-C(206)-C(207)
101.9(15)
C(208)-C(207)-C(203)
87.5(15)
C(208)-C(207)-C(206)
134(2)
C(203)-C(207)-C(206)
98.7(16)
C(201)-C(208)-C(213)
115.0(14)
C(201)-C(208)-C(207)
99.5(14)
C(205)-C(210)-C(204)
85.6(16)
C(205)-C(210)-C(213)
102(2)
C(204)-C(210)-C(213)
97.8(17)
C(212)-C(211)-C(202)
115(2)
C(211)-C(212)-C(204)
103(2)
C(211)-C(212)-C(123)
92.2(17)

	C(207)-C(213)-C(210)		C(207)-C(213)-C(205)	
116(2)			90.8(17)	
	C(208)-C(213)-C(206)			
126.4(17)				

Table 3.   Anisotropic displacement parameters ($Å^2$ x 10^4) for the expression:

$$\exp\{-2\pi^2(h^2a^{*2}U_{11} + \ldots + 2hka^*b^*U_{12})\}$$

E.s.ds are in parentheses.

	U_{11}	U_{22}	U_{33}	U_{23}	U_{13}	U_{12}
Zn(1)	226(2)	258(2)	349(2)	-32.9(14)	5.4(14)	-39.6(15)
N(1)	240(11)	255(11)	324(12)	-17(9)	16(9)	-62(9)
C(2)	222(13)	261(13)	349(14)	11(11)	27(10)	-69(10)
C(3)	275(14)	293(14)	357(14)	-10(11)	51(11)	-103(11)
C(4)	400(17)	354(16)	345(15)	-1(12)	30(12)	-82(13)
C(5)	471(19)	405(17)	341(15)	-37(13)	1(13)	-72(14)
C(6)	420(18)	369(16)	365(15)	-65(12)	43(13)	-104(13)
C(7)	302(15)	302(14)	391(15)	-56(11)	46(11)	-72(12)
C(8)	220(13)	286(14)	364(14)	4(11)	41(10)	-74(11)
C(9)	210(13)	234(13)	357(14)	-34(10)	35(10)	-62(10)
C(10)	206(13)	235(13)	366(14)	-16(10)	36(10)	-58(10)
N(11)	218(11)	314(12)	369(12)	-43(9)	7(9)	-62(9)
C(12)	217(13)	235(13)	381(14)	-23(11)	33(10)	-56(10)
C(13)	243(14)	267(13)	369(14)	13(11)	-4(11)	-45(11)
C(14)	377(17)	331(15)	402(16)	18(12)	-9(12)	-77(13)
C(15)	466(19)	342(16)	481(18)	47(14)	-41(14)	2(14)
C(16)	500(20)	439(19)	432(18)	50(14)	-110(14)	-25(15)
C(17)	367(17)	404(17)	376(15)	-2(12)	-60(12)	-75(13)
C(18)	262(14)	295(14)	383(15)	-3(11)	21(11)	-63(11)
C(19)	250(14)	306(14)	368(14)	-14(11)	6(11)	-82(11)
N(20)	270(12)	318(12)	370(12)	-34(10)	-2(9)	-82(10)
N(21)	260(12)	291(12)	369(12)	-50(9)	8(9)	-74(9)
C(22)	262(14)	322(14)	375(14)	-41(11)	23(11)	-123(11)
C(23)	273(14)	328(15)	408(15)	-45(12)	26(11)	-112(12)

C(24)	339(16)	334(15)	426(16)	−52(12)	−8(12)	−128(12)
C(25)	371(17)	406(17)	398(16)	−83(13)	−7(12)	−159(13)
O(251)	529(15)	451(13)	505(13)	−151(10)	−95(11)	−110(11)
C(252)	600(20)	427(19)	505(19)	−155(15)	−29(16)	−159(17)
C(253)	670(30)	510(20)	720(30)	−138(19)	−130(20)	−200(20)
C(254)	720(30)	530(20)	670(30)	−185(19)	80(20)	−180(20)
O(255)	564(16)	424(13)	578(14)	−215(11)	−86(12)	−52(11)
C(26)	387(17)	345(16)	480(18)	−141(13)	40(13)	−134(13)
C(27)	320(16)	328(15)	454(17)	−70(12)	26(12)	−101(12)
C(28)	286(15)	322(14)	400(15)	−55(12)	35(11)	−119(12)
C(29)	260(14)	276(14)	402(15)	−54(11)	41(11)	−96(11)
N(30)	240(12)	254(11)	439(13)	−37(10)	23(10)	−74(9)
N(31)	241(12)	287(12)	404(13)	−45(10)	26(9)	−71(9)
C(32)	194(13)	256(13)	416(15)	−33(11)	34(11)	−45(10)
C(33)	219(13)	266(14)	477(16)	12(12)	−3(11)	−78(11)
C(34)	247(14)	248(14)	571(18)	−19(12)	17(12)	−52(11)
C(35)	227(14)	246(14)	610(19)	26(13)	28(13)	−43(11)
O(351)	287(11)	321(11)	728(16)	60(10)	−23(10)	−25(9)
C(352)	243(15)	345(17)	780(20)	118(16)	−27(15)	−44(13)
C(353)	301(18)	429(19)	1080(30)	280(20)	−92(19)	−118(15)
C(354)	312(17)	388(18)	890(30)	199(18)	−58(17)	−62(14)
O(355)	302(12)	360(12)	691(15)	103(11)	−108(10)	−45(9)
C(36)	230(14)	321(15)	557(18)	116(13)	−61(12)	−78(12)
C(37)	274(15)	294(14)	470(16)	51(12)	−38(12)	−78(12)
C(38)	219(13)	274(14)	460(16)	35(12)	−2(11)	−75(11)
C(39)	204(13)	307(14)	380(14)	−4(11)	30(10)	−84(11)
N(40)	228(12)	306(12)	364(12)	2(10)	30(9)	−64(9)
C(41)	229(13)	242(13)	352(14)	6(10)	−4(10)	−53(10)
C(42)	221(13)	245(13)	402(15)	1(11)	43(11)	−57(10)
C(43)	212(13)	272(14)	484(16)	−5(12)	42(11)	−55(11)

C(44)	261(14)	244(14)	495(17)	−43(12)	24(12)	−61(11)
C(45)	266(15)	283(14)	508(17)	6(12)	3(12)	−103(12)
C(46)	206(13)	311(14)	457(16)	−26(12)	37(11)	−71(11)
O(47)	270(11)	234(10)	669(14)	−41(9)	70(9)	−73(8)
C(48)	357(17)	298(15)	700(20)	19(14)	33(15)	−151(13)
C(49)	352(17)	270(15)	730(20)	23(14)	−70(15)	−91(13)
C(50)	337(17)	328(16)	680(20)	30(15)	−25(15)	−76(13)
C(51)	460(20)	360(18)	740(30)	−25(16)	27(18)	−57(15)
C(52)	760(30)	570(30)	740(30)	−90(20)	120(20)	−120(20)
O(51S)	288(10)	324(10)	383(11)	−59(8)	70(8)	−102(8)
C(52S)	421(18)	345(16)	401(16)	−59(12)	66(13)	−170(13)
C(53S)	510(20)	560(20)	455(18)	−106(15)	135(15)	−323(17)
C(54S)	368(17)	469(18)	427(17)	−64(14)	73(13)	−167(14)
C(55S)	480(19)	455(18)	368(16)	−110(13)	135(14)	−228(15)
Zn(2)	318(2)	271(2)	289(2)	−30.3(14)	55.9(15)	−80.9(15)
N(61)	325(13)	279(12)	289(11)	−26(9)	30(9)	−63(10)
C(62)	365(16)	246(13)	311(14)	−37(10)	−4(11)	−81(11)
C(63)	344(16)	317(15)	312(14)	−32(11)	1(11)	−59(12)
C(64)	428(18)	335(16)	420(16)	−96(13)	28(13)	−106(13)
C(65)	530(20)	412(18)	498(19)	−184(15)	59(15)	−140(16)
C(66)	530(20)	429(18)	459(18)	−181(14)	132(15)	−110(16)
C(67)	394(17)	399(17)	389(16)	−115(13)	100(13)	−90(14)
C(68)	366(16)	317(15)	316(14)	−37(11)	16(11)	−82(12)
C(69)	328(15)	285(14)	284(13)	−25(10)	33(11)	−44(11)
N(70)	319(13)	302(12)	292(11)	−37(9)	26(9)	−86(10)
N(71)	314(13)	287(12)	282(11)	−26(9)	34(9)	−59(10)
C(72)	275(14)	294(14)	264(13)	−23(10)	40(10)	−47(11)
C(73)	324(15)	279(14)	316(14)	−28(11)	13(11)	−79(11)
C(74)	313(15)	371(15)	324(14)	−62(12)	51(11)	−84(12)
O(751)	442(13)	584(15)	400(12)	−165(10)	144(10)	−265(12)

C(752)	348(17)	492(18)	379(16)	-101(13)	95(12)	-182(14)
C(753)	490(20)	550(20)	510(20)	-117(16)	-40(16)	-125(17)
C(754)	480(20)	490(20)	415(17)	-66(14)	30(14)	-123(16)
O(755)	453(13)	536(14)	418(12)	-160(10)	125(10)	-258(11)
C(75)	319(15)	405(16)	320(14)	-58(12)	69(11)	-127(13)
C(76)	355(16)	404(16)	352(15)	-45(12)	36(12)	-181(13)
C(77)	358(16)	330(15)	312(14)	-80(11)	30(11)	-103(12)
C(78)	290(14)	285(14)	277(13)	-23(10)	33(10)	-59(11)
C(79)	292(14)	257(13)	290(13)	1(10)	9(11)	-51(11)
N(80)	323(13)	238(11)	272(11)	-20(9)	16(9)	-37(9)
N(81)	345(13)	290(12)	284(11)	-21(9)	38(9)	-83(10)
C(82)	312(15)	285(14)	261(13)	11(10)	24(10)	-47(11)
C(83)	335(15)	264(13)	278(13)	2(10)	17(11)	-41(11)
C(84)	363(16)	329(15)	311(14)	-12(11)	28(11)	-80(12)
C(85)	480(19)	332(15)	298(14)	-46(11)	24(12)	-111(13)
O(851)	601(15)	461(13)	351(11)	-132(10)	129(10)	-205(12)
C(852)	630(20)	405(17)	314(15)	-84(13)	130(14)	-199(16)
C(853)	620(20)	480(20)	408(18)	-67(15)	30(16)	-159(17)
C(854)	840(30)	580(20)	349(17)	18(16)	-10(18)	-180(20)
O(855)	740(18)	477(14)	370(12)	-161(10)	228(11)	-271(13)
C(86)	518(19)	352(16)	283(14)	-61(12)	96(13)	-117(14)
C(87)	517(19)	353(16)	301(14)	-48(12)	121(13)	-161(14)
C(88)	397(16)	260(14)	306(14)	-13(11)	59(12)	-69(12)
C(89)	353(15)	277(14)	280(13)	-17(11)	50(11)	-57(12)
N(90)	401(14)	291(12)	325(12)	-23(9)	66(10)	-100(10)
N(91)	359(13)	290(12)	312(12)	-27(9)	47(10)	-96(10)
C(92)	397(17)	301(14)	315(14)	4(11)	57(12)	-101(12)
C(93)	365(16)	322(15)	353(15)	-20(12)	66(12)	-100(12)
C(94)	422(18)	344(16)	388(16)	-62(12)	126(13)	-119(13)
C(95)	417(18)	418(18)	460(18)	-24(14)	129(14)	-147(14)

C(96)	404(18)	385(17)	501(18)	−36(14)	75(14)	−155(14)
C(97)	434(18)	319(15)	430(16)	−30(12)	56(13)	−137(13)
C(98)	373(16)	290(14)	335(14)	−21(11)	66(12)	−90(12)
C(99)	358(16)	264(14)	342(14)	2(11)	50(12)	−103(12)
C(100)	356(16)	240(13)	341(14)	5(11)	−3(11)	−60(11)
C(101)	308(15)	312(14)	330(14)	−15(11)	21(11)	−89(12)
C(102)	362(16)	311(15)	357(15)	−11(11)	−41(12)	−100(12)
C(103)	408(17)	286(14)	392(16)	12(12)	−51(12)	−79(12)
C(104)	415(17)	309(15)	395(16)	−38(12)	−83(13)	−97(13)
C(105)	428(18)	344(16)	402(16)	3(12)	−99(13)	−92(13)
C(106)	373(16)	318(15)	394(16)	25(12)	−26(12)	−83(12)
O(107)	522(14)	292(11)	518(13)	−5(9)	−194(10)	−101(10)
C(108)	550(20)	289(16)	620(20)	−18(14)	−204(17)	−59(15)
C(109)	710(30)	346(18)	760(30)	−101(17)	−330(20)	−69(17)
C(110)	630(30)	480(20)	650(20)	−70(17)	−240(19)	−142(18)
C(111)	780(30)	460(20)	730(30)	−89(19)	−290(20)	−120(20)
C(112)	830(30)	640(30)	720(30)	−110(20)	−220(20)	−290(20)
O(121)	305(11)	354(11)	377(11)	−15(8)	2(8)	−83(9)
C(122)	540(20)	680(30)	910(30)	−340(20)	−240(20)	−20(20)
C(123)	730(30)	550(20)	670(30)	−30(19)	−200(20)	−170(20)
C(132)	530(50)	1020(70)	1160(70)	80(60)	−280(50)	−200(50)
C(133)	500(40)	1240(80)	810(50)	−160(50)	70(40)	−290(50)

Table 4. Hydrogen coordinates (x 10^4) and isotropic displacement
parameters (Å^2 x 10^3). All hydrogen atoms were
included in idealised positions with U(iso)'s set at
1.2*U(eq) or, for the methyl group hydrogen atoms,
1.5*U(eq) of the parent carbon atoms.

	x	y	z	U(iso)	S.o.f.#
H(4)	9554	3196	−1591	46	
H(5)	10135	1980	−2200	50	
H(6)	11093	646	−1835	47	
H(7)	11457	476	−865	41	
H(14)	12397	−412	1147	46	
H(15)	13203	−971	1962	55	

H(16)	13177	−70	2727	57
H(17)	12311	1425	2712	46
H(24)	11115	3985	3189	43
H(25A)	9932	7515	4215	92
H(25B)	10683	6675	4465	92
H(25C)	10826	7008	3764	92
H(25D)	8556	6752	4575	97
H(25E)	8638	5791	4338	97
H(25F)	9241	5876	4843	97
H(27)	8853	6447	2388	44
H(34)	7586	6995	880	44
H(35A)	4882	7406	−574	94
H(35B)	5431	6839	−52	94
H(35C)	4771	7821	62	94
H(35D)	5464	8724	−1136	84
H(35E)	5376	9186	−522	84
H(35F)	6371	8967	−962	84
H(37)	7992	5593	−980	42
H(42)	12964	551	−161	36
H(43)	13633	−922	−402	40
H(45)	11184	−1606	377	43
H(46)	10514	−119	582	40
H(48A)	11923	−2938	−51	55
H(48B)	12328	−2927	562	55
H(49A)	12971	−4345	261	54
H(49B)	13818	−3845	95	54
H(50A)	13633	−3657	−919	55
H(50B)	12714	−4060	−770	55
H(51A)	14616	−5049	−718	66
H(51B)	13727	−5472	−467	66
H(52A)	14390	−5918	−1434	108
H(52B)	13336	−5316	−1442	108
H(52C)	14226	−4892	−1693	108
H(52D)	9296	1454	1476	47
H(52E)	8920	1677	836	47
H(53A)	7839	1165	1783	59
H(53B)	7373	1862	1271	59
H(54A)	6873	2882	1966	51
H(54B)	7493	2240	2435	51
H(55A)	7956	3694	1823	52
H(55B)	8679	2924	2162	52
H(64)	4804	4620	3716	48
H(65)	6049	3952	2993	58
H(66)	7309	4610	2625	58
H(67)	7358	5969	2958	49
H(74)	8134	8146	3128	41
H(75A)	10937	9885	3529	77
H(75B)	10561	8990	3701	77
H(75C)	11069	9186	3029	77
H(75D)	10017	11141	2866	70
H(75E)	10135	10461	2357	70
H(75F)	9099	10985	2650	70
H(77)	7590	10212	4669	40
H(84)	5616	10512	6405	41
H(85A)	2624	12153	8198	77
H(85B)	3490	12565	7866	77
H(85C)	2944	12110	7483	77
H(85D)	3667	11111	8889	90
H(85E)	4611	10437	8592	90
H(85F)	4570	11484	8580	90

H(87)	3009	9225	7282	48
H(94)	1592	7660	6752	48
H(95)	435	6872	6719	54
H(96)	621	5914	5957	52
H(97)	1954	5702	5204	48
H(102)	3978	4531	5120	41
H(103)	3386	3378	4868	44
H(105)	2273	5033	3518	47
H(106)	2889	6166	3766	44
H(10A)	2678	2490	4633	58
H(10B)	3371	2363	3998	58
H(10C)	2497	1374	3978	70
H(10D)	1963	2227	3596	70
H(11A)	1331	1870	4865	68
H(11B)	768	2631	4435	68
H(11C)	453	1532	3914	76
H(11D)	1057	756	4315	76
H(11E)	-558	920	4662	104
H(11F)	-66	1173	5174	104
H(11G)	-670	1950	4772	104
H(12A)	2557	9544	4154	83
H(12B)	2397	8750	4647	83
H(12C)	2390	8352	3701	95
H(12D)	3433	8507	3482	95
H(12E)	3272	7711	3976	95
H(13A)	3872	3900	1560	108	0.6
H(13B)	4139	4335	2103	108	0.6
H(13C)	3210	3601	2755	102	0.6
H(13D)	3035	3090	2221	102	0.6
H(13E)	3861	1891	2600	128	0.6
H(13F)	4198	2442	3053	128	0.6
H(13G)	5146	1875	1944	100	0.6
H(13H)	5563	2233	2455	100	0.6

\# - site occupancy, if different from 1.

```
     Table 5.   Torsion angles, in degrees.   E.s.ds are in parentheses.
```

```
     C(9)-N(1)-C(2)-N(40)              177.4(2)
     Zn(1)-N(1)-C(2)-N(40)               1.7(4)
     C(9)-N(1)-C(2)-C(3)                -1.0(3)
     Zn(1)-N(1)-C(2)-C(3)             -176.68(16)
     N(40)-C(2)-C(3)-C(4)                1.0(4)
     N(1)-C(2)-C(3)-C(4)               179.5(3)
     N(40)-C(2)-C(3)-C(8)             -177.3(2)
     N(1)-C(2)-C(3)-C(8)                 1.2(3)
     C(8)-C(3)-C(4)-C(5)                 0.0(4)
     C(2)-C(3)-C(4)-C(5)              -178.0(3)
     C(3)-C(4)-C(5)-C(6)                -0.8(5)
     C(4)-C(5)-C(6)-C(7)                 0.9(5)
     C(5)-C(6)-C(7)-C(8)                -0.2(4)
     C(4)-C(3)-C(8)-C(7)                 0.7(4)
     C(2)-C(3)-C(8)-C(7)               179.2(2)
     C(4)-C(3)-C(8)-C(9)              -179.4(2)
     C(2)-C(3)-C(8)-C(9)                -0.9(3)
     C(6)-C(7)-C(8)-C(3)                -0.6(4)
     C(6)-C(7)-C(8)-C(9)               179.5(3)
     C(2)-N(1)-C(9)-C(10)             -178.4(2)
     Zn(1)-N(1)-C(9)-C(10)              -2.8(3)
     C(2)-N(1)-C(9)-C(8)                 0.4(3)
     Zn(1)-N(1)-C(9)-C(8)              175.98(16)
     C(3)-C(8)-C(9)-N(1)                 0.4(3)
     C(7)-C(8)-C(9)-N(1)              -179.7(3)
     C(3)-C(8)-C(9)-C(10)              179.1(2)
     C(7)-C(8)-C(9)-C(10)               -1.0(5)
     N(1)-C(9)-C(10)-C(12)              -6.9(4)
     C(8)-C(9)-C(10)-C(12)             174.6(2)
     N(1)-C(9)-C(10)-C(41)             172.9(2)
     C(8)-C(9)-C(10)-C(41)              -5.6(4)
     C(19)-N(11)-C(12)-C(10)          -175.3(2)
     Zn(1)-N(11)-C(12)-C(10)            14.9(3)
     C(19)-N(11)-C(12)-C(13)            2.0(3)
     Zn(1)-N(11)-C(12)-C(13)         -167.79(17)
     C(9)-C(10)-C(12)-N(11)             0.3(4)
     C(41)-C(10)-C(12)-N(11)         -179.5(2)
     C(9)-C(10)-C(12)-C(13)          -176.5(2)
     C(41)-C(10)-C(12)-C(13)            3.7(4)
     N(11)-C(12)-C(13)-C(14)          178.6(3)
     C(10)-C(12)-C(13)-C(14)           -4.2(5)
     N(11)-C(12)-C(13)-C(18)           -3.1(3)
     C(10)-C(12)-C(13)-C(18)          174.1(2)
     C(18)-C(13)-C(14)-C(15)           -2.1(4)
     C(12)-C(13)-C(14)-C(15)          176.0(3)
     C(13)-C(14)-C(15)-C(16)            0.9(5)
     C(14)-C(15)-C(16)-C(17)            0.8(5)
     C(15)-C(16)-C(17)-C(18)           -1.2(5)
     C(16)-C(17)-C(18)-C(13)           -0.1(4)
     C(16)-C(17)-C(18)-C(19)         -179.9(3)
     C(14)-C(13)-C(18)-C(17)            1.7(4)
     C(12)-C(13)-C(18)-C(17)         -176.9(3)
     C(14)-C(13)-C(18)-C(19)         -178.4(2)
     C(12)-C(13)-C(18)-C(19)            2.9(3)
     C(12)-N(11)-C(19)-N(20)          180.0(2)
     Zn(1)-N(11)-C(19)-N(20)          -10.2(4)
     C(12)-N(11)-C(19)-C(18)           -0.2(3)
     Zn(1)-N(11)-C(19)-C(18)          169.62(17)
     C(17)-C(18)-C(19)-N(20)           -2.1(5)
```

```
C(13)-C(18)-C(19)-N(20)        178.0(2)
C(17)-C(18)-C(19)-N(11)        178.0(3)
C(13)-C(18)-C(19)-N(11)         -1.8(3)
N(11)-C(19)-N(20)-C(22)          3.8(4)
C(18)-C(19)-N(20)-C(22)       -176.0(2)
C(19)-N(20)-C(22)-N(21)          1.7(4)
C(19)-N(20)-C(22)-C(23)        179.5(2)
C(29)-N(21)-C(22)-N(20)        177.3(2)
Zn(1)-N(21)-C(22)-N(20)          0.2(4)
C(29)-N(21)-C(22)-C(23)         -0.7(3)
Zn(1)-N(21)-C(22)-C(23)       -177.83(17)
N(20)-C(22)-C(23)-C(24)          0.8(5)
N(21)-C(22)-C(23)-C(24)        178.9(3)
N(20)-C(22)-C(23)-C(28)       -176.9(2)
N(21)-C(22)-C(23)-C(28)          1.2(3)
C(28)-C(23)-C(24)-C(25)          0.6(4)
C(22)-C(23)-C(24)-C(25)       -176.7(3)
C(23)-C(24)-C(25)-O(251)       177.7(3)
C(23)-C(24)-C(25)-C(26)         -1.8(4)
C(24)-C(25)-O(251)-C(252)     -174.7(3)
C(26)-C(25)-O(251)-C(252)        4.8(3)
C(25)-O(251)-C(252)-O(255)     -10.3(3)
C(25)-O(251)-C(252)-C(253)    -126.2(3)
C(25)-O(251)-C(252)-C(254)     105.5(3)
O(251)-C(252)-O(255)-C(26)      12.1(3)
C(253)-C(252)-O(255)-C(26)     128.5(3)
C(254)-C(252)-O(255)-C(26)    -104.6(3)
C(252)-O(255)-C(26)-C(27)      170.8(3)
C(252)-O(255)-C(26)-C(25)       -9.6(3)
C(24)-C(25)-C(26)-O(255)      -177.4(3)
O(251)-C(25)-C(26)-O(255)        3.1(3)
C(24)-C(25)-C(26)-C(27)          2.2(5)
O(251)-C(25)-C(26)-C(27)      -177.3(3)
O(255)-C(26)-C(27)-C(28)       178.2(3)
C(25)-C(26)-C(27)-C(28)         -1.3(4)
C(26)-C(27)-C(28)-C(23)          0.2(4)
C(26)-C(27)-C(28)-C(29)        179.3(3)
C(24)-C(23)-C(28)-C(27)          0.1(4)
C(22)-C(23)-C(28)-C(27)        178.1(2)
C(24)-C(23)-C(28)-C(29)       -179.2(2)
C(22)-C(23)-C(28)-C(29)         -1.2(3)
C(22)-N(21)-C(29)-N(30)        179.6(2)
Zn(1)-N(21)-C(29)-N(30)         -3.3(4)
C(22)-N(21)-C(29)-C(28)         -0.1(3)
Zn(1)-N(21)-C(29)-C(28)        177.04(17)
C(27)-C(28)-C(29)-N(30)          2.0(4)
C(23)-C(28)-C(29)-N(30)       -178.8(2)
C(27)-C(28)-C(29)-N(21)       -178.3(3)
C(23)-C(28)-C(29)-N(21)          0.8(3)
N(21)-C(29)-N(30)-C(32)         -7.2(4)
C(28)-C(29)-N(30)-C(32)        172.4(2)
C(29)-N(30)-C(32)-N(31)          3.4(4)
C(29)-N(30)-C(32)-C(33)       -175.1(2)
C(39)-N(31)-C(32)-N(30)       -177.1(2)
Zn(1)-N(31)-C(32)-N(30)         10.4(4)
C(39)-N(31)-C(32)-C(33)          1.6(3)
Zn(1)-N(31)-C(32)-C(33)       -170.96(16)
N(30)-C(32)-C(33)-C(38)        177.1(2)
N(31)-C(32)-C(33)-C(38)         -1.6(3)
N(30)-C(32)-C(33)-C(34)         -4.2(4)
N(31)-C(32)-C(33)-C(34)        177.0(3)
```

```
C(38)-C(33)-C(34)-C(35)           0.9(4)
C(32)-C(33)-C(34)-C(35)        -177.5(3)
C(33)-C(34)-C(35)-O(351)        177.9(2)
C(33)-C(34)-C(35)-C(36)          -1.6(4)
C(34)-C(35)-O(351)-C(352)      -162.1(3)
C(36)-C(35)-O(351)-C(352)        17.5(3)
C(35)-O(351)-C(352)-O(355)      -27.8(3)
C(35)-O(351)-C(352)-C(354)     -145.3(3)
C(35)-O(351)-C(352)-C(353)       89.2(3)
O(351)-C(352)-O(355)-C(36)       27.9(3)
C(354)-C(352)-O(355)-C(36)      145.3(3)
C(353)-C(352)-O(355)-C(36)      -89.5(3)
C(352)-O(355)-C(36)-C(37)       161.1(3)
C(352)-O(355)-C(36)-C(35)       -17.7(3)
O(351)-C(35)-C(36)-C(37)       -178.7(2)
C(34)-C(35)-C(36)-C(37)           0.9(4)
O(351)-C(35)-C(36)-O(355)         0.2(3)
C(34)-C(35)-C(36)-O(355)        179.8(2)
O(355)-C(36)-C(37)-C(38)       -178.1(2)
C(35)-C(36)-C(37)-C(38)           0.6(4)
C(34)-C(33)-C(38)-C(37)           0.6(4)
C(32)-C(33)-C(38)-C(37)         179.3(2)
C(34)-C(33)-C(38)-C(39)        -177.7(2)
C(32)-C(33)-C(38)-C(39)           1.0(3)
C(36)-C(37)-C(38)-C(33)          -1.3(4)
C(36)-C(37)-C(38)-C(39)         176.5(3)
C(32)-N(31)-C(39)-N(40)         179.7(2)
Zn(1)-N(31)-C(39)-N(40)          -7.8(4)
C(32)-N(31)-C(39)-C(38)          -0.9(3)
Zn(1)-N(31)-C(39)-C(38)        171.63(16)
C(33)-C(38)-C(39)-N(40)         179.3(2)
C(37)-C(38)-C(39)-N(40)           1.3(4)
C(33)-C(38)-C(39)-N(31)          -0.1(3)
C(37)-C(38)-C(39)-N(31)        -178.2(3)
N(31)-C(39)-N(40)-C(2)            0.8(4)
C(38)-C(39)-N(40)-C(2)         -178.5(2)
N(1)-C(2)-N(40)-C(39)             2.5(4)
C(3)-C(2)-N(40)-C(39)          -179.3(2)
C(12)-C(10)-C(41)-C(46)          88.0(3)
C(9)-C(10)-C(41)-C(46)          -91.8(3)
C(12)-C(10)-C(41)-C(42)         -90.3(3)
C(9)-C(10)-C(41)-C(42)           89.9(3)
C(46)-C(41)-C(42)-C(43)          -0.7(4)
C(10)-C(41)-C(42)-C(43)         177.7(3)
C(41)-C(42)-C(43)-C(44)          -1.7(5)
C(42)-C(43)-C(44)-O(47)        -177.3(3)
C(42)-C(43)-C(44)-C(45)           3.0(5)
O(47)-C(44)-C(45)-C(46)         178.5(3)
C(43)-C(44)-C(45)-C(46)          -1.8(5)
C(44)-C(45)-C(46)-C(41)          -0.7(5)
C(42)-C(41)-C(46)-C(45)           1.9(5)
C(10)-C(41)-C(46)-C(45)        -176.5(3)
C(45)-C(44)-O(47)-C(48)         -11.8(5)
C(43)-C(44)-O(47)-C(48)         168.5(3)
C(44)-O(47)-C(48)-C(49)        -171.7(3)
O(47)-C(48)-C(49)-C(50)         -72.9(4)
C(48)-C(49)-C(50)-C(51)        -174.1(3)
C(49)-C(50)-C(51)-C(52)         171.4(3)
C(55S)-O(51S)-C(52S)-C(53S)      37.9(3)
Zn(1)-O(51S)-C(52S)-C(53S)     -179.7(2)
O(51S)-C(52S)-C(53S)-C(54S)     -28.3(4)
```

```
C(52S)-C(53S)-C(54S)-C(55S)      9.3(4)
C(52S)-O(51S)-C(55S)-C(54S)    -32.0(4)
Zn(1)-O(51S)-C(55S)-C(54S)    -176.1(2)
C(53S)-C(54S)-C(55S)-O(51S)     12.9(4)
C(69)-N(61)-C(62)-C(100)        178.0(3)
Zn(2)-N(61)-C(62)-C(100)          3.5(4)
C(69)-N(61)-C(62)-C(63)           0.6(3)
Zn(2)-N(61)-C(62)-C(63)        -173.84(19)
N(61)-C(62)-C(63)-C(68)          -0.2(3)
C(100)-C(62)-C(63)-C(68)       -177.5(3)
N(61)-C(62)-C(63)-C(64)         175.0(4)
C(100)-C(62)-C(63)-C(64)         -2.3(6)
C(68)-C(63)-C(64)-C(65)           0.4(5)
C(62)-C(63)-C(64)-C(65)        -174.3(3)
C(63)-C(64)-C(65)-C(66)           0.1(6)
C(64)-C(65)-C(66)-C(67)          -0.5(6)
C(65)-C(66)-C(67)-C(68)           0.4(6)
C(66)-C(67)-C(68)-C(63)           0.1(5)
C(66)-C(67)-C(68)-C(69)         174.9(3)
C(64)-C(63)-C(68)-C(67)          -0.5(5)
C(62)-C(63)-C(68)-C(67)         175.6(3)
C(64)-C(63)-C(68)-C(69)        -176.4(3)
C(62)-C(63)-C(68)-C(69)          -0.2(3)
C(62)-N(61)-C(69)-N(70)        -179.8(3)
Zn(2)-N(61)-C(69)-N(70)          -5.2(4)
C(62)-N(61)-C(69)-C(68)          -0.7(3)
Zn(2)-N(61)-C(69)-C(68)         173.9(2)
C(67)-C(68)-C(69)-N(70)           4.3(5)
C(63)-C(68)-C(69)-N(70)         179.7(3)
C(67)-C(68)-C(69)-N(61)        -174.8(3)
C(63)-C(68)-C(69)-N(61)           0.6(3)
N(61)-C(69)-N(70)-C(72)           8.5(5)
C(68)-C(69)-N(70)-C(72)        -170.5(3)
C(69)-N(70)-C(72)-N(71)           1.6(5)
C(69)-N(70)-C(72)-C(73)         178.6(3)
C(79)-N(71)-C(72)-N(70)         175.3(3)
Zn(2)-N(71)-C(72)-N(70)         -12.9(4)
C(79)-N(71)-C(72)-C(73)          -2.0(3)
Zn(2)-N(71)-C(72)-C(73)         169.84(19)
N(70)-C(72)-C(73)-C(78)        -176.2(3)
N(71)-C(72)-C(73)-C(78)           1.2(3)
N(70)-C(72)-C(73)-C(74)           3.7(5)
N(71)-C(72)-C(73)-C(74)        -178.8(3)
C(78)-C(73)-C(74)-C(75)          -0.6(5)
C(72)-C(73)-C(74)-C(75)         179.4(3)
C(75)-O(751)-C(752)-O(755)       -9.7(3)
C(75)-O(751)-C(752)-C(753)      107.9(3)
C(75)-O(751)-C(752)-C(754)     -126.8(3)
O(751)-C(752)-O(755)-C(76)        9.3(3)
C(753)-C(752)-O(755)-C(76)     -107.3(3)
C(754)-C(752)-O(755)-C(76)      125.6(3)
C(752)-O(751)-C(75)-C(74)      -174.6(3)
C(752)-O(751)-C(75)-C(76)         6.7(4)
C(73)-C(74)-C(75)-O(751)       -177.5(3)
C(73)-C(74)-C(75)-C(76)           1.1(5)
C(752)-O(755)-C(76)-C(77)       175.8(3)
C(752)-O(755)-C(76)-C(75)        -5.5(4)
O(751)-C(75)-C(76)-O(755)        -0.7(4)
C(74)-C(75)-C(76)-O(755)       -179.5(3)
O(751)-C(75)-C(76)-C(77)        178.0(3)
C(74)-C(75)-C(76)-C(77)          -0.8(5)
```

295

```
O(755)-C(76)-C(77)-C(78)          178.4(3)
C(75)-C(76)-C(77)-C(78)            -0.1(5)
C(74)-C(73)-C(78)-C(77)            -0.2(5)
C(72)-C(73)-C(78)-C(77)           179.8(3)
C(74)-C(73)-C(78)-C(79)          -180.0(3)
C(72)-C(73)-C(78)-C(79)             0.0(3)
C(76)-C(77)-C(78)-C(73)             0.5(4)
C(76)-C(77)-C(78)-C(79)          -179.8(3)
C(72)-N(71)-C(79)-N(80)          -175.1(3)
Zn(2)-N(71)-C(79)-N(80)            13.6(4)
C(72)-N(71)-C(79)-C(78)             2.0(3)
Zn(2)-N(71)-C(79)-C(78)          -169.38(19)
C(73)-C(78)-C(79)-N(80)           175.9(3)
C(77)-C(78)-C(79)-N(80)            -3.8(5)
C(73)-C(78)-C(79)-N(71)            -1.2(3)
C(77)-C(78)-C(79)-N(71)           179.1(3)
N(71)-C(79)-N(80)-C(82)             0.3(4)
C(78)-C(79)-N(80)-C(82)          -176.4(3)
C(79)-N(80)-C(82)-N(81)            -2.9(4)
C(79)-N(80)-C(82)-C(83)           177.6(3)
C(89)-N(81)-C(82)-N(80)          -178.3(3)
Zn(2)-N(81)-C(82)-N(80)            -8.6(4)
C(89)-N(81)-C(82)-C(83)             1.3(3)
Zn(2)-N(81)-C(82)-C(83)           171.00(19)
N(80)-C(82)-C(83)-C(88)           178.4(3)
N(81)-C(82)-C(83)-C(88)            -1.2(3)
N(80)-C(82)-C(83)-C(84)            -0.5(5)
N(81)-C(82)-C(83)-C(84)           180.0(3)
C(88)-C(83)-C(84)-C(85)            -0.9(4)
C(82)-C(83)-C(84)-C(85)           177.8(3)
C(83)-C(84)-C(85)-O(851)          179.8(3)
C(83)-C(84)-C(85)-C(86)             0.0(5)
C(84)-C(85)-O(851)-C(852)         173.6(3)
C(86)-C(85)-O(851)-C(852)          -6.6(4)
C(85)-O(851)-C(852)-O(855)          9.6(4)
C(85)-O(851)-C(852)-C(854)        127.1(3)
C(85)-O(851)-C(852)-C(853)       -106.4(3)
O(851)-C(852)-O(855)-C(86)         -9.2(4)
C(854)-C(852)-O(855)-C(86)       -126.1(3)
C(853)-C(852)-O(855)-C(86)        107.6(3)
C(852)-O(855)-C(86)-C(87)        -174.5(4)
C(852)-O(855)-C(86)-C(85)           5.5(4)
C(84)-C(85)-C(86)-C(87)             0.5(5)
O(851)-C(85)-C(86)-C(87)         -179.3(3)
C(84)-C(85)-C(86)-O(855)         -179.5(3)
O(851)-C(85)-C(86)-O(855)           0.7(4)
O(855)-C(86)-C(87)-C(88)          179.9(3)
C(85)-C(86)-C(87)-C(88)             0.0(5)
C(84)-C(83)-C(88)-C(87)             1.4(5)
C(82)-C(83)-C(88)-C(87)          -177.6(3)
C(84)-C(83)-C(88)-C(89)           179.6(3)
C(82)-C(83)-C(88)-C(89)             0.6(3)
C(86)-C(87)-C(88)-C(83)            -0.9(5)
C(86)-C(87)-C(88)-C(89)          -178.7(3)
C(82)-N(81)-C(89)-N(90)           177.1(3)
Zn(2)-N(81)-C(89)-N(90)             6.7(4)
C(82)-N(81)-C(89)-C(88)            -0.8(3)
Zn(2)-N(81)-C(89)-C(88)          -171.23(19)
C(83)-C(88)-C(89)-N(90)          -178.0(3)
C(87)-C(88)-C(89)-N(90)             0.1(5)
C(83)-C(88)-C(89)-N(81)             0.1(3)
```

```
C(87)-C(88)-C(89)-N(81)          178.1(3)
N(81)-C(89)-N(90)-C(92)            2.8(5)
C(88)-C(89)-N(90)-C(92)         -179.5(3)
C(89)-N(90)-C(92)-N(91)            5.4(5)
C(89)-N(90)-C(92)-C(93)         -173.9(3)
C(99)-N(91)-C(92)-N(90)          179.2(3)
Zn(2)-N(91)-C(92)-N(90)          -21.2(4)
C(99)-N(91)-C(92)-C(93)           -1.4(3)
Zn(2)-N(91)-C(92)-C(93)          158.2(2)
N(90)-C(92)-C(93)-C(94)            3.1(5)
N(91)-C(92)-C(93)-C(94)         -176.3(3)
N(90)-C(92)-C(93)-C(98)         -180.0(3)
N(91)-C(92)-C(93)-C(98)            0.6(4)
C(98)-C(93)-C(94)-C(95)            0.1(5)
C(92)-C(93)-C(94)-C(95)          176.7(3)
C(93)-C(94)-C(95)-C(96)           -0.4(5)
C(94)-C(95)-C(96)-C(97)            0.1(5)
C(95)-C(96)-C(97)-C(98)            0.5(5)
C(96)-C(97)-C(98)-C(93)           -0.7(5)
C(96)-C(97)-C(98)-C(99)         -176.9(3)
C(94)-C(93)-C(98)-C(97)            0.4(5)
C(92)-C(93)-C(98)-C(97)         -176.8(3)
C(94)-C(93)-C(98)-C(99)          177.6(3)
C(92)-C(93)-C(98)-C(99)            0.4(3)
C(92)-N(91)-C(99)-C(100)        -178.6(3)
Zn(2)-N(91)-C(99)-C(100)          22.7(4)
C(92)-N(91)-C(99)-C(98)            1.7(3)
Zn(2)-N(91)-C(99)-C(98)         -157.0(2)
C(97)-C(98)-C(99)-N(91)          175.3(3)
C(93)-C(98)-C(99)-N(91)           -1.3(3)
C(97)-C(98)-C(99)-C(100)          -4.4(6)
C(93)-C(98)-C(99)-C(100)         179.0(3)
N(91)-C(99)-C(100)-C(62)          -3.7(5)
C(98)-C(99)-C(100)-C(62)         176.0(3)
N(91)-C(99)-C(100)-C(101)        174.4(3)
C(98)-C(99)-C(100)-C(101)         -5.9(5)
N(61)-C(62)-C(100)-C(99)         -10.1(5)
C(63)-C(62)-C(100)-C(99)         166.8(3)
N(61)-C(62)-C(100)-C(101)        171.7(3)
C(63)-C(62)-C(100)-C(101)        -11.4(4)
C(99)-C(100)-C(101)-C(102)       -76.2(4)
C(62)-C(100)-C(101)-C(102)       102.1(3)
C(99)-C(100)-C(101)-C(106)       106.0(3)
C(62)-C(100)-C(101)-C(106)       -75.7(4)
C(106)-C(101)-C(102)-C(103)        0.1(5)
C(100)-C(101)-C(102)-C(103)     -177.7(3)
C(101)-C(102)-C(103)-C(104)       -1.2(5)
C(102)-C(103)-C(104)-O(107)     -177.3(3)
C(102)-C(103)-C(104)-C(105)        1.7(5)
O(107)-C(104)-C(105)-C(106)      177.9(3)
C(103)-C(104)-C(105)-C(106)       -1.2(5)
C(104)-C(105)-C(106)-C(101)        0.1(5)
C(102)-C(101)-C(106)-C(105)        0.4(5)
C(100)-C(101)-C(106)-C(105)      178.2(3)
C(105)-C(104)-O(107)-C(108)      160.2(3)
C(103)-C(104)-O(107)-C(108)      -20.8(5)
C(104)-O(107)-C(108)-C(109)      176.2(3)
O(107)-C(108)-C(109)-C(110)      -81.0(4)
C(108)-C(109)-C(110)-C(111)     -172.6(3)
C(109)-C(110)-C(111)-C(112)      177.1(4)
Zn(2)-O(121)-C(122)-C(123)       -54.2(6)
```

```
O(121)-C(122)-C(123)-C(212)   -148(3)

C(135)-O(131)-C(132)-C(133)      2.0(13)
O(131)-C(132)-C(133)-C(134)      5.6(13)
C(132)-C(133)-C(134)-C(135)    -10.3(13)
C(133)-C(134)-C(135)-O(131)     11.2(13)
C(132)-O(131)-C(135)-C(134)     -8.6(14)
O(138)-C(137)-C(136)-C(139)    -14.0(13)
C(136)-C(137)-O(138)-C(139)     14.8(14)
```

Crystal structure analysis of a Zn-phthalocyanine complex with thf/EtOH ligands (101), plus solvents

Crystal data: $C_{54} H_{47} N_7 O_6 Zn$, $C_{52} H_{44} N_7 O_6 Zn$, $C_{3.6} H_{4.8} O$, *ca* 7.7C, M =1020.11. Triclinic, space group P-1 (no. 2), a = 14.7577(3), b = 15.4422(3), c = 22.5632(3) Å, α = 83.6288(12), β = 79.7051(13), γ = 75.3302(15) °, V = 4882.57(16) Å^3. Z = 2, Dc = 1.388 g cm^{-3}, F(000) = 2123, T = 100.3(8) K, μ(Cu-Kα) = 12.11 cm^{-1}, λ(Cu-Kα) = 1.54184 Å.

The crystal was a dark blue needle. From a sample under oil, one, *ca* 0.55 x 0.03 x 0.02 mm, was mounted on a small loop and fixed in the cold nitrogen stream on a Rigaku Oxford Diffraction XtaLAB Synergy diffractometer, equipped with Cu-Kα radiation, HyPix detector and mirror monochromator. Intensity data were measured by thin-slice ω-scans. Total no. of reflections recorded, to θ$_{max}$ = 70.00°, was 62,951 of which 18,253 were unique (Rint = 0.084); 14,581 were 'observed' with I > 2σ$_I$.

Data were processed using the CrysAlisPro-CCD and -RED (1) programs. The structure was determined by the intrinsic phasing routines in the SHELXT program (2A) and refined by full-matrix least-squares methods, on F^2's, in SHELXL (2B). There are two Zn-phthalocyanine units, with different axial ligands, in the crystal, and several solvent molecules (not fully resolved) in the lattice. In the Zn-complex molecules, the non-hydrogen atoms were refined with anisotropic thermal parameters and hydrogen atoms were included in idealised positions with their Uiso values were set to ride on the Ueq values of the parent carbon atoms. The atoms (some with partial site occupation) of the solvent molecules were included and most were refined isotropically. At the conclusion of the refinement, wR$_2$ = 0.198 and R$_1$ = 0.079 (2B) for all 18,253 reflections weighted w = [σ^2(F$_o^2$) + (0.1342 P)^2 + 0.31000 P]$^{-1}$ with P = (F$_o^2$ + 2F$_c^2$)/3; for the 'observed' data only, R$_1$ = 0.066.

In the final difference map, the highest peak (*ca* 0.9 eÅ^{-3}) was near Zn(2).

Scattering factors for neutral atoms were taken from reference (3). Computer programs used in this analysis have been noted above, and were run through WinGX (4) on a Dell Optiplex 780 PC at the University of East Anglia.

References

(1) Programs CrysAlisPro, Rigaku Oxford Diffraction Ltd., Abingdon, UK (2018).

(2) G. M. Sheldrick, Programs for crystal structure determination (SHELXT), *Acta Cryst.* (2015) A**71**, 3-8, and refinement (SHELXL), *Acta Cryst.* (2008) A**64**, 112-122 and (2015) C**71**, 3-8.

(3) 'International Tables for X-ray Crystallography', Kluwer Academic Publishers, Dordrecht (1992). Vol. C, pp. 500, 219 and 193.

(4) L. J. Farrugia, *J. Appl. Cryst.* (2012) **45**, 849–854.

Legends for Figures

Figure 1.   View of a molecule of the Zn-phthalocynine-thf complex, indicating the atom numbering scheme. Thermal ellipsoids are drawn at the 20% probability level.

Figure 2.   View of a molecule of the Zn-phthalocynine-EtOH complex, indicating the atom numbering scheme. Thermal ellipsoids are drawn at the 20% probability level.

Figure 3.   Projections on to the planes of the four coordinating N atoms of (a) the thf complex and (b) the ethanol complex.

Figure 4.   From the projections of Figure 3, rotation of the complexes about the horizontal axes in the page of 90°, shows (a) the side-on, neighbouring, parallel planes of the thf complex and (b) the corresponding views of the ethanol complex.

Figure 5.   View of the packing of molecules, along the *b* axis.

Notes on the structure

The two Zn-complex molecules have very similar core structures, and differ mostly in the axial ligand and peripheral orientation details. The thf ligand is well-defined as the axial ligand in the first complex; the ligand in the second complex appears to be an ethanol molecule, but there might be disorder around the methyl group with a nearby unresolved mass of solvent molecules. The ethanol (O)-H atom has not been identified, but the O(121)…N(80') distance is 2.773 Å and the trigonal planar geometry around O(121) indicates a likely hydrogen bond here.

The zinc centres lie 0.239 and 0.342 Å from the planes of the four coordinated isoindole N atoms and are directed towards the axially coordinated ligand, either the thf molecule or an ethanol molecule. The zinc coordination is therefore square pyramidal in both complexes, Figures 1 and 2.

Each of the two complexes has close links to a centrosymmetrically related molecule. The thf complex forms a back-to-back dimer with a long region, from C(10) to C(10'), showing close π…π contacts with its neighbour and the two zinc atoms 6.215 Å apart. In the EtOH complex, there is good overlap of half the phthalocyanine ligand, involving the isoindole rings of N(71) and N(81) and the related rings; the other half of the phthalocyanine ligand, with the rings of N(61) and N(91), is more twisted, presumably to accommodate the interactions of the C(97)–H and C(64)–H groups with the bisecting phenyl group of C(101-

106), but there are close C…C contacts between overlapping, approximately parallel rings, e.g. C(65)…C(93') at 3.548 Å.

The solvent sites comprise one molecule of THF, disordered in two orientations mostly resolved, plus an unresolved cluster of 12 sites occupied by a total of *ca* 7.7 carbon atoms.